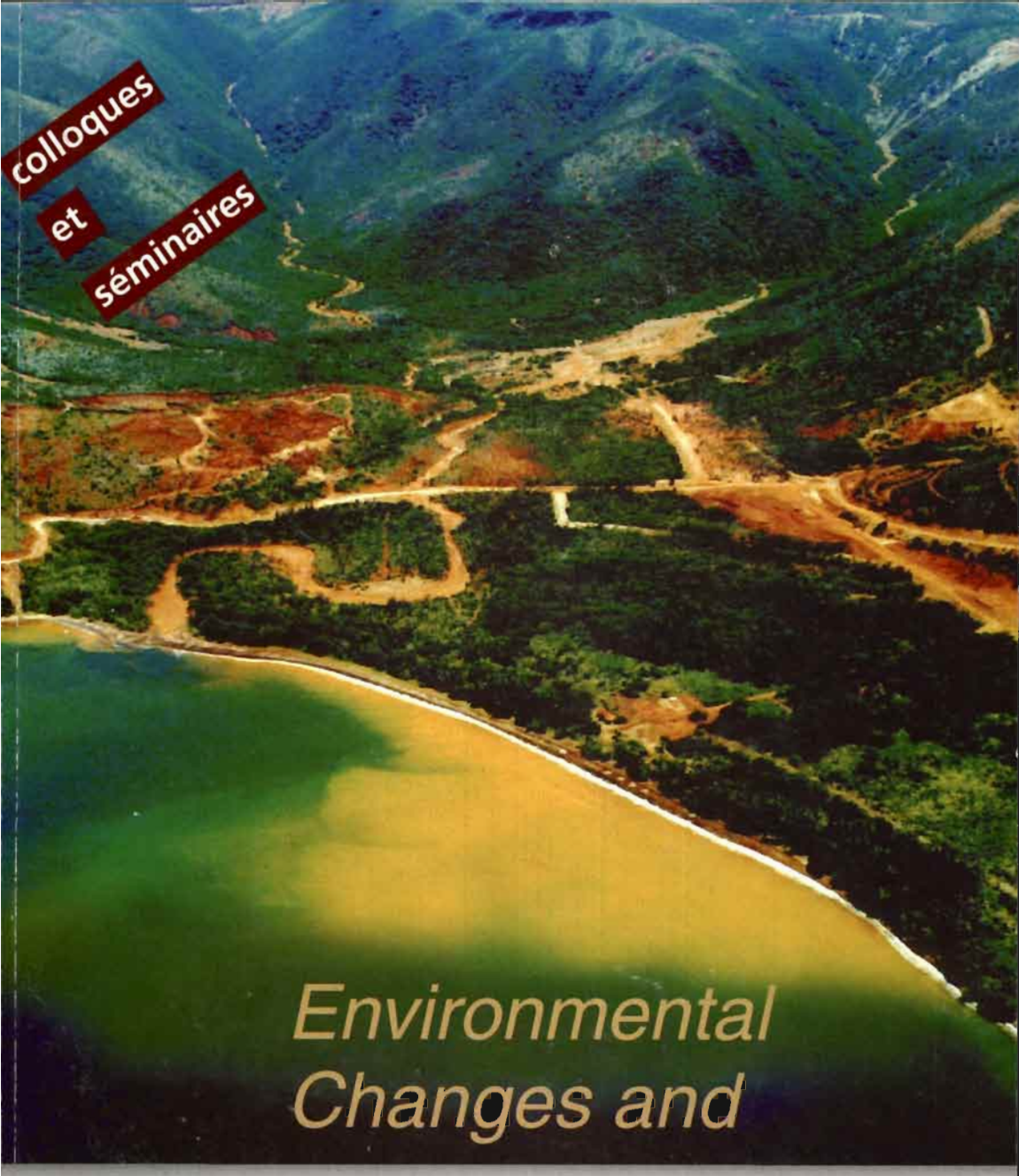

Environmental Changes and Radioactive Tracers

Scientific Editors
Jean-Michel Fernandez
Renaud Fichez

IRD Éditions

Environmental Changes and Radioactive Tracers

6th South Pacific Environmental
Radioactivity Association Conference
19-23 June 2000
Nouméa IRD Centre - New Caledonia

Environmental Changes and Radioactive Tracers

Scientific Editors
Jean-Michel Fernandez
Renaud Fichez

IRD Éditions
INSTITUT DE RECHERCHE POUR LE DÉVELOPPEMENT

collection Colloques et séminaires

Paris, 2002

Mise en page - Fabrication
Jean-Pierre Mermoud

Maquette de couverture
Michelle Saint-Léger

Maquette intérieure
Catherine Plasse

Photo de couverture
© QNI Limited: "Impacts on sea after high rainfall events"
Photo page 104
© CEA-Cadarache (DEN/DED)
Photos pages : 277, 363, 433
© IRD. J. P. Mermoud

ISSN : 0767-2896
ISBN : 2-7099-1493-X

Remerciements

La sixième conférence de la South Pacific Environmental Radioactivity Association (SPERA-2000) a été organisée grâce au soutien logistique et financier de l'Institut de recherche pour le développement (IRD) et l'implication active de Christian Colin, directeur du Centre IRD de Nouméa.

Cette conférence n'aurait pu avoir son plein succès sans la contribution financière de l'Institut de protection et de sûreté nucléaire (IPSN) dont Eugène Pauli a été le principal promoteur.

L'importance des coûts engendrés pour l'organisation d'une telle manifestation a également nécessité le soutien des partenaires tels que: l'Australian nuclear science and technology organisation (ANSTO-ED) ; Commissariat à l'energie atomique Direction des applications militaires - Département d'analyse et de surveillance de l'environnement, France (CEA-DAM/DASE) ; le National radiation laboratory (NRL), Nouvelle-Zélande.

Le Secrétariat permanent pour le Pacifique a permis par son aide, de prendre en charge les frais de déplacements et de séjour de plusieurs collègues, chercheurs dans les pays du Sud. Le Congrès de la Nouvelle-Calédonie, la Province Sud de la Nouvelle Calédonie, la ville de Nouméa ainsi que le Secrétariat Général de la Communauté du Pacifique (CPS) ont, pour leur part, amplement participé à l'accueil de la communauté internationale des chercheurs venus présenter leurs travaux.

La société Le Nickel (SLN) a contribué à la réussite de cette conférence tant par le soutien financier qu'elle a dispensé que par l'organisation de la visite mémorable du site minier du « Camp des Sapins ».

Les éditeurs tiennent également à remercier très sincèrement:

- les conférenciers invités qui ont ouvert chacune des sessions de travail;

- les présidents des différentes sessions et l'ensemble des intervenants qui ont permis le succès scientifique de la conférence;

- les présidents et chercheurs qui ont assuré la relecture et l'arbitrage des textes publiés dans ce document;

- le personnel des services administratifs du centre IRD de Nouméa ;

- le personnel de l'atelier de reprographie et en particulier Jacqueline Thomas responsable de la cellule de communication et Jean-Pierre Mermoud qui a assuré la mise en page des pré-actes et la mise en forme des textes.

Nous ne saurions oublier toute l'équipe du programme ECOTROPE qui s'est pleinement investie dans l'organisation du congrès.

Un clin d'œil cordial est adressé aux différents responsables du CEA-Cadarache (DEN/DED) ayant intercédé en faveur de l'achèvement de l'ouvrage pendant les « heures de travail ».

Acknowledgements

The Sixth Conference of the South Pacific Environmental Radioactivity Association (SPERA-2000) enjoyed the logistical and financial support of the Institute of research for development and benefited from the active involvement of Mr Christian Colin, the Director of IRD Nouméa centre.

This event could not have been such a success without the financial support of the *Institut de protection et de sûreté nucléaire* (Institute for nuclear protection and safety – IPSN) mainly represented by Mr Eugène Pauli.

The substantial cost of hosting such an event also required the support of sponsors such as the Australian nuclear science and technology organisation (ANSTO-ED); Commissariat à l'energie atomique; Direction des applications militaires - Département d'analyse et de surveillance de l'environnement, France (CEA-DAM/DASE) ; le National radiation laboratory (NRL), Nouvelle-Zélande.

The French permanent Secretariat for the Pacific covered the travel and accommodation costs of a number of colleagues working as researchers in southern countries. The Congress of New Caledonia, the Southern Province of New Caledonia, the City of Nouméa and the Secretariat of the Pacific Community (SPC) all generously helped to host the international community of scientists who came to present the results of their work.

The *Le Nickel* company (SLN) also contributed to the success of this conference through financial support and an unforgettable visit to their mining camp "Camp des Sapins".

The editors also wish to thank very sincerely:

- the invited speakers who opened each working session;

- the chairs of the various sessions and all the speakers who made this conference a scientific success;

- the chairpersons and scientists who reviewed and edited the texts published in this document;

- the administrative staff of the IRD Centre;

- the staff of the copying section, and also particularly Mrs Jacqueline Thomas, the IRD Communication Officer and Mr Jean-Pierre Mermoud, who laid out the book of abstracts and these published texts.

We should not forget the ECOTROPE Programme team, who played a full part in the organisation of the conference.

Thanks are also due to the various CEA-Cadarache (DEN/DED) staff who contributed to the completion of this publication during "working hours".

Authors list

C. **Alonso Hernández**, Radioecology and Environmental Surveillance Dpt, Central Radiological and Environmental Surveillance Laboratory, LVRAC AP #5, Ciudad Nuclear, CP 59 350, Cienfuegos, Cuba

Peter G. **Appleby**, Department of Mathematical Sciences, University of Liverpool, P.O. Box 143, Liverpool L69 3BX, U.K., email: appleby@liverpool.ac.uk

Gérard **Ardisson**, Laboratoire de radiochimie et radioécologie, université de Nice-Sophia Antipolis, Faculté des Sciences, 28 avenue Valrose, 06108 Nice cedex 2, France, email: ardisson@unice.fr

Christian **Badie**, Laboratoire d'étude et de surveillance de l'environnement, CEA/IPSN, BP 519, Papeete, Tahiti, Polynésie française

Geneviève **Barci-Funel**, Laboratoire de radiochimie et radioécologie, université de Nice-Sophia Antipolis, faculté des sciences, 28 avenue Valrose, 06108 Nice cedex 2, France, email: gbarci@unice.fr

Christian **Bernard**, Laboratoire d'étude et de surveillance de l'environnement, IPSN/CEA, BP 519, Papeete, Tahiti, Polynésie française

Michael **Bickel**, European Commission, Joint Research Centre, Institute for Reference Materials and Measurements, Geel, Belgium, email: michael.bickel@irmm.jrc.be

Lidia D. **Blinova**, V. G. Khlopin Radium Institute, Saint-Petersburg, Russian Federation, email: head@atc.sbor.spb.su

Alexandru **Bologa**, National Institute for Marine Research and Development "Grigore Antipa", RO-8700, Constanta, Romania, email: abologa@alpha.rmri.ro

Ludovic **Breau**, Centre IRD de Nouméa, BP A5, 98848 Nouméa, Nouvelle-Calédonie, email: breau@noumea.ird.nc

Francois **Bréchignac**, Institut de protection et de sûreté nucléaire (PSN), DPRE-SERLAB, CE Cadarache, BP1, 13108 Saint-Paul-lez-Durance, France, email: francois.brechignac@ipsn.fr

Greg **Brunskill**, Australian Institute of Marine Science, Townsville, Qld, Australia, email: g_brunskill@aims.gov.au

Paco **Bustamante**, université de La Rochelle, La Rochelle, France, email: pbustama@univ-lr.fr

H. **Cartas Aguila**, Radioecology and Environmental Surveillance Dpt, Central Radiological and Environmental Surveillance Laboratory, LVRAC AP #5, Ciudad Nuclear, CP 59 350, Cienfuegos, Cuba

Jaume **Casadesus**, Departament de Biologia Vegetal, Universitat de Barcelona Diagonal, 645 08028 Barcelona, Spain, email: jcasadesusb@campus.uoc.es

Alejandra **Castillo**, *Instituto de Física, Facultad de* Ciencias, Universidad Austral de Chile, Valdivia, Chile, email: acastillo@uach.cl

Douglas **Chitty**, Laboratoire de radiochimie et radioécologie, université de Nice-Sophia Antipolis, faculté des Sciences, 28 avenue Valrose, 06108 Nice cedex 2, France

Claude **Colle**, Institut de protection et de sûreté nucléaire, DPRE/SERLAB, Centre de Cadarache, bât. 186, BP 1, 13108 Saint-Paul-Lez-Durance cédex, France, email: claude.colle@ipsn.fr

Olivier **Cotret**, International Atomic Energy Agency, Marine Environment Laboratory, Monaco, email: o.cotret@iaea.org

Elvira **Cuingioglu**, National Institute for Marine Research and Development "Grigore Antipa", RO-8700, Constanta, Romania, email: elvis@alpha.rmri.ro

Bruno **Danis**, Laboratoire de biologie marine (CP 160-15), université libre de Bruxelles, 50 av. F.D. Roosevelt, B-1050 Bruxelles, Belgium, email: bdanis@ulb.ac.be

Jean-Paul **Deschamps**, Commissariat à l'énergie atomique, (DAM/DASE/SRCE, direction Ile-de France, département analyses surveillance environnement, service radioanalyses chimie environnement, BP 12, F-91680, Bruyères-le-Châtel, France, email: deschamps@dase.bruyeres.cea.fr

Misael **Díaz Asencio**, Radioecology and Environmental Surveillance Dpt, Central Radiological and Environmental Surveillance Laboratory, LVRAC AP#5, Ciudad Nuclear, CP 59 350, Cienfuegos, Cuba

Philippe **Dubois**, université libre de Bruxelles, 50 av. F. D. Roosevelt, B-1050 Bruxelles, Belgique, email: dubois.p@pg.com

David N. **Edgington**, Great Lakes Water Institute, University of Wisconsin-Milwaukee, Milwuakee, USA, email: dnedge@csd.uwm.edu

Marie **Ferland**, McNair Scholars Program, Central Washington University, Ellensburg, WA 98926-7439, USA, email: ferland_ma@yahoo.com

Jean-Michel **Fernandez**, Commissariat à l'énergie atomique, CEA/DED/SEP/LCD, bât. 352, CE Cadarache, BP1, 13108 Saint-Paul-Lez-Durance, France, email: FERNANDEZ@desdsud.cea.fr

Renaud **Fichez**, Centre IRD de Nouméa, BP A5, 98848 Nouméa, Nouvelle-Calédonie, email: fichez@noumea.ird.nc

Jacques **Foos**, CNAM, Laboratoire des sciences nucléaires, 292 rue Saint Martin, 75003 Paris, France, email: foos@cnam.fr

Sverker **Forsberg**, Swedish University of Agricultural Sciences, Uppsala, Sweden, email: sverker.forsberg@ausys.se

Scott W. **Fowler**, International Atomic Energy Agency, Marine Environment Laboratory, Monaco, email: s.fowler@iaea.org

Masami **Fukui**, Research Reactor Institute, Kyoto University: Noda, Kumatori-cho, 590-0494 Osaka, Japan, email: fukuim@rri.kyoto-u.ac.jp

Sitaram **Garimella**, Department of Physics, The University of the South Pacific, Suva, Fiji Islands, email: garimella@usp.ac.fj

Claire **Garrigue**, Centre IRD de Nouméa, BP A5, 98848 Nouméa, Nouvelle-Calédonie, email: garrigue@noumea.ird.nc

José Marcus de Oliveira **Godoy**, Instituto de Radioproteção e Dosimetria, Comissão Nacional de Energia Nuclear, Rio de Janeiro, Brazil, email: godoy@ird.gov.br

Valentin N. **Golosov**, Laboratory of Soil Erosion and Fluvial Processes, Department of Geography, Moscow State University, Moscow, Russia, email: golosov@river.geogr.msu.su

Marc André **Gonze**, Institut de protection et de sûreté nucléaire, DPRE/SERLAB, Centre de Cadarache, bât. 186,

BP 1, 13108 Saint-Paul-Lez-Durance cedex, France, email: marc-andre.gonze@ipsn.fr

Ron **Grazioso**, Dept. of Chemical and Nuclear Engineering, University of New Mexico, USA

Jacqui **Greaves**, opération Cétacés, BP12827, Nouméa, Nouvelle-Calédonie

Gary **Hancock**, CSIRO Land and Water, Canberra, ACT 2601, Australia, email: gary.hancock@cbr.clw.csiro.au

Koh **Harada**, National Institute for Resources and Environment, 16-3 Onogawa, 305-5869 Tsukuba, Japan, email: harada@nire.go.jp

John R. **Harries**, ANSTO, Environment Division, Australian Nuclear Science and Technology Organisation (ANSTO), Menai, NSW 2234, Australia, email: john.harries@ansto.gov.au

Elizabeth **Haworth**, Institute of Freshwater Ecology, Ferry house, Ambleside, Cumbria LA22 0LP, U.K., email: eyh@ceh.ac.uk

Hilde-Elise **Heldal**, Institute for Marine Research, Bergen, Norway, email: hilde.elise.heldal@imr.no

Ann **Henderson-Sellers**, ANSTO, Environment Division, Menai, NSW 2234, Australia, email: ahssec@ansto.gov.au

Antonio **Hernandez Benitez**, CIEMAT, Avenidad Complutense, 08000 Madrid, Spain, email: antonio.hernandez@ciemat.es

Parvis **Irannejad**, ANSTO, Environment Division, Australian Nuclear Science and Technology Organisation, Menai, NSW, Australia, email: parvis.irannejad@ansto.gov.au

Takashi **Itakura**, ANSTO, Environment Division, Menai, NSW 2234, Australia, email: takashi.itakura@ansto.gov.au

Peter J. **Kershaw**, CEFAS, Lowestoft, UK, email: p.j.kershaw@cefas.co.uk

Dejanira C. **Lauria**, Instituto de Radioproteção e Dosimetria, Comissão Nacional de Energia Nuclear, Rio de Janeiro, Brazil, email: dejanira@ird.gov.br

Gilbert **Le Petit**, Commissariat à l'énergie atomique (DAM/DASE/SRCE), direction Ile-de-France, département analyse surveillance environnement, service radioanalyses chimie environnement, BP 12, F-91680 Bruyères-le-Châtel, France, email: lepetit@ldg.bruyeres.cea.fr

Hugh D. **Livingston**, IAEA-MEL (Marine Environmental Laboratory), Monaco, email: h.livingston@iaea.org

Chantal **Madoz-Escande**, Institut de protection et de sûreté nucléaire, DPRE/SERLAB, Centre de Cadarache, bât. 186, BP 1, 13108 Saint-Paul-Lez-Durance cedex, France, email: chantal.madoz-escande@ipsn.fr

Olivier **Magand**, International Atomic Energy Agency, Marine Environment Laboratory, Monaco, email: o.magand@iaea.org

Joanna **Marchant**, Imperial College, London, United Kingdom, email: j.marchant@ic.ac.uk

Maxim Vladimirovich **Markelov**, Laboratory of Soil Erosion and Fluvial Processes, Department of Geography, Moscow State University, Moscow, Russia, email: river@river.geogr.msu.su

Alastair **McArthur**, Department of Physics, The University of the South Pacific, Suva, Fiji Islands, email: MCARTHUR_A@usp.ac.fj

Gordon D. **McOrist**, ANSTO, Environment Division, Menai, NSW 2234, Australia, email: gdm@ansto.gov.au

Hervé **Michel**, Laboratoire de radiochimie et radioécologie, université de Nice-Sophia Antipolis, faculté des sciences, 28 avenue Valrose, 06108 Nice cedex 2, France, email: hmichel@unice.fr

Pierre **Miramand**, université de La Rochelle, La Rochelle, France, email: pierre.miramand@univ-lr.fr

Benjamin **Moreton**, Centre IRD de Nouméa, BP A5, 98848 Nouméa, Nouvelle-Calédonie, email: moreton@noumea.ird.nc

Sandor **Mulsow**, International Atomic Energy Agency, Marine Environment Laboratory, Monaco, email: s.mulsow@iaea.org

Alain **Muñoz Caravaca**, Radioecology and Environmental Surveillance Dpt, Central Radiological and Environmental Surveillance Laboratory, LVRAC AP #5, Ciudad Nuclear, CP 59 350, Cienfuegos, Cuba, email: lvrac@perla.inf.cu

Sunun **Nouchpramools**, Office of Atomic Energy for Peace, Vibhavadee-Rangsit Rd, Chatuchak, Bangkhen, Bangkok, Thailand

Anselmo S. **Paschoa**, Pontifícia Universidade Católica do Rio de Janeiro (PUC-Rio), Physics Department, C.P. 38071,

Rio de Janeiro, RJ 22452-970, Brazil,
email: aspas@vdg.fis.puc-rio.br

Vasile **Patrascu**, National Institute for Marine Research and Development "Grigore Antipa", RO-8700, Constanta, Romania, email: vasile@alpha.rmri.ro

Tim E. **Payne**, ANSTO, Environment Division, Menai, NSW 2234, Australia, email: tim.payne@ansto.gov.au

Gillian **Peck**, ANSTO, Environment Division, PMB 1, Menai, NSW 2234, Australia, email: Gillian.Peck@ansto.gov.au

John **Pfitzner**, Australian Institute of Marine Science, Townsville, Qld, Australia, email: j.pfitzner@aims.gov.au

Riitta **Pilvio**, National Radiation Laboratory, Christchurch, New Zealand, email: Riitta_Pilvio@nrl.moh.govt.nz

Pavel **Povinec**, International Atomic Energy Agency, Marine Environment Laboratory, Monaco,
email: p.povinec@iaea.org

Pedro **Rivas Romero**, CIEMAT, Avenidad Complutense, 08000 Madrid, Spain, email: pedro.rivas@ciemat.es

Jacques **Rivaton**, Centre IRD de Nouméa, BP A5, 98848 Nouméa, Nouvelle-Calédonie

John A. **Robbins**, Great Lakes Environmental Research Laboratory, National Oceanic and Atmospheric Administration, Ann-Arbor, USA,
email: robbins@glerl.noaa.gov

Pedro F. **Rodríguez-Espinosa**, Instituto Politécnico Nacional, Domicilio provisional: Calle Reforma Nº 113 Col. Palmira, 62490 Temixco, Morelos, México,
email: pedrof@mail.cicata.ipn.mx

Teresa **Sauras**, Departament de Biologia Vegetal, Universitat de Barcelona Diagonal, 645 08028 Barcelona, Spain, email: sauras@porthos.bio.ub.es

Paulina **Schuller**, Instituto de Física, Facultad de Ciencias, Universidad Austral de Chile, Valdivia, Chile,
email: pschulle@uach.cl

Graeme **Shaw**, Imperial College, T H Huxley School, Silwood Park, Ascot, Berkshire, SL5 7PY, United Kingdom,
email: gg.shaw@ic.ac.uk

Yoko **Shibamoto**, National Institute for Resources and Environment, 16-3 Onogawa, 305-5869 Tsukuba, Japan,
email: harada@nire.go.jp

David E. **Smiles**, CSIRO Land and Water, Canberra, ACT 2601, Australia, email: david.smiles@cbr.clw.csiro.au

J. David **Smith**, Marine Chemistry Laboratory, School of Chemistry, University of Melbourne, Parkville 3052, Australia, email: jdsmith@unimelb.edu.au

John N. **Smith**, Bedford Institute of Oceanography, Department of Fisheries and Oceans, Dartmouth, B2Y 4A2, Canada, email: smithjn@mar.dfo-mpo.gc.ca

Oswin **Snehaleela**, Department of Physics, The University of the South Pacific, Suva, Fiji Islands

E. **Suárez Morell**, Radioecology and Environmental Surveillance Dpt, Central Radiological and Environmental Surveillance Laboratory, LVRAC AP #5, Ciudad Nuclear, CP 59 350, Cienfuegos, Cuba

Ali **Temara**, université libre de Bruxelles, Laboratoire de biologie marine, CP 160/15, 50 av. F. Roosevelt, 1050 Bruxelles, Belgium, email: temara.a@pg.com

Jean-Louis **Teyssié**, International Atomic Energy Agency, Marine Environment Laboratory, Monaco, email: jl.teyssie@iaea.org

Yves **Thiry**, SCK-CEN, Mol, Belgium, email: ythiry@sckcen.be

Marc **Trescinski**, Laboratoire d'étude et de surveillance de l'environnement, CEA/IPSN, BP 519, Papeete, Tahiti, Polynésie française

Rosa Eugenia **Trumper**, Instituto de Física, Facultad de Ciencias, Universidad Austral de Chile, Valdivia, Chile, email: rtrumper@valdivia.uca.uach.cl

Ramon **Vallejo**, University of Barcelona, Facultat Biologia-Principal, Diagonal, 645, 08028 Barcelona, Spain, email: vallejo@porthos.bio.ub.es

Francisco **Vidal Lorandi**, Grupo de Estudios Oceanográficos, Centro de Investigación en Ciencia Aplicada y Tecnología Avanzada, Instituto Politécnico Nacional, Domicilio provisional: A.P. 1-475 Centro, Cuernavaca, 62001, Morelos, México

Víctor **Vidal Lorandi**, Grupo de Estudios Oceanográficos, Centro de Investigación en Ciencia Aplicada y Tecnología Avanzada, Instituto Politécnico Nacional, Domicilio provisional: A.P. 1-475 Centro, Cuernavaca, 62001, Morelos, México

Nadia **Waegeneers**, SCK-CEN, Mol, Belgium,
email: nadia.waegeneers@agr.kuleuven.ac.be

Michel **Warnau**, International Atomic Energy Agency,
Marine Environment Laboratory, Monaco,
email: m.warnau@iaea.org

Stewart **Whittlestone**, ANSTO, Environment Division,
PMB1, Menai, NSW 2234, Australia,
email: Stewart.Whittlestone@ansto.gov.au

Wlodek **Zahorowski**, ANSTO, Environment Division, PMB1,
Menai, NSW 2234, Australia, email: wza@ansto.gov.au

Vladimir L. **Zimin**, V. G. Khlopin Radium Institute,
Saint-Petersburg, Russian Federation,
email: zimin@atc.sbor.spb.su

Referees list

Jean-Michel **Fernandez**
Gareth R. **Gilbert**
Gary **Hancock**
John R. **Harries**
Antonio **Hernandez-Benitez**
Ross **Jeffree**
Peter J. **Kershaw**
Gilbert **Le Petit**
Timothy **Quine**
Paulina **Schuller**
John N. **Smith**
Rick **Tinker**
John **Twining**

Contents

Radioactivity in sedimentary studies

Radioactivity in atmospheric studies

Radioactivity in soils and related issues

Radioactivity and water column

Préface

Cela fera bientôt 70 ans que Frédéric et Irène Joliot-Curie montrèrent ou décrivirent, grâce à la radioactivité dite « artificielle » qu'ils venaient de découvrir, les diverses applications possibles des traceurs radioactifs. La radioécologie allait naître tout logiquement quelques années après. C'est ainsi que l'utilisation des isotopes radioactifs, naturels ou artificiels, allait se montrer indispensable dans les études environnementales, aussi bien en hydrologie que dans les sciences de la terre ou les études atmosphériques. Depuis quelques décennies, les traceurs radioactifs sont aussi utilisés pour mieux comprendre les processus biologiques: sciences environnementales et sciences de la vie se retrouvent donc – et logiquement – liées. On retrouve là le programme scientifique du congrès SPERA 2000.

Les progrès de la radioécologie sont intimement liés aux compétences des radiochimistes, capables par diverses opérations chimiques de déceler des quantités infimes de matière, utilisant là les propriétés remarquables de la radioactivité mais aussi les nouvelles techniques d'analyse extrêmement performantes.

Je mentionnais plus haut isotopes naturels et artificiels. L'intérêt des seconds me semble considérable à plusieurs points de vue. Lorsque, en 1987, nous décidions Jean-Claude Guary, Pierre Guegueniat, et moi-même d'accueillir à Cherbourg, dans les locaux flambant neufs de l'Institut national des techniques de la mer (Intechmer) un congrès international intitulé « Radionucléides: un outil pour l'océanographie », à quelques brasses des centres nucléaires de la Hague, de Flamanville et de l'arsenal militaire, nous désirions mettre l'accent, en pleine polémique anti-nucléaire, sur les possibilités qu'offraient les infimes rejets de matière radioactive en terme de recherches. Ce congrès eut le succès que l'on connaît. C'est à peu près à cette même époque que l'association SPERA, créée en 1985, prit son envol.

J'ai été très heureux de constater, dans ce VI^{e} congrès international SPERA 2000, les progrès qui ont été réalisés dans tous les domaines évoqués plus haut, comment les techniques utilisées permettent de mieux comprendre l'environnement, et également permettent de mieux le contrôler. Ce congrès a réuni 70 participants de 24 pays pour 76 communications orales ou affichées, regroupées dans 6 rubriques. Sur le plan matériel, l'organisation a été en tous points

remarquable, aussi bien dans la maîtrise opérationnelle que dans la convivialité qu'a su transmettre et entretenir celui qui en a été l'élément moteur: Jean-Michel Fernandez, qui s'est dépensé sans compter pour que cette conférence internationale se déroule dans les meilleures conditions. Tous les congressistes savent l'énergie qu'il convient de dépenser pour réussir une telle organisation et je me fais leur interprète pour le remercier très chaleureusement: ce n'est que justice dans cette préface.

Pour conclure, j'ai le sentiment que ce congrès SPERA 2000 a su fédérer tous les thèmes de recherche associant les radionucléides et l'environnement. C'est maintenant la mission des congrès de ce nouveau siècle, dont on s'accorde à dire qu'il sera celui de l'environnement, de développer ces divers domaines. C'est là aussi la tâche, difficile mais primordiale, des radioécologistes d'aujourd'hui.

Professeur Jacques FOOS
Titulaire de la chaire
« Rayonnements, Isotopes et Applications »
au Conservatoire national des arts et métiers (CNAM)
directeur du Laboratoire des sciences nucléaires (CNAM)
Paris - France

Preface

It is now almost 70 years since Frederic and Marie Joliot-Curie demonstrated, using 'artificial' radioactivity, that they had just discovered various possible applications of radioactive tracers. Radio-ecology would logically emerge a few years later. The use of radioactive isotopes, natural and artificial, would become essential in environmental research, in the areas of hydrology, earth sciences and atmospheric studies. For several decades now, radioactive tracers have also been used to gain a better understanding of biological processes: environmental sciences and life sciences are therefore, logically, linked. This is basis of the scientific programme for the SPERA-2000 Conference.

Progress in radio-ecology is closely linked to the abilities of radio-chemists who, from various chemical operations, are capable of detecting infinitely small quantities of matter, using the outstanding properties of radioactivity but also new and very efficient analysis techniques.

I mentioned natural and artificial isotopes. Artificial isotopes seem particularly promising from several points of view. In 1987 when we decided (Jean-Claude Guary, Pierre Guegueniat and myself) to host an international Congress titled 'Radionuclides: a tool for oceanography' in the brand-new buildings of the National Institute for Ocean Techniques, just a few steps from the nuclear centres of La Hague and Flamanville and close to the Military Arsenal, while antinuclear feeling was running high, we wanted to reflect upon the research possibilities offered by tiny emanations of radioactive matter. This Congress was a success, as we all know. It was at about the same time that the SPERA Association, set up in 1985, really took off.

I was very happy to note during the sixth international Conference that progress has been made in every area referred to above and how the techniques used make it possible to understand the environment better and to manage it more effectively. This Conference brought together 70 participants from 24 countries to deliver 76 papers under six headings.

From the practical point of view, the organisation was excellent, both in operational terms and in the friendly atmosphere that prevails through the efforts of the driving force, Dr Jean-Michel Fernandez, who worked tirelessly to make this international conference run smoothly. All the participants know how much energy is needed to make a congress a success

and I speak on their behalf when I thank him very warmly. It is only fair to do so in this preface.

To conclude, I have the feeling that the 6th International Conference, SPERA-2000, managed to address all the research themes associating radionuclides and the environment. The work of future conferences in this new century, which everyone agrees is the century of the environment, is to further develop the work in these areas. This is the difficult but essential task of today's radio-ecologists.

Professor Jacques Foos
Chair of 'Radiation, Isotopes and Applications' at the
Conservatoire national des arts et métiers (CNAM)
Director of the Laboratory of Nuclear Sciences (CNAM)
Paris, France

Radioactivity in biological processes

Session 1

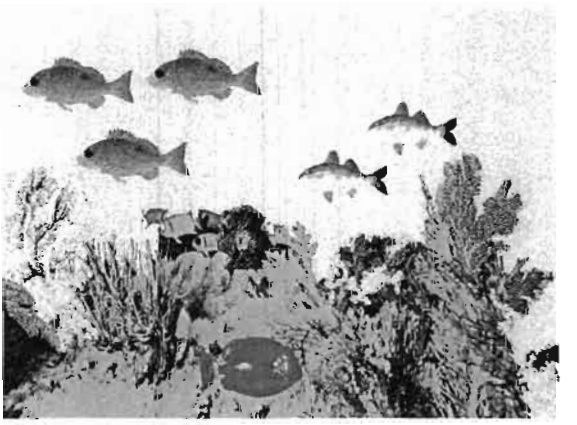

Chairman: J. Twining

Session opening: R. Jeffree

Fishes as radionuclide bioindicators in the area of Leningrad nuclear power plant (Gulf of Finland, Baltic Sea)

Vladimir L. Zimin

Lidia D. Blinova

Introduction

The radioactivity of the aquatic environment comprises radionuclides of natural origin, global fallout from nuclear weapon tests, accidents at nuclear facilities and also everyday leakage of radioactive substances from nuclear power plants.

The area under investigation is characterized by a high concentration of nuclear facilities. Leningrad NPP (LNPP) with 4 RBMK-1000 reactors, North-west regional storage facility of low and intermediate level radioactive wastes (LSK "Radon") and the North-west science and industrial center of atomic energy (Figure 1).

Radioecological monitoring of the Koporskaya Bay coastal waters (LNPP cooling water body) as well as rivers and lakes of the bay drainage basin, is a part of the integral ecological monitoring of Sosnovy Bor Region. The work was carried out at the Regional environmental monitoring laboratory of the V.G. Khlopin Radium Institute.

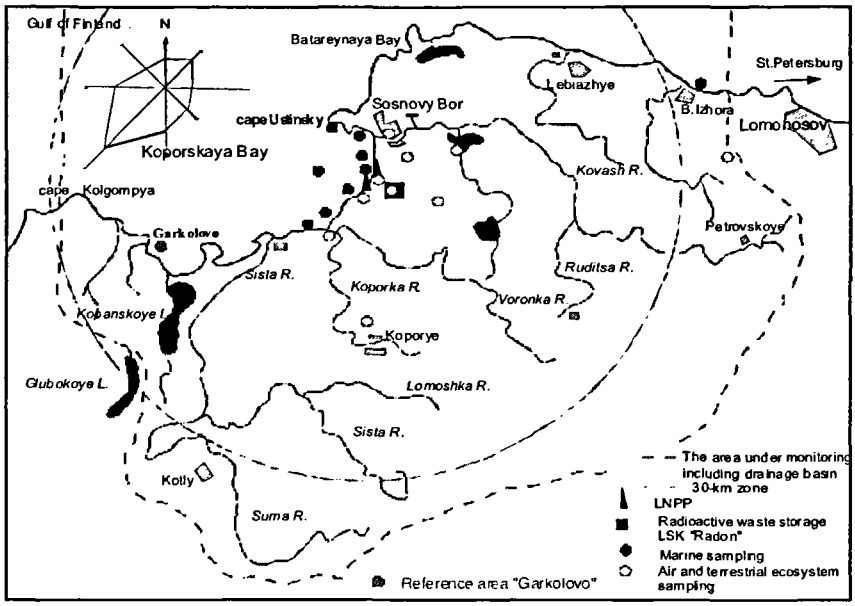

Figure 1
The area under monitoring (Sosnovy Bor Region), including Leningrad NPP 30-km zone.

Materials and methods

Most of the fish samples were collected in 1982-1999. In that period, 462 samples of 25 fish species were analyzed for radionuclide content. Fish were caught by our own efforts or collected from local fishery company catches. The locations of sampling sites are shown in Figure 1. A substantial portion of our catches comprised samples from the LNPP water input area. Fish samples were analyzed by routine biological methods before treatment for radioactivity measurement.

After biological analysis the samples were prepared to determine gamma-emitting radionuclides by means of generally accepted methods (Marey & Zykova, 1980), in particular: "wet" ashing of

fish samples in the presence of nitric acid and hydrogen peroxide mixture in 3:1 proportion, with the subsequent ash calcination at 450°C to produce mineral compounds.

Semi-conductor spectrometers with DGDK detectors type and ÀI-1024-95 multi-channel analyzers as well as a Canberra HPGe-detector (20% efficiency) were used for the purpose of gamma-emitting radionuclides determination in the energy range from 50 keV up to 2000 keV. The low detection limit of measurements of gamma-emitting radionuclides volumetric activity in fish samples was 1.0 $Bq.kg^{-1}$ fresh weight. The activity determination error was equal to 10-30% at the 95% confidence level.

Results and discussion

The influence of nuclear power plants on radioactivity of water and aquatic ecosystem components of the cooling water bodies is evident mainly in heated water outlet canals and adjacent sea areas. Moreover, technogenic radionuclides content is substantially lower than the content of radionuclides of natural origin (e.g., ^{40}K, ^{232}Th, ^{7}Be), and also it is lower than levels of radioactivity allowed by the Radiation Safety Standards (1996).

Activation products (mainly: ^{51}Cr, ^{58}Co, ^{60}Co, ^{59}Fe, ^{54}Mn) account for most of the radionuclide contribution to the artificial radioactivity of the aquatic environment in NPP areas. Since the probability of detection of radionuclides in hydrobionts is significantly higher than in water samples, fish were used as indicators of technogenic radionuclides discharged into the aquatic environment. The main results of the investigations, conducted in Sosnovy Bor Region, are presented in the papers and reports of the Laboratory (Kryshev, 1992; Blinova, 1994; Blinova, 1996; Zimin *et al.*, 1997; Blinova *et al.*, 1998; Blinova *et al.*, 1999; Blinova *et al.*, 2000).

Biological transfer of radioactivity

Activation products were often detected in fish samples from the bay, but these elements were of infrequent occurrence in fish collected in rivers of the Koporskaya Bay drainage basin. The occurrence of activation products in few fish samples from the Kovash River due to fish migration (more often - during spawning). From Table 1 it is clear, that the most frequent occurrence of the above mentioned elements was in fish samples from the LNPP outlet canal.

The occurrence frequency of these radionuclides in fish samples from the sea sites, spaced at 3-5 km from the nuclear plant, was lower than in the LNPP outlet canal. In the Kovash River (1 km upstream of the river mouth) near 3 km downstream from the LNPP heated water outlet, activation products were detected only a few times. It should be kept in mind that very few fish species are real

Fish species and location	^{54}Mn	^{60}Co	^{65}Zn
LNPP outlet canal			
roach	18 (30 %)	11 (52 %)	70 (43 %)
threespined stickleback	1.4 (38 %)	5.6 (62 %)	30 (56 %)
Koporskaya Bay			
roach	1.5 (7 %)	10 (14 %)	60 (28 %)
threespined stickleback	<	0.4 (5 %)	0.4 (5 %)
Kovash River, down stream			
roach	3.7 (17 %)	1.9 (17 %)	34 (17 %)
Kovash River, upper stream			
dace	<	0.4 (10 %)	13 (40 %)

Note: 1) <- below the detection limit;
2) detection frequency is indicated in parentheses

Table 1
The mean specific activity of NPP originated radionuclides (Bq. kg^{-1} fresh wt.) in fish from the Leningrad NPP area between 1976-1984. The value in brackets indicates the proportion of fish in which these radionuclides were detected.

migrating species. Except for anadromous species, namely *Lampetra fluviatilis*, *Salmo salar*, *Salmo trutta*, most species migrate only to the down stream sites for spawning or feeding. Thus

roach (*Rutilus rutilus*) dwelling in the Koporskaya Bay never migrate to the upper stream part of the river.

In the upper stream of the Kovash River radionuclides originated from the LNPP were registered in only one fish species, namely dace (*Leuciscus leuciscus*). This may be evidence of the radionuclide bio-transfer from the nuclear power plant to the river. Dace usually dwells at streams; its occurrence in the Koporskaya Bay is of low frequency; nevertheless this species, the activation products in the samples confirm the far migration of this species.

age	^{137}Cs	^{51}Cr	^{54}Mn	^{60}Co	^{58}Co	^{65}Zn	^{59}Fe
0+	1.0	32.0	42.3	30.9	13.4	16.6	45.9
2+	1.0	27.2	32.6	21.1	10.5	82.8	27.9
3+	0.8	9.0	19.6	14.1	5.3	<	20.8
4+	1.2	<	7.6	5.4	3.0	<	7.4

Note: 1) <- below the detection limit;

Table 2
Radionuclide concentrations (Bq.kg^{-1} fresh wt.) in roach (*Rutilus rutilus*) of different age groups collected in the NPP outlet canal on 12.08.1983.

Special features of radionuclide accumulation in connection with fish age

Table 2 shows the content of ^{54}Mn, ^{51}Cr, ^{60}Co and other activation products in roach collected at the LNPP heated water outlet in the summer of 1983. The unusual character of accumulation of radionuclides was registered for the roach of different age groups collected on 12.08.1983. All concentrations of the radionuclides, except for ^{65}Zn, clearly decreased in the series "young fish - old fish".

This phenomenon is presumed to be explained by the significant contribution of the radionuclides absorbed by mucous skin epithelium to the whole radionuclide content. In view of the fact, that small-sized fish have a relatively larger skin surface areas than big-sized ones, young fish individuals can absorb more radionuclides than old fish individuals of the same total body weight. It is known, that the mean concentration factor of radionuclides and the mean body length (or age) of fish

correlate positively (Rowan & Rasmussen, 1994; Kasamatsu & Ishikawa, 1997), which is associated mainly with food habits and trophic level. Since, as a rule, an opposite situation takes place.

The fact that the roach was immediately exposed to heated water with ^{54}Mn, ^{51}Cr, ^{60}Co and other radionuclides, discharged from the LNPP, at the outlet canal, plays, of course, the important part in the process of radionuclide accumulation.

Long time dynamics of ^{137}Cs content in fish

The radiocesium dynamics in populations of some fish species from the Koporskaya Bay, as well as from rivers and lakes of the bay drainage basin, was reviewed. The data available, partly presented in Table 3, made it possible to characterize radionuclide accumulation by fish of different ecological groups and trophic levels and to trace its dynamics. Since 1986 (after the accident at Chernobyl NPP) up to nowadays, the major contribution to cesium content in fish was via radionuclides from the Koporskaya Bay drainage basin, which was subjected to Chernobyl fallout mainly in the west part.

At the present time, considerable radiocesium concentrations were registered only in fish caught in Lake Glubokoye (the Koporskaya Bay drainage basin); both ^{137}Cs and ^{134}Cs were registered there (Figure 2). The isotope ratio ^{137}Cs: ^{134}Cs in fish samples from Lake Glubokoye indicated the Chernobyl origin of these radionuclides. In 1997 and 1998 ^{137}Cs concentrations in perch and roach from Lake Glubokoye were roughly two orders of magnitude greater than concentrations in the same species from the Koporskaya Bay coastal waters.

Koporskaya Bay has a wide water exchange with the open part of the Gulf of Finland, that is why radiocesium contents in coastal water and hydrobionts, including fish, were significant only in the first years after the accident at Chernobyl NPP, with their subsequent fast reduction.

The processes of intake and elimination of ^{137}Cs by fish of different food habits and trophic levels were different in their character. The maximum ^{137}Cs concentrations in prey fish species were registered in 1986-1987. In comparison, predatory species maxima occurred a

year	Baltic herring				perch				threespined stickleback			
	n	min	max	ave	n	min	max	ave	n	min	max	ave
1982	6	1,5	5,6	2,9	2	0,4	2,2	1,3	13	0,8	11,6	4.2
1883	7	0,8	4,3	1,7	4	1,6	4,0	2,8	15	0,3	2,9	1.4
1984	8	1,3	2,1	1,6	3	2,3	4,8	3,1	11	0,7	2,9	1.6
1985	7	0,5	3,7	1,7	-	-	-	-	9	1,3	3,0	2.0
1986	2	21,1	33,2	27,1	1	21,7	21,7	21,7	5	95,6	233,5	134.9
1987	4	21,0	50,7	32,6	2	83,3	163,4	123,3	6	27,5	255,2	99.2
1988	2	14,1	24,6	19,4	7	29,2	196,8	102,4	-	-	-	
1989	-	-	-	-	2	75,9	149,5	112,7	20	1,6	45,9	30.7
1990	3	13,3	24,1	19,2	2	54,0	178,3	116,2	24	10,9	54,0	30.3
1991	3	14,1	23,9	17,9	1	15,7	15,7	15,7	14	12,6	34,0	20.9
1992	2	9,2	13,7	11,4	-	-	-	-	7	15,3	21,8	18.4
1993	-	-	-	-	-	-	-	-	1	14,0	14,0	14.0
1994	1	9,3	9,3	9,3	-	-	-	-	1	10,9	10,9	10.9
1995	1	7,4	7,4	7,4	-	-	-	-	-	-	-	
1996	1	6,7	6,7	6,7	-	-	-	-	4	1,2	22,2	12.6
1997	1	10,8	10.8	10,8	5	17,3	23,4	21,2	2	12,7	13,4	13.1
1998	-	-	-	-	1	16,3	16,3	21,2	3	8,5	11,5	10.1
1999	1	6,1	6,1	6,1	1	7,4	7,4	7,4	3	8,7	13,4	11.3

Table 3
^{137}Cs concentrations (Bq.kg^{-1} fresh wt.) in Baltic herring (*Clupea harengus membras*), perch (*Perca fluviatilis*) and threespined stickleback (*Gasterosteus aculeatus*) collected in the Koporskaya Bay during the investigation period.

year later (Figures 3-6). In 1987-1990, average ^{137}Cs concentrations in perch (predatory species) varied from 100-120 Bq.kg^{-1}. Whereas, the planktivore Baltic herring, the most important commercial fish species in the Eastern Baltic, registered 20-30 Bq.kg^{-1} ^{137}Cs. 7-50 Bq.kg^{-1} it was registered in benthivore roach, a popular sport fishing and also a commercial species.

Substantially higher ^{137}Cs concentrations in samples of threespined stickleback in comparison with Baltic herring, species with similar feeding habits, are worthy of attention (Figure 3). Threespined stickleback is a resident omnivore fish species, feeding predominantly on plankton and meiobenthos. Most of this species samples

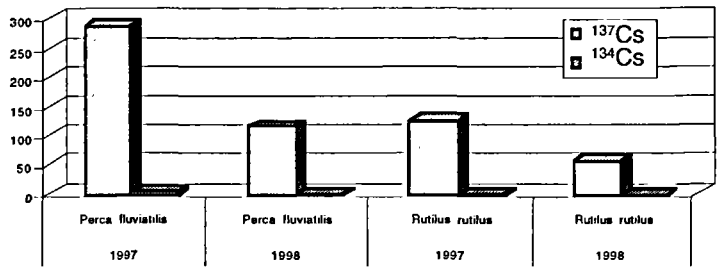

Figure 2
^{137}Cs and ^{134}Cs in prey fish *Rutilus rutilus* and predator fish *Perca fluviatilis* samples (Bq.kg^{-1} fresh wt.) from Lake Glubokoye contaminated with Chernobyl fallout.

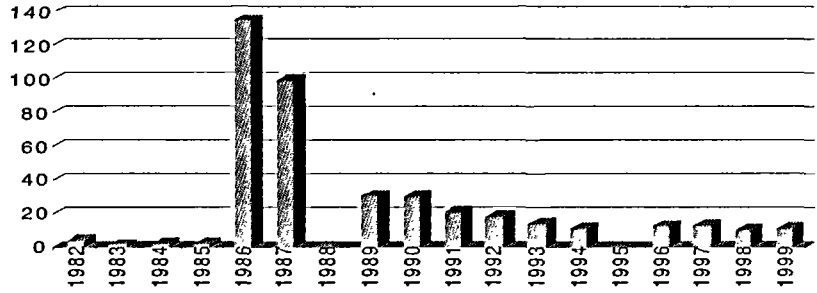

Figure 3
Long time dynamics of ^{137}Cs in omnivore fish *Gasterosteus aculeatus* samples (Bq.kg^{-1} fresh wt.) from the Koporskaya Bay (Leningrad NPP environs).

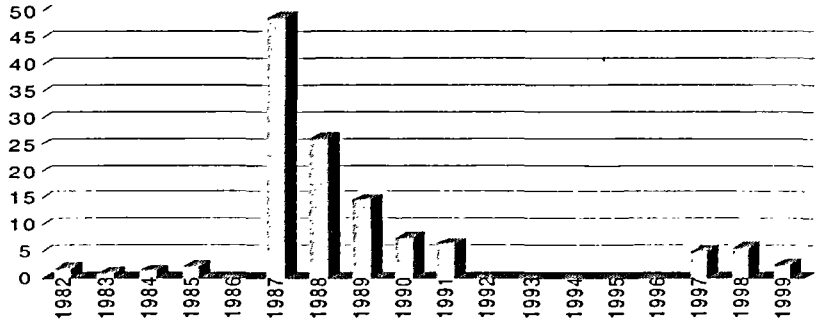

Figure 4
Long time dynamics of ^{137}Cs in benthivore fish *Rutilus rutilus* samples (Bq.kg^{-1} fresh wt.) from the Koporskaya Bay (Leningrad NPP environs).

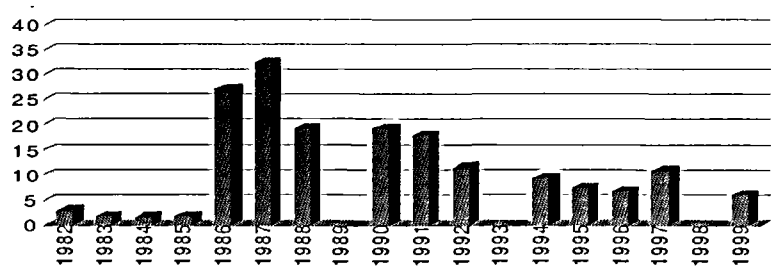

Figure 5
Long time dynamics of ^{137}Cs in planktivore fish *Clupea harengus membras* samples (Bq.kg^{-1} fresh wt.) from the Koporskaya Bay (Leningrad NPP environs).

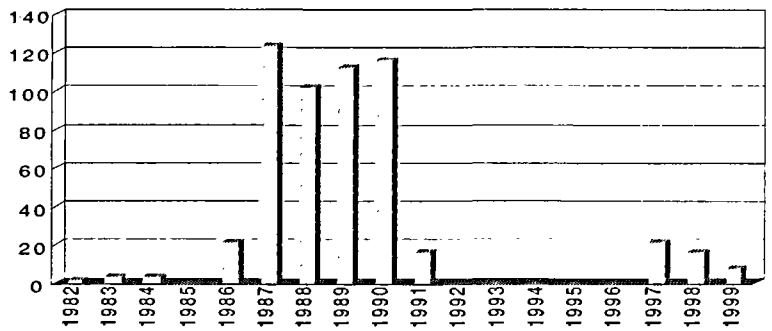

Figure 6
Long time dynamics of ^{137}Cs in piscivore fish *Perca fluviatilis* samples (Bq.kg^{-1} fresh wt.) from the Koporskaya Bay (Leningrad NPP environs).

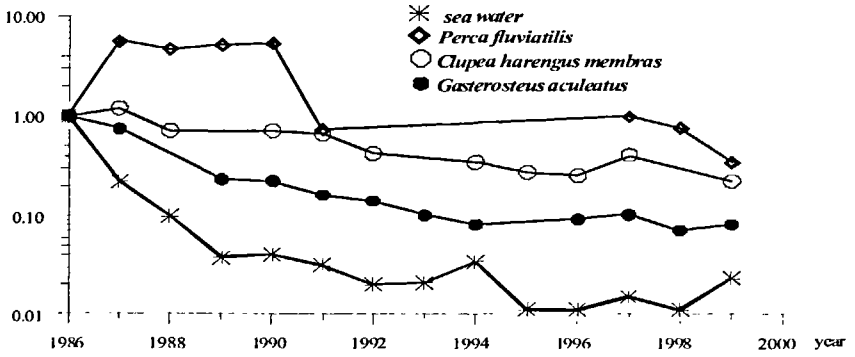

Figure 7
Relative ^{137} Cs concentrations in marine ecosystem components of the Koporskaya Bay, normalized to the data of 1986.

were collected at the water-input area, near the LNPP pump station, where a significant quantity of detritus and silt is accumulated. These are an appropriate substrata for radiocesium retention. The diet of the threespined sticklebacks from that site seems to contain a marked share of suspended organic matter as well as hydrobionts feeding on detritus. Hence, the high ^{137}Cs concentrations in this fish seems to owe their origin to diet.

Figure 7 demonstrates dynamics of ^{137}Cs content in prey and predatory fish after Chernobyl accident in 1986-1999. The steady reduction of ^{137}Cs concentrations in Baltic herring, planktivore species, and also in threespined stickleback, species with wide feeding spectrum (predominantly - planktivore), correlated positively with dynamics of ^{137}Cs content in the sea water. In contrast, most high concentrations of ^{137}Cs in predatory species, namely perch, were registered in 1987, a one year after the accident fallout. Then ^{137}Cs concentrations in perch decreased only after 1991, after a long period of retention.

Internal exposure doses for the population from consumption of local fish

It is important to estimate the internal exposure doses for the human population from consumption of $^{134, 137}Cs$ with local fish. A preliminary evaluation of internal exposure doses for the human population, inhabiting the Sosnovy Bor Region, was made in 1998. The consumption of local fish contaminated with $^{134, 137}Cs$ in consequence of the Chernobyl NPP accident now accounts for most of the expected doses of internal exposure for the population living on the southern coast of the Eastern Gulf of Finland. These doses vary over the range from 0.16 μSv from consumption of 1 kg of sea fish up to 20 μSv from consumption 1 kg of freshwater predatory fish (averaged for freshwater fish 3.0 μSv), (ISTC Project, 1999).

The annual per capita fish consumption is proposed to be 5 kg according "The Methods of Calculation of Distribution of Radioactive Substances from NPP and Exposure of the Local Population" (Normative Technical Document, 1984), but such a rate seems to be an underestimate, especially for the sea coast areas. However, calculations were made in accordance with the above

cited guidelines; and taking into account this fish consumption rate, the expected doses were evaluated as 0.8 μSv from consumption of sea fish or 15.0 μSv from the freshwater fish.

According to "Sanitary regulations in the design and exploitation of nuclear power plants (1993)" adopted in the Russian Federation, the annual limit for population exposure to radioactive substances, originated from all kinds of water usage equals 50 μSv. Thus the consumption of freshwater fish, caught in the contaminated water bodies of the Koporskaya Bay drainage basin, may be considered the most significant radioactive source in the region.

Bibliography

BLINOVA L. D., 1994 — St. Petersburg (Leningrad) NPP's region radioecological state estimation. ENC' 94 International nuclear congress-Atoms for Energy. *Transactions.*, 2: 37-39.

BLINOVA L. D., 1996 — "Littoral ecosystem radioecological monitoring in the region of atomic energy enterprises". *In: Protection of the Natural Environment,* Proceedings of International Symposium on Ionizing Radiation, Stockholm, 20-24 May 1996, 2: 497-503.

BLINOVA L. D., DUSHIN V. N., GOLUBEVA L. V., MICHURINA T. G., 1998 — "Radioecological Monitoring and Radiological Control in the Region of Sosnovy Bor Nuclear Facilities as Baltic Sea Region Safety Basis. – Radiation protection No110". *In: The radiological exposure of the population of the European Community to radioactivity in the Baltic Sea*, EUR 19200, Proceedings of Marina Balt Seminar. Stockholm, Sweden, 1998: 365-372.

BLINOVA L. D., DUSHIN V. N., GOLUBEVA L. V., MICHURINA T. G., 1999 — The development of environmental protection approaches in the region of nuclear facilities at the Russian coast of the Baltic Sea. *In: Radiation. Environmental Protection Approaches for Nuclear Facilities.* Proceedings of the Second Int. Symposium on Ionizing, Canada, Ottawa, 1999, section 6.

BLINOVA L. D., DUSHIN V. N., ZIMINA L. M., 2000 — Methodological approaches to the environmental protection in the area of nuclear power plant on the Russian coast of the Baltic Sea. *In: Problems of development of atomic energy in the Don Region.* Materials of science conference. Rostov-on-Don, 29 February 1 March, 2000. 2: 169-175.

ISTC Project, 1999 — "Ecological assessment of the region, where radioactivity dangerous enterprises are located. North-west region of Russia". *In: Methodological approaches to the organization of ecological monitoring*

system in the vicinity of nuclear facilities. (1999) Final report, #535-97, 149 p.

KASAMATSU F., ISHIKAWA Y., 1997 — Natural variations of radionuclide ^{137}Cs concentration in marine organisms with special reference to the effect of food habits and trophic level. *Mar. Ecol. Progr. Ser.*, 160: 109-120.

KRYSHEV I. I., (ed.), 1992 — *Radiological consequences of the Chernobyl accident.* Moscow, Nuclear Society International: 142 p.

MAREY A., ZYKOVA A., (eds), 1980 — *Methodical recommendations for sanitary monitoring of radioactive substances content in the environment.* Moscow.

NORMATIVE-TECHNICAL DOCUMENT 38.220.56-84, 1984 — *Safety in Atomic Energy. General principles of NPP safety. The Methods of Calculation of Distribution of Radioactive Substances from NPP and Exposure of the Local Population.* Moscow, Energoatomizdat.

Radiation Safety Standards, 1996 — NRB-96, Hygienic standards GN 2.6.1.054-96, Moscow, 127 p.

Regulations and Standards in Atomic Energy, 1993 — Sanitary regulations in the design and exploitation of nuclear power plants. SP-AS-88/93, Moscow.

ROWAN D. J., RASMUSSEN J. B., 1994 — Bioaccumulation of radiocesium by fish : the influence of physicochemical factors and trophic structure. *Can. J. Fish. Aquat. Sci.*, 51: 2388-2410.

ZIMIN V. L., BLINOVA L. D., ZIMINA L. M., 1997 — "Ecological monitoring in the vicinity of nuclear facilities for risk assessment and decision making". *In: New risk frontiers. Proceedings of the Annual meeting of the Society for Risk Analysis-Europe.*, 15-18 June 1997, Stockholm, Sweden: 746-754.

Synthetic results in the radioactivity assessment of the Romanian Black Sea sector after 1992

Vasile Patrascu

Alexandru S. Bologa

Elvira Cuingioglu

1 Introduction

A semi-enclosed tideless basin bordering six countries, the Black Sea is still considered a *"unicum hidrobiologicum"* because of its physical, chemical, and biological peculiarities; unlike any other sea, the Black Sea is permanently deficient in oxygen, or anoxic below a depth of 150-200 m (Bologa, 1994).

Major factors contributing to the deterioration of the Black Sea environment are pollution and improper use of natural resources (Osvath *et al.,* 1998). The Black Sea is an unique marine environment, one especially exposed to anthropogenic impact. Almost landlocked, besides the link with the shallow inland Azov Sea, its only exchange of water with the World Ocean is through the narrow Bosporus Strait.

The Black Sea encloses the largest body of permanently anoxic water in the world: some 90% of the sea's 5.37 x 10^5 km^3 total volume is deprived of oxygen and rich in hydrogen sulphide. Only the remaining 150 m thick surface water layer is capable of supporting marine life. The Black Sea drains a surface of land five time larger

than its own area, shared by 17 countries and inhabited by over 160 milion people. Rivers, notably the Danube, Dnieper, Don, Kuban and Bug, bring in about 80% of the pollutants (50% from the Danube alone). They include agrochemicals, poorly treated industrial liquid effluents, and domestic wastewater. Atmospheric transport, predominantly from Europe, and coastal sources, such as direct industrial waste and sewage discharges or dump sites, account for the remaining 20%. Riverine input of nutrients, heavy metals, radionuclides, organic compounds and oil is a severe problem (Osvath *et al.*, 1998).

As to radioactive contamination, different IAEA programmes showed that concentration of anthropogenic radionuclides in the Black sea environment, although considerably higher than in other parts of the World Ocean, are such that no significant radiological consequences can be expected for the public (Osvath *et al.*, 1998).

Fallout from atmospheric weapon tests and from Chernobyl accident provided excellent radiotracers for the Black Sea, such as ^{90}Sr, ^{137}Cs and plutonium isotopes (Osvath *et al.*, 1998). The main input occurred through direct deposition on the sea surface. For strontium-90, the Dnieper river became a significant source after the nuclear accident.

Various radiotracers can be used to trace water mixing and circulation, as time markers to provide sediment deposition chronologies, to provide information on fluxes of particles and particle-reactive pollutants, and in planktonic primary production estimates by ^{14}C (relevant to eutrophication).

The Black Sea's radioactivity levels have been the subject of rigorous research in the riparian countries and among organisations participating in various international oceanographic cruises. After the Chernobyl accident interest in radiological research of the Black Sea increased. Studies have included both radioactivity surveys on abiotic and biotic compounds, and experiments on the biokinetics of radionuclides in the marine environment.

For the Romanian Black Sea sector such work has carried particular importance. The need for monitoring radioactivity level's is mainly explained by the continuing existence of fallout, by the Danube river's presence and by the use of nuclear energy in elec-

tricity generation (Bologa, 1994). The Danube continues to be the main collector of radioactive wastes from seven riparian countries before flowing into the Black Sea; this important river flow (80% of the total input of fresh water to the sea) contributes to radiocontamination of the marine ecosystem as well. The utilization of nuclear energy, following the completion of the CANDU nuclear power plant at Cernavoda/Romania will require environmental monitoring including the marine areas.

Studies of radioactivity in environmental components in the Romanian marine sector date back in 1962. Beginning in 1976, the Romanian Marine Research Institute (RMRI, later National Institute for Marine Research and Development *"Grigore Antipa"* – NIMRD) initiated the country's systematic study of marine radioactivity using a network of permanent stations located between the Danube mouths, the southern extremity of the Romanian littoral, and occasionally offshore up to 90 nautical miles (Bologa *et al.*, 1994; 1995). The monitoring programme has resulted in a fairly extensive database covering the last 20 years.

The monitoring is being done for a number of reasons. One objective was to define the levels of radioactivity in the marine environment as a baseline before the new NPP started operating. Another objective was the identification of bioindicators for studying radiocontamination of the marine ecosystem, and experimentally determining possible levels of accumulation of critical radionuclides in marine biota and biological systems having direct or indirect influences on the environment and human health.

The main research tasks have included completion of the database on marine radioactive levels. Data have been also used for studies of distribution coefficients (Kds) for marine sediments and seawater and of concentration factors (CFs) for relevant local species. Assessment of external and internal individual and collective doses from marine radioactivity due to immersion in seawater and/or sea food consumption is also being made (Patrascu and Bologa, 1990).

Several applications of use of radiotracers in marine research were promoted by RMRI/NIMRD, in co-operation, since 1970: determination of sediment transport in the nearshore area, determination of the turbulent diffusion coefficients, estimation of planktonic primary production.

Material and method

A network of stations including the whole area between the Danube mouths (Sulina) and the southern limit (Mangalia), from the shoreline to 90 n.m. offshore has been used for radioactivity monitoring in the Romanian Black Sea sector.

Samples of sediments, seawater, and biota (macrophytes, molluscs, benthic and pelagic fish have been continuously collected, at monthly, quarterly, and semi-annual intervals, using common methods on board (R/V "Steaua de mare"). The material has been prepared for measurement in the laboratory. The sediment samples were dry, the water samples were dried by evaporation under infrared lamp, and the organic samples were dried and then ashed, all those operations being followed by weighing.

Beta and gamma measurements have been used in accordance with international methodology. The method of radiochemical separation in the presence of carriers was used for ^{90}Sr measurements; the beta activity of its daughter ^{90}Y was measured after it had been kept at least for 21 days reaching $^{90}Sr - ^{90}Y$ equilibrium (Cuingioglu *et al.*, 1996; 1997). Total beta counts can be an indicator to select samples for radiochemical and gamma investigations.

Nuclear techniques used for beta measurements have been two instrument lines with plastic detectors: NE102A and ND304. Gamma spectrometry analyses were carried out on HPGe Pop Top ORTEC (12% eff, 1.85 keV resolution at 1332 keV), ORTEC-NORLAND 5500 multichannel analyzer and NIM associated electronics.

The standards used for calibration are volume sources (^{137}Cs, ^{152}Eu, KCl) produced at the Atomic Physics Institute in Bucharest. The measuring times are usually between 40,000-100,000 s for gamma and between 1,000-6,000 s for beta measurements.

The measuring geometry is cylindrical with F 80x35 mm – gamma and F 50x5 mm for beta (^{90}Sr is measured on cellulose filter)

Gamma spectrometry was used for analysing emerged and submerged sediments, seawater, macroalgae, invertebrates and fish of marine origin (Bologa *et al.*, 1991).

For all seawater samples, some physico-chemical parameters such as temperature, salinity, pH, and O_2 concentration were also measured. Gross beta activity, gamma radioactivity of sediments, seawater and biota have been determined.

Results and discussion

Previous studies revealed significant radionuclide CFs for the uranium-radium and thorium series in some seaweeds. They further found fission product concentration (originating from earlier atmospheric nuclear tests and post-Chernobyl environmental contamination) in different living and non-living marine components. Given their importance, special attention was paid to caesium-134 and 137, strontium-90 and plutonium isotopes, for which international organizations established maximum permissible limits for food products. Romanian studies thus particularly focused on computing the concentration of caesium-137 and strontium-90 for sediment and seawater in the pre-Danubian sector of the Black Sea.

The highest content of artificial gamma emitters was noticed in 1986, followed by its subsequent decrease in all components, excepting submerged sediments that are a sink for the isotopes. Environmental CFs for caesium-137 and strontium-90 in different Black Sea biota were also estimated (Figure 1). The radiometric investigations of the coastal marine ecosystem showed the presence of the long-lived anthropogenic radionuclides ^{90}Sr and ^{137}Cs (Table 1).

Significant ^{90}Sr activities (0.53-8.6 Bq.kg^{-1} dry weight (d.w.)) were found in the submerged sediments collected from seven profiles between the northern and southern limits of the Romanian littoral (Table 1). The maximum values were recorded at the pre-Danubian zone, in good generally correlation with quality and origin of the sediments. For 1998 the ^{90}Sr level ranged from 2.1 to 7.8 Bq.kg^{-1} d.w. in 1999 from 3.1 to 8.3 Bq.kg^{-1} d.w. Emerged sediments were under lower limit of detection (<1.8 Bq.kg^{-1} d.w.), emphasizing small influence of the aquatic environment and their processes.

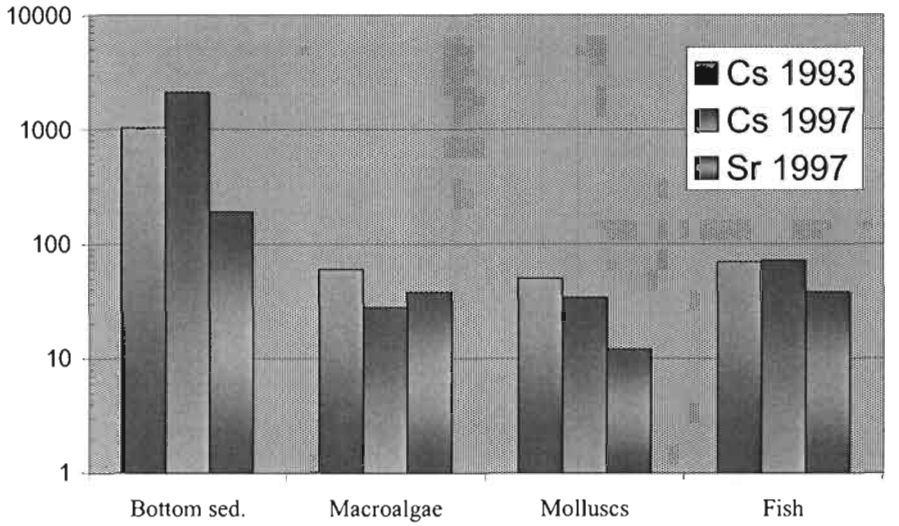

Figure 1
Concentration Factors for marine components.

Component	N	Gross beta	^{90}Sr	^{137}Cs
Sediment				
Emerged	141	30 -:- 1300	< 1.8	1.1 -:-11
Submerged	154	95 -:- 1470	0.53 -:-8.6	3.7 -:- 257
(Bq.kg^{-1}dryw.)				
Seawater	62	3300 -:- 7500	10.9 -:- 26	0.1 -:- 120
(Bq.m^{-3})				
Macroalgae	52	39 -:- 683	< 0.16 -:-	0.2 -:-
(Bq.kg^{-1}f.w.)			12.3	81.4
Molluscs	41	12 -:-192	< 0.13 -:-	0.4 -:- 2.6
(Bq.kg^{-1}f.w.)			0.7	
Fish	42	17 -:- 251	< 0.15 -:-	1.2 -:- 7.2
(Bq.kg^{-1}f.w.)			1.1	

Table 1
Results on radioactivity level for marine components (1992-1997).

In surface seawater, ^{90}Sr recent content varied over a very narrow range, 19.2-21.8 $Bq.m^{-3}$ in 1997 and 18.6-21.6 $Bq.m^{-3}$ in 1998.

The green and red macrophytes had a ^{90}Sr content of 0.3-1.9 $Bq.kg^{-1}$ fresh weight (f.w.).

Molluscs low values had 0.17 ± 0.09 $Bq.kg^{-1}$ f.w in 1998 and 0.25 ± 0.12 $Bq.kg^{-1}$ f.w. in 1999. The recent measurement of ^{90}Sr in the most frequently collected benthic fish species resulted in significant values of 0.4-1 $Bq.kg^{-1}$ f.w. in 1998, and 0.5-1.1 $Bq.kg^{-1}$ f.w. in 1999.

In all samples caesium-137 persisted after 1986; thus it was possible to track the temporal changes in concentrations of caesium-137 (Patrascu, 1996; 1997).

The numerous investigations carried out on environmental pollution indicated ^{137}Cs concentrations of 3.7-257 $Bq.kg^{-1}$ d.w. in submerged sediments from the Romanian Black Sea sector until 1997. After this year, the range has been 21-139 $Bq.kg^{-1}$ d.w. for 1998 and 16-88 $Bq.kg^{-1}$ d.w. in 1999 (Figure 2). The maximum value was found off the Danube mouths. The local variations are remarkable and correlate with the hydrodynamic conditions and sediment quality, a fact which could explain the minimum value found in a nearshore area. The observations were extended along the entire coast in bottom sediments up to 70 m depth, resulting in radionuclide concentrations of up to 249 $Bq.kg^{-1}$ d.w.; the maximum value found at a depth of about 50 m indicated that other marine processes or phenomena may have been involved (e.g. sediment transport).

The most recent analyses carried out on the emerged sediments showed concentrations between 3.7-6 $Bq.kg^{-1}$ d.w. (in 1998).

The relatively slow decrease of caesium-137 concentrations in sediment compared to seawater confirmed the ability of sediments to concentrate radionuclides.

The determination of ^{137}Cs concentrations in a reference seawater samples (Constanta, offshore and Odessa offshore) showed a level between 18-36 $Bq.m^{-3}$ (Figure 2).

Marine biota had low caesium-137 concentrations of only a few $Bq.kg^{-1}$ f.w. The macrophytes had a radionuclide average content of 1.4 ± 0.8 $Bq.kg^{-1}$ f.w, the molluscs of 1.3 ± 0.3 and the fish of 2.4 ± 0.7 $Bq.kg^{-1}$ f.w. (in 1998). *Bryopsis plumosa, Ceramium rubrum, Mya*

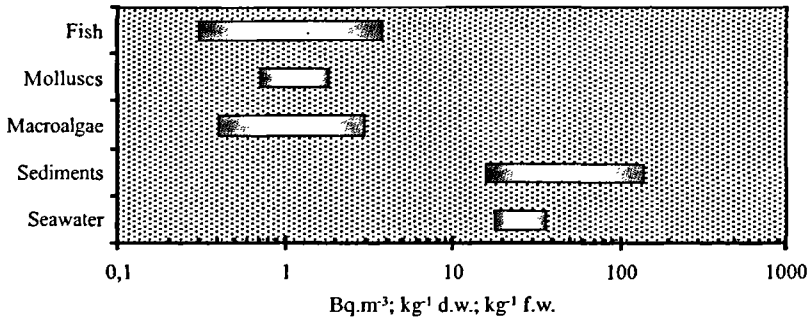

Figure 2
^{137}Cs level in marine components between 1998-1999.

arenaria, Mytilus galloprovincialis, Sprattus sprattus, Gobius melanostomus can be good bioindicators for radioactivity level in marine environment.

The highest caesium-137 and strontium-90 concentrations in edible marine biota (fish, molluscs) always ranged below the maximum permissible level allowed by FAO in 1987 and later.

The gross beta is a basic parameter in the routine control of environmental radioactivity. Gross beta measurements have been carried out in the Romanian Black sea sector for the main components of the coastal ecosystem (Table 1).

The results obtained for marine water in the reference point Mamaia have indicated values of 3,300-7,500 $Bq.m^{-3}$. The contribution of potassium is obvious. A comparative analysis effected on fresh water samples from the Danube-Black Sea Canal has shown this fact, as the values of gross beta were from 180-240 $Bq.m^{-3}$. In a sample collected from the neighbourhood of the nuclear power plant during the evacuation of the cooling agent has not indicated a significant increase of gross beta.

The emerged and interface sediments had gross beta values of 30-1300 $Bq.kg^{-1}$ d.w. (Table 1). The submerged sediments have values of 95-1470 $Bq.kg^{-1}$ d.w. The differences depend on the zone, depth, sediment quality.

The fish has a mean value of 100 $Bq.kg^{-1}$ f.w., an intermediate value between minimum for molluscs (25 $Bq.kg^{-1}$ f.w.) and maximum for algae (146 $Bq.kg^{-1}$ f.w.)

The continued monitoring of marine radioactivity is necessary either for avoiding of any nuclear risk and for comparative radiometric studies in the coastal zone (Patrascu and Bologa, 1990; Bolosa and Patrascu, 1998; Bologa *et al.*, 1998b).The knowledge and conservation of the environmental factor quality can be supported only by concrete results.

Romanian monitoring data of the annual concentrations of gamma emitting radionuclides were used in the IAEA and national data bases.

Conclusions

Several main conclusions resulted from this monitoring in the Romanian Black Sea Sector:

- the radioactivity monitoring in the Romanian marine sector has enabled the establishement of reference values for all categories of marine components;

- the Danube River mouths produce an additional impact zone owing to the Danube contribution;

- the abiotic and biotic components significantly concentrate artificial radionuclides in relation to the environmental concentrations;

- there is a remarkable concentration of caesium-137 in the submerged sediments, as a consequence of recent human activities dealing with nuclear material;

- the maximum concentration of ^{137}Cs and ^{90}Sr in edible marine biota (i.e. fish and molluscs) were always below "action level" or highest permissible limits enforced by FAO;

- background references on the present marine environmental contamination are required for the characterization of the impact of future nuclear activities near the Romanian coast (Cernavoda NPP, Danube-Black Sea Canal, Constanta-Agigea harbour).

Bibliography

BOLOGA A. S., 1994 — Radioecological research of the Black Sea: Report from Romania. *IAEA Bulletin.*, 2: 36-38.

BOLOGA A. S., OSVATH I., PATRASCU V., 1994 — "Monitoring of marine water, sediment and biota radioactivity in samples from the Romanian sector of the Black Sea by means of gamma spectrometry". *In* POVINEC P. P., (ed.): *Sources of Radioactivity in the Marine Environment and their Relative Contribution to Overall Dose Assessment from Marine Radioactivity (MARDOS).* IAEA-MEL-R2/94, June.

BOLOGA A. S., OSVATH I., DOVLETE C., 1995 — ^{137}Cs monitoring in the Romanian sector of the Black Sea. *Rapp. Comm. Int. Mer. Medit.*, 34: 224.

BOLOGA A. S., PATRASCU V., 1998 — "Radioactivity in the Romanian Black Sea sector one decade after Chernobyl". *In: One Decade after Chernobyl: Summing up the Consequences of the Accident*, IAEA-TECDOC-964., 2, Vienna, 469-475.

BOLOGA A. S., PATRASCU V., CUINGIOGLU E., 1998a — Distribution of total beta radioactivity, ^{90}Sr and ^{137}Cs content in the Romanian and NW Black Sea coast. *Rapp. Comm. Int. Mer. Medit.*, 35 (1): 234-235.

BOLOGA A. S., APAS M., COCIASU A., CUINGIOGLU E., PATRASCU V., PECHEANU I., PIESCU V., POPA L., 1998b — Present level of contaminants in the Romanian Black Sea Sector. IAEA-TECDOC-1094., Vienna, 58-63.

CUINGIOGLU E., BOLOGA A., BALABAN D., DOBRESCU E., PATRASCU V., 1996/1997 — Distribution of total beta radioactivity and ^{90}Sr in the Romanian Black Sea sector between 1994-1995. *Cercetari marine – Recherches marines.*, 29-30: 23-35.

OSVATH I., SAMIEI M., CARVALHO F., VILLENEUVE J. P., 1998 — Sustaining development in the Black sea region: A sea of changing fortunes. *IAEA Bulletin.*, 40 (3): 31-36.

PATRASCU V., 1996/1997 — Évolution post-Chernobyl de la concentration du ^{137}Cs dans le sédiments du littoral roumain de la mer Noire. *Cercetari marine Recherches marines.*, 29-30: 37-61.

PATRASCU V., BOLOGA A. S., 1990 — Evolution actuelle concernant l'irradiation humaine par certaines composantes marines. *Cercetari marine – Recherches marines.*, 23: 165-170

Impact of the human activities on cetaceans in the South West Pacific Ocean by measuring ^{137}Cs, ^{40}K and ^{210}Pb

Claire Garrigue

Jean-Michel Fernandez

Christian Badie

Christian Bernard

Jacqui Greaves

Jacques Rivaton

Marc Trescinski

Introduction

Radionuclides occur naturally in the environment but recently some artificial radionuclides have been introduced. One of the most widespread is the ^{137}Cs isotope. Its major sources come from the atmospheric deposition of debris from atmospheric nuclear explosions that occurred in the 50 and 60's and in the northern hemisphere from nuclear accidents in particular Tchernobyl power station accident that took place in 1986.

The analyses of long-lived artificial radionuclide ^{137}Cs is used as an indicator of radioactive pollution in the marine environment. Along time after the nuclear weapons test were stopped, this radionuclide can be traced in tissues of living organisms.

Many data are available on ^{137}Cs concentrations in pelagic fish, especially tuna species (Suzuki *et al.*, 1973; Young *et al.*, 1975). Some measurements were realized on marine invertebrates (Kasamatsu and Ishiwaka, 1997) but little information is available on marine mammals. Osterberg (1964) and Samuel *et al.* (1970) gave concentrations on mysticetes and Calmet *et al.* (1992) Berrow *et al.* (1998) and Kasatmatsu *et al.* (1999) did measurements on odoncetes. The diet of these two groupes of marine mammals come from different trophic level. Most of the mysticetes feed on plankton whereas the odontocetes or toothed cetacea feed on fish, squid and shrimps.

Recently some studies (Kasatmatsu and Ishiwara, 1997; Watson *et al.*, 1999) examined the mechanisms of transmission of the radionuclides in the marine community showing that in fish the ^{137}Cs concentration increased with rising trophic level and that the biomagnification factor (Cs predator/ Cs prey) equals 2.0.

In marine mammals the bioconcentration is thought to be high. Measurements of radionuclides are necessary on the mammals from the top of the food chain in order to quantify this bioconcentration.

This paper will present results of data analysis of ^{137}Cs, ^{40}K and ^{210}Pb realized on four cetaceans stranded in 1997 on the coast of New Caledonia marine mammals.

Materials and methods

New Caledonia is situated in the South West of the Pacific Ocean between 18° and 23° latitude South and 158° to 170° longitude East. In 1997, four marine mammals stranded on the coast of the island: two pilot whales (*Globicephala macrorhynchus*) and two pygmy sperm whales (*Kogia breviceps*). The conditions of the cadavers varied from fresh to good for stranded animals dead for a few days prior to sampling. During post-mortem examination, morphological data were noted and stomach contents were collected for diet analyses. Skin samples were taken for genetic analyses and teeth were extracted to determine the age by counting the growth layer groups (GLG) (Lockyer, 1995). Then carcasses were dissected and samples

of muscle, blubber and liver were taken in order to measure the concentrations of heavy metals and radionuclides ^{137}Cs, ^{40}K and ^{210}Pb. These tissues were weighted to get the wet weight. They were then freeze-dried and finely grounded. Direct measurements of ^{137}Cs, ^{40}K and ^{210}Pb were carried out by gamma spectrometry on the respectively energy rays, 0.661 MeV 1.460 MeV and 0.046 MeV. The counting time ranged between 50,000 and 80,000 seconds.

Concentrations were expressed in $Bq.kg^{-1}$ wet weight and the Cs concentration factor (CFs) was defined as the ratio concentration in the animal on the concentration in the sea water. As the sea water concentration hasn't been measured around New Caledonia, the value of 1.3 $mBq.l^{-1}$ recommended for the SW Pacific by IAEA technical document (1995) was used to calculate the CFs.

Results

The total length of each animal, its sex, the concentrations of ^{137}Cs, ^{40}K and ^{210}Pb and the Cs concentration factors (CFs), are presented in Table 1 for the different tissues of the two marine mammals species sampled.

The ^{40}K concentrations were greater than the ^{137}Cs concentration in the four animals sampled. For the pygmy sperm whales the concentration of ^{137}Cs were higher in the muscle than in the liver than in the blubber. All the measurements done in the blubber were at the detection limits. The ^{40}K concentrations followed the same pattern. For the short-finned pilot whales the concentrations of ^{137}Cs measured in the liver of the two individuals were in the same order of magnitude than those measured in the pygmy sperm whales. Concerning the female it is interesting to note that the concentration found in its muscle was equal to the value measured in its liver whereas for the ^{40}K the concentration was higher in the muscle than in the liver.

The concentrations of ^{210}Pb measured in the muscles and the blubber were very small compared to those found in the liver. In all the measurements, the highest concentrations of ^{210}Pb appear in the liver.

Species	Sex	Length (m)	Tissue	210 Pb (mBq.kg^{-1})	Cs 137 (mBq.kg^{-1})	K 40 (mBq.kg^{-1})	Cs CF
Globicephala	M	5.4	Liver	39±5	0.09±0.02	91±9	70
macrorhynchus	F	3.5	Muscle	<5	0.08±0.03	132±14	62
			Liver	53±12	<0.08	72±10	<62
	M	3.1	Liver	24±6	<0.11	81±11	<82
			Blubber	<1	<0.04	26±4	<30
Kogia breviceps			Muscle	<6	0.26±0.04	171±17	200
	F	3.0	Liver	10±3	0.08±0.03	84±9	62
			Blubber	<7	<0.05	28±5	<38
			Muscle	<6	0.16±0.03	110±11	123

Table 1
Total length, radionuclide concentrations and Cs concentration factors in different tissues of *Kogia breviceps* and *Globicephala macrorhynchus*.

The analyses of stomach contents showed that pygmy sperm whales feed mainly on squid and crustaceans whereas the pilot whales feed mainly on mesopelagic fish and squid. The list of the species identified in the stomach are presented in Table 2. These prey suggested that these marine mammals occupied a high position in the marine community.

The result of the teeth study showed that the two females were old. The male of Kogia was a young animal.

The concentration factors for ^{137}Cs have been calculated using the value for the sea water recommended by IAEA (1995) given as 1.3 mBq.l^{-1} for the South West Pacific in 1995. They are presented on Figure 1. For the pygmy sperm whales the CF ranged from 123 to 200. For the female short finned pilot whales it reached 62.

Discussion

There is no published information on ^{137}Cs levels in short-finned pilot whales or pygmy sperm whales but there are information on harbour porpoises (*Phocoena phoceona*) in North Atlantic, Dall's

Species	Sex	Stomach contents
Globicephala macrorhynchus	M	Fishes : *Bathyclupea malayana* (Bathyclupeidae) *Antigonia sp.* (Caproidae) *Synagrops sp.* (Acropomatidae) *Diaphus sp.* (Myctophydae) *Cubiceps sp.* (Nomeidae) *Chlorophthalmus sp.* (Chlorophthalmidae) Cephalopods : *Stenoteuthis sp.* (Ommastrephidae) 3 unidentified species (Ommastrephidae) *Moroteuthis sp.* (Onychoteuthidae) *Lycoteuthis sp.*? (Lycoteuthidae) *Histioteuthis sp.* (Histioteuthidae) 5 unidentified species (Histioteuthidae)
Globicephala macrorhynchus	F	Stomach empty
Kogia breviceps	M	Shrimps : *Pasiphea sp.* (Pasiphaeidae), *Gnathophausia ingens* Dohrn, 1870 (Mysidacea) *Meningodora sp.* (Oplophoridae). Cephalopods : Taonius sp. (Cranchidae) Octopoteuthidae Histioteuthidae Enoploteuthidae
Kogia breviceps	F	Shrimps : *Pasiphea sp.* (Pasiphaeidae), *Gnathophausia ingens* Dohrn, 1870 (Mysidacea) *Meningodora sp.* (Oplophoridae). Cephalopods : *Histioteuthis sp.* (Histioteuthidae) *Enoploteuthis sp.* ? (Enoploteuthidae) 2 unidentified species

Table 2
Prey identified from the stomach contents.

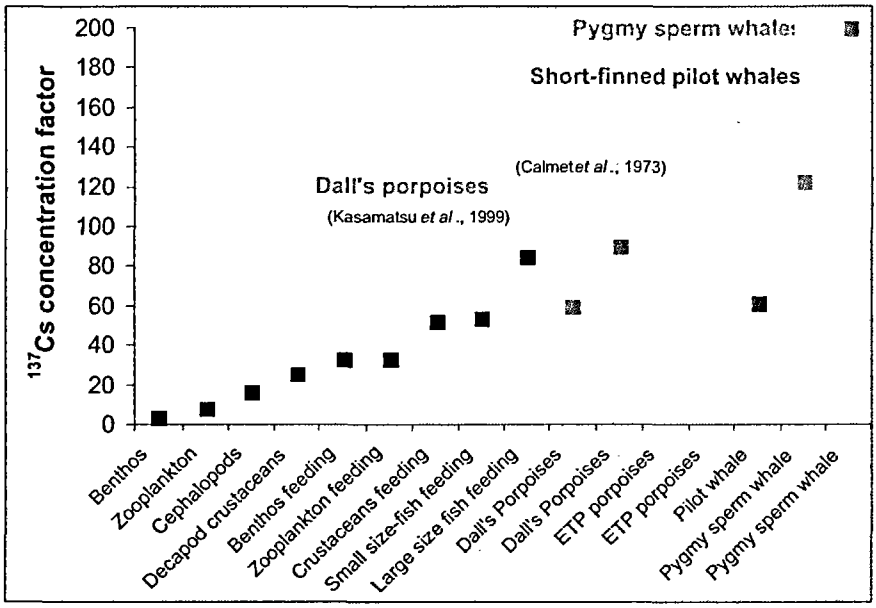

Figure 1
Caesium concentration factor in cetaceans in ETP (Eastern Tropical Pacific), from Kasamatsu and Ishiwaga (1997).

porpoises (*Phocenoides dalli*) in Japan and three species of dolphins in the Eastern Tropical Pacific (*Stenella longirostris, S. attenuata, Delphinus delphis*) (Calmet *et al.*, 1992; Berrow *et al.*, 1998; Watson *et al.*, 1999; Kasamatsu *et al.*, 1999). These information are summarized in Table 3.

The ^{137}Cs concentrations observed in New Caledonia are lower than those measured in the North Atlantic on harbour porpoises and especially when compared to the measurements carried out in the Irish sea. The measurements on the pygmy sperm whales are consistent to the results found by Kasamatsu *et al.* (1999) in Japan on Dall's porpoises and slightly lower to the ones found in dolphins from eastern tropical Pacific (Calmet *et al.*, 1992).

Our sampling is too small to discuss the possible relation between ^{137}Cs concentration and size or age of the animal. Nevertheless we can suggest that the very low ^{137}Cs concentration in the muscle of the female pilot whale could be due to its particular physiologic preg-

Species	Locations	Cs-137 Bq.kg^{-1}	K-40 Bq.kg^{-1}	CFs	Authors
Harbour porpoises	Ireland Sea	5.3-45.0	54 - 99.7	300 - 400	Berrow *et al.*,
	Atlantic seaboard	<1.0-3.4	85.4 - 108.7	500 - 600	1998
	Celtic sea	<1.0-2.4	66.8- 125.9	300 - 400	
	North Sea	2.2-2.7	90.3 - 106.5	100 - 200	
Dall porpoise	Japan	0.153 - 0.234	104.0 - 107.8	59-90	Kasamatsu *et al.*, 1999
Eastern tropical porpoise	Eastern Tropical Pacific	0.37 - 0.62	125 - 144	30 - 100	Calmet *et al.*, 1992
Common porpoise	Irish sea, UK	37.6	85.0		Kershaw, pers.
	Coastal waters of Wales, UK	6.69	97.5		com.
Short finned pilot whale	New Caledonia	0.08	132	62	Present study
Pygmy sperm whale	New Caledonia	0.16-0.26	110-171	123 - 200	

Table 3
^{137}Cs and ^{40}K concentrations measured in the muscle of marine cetaceans species (Bq.kg^{-1} wet weight).

nancy conditions. Samuels *et al.* (1970) showed that juvenile harp seals had higher concentration than the adults. They suggested that a significant quantity of ^{137}Cs could be transferred to the calf by lactation, like for humans. It is also probable that radionuclides may be transferred during pregnancy. Unfortunately it has not been possible to carry out measurements on the fetus for technical reasons.

The predominance of ^{137}Cs in muscle compared to the other tissues have been shown by Osterberg *et al.* (1964) and Samuels *et al.* (1970) in their studies of the distribution of radionuclides within the body of baleen whales and pinnipeds. This was confirmed for pinnipeds and toothed whales by Calmet *et al.* (1992) and Watson *et al.* (1999).

The values of ^{40}K in short-finned pilot whales and pygmy sperm whales are in the same order of magnitude of the concentrations measured in the other studies.

In all the measurements, there is a higher concentration of ^{210}Pb in the liver than in the muscle. This data shows that liver appears to be a privileged organ for the accumulation of trace metals. Similar results have been found by Calmet *et al.* (1992) in dolphins.

The caesium concentration factor calculated for the stranded cetaceans are in the same order of magnitude as for those found in dolphin in the eastern tropical Pacific (30 to 100) and in the Dall's

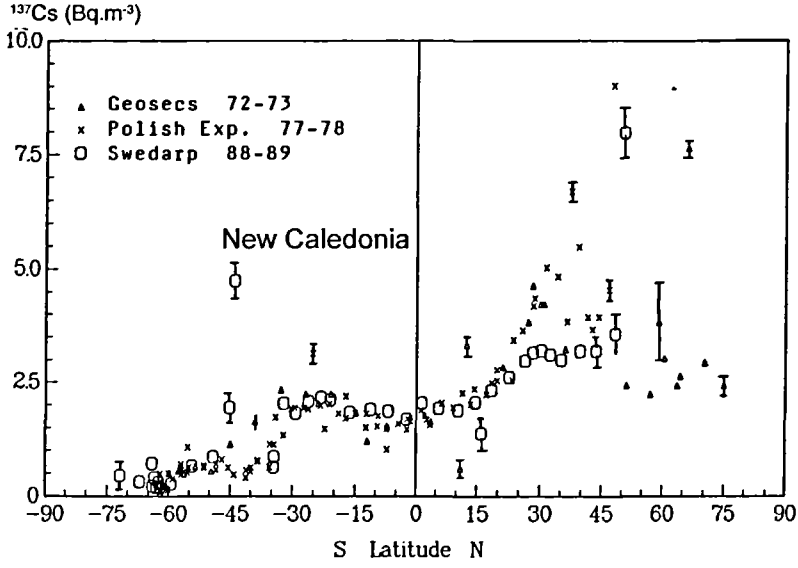

Figure 2
Caesium-137 activity concentrations (Bq.m^{-3}) in surface waters from the North and the South Atlantic in 17972/73 (GEOSECS expedition), 1977/78 (Polish expedition) and 1988/89 (SWEDARP expedition). Extracted from Holm *et al.* (1991).

porpoises in Japan (59 and 90). Kasamatsu and Ishiwaga (1997) wrote that ^{137}Cs falls to earth in a readily soluble form and is transferred up the food chain. Therefore this radionuclide is available to marine mammals via concentration phenomena. Pygmy sperm whales feed on squid and shrimps and short finned pilot whales feed on fish and squid. These two species occupy a high trophic level. The weak concentration factor for the ^{137}Cs in the female short finned pilot whales could be explained by its physiological state as the animal was pregnant. Hence a great part of the ^{137}Cs could have been transferred to the foetus.

Conclusions

The ^{137}Cs concentrations measured in the four stranded marine mammals are low compared to the measurements realised elsewhere. We could hypothesis that this is due to the variation of the radioactivity concentrations in different parts of the ocean, reflecting latitudinal impacts (Young *et al.*, 1975) as shown on the Figure 2 (Holm *et al.*, 1991) due to the difference in the nuclear past between the two hemispheres (lower fallout in the southern hemisphere than in the northern hemisphere).

Acknowledgements

We would like to thank Dr Crosnier from MNHM for his help in the determination of the shrimps and Dr R. Young from the University of Hawaii for his help in the determination of cephalopods.

Bibliography

BERROW S. D., LONG S. C., MCGARRY A. T., POLLARD D., ROGAN E., LOCKYER C., 1998 — Radionuclides (^{137}Cs and ^{40}K) in harbour porpoises *Phocoena phocoena*) from Bristish and Irish coastal waters. *Marine Pollution Bulletin*, 36 (8): 569-576.

CALMET D., WOODHEAD D., ANDRÉ J. M., 1992 — ^{210}Pb, ^{137}Cs and ^{40}K in three species of porpoises caught in the Eastern Tropical Pacific. *J. Environ. Radioactivity*, 15: 153-169.

HOLM E., ROOS P., PERSSON R. B. R., BOJANOWSKI R., AARKROG A., NIELSEN S. P., LIVINGSTON H. D., 1991 — "Radiocaesium and plutonium in Atlantic surface waters from 73°N to 72°S". *In* Kersahw P.J., Woodhead D.S. (eds): *Radionuclides in the study of marine process.* Amsterdam, Elsevier: 3-11.

KASAMATSU F., KAWABE K., INATOMI N., MURAYAMA T., 1999 — A note on radionuclide ^{137}Cs and ^{40}K concentrations in Dall's porpoises, *Phocoenoides dalli*, in coastal waters of Japan. *J. Cetacean Res. Manage.*, 1 (3): 275-278.

KASAMATSU F., ISHIWAKA Y., 1997 — Natural variation of radionuclide 137Cs concentration in marine

organisms with special reference to effect of food habits and trophic level. *Mar. Ecol. Prog. Ser.*, 160: 109-120.

LOCKYER C., 1995 — *A review of factors involved in zonation in environmental factors and major life events on harbour porpoise tooth structure.* Rep. Int. Whaling Commission Social Issue, 16: 511-529.

OSTERBERG C., PEARCY W., KUJALA N., 1964 — Gamma emitters in a Fin Whale. *Nature*, 204: 1006-1007.

SAMUELS E. R., CAWTHORN M., LAUER B. H., BAKER B. E., 1970 — Strontium-90 and Caesium-137 levels in tissues of fin whale (*Balaenoptera physalus*) and harp seal (*Pagophilus groenlandicus*). *Can. J. Zool.*, 48: 267-269.

SUZUKI Y., NAKAMURA R., UEDA T., 1973 — Caesium-137 contamination of marine fishes from the coasts of Japan. *J. Radiat. Res.*, 14: 382-391.

YOUNG D. R., FOLSOM T. R., HODGE V. F., 1975 — ^{137}Cs and ^{40}K in the flesh of Pacific Albacore. 1964-1974. *Health Physics*, 29: 689-694.

WATSON W. S., SUMNER D. J., BAKER J. R., KENNEDY S., REID R., ROBINSON I., 1999 — Radionuclides in seals and porpoises in the coastal waters around the UK. *The Sci. Tot. Environ.*, 234: 1-13.

^{14}C radiolabelling: a sensitive tool for studying PCB bioaccumulation in echinoderms

Bruno Danis

Olivier Cotret

Jean-Louis Teyssie

Paco Bustamante

Scott W. Fowler

Michel Warnau

Polychlorinated biphenyls (PCBs) are strictly anthropogenic chemicals that constitute one of the most problematic and widespread group of marine contaminants. These xenobiotics (represented by 209 congeners) are extremely resistant to any kind of degradation, are bioconcentrated by living organisms, and can cause various adverse effects depending on their pattern and degree of chlorine substitution (e.g., Harding & Addison, 1986; Livingstone, 1992; Metcalfe, 1994).

Being under the influence of heavy industrialisation and important urbanization, the North Sea is generally considered as a region highly contaminated by numerous contaminants, including PCBs. Therefore, there is a constant need to survey and monitor the quality status of the marine environment in the North Sea. This is particularly true for the benthic ecosystems since, due to their very low solubility, PCBs mainly accumulate in the sediments where they may become a threat to organisms and ecosystems. However, information on PCB bioaccumulation rates in marine benthic organisms

is scarce and is generally of limited value, since data are mainly derived from studies using sediments experimentally contaminated with high (unrealistic) PCB concentrations (Meador *et al.*, 1995; Boese *et al.*, 1997).

The asteroid *Asterias rubens* qualifies as a potential bioindicator species of PCB contamination in the marine environment. Widely distributed, abundant, and preying upon filter-feeders, *A. rubens* is a key species of various benthic ecosystems in the North Sea (Menge, 1982; Hostens & Hammerlynck, 1994). It is also an excellent choice for ecotoxicological studies, since it is a proven bioindicator for other contaminants (e.g. heavy metals; Temara *et al.*, 1998) and it can provide early warning signals for the presence of organic contamination (Everaarts *et al.*, 1998). This species was therefore selected as a model for an experimental study of PCB bioaccumulation.

Many studies have considered PCB bioaccumulation using commercial mixtures (e.g. Arochlor) which are not always representative of environmental contamination (Metcalfe, 1994). In the present work, bioaccumulation potential was investigated using a congener-specific approach and an extremely sensitive method (radio-analysis using β-spectrometry), which allowed us to study low (realistic) contaminant concentrations and to directly measure bioaccumulation in all the body compartments of the starfish (including very minute organs). PCB congener #153 (2,2',4,4',5,5' hexachloro-biphenyl) is the most abundant congener found in marine biota (NSTF 1993). It is therefore a good model to investigate PCB bioaccumulation and its ^{14}C-labelled form was used in the present study.

Asteroids were collected in Audresselles (Nord Pas-de-Calais, France). After being acclimatized for 1 month to laboratory conditions, starfishes were exposed for 34 days to sea water or sediments

contaminated with the radio-labelled PCB congener. Contaminant concentrations were adjusted in order to correspond to an environmentally realistic level of contamination in the North Sea (Stebbing *et al.*, 1992). During the exposure period, bioaccumulation of PCB #153 was followed in eight body compartments (oral body wall, aboral body wall, pyloric caeca, central digestive system, rectal caeca, gonads, podia, and coelomic fluid) using β-spectrometry and concentrations were expressed on a lipid weight basis.

Results showed that the observed kinetics generally tended to go through an initial latency phase and then to reach a saturation concentration (steady state) after an exponential increase. The latency phase duration and the time to reach steady state were body compartment as well as exposure mode-dependent. Both body walls (oral and aboral) accumulated the PCB most efficiently (intensity and rapidity). For each body compartment, equilibrium was always reached more rapidly during seawater exposure. Most generally, uptake fitted an asymptotic sigmoid model (corrected R^2 ranged between 0.27 and 0.84), the best fit being observed for oral body wall of starfish exposed via sea water. For each body compartment, uptake was more efficient when *A. rubens* was exposed directly in seawater than via sediments, especially in the body wall compartments.

The present study constitutes a first attempt to use a radiolabelled PCB congener to examine contaminant uptake kinetics in echinoderms. This radiotracer technique is a very promising tool for the study of PCB biokinetics. It is extremely sensitive and allows directly measuring bioaccumulation of PCBs at environmentally realistic concentrations. It also allows assessing uptake into key organs which are sometimes too minute for classical analytical measurements, such as HRGC-ECD or HRGC-MS, which require large amounts of sample material (Metcalfe, 1994).

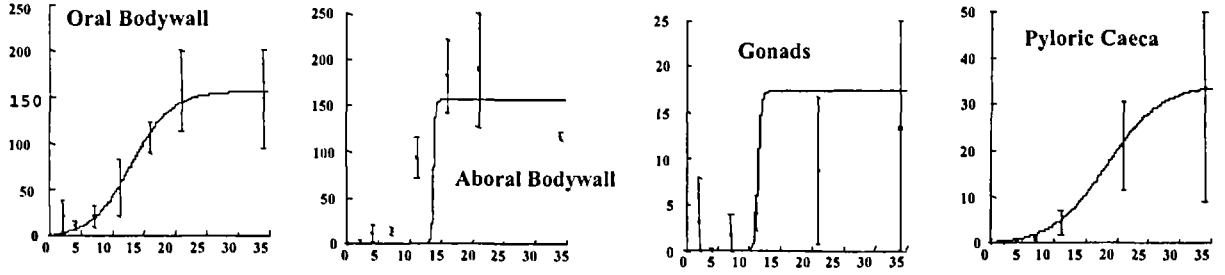

Figure 1
Uptake kinetics in *Asterias rubens* exposed via seawater (mean concentration (ng.g^{-1} total lipids) ± SD, n=3).

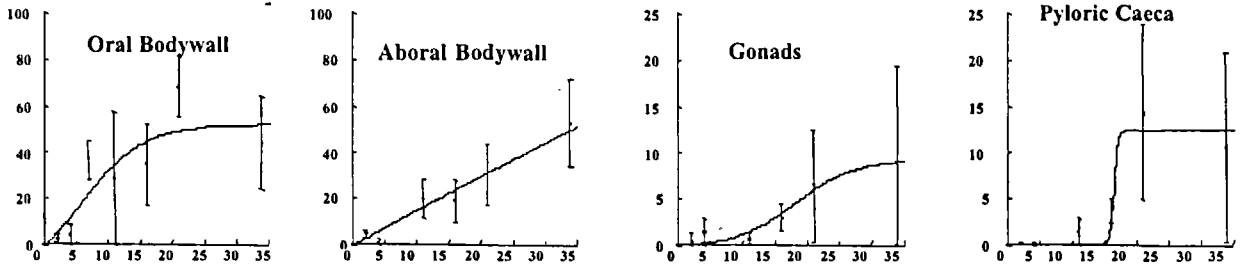

Figure 2
Uptake kinetics in *Asterias rubens* exposed via sediments (mean concentration (ng.g^{-1} total lipids) ± SD, n=3).

Bibliography

BOESE B. L., LEE H., ECHOLS S., 1997 — Evaluation of a first order model for the prediction of the bioaccumulation of PCBs and DDT from sediment into the marine deposit-feeding clam *Macoma nasuta*. *Environ. Toxicol. Chem.*, 16: 1545-1553.

EVERAARTS J. M., DEN BESTEN P. J., HILLEBRAND M. T. J., HALBROOK R. S., SHUGART L. R., 1998 — DNA strand breaks, cytochrome P450-dependant monooxygenase system activity and levels of chlorinated biphenyl congeners in the pyloric caeca of the seastar (*Asterias rubens*) from the North Sea. *Ecotoxicology*, 7: 69-79.

HARDING G. C., ADDISON R. F., 1986 — "Accumulation and effects of PCBs in marine invertebrates and vertebrates". *In*: Wood J.S. (ed): *PCBs and the environment*, CRC Press, 2: 9-30.

HOSTENS K., HAMMERLYNCK O., 1994 — The mobile epifauna of the soft bottoms in the subtidal Oosterschelde estuary: structure, function and impact of the storm-surge barrier. *Hydrobiologia*, 282/283: 479-496.

LIVINGSTONE D. R., 1992 — "Persistent pollutants in marine invertebrates". *In*: Walker C.H., Livingstone D.R. (eds). *Persistent pollutants in marine ecosystems*. Oxford, Pergamon Press: 3-34.

MENGE B. A., 1982 — "Effects of feeding on the environment: Asteroidea". *In*: Jangoux M., Lawrence J.M. (eds): *Echinoderm nutrition*. Rotterdam, Balkema: 521-551.

METCALFE C. D., 1994 — "Polychlorinated biphenyls". *In*: Kiceniuk J.W., Ray S. (eds): *Analysis of contaminants in edible aquatic resources*, VCH Press : 305-338.

MEADOR J. P., CASILLAS E., SLOAN C. A., VARANASI U., 1995 — Comparative bioaccumulation of polycyclic aromatic hydrocarbons from sediment by two infaunal invertebrates. *Mar. Ecol. Prog. Ser.*, 123: 107-124.

NSTF-North Sea Task Force, 1993 — *North Sea quality status report 1993*. Oslo & Paris Commission, ICES, London, 132 p.

STEBBING A. R. D., DETHLEFSEN V., CARR M., 1992 — Biological effects of contaminants in the North Sea. *Mar. Ecol. Prog. Ser.*, 91 (special edition).

TEMARA A., SKEI J. M., GILLAN D., WARNAU M., JANGOUX M., DUBOIS P., 1998 — Validation of the asteroid *Asterias rubens* (Echinodermata) as a bioindicator of spatial and temporal trends of Pb, Cd, and Zn contamination in the field. *Mar. Environ. Res.*, 45: 341-356.

Cadmium bioaccumulation at different stages of the life cycle of cephalopods: a radiotracer (^{109}Cd) investigation

Paco Bustamante
Olivier Cotret
Bruno Danis
Jean-Louis Teyssié
Scott W. Fowler
Pierre Miramand
Michel Warnau

Introduction

High levels of cadmium in the liver and kidney of marine mammals and seabirds have been reported in polar and sub-polar regions, areas which are not known to be subjected to particularly high inputs of cadmium (Schneider *et al.*, 1985; Wagemann *et al.*, 1990; Caurant & Amiard-Triquet, 1995). Similarly, very high cadmium concentrations in polar and sub-polar cephalopods have been recorded (Bustamante *et al.*, 1998). Since cephalopods are a primary food source for many cetaceans and seabirds, it has been

proposed that a cephalopod-rich diet may be linked to the high metal concentrations found in these top predators (Honda & Tatsukawa, 1983; Muirhead & Furness, 1988; Bustamante *et al.*, 1998).

Despite the probable crucial role of cephalopods in the transfer of cadmium along food webs, only very few studies have examined heavy metal behaviour and fate in cephalopods. For example, these organisms are well known to concentrate cadmium to extremely high levels in their digestive gland (Martin & Flegal, 1975; Finger & Smith, 1987; Miramand & Bentley, 1992); however, the reason for such a high bioaccumulation is still poorly understood. Therefore, the present study has examined the biokinetics of uptake and loss of cadmium in a typical cephalopod, the common cuttlefish *Sepia officinalis,* in order to characterise the bioaccumulation and retention potential of cadmium in this organism. In the present work, bioaccumulation in *S. officinalis* was investigated using ^{109}Cd in combination with low (realistic) cadmium concentrations in order to directly measure Cd bioaccumulation in various body compartments of the cuttlefish.

Adult individuals, collected by net fishing off Monaco or provided by the « Musée Océanographique de Monaco »; were acclimatised for several weeks to laboratory conditions before experimentation. Numerous eggs were obtained during acclimation of adults and they were maintained at constant temperature (17±1°C) in continually aerated sea water. After 8 to 10 weeks, hatching of the cultured eggs furnished several dozen juvenile cuttlefish.

Cadmium bioaccumulation could thus be studied at different stages of the life cycle of *S. officinalis, viz.* in embryos, early juveniles and adults. In addition, bioaccumulation was investigated following exposures to the metal via sea water, sediment, or food.

At the end of the exposure periods, ^{109}Cd was measured by g-spectrometry in 3 compartments of eggs (capsule membrane, perivitellin liquid, and embryo), 3 body compartments of juveniles (digestive gland, cuttlebone, and remainder), and 13 body compartments of adults (digestive gland, branchial hearts, branchial appendages, gills, kidneys, ink sack, digestive tract, genital tract, ovocytes, skin, muscles, cuttlebone, and remainder).

Results and discussion

Results showed that during embryonic development, cadmium was efficiently taken up from sea water by the eggs (concentration factor reaching 46 after 8 days of exposure). However, most of the ^{109}Cd burden was found associated with the capsule membrane of the egg. Thus, the capsule most probably acts as a very efficient shield against internal cadmium incorporation, which in turn suggests that this metal could be highly toxic for early embryos.

Once this shield is lost (after hatching), the cuttlefish bioconcentrates waterborne cadmium. Indeed, juveniles as well as adults take up cadmium quite efficiently, particularly in muscles (62% of body burden) and digestive gland (25%). When non-contaminated conditions are restored, whole-body loss of cadmium in *S. officinalis* is relatively slow (biological half life: ca. 65 days) and its kinetics are best described by a two-compartment exponential model. In addition, the ^{109}Cd burden increases in digestive gland during the depuration period reaching 70% of the total body burden after one month of depuration. This would indicate either a higher retention efficiency of cadmium in digestive gland than in the other organs, or a preferential translocation of cadmium from different organs to the digestive gland.

Despite their habit to spend most of their time on the bottom sediments, bioaccumulation of ^{109}Cd from contaminated sediment remained very low after one month of exposure. Among the different organs, the digestive gland contained most of the metal at the end of the exposure period.

Regarding cadmium exposure through the food, data analysis indicates that ingested cadmium is taken up very efficiently by *S. officinalis* (Figure 1). Calculated assimilation efficiencies (AE) were as high as 60% for both age groups. Loss of ^{109}Cd ingested with food (brine shrimps *Artemia sp* for juveniles; mussels *Mytilus galloprovincialis* for adults) was much slower than loss of cadmium taken up via sea water, indicating a very strong retention efficiency of dietary cadmium by juvenile as well as adult *S. officinalis*. As for the other exposure modes tested (sea water and sediments), most of

the cadmium ingested with food was found in the digestive gland. The proportion of ^{109}Cd body burden in the digestive gland reached 90% after one month of loss.

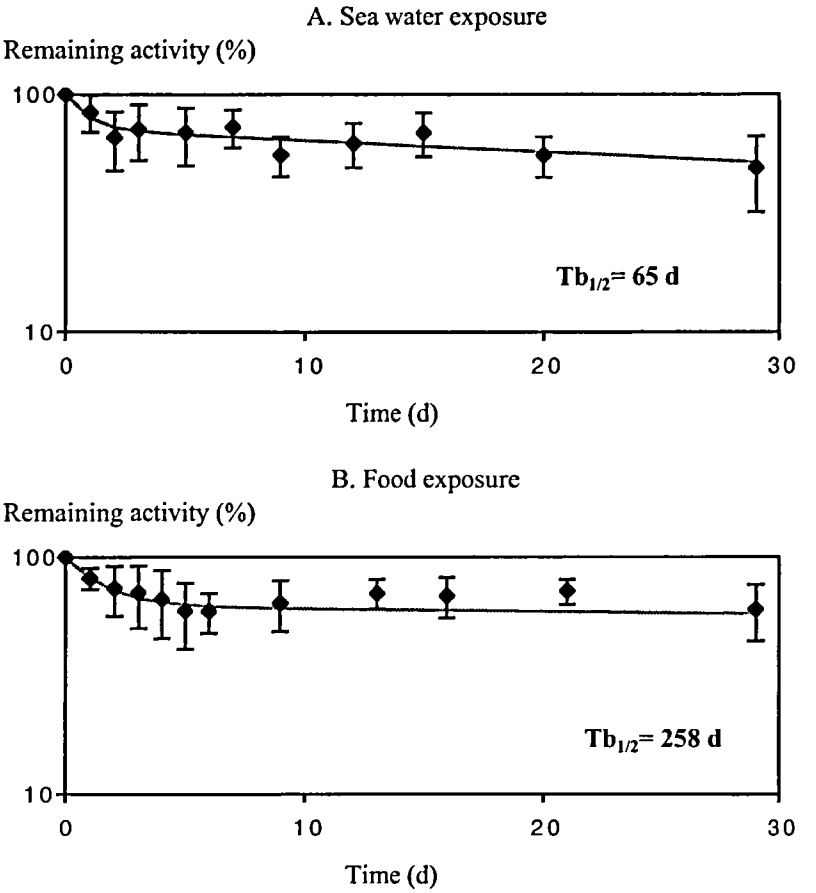

Figure 1
A. Loss of ^{109}Cd in whole juvenile cuttlefish previously exposed to radiolabelled sea water for 36 h (mean remaining activity ± SD, n =8 at day 0 and n=4 at day 29) B. Loss of ^{109}Cd in whole cuttlefish previously fed with radiolabelled *Artemia salina* (mean remaining activity ± SD, n =8 at day 0 and n=5 at day 29).

Our results clearly demonstrate that food is a major route of cadmium bioaccumulation in the cephalopod *S. officinalis*. Whatever the source of cadmium (water or food), the digestive gland is always the primary organ that accumulates the metal. This form of metal storage may be related to the detoxification function of the digestive gland (e.g., metal trapping by metalloproteins), which could explain why cadmium reaches extremely high concentrations in this organ.

Bibliography

BUSTAMANTE P., CAURANT F., FOWLER S. W., MIRAMAND P., 1998 — Cephalopods as a vector for the transfer of cadmium to top marine predators in the north-east Atlantic Ocean. *Sci. Tot. Environ.*, 220: 71-80.

CAURANT F., AMIARD-TRIQUET C., 1995 — Cadmium contamination in pilot whales *Globicephala melas*: source and potential hazard to the species. *Mar. Pollut. Bull.*, 30 (3): 207-210.

FINGER J. M., SMITH J. D., 1987 — Molecular association of Cu, Zn, Cd and ^{210}Po in the digestive gland of the squid *Nototodarus gouldi*. *Mar. Biol.*, 95: 87-91.

HONDA K., TATSUKAWA R., 1983 — Distribution of cadmium and zinc in tissues and organs, and their age-related changes in striped dolphins, *Stenella coeruleoalba*. *Arch. Environ. Contam. Toxicol.*, 12: 543-550.

MARTIN J. H., FLEGAL A. R., 1975 — High copper concentrations in squid livers in association with elevated levels of silver, cadmium, and zinc. *Mar. Biol.*, 30: 51-55.

MIRAMAND P., BENTLEY D., 1992 — Concentration and distribution of heavy metals in tissues of two cephalopods, *Eledone cirrhosa* and *Sepia officinalis*, from the French coast of the English Channel. *Mar. Biol.*, 114: 407-414.

MUIRHEAD S. J., FURNESS R. W., 1988 — Heavy metal concentrations in the tissues of seabirds from Gough Island, South Atlantic Ocean. Mar. Pollut. Bull., 19: 278-283.

SCHNEIDER R., STEINHAGEN-SCHNEIDER G., DRESCHER H. E., 1985 — "Organochlorines and heavy metals in seals and birds from the Weddell Sea". *In* Seigfried W. R., Condy P. R., Laws R. M., (eds) *Antarctic nutrient cycles and food webs*. Springer, Berlin, Heildeberg, New York: 652-655.

WAGEMANN R., STEWART R. E. A., BÉLAND P., DESJARDINS C., 1990 — "Heavy metals and selenium in tissues of beluga whales, *Delphinapterus leucas*, from the Canadian Arctic and the St. Lawrence estuary". *In* Smith T.G., ST AUBIN D. J., GERACI J. R. (eds) *Advances in research on the beluga whale, Delphinapterus leucas*. Can. Bull. Fish. Aquat. Sci., 224: 191-206.

Heavy metals in the sea star *Asterias rubens* (echinodermata): basis for the construction of an efficient biomonitoring program

Ali Temara

Michel Warnau

Philippe Dubois

Introduction

The heavy metals that enter marine trophic chains are naturally directed towards the benthos in a multiple-step sequence. Physico-chemical processes such as precipitation, adsorption, and complexation, incorporate them into the seston. Through grazing and predation, zooplankton organisms ingest the heavy metals present in the seston (Bremer *et al.*, 1990). Only a small proportion of these metals is absorbed by the zooplankton, the major part is eliminated with the fecal pellets. Being denser than seawater, the fecal pellets sink. A large proportion of these pellets is swallowed (up to 40%, Joiris *et al.*, 1982) with dead plankton by benthic (micro)heterotrophic organisms. Similarly, these benthic organisms absorb only a small fraction of the metals present in their diet. Their excrements thus have a high content heavy metals as well. Therefore, both abiotic and biotic processes direct metals

towards the sediments. Heavy metals associated with the sediments are bioavailable to benthic organisms through exchanges between the water column and the interstitial water, ingestion and through sediment resuspension. As resuspension is stimulated by activity of the in fauna, by human activity (e.g. dredging), and by hydrodynamics, the sediments become a secondary source of contamination. Such a source can sometimes be detected much later than the primary contamination (Skei, 1981). Because of this secondary source of contamination, the benthic zone of littoral ecosystems is particularly exposed to metal contaminants. As an example, the loads of Cd, Pb, and Hg accumulated in the macrobenthos of the North Sea exceed 8 tons (T) Cd, 4T Pb, and 1T Hg, mainly from anthropogenic origin (Karbe *et al.*, 1994).

Heavy metal pollution is a major problem in several sites of the NE Atlantic, particularly in coastal zones and in zones of sedimentary deposits (NSTF, 1993). These zones are generally ecologically sensitive and are economically important because they include fisheries and recreational areas. According to Kröncke & Rachor (1992), the macrobenthic communities of the NE Atlantic are affected by the presence of multiple pollutants including heavy metals. The disrupted communities typically have larger numbers of species that are of smaller size and shorter lifespan than the healthy communities. According to NSTF, (1993), four metals constitute a major threat to the animal communities in the NE Atlantic: Sn (as tributyltin) affects bivalves and gastropods through endocrine disruption, Cd and Hg constitute a major threat to the top-predators, and Pb is a major threat to mollusc predators.

Bioindicators and complementarity

It is no longer accepted that marine systems can receive an unregulated load of heavy metals, and programs monitoring the health of ecosystems are required. It is generally recognised that biological parameters should be studied in such programs in conjunction

with both chemical and physical measurements. Nowadays, ecotoxicological risk assessment has become a tool in several regions of the world and is used by decision-makers in chemical regulation. Environmental decision making can be a multi-million dollar/euros issue and efficient biomonitoring programs must therefore be based on carefully calibrated bioindicators.

Two types of organisms can be selected for biomonitoring programs. If the aim of the program is to protect human health, edible species should be considered. Alternatively, if the aim of the program is to determine temporal or geographical trends of a contamination, ubiquitous species should be considered. Mussels *Mytilus* spp have a double advantage from the standpoint of ecotoxicology: they are both edible and have a wide distribution. This is why they are so often used by ecotoxicologists. But mussels cannot be considered as the ultimate bioindicator because they are not ubiquitous [e.g.: limited bathymetric distribution, absence from some biotopes, such as seagrass meadows (Hayward & Ryland, 1990)], and because they do not always indicate environmental conditions. Indeed, according to Coleman *et al.* (1986), there is no simple relationship between the Cd concentrations in *Mytilus edulis* and the concentrations in the seawater. Similarly, Cd, Pb, Cu, and Zn concentrations in the mussels of Sørfjord (Norway) were not correlated to contamination gradients along the fjord (NSTF, 1993). If mussels are not the ideal bioindicator, it is likely that no organism is. Indeed, in each organism, the body concentrations indicate the specific local bioavailability of the heavy metals rather than the global environmental conditions. A sub-optimal bioindicator should not be replaced by another one. However, in Sørfjord, the asteroid *Asterias rubens* better indicated the environmental conditions than any other species (including *M. edulis*); the measured body concentrations being highly correlated to metal concentrations in the sediments, which represent the major source of contamination in the area (Temara *et al.*, 1998c). Even so, analyses of metal concentrations in mussels have been of importance to public health: the detection of highly elevated levels all along the fjord led the regional authorities to ban their consumption (Skei, 1995). According to Gray (1989), several species should thus be included in biomonitoring programs. Phillips (1990) reviewed the bioindicators widely used at the time of his

writing; bioindicators were gathered in three groups: macrophyte algae, crustaceans, and molluscs. Each of these groups had both advantages and disadvantages.

To select an adequate taxon, it has been proposed to focus on the species that qualitatively or quantitatively structure the biocenosis (key-species) (Gray, 1989). This approach could also assist in assessing the impact of contamination on the whole ecosystem (if one or several key-species are affected, the whole ecosystem is affected). However, according to Hurlbert (1997), the concept of keystoneness has hardly been demonstrated for most organisms and in the ecotoxicological perspective, the concept of complementarity might be more appropriate as far as selection of bioindicators is concerned. To be complementary, species should be chosen among biologically distanced taxa. In this view, *M. edulis* and *A. rubens* are complementary. The first one is a filtrating protostome with an exoskeleton that keeps the other tissues out of contact with the sediments [mussels settle on hard bottoms as well as on soft bottoms as aggregates (Hayward & Ryland, 1990)]; the second one is a predatory deuterostome with an endoskeleton; the respiratory surfaces, the podia, are in close contact with the sediments. Contact with heavy metals, metal bioaccumulation, and sensitivity to metals will thus be dramatically different for these two species. The joint study of such species would thus be more representative of the biodiversity in marine ecosystems. Macrophyte algae would favourably complement these two species as these organisms mainly bioaccumulate metals from the dissolved phase (e.g. Phillips, 1990; Warnau *et al.*, 1996a).

The ecotoxicology of *M. edulis* has extensively been reviewed (see *e.g.* references above) and the present paper describes the ecotoxicological information available for *A. rubens*. It is a top-predator feeding mainly on molluscs and is regarded as a keystone predator in several communities (see hereafter). Therefore, the effects of Cd, Pb, and Hg on this species are likely to have an impact on whole communities (see above). The present paper reviews the modes of bioaccumulation and loss/detoxification of such metals in *A. rubens* in order to ascertain the value of the species as a bioindicator of metal contamination.

Asterias rubens, a key-species in NE Atlantic macrobenthic communities

Asterias rubens is euryhaline while most other echinoderms are generally stenohaline. Thus, it commonly settles in low salinity zones such as the Baltic Sea or estuaries. It is precisely such low salinity zones that are likely to be exposed to human activities and where the most dramatic heavy metal-related problems are found in the marine environment.

In some NE Atlantic littoral ecosystems, *A. rubens* can represent the most significant fraction (up to 40 %) of the mobile epifauna biomass (Hostens & Hammerlynk, 1994). Other species of the same genus (e.g. *A. amurensis*) that would presumably share some ecotoxicological characteristics together with *A. rubens*, are dominant benthic predators in the other oceans of the North hemisphere and are invasive organisms in the Southern Pacific (Byrne *et al.*, 1997). The position of the species in the benthic trophic webs of these ecosystems is strategic (Menge, 1982). *A. rubens* is a major predator (it feeds on bivalves, filter-feeders that are known to accumulate metals) and is also an opportunistic species. The ecological pressure due to the presence of the predator (in addition to the predation by itself) affects the fitness of its prey (Reimer *et al.*, 1995). Eventually, it is an important intermediate link in several trophic webs: (1) within its own community, through predation by other echinoderms (Menge, 1982); (2) to the endofauna, through *post-mortem* decomposition; (3) to other benthic and pelagic communities, through predation by flat fishes (Keats, 1990) and, due to fishery activities, indirectly to man; and (4) to the terrestrial communities, through predation by sea birds such as the laridae (sea gulls) or the eider *Somateria mollissima* (Bustnes & Erikstad, 1983).

All of this data indicates that predation by and on *A. rubens* is a major selective factor on benthic communities; this asteroid has therefore been identified as a key-species (Menge, 1982).

Heavy metal bioaccumulation in *A. rubens*

Baseline studies on heavy metal contamination of *A. rubens* have been conducted in the field by several authors (e.g. Everaarts & Fisher, 1989; Everaarts *et al.*, 1990; Vyncke *et al.*, 1991; Temara *et al.*, 1997a) and the asteroid is now recognised as one of the species that can bioindicate metal contamination of an ecosystem (NSTF, 1993).

A sampling of *A. rubens* from the coastline of the Netherlands to the Dogger Bank (central North Sea) showed that the populations in the Dogger Bank (a region with high sediment deposition rate, elevated organic content, and where metal bioavailability is elevated; Kersten & Kröncke, 1991) had significantly higher Cd concentrations than the other populations studied (Everaarts *et al.*, 1990), while Zn and Cu concentrations did not vary significantly along the transect (Everaarts & Fisher, 1989). According to Vyncke *et al.* (1991), *A. rubens* would be the most suitable species to bioindicate heavy metal (Pb, Cr, Hg, Ni) contamination among the organisms studied (these organisms were the crustaceans *Pagurus berhnardus* and *Macropipus holsatus*, the ophiuroid *Ophiura texturata*, the bivalve *Spisula subtruncata*, and *A. rubens*). According to the latter authors, metal concentrations in asteroids collected close to the European coast were significantly higher than the metal concentrations in asteroids collected offshore.

It is worth noting that in the early studies that have used *A. rubens* to monitor heavy metal contamination in the field, the metal concentrations were analysed in total asteroid body, without any distinction of body compartments [an exception is the work by Riley & Segar (1970) who separated several body compartments]. However, *A. rubens* has well differentiated body compartments, and it has since been shown that they do not accumulate metals similarly (den Besten *et al.*, 1990; Sorensen & Bjerregaard, 1991; Hansen & Bjerregaard, 1995; Temara *et al.*, 1996a, b; 1998a; Warnau *et al.*, 1999).

The importance of the factors (body compartment, season, sampling site, sex) influencing heavy metal concentrations were investigated in adult asteroids in the southern bight of the North Sea. According to multi-way analyses of variance, the considered factors accounted for a significant proportion of total variability in Pb (93%), Cd (88%), and Hg (27%) concentrations. Body compartment appeared as the most critical factor (Pb: 88%, Cd: 40%, Hg: 10%) in background environments (Temara *et al.*, 1997a). Concentration ratios towards prey (invertebrates of various trophic categories) were lower than 1 for Pb, around 1 for Hg, and up to 7.8 for Cd, indicating that limited biomagnification may occur in the trophic web *A. rubens* belongs to (Temara *et al.*, 1997a). The same study showed that sex-related differences were significant for Cd concentrations (1.75 times higher in female than in male gonads). Significant allometric relationships were measured and statistically fitted models were positive (Cd concentrations in the body wall and the digestive system) or negative (Pb concentrations in the digestive system) power functions.

According to Temara *et al.* (1997a), Pb is particularly concentrated in the skeleton while its concentration in the other tissues is rather low in background environments. Pb is known as a calcic skeletal-seeking element [calcic skeletons represent the vast majority of types of mineralised skeletons in the metazoans], regardless of the nature of the calcic skeleton [e.g. phosphate skeletons of vertebrates, carbonate skeletons of molluscs]. Among the carbonate skeletons, the crystallographic structure seems surprisingly inconclusive for Pb bioaccumulation that occurs in aragonitic skeletons as well as in calcitic skeletons (Kröncke, 1987; Temara *et al.*, 1995; Warnau *et al.*, 1995a). According to Sorensen (1991), the accumulation of Pb in calcitic skeletons is facilitated by the similarity between the ionic radius of Pb and Ca.

In *A. rubens*, Cu, Zn, and Fe, which are cofactors of several enzymes, were preferentially concentrated in body compartments that are characterised by high metabolic activity. Concentrations were significantly higher in the pyloric caeca (Temara *et al.*, 1997a), nutrient storage organs that have high metabolic activity (Oudejans *et al.*, 1979). Cu and Zn, as well as other Ib and IIb elements (Cd, Hg, Ag), generally have a high affinity for the -SH pep-

tidic groups of the tripeptide glutathione and of metallothioneins (MTs) (Roesijadi, 1992). In *A. rubens*, the quantification of MTs in the pyloric caeca (Temara *et al.*, 1997b) confirmed the presence of this ligand in sufficient quantity to fix accumulated Cd. In contrast, MTs are absent from the gonads (den Besten *et al.*, 1990), accounting for the low Cd concentrations in this compartment. However, Hg concentrations were high in the gonads (Temara *et al.*, 1997a). As opposed to the MTs of most other organisms studied so far, the MTs in the pyloric caeca of *A. rubens* showed a low affinity for Hg (Sorensen & Bjerregaard, 1991), which could account for its rapid transfer to the gonads. Such transfer could take place via the haemal system (Rouleau *et al.*, 1993) which is part of the circulatory system in echinoderms (Ruppert & Barnes, 1994).

Metal sources for the organism can vary according to the element and are debatable. According to Voogt *et al.* (1987), the principal source of Cd for *A. rubens* was the water. In contrast, den Besten *et al.* (1990) showed that Cd seemed to be accumulated by *A. rubens* mainly from its diet. According to experimental exposures (Temara *et al.*, 1996a), Cd accumulated in the pyloric caeca was mainly of dietary origin (Figure 1). However, the importance of diet as a source of Cd is apparently not a rule in echinoderms. Indeed, the contribution of diet to the Cd load of the echinoid *Paracentrotus lividus* (grazing sea urchin) is comparatively much lower (Warnau *et al.*, 1995b; 1996b).

The sources of Pb can be ions dissolved in seawater, Pb present in the diet, and Pb adsorbed on particules in suspension. Such particules enter the body *via* the microphagic activity of *A. rubens* (Jangoux, 1982). The relative importance of such sources has not yet been evaluated. In contrast to Cd that is taken up through the integument and the digestive tract (Temara *et al.*, 1996), recent studies (Temara *et al.*, 1998a) have shown that the main entry route of Pb in the organism would be the digestive wall (Figure 2), possibly through an antiporter system. Secondary entry routes could be the podia, the papulae, and the madreporite, viz. structures that control the equilibrium of internal fluids and that are involved in respiratory exchanges. The metal ions associated with dissolved organic matter could also enter the asteroid through the epidermis of the body wall, whose role in the absorption of dissolved organic molecules has been demonstrated by Fergusson (1982).

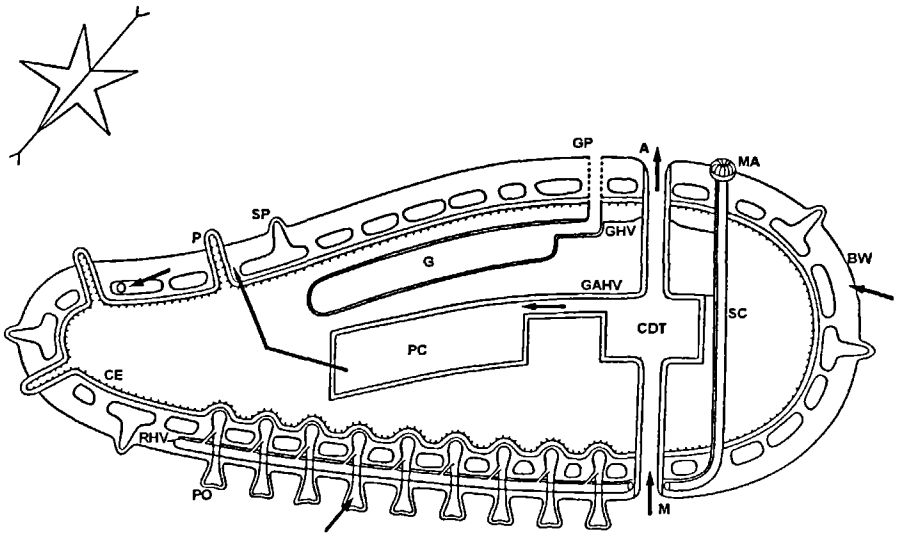

Figure 1
Sagital section through an asteroid arm showing known and supposed routes of in- and out-fluxes of Cd. Direction of section is shown on the small asteroid. A: anus. BW: body wall. CDT: central digestive tract. CE: coelomic epithelium. G: gonad. GAHV: gastric hemal vessel. GHV: genital hemal vessel. GP: gonopore. MA: madreporite. M: mouth. O: ossicle. P: papula. PC: pyloric caecum. PO: podion. RHV: radial hemal vessel. SC: stone canal. SP: spine.

Impact and detoxification of heavy metals in *Asterias rubens*

Preliminary studies on Mn assessed the survival of exposed asteroids. The lowest observed effective concentration (50 $mg.l^{-1}$.Mn) calculated in aquarium (Hansen & Bjerregaard, 1995) was well above the concentrations that can be observed in the most contaminated sites in the field (800 $\mu g.l^{-1}$.Mn in few heavily contaminated sites of the Baltic Sea; Kremling, 1983). Cu did affect the oxygen consumption in *A. rubens* at concentrations = 25 $\mu g.l^{-1}$ Cu (Gerets *et al.*, 1972). Cd disrupted steroid metabolism (Voogt *et al.*, 1987),

reproduction, and larval development in *A. rubens* at concentrations = 25 µg Cd l^{-1} (den Besten *et al.* 1989). Lower concentrations (1 µg.l^{-1} Cd) could disrupt Zn metabolism (Temara *et al.*, 1998b). Considering these relatively high effective concentrations, it can be proposed that detoxification systems (including constitutive MTs, synthesis of inducible MTs, incorporation of heavy metals into the skeleton) appear relatively efficient in *A. rubens* and that the species is particularly resistant to the heavy metals studied so far. This is confirmed by a study in the field, as *A. rubens* is one of the few macro-invertebrates that survive in the most polluted sites of Sørfjord where they can be found in dense populations around, and on, mussel beds (Temara, personal observations). However, sublethal effects have been detected (partial inhibition of alkaline phosphatase function and disruption of skeletogenesis, larval settlement, and/or growth, Temara *et al.*, 1997c; 1998c).

A route of Pb elimination in *A. rubens* has been proposed (Figure 2): the transfer of the metal from the digestive system (the main route of entry in the organism) to the gonads and its probable expulsion

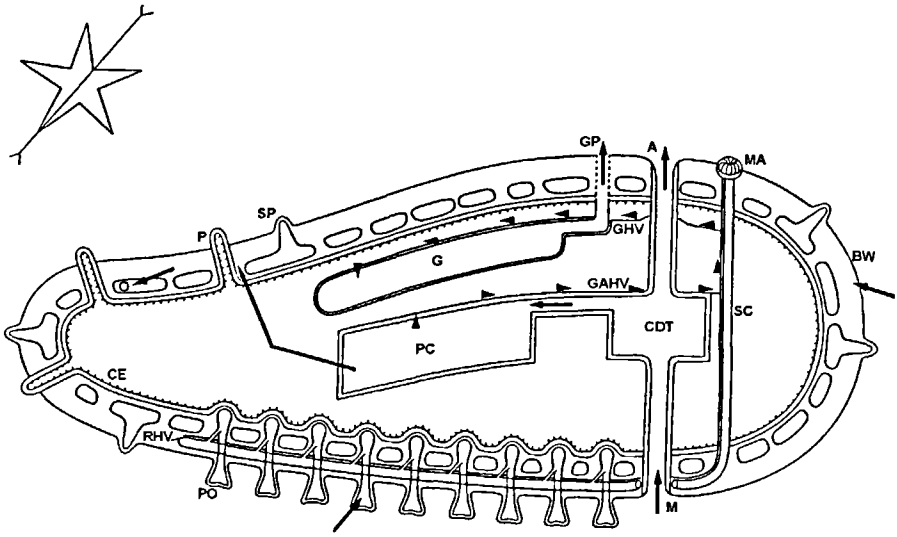

Figure 2
Sagital section through an asteroid arm showing known and supposed routes of in- and out-fluxes of Pb. Caption as in Figure 1.

during spawning (Temara *et al.*, 1998a). The toxicity of Pb accumulated in the gonads towards the maturing gametes depends on its chemical speciation and on the type of tissues (somatic or germinal) in which it is stored. It is noteworthy that Pb presented low toxic effects to mature echinoid gametes (Dinnel *et al.*, 1989.

The use of biomarkers to detect the biological impact of pollutants in asteroids has received little attention (Everaarts *et al.*, 1998). According to Everaarts (1995), assessment of DNA integrity is a valuable method as a biomarker of polycyclic aromatic hydrocarbon and polychlorinated biphenyl effects in *A. rubens*, but no correlation with metal content has been calculated. Similarly, P450 induction by planar compounds has been reviewed by den Besten (1998). According to Temara *et al.* (1997b), the quantification of MT content in *A. rubens* is not a valuable biomarker of Cd or Zn exposure in asteroids as opposed to several other taxa.

Bioindicative value of *A. rubens*

In Sørfjord (SW Norway), one of the most heavily metal-polluted sites in the NE Atlantic, the asteroid populations studied in the 1970s had very high Cd (18 $\mu g.g^{-1}$ Cd dw), Pb (460 $\mu g.g^{-1}$ Pb dw), and Zn (1500 $\mu g.g^{-1}$ Zn dw) concentrations, i.e. respectively 11, 200, and 7 fold the measured values in populations living at the same period in background regions (Bryan, 1984). After remedial actions in the fjord, concentrations have considerably decreased but are still significantly higher than background levels (Temara *et al.*, 1998c).

The characteristic features of an ideal bioindicator of heavy metal contamination have been described by several authors including Phillips (1990), Bryan & Hummerstone (1977). It has been reported that *A. rubens* is characterised by most of these features (Table 1).

The use of an organism as a bioindicator requires that its body concentrations reflect environmental conditions. An organism that is able to regulate the body concentrations of the metal studied could not be used as a valuable bioindicator (some decapod crustaceans, for example, control their internal Zn and Cu concentrations.

Qualities of an ideal bioindicator *	Characteristic features of *Asterias rubens*	References
• Ubiquity	Distribution of *Asterias* spp covers the Northern hemisphere, from the tidal zone down to -650 m; euryhaline species; invasive *A. amurensis* in Southern hemisphere	Hayward & Ryland, 1990 Byrne *et al.*, 1997
• Stability of populations over the year	Life expectancy up to 7 years	Guillou & Guillaumin, 1985
• Permanence of localization	Sedentary behaviour	Hostens & Hammerlynck, 1994
• Abundance	Large populations (thousands of individuals)	Hostens & Hammerlynck, 1994
• Ease of sampling	Seashore fishing, dredging, diving	
• Large size for analyses	Body compartments of ecotoxicological interest weigh several grams dw	
• Good knowledge of the general biology of the organism	Thousands of publications about its biology from the end of the 19th century	
• Easy study	Rapid acclimatization to laboratory conditions	
• High affinity for heavy metals	Shown for Sr, Pu, Cd, Hg, Se, Mn, Pb, Zn, Ag, Am, Cs, Co	Binyon, 1978; Guary *et al.*, 1982; den Besten *et al.*, 1990; Sorensen & Bjerregaard, 1991; Rouleau *et al.*, 1993; Hansen & Bjerregaard, 1995; Temara *et al.*, 1996a; 1998c; Warnau *et al.*, 1998a; 1999.
• Measurable tissular concentrations	Easy detection of tissular concentrations by absorption or emission spectrometry	den Besten *et al.*, 1990; Sorensen & Bjerregaard, 1991; Everaarts & Fischer, 1989; Temara *et al.*, 1997.
• Sensitivity to heavy metals	Demonstrated for Cu, Pb, and Cd	Gerets *et al.*, 1972; den Besten *et al.*, 1989; Temara *et al.*, 1997b; 1998c.
• Direct relationships between tissular and environmental concentrations	Shown for Cd and Pb	Bjerregaard, 1988; Temara *et al.*, 1996a; 1998a,c.
• Presence in polluted zones	Presence in heavily polluted sites, e.g. Sørfjord (SW Norway)	Temara *et al.*, 1997b; 1998c.

*: From Phillips (1976; 1990), Bryan & Hummerstone (1977), and Bryan (1984).

Table 1
The characteristic features of *Asterias rubens* making the species an ideal bioindicator of heavy metal contamination.

In *A. rubens*, Cd concentrations in the pyloric caeca were directly proportional to contaminating concentrations in the range of 0.025 to 2.5 $\mu g.l^{-1}$ Cd (Bjerregaard, 1988). The bioconcentration factor decreased only with higher environmental concentrations according to a threshold effect (Bjerregaard, 1988; Temara *et al.*, 1996a). Moreover, Cd concentrations in the skeleton of asteroids collected along a well-marked contamination gradient in the field (Sørfjord, Norway) were significantly correlated to concentrations in the sediment (Temara *et al.*, 1998c).

The study of elimination kinetics provides information on the temporal scale of a bioindicator. While the pyloric caeca rapidly eliminated a significant proportion of the accumulated Cd (65% within a few days), the skeleton kept Cd for a longer time (elimination of 30% over a period of 6 weeks) (Temara *et al.*, 1996a). However, a study of the asteroids from the Sørfjord showed that the skeleton was not able to indicate variations in Cd concentrations over a period of several years. Therefore, according to observations by Temara *et al.* (1996a; 1998c), the Cd retention time in the skeleton is rather a few months. Further study on the retention capacity of Cd by the skeleton over a long period of time is needed in order to ascertain the half-time of the metal in this compartment. It is worthwhile noting that in the echinoid *Paracentrotus lividus*, the biological halftime has been estimated to a few months (Warnau *et al.*, 1995b). The pyloric caeca of *A. rubens* should thus be considered as a short-term bioindicator of Cd contamination, while the skeleton should be used as a mid-term bioindicator.

Because of the wide distribution of Asterias spp. (see Table 1), it is tempting to propose them as valuable bioindicators over the whole Northern hemisphere, including arctic regions where asteroids represent a significant proportion of the benthic biomass and which are increasingly polluted. However, biokinetics of Cd and Pb in *A. rubens* have been studied at temperatures characteristic of temperate regions only (i.e., 5-20 °C). According to Hutchins *et al.* (1996), elimination kinetics of radionuclides from *A. forbesi* were much slower at temperatures characteristic of northern habitats and extrapolation of conclusions drawn from observations in warmer ecosystems might be invalid in such extreme environments.

The Pb accumulation ratios in the asteroid body compartments were directly proportional to the environmental contaminating concentrations (Temara *et al.*, 1998a). Study of the contamination of asteroids from the Sørfjord showed that after long-term exposures, the body concentrations were in good agreement with environmental conditions at steady-state (Temara *et al.*, 1998c). The digestive organs accumulated and eliminated Pb rapidly; in contrast, the skeleton integrated the variations over the lifespan of the asteroid (*i.e.* several years, Temara *et al.*, 1998a, c).

Based on the information available so far, a sampling strategy of *A. rubens* may be proposed for future biomonitoring programs.

Sampling strategy

The variations in heavy metal concentrations in the body compartments of asteroids living in sites located far from any point sources of contamination have clearly shown that some precautions have to be taken in a biomonitoring program based upon that species.
(1) It is not advised to use *A. rubens* as an homogeneous compartment since the distribution of metals within the organism is selective.
(2) The gonads should not be included in biomonitoring programs: they are not present during part of the reproductive cycle, which limits extemporised samples. Furthermore, gametogenesis in *A. rubens* depends closely on water temperature and on food availability, which means that asteroids sampled at the same time but at different latitudes could present different metal concentrations in the gonads due to differences in gametogenic stages.
(3) The central digestive system is of limited use because of its small mass that does not allow various analyses on any one organism. Its analysis could, however, be useful in the frame of a biomonitoring program focused on Pb contamination due to its rapid elimination from that compartment.
(4) Heavy metal concentrations do vary with the size of the asteroid. Therefore, it is advised to sample asteroids of the same size-class. The amplitude of the allometric variations being minimal in the lar-

gest size-class, asteroids should be collected among individuals of this size-class in each population.
(5) As a rule, the advised body compartments are the pyloric caeca and the skeleton (prepared as described in Temara *et al.*, 1996a); they should be sampled on asteroids belonging to the largest size-class in the same gametogenic stage.

The results obtained so far during our study of the natural variations in metal concentrations in *A. rubens* populations in the NE Atlantic (deposited in the database of the International Council for the Exploration of the Sea, and that of the Management Unit of the North Scheldt and North Sea Mathematical Model, Belgium; Reference MUMM 94 CF. BE) provided a set of data corresponding to a range of concentration variations in relatively non-contaminated environments. The 95th percentile of such distributions has been chosen (for each metal) as a critical value beyond which any mean concentration can be considered as an indication of contamination. According to the variations between compartments, it is necessary to define different critical values for each of the compartments. These values are shown in Table 2 for the body compartments selected previously and for two of the metals whose concentrations are known to vary with environmental conditions (Cd and Pb).

	Skeleton	Pyloric caeca	Central digestive system
Pb	10	1.1	1.5
Cd	1.2	5.1	-

Table 2
Critical values (µg.g^{-1} dw) of heavy metals in the body compartments of adult *A. rubens*. (The central digestive system is necessary for Pb analyses).

Taking into account the critical values of Table 2 and uptake and elimination kinetics of Pb, concentrations in the digestive system and in the skeleton may thus indicate different situations.

(1) Pb concentrations in the central digestive system and in the skeleton are lower than the critical values: the ecosystem has not been sub-

jected to a major contamination for years before the sampling (up to 7 years, *i.e.* the lifespan of asteroids). It is noteworthy that a limited or a minor past contamination might not be detectable due to the dilution effect of skeletal growth.

(2) Pb concentrations in the central digestive system are higher than the critical values while concentrations in the skeleton are lower than the critical values: the ecosystem has been submitted to a recent contamination (early signal).

(3) Pb concentrations in both compartments are higher than their respective critical values: there is current long-lasting contamination.

(4) Pb concentrations in the central digestive system are lower than the critical values while concentrations in the skeleton are higher than the critical values: the ecosystem had been contaminated but the source has disappeared.

Taking into account the size/age relationship observed in asteroids and the long retention time of Pb in the skeleton, an allometric study of Pb concentration in the asteroid skeleton can provide further information on the history of the contamination of the site studied, as it has been undertaken in Sørfjord (Temara *et al.*, 1998c). Similarly, further investigations might determine the validity of assessing the remote history of contamination by studying the metal content of echinoderm fossils as proposed by Ferrara *et al.* (1997). The biokinetics in the various body compartments were quite different for Cd and a similarly precise approach to biomonitoring cannot be applied for this metal.

Conclusions

The main route of Cd and Pb uptake in *A. rubens* would be the digestive wall. Transfers to other body compartments including the body wall and the gonads have been observed. At steady state, the distribution of metals in the asteroid depends mainly on the type of body compartment. The pyloric caeca are the main target of classes Ib and IIb elements. The skeleton is the main target of

Pb. For the two elements that have been studied in detail (Pb and Cd), there is a simple relationship between the body concentrations and the concentrations in the environment (Bjerregaard, 1988; Temara *et al.*, 1996a; 1998a, c). Uptake and elimination of Pb and Cd by the pyloric caeca are rapid processes. In contrast, the retention periods are longer in the skeleton (Cd: several months, Pb: up to several years). Because of the satisfactory relationship between the ecotoxicological parameters of metals in *A. rubens* and the selection criteria of bioindicators, this species should be included in biomonitoring programs (such programs are currently underway in the Southern Bight of the North Sea by our own team as well as teams in the Netherlands, Everaarts *et al.*, 1998). Analysis of concentration variability in the populations located far from any point sources of contamination allowed definition of a sampling strategy as well as critical values. Mean concentrations exceeding such values indicate a contamination in the ecosystem at the 95% confidence level. The body compartments "pyloric caeca" and "skeleton" are proposed as complementary bioindicators of Cd and Pb contamination: the pyloric caeca as a short-term bioindicator, the skeleton as a mid- to long-term bioindicator. Concerning Pb, an allometric study of the skeleton can indicate temporal variations in environmental contamination on the scale of the decade.

Detoxification systems of Cd and Pb are relatively efficient in *A. rubens*, which is therefore fairly resistant to these metals. The major detoxification system of Cd would be its complexation to inducible proteins, the metallothioneins. Incorporation into the skeleton seems to be the major detoxification route for Pb.

Acknowledgements

Our thanks are due to K. Ryder (RMIT-University) for critical reading of the manuscript. Research was supported by the Impulse Program in Marine Sciences, financed by the Belgian government (SSTC, MS/11/020). P. Dubois and M. Warnau are Research Associates of the National Fund for Scientific Research (NFSR, Belgium). Contribution of the "Centre interuniversitaire de biologie marine" (CIBIM).

Bibliography

BEIJNINCK F. B., VAN DER SLUIS I., VOOGT P. A., 1984 — Turnover rates of fatty acid and amino acid in the coelomic fluid of the sea star *Asterias rubens* : implications for the route of nutrient translocation during vitellogenesis. *Comp. Biochem. Physiol.*, 78B: 761-767.

BJERREGAARD P., 1998 — Effect of Selenium on Cadmium uptake in selected benthic invertebrates. *Mar. Ecol. Prog. Ser.*, 48: 17-28.

BREMER P. J., BARKER M. F., LOUTIT M. W., 1990 — A comparison of the roles of direct absorption and phytoplankton ingestion in accumulation of chromium by sea urchin larvae. *Mar. Environ. Res.*, 30: 233-241.

BRYAN G. W., HUMMERSTONE L. G., 1977 — Indicators of heavy-metal contamination in the Looe Estuary (Cornwall) with particular regard to silver and lead. *J. Mar. Biol. Ass. UK.*, 57: 75-92.

BUSTNES J. O., ERIKSTAD K. E., 1983 — The diets of sympatric wintering populations of common eider *Somateria mollissima* and king eider *S. spectabilis* in Norway. *Ornis Fennica.*, 65: 163-168.

BYRNE M., MORRICE M. G., WOLF B., 1997 — Introduction of the northern Pacific asteroid *Asterias amurensis* to Tasmania: reproduction and current distribution. *Mar. Biol.*, 127: 673-685.

COLEMAN N., MANN T. F., MOBLEY M., HICKMAN N., 1986 — *Mytilus edulis planulatus*: an "integrator" of cadmium pollution? *Mar. Biol.*, 92: 1-5.

DEN BESTEN P .J., 1998 — Cytochrome P450 monooxygenase system in echinoderms. *Comp. Biochem. Physiol.*, C 121: 139-146.

DEN BESTEN P. J., HERWIG H. J., ZANDEE D. I., VOOGT P. A., 1989 — Effects of cadmium and PCBs on reproduction of the sea star *Asterias rubens*: aberration in the early development. *Ecotoxicol. Environ. Saf.*, 18: 173-180.

DEN BESTEN P. J., HERWIG H. J., ZANDEE D. I., VOOGT P. A., 1990 — Cadmium accumulation and metallothionein-like proteins in the sea star *Asterias rubens*. *Arch. Environ. Contam. Toxicol.*, 19: 858-862.

DINNEL P. A., LINK J. M., STOBER Q. J., LETOURNEAU M. W., ROBERTS W. E., 1989 — Comparative sensitivity of sea urchin sperm bioassays to metals and pesticides. *Arch. Environ. Contam. Toxicol.*, 18: 748-755.

EVERAARTS J. M., 1995 — DNA integrity as a biomarker of marine pollution: strand breaks in seastar (*Asterias rubens*) and dab (*Limanda limanda*). *Mar. Pollut. Bull.*, 31: 431-438.

EVERAARTS J. M., FISCHER C. V., 1989 — *Micro-contaminants in surface sediments and macrobenthic invertebrates of the North sea.* NIOZ-Rapport 1989 (6). Nederlands Instituut voor Onderzoek der Zee. North Sea Benthos Survey (ICES), 44 p.

EVERAARTS J. M., OTTER E., FISCHER C. V., 1990 — Cadmium and polychlorinated biphenyls: different distribution patterns in North Sea benthic biota. *Neth. J. Sea Res.*, 26: 75-82.

EVERAARTS J. M., DEN BESTEN P .J., HILLEBRAND M. T. J., HALBROOK R. S., SHUGART L. R., 1998 — DNA strand breaks, cytochrome P-450-dependent monooxygenase system activity and levels of chlorinated biphenyl congeners in the pyloric caeca of the seastar (*Asterias rubens*) from the North Sea. *Ecotoxicology*, 7: 69-79.

FERGUSSON J. C., 1982 — A comparative study of the net metabolic benefits derived from the uptake and release of free amino acids by marine invertebrates. *Biol. Bull.*, 162: 1-17.

GERETS C., DELAHAYE W., PERPEET C., VLOEBERGH M., JANGOUX M., 1972 — *Intoxication des moules et des astéries (Asterias rubens) par les métaux lourds. CIPS. Mathematical Model of the Pollution in the North Sea.* Technical Report, Brussels.

GRAY J. S., 1989 — Do bioassays adequately predict ecological effects of pollutants? *Hydrobiologia*, 188/189: 397-402.

GUILLOU M., GUILLAUMIN A., 1985 — "Variations in the growth rate of *Asterias rubens* (L.) from west and south Brittany (France). Echinodermata". *In* Keegan B. F., O'Connor B.S.D. (eds) *Proceedings of the Fifth International Echinoderm Conference*, Galway. A.A. Balkema, Rotterdam: 513-521.

HANSEN S. N., BJERREGAARD P., 1995 — Manganese kinetics in the sea star *Asterias rubens* (L.) exposed via food or water. *Mar. Pollut. Bull.*, 31: 127-132.

HAYWARD J. M., RYLAND J. S., 1990 — *The marine fauna of the British Isles and north-west Europe. II - Molluscs to Chordates.* Oxford Science Publications, New York.

HOSTENS K., HAMMERLYNCK O., 1994 — The mobile epifauna of the soft bottoms in the subtidal Oosterschelde estuary: structure, function and impact of the storm-surge barrier. *Hydrobiologia*, 282/283: 479-496.

HURLBERT S. H., 1997 — Functional importance *vs* keystoneness: reformulating some questions in theoritical biocenology. *Austral. J. Ecol.*, 22: 369-382.

HUTCHINS D. A., STUPAKOFF I., FISHER N. S., 1996 — Temperature effects on accumulation and retention of radionuclides in the sea star, *Asterias forbesi*: implications for contaminated northern waters. *Mar. Biol.*, 125: 701-706.

JANGOUX M., 1982 — "Food and feeding mechanisms: Asteroidea". *In* Jangoux M., Lawrence J.M. (eds): *Echinoderm nutrition.* Balkema, Rotterdam: 117-159.

JOIRIS C., BILLEN G., LANCELOT C., DARO M.H., MOMMAERTS J.P., BERTELS A., BOSSICART M., NIJS J., HECQ J.H., 1982 — A budget of carbon cycling in the Belgian coastal zone: relative roles of zooplankton, bacterioplankton and benthos in the utilization of the primary production. *Neth. J. Sea Res.*, 16: 260-275.

KARBE L., ALETSEE L., DÜRSELEN C. D., HEYER K., KAMMANN U., KRAUX M., RICK H. J., STEINHOUT H., 1994 — "Bioaccumulation and effects of plankton and benthos on the fate of contaminant". *In* Sünderman, J. (ed.): *Circulation and contaminant fluxes in the North Sea*, Springer-Verlag, Berlin: 556-597.

KEATS D. W., 1990 — Food of winter flounder *Pseudopleuronectes americanus* in a sea urchin dominated community in eastern Newfoundland. *Mar. Ecol. Prog. Ser.*, 60: 13-22.

KERSTEN M., KRÖNCKE I., 1991 — Bioavailability of lead in North sea

sediments. *Helgoländer Meeresunters*, 45: 403-409.

KREMLING K., 1983 — The behaviour of Zn, Cd, Cu, Ni, Co, Fe and Mn in anoxic baltic waters. *Mar. Chem.*, 13: 87-108.

KRÖNCKE I., 1987 — Lead and cadmium contents in selected macrofauna species from the Dogger Bank and eastern North Sea. *Helgoländer Meeresunters*, 41: 465-475.

KRÖNCKE I., RACHOR E., 1992 — Macrofauna investigations along a transect from the inner German Bight towards the Dogger Bank. *Mar. Ecol. Prog. Ser.*, 91: 269-276.

MENGE B. A., 1982 — "Effects of feeding on the environment: Asteroidea". *In* Jangoux M., Lawrence J. M. (eds): *Echinoderm nutrition*. Balkema, Rotterdam: 521-551.
NSTF, 1993 – *North Sea Quality Status Report*. Oslo and Paris Commissions, London.

OUDEJANS R.C.H.M., VAN DER SLUIS I., VAN DER PLAS A. J., 1979 — Changes in the biochemical composition of the pyloric caeca of female seastars, *Asterias rubens*, during their annual reproductive cycle. *Mar. Biol.*, 53: 231-238.

PHILLIPS D. J. H., 1990 — "Use of macroalgae and invertebrates as monitors of metal levels in estuaries and coastal waters". *In* Furness R. W., Rainbow P.S. (eds): *Heavy Metals in the Marine Environment*. CRC Press, Boca Raton, FL: 81-99.

REIMER O., OLSSON B., TEDENGREN M., 1995 — Growth, physiological rates and behaviour of *Mytilus edulis* exposed to the predator *Asterias rubens*. *Mar. Fresh. Behav. Physiol.*, 25: 233-244.

RILEY J. P., SEGAR D. A., 1970 — The distribution of the major and some minor elements in marine animals. I. ECHINODERMS and Coelenterates. *J. Mar. Biol. Ass. UK.*, 50: 721-730.

ROESIJADI G., 1992 — Metallothioneins in metal regulation and toxicity in aquatic animals. *Aquat. Toxicol.*, 22: 81-114.

ROULEAU C., PELLETIER E., TJÄLVE H., 1993 — The uptake and distribution of $^{203}HgCl_2$ and CH_3HgCl_2 in the sea star *Asterias rubens* after 24-h exposure studied by impulse counting and whole body autoradiography. *Aquat. Toxicol.*, 26: 103-116.

RUPPERT E. E., BARNES R. D., 1994 — *Invertebrate Zoology*. Saunders College Publishing, New York.
SKEI J. M., 1981 – *Dispersal and retention of pollutants in Norwegian fjords*. Rapp. P-v. Réun. Cons. Int. Explor. Mer., 181: 78-86.

SKEI J. M., 1995 — *Tiltaksorienterte undersøkelser i Sørfjorden og Hardangerfjorden 1994*. Delrapport 1. Vannkjemi. NIVA-report (in norvegian), 1, (3263).

SORENSEN E. M. B., 1991 — *Metal poisoning in fish*. CRC Press, Boca Raton.

SORENSEN M., BJERREGAARD P., 1991 — Interactive accumulation of mercury and selenium in the sea star *Asterias rubens*. *Mar. Biol.*, 108: 269-276.

TEMARA A., ABOUTBOUL P., WARNAU M., JANGOUX M., DUBOIS P., 1995 — "Kinetics of lead uptake by the skeleton of the asteroid *Asterias rubens* (Echinodermata)". *In* Emson R. H., Smith A. B., Campbell A. C. (eds): *Echinoderm Research 1995*, Balkema, Rotterdam: 79-82.

TEMARA A., LEDENT G., WARNAU M., PAUCOT H., JANGOUX M., DUBOIS P., 1996a — Experimental cadmium contamination of *Asterias rubens*, L. (Echinodermata). *Mar. Ecol. Prog. Ser.*, 140: 83-90.

TEMARA A., WARNAU M., JANGOUX M., DUBOIS P., 1997a — Factors controlling heavy metal concentrations in the asteroid *Asterias rubens* (Echinodermata). *Sc. Total Environ.*, 203: 51-63.

TEMARA A., WARNAU M., DUBOIS P., LANGSTON W.J., 1997b — Quantification of metallothioneins in the common asteroid *Asterias rubens* (Echinodermata) exposed experimentally or naturally to cadmium. *Aquat. Toxicol.*, 38: 17-34.

TEMARA A., NGUYEN Q.A., HOGARTH A.N., WARNAU M., JANGOUX M., DUBOIS P., 1997c — High sensitivity of skeletogenesis to Pb in the asteroid *Asterias rubens*. *Aquat. Toxicol.*, 40: 1-10.

TEMARA A., ABOUTBOUL P., WARNAU M., JANGOUX M., DUBOIS P., 1998a — Uptake and fate of lead in the common asteroid *Asterias rubens* (Echinodermata). *Water Air Soil Pollut.*, 102: 201-208.

TEMARA A., WARNAU M., JANGOUX M., DUBOIS P., 1998b — "Effects of exposure to cadmium on the concentrations of essential metals in *Asterias rubens* (Asteroidea)". *In* Mooi R., Telford M. (ed) *Echinoderm: San francisco.* Balkema, Rotterdam: 307-310.

TEMARA A., SKEI J. M., GILLAN D., WARNAU M., JANGOUX M., DUBOIS P., 1998c — Validation of the asteroid *Asterias rubens* (Echinodermata) as a bioindicator of spatial and temporal trends of Pb, Cd, and Zn contamination in the field. *Mar. Environ. Res.*, 45: 341-356.

VOOGT P. A., DEN BESTEN P. J., KUSTERS G. C. M., MESSING M. W. J., 1987 — Effects of Cadmium and Zinc on steroid metabolism and steroid level in the sea star *Asterias rubens* L. Comp. Biochem. Physiol., 86C: 83-89.

VYNCKE W., BAETEMAN M., GUNS M., VAN HOEYWEGHEN P., GABRIELS R., 1991 — Trace metals in the Belgian dumping area for acid wastes from the titanium dioxide industry (1985-89). *Revue de l'Agriculture-Landbouwtijdschrift*, 44: 1277-1291.

WARNAU M., LEDENT G., TEMARA A., JANGOUX M., DUBOIS P., 1995a — Allometry of heavy metal bioconcentration in the echinoid *Paracentrotus lividus*. *Arch. Environ. Contam. Toxicol.*, 29: 393-399.

WARNAU M., LEDENT G., TEMARA A., JANGOUX M., DUBOIS P., 1995b — Experimental cadmium contamination of the echinoid *Paracentrotus lividus:* influence of exposure mode and distribution of the metal in the organism. *Mar. Ecol. Prog. Ser.*, 116: 117-124.

WARNAU M., TEYSSIÉ J. L., FOWLER S. W., 1996a — Biokinetics of selected heavy metals and radionuclides in two marine macrophytes: the seagrass *Posidonia oceanica* and the alga *Caulerpa taxifolia*. *Mar. Environ. Res.*, 41: 343-362.

WARNAU M., FOWLER S. W., TEYSSIÉ J. L., 1999 — Biokinetics of radiocobalt in the asteroid *Asterias rubens* (Echinodermata): sea water and food exposures. *Mar. Pollut. Bull.*, 39: 159-164

Oral/Poster presentations

Session 1

Effect of marine oligotrophy on the biogeochemistry of radionuclides

Ross A. Jeffree

Oligotrophic or low productivity waters comprise more than 50% of the world's oceans. Moreover, their extent and degree of oligotrophy has increased in one region over the past 50 years. Oligotrophic waters are characterised by greater a) thermal stratification of the water column, b) temporal stability in phytoplankton and zooplankton abundances, and c) prominence of picoplankton. With regard to the presence of nuclides in these waters our studies have focussed on i) ^{210}Po bioaccumulation in marine organisms, relevant to its preeminence in human radiological dose from the consumption of seafoods, and ii) the use of naturally occurring nuclides, such as ^{234}Th, as tracers of biogeochemical processes in the euphotic zone. A study of ^{210}Po concentrations in zooplankton collected from the low productivity waters of French Polynesia during 1990-1992 has demonstrated their enhanced uptake of ^{210}Po when zooplankton biomass is low. ^{210}Po in zooplankton increases exponentially to previously unreported levels up to 3200 Bq.kg^{-1} dry weight, as their biomass decline to levels as low as 0.14 mg dry weight/cubic metre. A validated mathematical model, incorporating the established role of zooplankton in the removal of ^{210}Po from the water column, captures the shape of this empirical relationship and also explains this biomass-related mechanism that increases ^{210}Po concentrations in zooplankton. In a further study the model structure was reviewed to determine a set of biogeochemical behaviours of ^{210}Po, proposed to be critical to its environmental enhancement under oligotrophy: this set was then used to identify 25 other elements with comparable behaviours to ^{210}Po. Field investigation in the Timor Sea showed that four of these a *priori* identified elements *viz.* Cd, Co, Pb and Mn, as well as Cr and Ni, showed elevated water concentrations

with reduced particle removal rates in the euphotic zone, results that are consistent with those previously obtained for ^{210}Po and the proposed explanatory model. These findings point to the enhanced susceptibility to contamination with particle-reactive elements of oligotrophic marine systems, whose degree and geographic extent may be enhanced by projected increases in sea surface temperatures from global warming. Alternative interpretations of the inverse relationship between biomass and environmental concentrations of particle-reactive elements in the euphotic zone will also be discussed.

Accumulation and releasing of radium in *Thypha sp.* leaves and detrital materials

Dejanira C. Lauria

V. R. G. Reis

José Marcus O. Godoy

The radium accumulation and liberation in *Thypha dominguenes* Pers. green leaves and leaf detritus from a coastal lagoon was studied by in situ and lab experiments. From results of leaf sample analysis collected in different locals of the lagoon and the lab experiments, adsorption experiments followed by sequential extraction, it was observed the importance of the ionic exchange for the foliar accumulation. So the salinity plays a very important role in the dynamic of radium accumulation/releasing in the leaf. Decomposition of the leaves was studied by litter bag methods during a period of 6 months. At the end of the experiments the major cation losses were 96% of K, 76% of Na and 51% of Mg. On the other hand the amount of Ca in the residue increased three times (means a concentration increases of seven times) as well as increased the total activity of ^{226}Ra and of ^{228}Ra (seven and at least three times, respectively). In agreement with this observation, lab experiments showed that the material was able to adsorb quite a 100% of the added Ra and its adsorption capacity was estimated as 5 meq $(Ba^{2+})/g_{detritus}$. Radionuclide releasing by sequential extraction of the detrital material followed a little bit different dynamic from the green leaf, showing that important fraction of the radium can be retained in the litter by carbon mineralization.

Biokinetics of selected metals and radionuclides in echinoderms: a multitracer approach

Michel Warnau

Jean-Louis Teyssie

Scott W. Fowler

The common sea star Asterias rubens and sea urchin Paracentrotus lividus are widely distributed and abundant species in European seas. They have been shown to efficiently accumulate metals and were identified as valuable bioindicators of metal contamination. However, few studies have investigated bioaccumulation in these organisms using realistic contaminant concentrations. Here, biokinetics were investigated using radiotracer techniques in order to study element concentrations representative of those encountered in the marine environment. High-resolution g-spectrometry allowed the investigation of several elements simultaneously (multitracer experiments). Seven radiotracers were selected: ^{54}Mn, ^{57}Co, ^{65}Zn, ^{110m}Ag, ^{109}Cd, ^{134}Cs, and ^{241}Am. Bioaccumulation and depuration were followed in sea stars and sea urchins exposed via sea water, food, or sediments in order to determine predominant uptake route(s) and biological retention time of the tracers. Except for ^{134}Cs, organisms efficiently bioaccumulated all the elements examined. Bioconcentration was found to be strongly body-compartment dependent. Biological half-lives ranged from a few days to several months depending upon the element and the exposure route considered. Sea urchins bioconcentrated most tracers mainly from sea water. For sea stars, sea water and food constituted the two main routes of uptake (sediments generally accounted for only a small proportion in the contamination of the organisms).

Difference of ^{137}Cs concentration between sex of marine fishes

T. Iibuchi

Y. Suzuki

Y. Ishikawa

F. Kasamatsu

Monitoring on the artificial radionuclides concentrations of marine organisms in coastal waters of Japan has been conducted since 1984 as a part of the marine environmental radioactive monitoring program sponsored by the Science and Technology Agency of Japan. The variations of ^{137}Cs concentration in marine organisms and the factors affecting the variations have been investigated. Concentration of ^{137}Cs in marine fishes varied by species, sex, size, and food habits. In this presentation, we demonstrate the difference of ^{137}Cs concentrations by sex in rockfish and flounder together with the difference of stable Cs and stable nitrogen isotope ratio (delta 15N) in these fishes, and we discuss the possible factors affecting sexual difference of ^{137}Cs concentrations in marine fishes.

RadCon: A new Australasian radiological dose assessment model

J. Crawford

R. U. Domel

J. R. Twining

F. F. Harris

ANSTO developed and implemented a radiological dose assessment model, RadCon, with the emphasis on tropical and subtropical climates. An overview of RadCon will be given in this paper.

Models for dose assessment were developed using information on the distribution, transport and biological effects from studies mainly in the temperate and cold regions of the world, almost exclusively in the Northern Hemisphere. Only limited information is currently available for tropical and subtropical regions.

The original motivation of this work was to investigate these information deficiencies and commence targeted research into that data with the most significant effect on the radiological consequences for the Australian and South East Asian region. Aside from the identification and acquisition of the available data, a computational tool, RadCon, was developed and implemented at ANSTO, to be used in dose assessment and to assist in the identification of the most relevant data.

RadCon was developed as a simple and flexible model to assess the radiological consequences, as dose, to humans resulting from short-term release or accidental release of radionuclides to the atmosphere. RadCon implements internal exposure from inhalation and ingestion as well as external exposure from the passing cloud and from radionuclides deposited on the ground. Atmospheric dispersion and ground deposition is estimated externally to the program using meteorological models or measured data. RadCon accepts time-dependent air and ground concentration which would be the output of an atmospheric transport model suitable for the assessment site.

In designing RadCon, the variability of the region (e.g. lifestyle and diets of groups of the population, soil types, etc.) was taken into

account. RadCon presents a graphical interface to the user, which allows the user to set optional parameters over the region under study. In a manner similar to a geographic information system, the user specifies site specific information over the two-dimensional region of interest, such as soil type, dietary components of humans and animals, race and lifestyle.

RadCon was written in the Java programming language, resulting in portability across computer platforms. The estimated dose to man is displayed in coloured concentration contours, stepping through time, superimposed on the area of interest and the actual values at a particular location can be obtained by selecting the particular grid location.

To evaluate the RadCon mathematical model and its implementation, ANSTO is participating in the BIOMASS (BIOsphere Modelling and ASSessment) model inter-comparison program. BIOMASS is a program sponsored by the International Atomic Energy Agency. ANSTO is participating with the RadCon model in a case study of a contaminated area from the Chernobyl accident. The results generated by RadCon for this case study were very encouraging. Areas of potential model improvement were identified and some have been incorporated. Data sensitivity analysis was implemented in RadCon, allowing the user to identify which parameter entered into the model has the most impact on the estimated dose, under the conditions of the study.

Soil-to-plant transfer of radioactivity in tropical systems: development of field study in Northern Australia

John Twining

Previous work carried out within an IAEA CRP to evaluate tropical transfer of radionuclides into human food showed that soil-to-plant transfer factors were not, on average, different to those measured in temperate regions (particularly within the Northern Hemisphere). However, closer examination of the data showed that some systems gave extreme transfer factor values. There also seemed to be a higher proportion of environments within the tropics and sub-tropics that tended towards the extreme. This is to be expected given the much wider range of conditions and climatic differences observed when comparing tropical and temperate regions.

The observed differences were isotope specific but not plant specific. That is, if transfer factors were appreciably higher (or lower) than average for any particular isotope then that factor was observed in all samples taken, irrespective of the type of plant. However, it was not necessary that any other isotope would behave similarly.

Soil type was identified as the most probable reason behind the observed differences. Hence, a follow-up study has been designed to identify which soil types are extreme by observing bioaccumulation by an agreed sub-set of two plants (a leafy vegetable and a grain, which typically give the highest and lowest factors respectively) growing on a range of different soil types. The study is also designed to identify the specific characteristics of the soil, the climate and the agricultural practices that have most influence on transfer to crops.

This presentation will outline the background and design of the current IAEA CRP with specific reference to the Australian contribution that involves a field study of plant uptake following an addition of Cs, Sr and Zn to two soils in the Northern Territory of Australia. Results-to-date from the recently established site will also be discussed.

Radioactivity and waste disposal

Session 2

Chairman: G. E. Gilbert

Session opening: A. I. Hernandez-Benitez

Radioactive waste management: the role of CIEMAT in the Spanish and European R+TD programs for radwaste disposal

Pedro Rivas Romero

Antonio I. Hernandez Benitez

Introduction

Waste production is a direct consequence of welfare and industrial development. The waste volume produced and the hazards some of them represent have turned out in an appeal to rationale production, recycling and the storage of the final products under safe conditions.

Radioactive wastes have created the greatest social sensibilization, even though they must come from activities closely linked to welfare and development, such as nuclear energy production, industrial and diagnostic or therapeutic medical uses.

The "social" positioning on radioactive wastes is sometimes on the edge of rationality. The military use of nuclear energy, the lack of knowledge dissemination and biased information are giving place to reactions that go beyond the more elementary social and common senses.

Radioactive wastes exist and therefore, they must be adequately managed (recycling or transmutation) or stored. in a safe way. Their potential hazard and long life of some of them impose on our generation the moral obligation to avoid passing the problem to future generations.

The possibility of a permanent storage for high level radioactive wastes on deep geological formations have been intensively studied during the past twenty years in many countries. These studies are generating the knowledge and technical capabilities needed for building and managing a final storage site.

The exercises on long term performance assessment carried out up to date for real or hypothetical scenarios, defined from the knowledge of natural systems, give a reasonable level of confidence on the long term safety of the storage system.

The long term (10^4-10^6 years) assessment is the problem arising more doubts on the storage system and decreasing its confidence level. On that sense, the studies on natural analogues have a great relevance for the conceptual contributions, qualitative and quantitative, that they offer to the long or very long term evolution of natural processes and materials.

Any of the options that might be finally chosen for the final waste management, will finally end on the necessity of a definitive storage site.

The design of a Radioactive Waste Geological Storage is based on a multibarrier system concept (Figure 1). This is established so every barrier will provide mutual protection to the others. In the case of failure of any of the barriers all the others will act to solve this failure.

The barriers considered are the spent fuel matrix, the canister filling, the storage canister itself, the bentonite seal, the gallery backfill and the host rock. The ultimate function of the multibarrier system is to avoid or to retard as long as possible the arrival of the radionuclides to the biosphere with the aim of maintaining a dose to the public below the levels of the natural radioactive background for that host rock.

Objectives

The general objective of the Hydrogeochemical Site Characterisation Program of CIEMAT is to study the Long Term Behaviour of the Components of the Radioactive Wastes Storage

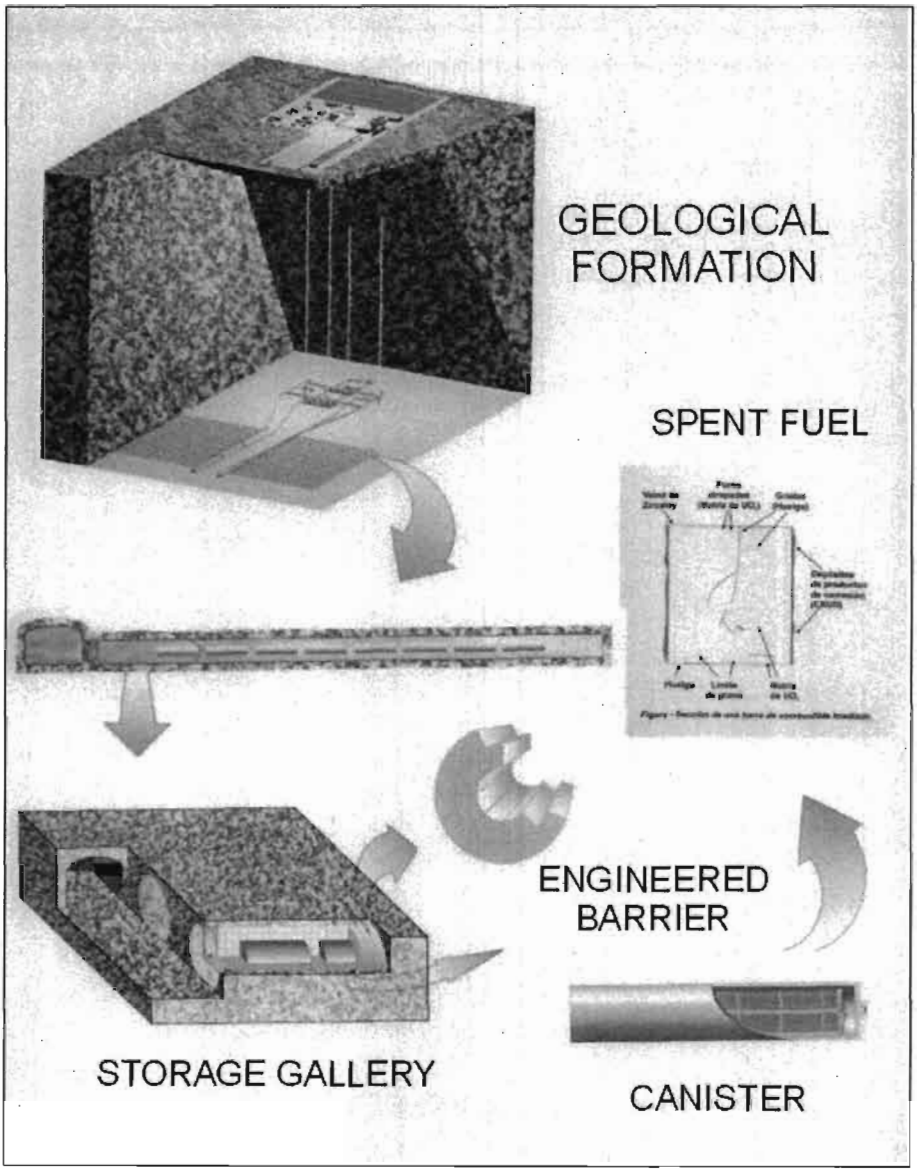

Figure 1
Conceptual design of a radioactive waste Deep Geological Storage system. Multibarrier system option.

Systems. This objective is focused on the study of the processes that determine the behaviour of the backfill and sealing materials, of granitic and clayish rocks and of natural analogues, in order to provide a sound scientific understanding of their role.

In the past four years, this objective has broadened to the study of spent fuel analogues, waste package filling materials and canister corrosion products. For all the materials considered, the most relevant aspect taken into account is their potential capability to decrease radionuclide mobility towards the environment, as they interact with the multibarrier system. This retardation or retention mechanisms may be of physical or chemical nature or a combination of different processes.

Results

The key processes controlling the long term behaviour and safety of a site act in a coupled way in the system as a whole, presenting a specific relevance for each of the barriers considered. The general objective of the Program is to identify those processes, to asses the manner in which they act and to provide a sound scientific understanding of their role. The results being obtained, presented below, are oriented to fulfil this general objective.

Long term stability of the spent fuel

The key process is the solubilization of the fuel matrix, the release of uranium and fission products in an almost dry, reducing, neutral and moderate temperature environment.

The study is carried out on natural UO_{2+x} (Uraninite and Pitchblende) as a fuel analogue, that has been exposed for millions of years to the evolution of a natural geochemical environment. The uraninites and pitchblendes studied correspond to the ore deposits of Oklo (Gabon), Palmottu (Finland) (Perez del Villar, 2000), Margnac and La Crouzille (France), Sierra Aabarrana, Los

Ratones and Mina Fe (Spain). They have been dated between 2000 (Oklo) and 50 Myears (Mina Fe). The more relevant results are the following:

for all the ore deposits it has been considered that most of the UO_{2+x} (Uraninite and Pitchblende) is original, even if it has undergone hydrothermal and/or meteoric weathering processes;

all uraninites and pitchblendes are affected by a relatively intense microfissuration that would had enhanced the weathering processes;

weathering has occurred mainly by pseudoisomorphic replacement of the original mineral specie (Uraninite and Pitchblende) by the new Uranium mineral without any apparent transport involved;

the kind of weathering depends on the geochemical environment in which it has happened. In high silica reduced environments Coffinite (U(IV) silicate) has replaced Uraninite or Pitchblende (Oklo, Mina Fe, Margnac and La Crouzille). In a pegmatitic oxidising environment such as Sierra Albarrana the gummites (complex hydrated U(VI) oxides) have partially replaced Uraninite;

all the weathering processes mentioned imply the mobilisation of part of the Uranium from the Uraninite or Pitchblende. The maximum mobilisation happens in the weathering to Uranyl phosphates. The leaching rate and the Uranium concentration in the rock interstitial water in contact with the ore do not vary significantly from those obtained in Uraninite leaching (10^{-9}–10^{-7} g.yr^{-1} for weathering ages of 50 and 1 Myears respectively). Those values imply Uranium concentrations of 10^{-7} to 10^{-6} M in the pore water in contact with the mineral;

in the natural reactor of Bangombé (Gabon) the Uraninite is impoverished in ^{235}U due to the fission reaction. However the $^{234}U/^{238}U$ and $^{230}Th/^{234}U$ ratios, with a unity value, indicate that Uraninite has remained unaltered for at least the last 1.7 Myears. The ^{206}Pb has not been mobilised over the last 740 Myears and the Zr, (Tc), Ru and ^{138}Ba have remained in the Uraninite where the fission occurred. However, Cs and Sr have migrated from that mineral (Gauthier-Lafaye *et al.*, 1999).

From the results showed above one of the main considerations is that the U mobilisation from natural minerals reflects the behaviour of spent fuel, and the resulting rate of U release from the waste

package will be very low with an almost immediate retention on the materials surrounding the waste. This should constitute an encouraging aspect concerning long term radionuclide mobility. In Figure 2 (Roubault, 1962) are shown some of the weathering processes affecting Uranium minerals.

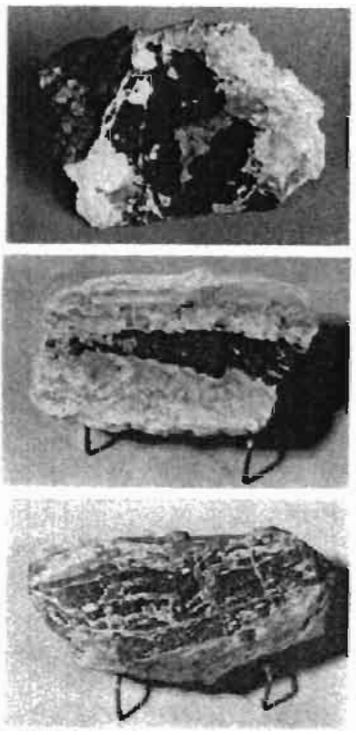

Figure 2
Examples of Uranium minerals weathering from different formations.
Top: Henriette mine (pitchblende oxidized to autunite).
Middle: Brugeaurd-Ouest mine (pitchblende to gummite).
Bottom: Margnac II (pitchblende to yellow gummite).

Canister filling materials

The function of these materials is to contribute to enhance the canister safety. It is planned to place an additional barrier, taking advantage of the small free space between the fuel elements and the canister inner wall, and several candidate materials are being con-

sidered according to the specific function assigned to them. In ENRESA's conceptual design this barrier would be made of borosilicate glass beads, but the study of other materials that retard the escape of Iodine (^{129}I) and Chlorine (^{36}Cl) from the canisters is also being carried out. Based on the laboratory data (sorption, diffusion, migration) is expected that these two isotopes, not retained in the clay seal and the geological barriers, will contribute the most to the long term average estimated dose, for a million years, in the safety and performance assessment exercises done for a deep geological repository.

Phosphates (apatites) and zeolites have been studied as alternative materials, because they are the natural materials with the higher geochemical contents of Iodine and Chlorine. Apatites also incorporate in their structure a large number of metals and zeolites have a very high ionic exchange capacity.

Partial conclusions from this study indicate that both phosphates and zeolites might contribute to retard the migration of Iodine and Chlorine from the waste canisters. The distribution coefficients for Iodine reach values of 20 $ml.g^{-1}$ in comparison with the zero value assigned to this element in previous Performance Assessment exercises (Stenhouse, 1995). Although the sorption mechanisms are not well defined it has been confirmed that between 75 and 90% of the Iodine remains retained in the solid phase after desorption with a reference granitic groundwater. Pre-treatment procedures to decrease the natural salt content, the homoionisation with reactive cations or the increase of specific area enhance the reactive capacity of these materials (De la Cruz *et al.*, 1999).

Both phosphates and zeolites have shown to be structurally stable under the thermal treatment conditions that they have undergone. The textural modifications detected, increase of surface and rearrangement of the pore distribution seem to stabilise at 150°C after two weeks. However, at 200°C over a year, most zeolites showed an structural alteration between 10 and 30% while for phosphates is negligible. The densities obtained by uniaxial compaction and the granulometric distribution of the natural materials indicate the feasibility of obtaining high density granulates of size above 1 mm. This type of preparation would facilitate the manipulation of the material avoiding the formation of a dusty environment during handling.

Phosphates most unfavourable characteristic is its low thermal conductivity, in the range 0.2 $W.m^{-1}.°K^{-1}$. It would be necessary to adjust this parameter through treatment or mixtures with other materials.

Behaviour of the canister materials

In the Spanish conceptual design of the Deep Geological Storage the canister material will be constituted by carbon steel or copper alloys (ENRESA, 1997 & 1999). In the case of steel there exist both localised and general corrosion phenomena, with an estimated mean rate of about 6.5 mm/ year, (Hernandez Benitez, 1999). Amongst the dominant corrosion products observed in 18 months experiments under saturated bentonite conditions with high HCO_3^- concentrations are Siderite ($CO_3Fe(s)$), Magnetite (Fe_3O_4) and Haematite (Fe_2O_3) (Azkarate *et al.*, 2000).

These studies have been carried out for gathering data on canister behaviour, under different corroding conditions. These results will be implemented in the framework of the Geochemical Mock Up test to be carried out along with the FEBEX II Project.

Behaviour of the clay barrier

In relation with this research line has been carried out the FEBEX (Full-scale Engineered Barriers Experiment) project (ENRESA, 2000). This project aims at demonstrating the technical feasibility and studying the behaviour of near-field components of a high level radioactive waste repository in crystalline rock. It consists of an "in situ" test (Grimsel), a "mock-up" (CIEMAT) test and a series of complementary laboratory tests as well as modelling work. In Figure 3 are shown the two experimental set-up for both tests. (Huertas *et al.*, 2000).

The clay barrier functions are the following: to facilitate the transfer of the heat generated by the waste, to act as a low hydraulic conductivity medium between the canister and the host rock, to seal the building discontinuities and fissures of the host rock, to retard the diffusive transport phenomena of the released radionu-

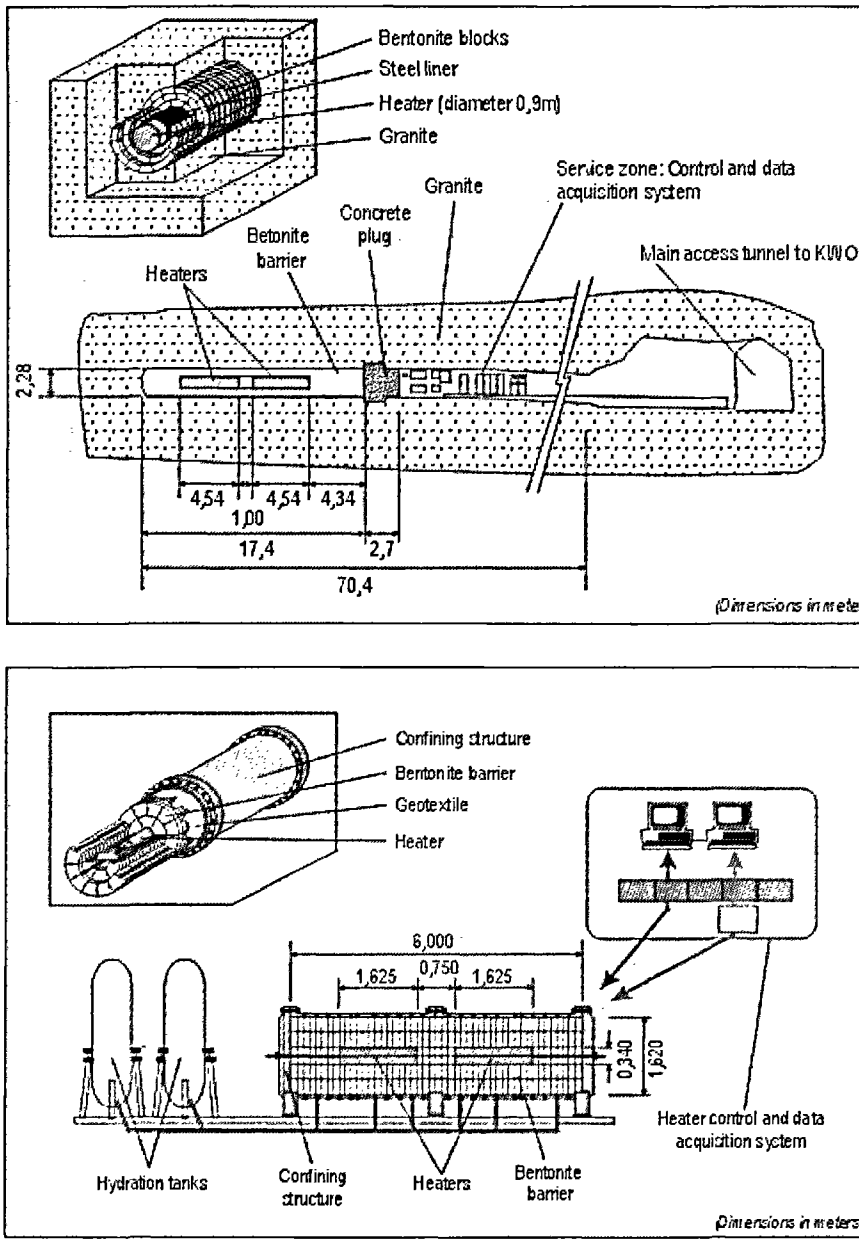

Figure 3
Experimental set-up for FEBEX experiments.
Top: *In situ* experiment at Grimsel Test Site (Switzerland).
Bottom: Mock-up experiment at CIEMAT facilities (Spain).

clides and to provide mechanical support to the host rock protecting the canister of possible shear movements of the geological formation.

The thermal gradient generated by the radioactive decay and the hydraulic gradient of the rock start the heat flow and water transport in the clay barrier. These two processes give place to the mechanical reaction of the bentonite and the chemical interactions in the mineral/water complex system that form the barrier. The four main basic processes (thermal, hydraulic, mechanical and geochemical) function in a coupled manner, producing new mineral phases and gradients and intrinsic modifications of the porous medium, until the general equilibrium of the system is reached.

Therefore, the long term performance assessment requires a deep knowledge of the short term behaviour, identifying and understanding the governing processes and parameters. This is necessary to prepare a conceptual model as a basis of a numerical model, calibrated for natural and experimental evidences, that will guarantee its long term predictive capacity.

The research work on the behaviour of clay barriers is being carried out mainly with the spanish reference bentonite (Serrata de Nijar, Almería) through laboratory experiments and large scale experiments in the "mock-up" (CIEMAT) and "in situ" (Grimsel, Switzerland) tests, that are becoming essential to calibrate the thermo-hydro-mechanical and geochemical coupled numerical models (ENRESA, 2000).

The most relevant results, for the basic processes and function of the barrier previously mentioned are the following:

Thermal behaviour

In a very short time the clay barrier will reach a quasi-stationary state and a very regular temperature distribution, with extreme values of about 100°C in the canister interface and 35°C in the contact with the host rock. The expected mean gradient is on the range $1°C.cm^{-1}$.

The heat transfer takes place by convection through water and water vapour phases and during the phase change processes produced by cooling as the distance from the heat source increases.

The characteristic empirical functions of the clay barrier have been set, relating the thermal conductivity with the hydration state, the specific heat with temperature, and the deformation also with the temperature (thermal linear expansion coefficient).

The predictive capacity of the numerical modelling is very good (Gens *et al.*, 1998).

Hydraulic behaviour

The barrier hydration takes place in a radial and centripetal fashion with a relatively homogeneous distribution of relative humidity and presumably of the saturation degree. The construction discontinuities (block joints), the structural heterogeneities and of water supply from the host rock do not seem to produce significant anomalies in the process.

In relatively short time periods the peripheral external annulus, of centimetric depth, reaches a near saturation while the inner annulus in contact with the canister dries out. However, the hydration rate reaches extremely low values, due to the low permeability, and the suction capacity decrease, due to hydration, of the clay. Therefore the clay saturation of the clay barrier will be a process taking several decades. For the mock-up experiment it has been predicted a 12 years time to reach a saturation value of 95%.

The hydraulic processes acting are water flow, water vapour diffusion, gas flow, air dissolution in water and dissolved air diffusion.

Up to this moment, to achieve the best fitting level between numerical predictions and results for the "mock-up" (CIEMAT) and "in situ" (Grimsel) experiments, it has been indispensable to obtain characteristic functions for bentonite; such as permeability as a function of dry density (ρ_d), of the saturation degree and temperature; the retention curves expressing the relationship between suction and the saturation degree at free and constant volumes, or the tortuosity coefficient and gas permeability as a function of dry density and saturation degree.

Although the predictive capacity for the barrier hydration process offers a great degree of confidence, it will be necessary in the next years to optimise the adjustments of the characteristic functions and to deepen in the study of microestructural modifications and their impact on the characteristic parameters of the barrier (UPC-DIT. 1999).

Mechanical behaviour

Processes governing the mechanical behaviour of the barrier are the thermal expansion and the bentonite porosity variations depending on the stress, suction (saturation degree) and temperature fields.

Bentonite has a strong avidity for water, and reacts mechanically, in such a way that in an open system regime volume can increase up to 200%. In a closed system regime this process can develop a swelling pressure during hydration that exponentially depends on the initial dry density (Lloret *et al.*, 1999). For the final dry density (ρ_d = 1.60 g.cm^{-3}) of the clay barrier the swelling pressure is about 5Mpa.

The first mechanical reaction of the clay barrier is the sealing of the bentonite-rock interface annulus and of the discontinuities between blocks where the free water arrives. From this point the development of pressure is a function of the hydration state, that homogeneously progresses in a radial and centripetal way as indicated: Hydration implies porosity modifications and therefore of a considerable amount of bentonite characteristic parameters (water and gas permeability, thermal conductivity, diffusion coefficient, swelling pressure, etc.).

Prediction of the barrier mechanical behaviour has an acceptable adjustment with experimental results. However, is not yet possible to rigorously analyse the predictive capacity of the models because the total pressure sensors response for the mock-up and "in situ" experiments is under local stress adjustments depending on location and because the hydration state has not produced significant responses for many of them.

The bentonite mechanical behaviour study has followed an extensive experimental programme from which the deformation parameters as a function of effective stresses, suction and temperature. This has allowed the development on the bentonite thermo-plastic-elastic behaviour model.

There have been determined the resistance parameter and the elastic shear modulus and the functions relating swelling pressures with dry density and suction have been adjusted, as well as the deformations under load.

Geochemical behaviour

The geochemical evolution of the clay barrier is produced by the heat flow from the canister and the water flow coming from the rock (granite). At short and medium term the effect of the granitic water chemistry on the geochemistry of the clay barrier is not significant.

The bentonite minor components solid phases that govern the geochemical processes by interacting with the hydration water are Halite Gypsum, Dolomite and Chalcedony. The dissolution kinetics of other mineral components is so slow that they would only would affect the system on a very long term.

Experimental data indicate that during the hydration transitory state Cl^- and SO_4^{2-} are transported by the hydration front. As a conservative ion, Cl^- moves accordingly to the effective porosity determined with HTO, while SO_4^{2-} movement is retarded and its concentration levels in the advancement front must be regulated by its equilibrium with Gypsum. Precipitation of Anhydrite occurs in contact with the heat source.

Bicarbonate concentration is controlled by dissolution/precipitation of Calcite and it remains almost practically constant in time for the duration of the experiments. Na^+, Ca^{2+}, Mg^{2+} and K^+ show a similar trend of mobilisation and concentration around the heat source. However, the analyses of their stochiometric relationships with their corresponding anions and of the composition of the bentonite ionic exchange complex show that during transport the exchange reactions with the smectite have occurred. The general trend indicate that the smectite is enriched in Ca^{2+} and Mg^{2+} released by carbonates dissolution and looses Na^+ and K^+. This is a very favourable aspect because it would exclude the possibility of smectite illitisation.

The ionic strength of the interstitial water varies from 0.07 M in the inlet zone to 1.2 M at the hottest zone, during the hydration transitory regime.

Bentonite buffers pH at values close to 8 and the Eh must evolve towards negative potentials when the residual Oxygen from building and emplacement is consumed.

Diffusion is the dominant transport process once saturation is reached. This fact, together with the concentration gradients created

by precipitates dissolution gives place to salt redistribution and their leaching by the granitic waters (Cuevas *et al.*, 1998).

The estimation of the barrier interstitial water evolution time seem to indicate that the bentonite water salinity will be maintained at a level similar to the initial up to 5000 or 10000 years. So, this time interval will be higher than the estimated lifetime of the canisters.

The geochemical processes described do not seem to affect the basic properties of specific area, hydraulic conductivity and swelling pressure of bentonite, according to the measurements performed after the thermal-hydraulic treatment.

The clay barrier is an efficient filter for the colloids that can be generated as a consequence of fuel alteration. On the other hand, the high ionic strength of the interstitial water and the pH, close to the point of zero charge (PZC) of many interesting colloids, provokes their immediate aggregation. A different situation occurs at the clay barrier/granite interface, where bentonite and silica colloids can be present and are very stable under the physicochemical conditions existing in the granitic formation.

The radionuclides will migrate through the barrier by diffusion, and their movement will be retarded due to sorption reactions with the clay surface (adsorption/desorption, precipitation, ion exchange, colloid filtration, etc.). Diffusion data obtained in laboratory experiments with compacted bentonite at the barrier density vary from 10^{-11} m^2/s for tritiated water (HTO) to 10^{-14} $m^2.s^{-1}$ for Re(VI), as ReO_4^{2-}, and Tc(VII), as TcO_4^-. Sorption experiments performed on loose bentonite (batch method) have demonstrated that Eu(III), Nd(III) and Th(IV) result completely retained by bentonite; Cs, Sr and Co have high values of the distribution coefficient, K_d (Yllera *et al.*, 1998); U(VI) is slightly retained, and Re(VI), Tc(VII) and I- are not sorbed at all (Garcia *et al.*, 1999A). In Figure 4 are shown some of the different type of diffusion experiments carried out in clay materials.

It is clear that there it has been a great advance in the knowledge of the integrated behaviour of the clay barrier. There are still some uncertainties, that might be solved in the next research programme. On the other hand, the geochemical models have not been calibrated for the evolution of the key parameters in the large scale experiments. With this aim it has been proposed the establishment of a geochemical mock-up experiment.

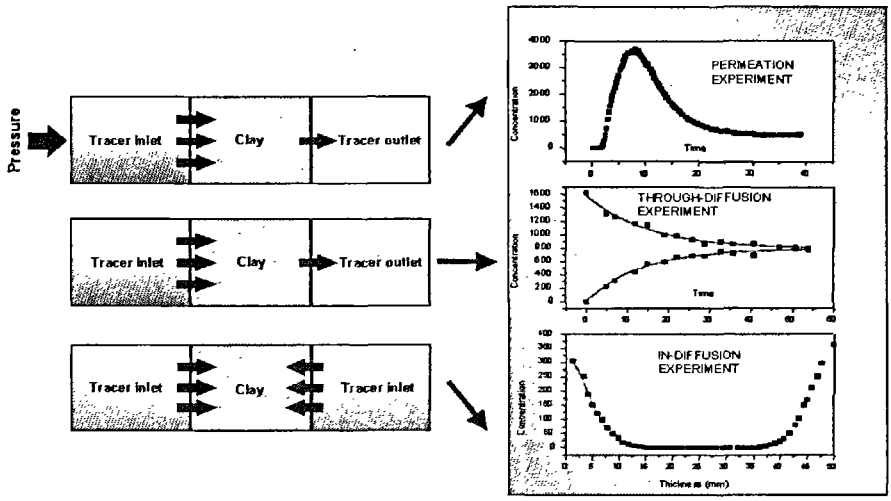

Figure 4
Different diffusion experimental set-up used for geological material characterization.

Geosphere behaviour

The role of the geological formation for site emplacement is the chemical and mechanical protection of the other barriers and to retard the radionuclide transfer to the geosphere. This is achieved as a consequence of the structural, hydraulic and geochemical properties of the geological barrier.

According to the above mentioned functions, the study of the geological formation is mainly focused on the obtention of a structural model of the discontinuity network, acting as potential flow paths; a groundwater flow model, a geochemical rock-water interaction model and a transport model.

The program mainly addresses the geochemical model, and provides the basic parameters related to the radionuclide transport. In the current program, work is being carried out in granitic, clay and natural analogue formations.

Some of the most remarkable results are presented in the following section:

Granitic formations

The first research work in this field made in Spain was started in 1989 with the El Berrocal Project (Rivas *et al.*, 1997). The project was carried out in a granitic pluton that hosts a number of U mineralisations, which were mined over a period of several years, although the mines were definitely abandoned by the late 1960's. The project was an integrated international exercise in geological, geochemical, and hydrogeological characterisation and had the aim of understanding and modelling the past and present-day migration processes that control the behaviour of distribution of naturally occurring radionuclides in a fractured granitic environment.

Work at the El Berrocal during the project was extensive. It included geological mapping, structural analysis, mineralogical, lithogeochemical and hydrogeochemical investigations, considering both stable and radioactive isotopes, colloid and microbial studies. Several methodologies and instrumentation were developed for *in situ* tracer tests, application of downhole probes, hydrogeological characterisation and coupled flow and transport modelling. The fieldwork was supported by a wide laboratory program, which generated valuable data for the interpretation of those phenomena observed at natural scale. In Figure 5 are shown the experimental and modelled results for the first tracer test performed between boreholes S-13, S-15 and S-2.

This research constitutes the basis for implementing a methodology that is used for characterisation of crystalline formations affected by U mobilisation processes. Specially in the case of restoration programs for abandoned mines, or mill tailings environmental impact studies (Project Ratones, Project MATRIX (Perez del Villar *et al.*, 2000), etc.).

The deep groundwater ($\cong$ 500 m) of the reference granite (Gomez *et al.*, 1999) used for ENRESA 2000 Performance Assessment exercise has a sodium/bicarbonate composition presenting a residence time of about 20,000 years. The pH is regulated by the equilibrium with carbonates with neutral or slightly alkaline values. The measured redox potential is regulated by the reaction of the redox pair Ankerite (15% Fe)/Goethite presenting a value of -175 mV.

The processes controlling the concentration of the major components of the groundwater are dissolution/precipitation of carbon-

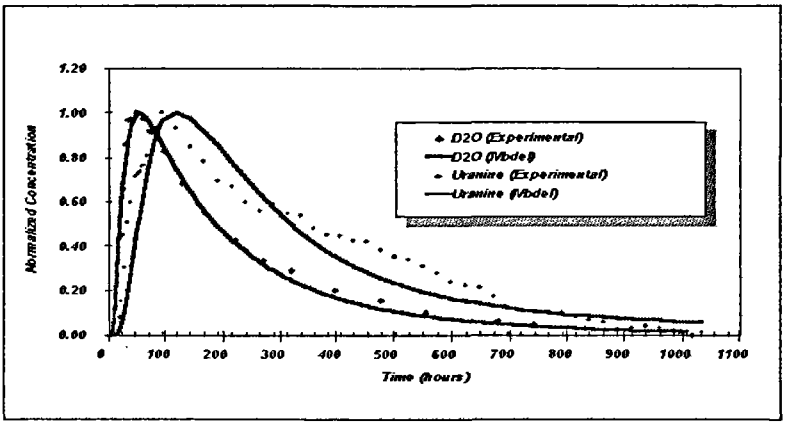

El Berrocal Project: results of the *in situ* Tracer Test

Figure 5
Tracer test modelling and experimental results in El Berrocal granite. First tracer injection /D_2O and Uranine)

ates, the ionic exchange (Ca/Na and Mg/Na), montmorillonitisation and precipitation of goethite-like iron oxide.

Given the redox potential of this groundwater, uranium concentrations are below the detection limits, even in the presence of residual Uranium mineralization existing in the granite. Those characteristics are considered as highly favourable to minimise the radionuclide mobilisation processes.

The sorption parameters obtained, under oxic conditions, indicate that more than 90% of Cs, Co and Eu and about 30% of Sr and Se(IV) are retained by the granite minerals, while Tc is not retained at all (Garcia *et al.*, 1999b).

Clay formations

The first studies on clay formations for their characterisation to act as geological barriers have been carried out.

The Spanish reference clay formation has a thickness close to 280 m., being very homogeneous. These sediments have a lacustrine origin,

and are limited, at top and bottom, by fluvio-alluvial sediments and lacustrine-palustrine carbonates, respectively.

Illite and smectite represent more then 80% of the mineralogical composition of the formation. The minor minerals that regulate the groundwater characteristics are Calcite, Dolomite and Gypsum. The organic matter content is near 1.5%.

The values of total cation exchange capacity, specific area and hydraulic conductivity are coherent with the mineralogical composition. As a whole, these values provide this formation with a high index of favourability as a site emplacement host rock.

The interstitial waters have a sodium/sulphate nature with pH values around 7.5. The geochemical modellisation is being performed.

The radionuclide retention capacity is higher than for the reference granite. For Cs, Sr, Co and Eu the value of the distribution coefficient increases in one or several orders of magnitude.

In the Mt. TERRI Project (Thury & Bossart, 1999), intercomparison exercises have been carried out for the extraction and analyses of the interstitial water, the geochemical modelling and the determination of diffusion coefficients 1.3-2.3 10^{-11} $m^2.s^{-1}$ for HTO and 2.3-3.0 10^{-12} $m^2.s^{-1}$ for I^- (Yllera *et al.*, 2000). All this work has been carried out with the Mt TERRI Opalinous Clay formation, a very consolidated clay of marine origin.

As a consequence of the start of this research line on bentonite engineered barriers, a participation in the GMT Project exists, financed by Japan, to study the gas transport in the reference japanese bentonite. Also, in the framework of the FEBEX II Project, gas transport essays in the "in situ" (Grimsel) and in the "geochemical mock-up" experiments have been proposed.

Radionuclides behaviour in the geosphere (natural analogues)

In the host rock of the Bangombé (Gabon) reactor, the Uranium has its natural isotopic composition, thus, indicating that the Uranium from the reactor has practically not been mobilised. Neither are there evidences of isotopic data that indicate Sr of Mo retention.

The fissiogenic Ba and the Ba decaying from Cs have migrated from the reactor area and have been retained in the phyllosilicate-rich zones. There is also evidence of Zr migration and retention in the host rock, although it has not been possible to determine the minerals where this element was incorporated.

Based on the fluid inclusion analyses, the different fluid phases and the formation temperatures of the mineralization and weathering processes identified in the host rock of the natural reactor are known.

In the MATRIX project (Perez del Villar *et al.*, 2000), once the structural framework of the Boa fault was established, and knowing the weathering and Uranium distribution in the exploitation front of that fault, the drilling of four boreholes was carried out to study the Uranium mobility as a function of the oxidising-reducing environment.

Conclusions

In Spain, for the last fifteen years, it has been studied the problem of radioactive waste Deep Geological Storage. In that time it has been achieved a great advancement on the understanding of components and processes that must initially regulate the behaviour of the storage system. International research has progressed too in the same direction.

The research on the problems arisen from the storage activity, gives place to new questions on the system. Despite this situation, the solution of the problems from the scientific or technological point of view in which they are approached, it produces a reasonable confidence on the storage safety and viability. This consciousness is someway supported by the Safety and Assessment exercises (PA) carried out on several geological formations.

Several important uncertainties exist, and their resolution will come through the unification, in experiments under natural conditions at a real scale, of the basic knowledge generated on the laboratory experimental programs and the theoretical knowledge developed for the modelling of natural processes.

On the other hand, all the methodologies and knowledge obtained in the field of radioactive wastes is applicable to any of the environmental fields that appear every day. In that way CIEMAT has participated in several projects involving both natural radionuclides of even metallic contaminants. One of these cases was the study of the contaminated soils from the Aznalcóllar area, after a mining slurry spill at the end of April, 1998.

Aknowledgements

The different research programs reflected in this document have been carried out in the framework of ENRESA R+D programs since 1988, and of the consecutive Framework Programs of the European Union.

Bibliography

AZKARATE I., MADINA V., INSAUSTI M., 2000 — "Estudio de los productos de corrosión de la cápsula y su interacción con la barrera arcillosa de ingeniería". *In: Proyecto CORROBEN*, Informe Final 1997-1999, INASMET, San Sebastian (España), 51 p.

CUEVAS J., VILLAR M. V., MARTIN M., COBENA J. C., LEGUEY S., 1998 — "Thermal-hydraulic gradients on bentonite; time dependent distribution of soluble salts, microestructural effects and modification of the hydraulic and mechanical behaviour". *In: Key Issues in Waste Isolation Research*, Barcelona, 2-4 December 1998. CIEMAT/DIAE/54111/18/98.

DE LA CRUZ B., RIVAS P., HERNÁNDEZ A., MARÍN C., VILLAR M. V., DE LA IGLESIA A, 1999 — "Materiales alternativos de relleno de la cápsula de almacenamiento de residuos radiactivos de alta actividad". *In: Proyecto RELLENOS*, Informe Técnico ENRESA 1/99, Madrid, 1999), 93 p.

ENRESA, 1997 — *Evaluación del comportamiento y la seguridad de un almacenamiento geológico profundo en granito.* Informe Técnico ENRESA 6/97, Madrid, 1997), 179 p.

ENRESA, 1999 — *Evaluación del comportamiento y la seguridad de un almacenamiento profundo en arcilla.* Informe Técnico ENRESA 3/99, Madrid, 1999), 219 pp.

ENRESA, 2000 — "Full-scale Engineered Barriers Experiment for a deep geological repository for high level radioactive waste in crystalline host rock". *In: FEBEX Project*, Informe Final ENRESA 1/00 (ISSN-1134-380X, Madrid, 2000), 354 p.

Huertas F., Fuentes Cantillana J. L., Julien F., Rivas P., Linares J., Fariña P., Ghoreychi M., Jockwer N., Kickmaier W., Martinez M. A., Samper J., Alonso E., Elorza F. J. 2000 — "Full-scale engineered barriers experiment for a deep geological repository for high-level waste in crystalline host rock". *In: FEBEX Project*, Informe Final Contract FI4W-CT95-0006 (EUR 19147 EN, Belgium), 362 p.

Garcìa Gutiérrez M., Missana T., Yllera A. Mingarro M., 1999a — "Sorption and diffusion experiments in FEBEX bentonite". *In: FEBEX Project*, Informe Tecnico CIEMAT/DIAE/54111/3/99, Madrid.

Garcìa Gutiérrez M., Yllera A., Fernàndez V., Mingarro M., Missana T., 1999b — "Cuantificación de parámetros de sorción y difusión en granitos y arcillas españolas". *In: MYCO Project*, Informe Final CIEMAT/DIAE/54231/8/99, Madrid.

Gauthier-Lafaye F., Ledoux E., Smellie J., Louvat D., Michaud V., Perez del Villar L., Oversby V., Bruno J., 1999 — *Behaviour of nuclear reaction products in a natural environment (the Oklo site, Gabon, Western Africa).* Final Report CIEMAT/DIAE/54312/13/99, Madrid.

Gens A., Garcìa Molina A. J., Olivella S., Alonso E. E., Huertas F., 1998 — Analysis of a full scale in situ test simulating repository conditions. *Int. J. Num. Anal. Meth. In Geomech.*, 22: 515-548

Gomez P., Garralòn A., Turrero M. J., Sànchez L., Melòn A., Ruiz B., Fernàndez F., 1999 — *Impacto medio-ambiental de la restauración de la Mina Ratones en las aguas subterráneas. Modelo hidrogeoquímico.* Informe Final CIEMAT/DIAE/54211/7/99, Madrid.

Hernàndez Benìtez A., 1999 – *Empleo de mezclas de productos de corrosión/bentonita en la maqueta geoquímica del Proyecto FEBEX-II: Estudio bibliográfico y aproximaciones realizadas.* Informe Técnico FEBEX, CIEMAT 70-IMA-I-0-05, Madrid, 29 p.

Lloret A., Villar M. V., Pintado X., 1999 — *Ensayos THM: Informe de síntesis.* Informe Técnico FEBEX, CIEMAT/DIAE/54111/15/99, Madrid.

Perez del Villar L., 2000 — *CIEMAT contribution to the Palmottu international project.* Final Report Palmottu Project, CIEMAT/DIAE/54321/5/00, Madrid.

Perez del Villar L. Cozar J. S., Pardillo J., Buil B., Pelayo M., Labajo M. A., 2000 — *Mineralogía y geoquímica de los rellenos fisurales del Proyecto MATRIX; Implicación para los procesos de disolución, migración y retención de los radionucleidos naturales y otros elementos análogos (Mina Fe, Ciudad Rodrigo).* Informe Final Proyecto MATRIX, CIEMAT/DIAE/54331/1/00, Madrid.

Rivas P., Hernàn P., Bruno J., Carrera J., Gòmez P., Guimera J., Marìn C., Perez del villar L., 1997 — *El Berrocal Project: Characterization and validation of natural radionuclide migration processes under real conditions on the fissured granitic environment.* Final Report. Contract FI2W-CT91/0080 (EUR 17478 EN, ISBN 92-827-9673-6), Luxembourg, 522 p.

Stenhouse M. J., 1995 — *Sorption databases for Crystalline, Marl and Bentonite for Performance Assesment.* Nagra Technical Report NTB-93-06.

ROUBAULT M., 1962 — *Les Mineraux Uranifères français et leur gisements.* Saclay, institut nationale des sciences et techniques nucléaires, t.II, 419 p.

THURY M., BOSSART P., 1999 — The Mont Terri rock laboratory, a new international research project in a Mesozoic shale formation, in Switzerland. *Engineering Geology*, 52: 347-359.

UPC-DIT, 1998 — *Febex Project: Thermo-hydro-mechanical (T-H-M) modelling of the "mock up" and "in situ" tests.* FEBEX Technical Report 70-UPC-M-0-05, Barcelona.

YLLERA DE LLANO A., HERNÀNDEZ BENITEZ A., GARCÌA GUTIÉRREZ M., 1998 — Caesium Sorption Studies on Spanish Clay Materials. *Radiochimica Acta*, 82: 275-278.

YILLERA DE LLANO A., MINGARRO SAINZ-EZQUERRA M., GARCÌA GUTIÉRREZ M., 2000 — *DI Experiment: Results of the Laboratory Diffusion Experiments. Mont TERRI Project.* Technical Note 99-50, 25 p.

Radionuclide migration in arid soils

John R. Harris

Takashi Itakura

Gordon D. McOrist

Tim E. Payne

David E. Smiles

Introduction

Australia is siting and establishing a national radioactive waste repository for the disposal of low level and short lived intermediate level waste. The repository will be a near surface facility located in an arid climate. A code of practice for such a facility in Australia, including site selection criteria, was issued by the National Health and Medical Research Council (NHMRC, 1992). In February 1998, a region in the central north of South Australia (CNSA region) was selected for detailed assessment (BRS, 1997).

The site selection criteria for the repository include requirements that the geological structure and hydrogeological conditions of the site should enable prediction of radionuclide migration times and patterns and that the geochemical and geotechnical properties of the site should inhibit migration of radionuclides. Migration of radionuclides depends on the rate of water movement and the retardation of the radionuclides by chemical reaction with, and adsorption on, the regolith material.

The climate of the CNSA region is characterised by irregular low rainfall with an average of 198 $mm.yr^{-1}$, low relative humidity, high

evaporation and high summer temperatures. Based on rainfall and evaporation in the region, Harries *et al.* (1999) calculated that the deep drainage for typical soils was between 0.004 mm.yr^{-1} and 1.3 mm.yr^{-1} in the presence of vegetation and between 1.4 mm.yr^{-1} and 7 mm.yr^{-1} in the absence of vegetation. Limited field measurements were consistent with these estimates. These low water fluxes indicate that the transit time of water moving from the repository towards the water table is expected to be many thousand years.

This paper describes technical studies on the retardation of radionuclides undertaken in support of the site selection and to provide information needed for the safety assessment.

Radionuclide retardation

The migration of most radionuclides in groundwater is slower than the rate of water movement because chemical precipitation and adsorption remove the radionuclide from the aqueous phase and deposit it on the solid matrix. Adsorption, by which a solute is bound by the surfaces of minerals and organic matter in the soil, significantly retards the movement of all radioisotopes including those that are relatively or highly soluble. The complex sorption interaction can be expressed as a distribution coefficient (K_d), which is the ratio of the amount of the radionuclide sorbed by the solid (g.g^{-1}) divided by the concentration in the equilibrium solution (g.ml^{-1}). The K_d value is commonly used as a means of assessing the mobility of radionuclides in the environment and for comparing adsorption data obtained from different sources (McKinley and Scholtis, 1992; Sheppard and Thibault, 1990).

The value of the K_d depends on the element in question, the chemical conditions of the regolith solution, and properties of the solid (such as its surface area, surface charge, mineralogy, etc). Some elements (such as iodine) have relatively low K_d values in a range of geochemical environments, whereas others (such as thorium) have very high K_d values and are virtually immobile in most natural environments. However even for a single element, the value of K_d can

cover many orders of magnitude depending on the system in question. We have measured K_d values and retardation over a range of chemical conditions using two different types of experimental procedure: batch and column experiments.

Batch experiments

Batch experiments assess geologic materials in terms of their ability to adsorb radionuclides under a range of experimental conditions. The batch technique measures adsorption of radionuclides from a standard solution at a high liquid-to-solid ratio (10:1 or 100:1). These high solid-to-liquid ratios are dissimilar to field conditions in the unsaturated zone of the arid environment, but the measurement is rapid, reproducible and relatively inexpensive. The column experiments described in Section 4 use liquid-to-solid ratios more comparable to field conditions. In the batch experiment, solid, radionuclide and aqueous phases are mixed for 48 hours, the liquid phase separated by centrifugation and the radionuclide concentration in aqueous phase measured.

Batch experiments have been used to measure the sorption of ^{60}Co, ^{137}Cs and ^{238}U. The experimental duration was three days. In the first 24 hours, the solids were pre-equilibrated with the background electrolyte. The radionuclide, which is supplied in an acid solution, was then added, and the system immediately adjusted to the required pH value. The samples were gently shaken in unsealed centrifuge tubes at room temperature. After 48 hours contact time, the solid and liquid phases were separated by centrifugation and the ^{60}Co, ^{137}Cs and ^{238}U content of the clear supernate was measured by g-spectrometry or kinetic phosphorimetry.

Batch experiments with cesium were performed with two different concentrations of radionuclide. Trace cesium experiments were undertaken with carrier-free cesium-137, and experiments at a higher total cesium (ΣCs) of 1 $mmol.l^{-1}$ were carried out after adding CsCl. The different concentrations of cesium enable chem-

ical controls on sorption of cesium to be measured. The higher concentration value (1 mmol.l^{-1} total cesium) provided a clear indication of the effect of total concentration, even though this concentration is much greater than would be expected near a repository.

The measured K_d values for cesium on the near-surface materials from the CNSA region are summarised in Table 1. Over the range of variables considered in the present study, pH had almost no effect on cesium adsorption. This is because the aqueous speciation of cesium is limited to the Cs^+ species under most environmental conditions. These results indicate that the migration of trace cesium in these materials would be greatly retarded relative to water movement. For K_d values greater than 200 ml.g^{-1}, the radionuclide would be retarded by at least 3 orders of magnitude compared to water flow. At a total concentration 1 mmol.l^{-1} total cesium, the results in Table 1 indicate that the efficiency of adsorption is reduced. The increase of total cesium by several orders of magnitude greatly reduced the measured K_d values.

The pH is a significant factor influencing the adsorption of uranium (Figure 1). This reflects the speciation of U(VI), which is strongly dependent on pH and on the presence of carbonate. The very weak sorption of U at high pH values under these conditions is a consequence of the stability and weak sorption of aqueous uranyl carbonate complexes. As with cesium, the sorption of U(VI) also decreases at higher radionuclide concentrations, although the effect is significant only in the low pH region, at pH values below about 5 (Figure 1). This effect has been attributed to the presence of a range of sorption sites of varying affinity for adsorbing uranyl (Waite *et al.*, 1994). A similar dependence on total uranium may occur near the high pH desorption edge, but this pH edge is very steep and the experimental uncertainty precludes identifying a concentration effect.

The results of batch sorption experiments with ^{60}Co with materials from the CNSA region indicate that the K_d for cobalt is strongly pH dependent. The K_d of cobalt increases from approximately 1 ml.g^{-1} at a pH of 4.0 to 1000 ml.g^{-1} at pH of 8.0. In addition to the role of pH, there is some dependence on mineralogy.

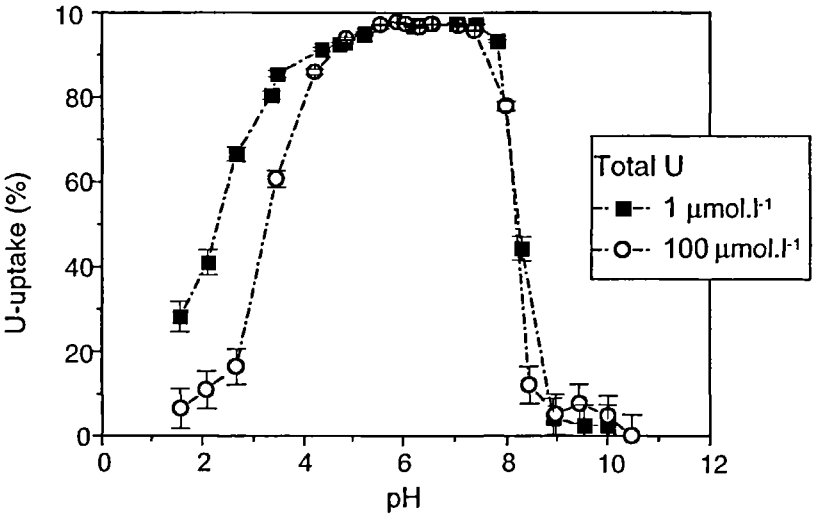

I Figure 1
Percentage of uranium adsorbed on the W2 soil sample from the CNSA region as a function of pH and total uranium (ΣU). Data were obtained in 0.02 M NaCl and equilibrated with air ($pCO_2 = 10^{-3.5}$ atm.). Note the very strong pH dependence and the effect of ΣU on the position of the low-pH edge.

Colum measurements

The column experiments are based on a liquid-to-solid ratio of about 0.3:1. In these experiments, saturated $CaSO_4$ solution containing radionuclides (^{60}Co, ^{137}Cs and ^{3}H) was absorbed by a uniform and relatively dry soil column. The advance of the wetting front was observed and, at different elapsed times, experiments were terminated to measure the spatial distributions of water and solute. The chemical conditions in the experimental column are expected to be similar to conditions in the field.

The column experiments were conducted with material that passed a 2-mm sieve. The $CaSO_4$ was used to maintain the structural sta-

bility of these materials; it is expected to be present in the field. All experiments involving nuclide traces in solutions are therefore based on saturated $CaSO_4$ (≈30 millimoles of charge $.l^{-1}$).

Some swelling occurred in the experiments, which makes a physical space coordinate system unreliable. The experiments were analysed in terms of both solid based space and a material coordinate based on the distribution of the water in the soil. The solid-based coordinate is the cumulative mass of solid per unit area of cross section, measured away from the inflow surface. A water-based coordinate system is used to compare mobility of nuclides. The use of these coordinate systems (Smiles, 2000) gets over the swelling problem; it also reduces the effects of inevitable slightly different column packing. The data are scaled in terms of material distance divided by the square root of time. The coherent set of data for experiments terminated at substantially different times indicates that basic initial and boundary conditions on the experiments are realised and that diffusion equation theory can be applied to extend the experimental data in both distance and time.

The experimental methods, based on sectioned columns of unsaturated but uniformly moist fine soil, and the theoretical analysis, are described by Smiles *et al.* (1981) and Bond *et al.* (1982).

Illustrative results for a set of column experiments terminated after various time intervals are shown in Figure 2. The tritium is a tracer for water. Thus, the tritium front, identified with an inflection in the concentration curve, corresponds to an inflection in the receding soil solution salt profile (Figure 2). This is consistent with the notion that the tritium front should correspond with a "piston front" which would exist if the invading solution displaced, in its entirety, the soil water originally present. Displacement of solute front relative to the "piston front" reflects the degree to which the solute is retarded relative to the moving soil water.

Comparison of the profiles for ^{60}Co with the tritium indicates the rate of movement of cobalt relative to the water. The column experiments involved both ^{137}Cs and ^{60}Co. However, the cesium experimental data are not shown because the ^{137}Cs did not travel past the first section of the column. This is consistent with strong association of cesium with the soil indicated in the batch experimental data

(Table 1) where typical K_d values for trace cesium exceed 10^3 ml.g^{-1}. In contrast, cobalt does progress through the column to some extent, as is shown by the profile in Figure 2.

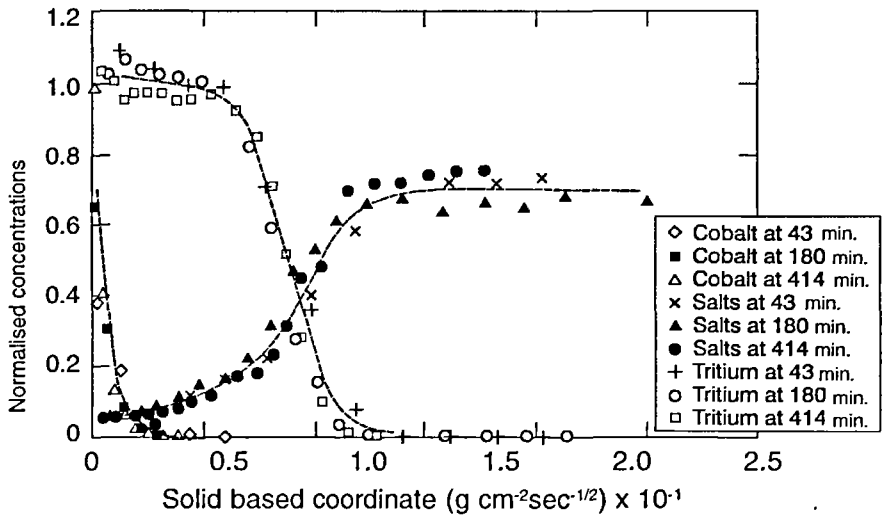

I Figure 2
Illustrative results from a set of column experiments.
Water-soluble salts, tritium and ^{60}Co concentrations are graphed as functions of solid distance divided by the square root of time.
To facilitate presentation on the same diagram,
the concentrations are normalised (Smiles and McOrist, 2000).

Preliminary batch experimental data for materials from the CNSA region indicate that the K_d for cobalt is strongly pH dependent, with the K_d increasing with increasing pH. The input tracer solution for the column experiments has a pH of 6.0, and measured K_d values in batch experiments for these materials in the pH range from 5.5 to 6.5 were between approximately 10 and 100 ml.g^{-1}. Thus the batch experiments and column experiments both indicate that the cobalt should be more mobile than the cesium, but substantially retarded relative to the tritium. This behaviour is illustrated in Figure 2.

Total Cesium	pH	Measured range of K_d
Trace Cs	7.0	4000 to 9000 ml.g^{-1}
Trace Cs	8.0	2000 to >10000 ml.g^{-1}
Trace Cs	9.0	3000 to > 10000 ml.g^{-1}
ΣCs = 1 mmol.l^{-1}	various	170 to 330 ml.g^{-1}

Table 1
Summary of Kd ranges for 11 experiments with Cesium on W1 and W2 soils from the Australian arid zone (mass loading 0.3 g/ 30 ml). Note the lack of significant pH dependence but a strong effect of total cesium (ΣCs).

Conclusions and recommendations

Measurements of radionuclide adsorption in batch experiments, and measurements of nuclide retardation during absorption of water by columns of relatively dry soils, have been undertaken. The batch experiments enable dependence of retardation on geochemical conditions to be investigated, whilst the column experiments enable retardation under specific conditions to be measured under unsaturated conditions similar to field conditions.

Repository safety assessment requires prediction of the behaviour of any radionuclides released from the repository. For an arid zone repository, this needs to be based on knowledge of water flow and radionuclide retardation in materials at the site. A combination of batch and column experiments can provide the required information on radionuclide retardation for site specific samples.

Aknowledgements
Support for some of this work was provided by the Bureau of Rural Sciences and the Department of Industry, Science and Resources.

Bibliography

BOND W. J., GARDINER B. N., SMILES D. E., 1982 — Constant Flux Absorption of a Tritiated Calcium Chloride Solution by a Clay Soil. *Soil Science Society of America Journal.*, 46: 1133-1137.

BRS 1997 — A Radioactive Waste Repository for Australia: Site Selection Study æ Phase 3: Regional Assessment: A Public Discussion Paper. Bureau of Resource Sciences, Canberra.

HARRIES J. R., PAYNE T. E., KIRBY J. M., SMILES D. E., 1999 — "Studies for Selecting a Site for an Australian Near-Surface Repository". *In: 7th International Conference on Radioactive Waste Management and Environmental Remediation*, Nagoya, Japan, 26-30 September 1999, American Society of Mechanical Engineers (AMSE International).

MCKINLEY I. G., SCHOLTIS A., 1992 — "Compilation and Comparison of Radionuclide Sorption Databases used in Recent Performance Assessments". *In: Proceedings of a NEA Workshop on Radionuclides from the Safety Evaluation Perspective*, 16-18 October 1991, Interlaken Switzerland, OECD.

NHMRC (NATIONAL HEALTH AND MEDICAL RESEARCH COUNCIL), 1992 — *Code of Practice for the Near-Surface Disposal of Radioactive Waste in Australia.* Radiation Health Series No. 35, AGPS, Canberra, 44 p.

SHEPPARD M. I., THIBAULT D. H., 1990 — Default Soil Solid/Liquid Partition Coefficients, Kds, for Major Soil Types: a Compendium. *Health Physics.*, 59: 471-482.

SMILES D. E., 2000 — Material coordinates and solute movement in consolidating clay. *Chem. Eng. Sci.*, 55: 773-781.

SMILES D. E., PERROUX K. M., ZEGELIN S. J., RAATS P. A. C., 1981 — Hydrodynamic Dispersion During Constant-rate Absorption of Water by Soil. *Soil Science Society of America Journal.*, 45: 453-458.

SMILES D. E., MCORIST G. D., 2000 — "Radionuclide movement during unsteady unsaturated soil water flow". *In: Proceedings of 24th International Symposium on the Scientific Basis for Nuclear Waste Management*, Sydney.

WAITE T. D., DAVIS J. A., PAYNE T. E., WAYCHUNAS G. A., XU N., 1994 — Uranium(VI) Adsorption to Ferrihydrite: Application of a Surface Complexation Model. *Geochim. Cosmochim. Acta.*, 58: 5465.

Actinide separations using extraction chromatography

Riitta Pilviö

Michael Bickel

Introduction

Radiochemistry has always been and still is a crucial tool in the field of radionuclide determination; this holds particularly in the case of alpha and beta emitters. In environmental samples the concentrations of actinides are very low. Therefore special chemical procedures are needed for preconcentration and separation of these nuclides from different matrices and from each other.

Separation methods based on extraction chromatography have become increasingly popular in radiochemical analysis. This is due to their simplicity, rapidity and the savings in reagent and waste disposal costs compared to the traditional separation methods based on, e.g., anion exchange and liquid-liquid extraction.

In solvent extraction, an ion is transferred from the aqueous phase to the organic phase. Extraction chromatography is a combination of liquid/liquid extraction and the chromatographic technique. The mobile phase is an aqueous solution and the stationary phase is an organic solution loaded onto an inert support. In the majority of cases the compounds to be analysed, flowing through the column with the eluent, form an extractable species at the boundary of the aqueous and organic phases. The transfer of the species between the phases happens simultaneously with the complex formation or association processes (Siekeirsky *et al.*, 1975).

Philip Horwitz and co-workers have developed special extraction chromatographic resins for the separation of actinides from different sample matrices. They are commercially available from Eichrom Industries, Inc., U.S.A. These resins are comprised of different organic stationary phases sorbed onto inert polymeric supports.

The resins used in this work were UTEVA Resin, TRU Resin and TEVA Resin. The UTEVA Resin was developed for the separation of *u*ranium and *te*tra*v*alent *a*ctinides from different matrices. It consists of diamyl amylphosphonate sorbed onto an inert polymeric support called Amberlite XAD-7 (Horwitz *et al.*, 1992).

The TRU Resin is used for separation of *tr*ans*u*ranic elements. It consists of octyl(phenyl)-*N,N*-diisobutylcarbamoylmethylphosphine oxide (CMPO) dissolved in tributyl phosphate (TBP) supported on an inert substrate Amberlite XAD-7. In addition to sequental separation of actinides the TRU Resin can be used for group separation of actinides from large amounts of impurities and other radio-isotopes, e.g. Sr (Horwitz *et al.*, 1990).

The TEVA Resin will strongly adsorb all *te*tra*v*alent *a*ctinides. This resin is comprised of an aliphatic quarternary ammonium salt called Aliquat 336N supported on Amberlite XAD-7 (Horwitz *et al.*, 1993).

A method has been developed for the separation of Th, U, Pu, and Am, all from a single sample (Pilviö *et al.*, 1998; 1999). However, in environmental samples the natural radionuclides of Th and U are often present in far greater quantities than Pu, and Am, which are of artificial origin. An average concentration of natural U in seawater is 3.3 ppb, corresponding to 41 $mBq.l^{-1}$ (Ivanovich *et al.*, 1982), while Pu and Am concentrations in most seas are orders of magnitude less. (Sholokovitz *et al.*, 1983; 1989). Th and U are also enriched in certain minerals, compared to Pu and Am which originate only from man-made sources. (Hardy *et al.*, 1982; Eisenbud, 1987). Therefore two separate methods are also presented: first for the determination of Pu and Am and the second for Th (and U). These methods were adapted and optimised from previously published methods (Pilviö *et al.*, 1998; 1999; Maxwell, 1997) and applied to (i) the determination of Pu and Am in diluted MOX material and (ii) the analyses of ^{230}Th from soil. The activities of the samples were determined using alpha spectrometry.

Analytical methods

Separation of Th, U, Pu and Am from bone ash

Bone is a critical organ for accumulation of many radionuclides including ^{90}Sr and actinides. The National Institute of Standards and Technology (NIST) prepared bone ash samples in view of producing a standard reference material. The determination of the actinide concentration in this material was performed using TRU Resin for the group separation of actinides from Sr and other major impurities, e.g. Ca and phosphates. After this UTEVA and TRU resins were used for the sequental separation of Th, U, Pu and Am. The source preparation for alpha spectrometry was done by electrodeposition (Talvitie, 1972) (U and Pu) and NdF_3 coprecipitation (Hindman, 1983) (Th and Am). The separation scheme for the method used is presented in Figure 1. The details are presented elsewhere. (Pilviö *et al.*, 1998-1999).

Separation of Pu and Am from MOX

The separation of Pu and Am from a diluted MOX material was performed using TEVA and TRU Resins, according to a procedure published earlier. (Maxwell, 1997; Pilviö *et al.*, 2000). The source preparation for alpha spectrometry was performed by NdF_3 coprecipitation. (Hindman, 1983). The scheme for the separation of Pu and Am is presented in Figure 2.

Separation of Th from soil

Thorium-230 concentrations in soil samples were analysed using a procedure shown in Figure 3. Th was coprecipitated with $Fe(OH)_3$ and the sample loaded into an anion exchange column in 8 M HNO_3. Th was eluted from the column with 37% HCl. The chemical separation of Th from the impurities and other radionuclides still present in the sample was performed using UTEVA Resin columns.

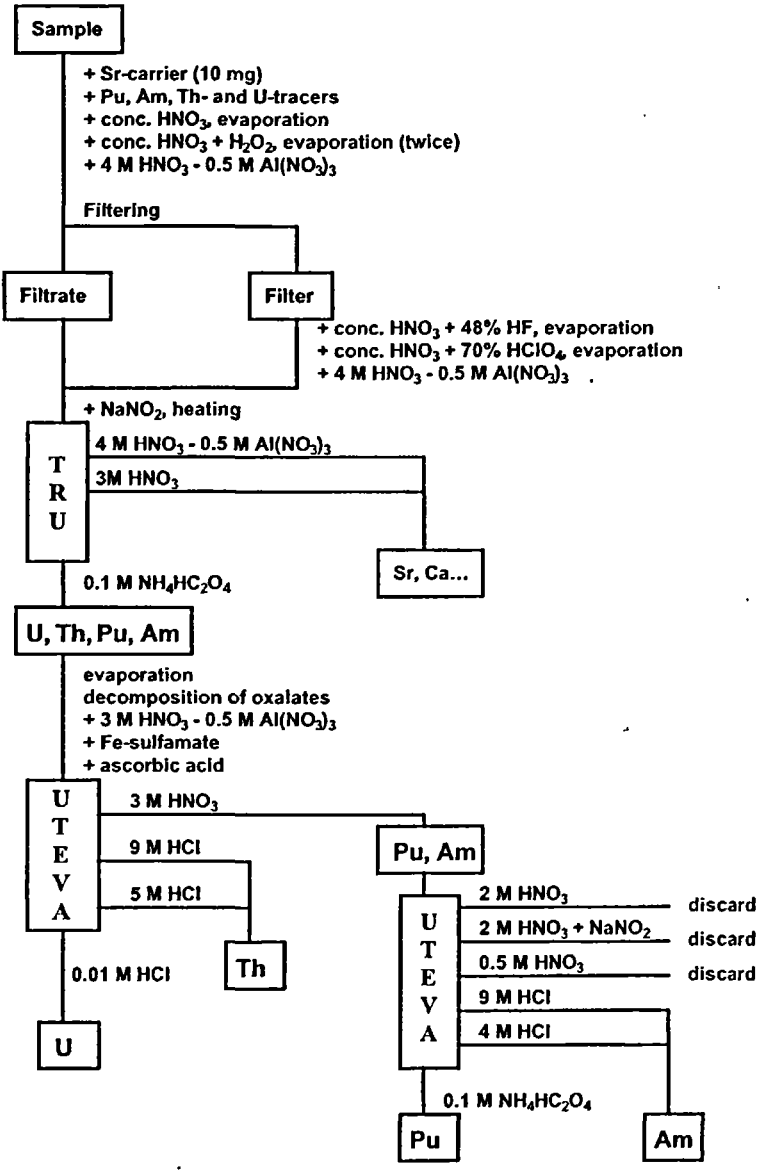

Figure 1
Scheme for the separation of Th, U, Pu and Am from bone ash.

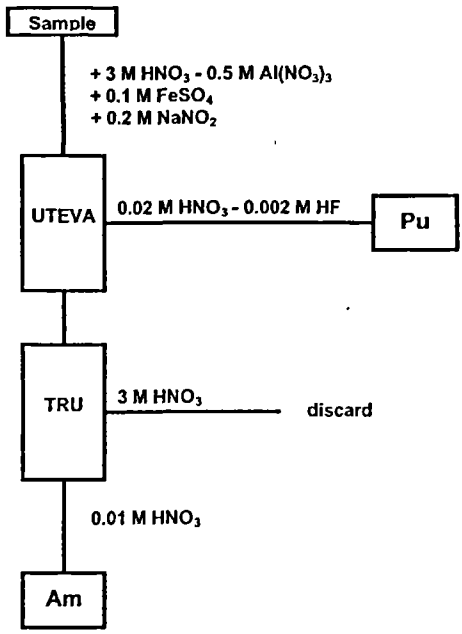

Figure 2
Scheme for the separation of Pu and Am from MOX material.

If requested U concentrations can also be determined using this method. The source preparation for alpha spectrometry was performed by NdF_3 coprecipitation. (Hindman, 1983).

Results and discussion

Pure alpha spectra were achieved for all the nuclides concerned. The summary of the recoveries for the actinides determined in bone ash, MOX material and soil are presented in Table 1. The recoveries were all high. The variations in the Th results were due to large differences in the composition of the 19 soil samples analysed. The measured actinide concentrations in bone ash agreed well with the NIST certified values, as shown in Figure 4.

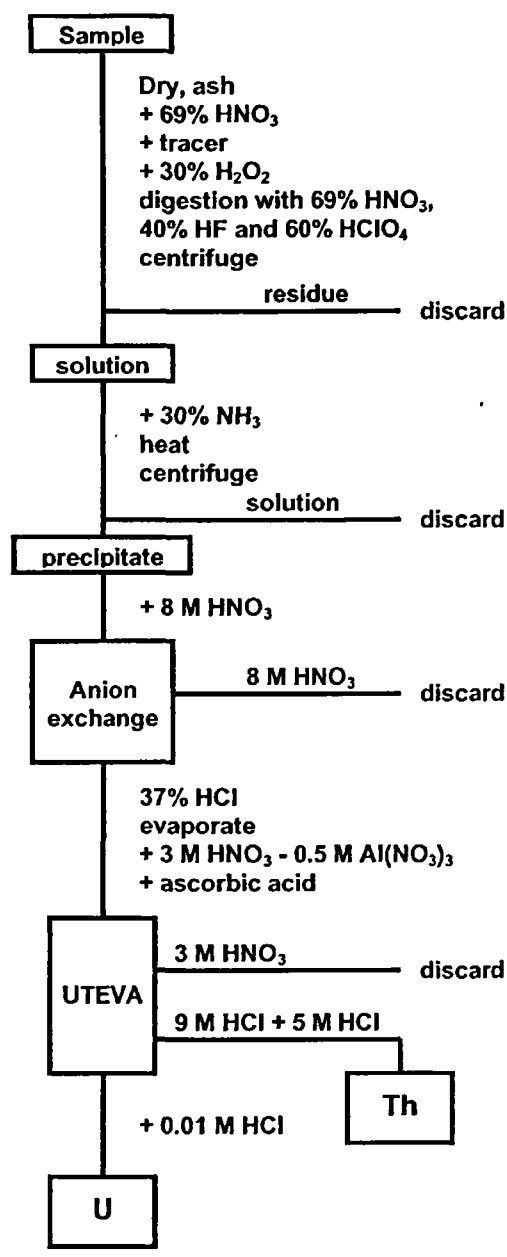

Figure 3
Scheme for the separation of Th from soil.

Sample	Th	U	Pu	Am
Bone ash	89 ± 3	86 ± 5	81 ± 5	87 ± 4
Soil	75 ± 20			
MOX material			94 ± 4	100 ± 2

Table 1
A summary of the recoveries for the determinations of Th, U, Pu and Am in bone ash, Pu and Am in MOX material and Th in soil.

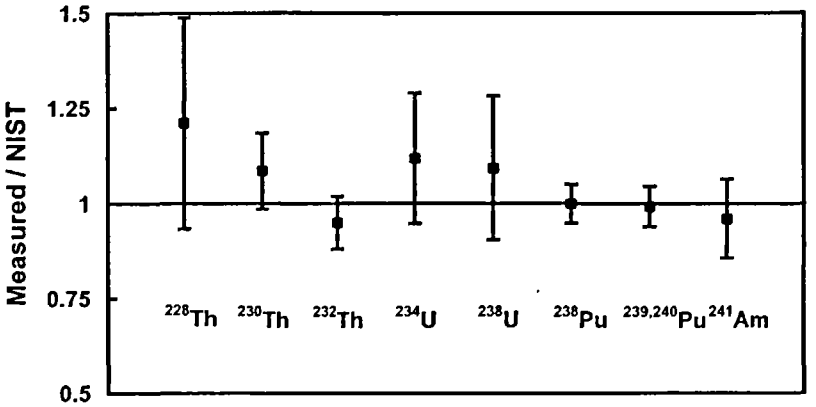

Figure 4
Ratios of the measured activity concentrations for Th, U, Pu and Am isotopes to the NIST certified values. The uncertainties are shown at the 1 s level.

Hydrochloric acid (4-9 M) was used for the elution of the Th and Am fractions in two of the methods. Some bleeding of the organic extractant from the columns was observed during these separation steps. These organic residues could be destroyed by hot digestion with 1-2 ml of 65% HNO_3, 37% HCl, 48% HF and/or 70% $HClO_4$, thereby eliminating the interferences in the sample preparation by the coprecipitation method.

The separation of Pu and Am from MOX material was performed using TEVA and TRU Resins. Therefore the oxidation state of Pu

needs to be quantitatively adjusted to Pu(IV). For this purpose several redox reagents were tested. A commonly used agent is $NaNO_2$ together with heating. However, our experiments showed that an addition of 100 mg $NaNO_2$ to the sample and heating it up to boiling for 30 minutes left up to 10% of the Pu in the oxidation state Pu(III) and quantitative separation from Am(III) was not achieved. Increasing the amount of $NaNO_2$ only reduced the Am recovery.

H_2O_2 has also been used for the redox adjustment of Pu to Pu(IV) before separation of Pu from U with UTEVA Resin. (Apostolidis *et al.*, 1998). An addition of 350 ml of 30% H_2O_2 to a 5 ml sample, heating at 80°C for 25 minutes and cooling the sample for 10 minutes left up to 6% of the Pu to Pu(III).

A quantitative redox adjustment was achieved when Fe(II) was first used to reduce all the Pu present to Pu(III). After this $NaNO_2$ was added to oxidise Pu(III) to Pu(IV). (Maxwell, 1997). These reactions are rapid in room temperature and no heating or cooling is needed.

Th adsorbs very easily onto surfaces. There are many individual steps involved in the Th determination and strong adsorption onto e.g. the glass beaker walls may occur during the evaporation steps. To prevent this, 1 ml of $NaHSO_4$ solution (50 $mg.ml^{-1}$) was added to the sample before the last evaporation. In addition, all glassware used was cleaned by exposing it to 65% nitric acid fumes for a minimum time of 5 hours between analyses, to avoid cross contamination. (Holmes *et al.*, 2000).

Conclusions

The methods presented gave high recoveries and showed good reproducibility for Th, U, Pu and Am determinations. The method for the determination of Pu and Am has an advantage compared to previous extraction chromatography based methods, i.e. that no bleeding of organic residues from the column was observed because diluted acids were used for the elution of these radionuclides.

Quantitative redox adjustment of Pu to Pu(IV) was only achieved when Fe(II) was used to reduce Pu to Pu(III) and $NaNO_2$ to oxidise Pu(III) to Pu(IV). Both $NaNO_2$ and H_2O_2, together with heating, left part of the Pu to Pu(III).

These separation procedures can easily be adapted to different sample matrices by using modern or traditional digestion methods before loading the samples to the columns.

Bibliography

Siekiersky S., 1975 — *In* Braun T., Gershini G. (eds): Extraction Chromatography. Elsevier Scientific Publishing Company, Budabest, p.1-6.

Horwitz E. P., Dietz M. L., Chiarizia R., Diamond H., Essling A. M., Graczyk D., 1992 — Separation and preconcentration of uranium from acidic media by extraction chromatography. *Anal. Chim. Acta.*, 266: 25-37.

Horwitz E. P., Dietz M. L., Nelson D. M., LaRosa J. J., Fairman W. D., 1990 — Concentration and separation of actinides from urine using a supported bifunctional organophosphorus extractant. *Anal. Chim. Acta.*, 238: 263-271.

Horwitz E. P., Chiarizia R., Dietz M. L., Diamond H., Nelson D. M., 1993 — Separation and preconcentration of actinides from acidic media by extraction chromatography. *Anal. Chim. Acta.*, 281: 361-372.

Pilvió R., Bickel M., 1998 — Separation of actinides from a bone ash matrix with extraction chromatography. *J. Alloys Comp.*, 271-273: 49-53.

Pilvió R., LaRosa J. J., Mouchel D., Wordel R., Bickel M., Altzitzoglou T., 1999 — Measurement of low-level radioactivity in bone ash. *J. Environ. Radioactivity.*, 43: 343-356.

Ivanovich M., Harmon R. S., 1982 — *Uranium Series Disequilibrium: Application to Environmental Problems.* Oxford, Claredon Press, 40p.

Sholkovitz E. R., 1983 — The geochemistry of plutonium in fresh and marine water environments. *Earth-Sci. Rev.*, 19: 95-161.

Suutarinen R., Jaakkola T., Paatero J., 1989 — "The behaviour of transuranic elements in Lake Päijänne after the Chernobyl accident". *In: Proceedings of the XVth Regional Congress of IRPA*, Visby, Sweden, 10-14 September, 1989.

Hardy, E. P., Krey, P. W., Volchok, H. L., 1973 — Global Inventory and distribution of Fallout Plutonium. *Nature.*, 241: 444-445.

Eisenbud M., 1987 — *Environmental Radioactivity, From Natural, Industrial and Military*

Sources. 3rd ed., Academic Press, New York, 343p.

MAXWELL S. L. 1997 — III, Rapid Actinide Separation. *Radioactivity and Radiochemistry.*, 8: 36-44.

TALVITIE A., 1972 — Electrodeposition of actinides for alpha spectrometric determination. *Anal. Chem.*, 44: 280-283.

HINDMAN F. D., 1983 — Neodymium fluoride mounting for spectrometric determination of uranium, plutonium and americium. *Anal. Chem.*, 55: 2460-2461.

PILVIÖ R., BICKEL M., 2000 — Actinoid separation by extraction chromatography. *Appl. Radiat. Isot.*, 53: 273-277.

APOSTOLIDIS C., MOLINET R., RICHIR P., OUGIER M., MAYER K., 1998 — Development and validation of a simple, rapid and robust method for the chemical separation of uranium and plutonium. *Radiochim. Acta.*, 83: 21-25.

Holmes L., Pilviö R., 2000 — Determination of thorium in environmental and workplace materials by ICP-MS. *Appl. Radiat. Isot.*, 53: 63-68.

Oral/Poster presentations

Session 2

Project Chariot, a nuclear excavation project in Northern Alaska

G. E. Gilbert

In the mid-1950's, American nuclear scientists, especially those at the Livermore Nuclear Laboratory as well as many within the Atomic Energy Commission, were extremely interested in initiating a variety of projects involving underground nuclear detonations ostensibly to promote peaceful uses of atomic energy. This interest resulted in the establishment in 1957 of a program entitled Project Plowshare (or PNE, Peaceful Uses of Nuclear Explosives). It was reported (Ogle) that if successful this program would counteract the fear of nuclear detonations, at least to some extent. Also, it might keep nuclear explosive design and experimental work continuing during a moratorium or test ban period. About a dozen specific projects were established within Project Plowshare including the excavation of a channel through the reef at Kapingamarangi (an atoll in the Caroline Islands), a sea-level Panama Canal and the excavation of a harbor along the northwest coast of Alaska. The latter project was entitled Project Chariot. Of all the Plowshare Projects, Project Chariot became the closest to fruition. The objective was to create a harbor for the shipment of natural resources in the area and, in the process, develop a better understanding of the use of nuclear energy for large excavation projects. An outstanding feature of Project Chariot was the conduction of approximately 50 in-depth physical and biological studies of the terrestrial, coastal, oceanic and atmospheric components of the study area. As a result, the Project Chariot study area could possibly be the most deeply and widely studied sizeable area in the biosphere. Collectively these studies would have provided an excellent baseline to evaluate the impact of the use of nuclear detonations for excavation and cratering projects.

Environmental remediation of uranium mining tailings ponds

P. Szerbin
L. Juhász
Zs. Lendvai
M. Csõvári
I. Benkovics
A. Várhegyi
B. Kanyár
Z. Várkonyi
F.-J. Maringer

After more than 35 years operation the uranium mining and milling facilities near Pécs city in Hungary were finally shut down in 1997. A complex plan and appropriate strategy have been prepared for restoration tasks. The main principle of the restoration planning is the applying of step by step solutions of each task. Most of the waste rock and heap leaching piles have been already restored or the restoration is in progress now. One of the most important and most complicated tasks is the remediation of tailings ponds because of the complexity of chemical, radiological and geotechnical requirements of the restoration. Material in the tailings ponds contains the residuary isotopes of the uranium decay series after the ore processing, and the ponds are potential sources of radioctive contaminants through both aerial and terrestrial pathways. The potential risk of environmental contamination from the latter route has been substantially decreased by pretreatment of the soil (liming) before construction. The main task of the presented study is development of a covering technology that ensures the radon emanation reduction from the surface of the pond below the established limit. Besides, the cover should solve problems of wind erosion of the ponds, the cover is expected to give an environmental friendly shape to the resulting pile and should prevent soil erosion from the slopes. The presentation gives details on investigation of different covering options of tailings ponds. In the first pilot study concrete rings of 1

m diameter filled with test layers of different materials were used for in situ examination of radon infiltration. In total 11 columns were studied, including the uncovered pond as a reference point. Radon concentrations of the layers were measured by monitors equipped with scintillation soil probe, and in parallel radon flux was measured on the top of each column. On the basis of the evaluation of the results two covering options have been designed for detailed studies on in-field on territories cover about 2000 m^2. Radon concentration in the layers, radon emanation from the surface of the cover were measured. Results of the described above pilot studies are discussed in the presentation.

Purification and decontamination for waste containing radioactive, natural or artificial, trace element

A. Favre-Reguillon *et al.*

Despite recent improvements in both sensitivity and selectivity of analytical methods, separation and preconcentration remain essential steps in many chemical analyses. In the determination of radionuclides in environmental and biological samples, the low level of the nuclides typically encountered and the complexity of the sample matrix often preclude direct determination. Separation and preconcentration are also important in the processing of nuclear waste. They make it possible to reduce the volume of materials requiring final disposal and, therefore, lower the cost of waste handling and treatment. We have been working on partitioning for high-level liquid waste during the past 10 years. Our objectives involved the selective extraction of alkali, alkaline-earth metals and platinum group's metals and more recently the group separation of actinides and lanthanides. To reach these objectives, macrocyclic compounds, such as crown ether, thia-crown ether, calixarene and pyridinium containing aza-macrocyclic have been synthesized. Depending on their hydrophilicity, ligands were used in liquid/liquid extraction or nanofiltration-complexation. Characterisation and results obtained with the new compounds and systems are reported. Decontamination of liquid waste as well as gaseous effluent by chelating resins was also studied. Immobilisation of macrocycles on various inert supports, design of new ion-exchange resins with the "template effect" technique and trapping of gaseous radionucleides will be also presented. We describe recent advances in laboratory and process-scale separation techniques for removing and recovering several of the more hazardous elements of the waste constituents.

Radioactivity in sedimentary studies

Session 3

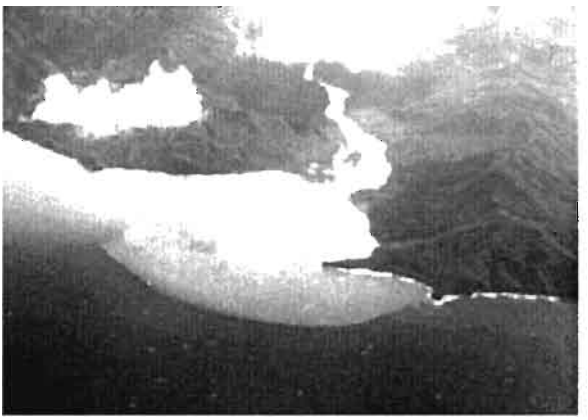

Chairman: J.-M. Fernandez

Session opening: J. N. Smith

Seasonally modulated sedimentation in an estuarine depositional regime

John N. Smith

Introduction

One commonly employed assumption used to simplify the modelling of sediment dynamics and the determination of geochronologies in complex, estuarine depositional regimes is that of a constant sedimentation rate. However, in most river-estuarine systems, periodic phenomena, such as the seasonal cycle in river discharge or annual phytoplankton blooms, can produce a seasonal variability in the transport or production of suspended material and a corresponding variation in sedimentation rates in downstream environments. Less predictable "catastrophic" phenomena such as storm events, landslides, etc. can also contribute to seasonally "pulsed" sediment discharge events. Short, periodic "bursts" of high sediment deposition can, in some instances, provide the majority of sediment transport compared to that delivered during the longer intervening quiescent periods of sedimentation. Under these conditions, the mean sediment accumulation rate can be very much different (usually, greater) than the most probable rate. The degree to which a sedimentation regime is skewed from its mean value, ie., the dispersion of its instantaneous rate distribution with respect to its mean sedimentation rate, may have an important effect on other environmental variables such as the composition and activity of benthic community assemblages, the rates of sediment diagenesis and the

efficiency of particle and contaminant transport from the water column to the sediments.

The annual variability in estuarine sedimentation rates could be determined synoptically using sediment traps. However, this method will provide only the most recent record and will invariably reflect contemporary climatological and hydrological conditions. An alternative method, employed in the present study in the Saguenay Fjord, Quebec, utilises the sequence of variations in sedimentation rate recorded in the sediments in the form of textural varves or particle size unconformities. This type of analysis can be carried out in estuarine systems having a bi-modal depositional mechanism in which pulsed inputs of coarser-grained sands and silts during high Spring river discharge conditions are superimposed on the ambient sedimentation of finer-grained clays and organic material. In the present case, the quantity of sediment pulsed into the system is estimated by the extent of dilution of the ^{210}Pb signal, assuming that ^{210}Pb transport can be simulated using a Constant Flux (CF) technique. The applicability of the CF technique to the Saguenay Fjord sediment regime is validated using time-stratigraphic horizons associated with landslide events and the thresholds for anthropogenic contaminant loadings. The purpose of this study is to evaluate the historical importance of sediment deposition during high energy, Spring river discharge conditions compared to ambient sedimentation patterns that prevail during the remainder of the year.

Methods and environmental setting

The Saguenay Fjord is a deep (250 m) glaciated valley carved into the crystalline rocks of the Canadian Shield, located 300 km Northeast of Montreal, Quebec (Figure 1). Sedimentation rates in the fine-grained clayey sediments covering the bottom of the fjord decrease exponentially with increasing distance from the mouth of the Saguenay River. The highest sedimentation rates (> 4 $g.cm^2.yr^{-1}$; Smith and Ellis, 1982) occur at the head of the fjord where an abrupt decrease in river water velocity caused by the widening and

deepening of the river channel as it enters the fjord promotes the rapid deposition of suspended material and bedload. Further, a high flux of terrigeneous organic matter derived from upstream pulp and paper mills and sawmills located near Arvida (Figure 1) has produced an extremely anoxic benthic environment, almost totally devoid of bioturbating organisms. This unique combination of high sedimentation rate and the absence of sediment mixing has resulted in well-preserved sediments containing an excellent record of chronological events during the past 100 years.

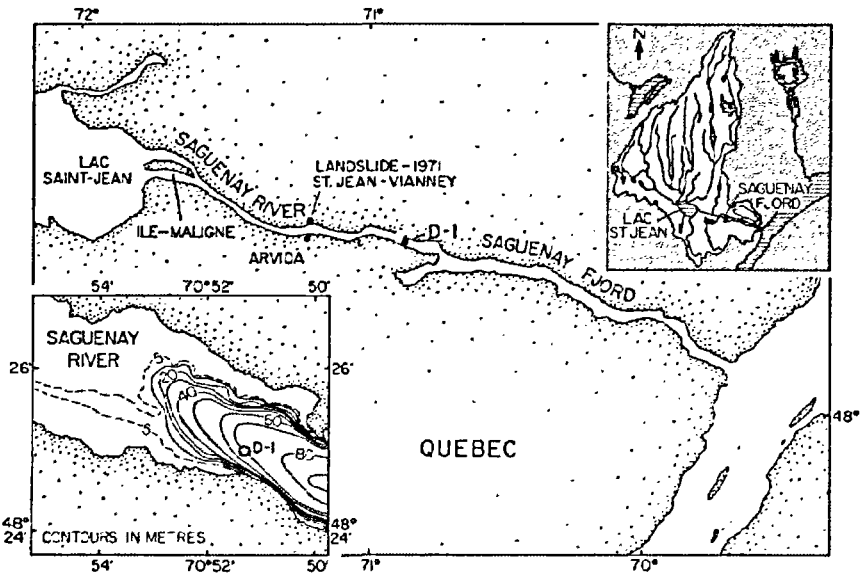

Figure 1
Sediment cores D-1, 007 and C-7 were collected from Station D-1 in the Saguenay Fjord in 1979, 1982 and 1997, respectively.

Two depositional events have had a pronounced impact on sediment accumulation rates in the Saguenay Fjord. In 1971, a landslide at Saint-Jean Vianney (Figure 1) resulted in the displacement of 25 million tonnes of ancient marine clays into the Saguenay River and produced a distinct 1971 clayey horizon distinguishable by abrupt

changes in texture, colour and geochemical profiles in all sediment cores in the upper arm of the fjord (Smith and Walton, 1980; Schafer and Smith, 1987). Massive flooding in the Saguenay region in 1996 produced a second, clayey time-stratigraphic horizon in more recently collected cores from the fjord.

A 2 metre, Lehigh gravity core (10 cm I.D.) was collected at Station D-1 in the upper arm of the fjord (Figure 1) in 1979. This core was X-radiographed, subsampled at 1 cm intervals and analysed for a range of geochemical properties and contaminants at one cm intervals, including the radionuclide tracers, ^{137}Cs, $^{239,240}Pu$, ^{226}Ra and ^{210}Pb using alpha and gamma spectrometric methods outlined in Smith *et al.* (1987). Organic matter, porosity and particle size measurements were also carried out using methods outlined in Smith and Schafer (1987). The station was re-occupied in 1982 and 1997 when a piston core (core C-7) and another Lehigh gravity core (core 007), respectively, were collected.

Previous studies in the upper arm of the Saguenay Fjord have indicated that, despite the seasonal modulation of the ^{210}Pb signal, the annual flux of ^{210}Pb remains relatively constant. This is due to the fact that the enhanced inputs of sands and silts during the Spring river discharge carry comparatively little additional excess ^{210}Pb owing to their inefficient scavenging of this particle-reactive tracer from the water column. As a result, it has been shown (Smith *et al.*, 1987) that it is feasible to apply a Constant Flux (CF) ^{210}Pb technique (Robbins, 1978) to the interpretation of the experimental results. The geochronology for a core is then given by;

$$T = \frac{1}{\lambda} \ln(1 - I(m) / I^{\circ})^{-1} \qquad 1$$

where, T is the time, λ is the radioactive decay constant for ^{210}Pb (0.0311 y^{-1}), I(m) is the inventory of excess ^{210}Pb above a sediment depth, m and I^{∞} is the total inventory of ^{210}Pb in the sediments. The sediment accumulation rate, w, is given by;

$$\omega = \frac{\lambda}{A} (I^{\circ} - I(m)) \qquad 2$$

where, A is the ^{210}Pb activity at a depth, m. The time-invariant ^{210}Pb flux for the CF technique is;

$$F = I^{\circ} / \lambda \qquad 3$$

As noted by Robbins *et al.* (2000), the CF technique is actually a mapping method and not a model, because it simply uses an algorithm to convert excess ^{210}Pb activities into dates and sediment accumulation rates and has no predictive value.

Results

The ^{210}Pb sediment-depth distributions for the three sediment cores are illustrated in Figure 2. The impact of the 1971 St. Jean Vianney landslide is defined by a depositional unconformity of grey clay having reduced ^{210}Pb activities in each core. The bottom of this layer was located at depths of approximately 40 cm, 55 cm and 165 cm in 1979, 1982 and 1997, respectively corresponding to a mean sedimentation rate of about 6 cm.yr^{-1} at this location. The 1996 flood event has produced a similar, ^{210}Pb -deficient unconformity near the top of core 007 (collected in 1997). The peaks and troughs in ^{210}Pb distributions (apart from the landslide/flood layers) reflect seasonally-modulated inputs of coarser-grained silts and sands during the spring river discharge of each year, characterised by reduced ^{210}Pb levels, alternating with the ambient deposition of finer-grained clays and organic matter having higher concentrations of ^{210}Pb.

The total ^{210}Pb inventory, I$^{\circ}$, and inventories above a given depth m, I(m), were measured through cores D-1 and 007. These results were then used to determine the core geochronology, sediment accumulation rates and the ^{210}Pb flux from equations 1, 2 and 3, respectively. The values of ω for each core are plotted as a function of T in Figure 3. The entire inventory of excess ^{210}Pb is not contained in the upper 260 cm of core C-7, and an alternative method must be employed in order to estimate I$^{\circ}$. Since the 1971 landslide event is pronounced and easily defined, then this time-stratigraphic horizon was used to calculate I$^{\circ}$ from Equation 1. This value of I$^{\circ}$ was then used in equations 2 and 3 to calculate the core geochronology.

Obviously, any geochronology determined using the CF technique must be validated using independent time-stratigraphic horizons (Robbins and Edgington, 1975), because there is no external con-

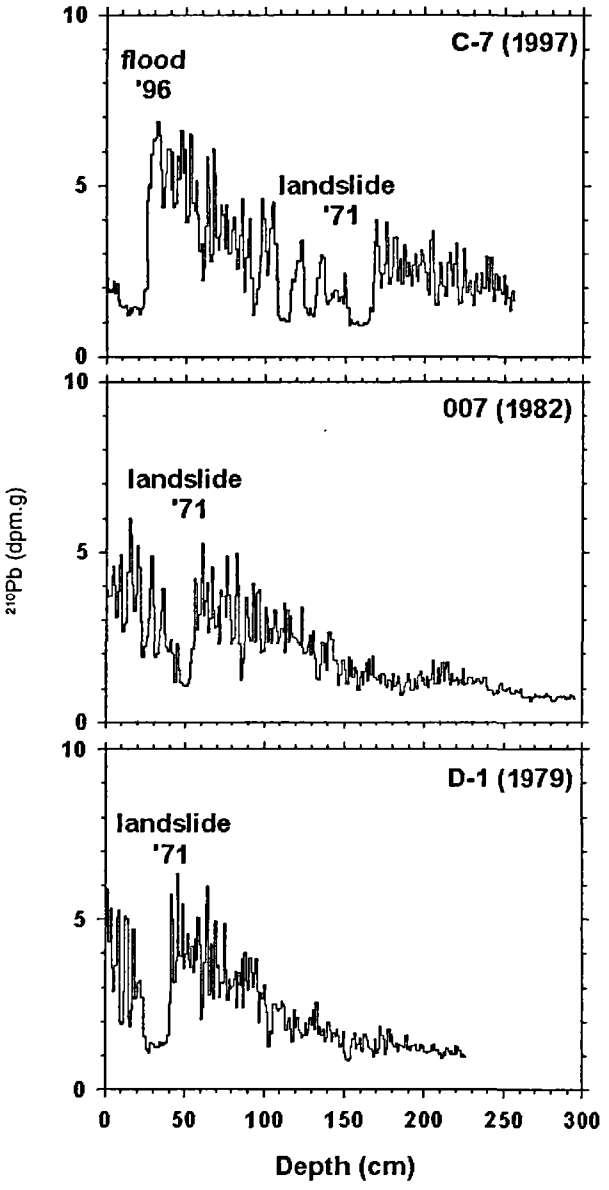

Figure 2
^{210}Pb sediment-depth distributions for the three cores, D-1 (collected in 1979), 007 (1982) and C-7 (1979) were measured at 1 cm intervals for the entire length of each core.

straint imposed on the data, ie. each ^{210}Pb data point is equally valid regardless of its actual value. For cores D-1 and 007, the agreement of the landslide horizon with a date of 1971 is sufficient validation for the CF technique. However, an alternative horizon must be employed for core C-7, because the 1971 horizon was used to estimate the ^{210}Pb flux, itself. Numerous geochemical and textural horizons have been identified in each of these cores, but a series of horizons common to all are those associated with the deposition and transport of fallout radionuclides. Specifically, the initial introduction of measurable levels of ^{137}Cs in 1954 and the maximum ^{137}Cs flux to the sediments in 1964 provide geochemical markers whose positions in each core are in good agreement with calculated geochronologies (Figure 3). This independent validation of the CF results provides some assurance that the ensemble of sediment accumulation rates shown in Figure 3 for each core bear some semblance to reality. In fact, there are numerous additional horizons that have also been used to validate the geochronologies for these cores including; (1) a 1947 Hg horizon associated with the construction of a chlor-alkali plant at Arvida (Smith and Loring, 1981; Smith and Schafer, 1999); (2) a 1924 clay landslide horizon associated with a landslide at Kenogami (Smith and Schafer, 1987), and; (3) a 1910 organic matter horizon resulting from the beginning of the pulp and paper industry in the Saguenay region (Smith and Schafer, 1987).

The results from these three cores show that the 1971 landslide unconformity has survived intact and continues to provide an important time-stratigraphic horizon in Saguenay Fjord sediments. It was joined by a second, flood-produced unconformity in 1996 and, together, the two horizons can produce geochronological reference points throughout the fjord sediments. This time series of sediment cores also shows that the history of seasonally modulated maxima in ^{210}Pb sedimentation rates are preserved over relatively long periods. Sedimentation rate maxima and minima can be cross-correlated between the sediment cores and can be related to the history of river discharge (Smith and Schafer, 1987). The ultimate goal of this study is to use the record of river discharge events preserved in the sediments of the fjord to resolve the history of river discharge during the 18th and 19th centuries and thereby provide new insights into the history of temperature, precipitation and climate change in Eastern Canada.

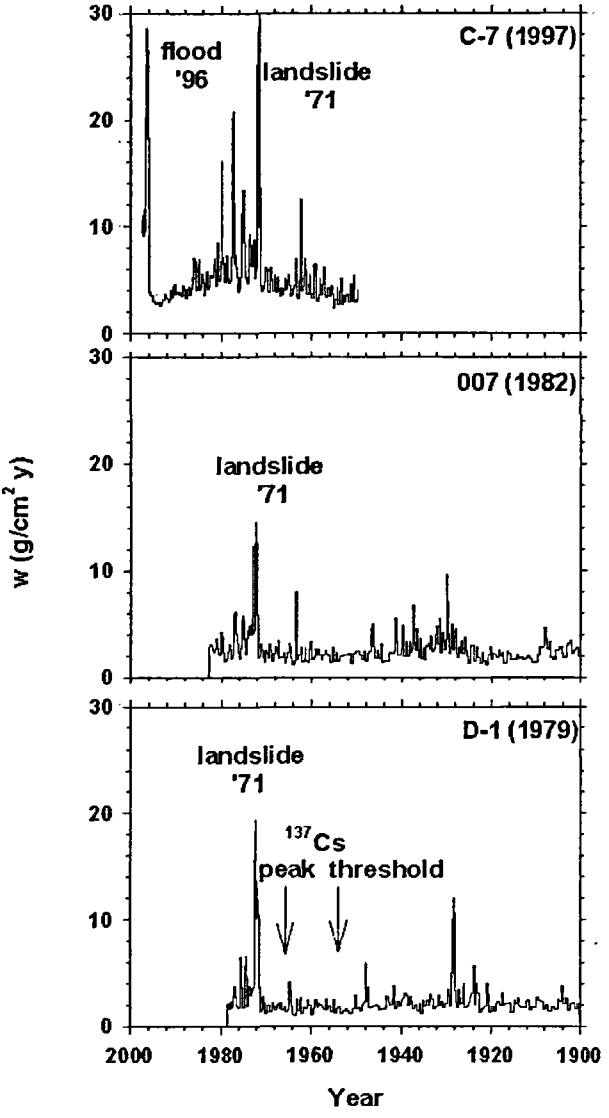

Figure 3
Sediment accumulation rates, w ($g.cm^{-2}.yr^{-1}$) were calculated from the ^{210}Pb distributions using a constant flux technique and equations 1,2 and 3 given in the text. The geochronologies for each core were validated using horizons associated with the initial appearance of fallout ^{137}Cs (1954) and the maximum flux of fallout ^{137}Cs (1964). The 1971 landslide and 1996 flood event horizons are also in agreement with the ^{210}Pb constant flux geochronologies.

Bibliography

ROBBINS J. A., EDGINGTON D. N., 1975 — Determination of recent sedimentation rates in Lake Michigan using ^{210}Pb and ^{137}Cs. *Geochimica et Cosmochimica Acta*, 39: 285-304.

ROBBINS J. A., 1978 — "Geochemical and geophysical applications of radioactive lead isotopes". *In* J.O. Nriagu (Ed.): *Biochemistry of Lead*, Amsterdam, Elsevier: 285-393.

ROBBINS J. A., HOLMES C., REDDY K., NEWMAN S., 2000 — "Mapping schemes versus process models for ^{210}Pb dating soil cores: an example from the Everglades of South Florida, U.S.A". *In: South Pacific Environmental Radioactivity Conference*, Noumea June 19-23, New Caledonia.

SMITH J. N., WALTON A., 1980 — Sediment accumulation rates and geochronologies measured in the Saguenay Fjord using the ^{210}Pb dating method. *Geochimica et Cosmochimica Acta*, 44: 225-240.

SMITH J. N., LORING D. H., 1981 — Geochronology for mercury pollution in the sediments of the Saguenay Fjord, Quebec. *Environmental Science and Technology*, 15 (8): 944-951.

SMITH J. N., ELLIS K. M., 1982 — Transport mechanism for ^{210}Pb, ^{137}Cs and Pu fallout radionuclides through fluvial-marine systems. *Geochimica et Cosmochimica Acta*, 46: 941-954.

SCHAFER, C. T., SMITH J. N., 1987 — Hypothesis for a submarine landslide and cohesionless sediment flows resulting from a 17th century earthquake-triggered landslide in Quebec, Canada. *Geo-marine Letters*, 7: 31-37.

SMITH, J. N., SCHAFER C. T., 1987 — A 20th century record of climatologically-modulated sediment accumulation rates in a Canadian fjord. *Quaternary Research*, 27: 232-247.

SMITH, J. N., ELLIS K. M., NELSON D. M., 1987 — Time-dependent modelling of fallout radionuclide transport through a drainage basin; significance of «slow» erosional and «fast» hydrological components. *Chemical Geology*, 63: 157-180.

SMITH, J. N., SCHAFER C. T., 1999 — Radionuclide modelling of sedimentation, bioturbation and Hg uptake in the sediments of the Estuary and Gulf of St. Lawrence. *Limnology and Oceanography*, 44, No. 1, 207-219.

Regionalization of natural and artificial radionuclides in marine sediments of the Southern Gulf of Mexico

Pedro Francisco Rodríguez-Espinosa

Francisco V. Vidal Lorandi

Víctor M. V. Vidal Lorandi

Introduction

This paper summarizes the results of regional studies of radioactivity (^{40}K and ^{137}Cs) in marine sediments of the Southern Gulf of Mexico. These investigations were initiated in 1993 and the first results were published by Rodríguez-Espinosa P.F *et al.*, in 1998, 1999a, 1999b and 1999c. They found that the ^{137}Cs, ^{40}K and ^{214}Bi concentrations measured in five sediment-cores sampled in the southern Gulf of Mexico are similar to those reported in the world inventory for same type of marine sediments. As would be expected, the radioactivity concentrations measured vary as a function of sedimentary environment. The highest ^{40}K concentrations are associated mainly with the sediments of the Panuco River, whose drainage basin inputs sediments from the Sierra Madre Oriental and Central Mexico, where intensive agricultural practices and heavy use of fertilizers take place. The mid-range ^{40}K concentrations were measured in sediments of the Grijalva-Usumacinta river fan, and reflected the characteristic properties of the Cenozoic and Paleozoic metamorphic rocks of its drainage basin. Finally, the highest ^{137}Cs concentrations found in the sediment-cores of the Grijalva-Usumacinta river fan sediments result from the higher

rainfall (3,000 mm.yr^{-1}) over its much greater drainage basin size, relative to that of the Pánuco River.

In this paper we now present the results of ^{40}K and ^{137}Cs concentrations in another twelve sediment-cores sampled in the Southern Gulf of Mexico. These new radioactivity concentration values will aid to further understand the nature and regional distribution of radioactivity in Southern Gulf of Mexico marine sediments.

Methods

Twenty five USNEL Box sediment-cores were collected in water depths between 20 to 2,000 m in the Southern Gulf of Mexico of which twelve of them are reported in this paper. The USNEL Box sediment-cores were collected aboard the R/V Justo Sierra during the OGMEX XI, XII and XIII oceanographic cruises, during the summers of 1993, 1994 and 1995 (Figure 1).

The 30-cm deep sediment-cores were sub-sampled in 2-cm thick slides, and frozen for later analyses. Sediment sub-samples were analyzed by XRD to determine mineral composition. The natural ^{40}K and artificial ^{137}Cs radionuclide concentrations were measured using a Ge-Hp Gamma-Spectrometer, and counting for 50-60,000 seconds with a ± 5 % uncertainty (95 % confidence limit). The measurements were made at the Laboratorio de Vigilancia Radiológica Ambiental del Centro at Cienfuegos, Cuba.

Results

We report natural and artificial radioactivity concentrations in twelve of the twenty-five sediment cores sampled. These results are representative of the regional radioactivity concentrations in the Southern Gulf of Mexico.

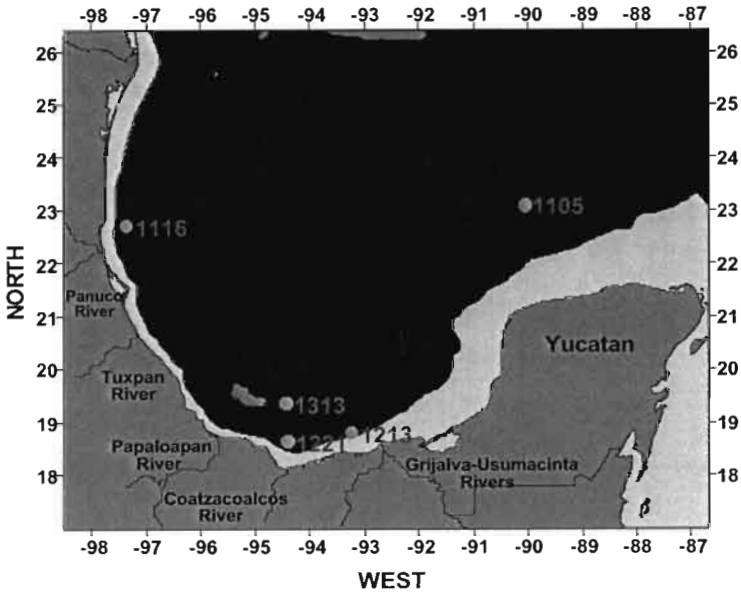

Figure 1
Sediment samples collected in the Gulf of Mexico during 1993, 1994 and 1995.

The ^{137}Cs and ^{40}K concentrations measured range from 2 to 6.5 $Bq.kg^{-1}$ and 100 to 800 $Bq.kg^{-1}$, respectively. The highest ^{137}Cs concentrations were found in the sediments of the Grijalva-Usumacinta river fan at 75 meters depth (stations 1213 and 1210). The lowest ^{137}Cs concentrations were found in the Yucatan Escarpment, in the intermediate carbonate and terrigenous regions at 100 m. (station 1221) and in the maximum depth sampled at 2000 m (station 1313).

The lowest ^{40}K (150-175 $Bq.kg^{-1}$) concentration was found in the Yucatan Escarpment sediments in the southeast Gulf of Mexico. This is basically a carbonated region with no-river influence (station 1105). The highest ^{40}K concentration (700-1000 $Bq.kg^{-1}$) was found in the southwest Gulf of Mexico in the Pánuco river fan (station 1116). The mid-range concentrations of ^{137}Cs (4-5 $Bq.kg^{-1}$) and ^{40}K (400-700 $Bq.kg^{-1}$) were found in the sediments of the southwestern continental shelf, in the Pánuco river fan (Figure 2). Figure 2 is a scatter diagram showing the concentration of ^{137}Cs vs ^{40}K.

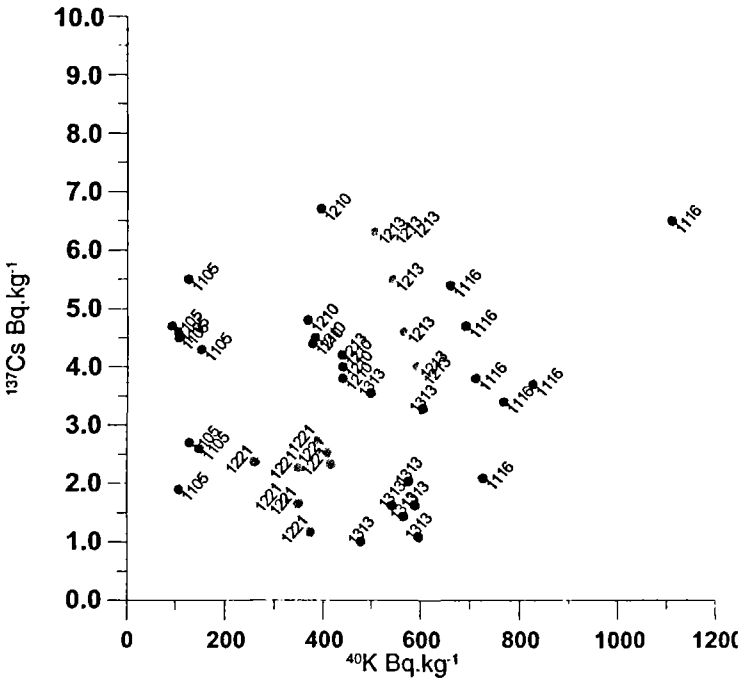

Figure 2
^{137}Cs vs ^{40}K concentrations in marine sediment cores sampled in the Gulf of Mexico.

Figure 3 shows the ^{137}Cs vs ^{40}K concentrations for the same data of figure 2 including error bars. This figure allows us to visualize the instrumental error associated with each measured value and to associate the different radioactivity concentration types with the different sedimentary provinces within the study area, including the influence of the big rivers.

In Figure 4 we show the error bars for the mean ^{137}Cs and ^{40}K concentrations. This figure provides a clear picture of the regional radioactivity distribution in marine sediments of the Southern Gulf of Mexico.

Figure 5 shows a plot of our mean data values compared to the different ^{137}Cs vs ^{40}K concentrations in marine sediments from other

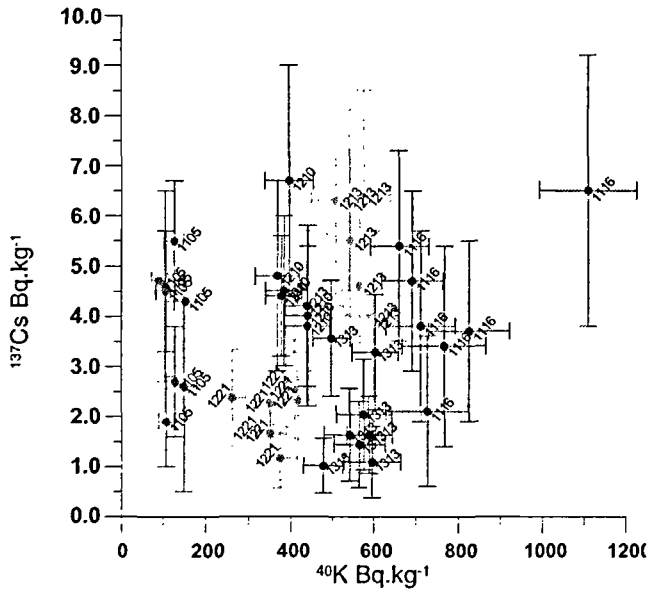

Figure 3
^{137}Cs vs ^{40}K concentrations error bars in marine sediment cores sampled in the Gulf of Mexico.

regions of the word oceans (Yu *et al.*, 1994; Albrecht and Beer, 1997; Pujol and Sánchez, 1997; Alonso *et al.*, 1998; Pérez-Sabino *et al.*, 1999.

Conclusions

Our results corroborate the findings reported by Rodríguez-Espinosa *et al.*, in 1998; 1999a; 1999b and 1999c, namely that the ^{137}Cs and ^{40}K concentrations measured in the sediment-cores sampled in the Southern Gulf of Mexico are similar to those reported in the world inventory for same type of marine sediments.

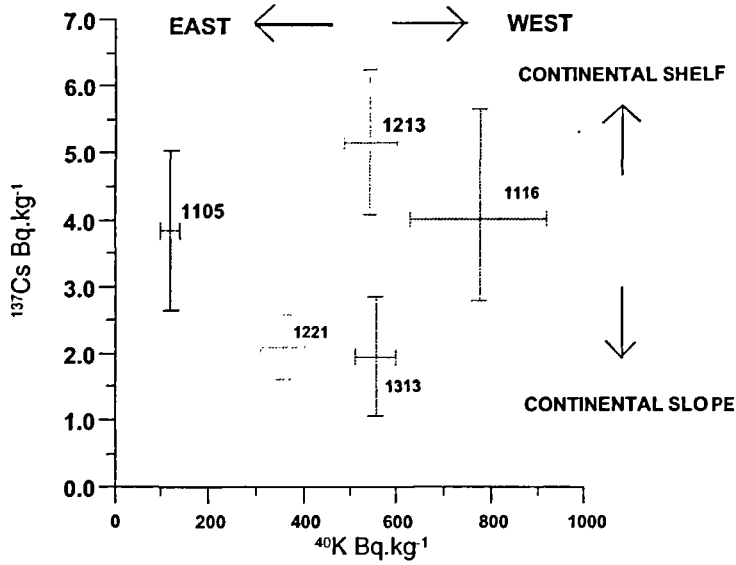

Figure 4
^{137}Cs vs ^{40}K mean concentrations of five marine sediment cores of the Southern Gulf of Mexico.

As would be expected, the radioactivity concentrations measured vary as a function of sedimentary environment.

The highest ^{40}K concentrations are associated mainly with the sediments of the Pánuco River, whose drainage basin inputs sediments from the Sierra Madre Oriental and Central Mexico, where intensive agricultural practices and heavy use of fertilizers takes place.

The mid-range ^{40}K concentrations were measured in sediments of the Grijalva-Usumacinta river fan, and reflected the characteristic properties of the Cenozoic and Paleozoic metamorphic rocks of its drainage basin.

The highest ^{137}Cs concentrations found in the sediment-cores of the Grijalva-Usumacinta river fan sediments result from the higher rainfall (3,000 mm. yr^{-1}) over its much greater drainage basin size, relative to that of the Pánuco River.

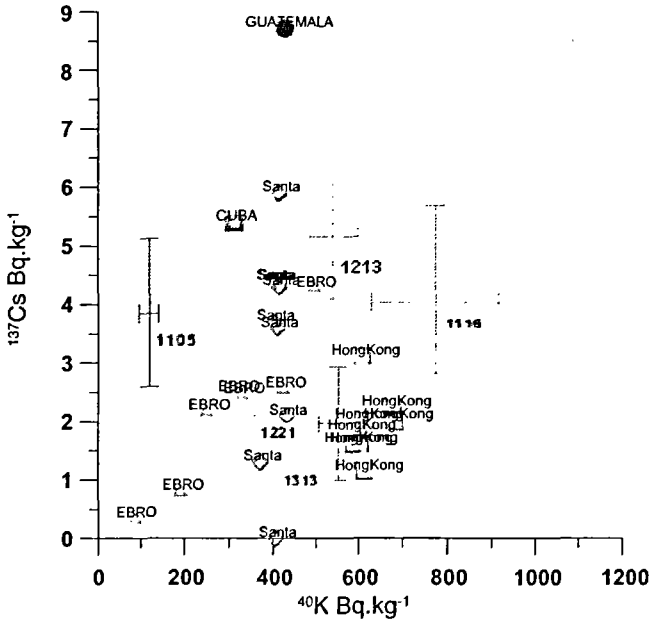

I Figure 5
Concentrations of ^{137}Cs vs ^{40}K in sediment cores from different locations of the World.

Finally the highest ^{137}Cs are found in continental shelf sediments, and the lowest in continental slope sediments.

Aknowledgements

Ing. Hector Cartas Radiometría y Contéo del Laboratorio de Vigilancia Radiológica Ambiental del Centro, Cienfuegos, Cuba. This research was sponsored by the Grupo de Estudios Oceanográficos, Centro de Investigación en Ciencia Aplicada y Tecnología Avanzada, The Comisión de Operación y Fomento de Actividades Académicas of the Instituto Politécnico Nacional and Dr. Elva Escobar Briones of the Universidad Nacional Autonoma de México for support the time of the O/V Justo Sierra UNAM for the DGAPA UNAM IN 213197, 217298 and finally CONACYT G27777B PÑ-50.

Bibliography

ALBRECHT A., BEER J., 1997 – Assessment of Radionuclide Distribution in Continental Shelf Sediments (the Gulf of Taranto, Mediterranean Sea). *Radioprotection-Colloques*, 32 C2: 277-285.

ALONSO H. C., DÍAZ A. M., MUÑOZ C. A., SUAREZ MORELL E., CLARO M R., 1998 – Levels of Radioactivity in the Cuban Marine Environment. *Radiation Protection Dosimetry*, 75 (1-4): 69-70.

DAVIES D.K., MOORE W.R., 1970 – Dispersal of Mississippi sediment in the Gulf of Mexico. *Jour. Sed. Petrology*, 40 (1): 339-353.

DAVIES D. K., 1972 – Mineralogy, petrology and derivation of sands and silts of the continental slope, rise and abyssal plain of the Gulf of Mexico. *Jour. Sed. Petrology*, 42 (1): 59-65.

PÉREZ-SABINO J. F., OLIVA DE SANDOVAL B. E., OROZCO-CHILEL R. M., AGUILAR SANDOVAL E., 1999 – "Radioactive Contamination of the Guatemalan Marine Environment". *In: International Symposium on Marine Pollution*, Monaco, 5-9 October 1998 (OIEA ISSN 1011-4289, Vienna, 1999): 550-552.

PUJOL T. LI., SÁNCHEZ C. J.A., 1997 – Radioactividad del Agua Superficial y los Sedimentos en la Cuenca del Ebro: Utilización del Tritio como Radiotrazador en el Tramo Catalán. *Radioprotección* 5 (15): 95-103.

RODRÍGUEZ ESPINOSA P. F., VIDAL LORANDI F. V., VIDAL LORANDI V. M. V., 1998 – "Natural and Artificial Radionuclides in Southern of Gulf of Mexico Marine Sediments". *In: International Symposium on Marine Pollution*, Monaco, 5-9 October 1998 (OIEA ISSN 1011-4289, Vienna, 1999): 612-613.

RODRÍGUEZ ESPINOSA P. F., VIDAL LORANDI F.V., VIDAL LORANDI V.M.V., 1999a – "Natural and Artificial Radionuclides in Southern of Gulf of Mexico Marine Sediments". *In: International Symposium on Marine Pollution*, Monaco, 5-9 October 1998 (OIEA ISSN 1011-4289, Vienna, 1999): 555-556.

RODRÍGUEZ ESPINOSA P. F., VIDAL LORANDI F.V., VIDAL LORANDI V.M.V., 1999b – "On the Concentration and Distribution of Natural (^{40}K, ^{214}Bi and ^{210}Pb) and Artificial (^{137}Cs) Radionuclides in Marine Sediments of The Southern Gulf of Mexico". *In: International Symposium on Nuclear and Related Techniques in Agriculture, Industry and Environment.* Proceeding of the 2nd NURT, V Workshop on Nuclear Physics, Havana, 26-29 October 1998 (ISBN 959-7136-04-X): 1-4.

RODRÍGUEZ ESPINOSA P. F., VIDAL F. V., VIDAL V. M. V., 1999c – "Radioactivity in sediments of the Western, Southern and Central-Eastern Gulf of Mexico". *In: EOS Trans.*, AGU, 80 (49), Ocean Sciences Meet. Suppl.: p OS14.

RODRÍGUEZ ESPINOSA P. F., VIDAL F. V., VIDAL V. M. V., 1996 – *Estudio de la Concentración y Distribución de Radionúclidos Naturales y Artificiales en Sedimentos Marinos del Golfo de México.* Informe Final IIE/UREN/13/5586/I01/F., 374 p.

VAN ANDEL TJ. H., 1960 – Sources and Dispersion of Holocene Sediments, in North west Gulf of Mexico. *Am. Assoc. Petroleum Geologists*, 1: 34-55.

YU K. N., GUAN Z. J., STOKES M. J., YOUNG E. C. M., 1994 – Natural and Artificial Radionuclides in Seabed Sediments of Hong Kong. *Nucl. Geophys.*, 8 (1): 45-48.

Mixing models (advection/diffusion/ non-local exchange) and ^{210}Pb sediment profiles from a wide range of marine sediments

Sandor Mulsow

Pavel Povinec

Introduction

Particles settling from the water column may enter the sediment below by physical or biological activity. Because these transport processes play a role during early diagenesis (Aller, 1990), their understanding and quantification is crucial in the fate of many sediment bound particles reaching the seafloor. Theoretically sediment accumulation rates depends only in the variable or constant supply of particles. For many years sediment bound tracers have been used to estimate sediment accumulation rates, a commonly used one is concentration profiles of excess ^{210}Pb (Nittrouer *et al.*, 1983; DeMaster *et al.*, 1994). This radiotracer is strongly bound to particulate material, hence its redistribution depends mainly on the supply at the sediment-water interface, *in situ* production from ^{238}U via ^{226}Ra decay, sediment accumulation and physical (earthquake, waves) or biological mixing. In nature most of the particles bearing ^{210}Pb are of organic origin, thus in only few cases biological mixing does not influence

activity concentration profiles. This fact is quite important because violate one of the prerequisite in using tracers as time clocks in sediments, that is, the immobilisation of the tracer upon arrival to the sediment-water interface (Kadlec and Robbins, 1984). Biological mixing in marine sediment has been estimated assuming that sediment reworking consist of a large number of small events, thus the result over time appears as diffusive and the activity can be quantify as biological diffusive mixing (Db) (Boudreau, 1986a; Mulsow and Boudreau, 1999). This coefficient is usually modelled from sediment-depth profiles of particle bound radioactive tracers. However, empirical data showed quite often-subsurface maximum (Smith *et al.*, 1986) that can not be accounted for as diffusive mixing. Alternative hypotheses are fluctuation in the input sources, burrows or tube's infilling or a mechanism that introduce surface (young) sediment at depth in the sediment column. This latter process is call non-local exchange (Boudreau, 1986b). Because of the complexity of such processes biological-mixing effect on ^{210}Pb sediment profiles is often ignored and not accounted for. One of the reasons is the lack of systematic models that could account for the main biological mixing activities in marine sediments. Soetaert *et al.* (1996) presented a family of bioturbation models including diffusive and non-local exchange processes and demonstrated its applicability and limitations in the interpretation of ^{210}Pb sediment profiles. In this study, we apply these mixing models to 10 sediment depth profiles of ^{210}Pb. The cores were collected from deep-sea stations (Northwest Pacific) to intermediate depths (Arabian Sea, Mediterranean Sea) and marginal sediments from Kara Sea.

2 Material and methods

Sediment collection

All the sediment was collected using a box corer and inserting a Plexiglas liner of 30 cm in length and 112 mm in diameter. The only exception was the sediment core collected in the Arabian Sea sedi-

ments. At this station the sediment was collected using a gravity corer. The sediment was sliced on board and freeze-dried. An aliquot of 100-200 mg of sediment was digested in a mixture of HF+HCL+HNO_3 in a Teflon bomb and microwave. The activity of ^{210}Pb was measured by alpha counting of its daughter ^{210}Po considered here as in secular equilibrium. ^{208}Po or ^{209}Po were used as chemical yield. Standard sediment sample as well as blanks were used with each batch of samples analysed. ^{210}Po were spontaneously deposited on silver discs. Bulk density and porosity were determined from the difference in wet and dried weight after correction for salinity content. The activity concentration of ^{210}Pb was expressed in dpm ml^{-1} of total activity in order to satisfy the model's requirement used here. The supported production is calculated as a parameter in the models.

Models

Basically, we used the models proposed by Soetaert *et al.* (1996) These authors proposed a family of models with increasing complexity (number of parameters added) of diffusive and non-local exchange mixing processes included in the models. The models require only a known sedimentation rate and total activity of the tracer profile. In our study we used the most close sedimentation rate from the literature for each one of the sites and ranged from 1-10 $cm.kyr^{-1}$. For details in the models see Soetaert, *et al.* (1996).

Results and discussion

The sediment cores studied come from a wide range of marine environments. Some stations are from coastal areas (Morocco, Kara Sea), others from intermediate depth water from the

Mediterranean Dyfamed and others from the Northwest Pacific and Arabian Sea deep-sea ocean (Table 1). The water depths ranged from 10 to > 4000 meter. In all instances the sediments were carefully collected and handled. The radiometric measurements were done at IAEA-MEL.

Station	depth	latitude	longitude	H_0: 1/ 2	H_0: 2/ 3	H_0: 3/ 4a	best fit
South Med.	900	35° 48N	9° 55E	***	ns		Model 2
Dyfamed	2300			**	**	ns	Model 3
Geosecs 413	2830	13° 21.8N	53° 15E	***	***	**	Model 4a
Kara Sea 1	195	69° 57.6N	61° 52E	***	**	ns	Model 3
Kara Sea 7	27	72° 59.9N	72°.58E	**	ns		Model 2
Kara Sea 9	30	73° 58.9N	73° 17E	***	*		Model 2
Kara Sea 13	17	72° 25.9N	80°.39E	***	ns		Model 2
NW Pacific 6	4577	11° 28.3N	164° 52E	***	**	ns	Model 2
NW Pacific 8	5390	15° 30.2N	159° 30E	***	ns		Model 2
NW Pacific 9	5002	22° 22.1N	152° 40E	***	ns		Model 3

Table 1
Name of the stations and statistical results of the F-test comparison among the models. *** p>0.9999; ** p 0.99-0.999 and * p 0.95-0.99.

None of the 10 cores measured for ^{210}Pb-concentration profiles could be interpreted as the result of only decay and sedimentation rate (Table 2; Figures 1-3). In 50 % of the cases a simple diffusion-like mixing coefficient addition was enough to better reproduce the observed data points. In 4 cores the addition of a non-local exchange parameter, injection of particles from the surface layer to a depth L, was necessary to improve the fitting of the observed activity profile. In only one instance, a more complex model was required to explain the observed data point (Arabian Sea Core; Geosec 413; table 2). In this latter case a subsurface layer is depicted of certain thickness $L \pm \delta x$, for the modeller this may suggest the result of homogeneously egested sediment by benthic organisms at this depth. This sediment core was collected using a gravity core of (10 cm OD). As it is shown in its porosity profile (Figure 4b) one can see that this particular core may have been

Station	best fit	$Sup.Flux_{mod3}$	Db_{mod3}	$Flux1_{mod3}$	$Flux2_{mod3}$	L_{mod3}	Db_{mod2}
South Med	Model 2	0.04	0.73	0.00	2.40	0.54	0.80
Dyfamed	Model 3	0.11	0.04	1.15	0.94	3.31	0.17
Geosecs 413	Model 4a	0.07	0.12	0.50	1.36	9.81	0.83
kara Sea 1	Model 3	0.05	0.03	0.20	1.43	3.20	2.44
kara Sea 7	Model 2	0.02	0.02	0.06	0.13	2.20	0.63
kara Sea 9	Model 2	0.00	1.39	0.34	0.96	5.79	4.32
kara Sea 13	Model 2	0.00	19.94	2.02	1.26	10.00	27.44
NW Pacific 6	Model 3	0.00	1.36	0.00	34.10	2.71	2.32
NW Pacific 8	Model 2	3.69	0.74	28.57	32.97	9.44	17.74
NW Pacific 9	Model 3	0.00	3.09	0.00	130.74	8.29	20.24

Table 2
Parameters calculated from the best-fitted models compared to the less complex model for each run. Supported.produtcion in $dpm.cm^{-3}.yr^{-1}$, Flux 1 and Flux 2 in $dpm.cm^{-2}.yr^{-1}$, Db in $cm^{-2}.yr^{-1}$, L in cm. Shaded area corresponds to best-fitted model's values.

affected by sampling and handling artefacts. In contrast, the cores collected using a box corer showed smooth porosity profiles as shown in Figure 4a. Thus, the feature depicted as a non-local exchange process by the model may be misleading. The inclusions of more complex models such as in model 4 and 5 (Soetaert *et al.*, 1996) were not adding any improvement in fitting the measured activity profiles. The shallower stations as expected, showed the highest bioturbation effects (model 2 and 3) in comparison with those from intermediate and deep water sediments. The mixing coefficients observed in the deep-sea sediments were slightly higher or similar to those observed at intermediate waters. This may suggests that at these particular places, mixing may be important while studying geochronology. However, the values are not high enough to have a real effect on other early diagenetic processes such as organic carbon decay constant estimations as it was shown in Mulsow *et al.* (1998) working on marginal sediment of the North East Atlantic coast.

In order to see if there was a relationship between Db and water depth, Db_{mode3} values were grouped by depth intervals in shallow stations (0-200 m), intermediate water depth stations (200-2500 m) and deep-sea stations (2500-6000 m) and plotted against water

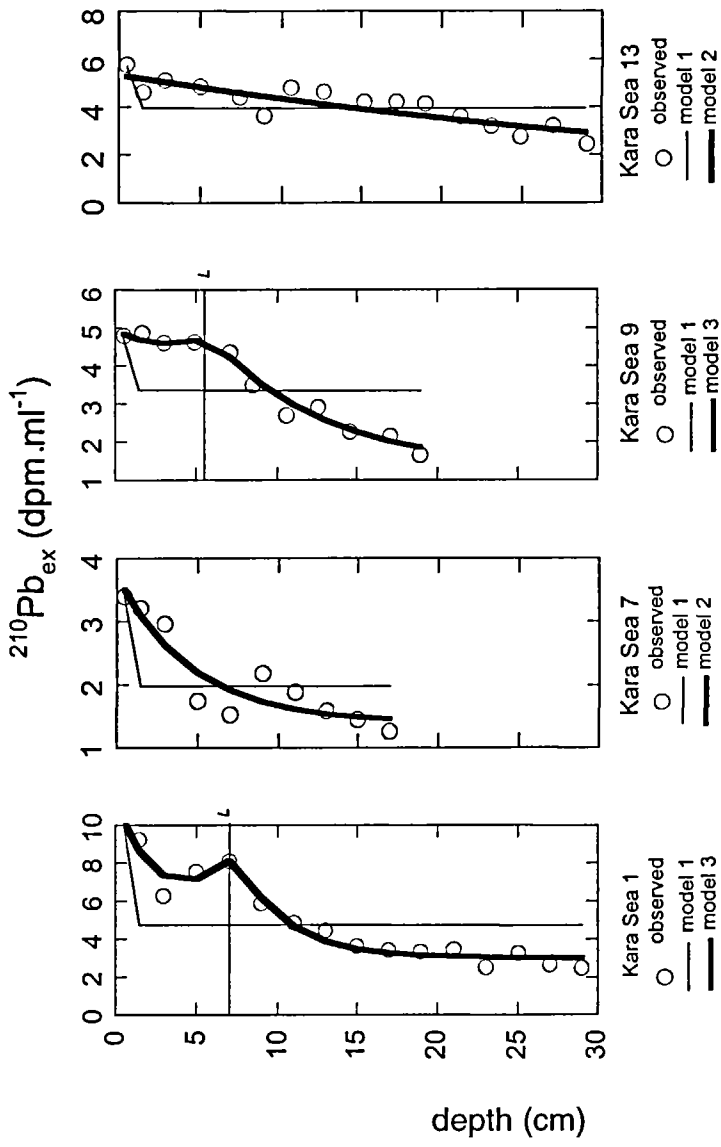

Figure 1
^{210}Pb-depth profiles observed compared to data expected from advection and decay only (model 1) and with the addition of bioturbation. Model 2: advection + diffusive mixing and Model 3: advection + diffusive +non-local mixing processes.

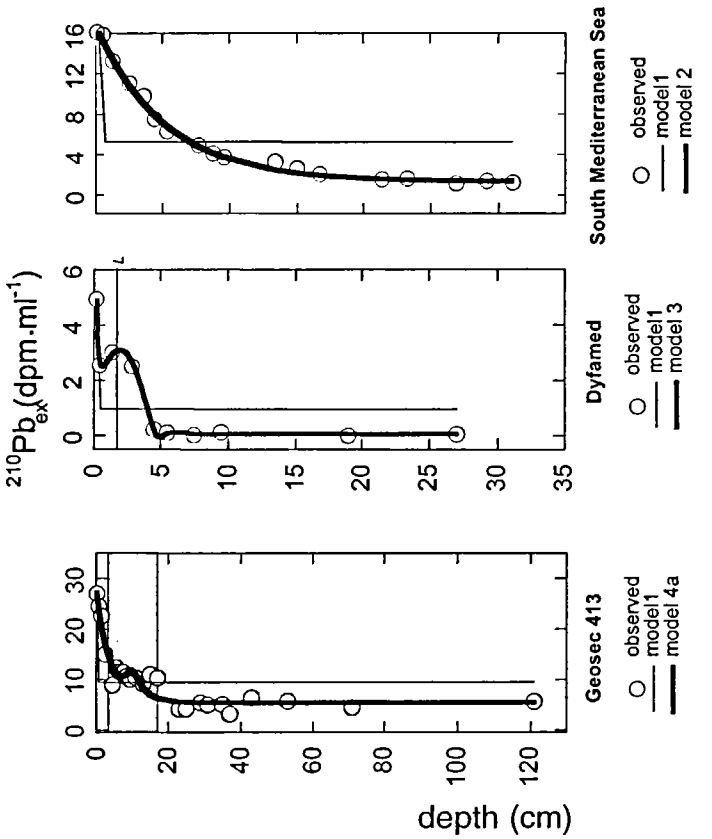

Figure 2
^{210}Pb-depth profiles observed compared to data expected from advection and decay only (model 1) and with the addition of bioturbation. Model 2 advection + diffusive mixing, Model 3: advection + diffusive +non-local mixing processes. Model 4a assumes that the flux injected is distributed homogeneously at depth (shaded area).

depth (Figure 5a). In general, the Db value decreased with depth as observed in other studies worldwide (Stoetaert *et al.*, 1996; Middelbourg *et al.*, 1997; Buffoni *et al.*, 1992). Although it is difficult to draw a conclusion with the few data point of this study, there is a clear tendency that the bioturbation influence decreases with

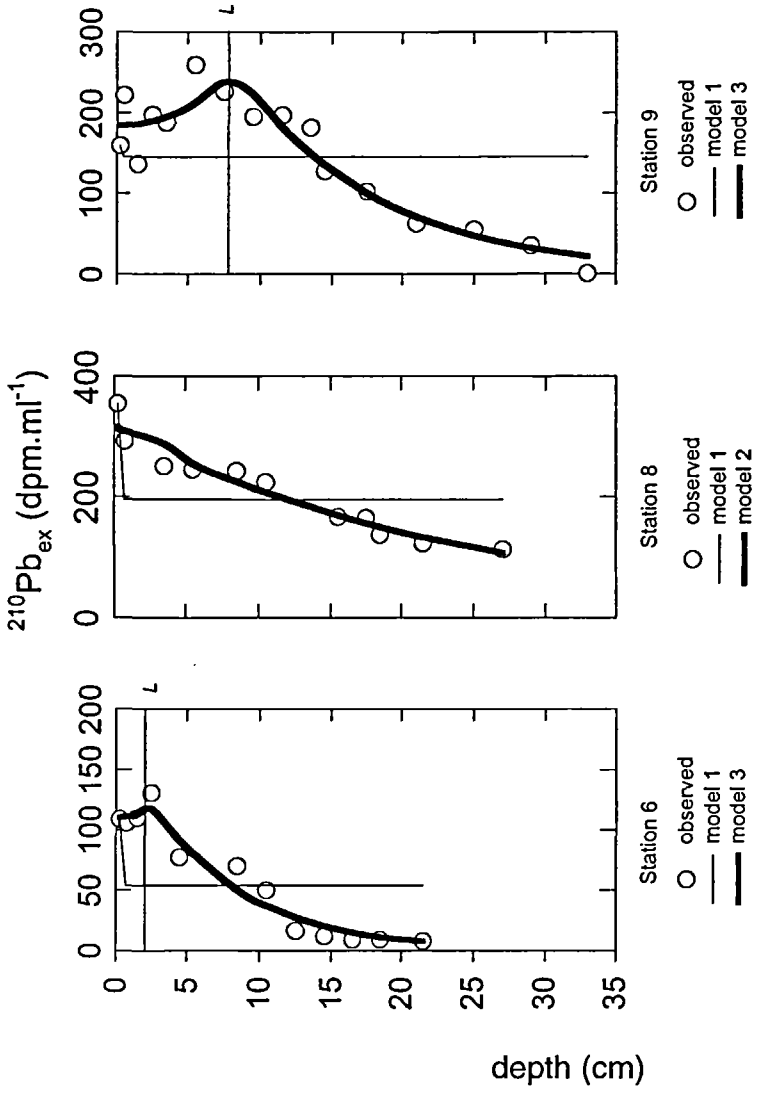

Figure 3
^{210}Pb-depth profiles observed compared to data expected from advection and decay only (model 1) and with the addition of bioturbation. Model 2 advection + diffusive mixing and Model 3: advection + diffusive +non-local mixing processes

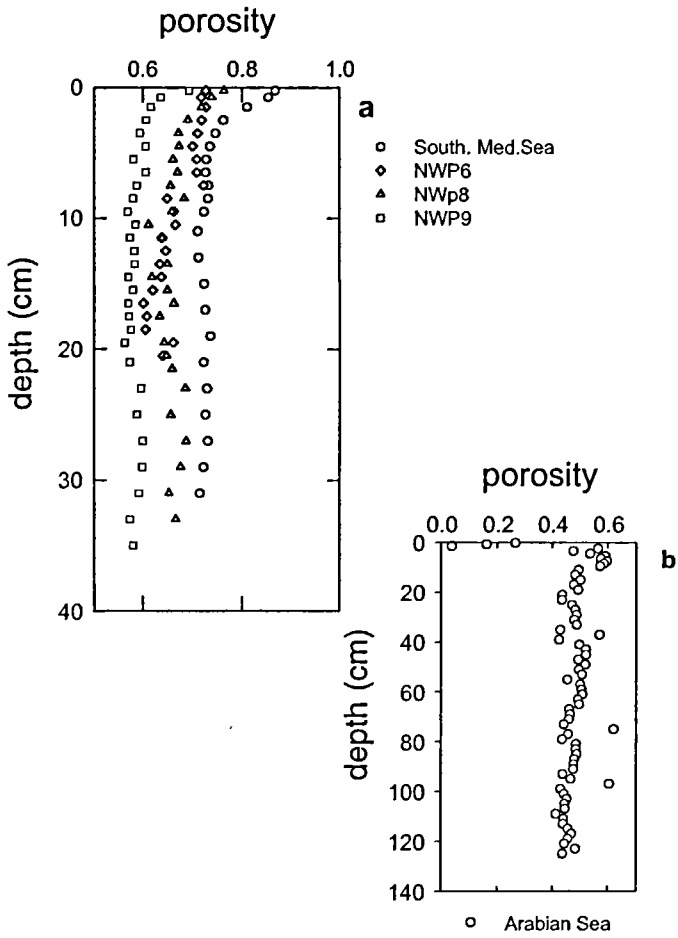

Figure 4
Sediment core porosity profiles. a) typical porosity-depth profiles observed in the studied sediments. b) Porosity profile of a sediment core collected with a gravity core.

increasing depth. Since in 40 % of the cases the best fit was obtained using Model 3, a plot of percentage of the injected flux from the total input of the tracer with depth will give and indication on how important non-local exchange processes are in the study sediments. The relationship is not clearly defined due to, in one hand, the few

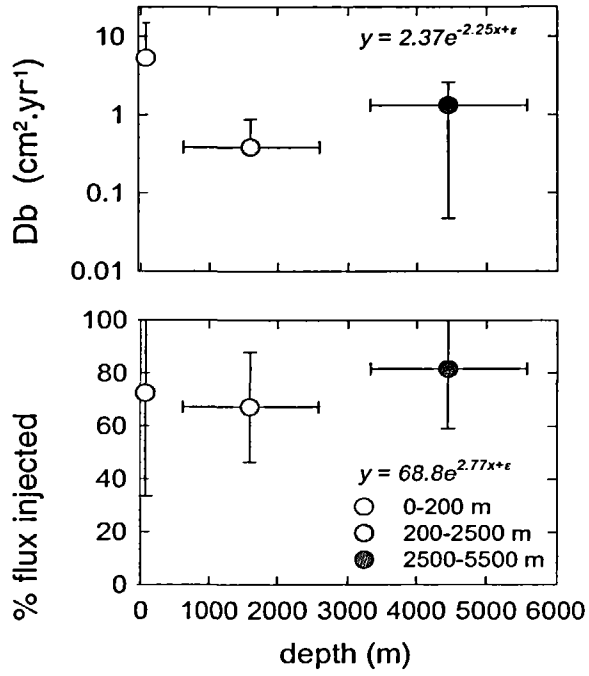

Figure 5
Estimated bioturbation coefficients and the percentage of the total flux which is directly injected into the sediments (flux 2), using model 3 parameters. The data were grouped by depth into shallow (white dot:10-200 m), mid depths (grey: 200-2800) and deep sea (dark grey: > 4000 m).

data available, and in other hand to perhaps a greater role of non-local exchange at those station from deep-sea, namely the Northwest Pacific's stations (Figure 5b). This may explain why in our study we found that the relation was opposite to bioturbation (Figure 5a). The sediment from the Northwest Pacific was very fine and in two stations, namely 8 and 9, they have an abundant cover of manganese nodules. Perhaps the turn over movement of nodules it is also a phenomenon that can increased the injection of younger sediment into the sediment column. In addition, at station 6, there was a two clearly distinctive facies with a contact at about 12 cm. The younger of them characterised by brown siliceous ooze and the older one by foraminifer ooze. We did not see any physical artefact

based on porosity profiles measured at each one of the stations as shown in Figure 1. Station 6 is also relatively close to Marshal Island region, thus perhaps physical mixing may be also playing a role in this diagenetic parameters.

Conclusion

In summary, none of the ^{210}Pb-depth profiles were better fitted if sedimentation rate and radioactive decay of the tracer was considered. Our finding agree with those found in the literature. Soetaert *et al.* (1996) found in marginal sediment cores that the ^{210}Pb profiles were best fitted using Db and non-local exchange mixing like in our case. However, in their study they clearly showed that Db decreased with depth, it is worth to mention that these authors analysed 16 cores and many of them seasonally. Two major conclusions can be drawn from our study. One of them is that the use of ^{210}Pb in geochronology is increasingly doubtful if only one tracer is used and no attempts to study systematically the effect of bioturbation. Secondly, it appears that mixing of tracers and therefore any other sediment bound particle, reaching the sediment-water interface at deep-sea ocean sediments are perhaps more affected by mixing (diffusive/non-local exchange) as previously thought. Smith *et al.* (1986) showed that when non-local exchange is included in the analyses of determining bioturbation rates they could be overestimated. It is clear that bioturbation in marine sediments during early diagenesis do play a quantitative role in the fate of sediment bound contaminants. From our study it is also clear that geochronology based uniquely on ^{210}Pb-depth profiles is not suitable for obtaining sound accumulation rate values. Although the models can depicted mixing processes (diffusive/non-local mixing) taking place in the sediment columns, the lack of knowledge on the actors (benthos) who mix solute and particles are often a major incognito. Perhaps, a different approach must be taken to bring some light to this uncoupling of sediment and biota. If one could model the feeding guild of a dominant group through time on a well define sediment column, the resulting profile of such an experiment may resemble those

found in our study. If this is possible then we can predict which feeding guild is responsible, for example, of a characteristic subsurface maxima peak often found on tracer-depth profiles and generally disregard as noise.

Bibliography

ALLER R. C., 1990 – Bioturbation and manganese cycling in hemipelagic sediments. *Phil. Transc.R.Soc.Lond.*, 331: 51-68.

BOUDREAU B., 1986a – Mathematics of tracer mixing in sediments: I spatially-dependent,diffusive mixing. *A.J.Sci.*, 286: 161-198.

BOUDREAU B., 1986b – Mathematics of tracer mixing in sediments: II non-local mixing and biological conveyor belt phenomena. *A.J.Sci.*, 286: 199-238.

BUFFONI G., DELFANTI R., PAPUCCI C., 1992 – Accumulation rates and mixing processes in the near-surface North Atlantic sediments: Evidence from C14and Pu-239-240 downcore profiles. *Mar.Geol.*, 109: 159-170.

DEMASTER D. J., HOPE R. H., LEVIN L. A., BLAIR N. E., 1994 – Biological mixing intensity and rates of organic carbon accumulation in North Carolina slope sediments. *Deep-sea Research*, 41: 735-753.

KADLEC R. H., ROBBINS J. A., 1984 – Sedimentation and sediment accretion in Michigan Coastal Wetlands (UAS), *Chem. Geol.*, 44: 119-150.

MIDDELBOURG J. L., SAETAERT K., HERMAN P. M. J., 1997 – Empirical relationships for use in global diagenetic models. *Deep-sea Research*, 44 (2): 327-344.

MULSOW S., BOUDREAU B., SMITH J. N., 1999 – Bioturbation and porosity gradients. *Limn. & Oceanogr.*, 43 (1): 1-9.

MULSOW, S., BOUDREAU B., SMITH J. N., 1998 – *Biological mixing models in the interpretation of ^{210}Pb sediment concentration profiles.* NSK-EKO-II. Helsinki, 1997: 1-8.

NITTROUER C. A., DEMASTER D. J., MCKEE B. A., CUTSHALL N. H., LARSEN I. L., 1983 – The effect of sediment mixing on ^{210}Pb accumulation rates for the Washington shelf. *Mar. Geol.*, 54: 201-221.

SMITH, J. N., BOUDREAU B. P., NOSHKIN V., 1986 – Plutonium and ^{210}Pb distributions in the Northeast Atlantic sediments: subsurface anomalies caused by non-local mixing. *Earth Planet. Sci. Lett.*, 81: 15-28.

SOETAERT K., HERMAN P. M. J., MIDDELBOURG J. L., HEIP G., DESTIGTER H. S., VAN WEERING T. C. E., EPPING E., HELDER W., 1996 – Modelling ^{210}Pb–derived mixing activity in ocean margin sediments: diffusive versus non-local mixing. *J.Mar. Res.*, 54: 1207-1227.

Advantages of combining ^{210}Pb and geochemical signature determinations in sediment record studies: application to coral reef lagoon environments

Jean-Michel Fernandez
Benjamin Moreton
Renaud Fichez
Ludovic Breau
Olivier Magand
Christian Badie

Introduction

During the past 150 years, terrestrial and coastal environments have been strongly modified by human activities. In the tropics, population growth and economic development imposed serious constraints on lagoon ecosystems (Hatcher *et al.*, 1989). Deforestation and mining, which are primarily responsible for hyper-sedimentation and metal pollution, are two of the major causes of disturbance in coral-lagoon environments (Carey, 1981; Naidu and Morrisson, 1994; Zan, 1994). Traces of these upheavals may be preserved in the sediment layers that gradually build up a memory of the various successive events affecting the environment.

Interpretation of these "sedimentary records" is mostly based on the dating of deposits, using natural timers such as radionuclides to establish a geochronology of sediment deposition. Most of the studies dealing with recent sedimentary records of environmental changes have been based on ^{210}Pb determinations, the decrease in unsupported ^{210}Pb permitting age determinations back to about 100 years (Faure, 1986). However, deciphering both the geochemical and sedimentological data collected from these layers is not always straightforward, with results often leading to misinterpretations due to a lack of converging information.

Four cores have been selected here to demonstrate that in most cases a combination of excess ^{210}Pb measurements, geochemical and sedimentary data is necessary to reach a solid interpretation of recorded environmental changes. This paper shows how excess ^{210}Pb values may be used to distinguish between real human effects and sampling errors or natural processes.

Materials and methods

Sediment cores were collected in the coral reef lagoons of New Caledonia and Fiji in the vicinity of Noumea and Suva towns (Table 1). Two cores were sampled in the New Caledonia Lagoon (Figure 1).The first core was taken adjacent to Noumea in Sainte Marie Bay (N12) and the second (M15) was extracted from the Dumbea sub-marine valley formed during the last glaciation, 20 000 years ago, when the sea level was roughly 120 m below present sea level. Sainte Marie Bay is a fairly enclosed system with two narrow passes connecting it to Boulari Bay in the northeast part, and the middle lagoon in the south part. The N12 core was extracted in an area where evidence of fine material deposition has been demonstrated (Dugas & Debenay, 1979, Chevillon unpublished results). Core M15 was extracted at the base of the northern slope of the submarine valley, close to the Dumbea pass.

In the lagoon of Fiji, two other cores were collected, in Suva Harbour (S14) and in Lauthala Bay (S31) (Figure 2). Suva Harbour is known to have experienced a large increase in industrial and urban developments in the coastal zone over the past 30-40 years. Lauthala Bay, where the other core was sampled, is a coral reef lagoon acting as a major recipient of the 2900 km^2 wide catchment area of the Rewa river.

Core	Geographical Coordinates	Depth (m)
N12	22° 17.66 E – 166° 27.74 S	13.5
M15	22° 18.25 E – 166° 15.69 S	45
S14	18° 07.34 E – 178° 24.78 S	18
S31	18° 08.89 E – 178° 28.66 S	11

Table 1
Geographical coordinates and collecting depths.

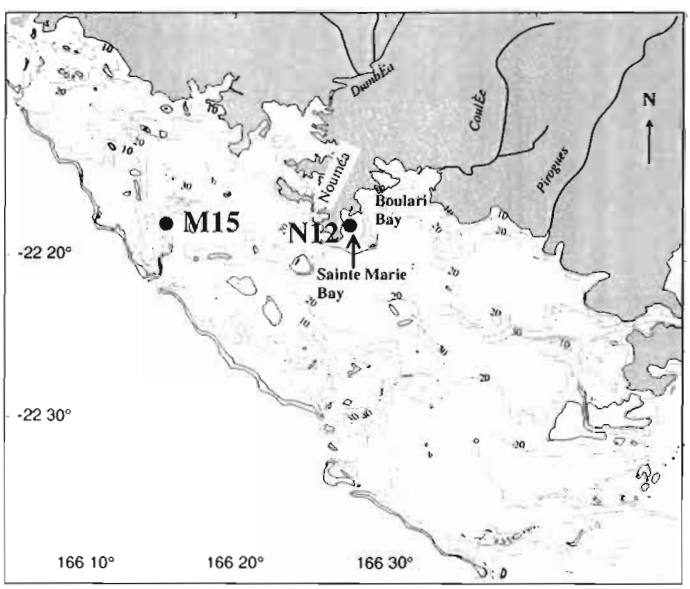

Figure 1
Sampling locations of sediment cores collected in the Noumea Lagoon, New Caledonia.

The sediment cores were sampled using a specially devised PVC corer operated by SCUBA divers (Harris *et al.*, 2001). The corer consisted of a 1.2 metre long PVC tube, 25 cm in diameter, which had been cut in half from top to bottom. The two halves were clamped together during coring and transportation to sustain the core until sampling. The corer was forced down into the sediment by hammering on a cap placed on the top of the corer to about half a meter deep. The sediment surrounding it was then pumped away until the bottom could be sealed with a second cap. The corer was then removed and kept vertical.

Once onboard the core was allowed to settle vertically, the top was then removed and the overlying water carefully pumped out. The first fluid layers were sampled using a spatula and the core was then laid horizontally and 2 cm slices taken for geochemical and sedimentalogical analysis. A sub-sample of each slice was used for ^{210}Pb measurements.

Finally, to obtain water content additional 10 ml sub-samples were taken and weighed before and after drying, in an oven at 110°C until constant weight. Results are expressed as a percentage of the initial sediment dry weight. This was subsequently used to calculate sediment accumulation in $g.cm^{-2}$.

The concentrations of three transition metals (Fe, Mn and Ni) were determined using a sequential extraction scheme (Tessier, 1979) on the pelitic (<40µm) fraction of the sample. The residual phase, primarily composed of terrigeneous material, was extracted with an acidic mixture ($HCl/HNO_3/HF$) in a high pressure vessels made of TFM (Anton Paar, MF100) and subject to micro-wave exposure in an Anton Paar Multiwave. Metals were analysed by ICP-OES (Perkin-Elmer, 3300DV model). Results are expressed in *absolute concentration* ($mg.g^{-1}$ extracted from the residual phase per mass unit of pelitic fraction) and *relative concentrations* ($mg.g^{-1}$ extracted from the residual phase per unit mass of residual phase).

Geochronology was defined using ^{210}Pb activity determined indirectly by measuring alpha emission from its granddaughter isotope ^{210}Po. Each sample was spiked with ^{208}Po in order to appraise possible losses incurred during application of the digestion protocol. The ^{210}Po measurement was performed in a NUMELEC gridded-chamber (NU 114B model) by alpha counting.

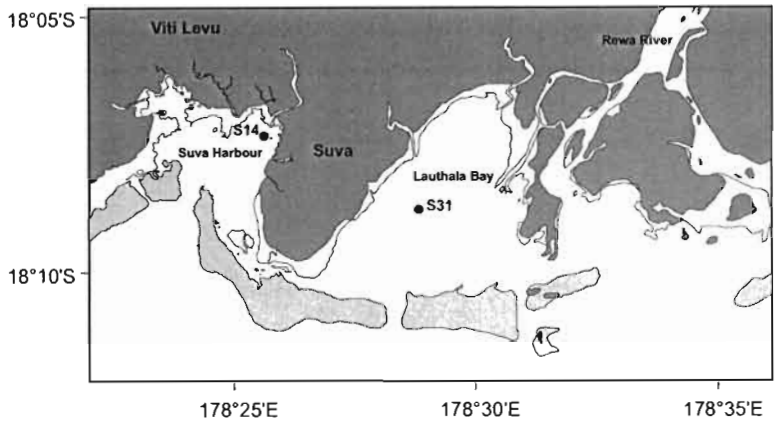

Figure 2
Sampling locations of sediment cores collected in the Suva Lagoon, Fiji.

Direct ^{210}Pb determination using gamma spectrometry at the 46.54 keV, was also conducted on the two Fijian cores. These measurements were carried out on an ORTEC X beryllium window Diode with a relative efficiency of 80%. The unsupported ^{210}Pb results were subsequently plotted for the 4 cores.

Results and discussion

The Lauthala Bay S31 core (Figure 3) core is one example where the data shows linear concentration profiles of Mn and Ni, in both relative and absolute values, indicating a regular supply in particulate matter (Schneider *et al.*, 1995). The ^{210}Pb measurements demonstrated the existence of a limited bioturbation layer extending down to 10 cm (5 g.cm^{-2}) as most commonly reported world-wide (Boudreau, 1998). Below 10 cm (5 g.cm^{-2}), a very good fit can be observed between the data and a "log (excess ^{210}Pb) vs. sediment

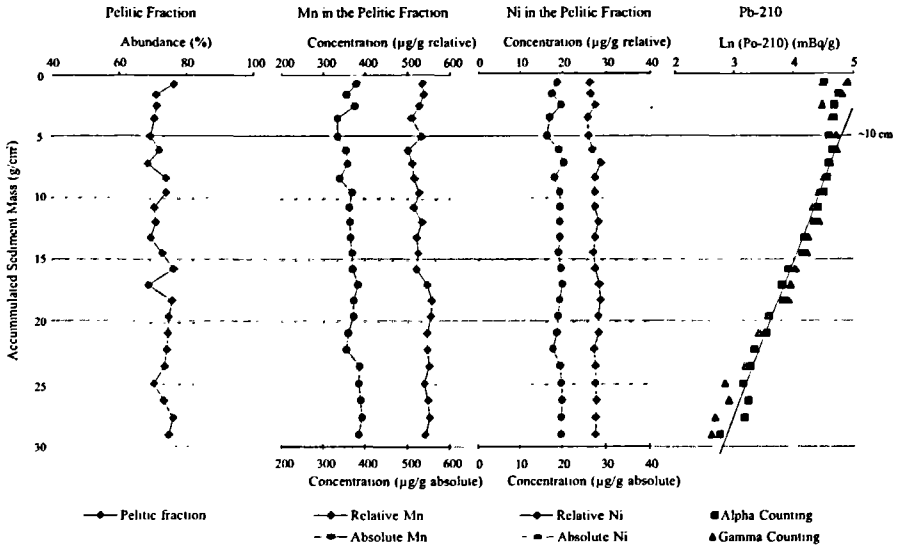

Figure 3
Physical, geochemical and ^{210}Pb profiles for the core S31, Luthala Bay, Fiji.

accumulation" regression giving an estimated accumulation rate of 0.39 $g.cm^{-2}.yr^{-1}$. In this very unambiguous case the excess ^{210}Pb and geochemical variables profiles converged to indicate that no changes in sediment deposition regime occurred during the last century and that sediment dating could be inferred from excess ^{210}Pb. This conclusion is consistent with other results demonstrating that the Rewa River basin experienced very little change during the recent past (Shorten, 1993).

In core S14 (Figure 4) a constant reduction in Ni concentrations down the core can be observed, in both relative and absolute values, together with a continuous increase in Mn between 0 and 33cm depth (0 and 17.5 $g.cm^{-2}$). Below 33 cm (17.5 $g.cm^{-2}$) a sharp increase in Ni and decrease in Mn was recorded in the deeper layers. The highest Ni and lowest Mn values measured in these deeper layers were equivalent to those measured in the two first centimetres of the core. This global trend was similarly marked when con-

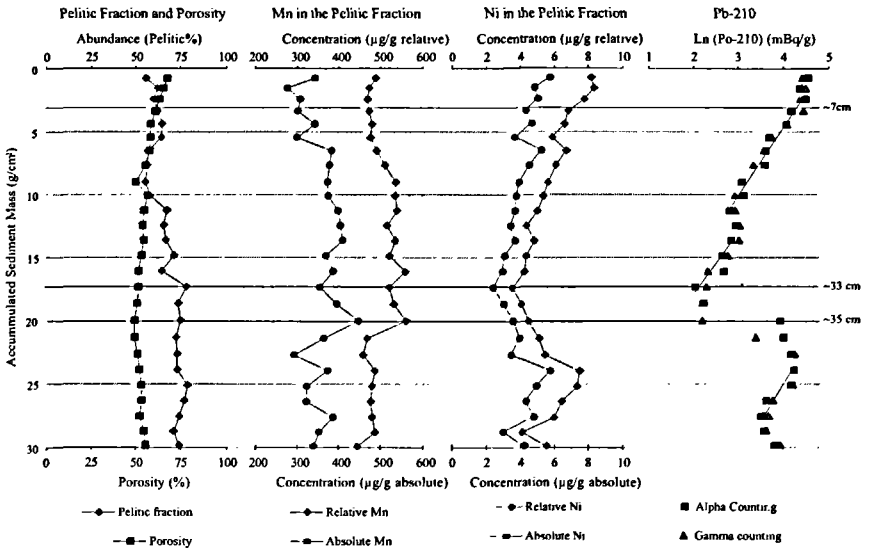

I Figure 4
Physical, geochemical and ^{210}Pb profiles for the core S14, Suva Harbour, Fiji.

sidering other transition metals profiles, leading to the hypothesis that major changes in particle supply occurred in the past over a short time period.

The excess ^{210}Pb profiles indicated that the main bioturbation layer did not extend beyond 6-8 cm (3-4 g.cm^{-2}). Excess ^{210}Pb activity exponentially decreased with depth down to 35 cm (20 g.cm^{-2}), where a strong anomaly was observed. At this depth, a strong increase in excess ^{210}Pb was recorded with values of a similar magnitude to those recorded in the top layers. This profile clearly indicated that the sediments in core S14 were not chronologically deposited and that the observed change at 35 cm (20 g.cm^{-2}), was most likely a result of an artificial disturbance of the sedimentary column. This interpretation was further sustained by the documented absence of drastic changes in sediment supply in the Suva Harbour during the early Holocene (Shorten, 1993).

Sample preparation for ^{210}Po alpha counting was the first potential source of error to be considered. Additional direct gamma spec-

trometry ^{210}Pb provided results consistent with alpha determination therefore ruling out analytical failure. Furthermore, ^{234}Th and ^{137}Cs activity profiles were also strongly consistent with the distribution pattern of ^{210}Pb. An increase in water content was also observed in the last 15 cm together with a change in mud colour from black to brown. These discrepancies reinforced the hypothesis of non-chronological sediment deposition.

Two hypotheses were suggested to explain the profiles. The first one, was based on the consideration that the sampling site was located next to the commercial port of Suva where ships are often anchored before berthing. The traction pull of an anchor may have led to the displacement of a sediment layer and its subsequent deposition on top of adjacent unaltered sediments, therefore resulting in the occurrence of two similar sedimentary interfaces in a single vertical sediment column. Even though this occurrence cannot be fully dismissed it seems unlikely that the displacement of such a sediment layer would occur without significant reworking. On the contrary the ^{210}Pb and the metal profiles show a superposition of two well-stratified layers. The second hypothesis arosed from the fact that divers had experienced some problems while removing the core from the sediment bed. During this process the core, once extracted, was momentarily settled on the bottom before bringing it back to the surface and during this period it is possible that the bottom stopper of the corer was not in place. In such a situation and considering that the upper layers of the sediment were mainly composed of fluid mud, the corer by its own weight might have sampled again a 15 cm thick section of surface sediment. This scenario, resulting in the occurrence of two similar overlaying sediment sections, appears the most likely explanation to account for the almost perfectly mirrored distribution of all sediment parameters studied. Whatever the interpretation, the bottom layer was dismissed as an artefact and the 0 to 35 cm depth (0 to 20 $g.cm^{-2}$) layer being solely useable to study sediment geochronology. In this layer the maximum accumulation rate calculated from the slope of the regression fit was 0.17 $g.cm^{-2}.yr^{-1}$.

The M15 core produced specific profiles (Figure 5); the pelitic fraction together with absolute and relative Mn and Ni concentrations core showed a relatively constant pattern between 25 and 42 cm depth (14 to 24 $g.cm^{-2}$). This trend demonstrates the sediments to be

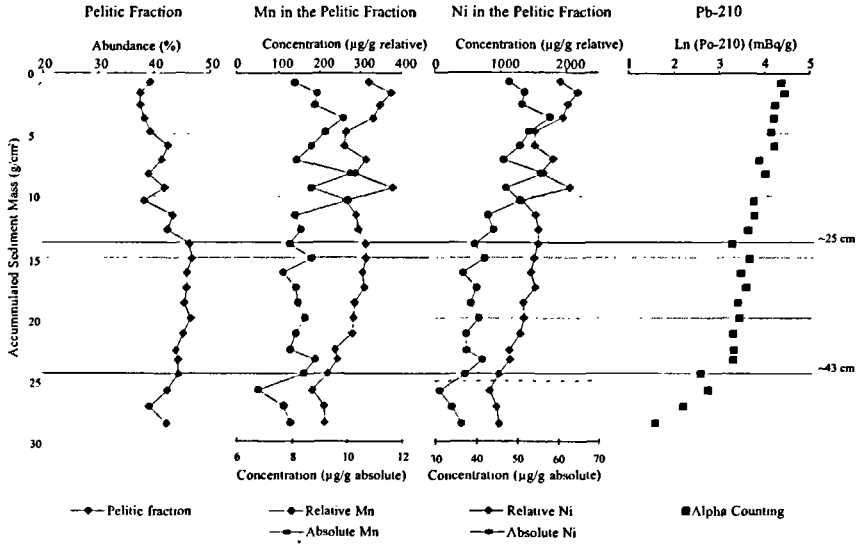

Figure 5
Physical, geochemical and ^{210}Pb profiles for the core M15, Dumbea canyon, New Caledonia.

fairly homogeneous over more than 18 cm section of the core. The unsupported ^{210}Pb profile display a very regular and slow decrease in activity with depth, down to 43 cm (24 g.cm^{-2}), followed by a rapid decrease below. In the upper layer, strong bioturbation is not evidenced as no homogeneous layer is observed.

A first analysis of the ^{210}Pb profile suggests a strong change in sediment deposition rate occurred at 43 cm depth. Considering this scenario, the corresponding sediment accumulation rates would have increase sharply from 0.11 g.cm^{-2}.yr^{-1} below 43 cm depth to 0.56 g.cm^{-2}.yr^{-1} in the upper layer and the age of change could be dated at around the year 1952.

A second interpretation of this data might be proposed based on the location of the sampling site. The core was sampled at 55 m depth in a submarine canyon that is delimited by steep slopes extending through a lagoon area with an average depth of 22 m. The canyon, formed by river erosion during the last low sea-level period, is now progressively filling up with sediments imported from the adjacent

and shallower lagoon bottoms. Under such conditions sediment slumps are a very likely occurrence and the presence of a very homogeneous 18 cm thick sediment layer in the middle of the core could be attributed to such an event. Similar homogeneous geochemical signatures have been documented in deposits resulting from sediment slides (Monaco *et al.*, 1982).

Interpretation of this core therefore calls for additional information which could be obtained from the study of grain size distribution throughout the core as slumps are known to cause gravimetric grain size sorting (Mear, 1984).

From the bottom to the top of the core, the pelitic fraction and the absolute Fe concentrations of the sieved sample increase in parallel with a corresponding decrease in carbonates. The Ni concentration profile clearly identifies a drastic change in the amount of the terrigeneous inputs, with a sharp increase in both absolute and relative concentrations between 12 and 11 $g.cm^{-2}$ corresponding to 31 and 30 cm depth, respectively.

The beginning of the ^{210}Pb profile of the N12 core indicates a large layer of almost invariable activities between 0 and 20 cm (0 to 7 $g.cm^{-2}$) reflecting intense bioturbation processes and/or large accumulation rates (Figure 6). The magnitude of this phenomena makes any interpretation difficult, particularly when considering the unsupported ^{210}Pb data alone. Below 20 cm (7 $g.cm^{-2}$), excess ^{210}Pb activity decreases roughly exponentially but using a single linear fit for the whole data set resulted in a poor regression fit. When comparing ^{210}Pb and metal data it appears possible to propose an environmental change scenario compatible with the ^{210}Pb profile. There is a clear shift in sediment composition and especially in Ni concentrations at 30 cm depth (11 $g.cm^{-2}$) which is very likely to be associated with change in deposition regime. Hence, the linear fit calculated for the ^{210}Pb data below 30 cm (11 $g.cm^{-2}$) was not extended to the above layer and another fit was drawn between 30 and 20 cm (11 and 7 $g.cm^{-2}$). Two regression lines were calculated for the ^{210}Pb distribution yielding different sediment accumulation rates and allowing this major environmental change to be dated at 1952 +/- 5 years.

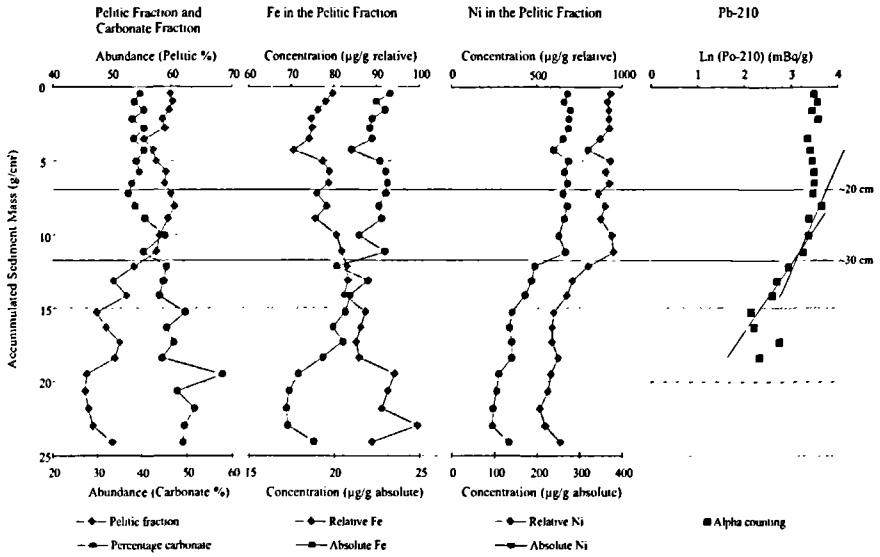

I Figure 6
Physical, geochemical and ^{210}Pb profiles for the core N12, Sainte Marie Bay, New Caledonia.

Despite large uncertainties regarding the calculation, the proposed date of sedimentation change corresponded with the beginning of large scale and extensive open-cast mining activities in the Southern part of New Caledonia (Bird *et al.*, 1984; Mermoud, 1994). Those past activities were responsible for the long term erosion of soils with the lagoon acting as a final reservoir of all eroded land material. The influence of the mining exploitation has also been clearly recorded in another core taken from the Dumbea Bay (Ambatsian, 1997), a Bay where sedimentation mechanisms have been widely studied in the past (Launay, 1972). The values from both Bays present converging results regarding the decrease in excess ^{210}Pb with sediment depth. Unlike Dumbéa Bay, Sainte-Marie Bay where our N12 core was sampled is not directly under the influence of river inputs, the nearest estuary being 11 km away, indicating that additional terrigeneous inputs related to poor mining practice affected the coastal zone on a large scale.

Conclusion

Most of the sediment cores we have been dealing with are not as easily interpreted as core S31. This relatively rare case seems to present the ideal conditions regarding particle supply and biological mixing to obtain reliable estimate of accumulation rates (consistent and constant particulate matter inputs and a reduced bioturbation layer) and therefore of dating. In sedimentary deposits subject to various sources of perturbation including the impact of the human activities, the combination of excess ^{210}Pb with geochemical data can provide necessary additional information to allow for a proper interpretation of sediment deposition processes.

Aknowledgements
This work was part of a research project financially supported by IRD and the French "Programme National Environnement Côtier" (PNEC).

Bibliography

AMBATSIAN P., FERNEX F., BERNAT M., PARRON C., LECOLLE J., 1997 – High metal inputs to closed seas: the New Caledonian Lagoon. *Journal of Geochemical Exploration.*, 59: 59-74.

BOUDREAU B.P., 1998 – Mean mixed depth of sediments: The wherefore and the why. *Limnol. Oceanogr.*, 43: 524-526.

BIRD E. C., DUBOIS J-P., ILTIS J. A., 1984 – *The impacts of opencast mining on the rivers and coasts of New Caledonia.* The United Nations University, NRTS-25 / UNUP-505, ISBN 92-808-0505-5, 53 p.

CAREY J., 1981 – Nickel minning and raffinery wastes in Coral Sea environs. *In: Proceed. 4th Intern. Coral Reef Symp., Manila,* 1: 137-146.

DUGAS F., DEBENAY J.-P., 1979 – Carte sédimentologique et carte annexe au 1/50 000e de Nouvelle-Calédonie. Orstom. Bondy.

FAURE G., 1986 – *Principles of isotope geology.* Wiley & Sons, New York, 374 p.

HARRIS P., FICHEZ R., FERNANDEZ J. M., GOLTERMAN H.L., BADIE C., 2001 – Phosphorus enrichment in the Papeete Lagoon (Tahiti, French Poynesia): using sediment geochronology to reconstruct the evolution of phosphorus inputs during the past century. *Oceanologica Acta*, 24: 1-10.

HATCHER B. G., JOHANNES R. E., ROBERTSON A. I., 1989 – Review of research relevant to the conservation of shallow tropical marine ecosystems. *Oceanogr. Mar. Biol. Annu. Rev.*, 27: 337-414.

LAUNAY J., 1972 – La sédimentation en baie de Dumbéa (Côte ouest - Nouvelle-Caledonie), *Cah. Orstom, ér. Géol.*, IV (1) : 25-51.

MEAR Y., 1984 – Séquences et unités sédimentaires du glacis rhodanien (Méditerranée occidentale). Thesis., University of Perpignan, 214 p.

MONACO A., ALOISI J. C., BOUYÉ C., GOT H., MEAR Y., BELLAICHE G., DROZ L., MIRABILE L., MATTIELO L., MALDONADO A., LE CALVEZ Y., CHASSEFIÈRE B., NELSON H., 1982 – Essai de reconstitution des mécanismes d'alimentation des éventails sédimentaires profonds de l'Ebre et du Rhône. *Bulletin de l'Institut de Géologie du Bassin d'Aquitaine*, 31 : 99-109.

NAIDU S. D., MORRISON R. J., 1994 – Contamination of Suva Habour, Fiji. *Mar. Poll. Bull Special Issue.*, 29: 52-61.

MERMOUD Y., 1994 – Processus de dégradation du milieu naturel dans le bassin versant de la Rivière des Pirogues. *Mémoire de Licence, Université française du Pacifique, centre de Nouméa.*

SCHNEIDER W., SCHMELZER I., WURTZ J., 1995 – *Sedimentoogical interplay of siliciclastic Rewa river input and organic carbonate production of the Suva barrier reef, Laucala Bay, Fiji.* Technical Report, Marine Studies 95/4, The University of the South Pacific eds, 12 p.

SHORTEN G. G., 1993 – Stratigraphy, sedimentology and engineering aspects of Holocene organo-calcareous silts, Suva Harbour, Fiji. *Marine Geology.*, 110: 275-302.

TESSIER, A., CAMPBELL P. G. C., BISSON M., 1979 – Sequential procedure for the speciation of particulate trace metals. *Analitycal Chemistry.*, 51: 844-851.

ZAN L. P., 1994 – The status of coral reefs in south western Pacific islands. *Mar. Poll. Bull Special Issue.*, 29: 52-61.

Concentrations of heavy metals and trace elements in the marine sediments of the Suva Lagoon, Fiji

Sitaram Garimella

Alastair McArthur

Marie Ferland

Oswin Snehaleela

Introduction

The Suva Lagoon (which includes the Suva Harbour and the Laucala Bay) is located in the south-east of Viti Levu, the largest of the Fiji islands. The lagoon is sheltered from the Pacific Ocean by a series of barrier reefs (Figure 1) which are submerged at high tide. Seawater enters the lagoon twice a day mainly through the harbour entrance and the Nukulau and the Nukubuco passages. Freshwater enters the lagoon predominantly through the Rewa river and to a lesser extent through the Tamavuva, Lami, Vatuwaqa and the Nasinu rivers. The Rewa river continuously brings a large volume of sediment into the Laucala Bay with the load increasing significantly during periods of heavy rain (Kyaw, 1982). The annual rainfall in the region is about 3000 mm and for most of the year the south-east trade winds prevail. The turbidity levels in the bay are high throughout the year.

There is considerable industrial and commercial activity in the Suva region (consisting the Lami town, Suva City and Nasinu town)

which has a population of about 170,000. The Suva Harbour is surrounded by two major industrial zones which contain shipyards, manufacturing plants, oil storage depots, food processing industries, and the Lami rubbish dump is located on the edge of the waterline. Two sewage treatment plants are located close to the Laucala Bay. A major plant at Kinoya discharges effluents directly into the bay via an outfall pipe 800 m offshore. A minor plant at Raiwaqa discharges into the Vatuwaqa river. Another rubbish dump is located along the Rewa river at Nausori town (not shown in the figure). Two minor industrial zones (at Vatuwaqa and Laucala Beach Estate) are also active around the Laucala Bay. These activities inevitably lead to the discharge of pollutants into the lagoon. According to Naidu and Morrison (1994), much of Suva is located on marl which does not allow septic tank effluents to seep into the ground. Most seepages move into the numerous creeks that discharge into the Suva Lagoon. Further, many storm water drains transport litter from the streets into the lagoon during periods of heavy rain.

A few studies have been done on contamination of the Suva Lagoon. Naidu *et al.* (1991) measured major sewage related contaminants, while Stewart and de Mora (1992) and Maata (1997) found high levels of TBT in the sediment of the Suva harbour. Using chemical methods, Narayan (1993) measured heavy metals in the sediment and shellfish of the Laucala Bay, while Naidu and Morrison (1994) measured the same in parts of the Suva Harbour (close to the Lami dump and the battery factory). Tabudravu (1995) measured Zn, Pb and Cu in sediments collected from the coastal waters of Lami.

The present study aimed to measure the concentration of heavy metals, as well as other trace elements, in sediments from the entire Suva Lagoon. Sediment samples were collected from a wide range of sites (Figure 2) such that the entire lagoon was well represented in terms of environment (shipping channel,reef and the harbour), water depth (range 1-66 m), likely sources of pollution input (industrial areas, shipyards, seafront hotels, Lami dump, sewage treatment plants outfalls) and rivers entrances (the Rewa, Nasinu, Samabula, Vatuwaqa, Tamavuva and Lami rivers). This is also the first major environmental study (in the Suva region) in which the nuclear technique of instrumental neutron activation analysis (INAA) has been used to determine elemental concentrations.

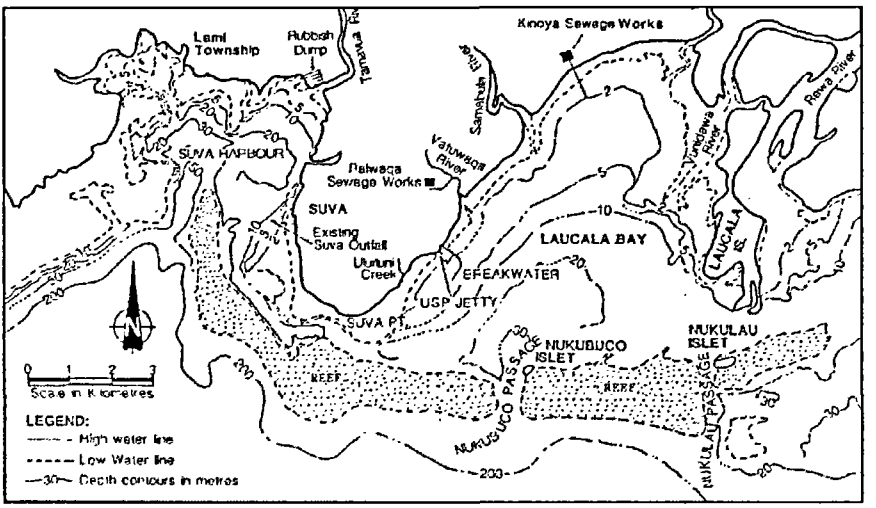

Figure 1
Map of the Suva Lagoon (Naidu *et al.*, 1991).

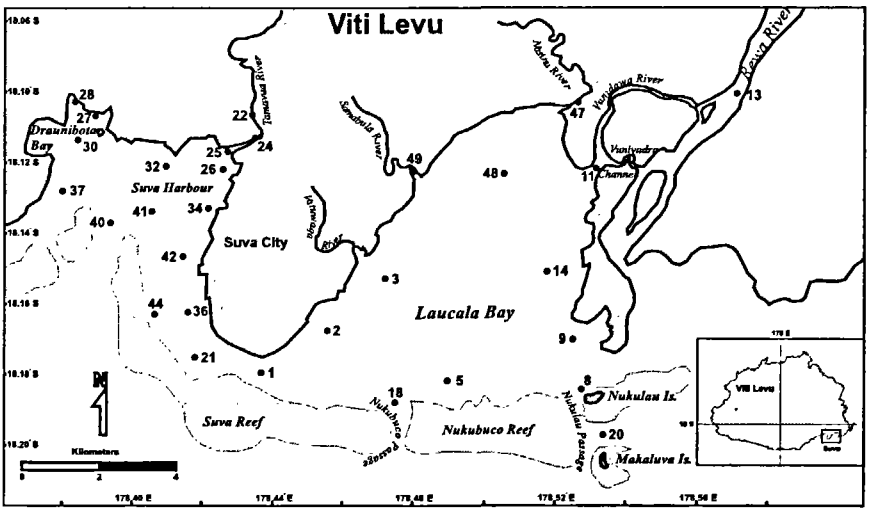

Figure 2
Suva Lagoon with the sampling sites (latitudes and longitudes in decimal notation).

Materials and methods

Method of INAA

In INAA, the irradiation of a multi-element sample with thermal neutrons produces radionuclides with long half-lives. The sample can then be transferred to a counting room for analysis of the induced radioactivity. The radionuclides are identified by their characteristic gamma-ray energies. The elemental abundances can be calculated from the measured activities, nuclear data and the irradiation conditions. Details of the method are described fully by Landsberger (1994), De Soete *et al.* (1972) and Adams and Dams (1970).

To eliminate possible errors in some of the nuclear data (gamma-ray transition probabilities and thermal neutron cross-sections) and irradiation conditions (constancy of irradiation flux over long irradiation periods), elemental abundances were determined by the comparator method. In this method, a 'standard' sample (of known elemental concentrations) and an unknown sample are stacked together and irradiated. Later, the two samples were analysed in the counting room, one after the other, under identical conditions by the same detector. The ratio of the number of gamma-rays counted in each sample for any given radioisotope (normalised to the same sample mass and after correction for the decay of the radionuclide due to delay time) is equal to the ratio of their respective elemental abundances. The accuracy of this method depends mainly on the counting statistics when a *good* standard is chosen, i.e. when its elemental abundances are known accurately.

Sample preparation and irradiation

Sediments were collected from 49 sites (Figure 2) by means of a grab sampler from a boat. Thirty of these sites were then selected for sediment analysis. All samples were dried and ground to a fine homogeneous powder. One aliquot of each was accurately weighed (about 100 mg) into clean polythene bags (12 x 12 mm) and heat sealed.

Each sample bag was then sealed into another polythene bag as a precaution. Three *United States Geological Survey* standards AGV-1 (andesite, four aliquots), RGM-1 (rheolite, two) and STM-1 (syenite, one) and two *Community Bureau of Reference* standards CRM-38 (flyash, one) and BCR-176 (citywaste, one) were similarly prepared. The standards and the sediments were put together into two stacks, with one aliquot of AGV-1 at the ends of each stack (to permit correction for the neutron flux gradient during irradiation). The stacks were then loaded into separate aluminium irradiation cans. Since Fiji does not have its own nuclear reactor, the samples were irradiated in a reactor of the *Australian Nuclear Science and Technology Organisation*, for 4.0 h at a thermal neutron flux of 4×10^{12} $cm^{-2}.s^{-1}$. The irradiated samples were allowed to cool for 5 d, and were flown back to Suva for analysis using a hyperpure germanium (HPGe) gamma-ray spectrometer (efficiency 24.5% and resolution 1.84 keV).

Measurements

The concentrations of 25 elements were measured in each of the 30 sediment samples using the nuclear data provided by Landsberger (1994). The activation products were identified by their characteristic gamma energies and were also confirmed later by their half-lives. The measurements on each sample were repeated one or more number of times, to ensure reproducibility of the data as well as to decrease the counting errors.

The first set of measurements was carried out immediately after the irradiated samples arrived in Suva. A gamma-ray spectrum for each sample was taken over a period of 4000 s. From this set, the short-lived radionuclides ($T_{1/2} < 7$ days) were analysed and the concentrations of As, Br, La, Lu, Mo, Na, Sb, Sm and U in the samples were determined.

A second set of measurements was carried out after about a cooling period of 3-4 weeks. A gamma-ray spectrum for each sample was taken over a period of 6000 s. In this set, the activities of the short-lived nuclides are practically absent and, therefore, the long-lived nuclides could be more accurately measured. From these measurements, the concentrations of Ce, Co, Cr, Cs, Eu, Fe, Hf, Hg, Nd, Rb, Sc, Sr, Ta, Tb, Th, Yb, Zn and Zr were determined.

Results

Table 1 presents the calculated concentrations of 25 elements present in the sediments from 4 sites in the Suva Lagoon. Two of these 4 sites (26 and 48) are likely to be fairly polluted. In order to check the accu-

Element	AGV-1*	RGM-1		Yacht Moorings SH26	Harbour Centre SH41	Off VatuwaqaRiver LB3	Kinoya Sewage Outfall LB48
		Measured	Ref.†				
As	0.88	2.3 ± 0.2	3.0	21	12	18	16
Br				22	32	14	32
Ce	67	44 ± 7	47	11.7	10.6	18.4	21.7
Co	15.3	2.0 ± 0.1	2.0	21	10	21	23
Cr	10.1	6.4 ± 1.5	3.7	48	33	88	64
Cs	1.3	11 ± 2	9.6	NP	NP	NP	NP
Eu	1.64	0.62 ± 0.02	0.66	1.30	0.60	1.30	1.20
Fe (%)	4.74	1.2 ± 0.3	1.3	7.1	3.6	5.8	6.8
Hf	5.1	5.6 ± 0.8	6.2	2.0	1.5	2.9	2.7
Hg	**	NP	0.02	0.7	0.6	NP	0.4
La	38	23.4 ± 0.6	24	5.6	4.4	9.9	8.8
Mo	2.7	7.3 ± 6.2	2.3	NP	0.7 ± 0.5	NP	NP
Na (%)	3.2	3.1 ± 0.1	3.05	1.7	1.9	2.1	3.0
Nd	33	17 ± 8	19	ND	ND	ND	ND
Rb	67.3	136 ± 38	149	NP	NP	NP	NP
Sb	4.3	1.3 ± 0.2	1.3	NP	NP	NP	NP
Sc	12.2	4.6 ± 0.6	4.4	31	16	24	28
Sm	5.9	4.1 ± 0.1	4.3	3.4	2.0	3.1	3.6
Sr	662	112 ± 21	108	NP	3155	369	NP
Ta	0.90	0.9 ± 0.3	0.95	ND	ND	ND	ND
Tb	0.70	0.7 ± 0.5	0.66	0.6	ND	0.5	0.6
Th	6.5	14 ± 2	15.1	0.4	0.4	1.1	1.0
Yb	1.72	2.5 ± 0.3	2.6	2.7	1.4	2.4	2.5
Zn	88	28 ± 15	32	219	111	122	149
Zr	227	257 ± 44	219	NP	NP	NP	NP

* used as standard. ND - not determined. NP - No peak observed.

** BCR-176 used as standard. † Govindaraju (1994)

Table 1
Concentrations of trace elements (ppm) measured in USGS standard RGM-1 and in four sediments of the Suva Lagoon.

racy and reliability of our analyses, the concentrations of these elements were also calculated for standards RGM-1, STM-1, CRM-38 and BCR-176, treating them as unknowns. As an illustration, the results thus obtained, together with counting errors (one standard deviation only), for RGM-1 are shown in Table 1 and compared with reference values (Govindaraju, 1994). The agreement (measured versus reference value) is generally good.

Table 2 shows calculated concentrations of some environmentally important elements (As, Cr, Fe, Hg, Zn and Sb) in all 30 sediments samples.

Discussion

The elemental concentrations reported in Table 2, were compared with the Environmental Protection Agency (EPA) Guidelines for Pollution Classification, and with the USGS Sediment Alert Levels (Batley, 1992). The EPA pollution guidelines prescribe margin concentration values, above which the element is said to be a pollutant in the environment. The USGS Alert Levels are concentrations above which the element could pose a threat to the ecosystem and its components. The status of heavy metal pollution in the lagoon will now be considered.

Arsenic

At most sites in the Suva Lagoon, the level of As is 3-7 times the EPA level. The highest level of As reported here, about 20 ppm, was observed near the Lami dump, near some seafront hotels in the Lami town, and at the two sewage treatment outflows. In comparison, Naidu and Morrison (1994) measured As levels of 27-45 ppm at sites close to the Lami dump, and 3-6 ppm at sites within 100 m of the dump (most of these sites have water depths less than 5 m). The fairly high levels of As reported in the present work at locations farther away from the dump indicate a general increase in As levels since 1994.

Site	As	Cr	Fe (%)	Hg	Zn	Sb
LB1	ND	41	2.5	NP	59	NP
LB2	14	160	4.9	NP	95	NP
LB3	18	88	5.8	NP	122	NP
LB5	21	38	4	0.3	84	NP
LB8	16	60	6.4	NP	136	NP
LB9	ND	75	11	NP	138	NP
LB11	ND	73	6.3	NP	135	NP
LB13	ND	198	6.7	NP	95	NP
LB14	ND	79	6.6	NP	138	NP
LB18	ND	20	1.5	NP	33	NP
LB20	16	69	5.8	0.3	128	NP
LB21	ND	26	1.3	NP	32	NP
LB47	19	89	7.3	0.55	172	NP
LB48	16	64	6.8	0.36	149	NP
LB49	18	78	6	0.7	188	0.49
SH22	ND	44	8.1	0.79	258	NP
SH24	ND	53	7.7	0.42	279	NP
SH25	ND	20	6.3	0.84	202	0.53
SH26	21	48	7.1	0.7	219	0.49
SH27	22	22	5.9	0.8	198	NP
SH28	16	88	3.2	0.48	88	NP
SH30	10	38	6.6	0.2	149	NP
SH32	ND	35	7.3	NP	301	NP
SH34	18	34	5.3	0.8	208	NP
SH36	15	71	4.1	NP	94	NP
SH37	18	30	2.2	0.5	64	0.22
SH40	ND	65	4	0.4	150	NP
SH41	12	33	3.6	0.64	111	NP
SH42	ND	79	4.6	0.5	155	NP
SH44	ND	48	2.8	0.9	76	NP
Range	10-22	20-198	1.3-11.0	0.2-0.9	32-301	?
Average	17	62	5.4	0.56	142	?
EPA Pollution Level*	3	25	1.7	1	90	No data
USGS Alert Level *	200	200	No data	20	5000	No data

Key: LB - Laucala Bay, SH - Suva Harbour, ND - Not determined, NP - No peak seen
EPA - Environmental Protection Agency, USGS - United States Geological Survey
* taken from Batley (1992)

Table 2
Concentrations (ppm) of some environmentally important elements in the sediments of the Suva Lagoon.

Chromium

The major sources of chromium are industries and workshops that use paints. The observed concentrations of Cr are more than three times the EPA levels at a third of the sites in the lagoon. Naidu and

Morrison (1994) reported chromium concentrations in the range 16-160 ppm in sediments. At sites close to the Lami dump, their values are in the range of 20-40 ppm. For comparison, our Cr values are 53, 20 and 48 ppm at sites 24, 25 and 26 respectively. Thus, there appears to have been a small increase in Cr levels in sediments since 1994. The highest concentration of 198 ppm for Cr, at site 13 (near mouth of the Rewa river) and down stream of the Nausori rubbish dump, is close to the USGS Alert Level.

Iron

The concentrations of Fe in the present work are in the range of 1.3-11.0%. Tabudravu (1995) reported Fe values in the range 0.13-0.24% in the sediment samples from the coastal waters of Lami. In the present study, the sediment sample from site 32 at the mouth of the Lami river had a much higher concentration of 7.3%. However, the Fe concentrations in our work are much below the EPA pollution levels.

Mercury

Mercury contamination in the lagoon may be due to the use of antifouling paints in the shipyards and other workshops. The concentrations measured in this work are in the range 0.2-0.9 ppm, consistent with those reported (0.3-1.34 ppm) by Naidu and Morrison (1994). Thus, mercury concentrations in sediments of the lagoon remain below the EPA levels.

Zinc

The principal uses of zinc in this region are in the manufacture of galvanised iron, white paint and wood preservatives (which contain $ZnCl_2$). The concentrations of zinc reported here are in the range 32-301 ppm, with 22 out of 30 sites showing levels higher than the EPA limit (90 ppm). Naidu and Morrison (1994) reported zinc concentrations in the range 200-487 ppm in sediments close to the Lami dump. Their figures are similar in magnitude to our Zn

values of 279, 202 and 209 ppm at sites 24, 25 and 26 (which are close to the dump), respectively. Tabudravu (1995) reported Zn values in the range 52-514 ppm in the sediment samples from the coastal waters of Lami. In the present study, the highest Zn concentration was 301 ppm in sediment from site 32 at the mouth of the Lami river.

Antimony

Naidu and Morrison (1994) reported Sb concentrations in the range 15-5625 ppm in sediments close to the seawall near a battery factory (Suva Harbour area). They concluded that the area could be declared a hazardous waste site. The concentrations of Sb observed in our study are much lower, in the range 0.2-0.5 ppm. No EPA and USGS values are available for comparison.

In addition to the above, we measured many trace elements (including the rare earth elements Ce, Eu, La, Nd, Sm, Tb and Yb), in the sediments of the Suva Lagoon (see Table 1). The significance of these elements to environmental studies is not known, but their concentrations are reported here for completeness.

Due to logistic problems (transportation of irradiated samples from abroad), the concentrations of several elements which involve radioisotopes with low half-lives (eg. As, Au, Mo, and Sb) could not be measured satisfactorily. The elements Cs, Se, Sr and Zr are detectable in sediments using NAA, but the technique is not sensitive enough to measure the existing concentrations. Lead (Pb), which is one of the most environmentally important elements, cannot be measured using NAA due to its closed-shell nuclear structure.

Conclusion

The present work, which was undertaken in the entire region of the Suva Lagoon, has shown considerable heavy element contamination in the sediments of the Suva Lagoon. The pollution levels at many

sites are higher than the EPA limits, but remain much below the USGS alert levels. Comparison with previous works suggests that contamination of the Suva Lagoon is increasing with time.

Aknowledgements
This work was supported by a generous research grant from the University of the South Pacific.

Bibliography

ADAMS F., DAMS, R., 1970 – *Applied gamma-ray spectrometery*, Pergamon Press, Oxford, 752 p.

BATLEY G. E. 1992 — "Toxicants". In Douglas N. Hall (ed.): *Port Phillip Bay Environmental Study: Status Review*, Melbourne, Csiro Port Phillip Bay Environmental Study, Technical Report 9: 80-111.

DE SOETE D., GIJBELS R., HOSTE J., 1972 – *Neutron activation analysis*, Wiley-Interscience, London, 836 p.

GOVINDARAJU K., 1994 – Compilation of Working Values and Descriptions for 383 Geostandards, *Geostandards Newsletter*, 18: 1 – 158.

LANDSBERGER S., 1994 – "Delayed instrumental neutron activation analysis". *In Z.B. Alfassi (ed.)*: Chemical analysis by nuclear methods. Chichester, John Wiley, 6.

MAATA M., 1997 – *The decomposition of tributyltin (TBT) in tropical marine sediments.* Unpublished Ph.D., thesis, The University of the South Pacific, Suva.

NAIDU S., AALBERGSBERG W.G.L., BRODIE J. E., FUAVOU V. A., MAATA M., NAQASIMA P., MORRISON R. J., 1991 – *Water quality studies on selected South Pacific Lagoons.* UNEP Regional Seas Reports and Studies No. 136, and SPREP Reports and Studies No. 49, South Pacific Regional Environmental Programme.

NAIDU S. D., MORRISON R. J., 1994 – Contamination of the Suva Harbour, Fiji. *Marine Pollution Bulletin*, 29 (1-3): 126-130.

NARAYAN S. P., 1993 – *Heavy metals in sediments and shellfish from Laucala Bay, Fiji.* Unpublished MSc thesis, The University of the South Pacific, Suva.

STEWART X., DE MORA Z., 1992 – Elevated tri(n-butyl)tin concentrations in shellfish and sediments from Suva Harbour, Fiji. *Applied Organometal. Chemistry*, 6: 507-512.

Tabudravu Z., 1995 – *Experimental and field evaluation of enteromorpha flexuosa as an indicator of heavy metal pollution by zinc, lead and copper in coastal waters of Lami, Fiji.* Unpublished MSc thesis, The University of the South Pacific, Suva.

Comparaison of ^{210}Pb chronology with $^{238,239\text{-}240}Pu$, ^{241}Am and ^{137}Cs sedimentary record capacity in a lake system

Hervé Michel

Douglas Chitty

Geneviève Barci-Funel

Gérard Ardisson

Peter G. Appleby

Elizabeth Haworth

Introduction

Transuranic elements have been released into the environment on a global scale since the early 1950s. The main source was atmospheric testing of nuclear weapons though releases from nuclear installations have been significant on local and regional scales. Large quantities of radioactive debris from the explosion of high-yield thermo-nuclear weapons were injected into the stratosphere and widely dispersed around the world. Gradual re-entry of this debris to the troposphere was followed by fallout onto the earth's surface. Fallout on lakes was deposited on the bed of lake as part of the sediment record.

The purpose of this paper is to report the results of a study of the transuranic radionuclides $^{238,239\text{-}240}Pu$, ^{241}Am in the sediments of

Blelham Tarn in Cumbria (UK) and forms part of a project concerned with the fate of transuranic elements deposited on lakes and their catchments.

As sediments accumulate they capture a high quality record of the changing levels of contamination. In this study sediment cores taken from the two locations in the lake were sectioned at 1 cm intervals and analysed by alpha spectrometry for $^{238,239-240}Pu$, ^{241}Am to determine the historical fallout record at this site. The sub-samples were also analysed by gamma spectrometry for the fission product ^{137}Cs and the natural radionuclide ^{210}Pb.

^{137}Cs was also part of the debris from nuclear weapons tests though further amounts were also deposited in 1986 as a result of fallout from the Chernobyl reactor accident. Comparisons between ^{137}Cs and the transuranic elements provide information on their relative transport rates through the environment.

The ^{210}Pb flux is proportional to the annual precipitation on the lake and provides a chronology of the sub-samples of the cores.

Site Description

Blelham Tarn is a small lake situated off the North-West shore of the North basin of Windermere. The basic morphometric characteristics are given in Table 1. It has a fairly simple bathymetry, with two main basins (figure 1). The lake is mildly enriched, receiving inputs from some of the area's naturally richer soils on the western side of Windermere. The streams are nutrient enhanced due to local agriculture and a small sewage works for Outgate (a small village 2 miles away). Blelham Tarn has been a site of scientific interest since the 1930's and has been the subject of many palaeolimnological studies including some of the earliest studies of fallout radionuclides in recent sediments (Pennington *et al.*, 1976).

	Blelham Tarn
Location	54° 24' N, 2° 59' W
Altitude	42
Max. Relief	284 m
Rainfall	1814
Catchment Area	4.27 km^2
Lake Area	0.102 km^2
Length	0.65 km
Width	0.17 km
Max. Depth	15 m
Mean Depth	6.8 m
Volume	0.693 x 10^6 m^3
Inflows	5 small streams

Table 1
Morphometry of Blelham Tarn.

Experimental

Sample collection

Two sediment cores were collected on 24 March 1997 from the deepest parts of the two sub-basins of the lake (sites A and B, Figure 1) using a 10.3 cm diameter Mackereth corer. The cores were extruded vertically at the Institute of Freshwater Ecology, Windermere, core A at 1 cm intervals down to the base of the core and core B at 1 cm down to 30 cm and thereafter at 2 cm. The wet sediment samples (excluding the sub-samples taken for algal analysis) were stored in sealed plastic bags and returned to the ERRC Liverpool where they were dried at 50°C to determine the water content and dry bulk density. Each sample was divided into two parts, one being retained at Liverpool for dating by ^{210}Pb and ^{137}Cs and the other sent to the Laboratoire de Radiochimie et Radioécologie, Université de Nice-Sophia Antipolis where they were analysed for Pu and Am analysis by alpha spectrometry and ^{137}Cs by gamma spectrometry.

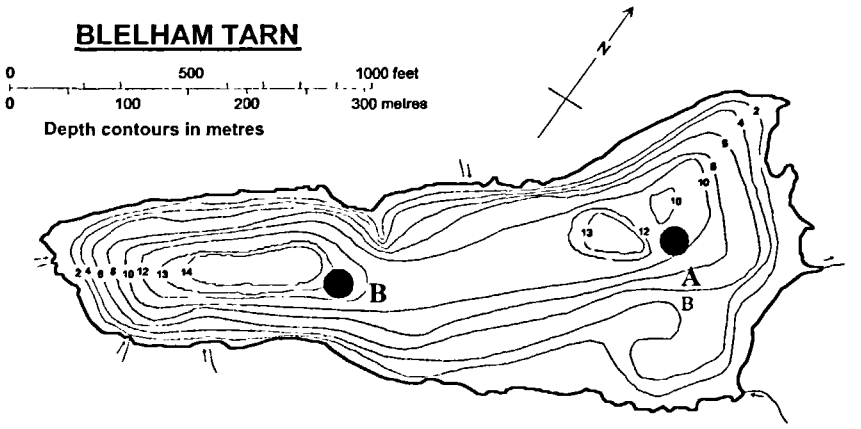

Figure 1a / b
The English Lake District showing (a) location and (b) the bathymetry of the lake. The locations of the sediment cores used in this study are marked.

Alpha spectrometry measurements

The radiochemical separation of Pu and Am in sediments is a complex procedure (Anonymous, 1989; Michel *et al.*, 1999a; 1999b). The first step is to pre-concentrate the radionuclides. The organic matter is removed by ashing and known quantities of the yield tracers ^{242}Pu and ^{243}Am are added to the residue. The transuranic elements are then removed by leaching with 8M HNO_3 and co-precipitation with ferric hydroxide in ammonia medium. This is followed by two extraction procedures: the first to separate the plutonium isotopes, the second to separate the fraction containing americium, before electrodeposition and counting by a-spectrometry. The separation of plutonium is achieved by elution with different acid solutions (8M HNO_3, 10M HCl and 10M HCl + 0.1M NH_4I) on an anionic exchange column mainly to discard thorium. After evaporation and addition of H_2O_2 in order to eliminate iodide, Pu isotopes are electrodeposited in sulfuric acid-ammonia media at pH = 2.4, on a stainless-steel disk, with a current of 1 A applied for 1 hour. The americium fraction is purified by co-precipitation with calcium oxalate. After extraction into HDEHP (diethylhexyl phosphoric acid) and elution through a two-layer exchange column (cationic + anionic), in order to separate remaining traces of Th and Pu, another anion-exchange process is used to eliminate rare earths. The eluate is evaporated and few drops of concentrated HNO_3 are added in order to eliminate thiocyanates. Americium is then electrodeposited two hours by the same procedure as for plutonium.

All reagents used in the separations were of analytical grade and solutions were prepared in unionized water. Anionic columns were: Bio Rad AGMP1 and Dowex 1 x 4 100-200 mesh in chloride form and cationic columns: Aldrich Dowex 50W x 8 100-200 mesh in chloride form.

The α-spectra were determined using EG & G Ortec 576A Dual Alpha Spectrometers equipped with boron implanted silicon detectors equipped with a multichannel buffer analyser (spectrum master ORTEC 919).

Gamma-spectrometry measurements

^{137}Cs measurements at Nice were carried out by standard g-spectrometry using methods described in (Barci-Funel *et al.*, 1988; 1992; Holm *et al.*, 1994). The sediment samples were oven-dried at 100°C, homogenized and packed into plastic containers and counted on a coaxial HPGe detector (EG&G ORTEC) of 17% relative efficiency with an energy resolution FWHM (Full Width at Half Maximum) of 1.9 keV at 1.33 MeV. The efficiency of detector was determined using standard sources with the same geometrical configuration as the samples being measured. Background radiation was reduced by placing the detector inside a 5 cm thick lead castle with a 2 mm thick copper lining. The spectra were collected using a multi-channel buffer analyzer (Spectrum Master ORTEC 919).

Results and discussion

Figure 2 plots concentrations of the transuranic radionuclides versus depth in core A. The corresponding results for core B are given in Figure 3. Figure 4 shows the ^{137}Cs results for both cores. The transuranic radionuclides all have a single well-resolved peak in their activity. In core A these occur at a depth of 14-16 cm. In core B they occur at 15-17 cm. The peaks in transuranic activity coincide with similar well-resolved peaks in the ^{137}Cs activity and almost certainly record the fallout maximum in 1963 from the atmospheric testing of nuclear weapons. Concern about fallout levels following the early tests resulted in a moratorium in atmospheric testing in 1958. Its breakdown in 1961 was followed by a period of intensive testing resulting in very high fallout during the years 1962-63. Implementation of the 1963 test ban treaty led to a rapid decline in fallout during the next few years and values in 1966 were just 10% of those in 1963. Nearly 50% of all fallout occurred during 1962-64, a space of just 3 years, giving rise to the very high concentrations recorded in the sediments of Blelham Tarn from this period.

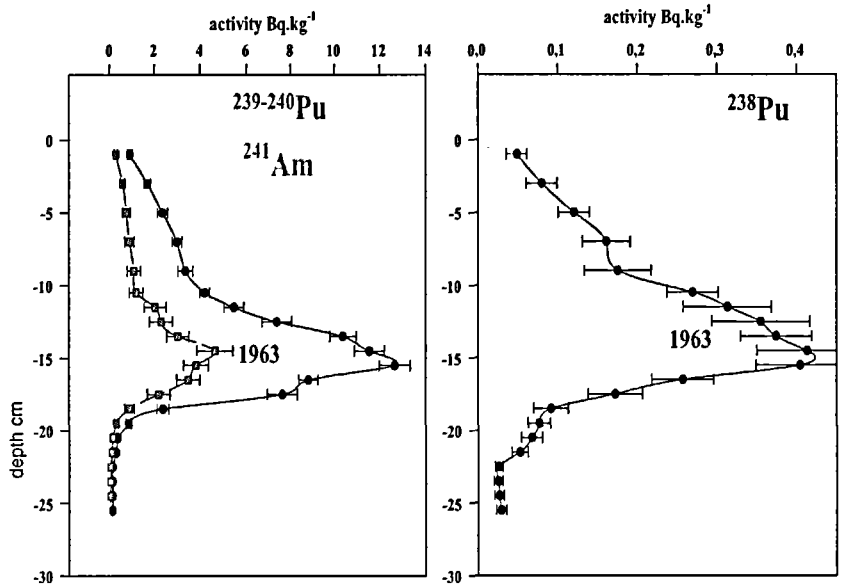

Figure 2
$^{238,239-240}$Pu and ^{241}Am profile in the dating core A.

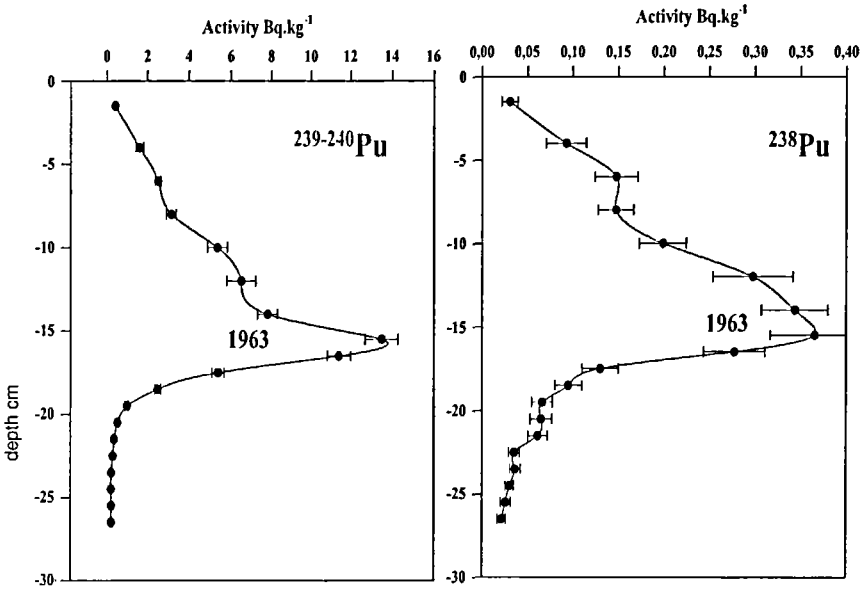

Figure 3
$^{238,239-240}$Pu profile in the dating core B.

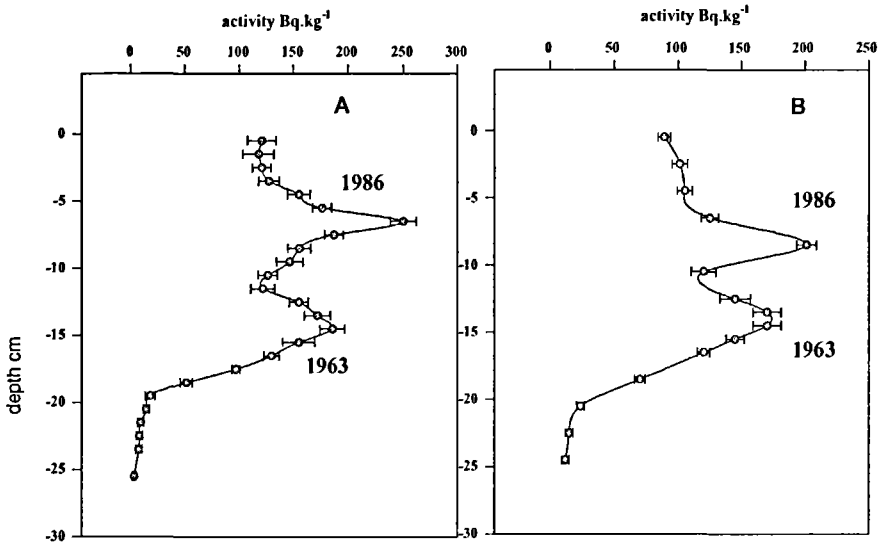

Figure 4
^{137}Cs profile in the dating core A and B.

In contrast to the transuranic elements, the ^{137}Cs profiles have a second more recent peak, at depths 6-7 cm in core A and 8-9 cm in core B. These features are almost certainly a record of fallout from the Chernobyl accident in 1986. Although the short-lived radionuclide ^{134}Cs associated with Chernobyl fallout was below limits of detection in the present cores, it was observed clearly in an earlier (1990) core from Blelham Tarn (van der Post, 1997). The ^{134}Cs peak in the 1990 core occurred at the same depth as the ^{137}Cs peak associated with Chernobyl fallout, and in the correct activity ratio. The absence of transuranic radionuclides in Chernobyl fallout is due to the fact that these radionuclides were mainly on heavier refractory particles and were deposited relatively near to the accident site.

Taken together the above results illustrate the extent to which sediments accurately recorded contamination of surface waters, in this case by radioactive fallout. They also show how dated events can be used to help provide accurate chronologies of recent sediments on timescales of just a few years. Sediments at 6-7 cm depth in core A

and 8-9 cm in core B can confidently be dated 1986. Sediments at 14-16 cm in core A and 14-17 cm in core B can be dated 1963. From these results the mean sedimentation rates at each core site during 1963-86 and 1986-97 are calculated to be:

Core A	Core B	
1963-86	0.079 ± 0.006 $g.cm^{-2}.y^{-1}$	0.100 ± 0.006 $g.cm^{-2}.y^{-1}$
1986-97	0.061 ± 0.008 $g.cm^{-2}.y^{-1}$	0.053 ± 0.002 $g.cm^{-2}.y^{-1}$

The date are compared to the ^{210}Pb chronology in the Figure 5. Using the ^{210}Pb chronology, the depths 15 cm and 7 cm respectively correspond to 1958±4 and 1983±4. The chronology is in good agreement with the transuranics and cesium dating profiles.

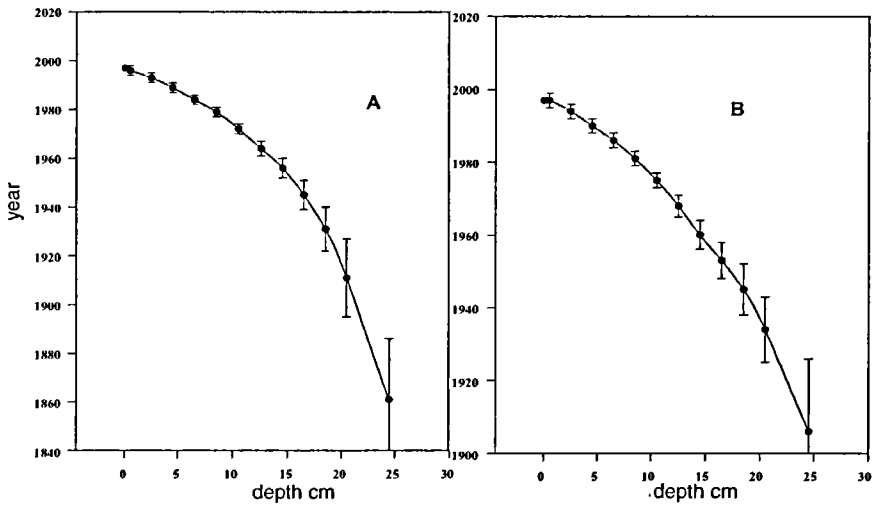

Figure 5
^{210}Pb chronology in the dating core A and B.

In conjunction with ^{210}Pb and other techniques such as diatom stratigraphy (Haworth, 1980) they can further be used to construct detailed sediment chronologies spanning the past 150 years.

Aknowledgements
This work is part of a research project financially supported by the European Commission, Nuclear Fission Safety Programme, Contract N° FI4P-CT96-0046 (DG12-WSMN).

Bibliography

ANONYMOUS, 1989 — *Measurement of Radionuclides in food and the environment.* Vienna, IAEA, Technical reports n° 295.

BARCI-FUNEL G., DALMASSO J., ARDISSON G., 1988 — Chernobyl fallout in some Mediterranean biotas, *Sci. Tot. Environ.*, 70, p. 373.

BARCI-FUNEL G., DALMASSO J., ARDISSON G., 1992 — Indirect determination of ^{241}Pu *activity in soils using low energy* photon spectrometer. *J. Radioanal. Nucl. Chem.*, 156, p. 83.

HAWORTH E.Y., 1980 — Comparison of continuous phytoplankton records with the diatom stratigraphy in the recent sediments of Blelham Tarn. *Limnol. Oceanogr.* 25, p. 1093.

HOLM E., BALLESTRA S., LOPEZ J. J., BULOS A., WHITEHEAD N. E., BARCI-FUNEL G., ARDISSON G., 1994 — Radionuclides in macroalgae at Monaco following the Chernobyl accident. *J. Radioanal. Nucl. Chem.*, 177, p. 51.

MICHEL H., BARCI-FUNEL G., DALMASSO J., ARDISSON G., 1999a — One step ion exchange process for the radiochemical separation of americium, plutonium and neptunium in sediments. *J. Radioanal. Nucl. Chem.*, 240, p. 467.

MICHEL H., GASPARRO J., BARCI-FUNEL G., DALMASSO J., ARDISSON G., 1999b. — Radioanalytical determination of *actinides and fission products in* Belarus soils. *Talanta*, 48, p. 821.

PENNINGTON W., CAMBRAY R. S, EAKINS J. D., HARKNESS D. D., 1976 — Radionuclide dating of the recent sediments of Blelham Tarn. *Freshwat. Biol.*, 6, p. 317.

VAN DER POST K. D., OLDFIELD F, HAWORTH E. Y., CROOKS P. J., APPLEBY P. G., 1997 — A record of accelerated erosion in the recent sediments of Blelham Tarn in the English Lake District. *J. Palaeolimnology,* 18, p. 103.

Excess ^{210}Pb and ^{210}Po in sediment from the Western North Pacific

Koh Harada

Yoko Shibamoto

Introduction

Particles in most surficial marine sediments are mixed mostly by the biological activities on the sea floors and the mixing is called as bioturbation. Knowledge of the mechanisms and rates of the bioturbation is critical to understand rates of the recycling and burial of organic matter, biogenic silica, carbonate and manganese (Berner, 1980; Emerson, 1985; Aller, 1990).

To determine the rate of the bioturbation, excess ^{210}Pb, which was produced ultimately from ^{226}Ra and scavenged by settling or resuspended particles, has been widely used (e.g., Nozaki *et al.*, 1977; Peng *et al.*, 1979; DeMaster and Cochran, 1982).

The western North Pacific has relatively high biological activity in surface water compared to the eastern North Pacific. This means rain rate of organic carbon to the sea floor in the western North Pacific is high and high bioturbation rate is expected. To clarify the rate, ^{210}Pb profile in the sediment from the western North Pacific was determined.

Activity ratio of ^{210}Po to ^{210}Pb in particulate matter in water column is generally over unity (Harada and Tsunogai, 1986). This suggests that significant amount of ^{210}Po reaches to the sea floor and some part of the ^{210}Po exists in the sediment even though half-life of ^{210}Po is short, 138 days. To test this hypothesis, ^{210}Po in the sediment was also determined.

Methods

Coring and sample treatment on board of the ship

Station KNOT (Figure 1), which is a station for time series observations of Japanese JGOFS activity, is located at 44°N, 155°E in the western North Pacific. Sediment core samples were collected at Stn. KNOT twice in cruises of R/V Hakurei-Maru #2 in October 1998 and

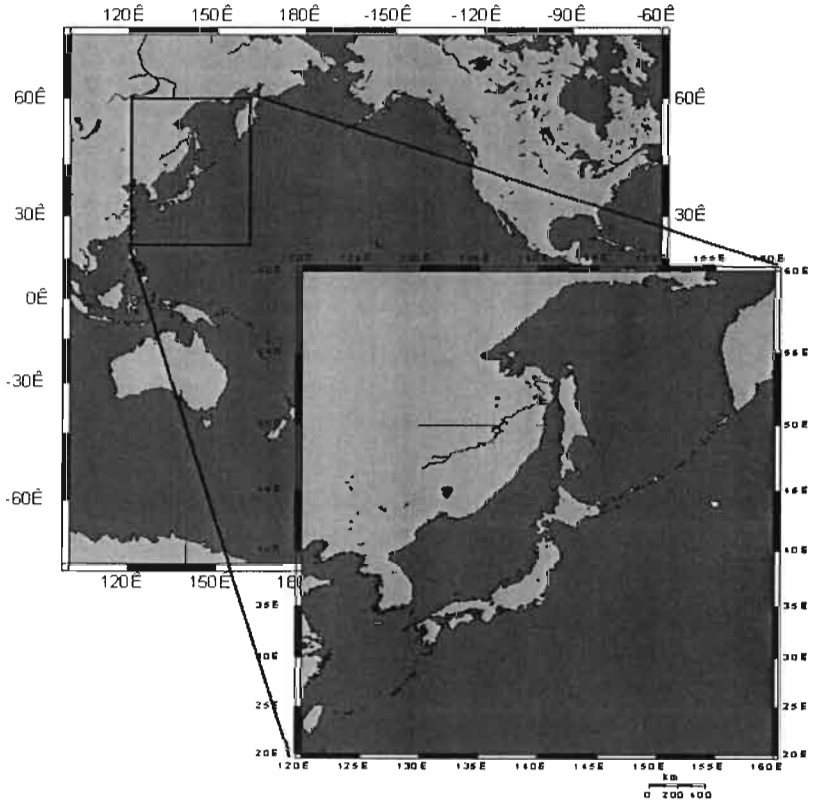

Figure 1
Map of the northwestern North Pacific showing a core location.

R/V Mirai in November 1998 using with a multiple corer (Figure 2). Immediately after recovery of the corer on the deck, the sediment core sample was sliced by 3 mm thickness for the top ten samples, by 6 mm thickness for the next 10 samples and by 12 mm thickness for the rest. The sliced samples were frozen and transferred to a land laboratory. In the laboratory, the samples were dried and powdered. Water content and porosity were calculated from weight loss after drying.

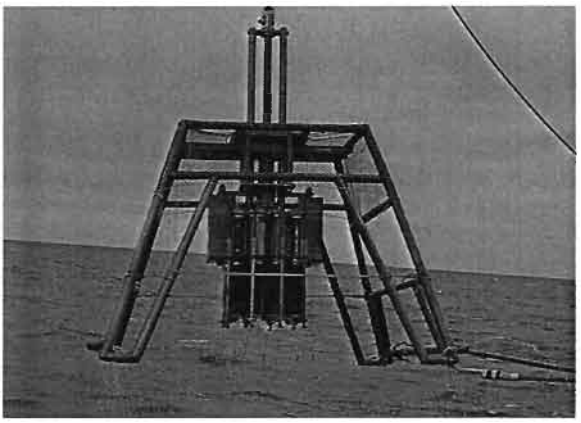

Figure 2
Picture of the Multiple Corer in the R/V Mirai cruise.

Radiochemical analyses

Radioactivities of ^{226}Ra and ^{210}Pb in the samples were determined by gamma spectrometry with a well-type intrinsic germanium detector. Efficiencies of the detector were calibrated by IAEA sediment standards.

Activity of ^{210}Po in the samples was determined by alpha spectrometry using ^{209}Po as a chemical yield monitor (Harada and Tsunogai, 1985). Aliquot amount of the sediment sample was leached in 6 M HCl solution and polonium was collected in hydroxide precipitate

from the leachate. Activities of ^{209}Po and ^{210}Po were determined by silicon surface barrier detectors after spontaneous deposition of polonium onto a silver disk from 0.1 M HCl that dissolved the precipitate.

Results and discussion

^{226}Ra and ^{210}Pb in the sediment at Stn. KNOT

Vertical distributions of ^{226}Ra and ^{210}Pb in the two sediment cores from Stn. KNOT were shown in Figure 3. Concentration of ^{210}Pb decreased rapidly from surface down to 1 cm depth, and then decreased gradually down to 6 cm depth. Below the depth, the concentration was almost constant, whereas there was a peak at 8 cm depth in the 1998 sample core. Contrastively, concentration of ^{226}Ra, which is a precursor of ^{210}Pb, was almost constant in the cores, ranging between 3.5 to 8.0 $dpm.g^{-1}$.

The vertical profiles of ^{226}Ra and ^{210}Pb showed that there was excess ^{210}Pb over its precursor ^{226}Ra from surface down to 6 cm depth. This excess ^{210}Pb must be supported by an input from outside of the sediment, which is an input of ^{210}Pb from the water column by settling particles.

Fluxes of ^{210}Pb from the bottom water to the sediment

Assuming a steady state condition, the ^{210}Pb flux from the overlying water column to the sediment can be calculated from inventories of ^{226}Ra and ^{210}Pb in the sediment from following relation,

$$F_i = \lambda_i I_i \qquad 1$$

where λ_i is a decay constant of nuclide i (day^{-1}) and I_i is an inventory in the sediment of the nuclide i ($dpm.m^{-2}$).

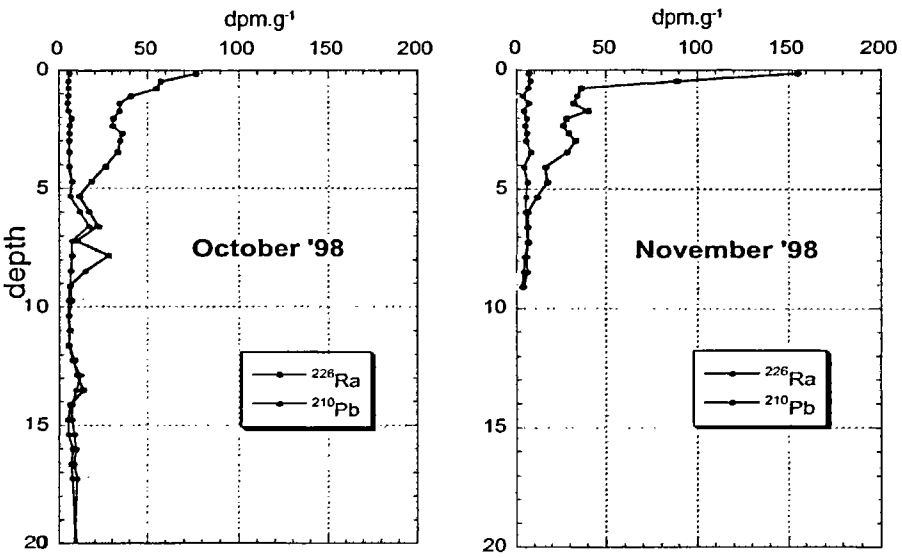

Figure 3
Vertical distibutions of ^{226}Ra and ^{210}Pb in the sediment core at Stn. KNOT.

The flux of ^{210}Pb was calculated as 81.9 and 64.2 dpm.m^{-2}.day^{-1} respectively from the October and November, 1998 profiles. This calculated flux can be compared with the flux observed by a sediment trap experiment. Unfortunately, ^{210}Pb in the sediment trap samples have not been determined so far, whereas the experiment at Stn. KNOT was carried out by the other group. Judging from previous papers, ^{210}Pb flux observed by the sediment trap in the North Pacific ranged from 20 to 100 dpm.m^{-2}.day^{-1}. The calculated fluxes from the profiles in the sediment seem to be comparable with the fluxes observed by the sediment traps in the biologically productive area in the North Pacific.

^{210}Po in the sediment

Using the sediment samples collected in November 1998, ^{210}Po was also determined, which is a daughter nuclide of ^{210}Pb. The vertical

profile of ^{210}Po showed in Figure 4 with ^{210}Pb. Excess ^{210}Po over ^{210}Pb seems to be exist in the top two sub-samples and between 7 and 10 cm depth. Generally speaking, the settling particles have high ^{210}Po/^{210}Pb ratio from 3 to 10 and this was explained by preferential scavenging of ^{210}Po from seawater to particulate matter. Although there still exist a possibility of calibration error of the counter because the excess ^{210}Po in the deeper samples is not explainable, the excess ^{210}Po in the core top seems to be caused by higher particulate flux of ^{210}Po from the water column than of ^{210}Pb. The ^{210}Po flux from the water column can be estimated from the inventory of the excess ^{210}Po in the sediment in the same method as ^{210}Pb flux mentioned above. The flux was calculated as 590 dpm.m^{-2}.day^{-1} showing the estimated ^{210}Po/^{210}Pb ratio in the settling particle was 7, which is comparable or a little higher than the observed one in the North Pacific.

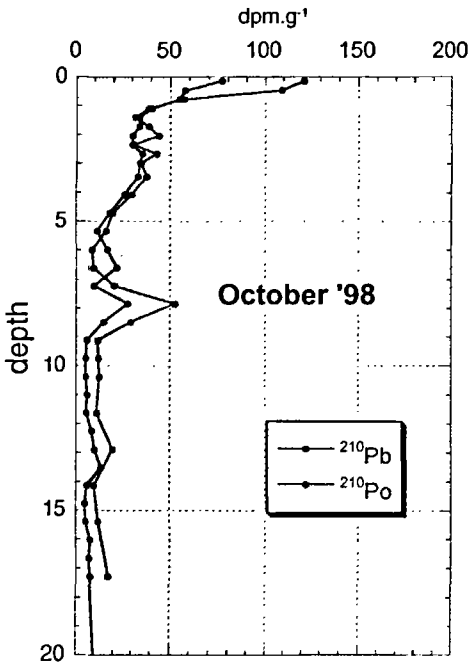

Figure 4 Vertical distibutions of ^{210}Pb and ^{210}Po in the sediment core collected in October.

Estimation of bioturbation rate from the vertical profiles of ^{210}Pb and ^{210}Po

As shown above, excess ^{210}Pb and ^{210}Po were detected in the sub-surface layers of the sediment core from the western North Pacific. Even though the excesses were supplied from the overlying water column by the settling particles, there must be some mechanisms in which surface sediment particles was mixed with sub-surface one since accumulation rate of pelagic sediment is very slow, <1 cm.kyr^{-1}, compared to the time scale of mean life of the nuclides. The particle mixing by organisms on sea floor, bioturbation, seems to be predominant although the mixing by bottom water current could be occur. If the nuclides is carried to the interior of the sediment only by the bioturbation, the concentration of the nuclides in the sediment can be expressed by the following equation,

$$\frac{dA}{dt} = D_B \frac{d^2A}{dz^2} + S\frac{dA}{dz} - \lambda A \qquad 2$$

where A is a concentration of nuclide i in the sediment, D_B is a bioturbation rate constant, S is a sediment accumulation rate and l_i is a decay constant of nuclide i. Since the second term in the right side in the Eq.(2) is negligible, the steady state concentration of the nuclide i can be expressed as follows;

$$A = C \cdot e^{-\sqrt{\frac{\lambda_i}{D_B}} \cdot z}$$

The concentrations of ^{210}Pb were plotted against depth semilogalismically (Figure 5). Judging from the linearity, the sediments were separated into three layers, surface to 1 cm, 1 to 2.5 cm and 3 to 6 cm depth and the biotubation coefficient in the layers was estimated to be 0.04, 0.4, 0.06 cm^2.yr^{-1}, respectively. It is very curious that the second layer has the largest coefficient, however, the reason is still unknown. Using the excess ^{210}Po profile, the coefficient was also calculated. The estimated value, 1.2 cm^2.yr^{-1}, is significantly larger than one obtained from the excess ^{210}Pb. To clarify the difference between the values from ^{210}Pb and ^{210}Po, further study is needed although the age dependent mixing of deep-sea sediments was reported (Smith *et al.*, 1993).

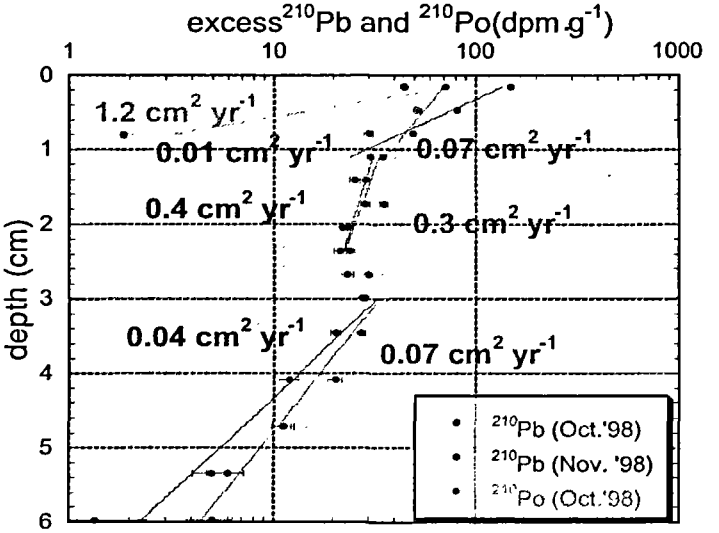

Figure 5
Semi logarithmic plots of ^{210}Pb and ^{210}Po in the sediment and estimation of D_B.

Conclusion

In the sediment in the western North Pacific,

1. excess ^{210}Pb and excess ^{210}Po existed down to 6 and 1 cm depth, respectively,

2. particulate fluxes of ^{210}Pb and ^{210}Po from the overlying water were estimated as 70 and 590 dpm.g^{-1}, respectively,

3. bioturbation mixing coefficient in the sediment was estimated to be from 0.004 to 0.4 cm^2.yr^{-1} and the highest value was observed in 1 – 2.5 cm layer.

Aknowledgements
The authors would like to thank scientists, technicians and crew members on R/V Mirai for their help of sample collection.

Bibliography

ALLER R. C., 1990 — "Bioturbation and manganese cycling in hemipelagic sediments". *In* H. Charnock *et al.* (eds) *The Deep Sea Bed: Its Physics, Chemistry and Biology*, Cambridge,University Press: 51-68.

BERNER R. A., 1980 — *Early Diagenesis: A Theoretical Approarch.* Prinston, University Press.

DEMASTER D. J., COCHRAN J. K., 1984 — Particle mixing rates in deep-sea sediments determined from excess ^{210}Pb and ^{32}Si profiles. *Earth Planet. Sci. Lett.*, 61: 257.

EMERSON S. R., 1985 — "Organic carbon preservation in marine sediments". *In:* Sundquist E.T., Broecker W.S. (eds): *The Carbon Cycle and Atmospheric CO2: Natural Variations Archean to Present*, AGU Geophys: 78-86.

HARADA K., TSUNOGAI S., 1985 — A practical method for the simultaneous determination of ^{234}Th, ^{226}Ra, ^{210}Pb and ^{210}Po in seawater. *J. Oceanogr. Soc. Japan*, 41: 98.

HARADA K., TSUNOGAI S., 1986 — Fluxes of ^{234}Th, ^{210}Po and ^{210}Pb determined by sediment trap experiments in pelagic oceans. *J. Oceanogr. Soc. Japan*, 42: 192.

NOZAKI Y., COCHRAN J. K., TUREKIAN K. K., KELLER G., 1977 — Radiocarbon and ^{210}Pb distribution in submersible-taken deep-sea cores from project FAMOUS. *Earth Planet. Sci. Lett.*, 34: 167.

PENG T. H., BROEKER W.S., BERGER W. H., 1979 — Rates of benthic mixing in deep-sea sediments as determined by radioactive tracers. *Quat. Res.*, 11: 141.

SMITH C. R., POPE R. P., DEMASTER D.J., MAGAARD L., 1993 — Age-dependent mixing of deep-sea sediments. *Geochim. Cosmochim. Acta*, 57: 1473.

Workshop on radiological techniques in sedimentation studies: methods and applications

Gary Hancock

David N. Edgington

John A. Robbins

John N. Smith

Greg Brunskill

John Pfitzner

The following document summarises the important issues raised during the 3 hour discussion period of the Workshop on "Radiological Techniques in Sedimentation Studies", held on June 22, 2000. The document includes contributions from the above authors summarising, and in some cases illustrating important features of the discussion. The discussion issues covered:

- problems associated with the use of "mapping" algorithms, particularly CRS, to give unsubstantiated ^{210}Pb "dates";

- the necessity to validate ^{210}Pb deposition histories;

- the trend in research journals to publish ^{210}Pb chronologies with supporting data;

- the effect of drainage basin residence times on fallout nuclide sediment profiles;

- the low activity of fallout tracers in the southern hemisphere, and the implications for sample core collection, analysis and geochronological usage.

These issues have been broadly divided into three sections; the first dealing with problems associated with interpretation and dating of ^{210}Pb profiles; the second describing some aspects of large scale processes and geographical features which affect the sediment profiles of excess ^{210}Pb and "bomb" nuclides. Finally some recommended sampling and analytical procedures are listed.

There was a collective recognition of the need for standards and consistency in reporting data and interpretations in publications. There was concurrence with the idea of trying to influence editorial policies of prominent research journals. Suggestions for editorial policy regarding the use of ^{210}Pb for sediment geochronology included (1) requiring at least one independent method to verify the chronology, (2) provision of all relevant data and details of computational methods to reviewers of submitted papers and (3) publication of relevant data and computational methods either within the paper (possibly as small-type appendices) or as reader-accessible electronic files.

Application of ^{210}Pb as dating tool

Introduction by J. A. Robbins

It has been 37 years since Ed Goldberg first used ^{210}Pb as a dating tool and nearly 30 years since the method was first applied to sediments. Not only did Goldberg introduce the method but, in a short paper presented at an IAEA meeting in Vienna, he proposed computational algorithms (yes, mappings) for obtaining dates – the very mappings popularised by Appleby and Oldfield 15 years later!

The round of applause given Gregg's tongue-in-cheek faulting of W. F. Libby for his "disservice" by development and promotion of the ^{14}C method, nicely underscored a division among those interested in ^{210}Pb: those who consider the radionuclide to be one among many that are enormously useful for understanding processes and associated time scales in lacustrine and marine systems on the one hand, and those who are primarily interested in temporal records of

chemical and biological changes in ecosystems on the other. I suspect the first group consists of mathematicians, physicists and chemists, comparatively well versed in quantitative process modelling, while the second group consists of biologists, ecologists and paleolimnologists. The first group is more inclined to think that when ^{210}Pb can provide chronological information it's nice but if not, it still may tell us something interesting about how a system works. The second group, with first or second hand knowledge of the comparative ease and benefits of ^{14}C dating, wants some analogous ^{210}Pb dates and maybe some associated uncertainties so as to tell a history, but wishes understandably to shun complexities, rigours and equivocations of quantitative process modelling. Of course with ^{210}Pb that's not possible – ever. Thus, while ^{210}Pb can be a valuable tool for dating sediments up to about a century old, its primary use is to evaluate processes of sediment transport, focusing, mixing and accumulation in lacustrine and coastal marine systems. The method is not analogous to ^{14}C dating, is never routine and chronological information culled from sediment ^{210}Pb profiles must always be verified by independent means. Perhaps the most important implication of a quite evident disparity in outlooks is that there should be more cooperation between the explicators of process and the tellers of history!

I am among those who are aggravated by the deterioration in reporting of ^{210}Pb data and interpretations in peer-reviewed publications. I applaud John Smith's forthcoming editorial in Journal of Environmental Radioactivity that addresses the problem and proposes standards for publication of ^{210}Pb results. I believe that we should use the SPERA-2000 Workshop summary document as another vehicle for promoting appropriate standards for journal publications.

Comment from D. N. Edgington

Over the last 20 years the measurement of ^{210}Pb in sediment cores has become a very popular method for determining sedimentation rates over a time-span of approximately 100 years. Unfortunately, this method appears to be far simpler than it really is and there is considerable misuse as evidenced by many papers appearing in the

literature. Based on my quick assessment of papers appearing in major journals in the field such as *Environmental Science & Technology* and *Limnology & Oceanography* approximately 75% of the papers published in the last year or so did not present any of the ^{210}Pb data or an age-depth relationship to justify their interpretation, merely presenting the y data versus a totally unsubstantiated x axis. This reflects a serious problem with quality of reviewing, or the understanding of the problems of using ^{210}Pb data to ascribe dates by reviewers, even for the most prestigious journals. It is now very common to assume that this method is so simple and cut-and-dried that it is no longer considered necessary to publish the derived age-depth relationships, let alone the data on which the dating is based. As a result there are many papers appearing in the literature in which the discussion of changes in contaminant concentrations or fluxes with time observed in sediment profiles based on dates derived from ^{210}Pb cannot be evaluated. This is because these discussions are based on an unreviewable or unevaluable time-scale, thus making these papers essentially meaningless. This situation is untenable and very unhealthy for our science.

Comment from G. Brunskill and J. Pfitzner

Libby gave us the ability to estimate the age of an organic or carbonate carbon sample from the ratio $^{14}C/^{12}C$, and Claire Patterson gave us the ability to estimate the age of the earth and meteorites from uranium/lead ratios. Despite the many sources of uncertainty and contamination of samples, the language used for results from these methods suggests that these methods give our best estimate of the real age of each sample analysed. These methods can be used to estimate a unique age (with associated uncertainty) of a single sample.

The use of sedimentation tracers such as excess ^{210}Pb, ^{234}Th, and ^{7}Be is a fundamentally different enterprise, as these particle-reactive tracers provide no unique "age" for one sample of mud. The information package from these tracer methods is contained in the magnitude and shape of the core profile over sediment depth, usually involving 20-100 samples in one sediment core. These isotopes are annually supplied to the sediment surface by natural production, and in most cases we do not know what sedimentary phases hosts

each isotope. The most obvious and useful parameters that can sometimes be derived from these sediment core profiles of short-lived nuclides are the rate of present day accumulation, the core horizons that are mixed, and the excess or depletion of these isotopes related to non-deposition, erosion, resuspension, and focusing of sediment labelled with these tracers. It is helpful to know the source and hopefully "steady state" rate of supply of these isotopes to the sediment column, and this can usually be estimated from atmospheric and water column measurements. If the rate of accumulation of bulk sediment can be estimated from more than one of these isotopes, then something approximating an "average age" for a given core slice can be calculated, and this average age uncertainty should include the time equivalent of the surface mixed layer, pore water diffusion smoothing, and all the analytical uncertainties of field sampling and measurement. Where other sedimentary information provides constraints on depositional history, such as varves, known contaminant inputs, or known natural episodic events, these isotopic tracers usually estimate accumulation rate in a reasonable manner. Except for very few unusual cases, it is inappropriate and misleading to provide a unique age for each sediment core sample.

Comment on Interpreting ^{210}Pb Profiles by J. A. Robbins

Profiles of ^{210}Pb are the end result of a complex of processes controlling the delivery of sediments and the radionuclide to coring sites over a time span of about one century. Proper quantitative modelling of profiles depends on an astute selection of a critical subset of those processes and an accurate mathematical representation of their role. This is not an easy task! ^{210}Pb sediment chronologies, if they can be established at all, should be the result of a self-consistent application of quantitative process models (QPMs) to ^{210}Pb and other ancillary data.

Because QPMs are difficult to develop, often require extensive supporting data as well as long observational (as well as computational) experience with specific systems, several simplified approaches have arisen for extracting chronologies from excess ^{210}Pb profiles: curve fitting and mappings.

In curve fitting, excess ^{210}Pb profiles are described by a simple function with a restricted number of parameters evaluated by least-squares optimisation methods: for example a fit of a roughly log-linear ^{210}Pb profile with depth using a straight line or several straight line segments. The value of curve fitting is its simplicity, provision of a test of goodness of fit to the data, and use of relatively large numbers of data points to generate age estimates with improved precision. The drawbacks are that simple functions may not represent the data well, relevant processes may go unrecognised and inaccuracies may result. Curve fitting invites laziness in reflection on system properties.

A mapping is a mathematical formula, algorithm, scheme or procedure by which each excess ^{210}Pb data point (or construction based on a set of data points) is used to calculate a corresponding age or accumulation rate (Robbins and Herche, 1993). Several mappings have appeared in the literature, most notably CRS or CIC, and have become methods of choice for extracting sediment age-depth relations. These are often referred to as "models" but they are not true models in the sense of QPMs. Mappings are relatively easy to use, can inform construction of QPMs, and can be of value in cases where true models are inaccessible. The principal drawback of mappings is that, by construction, they never provide a test of their validity. No comparison of theoretical and measured excess ^{210}Pb profiles ever results from use of a mapping. Mappings require little understanding of system processes, and can thus lead to false interpretations as well as irresponsible reporting of research results. CRS presents particular difficulties because even extremely erratic ^{210}Pb profiles can yield relatively smooth age-depth relations, sediment mixing as well as variability in rates of ^{210}Pb delivery may be mistakenly converted into changes in sediment accumulation rates, and, because the computation demands an accurate estimate of total excess ^{210}Pb inventory, sediment dates and accumulation rates can be incorrectly estimated, especially when supported levels are high.

Quantitative Process Models

The distinction between curve fitting, mappings and QPMs were illustrated at session and workshop presentations. An excess ^{210}Pb

profile in a sediment core from a reservoir from Lake Oahe in South Dakota (Callender and Robbins, 1993) that was constructed in 1958, while "noisy" nevertheless decreased roughly exponentially with depth to background at around 100 cm depth. Both conventional curve fitting and a CRS mapping incorrectly predicted the bottom of the core at 200 cm to correspond to about 1850, while the ^{137}Cs activity appeared down to 200 cm with a peak at 160 cm depth. In contrast a QPM, with an exponentially decreasing sediment accumulation rate since creation of the reservoir, explained both the ^{137}Cs and excess ^{210}Pb profile. Simple curve fitting and the CRS mapping failed because much of the information required by these calculations was lost in the high background of supported ^{210}Pb. In one presentation (Robbins *et al.*, 2001) four excess ^{210}Pb profiles from a high deposition area in Lake Erie collected in 1976, 1981, 1983 and 1991, exhibited progressively greater deviations from exponential with time in the upper 20 cm of core. This was shown to be the result of hypereutrophic conditions in the lake from about 1950 to 1975 and subsequent remediation of the system by reduction in P loads. During the hypereutrophic period near-bottom water in parts of the lake became seasonally anoxic. This resulted in the re-dissolution of Mn, Fe and probably excess ^{210}Pb and horizontal transport to the coring sites in adequately oxygenated depositional basin elsewhere in the lake. Here the CRS mapping failed because human-caused eutrophication had modified the rate of delivery of excess ^{210}Pb to the coring site. The CRS falsely interpreted changes as being due to altered sediment accumulation rates. In another presentation (Robbins *et al.*, 2000) excess ^{210}Pb distributions in highly organic peats from the Everglades (Florida) wetlands, showed almost classic features of mixing that CRS mappings attributed to increasing mass accumulation rates. Here the CRS algorithm was right but proof had to come through use of a QPM in which soil accretion rates were linearly coupled to historical P loadings to the system. Finally, during the Workshop Edgington et al. demonstrated the difficulties of selecting an appropriate computational method (either curve fittings, mappings) or reasonable QPMs in the case of sediment cores collected over more than a decade from Lake Tahoe (USA) even where ^{210}Pb and many radionuclides, as well as stable trace elements, had been determined.

Verification

In the absence of supporting information, no ^{210}Pb profile can be "explained" and no chronology derived from ^{210}Pb should be considered reliable! The proof of this is easy enough. A perfectly exponential decrease in an excess ^{210}Pb profile with depth can be due to radioactive decay plus sedimentation alone, uniform diffusive mixing alone or some combination of these two alternative transport processes. In the extreme case where there is no net sedimentation, an exponential ^{210}Pb profile cannot yield a chronology. Only independent information can resolve the profound ambiguity. Knowing the relevant process is critical to whether meaningful dates can be obtained even from an ideal ^{210}Pb profile.

It is common practice in the published literature to make limited use sediment profiles of fallout ^{137}Cs as a primary source of independent chronological information. Rather typically, ^{210}Pb chronologies are considered "verified" if subsurface ^{137}Cs peaks in sediments are located at depths where ^{210}Pb dates "agree" with the "date" fallout maximum, 1963-1964. Rarely is any attention paid to what constitutes acceptable agreement. The ^{137}Cs peak method is weak since it confirms, at best, merely one curve fitting or mapping date assignment. If mappings such as CRS or CIC are inappropriately applied to sediments subject to near-surface, steady-state mixing, they generate artificially high estimates of accumulation rates that can, in turn, falsely agree with ^{137}Cs peak locations which have been displaced downward by mixing. At minimum, one should also try to test the ^{210}Pb chronology by comparing the age assignment of the ^{137}Cs horizon (deepest level where activity can be detected) against a 1952 date of onset of atmospheric nuclear testing. Agreement strengthens the assertion of a valid ^{210}Pb chronology, while disagreement is an invitation to consider reasons and present them in published discussions. Horizon is more sensitive than peak depth to steady-state sediment mixing and diffusive migration. In the southern hemisphere horizons may be artificially closer to the surface in sediment cores due to detection problems.

More satisfactory approaches include building QPMs that account for entire ^{210}Pb and ^{137}Cs profiles, and the use of tracers such as stable Pb (at least in the northern hemisphere) where a well-developed,

roughly 100 year-long record of atmospheric Pb concentrations may be compared with sedimentary Pb temporal records based on ^{210}Pb dating. In this case, QPMs must account for ^{210}Pb, ^{137}Cs and Pb (Robbins *et al.*, 2000).

Comment on CRS and model validation by D. N. Edgington

The lack of published data supporting ^{210}Pb dates (outlined above) is made worse by the almost universal use of the Constant Rate of Supply mapping or transformation (CRS) to calculate ages, where each data point translates into an independent age or sedimentation rate. The method requires the assumption that the input of excess ^{210}Pb is invariant and the observed sediment column is in steady-state (i.e. the inventory of excess ^{210}Pb is constant). Under these conditions any variation from a perfect exponential decay of ^{210}Pb downcore must be ascribed to changes in sedimentation rate.

In most of the papers published where data have been presented, there has been no attempt either to validate the assumptions, or to show that age-depth relationships are reproducible from core to core or from sampling time to sampling time. The problem is confounded by the easy availability of ^{210}Pb data from a variety of commercial analytical services. It must be stressed that while gamma-ray spectrometry may be essentially a turn-key operation, the interpretation of the data is the crucial step in the assignment of sedimentation rates and requires a strong knowledge of local conditions. It must also be understood that all profiles are not interpretable. In those few cases where ^{210}Pb data were presented, there was no verification of the interpretation using either ^{137}Cs or other non-radiological markers in the sediment.

Several years ago John Robbins put together a set of "regrettable facts" regarding the use of ^{210}Pb for sediment dating. They deserve reiterating:

1 Not all cores have interpretable profiles;

2 Sediment dating is critical for paleolimnology. Often dating is given short schrift;

3 Assignments of dates requires calculations;

4 Calculations require appropriate models and reasonable assumptions;

5 Models require understanding the relevant processes;

6 Bad models lead to bad dates (garbage in = garbage out);

7 Defining appropriate models can be mathematically difficult;

8 Date assignments require verification;

9 Appropriate verification is generally non-trivial;

10 Self-consistency is a necessary but not a sufficient condition for model selection;

11 The ^{210}Pb method appears to be so easy and reliable that journals no longer require publication of even age-depth relationships – let alone the data.

Recommended standards for reporting ^{210}Pb results

Of course the general principle is that readers should be provided with all data and computations necessary to mount effective challenges to published data and interpretations at any future time.

It is beyond the scope of the workshop summary document to get into a lot of detail here. But we collectively recognised the need for standards and consistency in reporting data and interpretations in publications. There was concurrence with the idea of trying to influence editorial policies of journals such as L&O, ES&T, J. of Environmental Radioactivity, J. of Paleolimnology and perhaps Quaternary Research.

The following recommendations and are derived primarily from the text of an editorial by J.N. Smith to be published in the Journal of Environmental Radioactivity, probably next year. Similar recommendations have already been conveyed to editors of other Journals by D. Edgington.

Validation of ^{210}Pb geochronology

^{210}Pb geochronology must be validated using at least one independent tracer that separately provides an unambiguous time-stratigraphic horizon. This should be considered as fundamental to the validation of ^{210}Pb sedimentation models in as much as the use of radioactive tracers and standards is to the quality control and verification of analytical methodologies. Independent validation of ^{210}Pb geochronologies must become an integral part of the overall experimental methodology. If the validation is inconclusive, then either a more appropriate particle transport model must be formulated and applied to the interpretation of the experimental results or the core must be considered to be undateable.

Data Presentation

At the time of review, (1) all authors submitting manuscripts to research journals must be expected to provide figures of the data or a hard-copy appendix containing the data and a description of the methods of calculation, including verification, and (2) the editors publish the figures and/or this appendix in smaller type or provide an easily accessible electronic version for readers.

Large scale effects on ^{210}Pb and "bomb" nuclide sediment profiles

Comment on Drainage basin residence times by J. N. Smith

It has been shown over the past 20 years that radionuclide tracer distributions in sediments are a function of the rates of tracer transport through various phases (soils, water column, biota, transient sediment reservoirs, etc.) of the environment. For radionuclides

that can be considered to have a constant steady-state input flux (such as ^{210}Pb under many conditions), their retention in various environmental reservoirs will affect the overall flux to the sediments, but not necessarily the shapes of the sediment-depth profiles. In contrast, radionuclide tracers having time-dependent input functions (such as fallout ^{137}Cs and $^{239,240}Pu$) will have sediment-depth distributions whose both shape and magnitude are affected by their history of transport through the different phases of the environment.

In some cases, the effect of a "delay" of the fallout radionuclide in an environmental phase prior to final deposition in permanently deposited sediments can be simulated by a box model employing a single residence time representing tracer transport through the pertinent environmental phase. This is commonly observed in lake sediments having relatively small drainage basins where there is transient tracer pooling in near shore sediment regimes prior to resuspension and subsequent deposition in the deeper, permanent sediment deposits. In other types of aquatic or marine systems, several environmental phases having very different tracer residence times must be employed to simulate the experimental results. One example of this latter system is a lake or estuary with a relatively large drainage basin having a soil/litter phase in which tracers are delayed (on average) by thousands of years and a second environmental phase (eg. water column) that causes delays of only months to years.

One of the primary confounding factors of tracer "delay" in environmental phases prior to permanent deposition in the sediments may be to produce sediment distributions that appear to have undergone mixing. For example, the 1963-64 peak in the sediment-depth distribution of fallout radionuclides corresponding to the period of maximum atmospheric deposition will tend to be skewed towards the surface depending on the extent of tracer "delay" in various environmental phases. Further, recent sediments will be characterised by a significant depositional flux of fallout radionuclides despite the fact that the present-day atmospheric depositional flux is practically zero. The point is that these features can also be simulated by various combinations of sedimentation and

mixing and tracer delays in the environment can be mis-interpreted as having been caused by sediment mixing. It is therefore critical to properly evaluate tracer transport mechanisms and rates for their passage through the environment by comparisons of the distributions of tracers (such as ^{137}Cs) having time-dependent input functions with those of tracers (such as ^{210}Pb) having steady-state input functions.

Comment on Southern Hemisphere Fallout by G. Brunskill and J. Pfitzner

The flux of ^{210}Pb from the atmosphere to the land and sea is much smaller in the southern hemisphere, due to the large ratio of ocean/land. Rain fluxes and soil inventories suggest that the annual supply of excess ^{210}Pb in tropical Australia is about 50 $Bq.m^{-2}.yr^{-1}$, whereas European and North American excess ^{210}Pb supply is approximately 300-400 $Bq.m^{-2}.yr^{-1}$.

The situation is similar for "bomb" fallout nuclides, although for a different reason. Most of the bombs were exploded in the northern hemisphere, and many of the bomb nuclides commonly used as chronological markers in the northern hemisphere ($^{238, 239}Pu$, ^{241}Am) are very difficult to detect south of the equator. The history and magnitude of bomb fallout nuclide supply to North American ecosystems are known to be sharply focused in 1962-65, with a peak input that is 10+ times greater than 1950-60, and 1970-present activities (Figure 1). Inventories of ^{137}Cs in North American soils and sediments are typically 2-5 $kBq.m^{-2}$. Fallout history and magnitude is different in the southern hemisphere, and particularly in tropical Australia and New Zealand. The peak input is only 2 times greater than 1950-1960 or 1980-present, and the peak input was supplied over 1954-1974 as a result of smaller local bomb explosions (Murorora, Maralinga, Monte Bello Island) in the late 1950s and early 1970s. Undisturbed soil profiles in north Queensland usually have ^{137}Cs inventories of <400 $Bq.m^{-2}$. Therefore, we should not expect sediment core profiles of ^{137}Cs to have a sharp 1963 peak (as in North American examples), but rather a broad plateau of low activity (Figure 1).

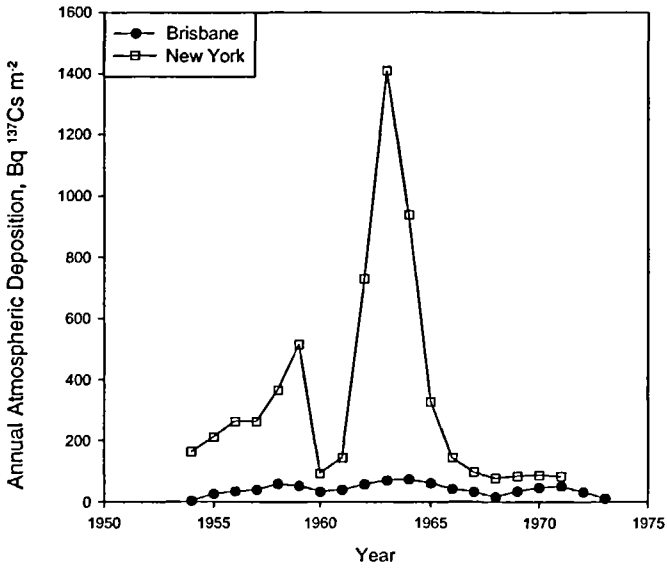

Figure 1
The history of bomb fallout ^{137}Cs deposition (as calculated from ^{90}Sr measurements) in New York city, NY, USA and Brisbane, Queensland, Australia. The data are from the Environmental Measurements Laboratory website (http://www.eml.doe.gov/databases/). The year 2000 inventory of ^{137}Cs in New York city is 2501 Bq.m^{-2}, and the corresponding value for Brisbane in the southern hemisphere is 352 Bq.m^{-2}. The peak/trough ratios for New York are 1964/1960, 15.0, and 1964/1966, 9.8, and for Brisbane are 1958/1955, 2.27, 1958/1960, 1.80, 1964/1967, 2.25, 1964/1967, 2.29, and 1971/1968, 3.23, 1971/1973, 4.94.

Comment on Large sediment fluxes by G. J. Hancock

Many South Pacific and other southern hemisphere countries share a common history of land use over the last 100-150 years. This can be summarised as large scale and rapid conversion of forested river catchments to European farming practices, mining activities, and urban developments. These changes have, in many cases, lead to the mobilisation of large amounts of sediment to lakes, water storages

and estuaries. The rapid rates of sediment accumulation associated with these catchment changes has resulted in the dilution of the activities of fallout tracers used in sediment dating (excess ^{210}Pb and ^{137}Cs), compounding the problem of low southern hemisphere activities of these nuclides described above by Brunskill and Pfitzner. The presence of ^{137}Cs and excess ^{210}Pb in undisturbed sediment usually means that layer has been deposited in the last 40 years and 100 years respectively, although chemical mobility of ^{137}Cs in some sediments may invalidate its use as a chronometer. However, the combined effects of high sediment fluxes and low fallout activities means that the lack of detectable ^{137}Cs and excess ^{210}Pb in sediments does not necessarily mean that the sediment has been deposited prior to the release of bomb ^{137}Cs into the atmosphere. This is illustrated by a core from the Murrah floodplain in SE Australia. Excess ^{210}Pb and ^{137}Cs is undetectable in the upper one meter layer of sediment. This layer overlies a deeper layer containing high ^{137}Cs activity, proving the upper one meter of sediment has been laid down within the last 40 years. This example illustrates the extreme effects that variable sediment fluxes can have on the sediment profiles of fallout nuclides, and highlights the necessity to corroborate dates by independent methods.

Recommended sample collection and analysis procedures

Comment on Core Collection by J. A. Robbins

Where possible we use modified Soutar type box cores and take open tube sub-cores from the box core and achieve alignment of interfaces inside and outside of the tube by hand regulated variations in a partial vacuum applied to the air space above sediments insider the tube.

We also have used piston coring in situations where there is visually verifiable preservation of the sediment-water interface.

Gravity coring, especially using core catchers or plunger type valves, can distort the sediment column and is not a desirable, although sometimes necessary collection method.

In many cases it is desirable to X-ray cores (or replicate ones) to characterise sediment stratigraphy.

Core Sectioning

Sectioning should be quantitative with respect to wet sediment content. Where it is necessary to trim an annulus from sediment sections, the trimmed material should be saved for calculating total sediment wet weight of each section.

Measurements

Section interval thickness, z (cm).

Section dry weight g, ($g.cm^{-2}$ of core cross-sectional area).

Fractional dry weight of section, fdw, (g.dry/g.wet).

Grain size distribution, (especially % less than ca. 65 microns). This is especially indicated where there appear to be localised anomalies in ^{210}Pb and other profiles.

Gamma counting of sealed whole-dry sediments, equilibrated for radon in-growth, preferably using detectors with enhanced efficiencies below 100 KeV, is the method of choice in many cases. Report ^{210}Pb, ^{7}Be, ^{226}Ra, ^{137}Cs and ^{40}K and sometimes ^{228}Th. At least near-surface samples should be counted soon enough to detect ^{7}Be ($t_{1/2}$ = 53.4 days). This radionuclide is useful for confirming recovery of surface sediments. However there are circumstances in which Be-7 may decay away before reaching sediments! There are cases where excess ^{228}Th ($t_{1/2}$=1.9 years) occurs in near-surface sediments. Lake Tahoe is an example. This nuclide may be useful for determining rates of near-surface mixing and/or sediment accumulation. Look for the ^{208}Tl peak at 583.19 KeV and the ^{212}Pb peak at 238.63 KeV. In the case of this latter peak, there may be a removable interference due to ^{214}Pb from ^{226}Ra at 241.98 KeV to deal with. The ^{40}K is use-

ful for identifying stratigraphic anomalies and should be reported when gamma counting is done. ^{226}Ra can best be determined from several peaks associated with decay of ^{222}Rn (295.21, 351.92 and 609.31 KeV) using a weighted average of activities. The gamma at 186.21 KeV arising directly from ^{226}Ra may be subject to interference from an unresolvable peak at 185.7 KeV from ^{235}U.

Enhanced efficiency gamma counting for ^{210}Pb (46.5 KeV) is generally not as rapid in terms of counting or as precise as the standard isotope-dilution alpha spectroscopy method in which ^{210}Po (in equilibrium with ^{210}Pb) in acid extracts of samples receiving calibrated ^{209}Po or ^{208}Po spikes are plated on to silver planchets and counted. We use this method in combination with gamma counting in many cases where establishing sediment chronologies as the primary goal.

A complete profile (with no missing intervals) should be generated and extend well into the background region of supported ^{210}Pb.

Estimating mean ages and time resolution of core sections

In cases where there is no evident mixing of near-surface sediments at a site, precision in mean ^{210}Pb ages of sediment sections can be calculated by conventional error estimation procedures including Monte Carlo methods for mappings and QPMs. However mean age precision can be somewhat misleading because it is not necessarily indicative of the time resolution with which historical records may be developed. Another time that we routinely calculate for " ^{210}Pb datable" cores is the ratio of the sediment section thickness ($g.cm^{-2}$) to the mass accumulation rate for the section ($g.cm^{-2}.yr^{-1}$). Since sections are presumably homogenized prior to analysis, this time indicates the best attainable time resolution for tracer "events" measured in a particular sectioned core. For example if the ratio is 5 years in a core section dated at 1945 ±1 year, then two spikes of a given tracer delivered to the sediment coring sites a times less than five years apart (say 1943 and 1946) cannot be separated (resolved) in the sedimentary record. Where there is evidence of mixing, mean age assignments, precision and time resolution can sometimes be meaningfully estimated by time averaging over appropriate QPM-

derived distributions of sediment deposition ages within sections. Finally, although it seems likely that most near-surface sediment mixing, as evidenced by ^{210}Pb profiles, must be steady state in character, it may not always be so. Consider an extreme example of sediments accumulating at a constant rate without mixing until last year, when Mayfly larvae populated coring sites. Their mixing actions (non-steady state by definition) may produce similar ^{210}Pb profiles, but QPMs as well as mean section ages, errors and time resolution estimates would, of course, be markedly different.

Special considerations for southern hemisphere (low activity) sediments by G. Brunskill J. Pfitzner and G. J. Hancock

The much lower fallout fluxes of ^{210}Pb and ^{137}Cs experienced in the southern hemisphere (described above) require special sampling and analytical considerations. Sampling requires large core barrel diameters to yield large samples of 1-2 cm slice thickness for radiochemical counting, and the resulting core profiles of excess ^{210}Pb have larger errors relative to ^{226}Ra. Because of these factors, we should anticipate more problems with the routine use of ^{210}Pb as a sedimentation tracer. Alpha spectrometry is the recommended detection system for both ^{210}Pb and ^{226}Ra, because it offers greater precision with a reasonable sample mass. We measure ^{210}Pb and ^{226}Ra by gamma counting, but we use large sample mass (>100 g dry weight), and accept larger error bars on the profile. In estuarine and marine sediment cores, we expect ^{137}Cs to have lower K_d than in freshwater sediments, and pore water diffusion of ^{137}Cs should be accommodated in geochronological models.

As noted above, a 1963 peak in ^{137}Cs profiles is not observed in the southern hemisphere. Where ^{137}Cs is assumed to have remained physically and chemically immobile in a sediment profile, such as freshwater flood-plain deposits which have remained mostly dry, the use of ^{137}Cs as a chronological marker equates its deepest penetration into the sediment profile to a date no earlier than the date where sufficient fallout activity has accumulated in sediments and soils to become detectable. Due to atmospheric circulation patterns,

and much lower fallout input, this date is later in the southern hemisphere than the northern. At CSIRO in Canberra we currently calculate the date of first detectable appearance of ^{137}Cs in Australian fine-grained soil and sediment to be 1958. This date is based on the performance of our gamma-ray detectors, counting system, sample geometry and sample weight. Because atmospheric input of ^{137}Cs has essentially ceased, the activity of ^{137}Cs in the landscape is decaying. The date of first detection is therefore not stable, and is moving forward at a rate dictated by the ^{137}Cs half-life and fallout history.

Bibliography

CALLENDER, E. C., ROBBINS J. A., 1993 — Radionuclide and trace element transport and accumulation in a Missouri River reservoir, Water Resources Res. 29: 1787-1804.

ROBBINS J. A., HERCHE L. R., 1993 — Models and uncertainty in Pb-210 dating of sediments, Verh. Internat. *Verein. Limnol*, 25: 271-222.

ROBBINS J. A., HOLMES C., HALLEY R., BOTHNER M., SHINN E., GRANEY J., KEELER G., TENBRINK M., ORLANDINI K. A., RUDNICK D., 2000 — Time-averaged fluxes of lead and fallout radionuclides to sediments of Florida Bay, *J. Geophys. Res. Oceans*, 105, C12: 28 805-28 821.

ROBBINS J. A., ROSMANN R., MUDROCH A., ROOD R., MOREHEAD N., EDGINGTON D. N., 2001 — "Effect of recurrent episodes of Lake Erie on accumulation of manganese and ^{210}Pb in sediments." *In:* Fernandez J. M., Fichez R. (eds): *Environmental Changes and Radioactive Tracers*, IRD Editions, Paris, p. 262.

Oral/Poster presentations

Session 3

Applications of radionuclide tracers to studies of mixing and accumulation in modern sediments

John N. Smith

The authors of the first paper on ^{210}Pb dating in marine sediments had the good sense to validate their method by performing their measurements in varved sediments in the Santa Barbara Basin, off California for which the time-stratigraphic horizons had been well established. Several years later, Robbins & Edgington (1975) pointed out that most sediment regimes in lake and marine environments undergo mixing or bioturbation in the upper 10-20 cm, mainly as the result of the feeding and physiological activities of benthic organisms. Mixing confounds the time-stratigraphic resolution of the sedimentary record and eliminates the possibility of determining 20th century, contaminant geochronologies in most marine and aquatic sediment regimes. The only recourse of the tracer geochemist is to formulate a model that simulates particle uptake and post-depositional mixing and apply it to the interpretation of radionuclide and contaminant sediment profiles. Geochemists accept this reality reluctantly, because of the enormous loss of chronological information resulting from even very low rates of sediment mixing. The interplay of sediment mixing and accumulation can be illustrated using examples from a variety of depositional regimes ranging from the slowly accumulating sediments of the Arctic Ocean basins to high sedimentation rate environments in the Saguenay Fjord, Quebec. The intention of this paper is to identify the pitfalls of ignoring the impact of mixing on the interpretation of geochemical features in marine sediments and to highlight the insights into animal-sediment interactions that can be gained from a more realistic approach to these types of studies.

Building a self-consistent interpretation of radionuclide profils in Lake Tahoe sediments: other geochemical parameters are required as well

David N. Edgington **A. Heyvaert**
John A. Robbins **D. Olaniyi**

^{210}Pb, $^{239+240}$Pu, ^{228}Th, ^{226}Ra, ^{235}U and ^{40}K were measured in a sediment core collected in 1998. The ^{210}Pb results may be compared with earlier profiles measured in 1982 and 1991. ^{137}Cs was measured in 1991 and 1998. Trace elements, e.g., Mn, Fe, and Pb, and organic carbon were measured in the same samples. The sediment record in Tahoe exhibits classical redox subsurface peaks of manganese, with iron immediately below (where phosphate also peaks), at depths from 2.5 to 4 cm., indicative of little mixing by organisms below this zone. The excess ^{210}Pb profiles are not a simple exponential, but may reflect a higher sedimentation rate since about 1975, corresponding to a factor of > 2 than in earlier times. This change in rate is consistent with the decrease in organic carbon content concomitant with the disturbance of low organic carbon soils resulting from construction activity in the basin. However, a comparison of the ^{137}Cs and ^{210}Pb profiles are also consistent with mixing down to 5-6 cm. But the $^{239+240}$Pu profile exhibits penetration and subsurface maximum at depths apparently consistent with sedimentation rates calculated from the ^{210}Pb data. The ^{228}Th profile shows mixing in the upper 2-3 cm of sediment, which is consistent with the position of the redox boundary. Geochemical changes associated with the redox zone lead to minimum values for ^{235}U and ^{40}K, and a small maximum for ^{226}Ra. Development of a self-consistent model needs to reconcile the large differences between the ^{137}Cs and $^{239+240}$Pu profiles in relation to their differences in geochemical properties in the water and interaction with sediments.

The time-dependent distribution of ^{137}Cs in the sediments of Lake Michigan

David N. Edgington **E. Taylor**
John A. Robbins **R. Rood**
S. Meyer **N. Morehead**

The spatial inventory of ^{137}Cs in Lake Michigan has been assessed in 1972, 1982, 1992, and 1994 - 1996. Early results indicated that by 1972 there had been extensive focusing of the atmospheric input into depositional zones corresponding to area where sediment had deposited since glacial times. Between 1972 and 1982, a period with little or no new inputs of ^{137}Cs, inventories in these zones increased to values greater than found in 1972. Between 1992 and 1996 in a definitive lakewide survey (134 sites within "depositional areas), cores collected were quantitatively sectioned into 1 cm intervals and mass per unit area, ^{210}Pb and ^{137}Cs measured for each section. Sedimentation and mixing rates, and mixing depths, were determined from the ^{210}Pb data . They were used to deconvolve the ^{137}Cs profiles into monthly (1955 to 1995) focusing factors (FF) (where FF = ratio of decay corrected inventories (dpm.cm-2) and mean integrated atmospheric deposition of ^{137}Cs), and these values were contoured. Over the whole lake, the average value of FF must equal 1. Within depositional areas, average FF increased from < 0.5 in the 50's to >4.0 in the 90's. Mass balance requires values of FF in "non-depositional" areas which extend outward from the shore (uncorable areas, 60% of lake surface) to decrease exponentially from 1.78 to ~0.5 respectively with a time constant of 37 years. These results will be discussed in terms of the geochemical properties of ^{137}Cs and scavenging from the water, resuspension and redistribution processes involved in this long-term transport of particles, and implications for recovery of closed systems from pollution episodes.

Time-average fluxes of lead and fallout radionuclides to sediments in Florida Bay, Florida, USA

John A. Robbins
C. W. Holmes,
R. Halley
M. Bothner
E. Shinn
J. Graney
G. Keeler
M. Tenbrink
K. A. Orlandini
D. Rudnick

Recent, unmixed sediments from mud banks of central Florida Bay were dated using $^{210}Pb/^{226}Ra$, and chronologies were verified by comparing sediment lead temporal record with Pb/Ca ratios in annual layers of a coral (*Montastrea annularis).* Dates of sediment lead peaks (1978 ± 2) accord with prior observations of a six-year lag between occurrences of maximum atmospheric lead in 1972 and peak coral lead in 1978. Smaller lags of 1-2 years occur between the year of maximum fallout and the sediment record of ^{137}Cs and Pu. Such lags are consequences of system-time averaging (STA) in which atmospherically derived material accumulates and mix before removal to the sediments and coral. Using time-dependant atmospheric inputs, STA model calculations produced optimized profiles in excellent accord with measured sediment ^{137}Cs, Pu lead and corals distributions. Derived residence times of these particle tracers (16 ± 1, 15.7 ± 0.7, 19 ± 3, and 16 ± 2 years, respectively) are comparable despite differences in sampling locations, in accumulating media, and in element loading histories and geochemical properties. For a sixteen-year, weighed-mean residence time, STA generates the observed six-year lead peak lag. This study shows that, when transient tracers are used to verify ^{210}Pb chronologies, potential lag effects resulting from STA processes must be considered. Because of reservoir effects, significant levels or non-degrad-

able, particle-associated contaminants can persist in Florida Bay for many decades following elimination of external inputs. Present results, in combination with STA-models analysis of previously reported radionuclide profiles; indicate that decade- scale time averaging may occur widely in recent coastal marine environments.

Sediment budget in the East China Sea elucidated from fallout nuclides

C. A. Huh

C.-C. Su

Using three fallout nuclides (^{210}Pb, ^{137}Cs and ^{239,240}Pu) as tracers, an attempt was made to elucidate the budgets, sources and pathways of sediments and these nuclides in the East China Sea (ECS). A large number of box and gravity cores were collected from this marginal sea and analyzed for this purpose. Multiplying the area of the ECS as defined in this study (353,000 km^2) by the ^{137}Cs-based mean sedimentation rate (0.372 g.cm^{-2}.yr^{-1}) yields an annual sediment flux of 1.3x10^9 tons.yr^{-1}. This is about twice the sum of the reported annual discharge from the Yangtze River (~5x10^8 tons.yr^{-1}) and erosion from Taiwan (~2 x10^8 tons.yr^{-1}). To account for the substantial imbalance, input from the Yellow River's dispersal system from the north is required. Spatial distribution of sediment inventories of ^{137}Cs and ^{239,240}Pu shows that input from the Yangtze Rivers's drainage basin constitutes the dominant source of these two anthropogenic nuclides in the ECS. As for the natural nuclide ^{210}Pb, boundary scavenging and atmospheric fallout are equally important whereas riverine input is negligible. By comparing the mean sediment inventories of ^{210}Pb, ^{137}Cs and ^{239,240}Pu in the study area (71, 5.2 and 0.72 dpm.cm^{-2}, respectively) with corresponding values expected from global fallout (37, 7.1 and 0.21 dpm.cm^{-2}, respectively), it can be seen that ^{210}Pb and ^{239,240}Pu precipitated from the atmosphere are effectively scavenging from the water column, whereas ^{137}Cs is not.

Reconstruction of Pleistocene history of metal pollution in a natural swamp using ^{210}Pb geochronometer

K. H. Kim

D. S. Moon

J. S. Yang

We report detailed profiles of ^{210}Pb and ^{137}Cs activities in a sediment core collected from Woopo Swamp, a 20 km^2-wide Pleistocene marshland in southern part of Korea. Activities of the two radionuclides were measured by non-destructive gamma spectroscopy utilizing a high-purity germanium detector. Since the bottom sediments of the swamp were highly anoxic with very high organic content derived from flourishing aquatic plants, no indication of biological particle mixing was recognized in the core. The excess ^{210}Pb activities showed an exponential decrease with depth as in the case of organic carbon content. A least-squares best-fit line drawn to the excess ^{210}Pb data points yielded a sedimentation rate of 0.44 ± 0.04 $cm.yr^{-1}$. This estimated rate was in a good agreement with the result from another stratigraphic marker, the depth of ^{137}Cs peak occurring around 15 cm below the surface. Fifteen elements including Al, As, Ba, Ca, Cd, Cr, Cu, Fe, Hg, Mn, Ni, Pb, Sr, Ti and Zn were determined as well in the same core by inductively coupled plasma atomic emission spectroscopy. They were classified into 3 groups: volatile (As, Cd, Hg, Ni, Pb), refractory (Al, Ba, Ca, Sr, Ti), and diagenetic groups (Cr, Cu, Fe, Mn, Zn). The concentrations of the refractory elements have remained relatively constant with time for last 160 years. On the contrary, the volatile and diagenetic elements showed increase since the beginning of the 20th century. The steep increase of volatile elements in swamp sediments may be due to the anthropogenic input associated with the population growth in Korea.

Effect of recurrent episodes of hypolimnetic oxygen depletion in Lake Erie on accumulation of manganese and ^{210}Pb in sediments

John A. Robbins
R. Rossmann
A. Mudroch
R. Rood
N. Morehead
David N. Edgington

The eastern depositional basin of Lake Erie (North America) would seem to be an ideal environment for ^{210}Pb dating. Sediment accumulation rates are high (~1 cm/year) and profiles of ^{137}Cs in four cores (collected in 1976, 1981, 1983 & 1991) have sharply defined peaks. However marked departures of ^{210}Pb profiles (0-20 cm depth) from ideal exponential shape, particularly by 1991, are not explained by mixing of surface sediments or by changing rates of sediment accumulation. In cores dated initially by ^{137}Cs, decay-corrected excess ^{210}Pb activities correlate well with Mn concentrations and with total phosphorus loading between 1800 and 1982. Evidently rate of supply of ^{210}Pb the eastern basin increased with human-caused eutrophication of the lake especially from the 1960s through early 1970s, and subsequently diminished in concert with reductions in phosphorus loads. Because of eutrophication, hypolimnetic waters over large areas of central lake were depleted in oxygen during the summer and early fall, causing Mn (and presumably ^{210}Pb) to dissolve from surface sediments. Subsequent mixing and re-oxygenation of the water column re-precipitated Mn that then was transported to the eastern basin and delivered to sediments. A quantitative model linearly coupling concentrations of excess ^{210}Pb and Mn produces excellent ^{210}Pb profile fits yielding accumulation rates consistent with those from ^{137}Cs. The Lake Erie case exemplifies the failure of mapping schemes, such as CRS, whose validity depends on a constant rate of supply of ^{210}Pb. Since mapping schemes do not yield model profiles for comparison with data, faults in derived age-depth relations may go unrecognized.

Mapping schemes versus process models for ^{210}Pb dating soil cores: an example from the everglades of South Florida, U.S.A.

John A. Robbins

C. Holmes

K. Reddy

S. Newman

Two contrasting approaches have emerged for extracting sediment age information from ^{210}Pb profiles: one using algorithms, such as CRS or CIC, to convert individual excess ^{210}Pb activities into dates; the other using process models to "explain" ^{210}Pb profiles and supply chronological information. These are illustrated using data from a nutrient-impacted area of the Everglades wetlands in south Florida. The study area (WCA2A) is bounded by a system of canals, one of which has been a long-term source of phosphorus from upstream agricultural activities. Near the canal, in the strongly impacted area, cattails (*Typha domingensis*) dominate the plant community. Further along a transect extending away from the canal, the community consists of a mix of cattails and sawgrass (*Cladium jamaicense*), and finally, beyond about 8 km, is dominantly sawgrass with interspersed open-water sloughs. A CRS mapping scheme applied to excess ^{210}Pb profiles in cores collected along the transect, generates age-depth relations consistent with depths of peak ^{137}Cs activity. The process model treats plant growth as being controlled by extraction of P from soils via anchoring root networks, and from water and surface soils by adventitious roots. By coupling net soil accretion rates, and indirectly biomass production, to near-surface soil total P concentrations, quite unusual ^{210}Pb profiles are quantitatively well described. Both process model and

mapping scheme yield sediment accumulation rates increasing exponentially at impacted sites during the past several decades. Although successful process models can potentially reinforce inaccurate notions of mechanisms producing observed ^{210}Pb profiles, mapping schemes should be nevertheless considered dating techniques of last resort.

^{210}Po and ^{210}Pb disequilibrium in mangrove coastal water and sediment

Y. Tateda

Y. Ikeda

K. Fukami

K. Kurosawa

^{210}Po concentrations in oligotrophic open water are generally controlled by density and size of zooplankton of high ^{210}Po affinity, because the rate of ^{210}Po removal from surface water is coincided with downward transport fluxes of ^{210}Po-rich biogenic debris originated to zooplankton. Thus the ^{210}Po levels in oligotrophic water are good index of zooplankton density and grazing activity in open waters. However, in coastal area, ^{210}Po is sometimes reported to be excess than ^{210}Pb, which ascribed to be the release from coastal sediment. In low latitude area of pacific ocean, the coastal area is mostly covered with coral reefs and mangroves, and the mangrove could be the significant ^{210}Po source because of its high organic and inorganic matter discharges. Briefly, the ^{210}Po and ^{210}Pb concentrations in mangrove coastal water are expected to be controlled by atmospheric deposition flux, in- and out-flux along with tidal water exchange, input flux originated from oxic-anoxic environment change of sediment, and from organic matter decomposition by heterotrophic benthos. To clarify the significant source of these nuclides, we analyzed the ^{210}Po and ^{210}Pb concentrations in coastal water and sediment of mangrove area at Fukidou River in Ishigaki Island Japan. By flux estimation, we estimate the balance of ^{210}Po and ^{210}Pb in the water column in and around the mangrove area and discuss the relation between these nuclides and other environmental component. The result indicated that the mangrove area is the source of ^{210}Po in coastal waters, and the organic matter decomposition or benthic biota activities are suggested to be important sources of ^{210}Po in mangrove area.

Isotopic constraints (^{228}Th, ^{210}Pb) on the age of resuspension episodes of contaminated sediments in a coastal lagoon from Northwestern Mexico

A. C. Ruiz-Fernández

C. Hillaire-Marcel

B. Ghaleb

F. Páez-Osuna

In order to document anthropogenic fluxes of trace metal contamination in the coastal lagoon system of Altata Ensenada del Pabellon, on the Pacific coast of Mexico, sediment push-cores up to ~ 70 cm-long were raised at the inner lagoons of Chiricahueto (CHI) and Caimanero (CAI) and at Culiacan estuary (ERC). The cores were subsampled at one-centimeter intervals for measurements of: ^{228}Th, ^{230}Th, ^{232}Th and ^{210}Pb (^{210}Po) through alpha-counting, ^{226}Ra by thermal ionization mass spectrometry and ^{137}Cs by gamma counting using a well-detector device. ^{137}Cs activity measurements were at background level for all samples. Based on ^{226}Ra data, the supported ^{210}Pb fraction was estimated to be ~ 1.1 dpm.g^{-1}, which corresponds to the minimum ^{210}Pb activities measured in the study cores; and this value was subtracted to total ^{210}Pb-measurements in order to calculate ^{210}Pb-excesses ($^{210}Pb_{xs}$). Core CHI shows a flat, ~ 0, $^{210}Pb_{xs}$ profile indicating the absence of recent sedimentation (i.e., less than ~ 100 yrs) and possibly erosion at the site. In opposition, core ERC shows an almost constant $^{210}Pb_{xs}$ of ~ 2 dpm.g^{-1} in the top 70 cm, overlying a section with a $^{210}Pb_{xs}$ ~ 0; this suggests the presence of relatively old sediment on top of a rather thick layer of recent material likely (re-)deposited during one single resuspension event, possibly triggered by high storminess conditions. Core CAI also shows flat but significantly lower $^{210}Pb_{xs}$, in its upper section, suggesting a

more older resuspension event at the origin of the corresponding layer, or the resuspension of sediment with a lesser $^{210}Pb_{xs}$. At site ERC, large ^{228}Th-excesses over ^{232}Th are observed, suggesting that the resuspension event, at the origin of the deposition of the upper high-$^{210}Pb_{xs}$ layer, occurred less than 10 years ago (i.e., less than 5 half-lives of ^{228}Th). It is concluded that the contaminated sediment of the lagoon are likely to be frequently resuspended, re-oxygenated, and therefore that the contaminating trace metal will continue to be easily remobilized in the food chain.

Patterns of ^{210}Pb and ^{137}Cs accumulation in sediments on australian/PNG coastal shelves of high and low continental sediment supply

Greg J. Brunskill

John P. Pfitzner

An overview of patterns of accumulation of ^{210}Pb (excess) and ^{137}Cs in continental shelf sediments of NE Queensland, the NW Shelf of Australia, and the Gulf of Papua is given. Atmospheric supply of these sedimentation tracer nuclides for NE Queensland is approximately 50 Bq $^{210}Pb.m^{-2}.yr^{-1}$ and a 1950-1990 inventory of 400 Bq ^{137}Cs m^{-2}, based upon terrestrial soil profiles and rain collections. These supply rates are much lower than in the northern hemisphere, and special efforts are required to use these sediment tracers in sedimentation models derived from high supply regions. The scavenging of these nuclides in coastal seas, and delivery to the sediment inventory, is probably a function of terrestrial sediment supply by rivers. River sediment plumes and resuspended fine sediments remove these atmospherically derived nuclides from the water column rapidly, whereas clear offshore waters that have low supply rates of fine particles deliver much smaller inventories of these nuclides to sediments. On the NW Shelf of Australia, river inflow is very small, and continental shelf sediment cores have low inventories of ^{210}Pb and ^{137}Cs. On the north Queensland continental shelf, small fluxes of water and terrestrial sediment are delivered to the inner shelf of the lagoon of the Great Barrier Reef. These river sediment inputs trap these tracer nuclides in fine riverine sediments of coastal estuaries, mangrove mud aprons, and shallow wind-protected embayments of the inner shelf, and we frequently find inven-

tories of both tracers 2-10 times greater than atmospheric supply rates. In the Gulf of Papua, where globally significant inputs of river water, solutes, and fine sediment are injected into the South Pacific Ocean, large fluxes (2-20 times atmospheric supply rates) of excess ^{210}Pb were found in the fine riverine sediments of the inner shelf and at the base of the continental slope. This region is a good example of an estuarine trap for particle reactive tracers, and exhibits ocean margin scavenging of continental slope-advected oceanic water from the Coral Sea and South Pacific Ocean.

Anthropogenic forces on distribution of heavy metals in the monsoon-dominated western continental margin of India

B. R. Manjunatha

Hazardous heavy metal concentrations and sediment accumulation rates measured by ^{210}Pb and ^{137}Cs, have been compiled to understand the impact of anthropogenic activities on monsoon dominated west coast of India. For the benefit of easy reference, the area of investigation can be divided into the northern Konkan Coast, the central Karnataka Coast and the southern Kerala Coast. Sediment accumulation rates increase from northern Konkan coast, through the Karnataka to Kerala coast (0.31-1.36, 0.38-1.91, and 2.9-3.8 $g.cm^2.yr^{-1}$ respectively). Conversely ^{210}Pb inventories also show the same trend in sediments of these three coastal tracts (0.5-5.82, 2.21-13.82 and 39.2-67.5 $dpm.cm^{-2}$ respectively). This suggests a southerly increase of land erosion perhaps be due to severe deforestation. The rates along the Kerala coast, particularly in Cochin Backwaters are considerably higher than that reported for other coastlines of the world, which could be ascribed as not due to the land erosion, but also due to dumping of solid wastes. In spite of high sediment accumulation rates, toxic heavy metals are remarkably higher in nearshore marine sediments bordering densely populated and industrialized cities like Bombay and Cochin. Toxic heavy metals like Cd, Pb and Zn are particularly higher in Cochin Backwater sediments (1.9-4, 40-284, 586-6296 ppm respectively) as compared to those in Mumbai estuarine sediments (1.7-6.1, 30-143 and 96-247 ppm respectively). Further, trapping of river-borne sediments together with contaminated heavy metals in the land-ocean margins. All these evidences indicate the dominance of

anthropogenic activities over the natural processes. Nevertheless, estuarine and marshy sediments along the Karnataka coast as well as inner shelf sediments off the West Coast of India these toxic metals are fairly within the background levels.

Dating sediment profiles using radionuclides: the need for corroborating evidence

Gary J. Hancock

Radionuclides provide important, and often unique ways of dating of soil and sediment profiles. However, changes in the rate and mechanism of delivery of radionuclides to sediments, and biogeochemical processes operating in the sediment profile invalidate many of the assumptions required for age determination. In these cases direct application of radionuclide dating models can yield spurious ages, and interpretation without corroborating evidence is risky. This presentation will explore the effects of some of these confounding processes by discussing a series of case studies. Lake Barrine, a tropical crater lake in Northern Australia exhibits many characteristics suitable for successful application of radionuclide dating techniques; ie. a small catchment relatively undisturbed by European settlement. Distinct laminations in the deposited sediment indicate little or no post-depositional mixing. Sediment core and frozen slabs samples covering a period of up to 5000 y^r BP have been collected and dated using ^{14}C, excess ^{210}Pb and ^{226}Ra, together with proxy age indications from charcoal, exotic pollen and meteorological data. These laminations are probably due to thermally induced water column overturn events, allowing the formation of excess ^{226}Ra in bottom sediment by co-precipitation of dissolved ^{226}Ra delivered from the catchment with Fe accumulated in anoxic bottom waters. In the period 1000-4000 yr BP ^{14}C and excess ^{226}Ra ages agree well. However in younger sediment the spread of ^{14}C ages increases to the point where many of the ^{14}C ages are clearly much too old. The spread is probably due to the delay in transport of organic material from the shallows to deeper water. Taking the youngest ^{14}C ages, and extrapolating the excess ^{226}Ra depth vs age

curve gives acceptable ages up to 1000 y^r BP. Sections of the ^{210}Pb profile closely approximate the exponential decline expected in a system where recent sedimentation rates have been approximately constant. However the profile is separated by a thick amorphous layer, below which the sediment ages estimated by the two commonly used dating models (the CRS and CIC models) differ. Exotic pollen and charcoal data support CRS ages for sediment below the amorphous band. The ^{210}Pb ages provide evidence for the ^{14}C 'contamination' of young sediment by organic material with an older ^{14}C signature. In many Australian lakes sediment profiles show ^{210}Pb profiles characteristic of highly variable sediment influx. Non-monotonic decreases in ^{210}Pb activity are common, and can be related to catchment disturbance associated with European settlement. In these sediments, the CRS model is usually the most appropriate, but ages should checked by independent means. Examples will be presented which show how dilution of ^{210}Pb activity by large sediment influxes could lead to the erroneously old ages. Mixing of the upper layers of sediments is common in near-shore marine sediment, and if not recognised can lead to the determination of spuriously young ages in the mixed zone. Mixing depths can vary greatly, as can the mixing process. Examples of simple 2-layer mixing models will be presented, where the sedimentation accumulation rate is determined from the ^{210}Pb below the mixing zone. Knowledge of the mixing time constant can help constrain the accumulation rate within the mixed layer, and the presence of second tracer with a half-life different to ^{210}Pb can allow the estimation of both mixing and accumulation rates. This approach has been applied in Port Philip Bay, using the decay profiles of excess ^{210}Pb and ^{228}Th.

A preliminary study of ^{210}Pb geochemistry in the Pearl River Estuary

S. Pan

Pearl River Estuary is a drainage basin of Pearl River system. The amount of yearly average runoff is totally $3.42x10^{10}$ m^3,and the amount of annual suspended silt is 83.36 million tons, 80% of which into the Pearl River Estuary. A large area of silt-clay or sandy deposits has been formed under the interaction of the river and the sea. A suite of sediment cores, collected between June 1995 and April 1998 from Pearl River Estuary, were analyzed for ^{210}Pb activities and textural parameters. It was found that both vertical and horizontal distribution of ^{210}Pb follow certain laws in this area. The vertical distribution of ^{210}Pb in Pearl River Estuary can be divided into two types (normal type and abnormal type). The normal type consists of three region, two region and one region forms, and the abnormal type consists of parallel, upside-down and disorder forms.The normal type of ^{210}Pb in sediment core reflects the relative steady sedimentary environment and the sedimentation rates can be determined. The abnormal profile of ^{210}Pb reflects the unsteady-state sedimentary environment, some events, such as bioturbation, resuspension, dredging, dumping and sliding, may take place in these stations, different environmental events caused the origin and genesis mechanisms of different anomalous fluctuations of ^{210}Pb. Sedimentation rates were calculated using constant flux/sedimentation rate(CFS) model.

Evidence of human induced environmental alteration: preliminary results from the study of sedimentary records in the Bay of Sainte Marie, New Caledonia

Jean-Michel Fernandez

Ludovic Breau

Renaud Fichez

Christian Badie

Past environmental changes have been studied in the sediments of the lagoon of New-Caledonian, sediments possess the capacity to integrate and store various information relative to modification and alteration. Extracting and deciphering those natural archives are central to the understanding of past and present sedimentary processes and provide a dynamic view on the evolution of environmental conditions. A core of 56 cm was extracted from the bottom of Sainte Marie Bay (New Caledonia) that is subject to significant urban inputs from the city of Noumea. The core was sampled in 2 cm thick slices and sediments were dated using ^{210}Pb unsupported radioactivity. Carbonate content was determined and 8 metals (Fe, Mn, Al, Ni, Cr, Co, Cu, Zn) were analysed in the oxidizable, acid-soluble, reducible and refractory phases. Carbonate distribution and grain size composition profiles, yielded evidence of a progressive decrease of the marine influence over the time in the bay. This assumption is supported by concentrations of Ni, Mn and Fe which underline a drastic change in the nature and the amounts of terrigeneous inputs. The distribution of nickel normalised by manganese, both in the refractory geochemical phase, versus depth confirms the alteration in sedimentary signatures during the last 100 years.

Despite the evidence of a significant bioturbation layer extending down to a maximum of 10 cm in depth, two average accumulation rates have been estimated : 0.2 $g.cm^{-2}.yr^{-1}$ from 1945 to the present day and 0.1 $g.cm^{-2}.yr^{-1}$ before 1945. These modifications demonstrate that the Sainte Marie Bay has been impacted on since the beginning of open-cast mining and deforestation activities in the Southern New Caledonia (La Coulée and Les Pirogues catchment basins).

Radioactivity in atmospheric studies

Session 4

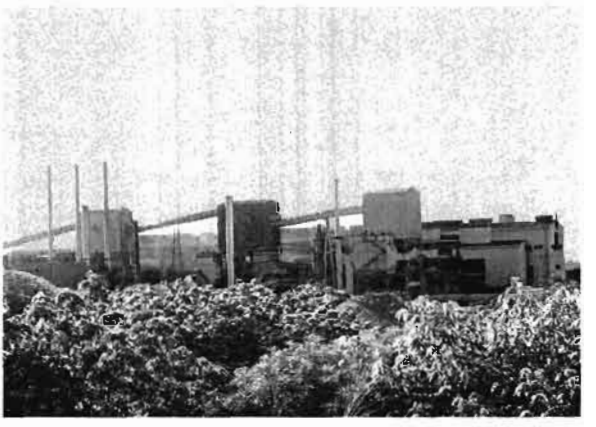

Chairman: G. Le Petit

Session opening: J. Harries

Radon measurements for atmospheric tracing

Wlodek Zahorowski

Stewart Whittlestone

John R. Harries

Introduction

Radon is a useful tracer of atmospheric dynamics because of its simple source and sink. Radon is a noble gas; as such it does not react chemically with other atmospheric species; its sink is predominantly by radioactive decay, with a half-life of 3.81 days. The half life of radon is comparable with the chemical lifetimes of short-lived air pollutants such as NO_x, SO_2, CO, O_3. It is also comparable with the resident times of such important atmospheric constituents like water and aerosols. Many important dynamic atmospheric features occur on a time scale in the order of days.

Radon comes from land. The flux depends on the mineralogy and varies depending on changes in atmospheric pressure and soil moisture. The oceanic radon flux is on average at least 100 times smaller than that from land. This makes radon present in air samples at characteristic levels indicative of contact with land within the previous few weeks.

Radon flux from the soil to the lower atmosphere is always positive or zero as in water saturated soils or in presence of surface barriers like ice sheets. The flux from the soil to the atmosphere is maintained by a strong concentration gradient with the concentration above the ground about 1000 times lower than a few cm below the ground.

Once injected into the atmosphere radon can be used as a tracer on local, regional and global scales. Sub-grid mixing processes as well as long-range transport cause significant changes in radon concentrations which can be analysed in the context of local mixing schemes or regional/global circulation models.

Changes in the radon concentration are characteristic of the mixing and transport processes in the atmosphere. These changes can be measured continuously with adequate precision in ground stations using automated detectors. Vertical profiles up to 13 km have also been measured using grab samples collected from aircraft platforms; detectors have been developed for in situ airborne measurements within the boundary layer.

Thoron (radon-220) and its decay product lead-212 complement very well radon tracing capabilities on smaller time and spatial scales. Thoron (half-life 55.6s) is a gas and like radon, emanates from land. It is used as an effective tracer within a few meters above the surface. Airborne lead-212 (half-life 10.6h) is indicative of contact with local land.

This paper will describe recent developments in the measurement and application of atmospheric radon for baseline air pollution stations, the characterisation of local and regional transport processes, and the development and verification of global transport models.

Instrumentation

Radon concentration in marine air can be as low as a few radon atoms per litre of air. This makes the task of measuring radon levels with a time resolution matching prevailing weather conditions a demanding task. Radon measuring techniques and commercially available instrumentation developed for radiation protection are inadequate for the atmospheric research.

The volume of air which needs to be analysed for radon has to be large since the expected radon concentrations can be very low. For instance, in the air at Cape Grim that has not been in contact with a

land mass has only 10 to 100 mBq.m^{-3} radon, which corresponds to between 5 and 50 radon atoms per litre of air. In a hypothetical detector of with a volume of 1 m^3, 100% counting efficiency for radon decays and no background, radon concentration at 10 mBq.m^{-3} level would result in 18 counts per half hour. In practice, counting efficiency is significantly lower than 50% and instrumental background is a serious problem for concentrations below 20 mBq.m^{-3}.

ANSTO detectors for measurement of radon times series

In the last decade, ANSTO has developed and commissioned two types of radon detectors with the sensitivity matching baseline concentrations (Whittlestone and Zahorowski,1995; Whittlestone and Zahorowski, 1998). Both designs are based on the two-filter method which relies on the sampled air being drawn continuously through one filter which removes all radon decay products, then through a delay chamber in which some new progeny are produced. Finally air passes through a second filter which collects the progeny at a rate proportional to the radon concentration. The larger the delay chamber volume, the more sensitive the detector will be since more progeny are produced in the chamber.

A major challenge in the design of high sensitive two filter detectors is to prevent the progeny from being plated out on the walls of the delay chamber. Most two-filter detectors use a high flow rate to ensure that the air passes from the inlet to the outlet filters in a time short compared to the mean plate-out time. In a detector with a volume of one or two cubic metres, the plate-out time is a few minutes. This implies that flow rates of about a cubic metre per minute would be necessary. As a result, pumping power and the second filter had to be unacceptably large.

One can solve this problem by injecting and maintaining a constant concentration of sub-micron particles in the delay chamber. This has been done in the first of the two designs (Whittlestone and Zahorowski, 1996). With particles in the chamber, the progeny become attached to the particles, which have a mean plate-out time of many hours in delay chambers of a volume greater than about 2 m^3.

This solution delivers excellent results as far as lower limit of detection is concerned but it cannot work unattended at remote sites and on mobile platforms.

The second design called dual flow loop wire screen radon detector addresses the plate out problem by introducing a division of the air flow into the low rate external and high rate internal components and the use of the wire screens as the second filter (Whittlestone and Zahorowski, 1998). Hence, the function of supplying filtered air to the detector has been separated from the function of delivering air to the collecting wire screen used for collection of the radon progeny. The high diffusivity of radon progeny makes it possible to use a wire screen to remove the progeny with high efficiency and very low flow impedance.

The principle of operation is show in Figure 1. The external flow takes the sampled air through the thoron delay volume that removes thoron and an inlet filter where existing radon progeny are filtered from the sample. The internal flow rate is high to maximise the likelihood of the progeny plating out on the wire mesh filter rather than on the walls of the chamber. The collected progeny decay by alpha decay which is detected in a scintillator/photomultiplier assembly.

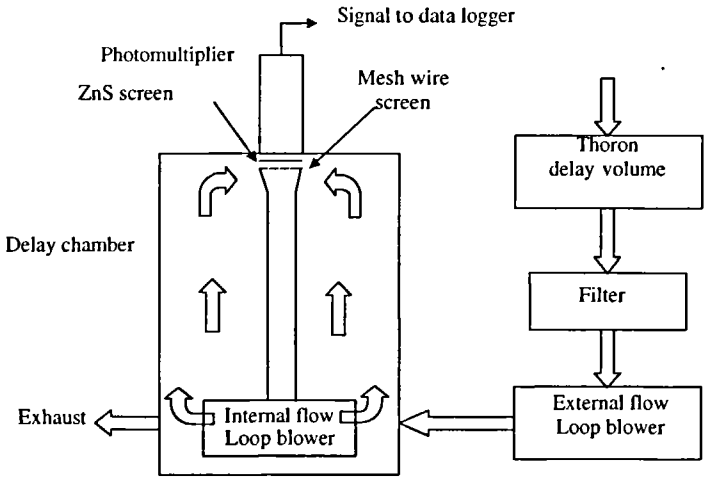

Figure 1
A schematic of the dual flow loop wire screen detector.

Dual flow loop wire screen radon detectors can measure radon concentration in air down to 5 $mBq.m^{-3}$ with a time response of about 45 minutes to 50% of the maximum after a step increase in radon concentration. Implementations of the design have varied delay volumes (from 750 l to about 5,000 l) to match different sensitivity requirements. A "middle of the range" 1,500 l detector has a lower limit of detection equal to 20 $mBq.m^{-3}$ with the internal flow rate at about 800 $l.min^{-1}$ and the external sampling flow rate at 80 $l.min^{-1}$.

Deployment of ANSTO radon detectors

Figure 2 shows locations where ANSTO radon detectors have been deployed. Three detectors (at Cape Grim, Mauna Loa and Cape Point) take part in Global Atmospheric Watch, a World Meteorological Organisation network of about 20 world-wide research stations for measuring atmospheric composition and long-lived pollutants. The stations' output underpins research into global climate change and stratosphere ozone depletion. Other locations point to installed detectors which serve ongoing air mass character-

Figure 2
Deployment of ANSTO's baseline detectors.
Locations in italics indicate a network of detectors under construction.

isation and recording of long term radon time series for model development and verification. A new set of detectors has been proposed and is now being established in the international Aerosol Characterisation Experiment (ACE-Asia) in East Asia and the Northern Pacific.

Local and regional land surface/ atmosphere characteristics derived from radon

Both radon and thoron have been used as a tracer of near-surface mixing processes.

At the soil-air interface the typical radon profile changes dramatically: above the surface at 1m height the radon concentration is 10 $Bq.m^{-3}$ and at 1000 m is half of that; below the surface at a depth of 5cm it is between 500-1000 $Bq.m^{-3}$ and the equilibrium concentration of between 70,000-90,000 $Bq.m^{-3}$ is reached at a depth of 2 m. For thoron, the concentration gradient is much steeper, owing to its much shorter half-life, with the depth and height at which half of the surface level are reached being 1.5 cm and 14 cm, respectively.

Local vertical mixing

Vertical distribution of a radioactive tracer concentration C(z) can be estimated using a simplified vertical diffusion equation:

$$\frac{\partial C}{\partial t} = \frac{\partial}{\partial z}\left(k_z \frac{\partial C}{\partial z}\right) - \lambda \cdot C$$

where k_z is the vertical eddy diffusivity and l is the decay constant of the tracer.

The vertical eddy diffusivities can be estimated from radon observations at different vertical scales within the boundary layer. Alternatively, modeled vertical eddy diffusivities can be validated by comparing calculated with observed profiles.

Lee and Larsen (1997) sampled radon profiles in the boundary layer as a function of altitude (up to the top of the layer) and time of day using an instrument designed for *in situ* aircraft measurements. The measured profiles were used to examine distributions of the profiles of the vertical eddy diffusivities $k_z(z,t)$. In particular, it was possible to validate modeled distributions of vertical eddy diffusivities by comparing measured radon profiles with simulated ones obtained by solving the above vertical diffusion model with the modeled profiles of the vertical eddy diffusivities.

In another study, radon was shown to provide an independent estimate of the trace gas exchange at the biosphere-atmosphere interface (Ussler *et al.*, 1993). Radon time series were recorded at different heights up to 18m of a micrometeorological tower located in a dry, open-canopy forest. Radon flux was estimated independently of the profile measurements. From the experimental data a time evolution of the forest canopy trace gas exchange coefficient was derived as well as the average total forest canopy resistance. The results compared well with those obtained by eddy correlation techniques. The study demonstrated that automated radon measurements of concentrations in air can be successfully employed in remote locations where daily maintenance required to standard micrometeorological equipment (such as a sonic anemometers) is not possible.

Butterweck *et al.* (1994) characterised vertical diffusion in the near-surface atmosphere (0-5m) from continuous measurement of radon and thoron concentrations within and above a wheat field over the complete vegetation cycle of the crop. They used the data to calculate vertical eddy diffusivities for two horizontal layers: one within the crop (0.14-1.5 m) and the other above the crop (1.5-5 m). Mean vertical diffusivities for three weather conditions and two vertical temperature gradient intervals were then calculated. When compared with results obtained from meteorological data for the above crop layer (1.4-5 m) good agreement was obtained. It was claimed that the tracer method was superior especially inside the crop where

meteorological methods are not effective. Thoron proved to be complementary to radon in the lower interval within the crop where the vertical change in radon concentration was to small to derive the gradient with a satisfactory precision.

Regional trace gas emissions

Trace gas emissions originating from large land areas can be estimated using radon as a marker for emission from soil. This has been demonstrated by Wilson *et al.* (1997). They used a 9 year database of nitrous oxide and radon recorded at Cape Grim to assess the origin of N_2O by examining the cross covariance between N_2O and radon signals originated from land surface. A clear maximum in the cross covariance very close to the zero time delay indicated the same source regions of the two gases. With the common origin of the investigated radon and N_2O signals established, they calculated the average flux of N_2O by assuming that the ratio of fluxes is directly proportional to the average ratio of the individual measurements of radon and N_2O from land:

$$\overline{f_{N_2O}} = \overline{f_{Rn}} \cdot \overline{\left(\frac{N_2O}{Rn}\right)} \cdot c$$

where c is a unit-dependent conversion factor. The precision of such estimates benefits from precision and accuracy of the radon concentration measurements. Another advantage is that such estimates are averaged over hundred of square km of land. Seasonal and inter-annual variations were also retrieved from the data with the authors showing that the nitrous oxide flux was higher for rainfall periods. Clear peaks in angular radon and N_2O signals made it possible to obtain independent flux estimates from two main land masses.

The uncertainties of the above method can be made smaller with a better knowledge of radon fluxes in regional areas. The study demonstrated that the method can be used as an independent method of evaluation of regional trace gases emitted from soil.

Radon time series at baseline stations

Baseline selection criteria

A world-wide network of baseline air pollution stations has been established to monitor long term trends in concentrations of climate-sensitive trace gases in the atmosphere. Above all, there is a need to characterise the origin of the air sample, or, more specifically, to develop baseline selection criteria. Air samples showing no recent contact with land (and hence with anthropogenic pollution) are termed "baseline". No generally accepted operational definition of baseline air has been formulated. Instead, site-and species-dependent baseline selection criteria have been proposed. For instance, Zahorowski *et al.* (1996) showed that in the case of ozone at Cape Grim a baseline criterion using exclusively radon concentrations rather than wind speed and direction selected a more consistent ozone subset for the baseline sector. In another study of baseline criteria, Gras and Whittlestone (1992) compared condensation nuclei (CN) and the radon concentration time series measured at two baseline stations (Cape Grim, Tasmania and Mauna Loa Observatory, Hawaii). They concluded that addition of CN and radon concentration to meteorological criteria significantly improved the objectivity of baseline selection. It was demonstrated that a combination of wind direction and CN concentration will indicate pollution from sources within a few km. At longer distances, the radon is a better indicator of fetch over land. Radon will be indicative of contact with land at distances greater than a thousand km, a situation when wind direction and CN are poor indicators.

Radon time series measured over a 10 day period in 1999 at Cape Grim is shown in Figure 3. Wind speed and sector indicators are shown at the top. The sector indicators are designated by the letters T (Tasmania), M (Mainland) and B (Baseline). All data points are hourly averages. As the source of radon changes, concentrations change from a few tens of $mBq.m^{-3}$ to more than 1 $Bq.m^{-3}$. These changes can occur within a few hours. This is well illustrated by two

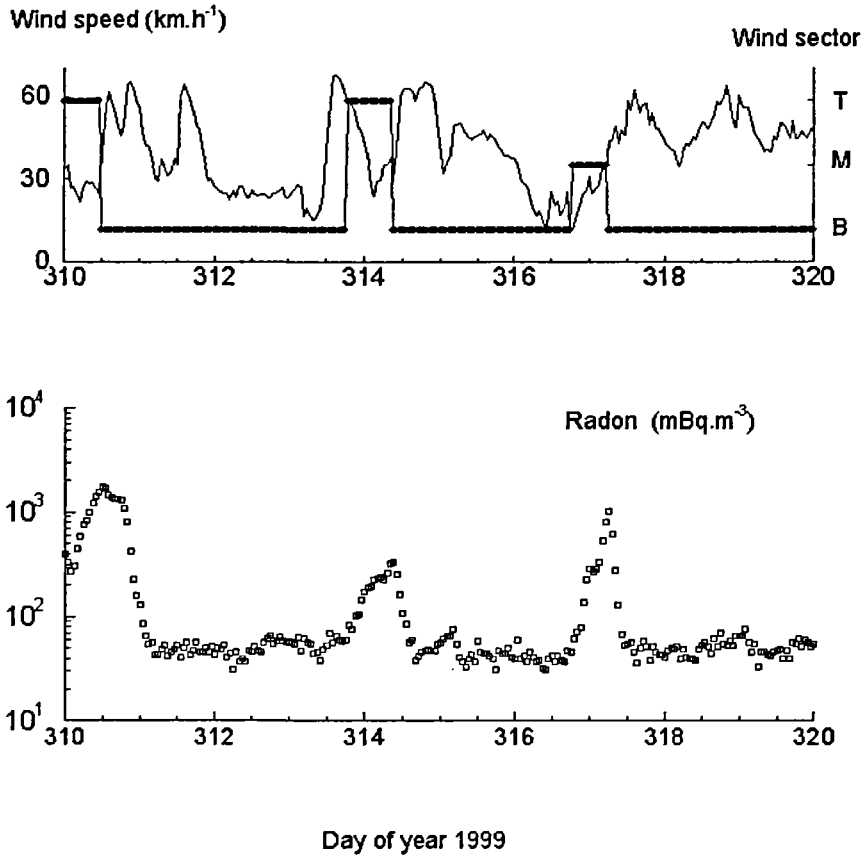

Figure 3
An example of hourly radon observations recorded at Cape Grim (see text for explanations).

events: in a relatively brief period, the change in wind direction from Baseline to Tasmanian (day 313/314) and Baseline to Mainland (day 316/317 resulted in increased radon concentrations of up to one order of magnitude. Both the radon range and rate of change impose demanding conditions on detection systems.

Local influence

An important issue in baseline observations is the problem of local influence on the chemical/elemental composition of air samples. The local influence is site-specific, depending on a combination of the location of the station, synoptic meteorology and availability and spatial distribution of local sources of radon and thoron. The problem of tracking and separation of the local signal is difficult to solve for continental sites. At coastal and island sites, lead-212 has been used in combination with radon to separate local from distant events (Polian *et al.*, 1986; Whittlestone *et al.*, 1996a). A local knowledge of radon and thoron fluxes in the vicinity of a baseline station can be important in this context. For instance, high sensitivity thoron flux measurements were required for an evaluation of the thoron source term from barren lava around the Mauna Loa Observatory in Hawaii (Whittlestone *et al.*, 1996b).

The problem of local influence also affects modelers who view it as a sub-grid source problem beyond their control. Mahowald *et al.* (1997) and Dentener *et al.* (1999) reported that in order to make meaningful model-observation comparisons they had to filter radon time series to remove the local influence. This needed to be done for Kerguelen and Crozet Is sites where about 13% of the radon data were rejected using simultaneous measurement of lead-212. In case of Mauna Loa Observatory data where the supporting in lead-212 data were not available for the investigated period only night data (12 pm till 7 am) were used to exclude daytime up slope conditions bringing local radon from the island (Dentener *et al.*, 1999). At some sites (Bermuda and Cape Grim) applying a wind sector criterion is sufficient to remove the locally influence from the data (Mahowald *et al.*, 1997 and Dentener *et al.*, 1999). However, concurrent measurements of lead-212 is always desirable: first, for an independent experimental verification of any data rejection scheme, second, for preservation of as much of the data as possible because the wind selection criterion is not precise and hence its effective application leads to rejection of some unaffected data.

Simulation of radon with global circulation models

The last decade has witnessed the first serious attempts to model radon concentrations on the global and regional scale and to compare the modeled results with observations. The purpose of radon simulations varied; some aimed at the development or validation of sub-grid mixing schemes and indication of regions associated with largest uncertainties (e.g. Jacob and Prather, 1990; Stockwell *et al.*, 1998), others at the comparison of models (e.g. Genthon and Armengaud, 1995; Jacob *et al.*, 1997) or the comparison of different meteorological input data sets (e.g. Mahowald *et al.*, 1997). More generally, a better understanding of all key atmospheric features which control the transport, mixing and distribution of radon has been sought by detailed comparisons of the modeled radon time series and vertical profiles with best available radon data sets (e.g. Mahowald *et al.*, 1997; Dentener *et al.*, 1999; Stockwell *et al.*, 1998).

The most comprehensive comparison between modeled and observed vertical radon profiles in the boundary layer and the troposphere covering the range 0-12 km was published by Stockwell *et al.* (1998). They parameterised radon emissions in a global offline three-dimensional chemical transport model forced using meteorological analyses. Sensitivity analysis was performed using two horizontal resolutions (2.8° x 2.8° and 7.5° x 7.5°). The effect of implementing vertical diffusion and moist convection was also tested. The inclusion of both vertical diffusion and moist convection as well as the higher resolution was necessary for a realistic simulation of radon. An analysis of model-observation correlations revealed that the modeled radon concentrations higher than those observed very close to the surface and generally much lower than those observed in the planetary boundary layer/lower troposphere. This was attributed to insufficient vertical mixing. An inclusion of a non-local vertical diffusion scheme was postulated, which was expected to give a better mixed planetary boundary layer.

Most recent extensive comparison between the simulated and observed radon time series recorded at a number of ground stations was published by Dentener *et al.* (1999). They utilised the data from 8 ground stations: 2 continental, 2 coastal under continental influence and 4 remote stations. Some vertical radon profiles were also compared with the model results. Similarly to Stockwell *et al.* (1998) and Mahowald *et al.* (1997) they constrained the two models used in the comparison with meteorological. The quantitative comparison was made using monthly means and correlation coefficients. To eliminate variations on time and spacial scales which cannot be reproduced by the models the monthly correlation coefficients were defined from daily averaged measurements and model results. Overall agreement was good for continental stations and coastal stations where correlation coefficients 0.6-0.8 were obtained. The highest monthly correlation coefficients of around 0.8 were obtained for Cape Grim, which was attributed to the fact that the model was constrained by observations performed on and near the Australian continent. Higher uncertainties in the meteorological fields constraining the models were indicated as a reason for lower correlation coefficient (0.5-0.6) for remote stations (especially for Crozet, Kerguelen, and Amsterdam Islands in the Indian Ocean) . A similar problem with the same remote sites (and also with the Macquarie Is site) was noted by Mahowald *et al.* (1997) who simulated successfully observed pollution events at Cape Grim but had difficulty to model events farther from continental source regions.

Radon source strength

Several processes may influence radon emissions to the atmosphere (e.g. Nazaroff, 1992; Holford *et al.*, 1993). These include the abundance of the parent radium-226 and soil properties with diffusion coefficient being the most important factor. The diffusion coefficient strongly depends on soil moisture, with the coefficient values ranging from 3×10^{-6} to 10^{-9} $m^2.s^{-1}$ for a typical dry soil and fully saturated soils, respectively. Although the predominant transport

mechanism responsible for delivering radon to the surface is by molecular diffusion, the flux is also sensitive to changes in atmospheric pressure. Soil freezing also affect the radon flux (Dörr and Münnich, 1990). The flux to the atmosphere is inhibited by snow and ice covers.

Even with this variability, there can be large areas where there is relative uniformity of radon emanation rate. However, a task of constructing radon emission maps is far from simple.

Spot measurement of radon flux

A radon flux survey aimed at covering large, frequently remote areas needs specific instrumentation. The main requirement, besides the lower limit of detection matching expected flux levels, is an adequate sampling frequency. ANSTO has developed a fast, general purpose emanometer for measuring radon and thoron fluxes (Zahorowski and Whittlestone, 1996). Figure 4 shows the essential features of the emanometer. The principle of operation of the instrument is as follows. At the start of the measurement the accumulation chamber (A) is placed over the ground. Air is drawn from the cham-

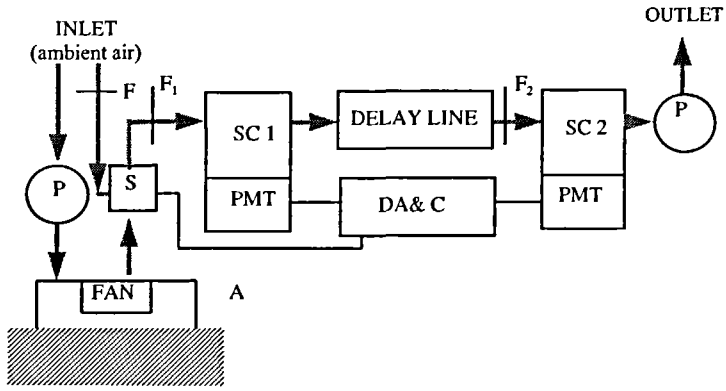

Figure 4
A simplified diagram of the fast emanometer.
A, accumulator chamber; DA&C, data acquisition and control; F, filter; PMT, photomultiplier tubes; SC, scintillation cells.

ber into the first scintillation cell (SC1) which records counts from both radon and thoron. From here, the air passes via a 6 minute delay tube in which thoron decays, into the second cell (SC2) which records radon counts. For a one hour measurement the lower limit of detection is 1 $mBq.m^{-2}.s^{-1}$ for radon and 20 $mBq.m^{-2}.s^{-1}$ for thoron. Lower limits can be achieved by counting for longer. One can set up the instrument for a semi-continuous flux monitoring by fitting an automatically operated ventilation lid to ensure a quick ventilation of the accumulator. Such a system is capable of unattended recording of hourly radon and flux measurements for many days.

It has been demonstrated (Whittlestone *et al.*, 1996b) that a high sensitivity thoron emanometer can be assembled in situations requiring thoron flux estimates down to 1 $mBq.m^{-2}.s^{-1}$. Due to thoron short half-life such an instrument has to operate at a high flow rate and mesh filters similar to the ones used in dual flow loop radon detectors have to be fitted for lead-212 collection.

Regional radon fluxes

Spot flux measurements are too resource intensive for construction of regional or continental radon emission maps.

Some large area estimates have been done in the past. Apart from some early coarse estimates (Turckian *et al.*, 1977) and some limited area studies, no large regional or continental emission maps was published. Nevertheless, a commonly held assumption is that the radon flux is quite uniform and equal to 1 $atom.cm^{-2}.s^{-1}$.

A map for the Australian continent has been constructed based on radon emissions combined with data from airborne gamma survey (Zahorowski and Whittlestone, 1997). In a first step maps were selected covering areas of 100x120 km for which both radon fluxes and airborne gamma data were available. An average gamma count for the area was found and converted to a map average radon flux. The maps were then matched as well as possible to the $5^{o}x4^{o}$ grid, and grid averages obtained.

The results of the flux evaluation procedure is shown in Figure 5. The top number in a cell is derived from spot radon measurements and the bottom from airborne gamma data. The two values, when

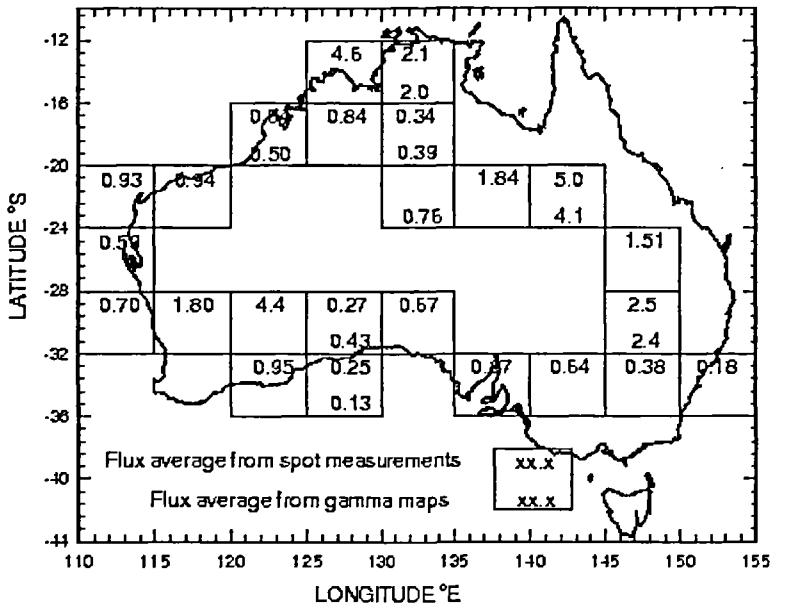

Figure 5
Average radon fluxes (in atom.cm^{-2}.s^{-1}) from 5o x 4o grid boxes.
1 atom.cm^{-2}.s^{-1} corresponds to about 21 mBq.m^{-2}.s^{-1}.

both are available for a cell, agree quite well. It is also clear that the 1 atom cm^{-2}.s^{-1} assumption is very inaccurate even on the 5°x4° grid basis. From the southern part of Australia, the average radon emission) is 1.1 atom.cm^{-2}.s^{-1}, but for the northern part of Australia it is 1.8 atom.cm^{-2}.s^{-1}. The whole data set gives 1.4 atom.cm^{-2}.s^{-1}.

Radon flux in global transport models

As radon time series become more frequently used for development and validation of global transport models, area-averaged radon fluxes are expected to attract more attention. In a recognition of the problem, the first radon emission scenario was recommended by the World Climate Research Programme (WCRP) in 1993. The only physical process taken into account, apart from

obvious effects related to ice covers, was an observation that radon flux depends on soil freezing. Global annual radon emission to the atmosphere was constrained to 72 mol of radon. The scenario was subsequently used as a basis for a comparison of 20 global models (Jacob *et al.*, 1997).

The WCR scenario has been useful as it allowed for intercomparison between results of simulations of radon concentrations obtained by different models. Most recent studies which adopted similar emission scenario (e.g. Mahowald *et al.*, 1997; Stockwell *et al.*, 1998; Dentener *et al.*, 1999) raised the problem of some obvious inadequacies of the scenario, which does not even allow for different source strengths on continental basis.

Some researchers attempted a simple sensitivity analysis involving the radon emissions. For instance, Stockwell *et al.* (1998) identified origins of radon in different altitude bands by varying continental radon source strengths within the prescribed global annual maximum emission value. Because of a constant emission source in their model the authors did not expect perfect agreement between the observed and the calculated values even if all transport processes were modeled perfectly. Their results suggested that the WCRP scenario might seriously underestimate the Asian radon source. Dentener *et al.* (1999) arrived at a similar conclusion regarding the Asian source while discussing reasons for large discrepancies between modeled and observed radon concentrations recorded at Mauna Loa Observatory.

Dentener *et al.* (1999) were also the first to address the source problem in a systematic way by parameterising the radon emission in their global model using a classification based on soil types (Dörr and Münnich, 1990). Although the flux used in the scheme varied significantly, from 0.4 to 1.5 atoms.cm^{-2}.s^{-1}, the measure did not lead to an improvement in the agreement between the modeled and observed data. Similar lack of response was also noted when the sensitivity of the model was tested to a reduced (3 times) flux due to snow cover.

Some modelers varied radon emissions with atmospheric pressure (e.g. Jacob and Prather, 1990; Lin *et al.*, 1996) but no significant improvement to model-observations comparison was reported.

Conclusions

The accuracy and precision of radon instrumentation is now more than adequate to provide the radon time series required for comparing with the simulated ones obtained from regional and global circulation models. The measured high quality radon time series data from selected locations will continue to contribute to the development and validation of the models.

Only a few limited sensitivity analyses involving continental radon sources have been performed. There are no systematic sensitivity analysis that consider variation of grid-averaged fluxes within experimentally derived constrains is required. Furthermore, circulation model performance strongly depends on the quality of the constraining meteorological data. Model-observation correlation coefficients fro radon levels as low as 0.5 and as high as 0.8 have been calculated depending solely on the quality of the meteorological input. Such a strong dependence of model performance on meteorological data indicates that radon is a sensitive tracer for model evaluation.

The present World Climate Research radon emission scenario needs to be improved by incorporating parameterisations of important factors controlling radon emanation like soil moisture. Improved area-averaged radon fluxes can be constructed from the geographical abundance of radium-226 (through airborne or car-borne radiometrics or geological data) with spot measurements providing a means to verify area emissions.

More observation stations will help to constrain the radon emissions. More regional stations will provide additional opportunities for pseudo-Lagrangian experiments and in new possibilities for model development and data interpretation.

Radon is a valuable tool for investigating atmospheric transport and mixing on different horizontal and vertical scales. In the last decade significant advances have been made both in radon instrumentation and simulation of radon concentration in the atmosphere using global circulation models.

Bibliography

BUTTERWECK G., REINEKING A., KESTEN J., PORSTENDÖRFER J., 1994 — The use of the natural radioactive noble gases radon and thoron as tracers for the study of turbulent exchange in the atmospheric boundary layer - Case study in and above a wheat field. *Atmospheric Environment*, 28: 1963-1969.

DENTENER F., FEICHTER J., JEUKEN A., 1999 — Simulation of the transport of ^{222}Rn using on-line and off-line global models at different horizontal resolutions: a detailed comparison with measurements. *Tellus*, 51B: 573-602.

DÖRR H., MÜNNICH O., 1990 — ^{222}Rn flux and soil air concentration profiles in West Germany. Soil ^{222}Rn as a tracer for gas transport in the unsaturated soil zone. *Tellus*, 42B: 20-28.

GENTHON, C., ARMENGAUD A., 1992 — Radon 222 as a comparative tracer of transport and mixing in two general circulation models of the atmosphere. *J. Geophys. Res.*, 100: 2849-2866.

GRAS J. L., WHITTLESTONE S., 1992 — Radon and CN: complementary tracers of polluted air masses at coastal and island sites. *J. Radioanal. and Nuclear Chemistry*, 161: 293-306.

HOLFORD D. J., SCHERY S. D., WILSON J. L., PHILLIPS F. M., 1993 — Modeling Radon Transport in Dry, Cracked Soil. *J. Geophys. Res.*, 98: 567-580.

JACOB D. J., PRATHER M. J., 1990 — Radon^{222} as a test of convective transport in a general circulation model. *Tellus* 42B: 118-134.

JACOB D. J., *et al.*, 1997 — Evaluation of intercomparison of global atmospheric transport models using ^{222}Rn and other short-lived tracers. *J. Geophys. Res.*, 102: 5953-5970.

KRITZ M. A., ROSNER S. W., STOCKWELL D. Z., 1998 — Validation of an off-line three-dimensional chemical transport model using observed radon profiles 1. Observations. *J. Geophys. Res.*, 103: 8425-8432.

LEE H. N., LARSEN R. J., 1997 — Vertical Diffusion in the Lower Atmosphere Using Aircraft measurements of ^{222}Rn. *J. Appl. Meteor.*, 36: 1262-1270.

LIN X., ZAUCKER F., HSIE E.Y., TRAINER M., MCKEEN S. A., 1996 — Radon^{222} simulations as a test of a three-dimensional transport model. *J. Geophys. Res.*,101 (19): 165-177.

MAHOWALD N. M., RASCH P. J., EATON B. E., WHITTLESTONE S., PRINN R. G., 1997 — Transport of ^{222}radon to the remote troposphere using the Model of Atmospheric Transport and Chemistry and assimilated winds from ECMWF and the National Center for Environmental Prediction /NCAR. *J. Geophys. Res.*, 102 (28): 139-151.

NAZAROFF W. W., 1992 — Radon transport from soil to air. *Rev. Geophys.*, 30: 137-160.

POLIAN G., LAMBERT G., ARDOUIN B., JEGOU A., 1986 — Long-range transport of continental radon in subantarctic and antarctic areas. *Tellus*, 38B: 178-189.

STOCKWELL D. Z., KRITZ M. A., CHIPPPERFIELD M. P., PYLE J. A., 1998 — Validation of an off-line three-

dimensional chemical transport model using observed radon profiles 2. Model results. *J. Geophys. Res.*,103: 8433-8445.

TUREKIAN K. K, NOZAKI Y., BENNINGER L. K., 1977 — Geochemistry of atmospheric radon and radon products. *Ann. Rev. Earth Planet. Sci.*,5: 227-255.

USSLER W., CHANTON J. P., — Radon 222 tracing of soil and forest canopy trace gas exchange in an open canopy boreal forest. *J. Geophys. Res.*, 99: 1953-1963.

WHITTLESTONE S., ZAHOROWSKI W., 1995 — "The Cape Grim huge radon detector". *In Baseline Atmospheric Program(Australia) 1992*: 26-30.

WHITTLESTONE S., SCHERY S. D., LI Y., 1996a — Pb-212 as a tracer for local influence on air samples at Mauna Loa Observatory, Hawaii. *J. Geophys. Res.*,101 (14): 777-785.

WHITTLESTONE S., SCHERY S. D., LI Y, 1996b — Thoron and radon fluxes from the island of Hawaii. *J. Geophys. Res.*,101 (14): 787-794.

WHITTLESTONE S., ZAHOROWSKI W., 1998 — Baseline radon detectors for shipboard use: Development and deployment in the First Aerosol Characterisation experiment (ACE 1). *J. Geophys. Res.*, 103 (16): 743-751.

WILSON S. R., DICK A. L., FRASER P J., WHITTLESTONE S., 1997 — Nitrous oxide flux estimates for South-Eastern Australia. *J. Atm. Chem.* 26: 169-188.

ZAHOROWSKI W., GALBALLY L. E., WHITTLESTONE S., MEYER C.P., 1996 — "Ozone and radon at Cape Grim: A study of their interdependence". *In Baseline Atmospheric Program (Australia) 1993*: 30-37.

ZAHOROWSKI W., WHITTLESTONE S., 1996 — A fast portable emanometer for field measurement of radon and thoron flux. *Radiat. Prot. Dosim.*, 67: 109-120.

ZAHOROWSKI W., WHITTLESTONE S., 1997 — "Application of sensitive and supersensitive radon detectors for radon flux density and radon concentration in environmental monitoring". *Proceedings of a Technical Committee meeting on Uranium exploration data and techniques applied to the preparation of radioelement maps*, Vienna, 13-17 May, 1996, IAEA-TECDOC-980: 223-236.

Trace elements in total atmospheric suspended particles in a suburban area of Paris: a study carried out by INAA

Gilbert Le Petit

Jean-Paul Deschamps

Sunun Nouchpramools

Introduction

Atmospheric pollution is a major concern world-wide, in particular for the inhabitants of certain large urban areas. Its many and varied components attack the environment and health directly or indirectly. The main pollutants are sulphur dioxide, carbon monoxide, reactive hydrocarbons, nitrogen oxides, ozone, lead and particulate matter. The primary contributions to atmospheric pollution in the form of solid aerosols come from either natural sources such as redispersion of crustal material, volcanic eruptions, aerosols of marine origin and pollens or from anthropogenic sources such as combustion of fuel oil and coal, combustion of fuels related to vehicular traffic, and various emissions related to industrial and human activities. It is generally accepted that the level in the atmosphere of particulate matter of natural origin is less than 10 $\mu g.m^{-3}$. In urban areas with high population density, such as the great megalopolises in developing countries, the concentrations in the atmosphere are regularly higher than the guideline values recommended by the World Health

Organisation (WHO), which considers that the annual mean concentration should not exceed 60 $\mu g.m^{-3}$. The long-term effects on health of a high concentration of atmospheric particulates, specifically the fraction smaller than 10 µm, are serious and insidious; moreover, the quantification of metals and certain anthropogenic trace elements present in the particulate matter is necessary in order to evaluate the hazards of the atmospheric pollution in terms of long-term exposure of the population and consequently implement the means to combat them and reduce them.

The preliminary study described here focuses on neutron activation analysis (INAA) of trace elements in atmospheric particulate matter (collected using a very high flow rate (approximately 600 $m^3.h^{-1}$) atmospheric sampling system fitted with a large filter. Weekly samples of approximately 100,000 m^3 of filtered air, collected during 1998 close to Paris, were used to determine the amplitude of seasonal fluctuations in pollutant concentrations, evaluate the enrichment factor of specific elements in the total atmospheric suspended particles (TSP) and, if possible, identify the origin of certain pollution sources.

Situation

The Service Radioanalyse Chimie Environnement (SRCE) of the Commissariat à l'Energie Atomique (CEA) has an atmospheric sampling station located at Montlhéry (2° 14' E, 48° 37' N), 35 km south-south-west of Paris and approximately 900 metres from a main road (N 20) with high traffic levels, approximately 70,000 vehicles per day (including 15% heavy good vehicles). The sampling station has a weather station recording the following data: wind speed and direction, precipitation, temperature, humidity; the wind rose established for 1998 is predominantly south-west, north-east. The locations of the main potential sources of atmospheric pollution emissions in the outer suburbs of Paris are shown in Figure 1.

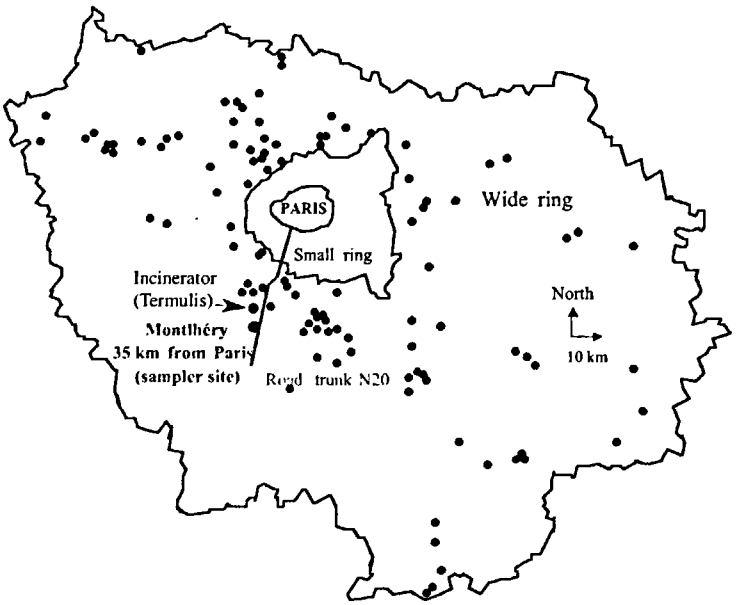

Figure 1
Air particulate sampler location and possible atmospheric emission source locations (black points).

Sampling apparatus and filter support

The atmospheric particulates sampling apparatus (Figure 2) used is the ASS500 P (Aerosols station ASS-500 Physic-Technik-Innnovation PTI & Central Laboratory for Radiological Protection CLRP (Poland), D.Fischer, Erlengen, Germany). This apparatus type equips the French Particulate Radionuclides Stations installed* as part of the world-wide network set up under the terms of the Comprehensive Test Ban Treaty (CTBT) (Schulze *et al.*, 2000) and

* An operational station is installed on the island of Tahiti in the South Pacific.

Figure 2
ASS500 P
type sampler.

intended to monitor atmospheric radioactivity (sensitivity: 10 mBq.m^{-3} for ^{137}Cs). The high flow rate sampling apparatus can operate continuously under severe meteorological conditions. The horizontal sampling head is protected by an aluminium hood. The polypropylene filter, with a surface density of approximately 125 g.m^{-2} and effective dimensions 43x43 cm, is mounted in an air-tight manner on a calibrated grid support. The filter retention efficiency, measured experimentally, is greater than 93% for 0.15 mm particles (French standard NF X 44011). Two infrared lamps are installed above the filter to prevent icing in winter. The ASS500 P has a system giving the filtered air volume at a given time and the instantaneous flow rate. The filtered air volume is corrected for the temperature and adjusted to standard conditions (STP). For this study 54 weekly samples covering 1998 were taken; the weekly mean air flow rate, approximately 600 m^3.h^{-1}, varied significantly according to

the meteorological conditions observed during sampling; at certain times of the year, when the temperature inversion layer is low, the resulting atmospheric dust level is higher, whereas at other times heavy rainfall can cause a substantial decrease in the flow rate. The weekly mean flow rates obtained during 1998 are shown in Figure 3; it can be seen that the minimum flow rate (440 $m^3.h^{-1}$) was obtained in winter.

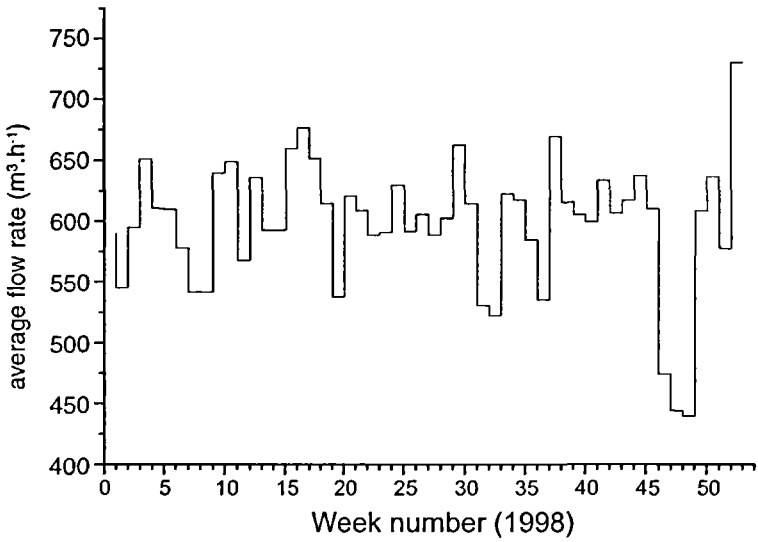

Figure 3
Average flow rate observed on the sampler during year 98.

Sample preparation protocol

The atmospheric particulate matter is sampled for one week, without particle-size cutoff. Each filter is oven-dried for 6 hours at 90° C, then weighed on a precision balance, before it is placed in the sampling apparatus. On withdrawal, the aerosol-loaded filter is dried and weighed again; the mean weight loss after drying is about 4%

of the total mass. The distribution of the aerosol masses ($mg.m^{-3}$ filtered air) collected on each weekly filter and measured in 1998 is shown in Figure 4. It can be seen that, in winter, atmospheric dust levels in the Paris region can reach 80 $mg.m^{-3}$ (weekly mean), a value that is slightly above the maximum annual limit adopted by the WHO (60 $mg.m^{-3}$).

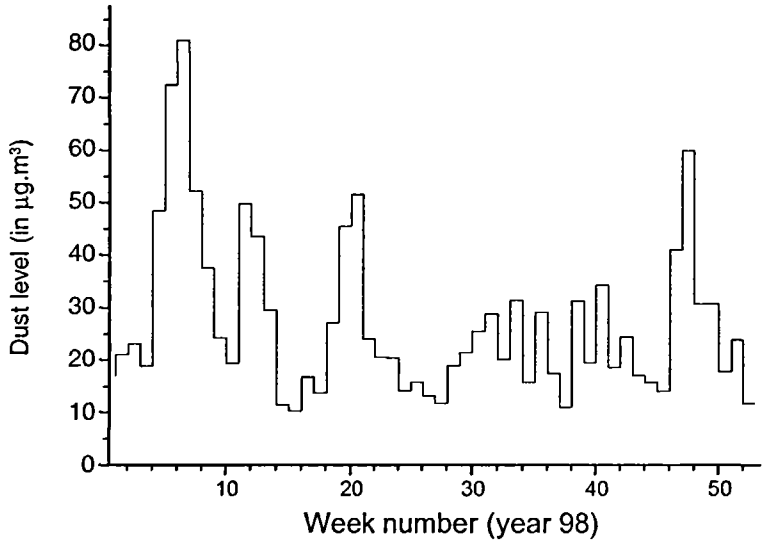

Figure 4
Dust concentration during year 98 observed at Montlhéry.

The filters are then compacted and reduced to ash in a programmable oven, using a protocol giving a slow temperature rise to 400 °C over a period of 8 hours. In parallel, blank filters loaded with stable tracers (standards), prepared under the same conditions as the samples and undergoing the same protocol, were used to determine the calcination yield after INAA analysis for each element investigated in the atmospheric aerosols (except Pb, analyzed by ICP-MS after solubilization). The reproducibility of the calcination yields obtained was verified by three independent values for each element.

After calcination, 50 mg of sample were placed in a high-purity polyethylene container and heat-sealed. A set of blank filters, prepared under identical conditions to the samples, was analyzed to identify and quantify impurities (major constituents: Al, Cl, Cu, Na, K). In addition, for the same purpose, impurity concentrations of the empty container were determined, as the gamma spectrometry measurements on the samples were made in the presence of the container (major constituents: Al, Mg). The results obtained were taken into account in the determination of the element concentrations in the atmospheric particulate matter.

Sample irradiation and induced activity measurements

Although the INAA technique cannot quantify certain elements such as Pb, Hg and S that are of particular interest as atmospheric pollutants, it is one of the most powerful non-destructive multi-element analysis techniques (Sarmani *et al.*, 1998; Djingova *et al.*, 1998), capable of determining some forty elements (lanthanides, rare earths, metals, K, Na, etc.).

The samples were irradiated using the HERMA pneumatic system installed on the periphery of the core of the OSIRIS reactor at the Centre d'Etudes Nucléaire at Saclay (CEA). This apparatus has a very fast transport system for shuttles carrying the container and the sample; the transfer time between the reactor core and the gamma spectrometry laboratory located in a peripheral gallery is about 2 to 3 seconds, which enables detection and measurement of radioelements with half-lives of a few minutes. A distributor managing eight shuttles simultaneously means that the irradiation system can sequence the irradiation cycles. The associated laboratory can perform two types of measurement: HPGe gamma spectrometry measurement and measurement of delayed neutrons by ^{3}He proportional counter for the fissile elements such as ^{235}U, ^{238}U, ^{239}Pu. The samples were irradiated in a thermal neutron flux of approximately

$1.2.10^{14}$ n.cm^{-2}.s^{-1} for 60 s. Each set of eight samples was framed by two flux guides made of ultra-pure Fe; experience has shown that, given the short duration of the irradiations, the neutron flux variation during the treatment of a set of samples can be considered negligible.

Two measurement procedures were used, depending on the elements to be analyzed. The short half-life radioelements (^{28}Al, ^{52}V, ^{66}Cu, ^{51}Ti, ^{80}Br, ^{38}Cl, ^{116m}In, ^{57}Mn, ^{56}Mn) were measured in the laboratory located close to the reactor by an HPGe detector, relative efficiency 30%, with a collimator 100 mm thick and a 10 mm aperture. The sample was positioned automatically in front of the detector by the pneumatic system. The detector was calibrated using a multigamma (^{152}Eu) solution placed and dried in a container identical to the ones used for sample irradiation; the calibration was checked using a Monte-Carlo code, taking into account the corrections due to summing effects. An initial measurement (T0) was made when the dead time of the acquisition electronics was less than 10%. Three measurements were then made at T_0+10, T_0+20 and T_0+30 min.

The medium and long half-life radioelements (^{46}Sc, ^{59}Fe, ^{51}Cr, ^{60}Co, ^{76}As, ^{65}Zn, ^{75}Se, ^{82}Br, ^{86}Rb, ^{99}Tc(Mo), ^{115}Cd, ^{122}Sb, ^{124}Sb, ^{131}Ba, ^{134}Cs, ^{140}La, ^{141}Ce, ^{110m}Ag, ^{152}Eu, ^{169}Y, ^{24}Na, ^{177}Lu, ^{181}Hf, ^{187}W, ^{198}Au, ^{233}Pa(Th), ^{42}K) were made in our laboratory at Bruyères le Châtel using HPGe detectors with relative efficiencies of 30 to 50%. The detector was calibrated using a multi-element gamma solution (AEA Technologie, Courtaboeuf, France) in the same geometry as the sample. All the measurements were made at a distance of 10 cm from the detector to minimize gamma summing effects. An initial measurement was made 1 day after irradiation (T_0), then further measurements at T_0+5, T_0+20 days.

The element concentrations, allowing for experimental conditions and including corrections for dead time and for decay during acquisition, are calculated (ng.m^{-3}) using the customary formula for activation analysis:

$$Conc = \frac{Ns \times A \times \lambda \times m_t \times k}{\varepsilon_{abs} \times A_b \times m_i \times I_\gamma \times N_v \times \varphi_{th} \times \sigma_{th} \times Y_c \times V_a \times (1 - e^{-\lambda \times t_i}) \times e^{-\lambda \times t_d} (1 - e^{-\lambda \times t_m})}$$

where:

k: constant
Ns: net area of the total gamma absorption peak
A: atomic number of the activated element
λ: decay constant of the activated element
ε_{abs}: absolute detection efficiency
A_b: isotopic abundance
m_i: mass of irradiated sample
m_t: total mass collected
I_λ: absolute gamma emission intensity
N_v: Avogadro's number
Y_c: calcination yield
V_a: volume of air sampled
φ_{th}: thermal flux
σ_{th}: thermal neutron absorption cross-section
t_i, t_d, t_m: irradiation, cooling and measurement times, respectively

The gamma spectrograms were processed using the GW software (Westmeir Gesellschaft für Kernspektrometrie mbH – Beratung Software). All the nuclear data (thermal neutron absorption cross-sections, gamma emission intensities) were taken from "*The K0-Consistent IRI gamma-ray Catalogue for Instrumental Neutron Analysis* (Menno Blaauw Interfacultair Reactor Instituut van de Technische Universiteit Delft, 1996) and the Neutron activation Tables (Gerhard Erdtmann, 1976). The Innovator in Elemental and Isotopic Mass Spectrometry relative. The Minimum Detectable Concentration (MDC) calculation was based on the definition of Currie (1968) and complies with the expressions defined by the international organization overseeing the CTBT (Schultze *et al.*, 2000).

$$MDC_{(mass/m^3)} = \frac{K_a \times 2.71 + 4.65 \sqrt{\sum_{ROI} count_i}}{t_m \times \varepsilon_{abs} \times V_a \times K_s \times K_w \times K_c}$$

where:

ROI is defined as ± 1.25 Full Width Half Maximum on either side of the hypothetical peak K_a, K_s, K_w, K_c: respectively factors related to the conversion mass/Bq, decay corrections during activation time, between end of activation and acquisition start, during acquisition time

The overall uncertainties assigned to the results are given by the following equation, for a standard deviation:

$$\Delta Conc = Conc \times \sqrt{\frac{\Delta N_s}{N_s} + 2\frac{\Delta N_b}{N_b} + \frac{\Delta I_\gamma}{I_\gamma} + \frac{\Delta \varepsilon_{abs}}{\varepsilon_{abs}} + \frac{\Delta m_i}{m_i} + \frac{\Delta m_t}{m_t} + \frac{\Delta V_a}{N_a} + \frac{\Delta Y_c}{Y_c} + \frac{\Delta \varphi_{th}}{\varphi_{th}}}$$

where N_b: area under the gamma peak.

Validation of the experimental method

The validity and the reliability of the results obtained using our experimental method were verified by irradiating an IAEA 1632A particulate matter standard (Table 1).

Element	Certified values IAEA 1632A(ppm)	Our work (ppm)	Detection limit (ppm)
As	9.3 ± 1.0	11.1 ± 1.0	0.55
Ce	29.0 ± 2 .0	28.5 ± 1.7	1.8
Cs	2.3 ± 0.2	3.0 ± 1.8	0.7
Cr	34.3 ± 1.5	31.5 ± 1.5	4.0
Eu	0.52 ± 0.04	0.52 ± 0.06	0.1
Fe	11100 ± 200	10755 ± 220	645
Hf	1.62 ± 1.00	1.67 ± 1.00	0.3
K	4110 ± 200	4063 ± 230	1.6
La	15 +/- 2	13.5 ± 2.0	0.06
Na	828 ± 77	834 ± 69	5.2
Rb	30 +/- 2	33.7 ± 2.1	1.5
Sc	6.3 ± 0.3	6.9 ± 0.6	0.04
Th	4.5 ± 0.1	5.3 ± 1.0	0.7
Yb	1.08 ± 0.09	1.3 ± 0.4	0.6

Table 1
Comparison of measured and certified values.

Atmospheric pollution monitoring in the Paris region

AIRPARIF (1998), the entity responsible for air quality monitoring in the Paris region, has three types of station for measuring the main primary atmospheric pollutants (CO, NO, NO_2, O_3, SO_2) covering a radius of approximately 100 km around Paris:

- *urban background stations:* installed away from the direct influence of any source of industrial or vehicular pollution, for example in parks, school grounds; the AIRPARIF network includes 60 stations of this type;
- *rural background stations:* installed on the edge of the Paris conurbation, intended to measure the impact of certain pollutants generated by chemical reaction, such as O_3; the network includes 3 stations of this type;
- *proximity stations:* installed in immediate proximity to vehicular traffic; the network includes 9 stations of this type.

The concentrations of primary pollutants measured by an urban background station (located in Paris, 500 metres from the Place d'Italie), representative of climatic events observed at the scale of the Paris region, were compared with the levels in the atmosphere of the stable elements determined by this study.

For this purpose the daily measurements made by AIRPARIF in 1998 have been matched to the corresponding weeks of ASS500 P atmospheric sampling.

Results and discussion

A certain number of elements present in the aerosols are used as markers of certain sources of atmospheric pollution, of anthropogenic or natural origin. The various sources of urban pollution

(main elements As, Se, Zn, Sb) and the natural sources, derived essentially from crustal material and the ocean, (main elements Al, Cl, Fe, La, Mn, Na, Ce, Sm) are listed in Table 2.

Sources	Markers
Crustal material	Al, Mn, Fe, Sc, Rare Earth Elements
Marine aerosols	Na, Cl
Coal combustion	As, Se, Hg
Oil combustion	V, La, Sm
Refineries	La, Sm
Motor vehicles	Br, Zn, Sb, Pb, Cu (La, Ce, Al, Fe)*
Wood burning	K
Incinerators	Na, K, Cl, In, Hg
Industrial urban areas	V, Zn, Se, Mo, Sb
Iron/steel works	Fe, Zn, Se, Mo, Sb,
Ni, Cu extraction	Hg, As, Se
Zn, Cd, Pb smelting extraction	In, As, Se, Co, Cd, Cr
Aluminium plants	Al, Mg, Hg
Paint	Ba, Ti
Precious metal	Au, Cr, Mo
	* *Catalytic converter*

Table 2
Sources of atmospheric particulates and their elemental markers (from reference [18]).

An effective approach for revealing any atmospheric pollution of anthropogenic origin consists in calculating an enrichment factor (EF) for each element, defined as the ratio of the element of interest in the sample to a reference element in the sample $(Xi/Ci)_{SAMPLE}$ divided by the same ratio in a reference material $(Xi/Ci)_{REF}$. In this work the table of crustal abundance given by Taylor (1972) was used, with respect to Sc as the reference element because of its low volatility and lack of anthropogenic sources. The mean enrichment

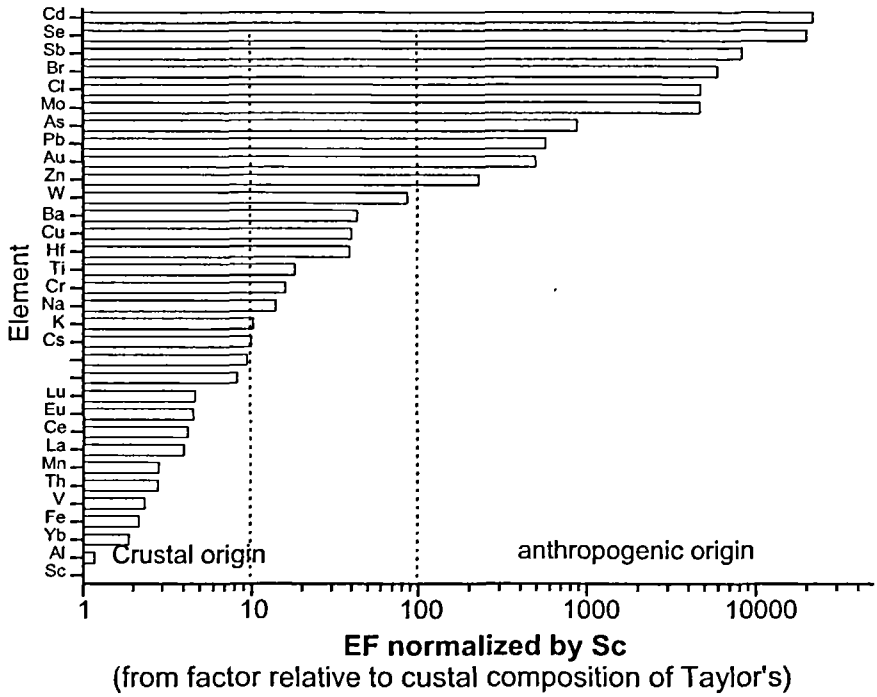

Figure 5
Enrichment factors related to TSP.

factor for each stable element, calculated from the 54 weekly atmospheric samples taken in 1998, is shown in Figure 5. The mean enrichment factors show a very wide range of variation (10^0 to 10^4). The hypothesis of emission sources of anthropogenic origin is highly probable for certain elements showing an EF greater than 10^2 (Cd, Se, Sb, Br, Cl, As, Pb, Mo, Au, Zn). Low enrichment factors, below 10, were observed for certain elements such as Al, Co, Cs, Hf, K, Mg, Mn, Th and the rare earths; it can be assumed that these elements correspond to the redispersion of materials from superficial layers of the ground in the investigated area. A few elements have moderate enrichment (Cr, V, Ti, Ba, Cu, W). Samples taken from the ground surface in the immediate vicinity of the sampling apparatus were sampled and analyzed by neutron activation. The EF values calculated as described above are given in Figure 6; it can be seen

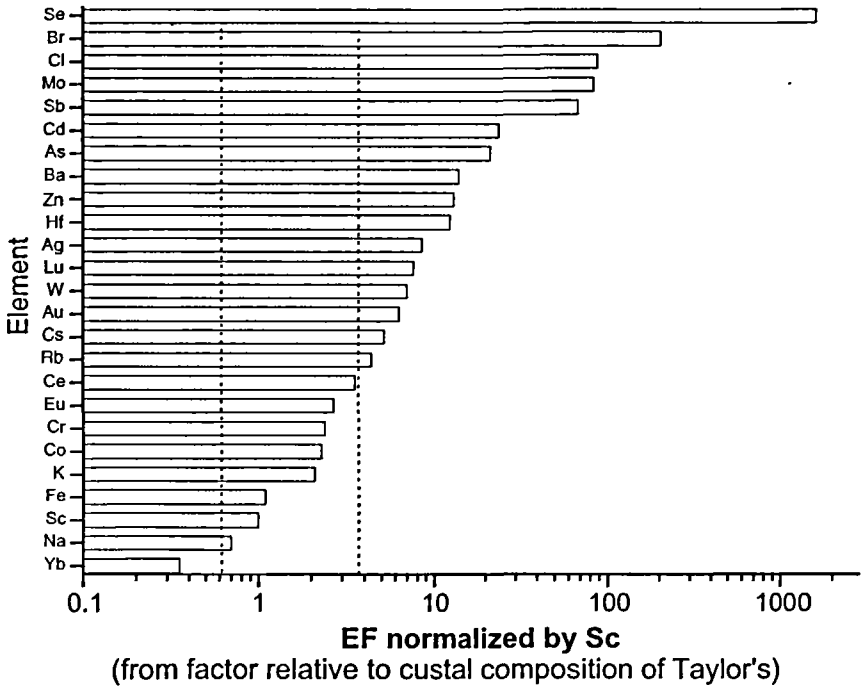

Figure 6
Enrichment factors in soils close to the sampler.

that the values obtained are, in general, an order of magnitude lower than those of the atmospheric aerosols; substantial marking of the ground samples for certain elements (Se, Br, Cd, Mo, Sb) is clearly apparent, corresponding with the highest EF values recorded for the aerosol samples. These results can be interpreted by considering a process of deposition of atmospheric aerosols enriched with stable elements under the effect of favourable climatic conditions. It should be noted that the concentration of the element Sc (10 ppm), used as reference for the enrichment factor calculations, is compatible with the value given by Taylor (20 ppm) (Taylor, 1972).

The trace element concentrations determined in TSP and presented in this work are in all cases equivalent to the levels found in industrialized suburban areas of the major European cities. The mean con-

centrations (1998) of stable elements measured in the Paris suburbs, expressed in $ng.m^{-3}$, the values published by several authors (Chung *et al.*, 1997; Gallorini *et al.*, 1998; Querol *et al.*, 1997; Krivan & Egger, 1986) for different cities in Europe and in Asia, and the minima and maxima for the USA are given in Table 3. The mean concentrations measured near Paris are characteristic of the major industrial cities and give an idea, despite the wide seasonal variation, of the total quantities of trace elements present in atmospheric aerosols in urban areas and of the nature of the main pollutants; these data, coupled with other parameters such as meteorological data, are essential clues for identifying the emission sources.

The mean Br/Na ratio calculated for 1998 (0.045) is an order of magnitude greater than the oceanic ratio (0.0062) (Nouchpramool *et al.*, 1998); this result indicates a local emission source for the element Na; the probable origin is an incinerator located 10 km from the sampling point (Figure 1), Na and Cl being characteristic markers of this type of pollution (Gone *et al.*, 2000).

The Cl/Pb ratio is an indication of fresh particles emitted in the exhaust by engines burning petrol; this ratio is about 0.14 (Ozben *et al.*, 1998). However, it should be noted that this ratio can be significantly different in France depending on the type of fuel produced. In this work the Cl/Br ratio was found to be 91, a very high value, which supports the hypothesis of the incinerator as potential emission source.

The Br/Pb ratio, a characteristic of fuel quality, can vary from 0.28 to 0.47 (Ozben *et al.*, 1998). The mean annual Br/Pb ratio found in this work is close to 2; this result, much higher than the expected value considering the sampling apparatus is located 800 metres from a main road with heavy traffic, may indicate the involvement of a substantial emission source for Br, independent of the one related to road traffic.

In contrast the high enrichment factors for elements Cd, Pb and Sb can be assumed to indicate pollution for which the main emission source is road traffic; other elements (Cu, Ce, La, etc.) could have the same origin, as suggested by Huang *et al.* (1994).

The elements As and Se, in trace amounts in the atmospheric aerosols but showing high EF values, could originate in the use of fossil fuels (district heating, etc.).

Element	Paris (our work) Median		Min	Max	MDC	Milan Median	Min	Max	Ulm Median	Castellon Median	Europe Min	max	Bangkok Median	Seoul Median	Mexico higher values	USA Min	Max
			ng.m^{-3}				ng.m^{-3}		ng.m^{-3}	ng.m^{-3}	ng.m^{-3}		ng.m^{-3}	ng.m^{-3}	ng.m^{-3}	ng.m^{-3}	
Al	286	(18%)	61	597	7.8								3950	2407			
As	4.1	(18%)	1.1	13	0.24	4.9	0.5	12	0.99	33	1	700	174.4	6.85		2	2320
Au	0.0035	(20%)	0.0010	0.0040	0.00060	0.12	0.005	0.6	0.017					0.007	3120		
Ba	55	(18%)	9.1	149	6.3				25	111							
Br	46	(19%)	6.3	136	0.11	387	43	872	71	72	24	433	23.79	12.1		32	1720
Cd	13	(19%)	1.2	33	1.5	8	3.3	45	1.33	1.8	1.3	27		6.96	270	0.2	7000
Ce	0.78	(18%)	0.15	2.3	0.11	1.8	0.3	2.8	0.62		0.4	14	3.26	0.44		0.8	13
Cl	1935	(20%)	30	5740	8.5	1350	150	3692			153	2500	995	639	3620	366	1500
Co	0.74	(22%)	0.14	2.0	0.05	4.3	0.8	16	0.32	4.2	0.25	18.3		0.81	60830	0.14	83
Cr	5	(21%)	0.90	12	0.19	70	2	264	16	34	3.7	6.7	3.01	1.86	15750	0.029	2.1
Cs	0.089	(23%)	0.020	0.22	0.030	0.14.	0.1	3.7	0.28		0.2	0.6	2.26	0.44			
Cu	15	(67%)	4.4	51	7.1	43	6	130	64	1.4	17	64			52	3	5140
Eu	0.029	(69%)	0.010	0.083	0.017	0.05	0.02	0.08	0.024		0.014	0.1				0.03	0.09
Fe	377	(21%)	385	931	12	2170	300	3600	930	1800	520	3500	2040	160		130	13800
Hf	0.093	(23%)	0.030	0.70	0.015	0.1	0.05	0.45	0.056	175	0.02	0.06		0.19			
K	675	(21%)	223	2460	25.5					5000				383	740		
La	0.37	(20%)	0.075	1.1	0.025	1.5	0.4	1.8	0.48		0.2	3.4	1.68	0.14		0.5	9.1
Lu	0.0070	(72%)	0.0030	0.016	0.006									0.11			
Mg	185	(19%)	87	272	42								212		320		
Mn	8.1	(18%)	2.1	17	0.089	40	16	282	20		13	390	58.74	13.7	190	23	850
Mo	1.5	(27%)	0.37	4.3	0.57				2.8	8.9							
Na	1020	(18%)	276	3500	50				370	5300			977.5	168	7880		
Pb	21	(15%)	1.6	86	3.2	775	75	4000	365		235	365				30	96270
Sb	5.0	(18%)	0.80	21	0.015	29	14	124	9.1	4.3	0.5	51	4.05	8.52		0.5	171
Sc	0.066	(20%)	0.026	0.11	0.0015	1.6	0.5	3.7	0.046	1.7	0.04	0.8	466	0.03		0.1	3.1
Se	3.0	(18%)	0.11	7.0		0.6	0.3	1.6	1	8.1			550.8	4.53			
Th	0.081	(30%)	0.017	0.21	0.03	0.03	0.01	0.08	0.095	4.9	0.05	0.1		0.2		0.02	0.42
Ti	307	(19%)	92	427	23	60	40	85					177.9			36	180
V	6.7	(19%)	2.2	8.2	0.21	31	9.1	61					19.65	14.5	7116	0.40	760
W	0.43	(28%)	0.036	1.8	0.08	1	0.08	3.5	<0.4		11	73					
Yb	0.017	(32%)	0.0030	0.065	0.005				0.022					0.12			
Zn	51	(20%)	2.1	156	0.75	85	31	270	170	256	80	200	282	0.0148		58	741

Table 3
Analytical results of Total Suspended Particles in suburban area of Paris and comparison with other studies.

Figure 7 shows the distribution of the concentrations of three heavy elements (Mo, Sb and Pb), characterized by high potential toxicity, in the 54 weekly atmospheric samples collected in 1998. As a comparison, the variation in a primary pollutant (SO_2) measured by AIRPARIF over the same period is shown. There is high seasonal variability; the maximum concentrations are observed in winter periods that favour temperature inversions and climatic episodes

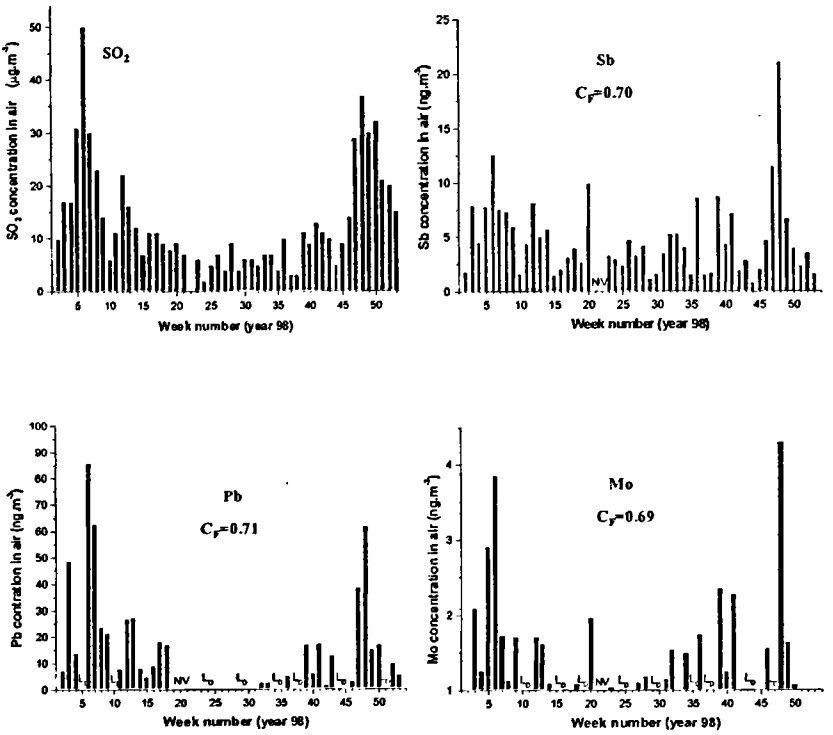

$$r = \frac{\frac{1}{n}\Sigma(x_i-\mu_x)(y_i-\mu_y)}{\sqrt{\frac{1}{n}\Sigma(x_i-\mu_x)^2} \times \sqrt{\frac{1}{n}\Sigma(y_i-\mu_y)^2}}$$

Correlation factor (C_r)

LD : Detection Limit
NV : None Value

with x_i, y_i observed data (SO_2 and stable element concentration)
μ_x, μ_y : means of populations x_i and y_i

Figure 7
Comparison between the variation of concentration of some trace heavy elements inTSP observed at Monthlery during year 98 and the variation of SO_2 measured by AIRPARIF at Paris arear.

involving anticyclonic stability and lack of wind. Moreover, there is considerable similarity between the annual variation of primary pollutants (SO_2, NO, etc.) and that of trace elements in the atmospheric particulates; as an example, analysis of the covariance of the data for SO_2 and for the metallic elements gives a correlation coefficient (r) close to 0.7. This can be explained by the fact that the stable particulate pollutants and the chemical pollutants come from emission sources that are very probably of different origins, but are produced in a diffuse manner, thus obeying the same dispersion rules dependent on the same climatic conditions. This hypothesis is plausible, since no correlation is observed between variation in Pb and Sb concentrations and variation in road traffic (Figure 8) in the immediate vicinity of the sampling apparatus.

The variation during the year of the concentrations of certain elements of non-anthropogenic origin is shown in Figure 9. No correlation with the variation of primary pollutants is observed; this is a

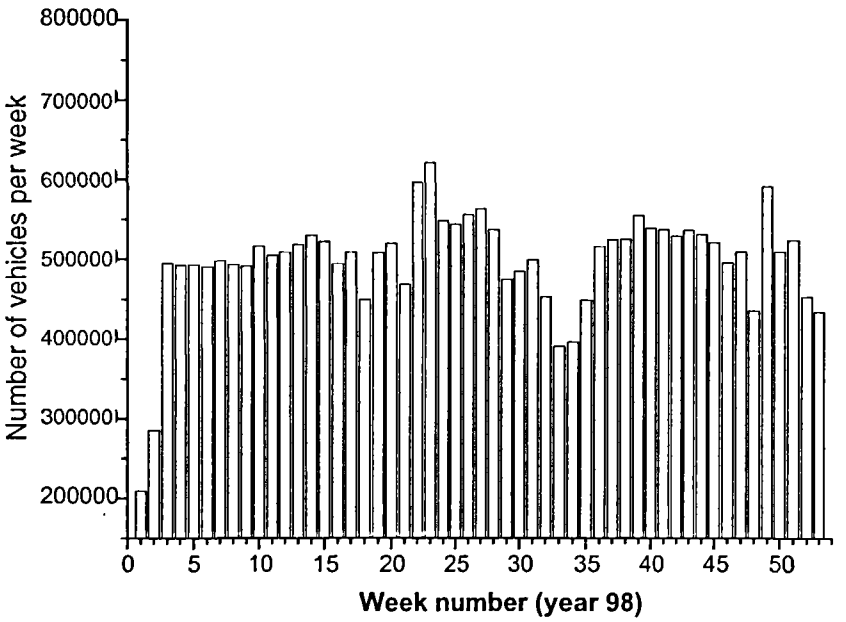

Figure 8
Trafic density related to the road trunk N20 located at 800 m of the sampler.

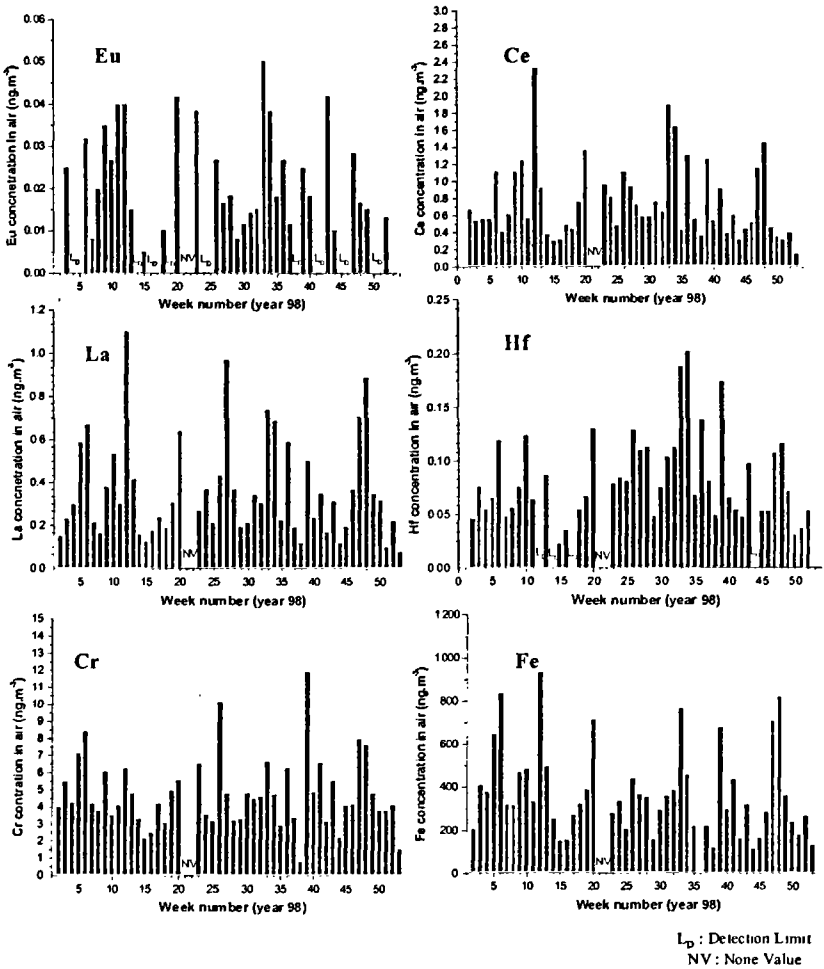

Figure 9
Variation of some trace element concentrations inTSP at Montlhery related to weak EF elements during year 98.

general trend for all the elements quantified in the atmospheric aerosols showing a low EF value and mainly of crustal origin. The low measured concentrations of these elements and the fact that the sampling apparatus is installed in a semi-urban area suggests a nearby origin, related to natural redispersion phenomena.

The annual variation of certain elements with high EF values is shown in Figure 10. Poor correlation of these elements with the variation of primary pollutants is observed, which might indicate the presence of a point source close to the sampling area.

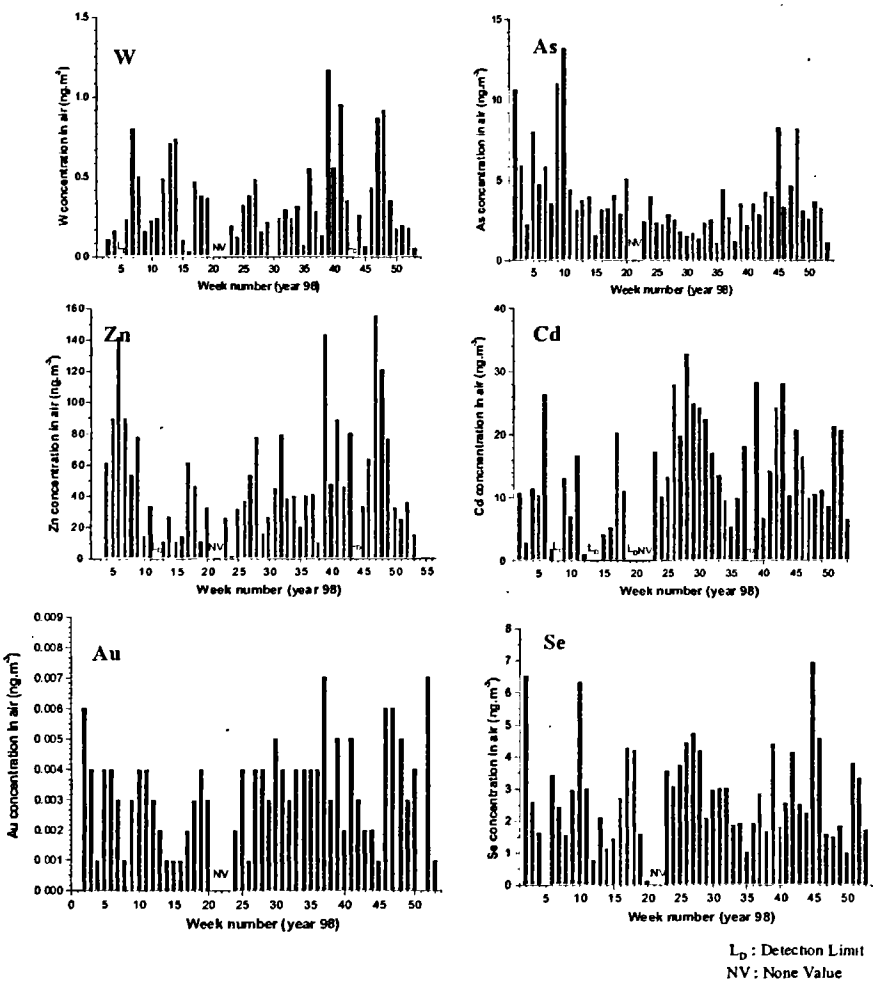

Figure 10
Variation of some trace element concentrations inTSP at Montlhery during year 98 related to high EF elements.

Conclusion

The characterization of trace elements in suspended particulate matter in major industrial cities has recently become a subject of research, since the public authorities became aware of the absence or deficit of data on possible toxicological and physiological impacts of certain elements on health. Furthermore, standards for maximum permitted concentrations in the atmosphere, including for the aerosol fraction smaller than 2.5 mm, the most harmful to the human respiratory system, are now being introduced. Although the data provided by this study concern only the total atmospheric suspended particulates (TSP), the entire particle-size range was included, as the efficiency of the filter medium remains high down to submicron particle sizes. However, the relationship between the analysis and the particle size class was not studied. The nature of the elements and the concentrations detected in the atmosphere during 1998 identify the major anthropogenic pollutants and show their seasonal variations. These data provide a guide for further investigation of the impact on man. This study is the first of its type carried out in France; the results obtained could be used as reference indicators for evaluating the long-term overall variation of atmospheric pollution in the Paris region, particularly the heavy metal levels.

Furthermore, in addition to the measurements provided by the type of study described here, it is necessary to set up collaborations with the various protagonists concerned to a greater or lesser extent by urban pollution in order to obtain the most complete possible synthesis of the available data, in particular those relating to the emissions of the various industrial activities, which are rarely published. Knowledge of these data, coupled with atmospheric modelling taking into account local weather, should enable more precise determination of the origin of emission sources for the major pollutants.

This study has also shown that neutron activation analysis remains a powerful, non-destructive, multi-element analysis method, with a measurement sensitivity that remains acceptable for this type of study. Nevertheless, although more than 30 elements were measured by this technique, knowledge of the atmospheric concentrations of

certain elements (Pb, Hg, S) that are of particular interest in terms of their impact on man necessitate the use of other techniques in addition to neutron activation (ICP-AE, ICP-MS, ED-XRF, AAS, etc.).

Acknowledgements

The authors wish greatly to thanks J. C. Carbonnelle, J. Moro, F. Raynaud and F. Mietlicki (AIRPARIF) for their participation in this work.

Bibliography

AIRPARIF, 1998 — *Surveillance de la qualité de l'air en Ile-de-France.* Rapport d'activité, 108 p.

CHUNG Y. S., CHUNG Y. J., JEONG E. S., CHO S. Y., 1998 — Study on air pollution monitoring in Korea using instrumental neutron activation analysis. *Journal of Rdioanalytical Nuclear Chemistry,* 217 (1): 83-89.

CURRIE L. A., 1968 — Abundances,of Naturally Occuring Isotopes. *Anal. Chem.,* 40: 586-593.

DE BIEVRE P., BRANES I. L., 1992 – Handbook of Chemistry and Physics 73rd Edition. CRC Press: 11,28 – 11,132.

DJINGOVA R., IVANOVA J. U., KULEFF I., 1998 — Comparative evaluation of the possibilities of INAA, ED-XRF, ICP-AES and AAS in the analysis of plants. *Journal of Rdioanalytical Chemistry,* 237 (1-2): 25-34.

GALLORINI M., BORRINI P. A., BONARDI M., ROLLA A., 1998 — Trace elements in the atmospheric particulate of Milan and suburban areas: a study carried out by INAA. *Journal of Radioanalytical and Nuclear Chemistry,* 235 (1-2): 241-247.

ERDTMANN G., 1976 — "Neutron activation Tables ". *In: Kernchemie in Einzeldarstellangen.* New York, Verlagchemie, t.VI.

QUEROL X., ALASTUEY A., LOPEZ-SOLER A., 1997 — Trace element contents in atmospheric suspended particules: Interferences from instrumental neutron activation analysis Fresenius. *J. Anal. Chem.,* 357: 934-940.

SARMANI S., ABUGASSA I., HAMZAH A., 1998 — Instrument neutron activation analysis of environmental samples using the K_0-standardization method. *Journal of Radioanalytical Chemistry,* 234 (1-2): 17-20.

SCHULZE J., AUER M., RWERZI R., 2000 — Low level radioactivity measurement in support of the CTBTO. *Applied Radiation and Isotopes,* 52: 23-30.

TAYLOR S. R., 1972 — Abundance of chemical elements in

the continental crust : a new table. *Geochim. and Cosmochim. Acta*, 28: 1973-1985.

Krivan V., Egger K. P., 1986 — Multielementanalyse von Schwebstäuben der Stadt Ulm und Vergleich der Lufbelastung mit anderen Regionen Frezenus Z. *Analytical Chemistry*, 325: 41-49.

Nouchpramool N., Sumitra T., Leenanuphunt V., 1998 — "Characterization of fine airbone particulates in Bangkok urban area by neutron activation analysis". *In: Nuclear Analytical Methods in the Life Sciences (NAMLS)*, Beijing, China, October 26-30, 5p.

Gone J. K., Olmez I., Ames M. R., 2000 — Size distribution and probable sources of trace elements in submicron atmospheric particulate material. *Journal of Radioanalytical and Nuclear Chemistry*, 244 (1): 133-139.

Ozben C., Belin B., Güven H., 1998 — Analysis of aerosols at the Bosphorus bridge of Istanbul. *Journal of Radioanalytical and Nuclear Chemistry*, 238 (1-2): 101-104.

Huang X., Olmez L., Aras N. K., 1994 — *Journal of Atmospheric Environment*, 28: 1385-1990.

Assessing soil moisture in global climate models: is radon a possible verification tool?

Ann Henderson-Sellers

Parvis Irannejad

Global Climate Model Evaluation

The natural greenhouse effect maintains the Earth's climate at temperatures hospitable to life. Human activities have been recognized as contributing radiatively active trace gases to the atmosphere for over a century (Henderson-Sellers and Jones, 1990). The potential impacts of human-induced global warming prompted the World Meteorological Organization (WMO) and the United Nations Environment Programme (UNEP) to establish the Intergovernmental Panel on Climate Change (IPCC) in 1988. Open to all member nations of the UNEP and WMO, the IPCC has a mandate to assess the scientific, technical and socio-economic information relevant for the understanding of the risk of human-induced climate change. It bases its assessment on published and peer reviewed scientific technical literature. Working Group I assesses the scientific aspects of the climate system and climate change. Working Group II addresses the vulnerability of socio-economic and natural systems to climate change, negative and positive consequences of climate change, and options for adapting to it. Working Group III assesses options for limiting greenhouse gas emissions and otherwise mitigating climate change. The Intergovernmental Panel on Climate Change (IPCC) Second Assessment Report published in 1996 stated:

"Our ability to quantify the human influence on global climate is currently limited because the expected signal is still emerging from the noise of natural variability, and because there are uncertainties in key factors. These include the magnitude and patterns of long term natural variability and the time-evolving pattern of forcing by, and response to, changes in concentrations of greenhouse gases and aerosols, and land surface changes. Nevertheless, the balance of evidence suggests that there is a discernible human influence on global climate." (Houghton *et al.*, 1996, p 5)

Thus it is established that human activities are impacting the climate system; in particular atmospheric concentrations of greenhouse gases are increasing at a rapid rate (e.g. Keeling *et al.*, 1976, 1995). Over the last few years, models and observations have combined to confirm that these increases are causing climate change (Houghton *et al.*, 1996). As a result, treaties and protocols are being developed and agreed which aim to reduce, and perhaps ultimately reverse, these human-induced disturbances to the climate system (e.g. Taplin, 1996; Wigley, 1998). The tools with which future climates are to be predicted are climate models. However, before models can be used with confidence, they must be tested against observations and their predictive skills verified (Gates *et al.*, 1996).

The IPCC includes a Task Force on National Greenhouse Gas Inventories which oversees the members' national efforts to account for and measure greenhouse gas sources and sinks. The IPCC has been at the forefront of international efforts to evaluate and verify global climate models. Its Second Assessment Report concluded that:

"The most powerful tools available with which to assess future climate are coupled climate models, which include three-dimensional representations of the atmosphere, ocean, cryosphere and land surface... (and)... More detailed and accurate simulations are expected as models are further developed and improved." Gates *et al.* (1996, p 233)

Climate models are tools employed to enhance understanding of the climate system and to aid prediction of future climates. The aim of all global climate models (GCMs) is the calculation of the full three-dimensional character of the climate comprising at least the global atmosphere, the continental surfaces and the oceans. If a model were to be constructed which included the entirety of our

knowledge on the atmosphere-ocean-land system, it would not be possible to run it on even the fastest computer. For this reason, GCMs, currently the most complicated numerical models, can only be simplifications of our current knowledge of the climate system (Figure 1).

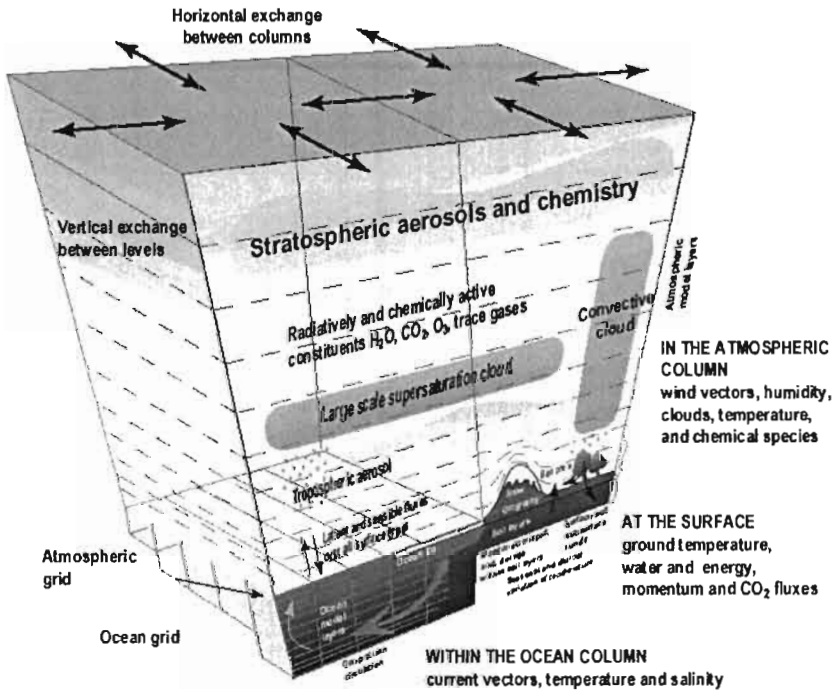

Figure 1
Illustration of the basic characteristics and processes within a general circulation model, showing the manner in which the atmosphere and ocean are split into columns. The atmosphere, land and ocean are modelled as a set of interacting columns distributed across the Earth's surface. The resolutions of the atmosphere, land and ocean models are often different because the processes differ and have different timescales and equilibration times. Typically many types of clouds, soils and vegetation are treated. In this example, soil moisture is modelled in a number of layers and tropospheric and stratospheric aerosols are included climate model schematic (after Henderson-Sellers and McGuffie, 2000).

Although there have been great advances made in the discipline of climate modelling over its forty year history, even the most sophisticated models remain very much simpler than the full climate system (e.g. Henderson-Sellers and McGuffie, 2000). Indeed, such simplicity is an intended attribute of climate models (e.g. Washington and Parkinson, 1986; McGuffie and Henderson-Sellers, 1997). Modelling of a system that encompasses such a wide variety of components as the climate system is a formidable task and it requires co-operation between many disciplines if reliable conclusions are to be drawn. Intercomparisons such as the Atmospheric Model Intercomparison Project (AMIP) Phase II (AMIP II) are now an integral part of climate science and an important means for advancement of understanding of the climate system (Gates *et al.*, 1999). For climate models to be accepted as useful tools for climate analysis their evaluation must progress beyond simply intercomparison to verification.

This process of verification is now termed model "evaluation", although many researchers still use the term "validation". The former term has been chosen over the latter by Working Group I of the IPCC for its Third Assessment Report, because it is argued that "evaluation" denotes a comparison while "validation" appears to offer some form of approval. In this paper, a novel method for the evaluation of predictions of large-scale soil moisture by climate models is proposed.

Why Investigate Radon as an Evaluation Tool?

Large-scale (roughly an American or Australian state or a European nation) soil moisture variability is now recognized as an important cause of variability in weather & climate systems (e.g. Beljaars *et al.*, 1993; Sellers *et al.*, 1997; Douville and Chauvin, 2000). The Global Energy & Water Cycle Experiment (GEWEX) and the Biospheric Aspects of the Hydrologic Cycle (BAHC) are developing interna-

tional programmes of soil moisture measurement, analysis & prediction (e.g. Sorooshian, 2000).

Arguably the most useful range of soil moisture verification for numerical model evaluation is for intermediate wetness conditions because very arid and permanently saturated soils behave in known and well-simulated ways (Shao & Henderson-Sellers, 1996; Wood *et al.*, 1998). Variations among land-surface simulations of latent heat fluxes are largest at intermediate soil wetnesses (Irannejad *et al.*, 1995). These temporally transient and spatially heterogeneous conditions are the most difficult conditions under which to try to measure "areal" soil moisture. Neither satellite-derived proxies for soil moisture nor summations of point-measured moisture contents can adequately deliver large-scale areal values of continental soil moisture (e.g. Robock *et al.*, 1998). The result is that the most important type of model prediction of continental soil moisture is the most difficult to evaluate because of the lack of appropriate observations.

Radon (^{222}Rn) is produced by the radioactive decay of radium (^{226}Ra) ubiquitous in rocks and soils. It is a noble gas with a half life 3.8 days: chemically inert & short-lived enough for tracking, radon has been successfully used in atmospheric tracer studies for e.g. vertical mixing and air mass history (Genthon and Armengaud, 1995; Jacob *et al.*, 1997). Radon escapes from the soil by plant transpiration and diffusion through soil pores (Armengaud and Genthon, 1993). The emanation of radon from land surfaces is known to be a function of soil temperature and also believed to be dependent upon: (i) soil porosity; (ii) depth of soil; (iii) soil moisture; (iv) vegetation - these probably in decreasing importance (Pearson and Jones, 1966; Stockwell *et al.*, 1998). Ocean fluxes are at least 100 times less than land fluxes (Broecker *et al.*, 1967) while ice cover strongly inhibits radon emanations and frozen soils exhibit much lower fluxes than non-frozen (Feichter and Crutzen, 1990).

Radon is believed to have a mean global land emission rate of ~1 atom.cm^{-2}.s^{-1} (Lambert *et al.*, 1982) with a rough constraint that total global annual radon source is around 15 kg (Stockwell *et al.*, 1998). Measurements of fluxes of radon range typically from ~0.004 atom.cm^{-2}.s^{-1} in New Zealand to ~2.5 atom.cm^{-2}.s^{-1} in Illinois (Turekian *et al.*, 1977) although Schery (1986) found fluxes of up to 5 atom.cm^{-2}.s^{-1}.

There are conflicting reports regarding the possible impact vegetation might have on radon fluxes (cf. Schery *et al.*, 1989). Pearson and Jones (1966) found a major enhancement of radon flux due to transpiration. Hinton and Whicker (1985) reported that their measurements of enhanced flux from vegetated tailings was probably due to increased porosity (Strong and Levins, 1982); and Schery *et al.* (1984 and 1989) both find that the effects of transpiration are small. Finally, it is known that precipitation can clog soil pores and air pressure fluctuations affect radon emanation rates over short timescales (Schery and Gaeddert, 1982).

Figure 2 shows the routes followed by radon once released to the atmosphere from the soil. Its short half-life makes it an excellent

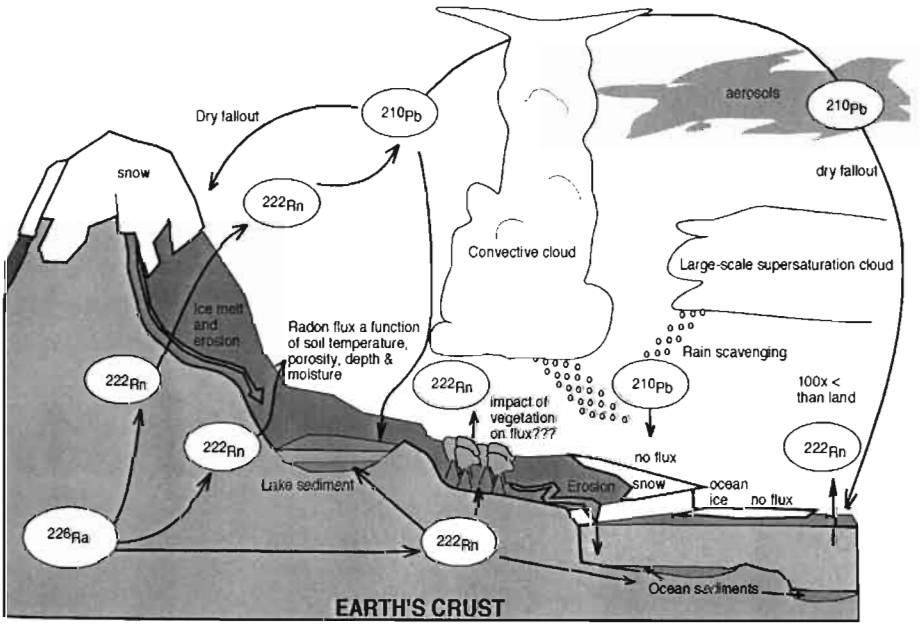

Half lives: ^{222}Rn = 3.8d, (0.33×10^{6}s); ^{210}Pb = 22.3y (0.694×10^{9}s); ^{226}Ra = 1,620 y, (0.511×10^{11}s)

Figure 2
Schematic illustrating the sources of (^{222}Rn) radon in the atmosphere and the paths of its decay product (^{210}Pb) lead from the atmosphere into terrestrial, lacustrine and marine sediments. Half lives are 1,620 years for radium; 3.8 days for radon; and 22.3 years for lead.

tool for atmospheric tracing and global modelling studies (e.g. Rind and Lerner, 1996). ^{222}Rn decays to ^{210}Pb which is removed from the atmosphere either directly by dry fall-out or by wash-out or rain-out following incorporation of the lead into cloud droplets and hence precipitation.

As well as the records of atmospheric radon from around the globe there are also archives of ^{210}Pb in ocean and lake sediments (e.g. Preiss *et al.*, 1996). Together, these radionuclide inventories form a powerful and synergistic archival record of continental-surface radon emanation to the atmosphere around the world and, thus, perhaps, of large-scale continental soil moisture variations over time.

Exploiting the Relationship between Radon and Soil Moisture for Climate Model Verification

Various initiatives of the UN-sponsored World Climate Research Programme (WCRP) are directed toward "validation and diagnosis" of GCM performance. Among these, the Atmospheric Model Intercomparison Project (AMIP) is an especially apt framework for assessing model performance at the atmosphere-land interface (Henderson-Sellers *et al.*, 1996; Gates *et al.*, 1999). Since 1992, for example, a Diagnostic Subproject on Land-surface Processes and Parameterizations has investigated AMIP model experiments with common specifications of radiative forcings and ocean boundary conditions. This subproject has analyzed selected 10-year climate simulations from the initial AMIP I phase of this intercomparison experiment (e.g. Love *et al.*, 1995, Qu and Henderson-Sellers, 1998), and currently investigations are being undertaken to validate and diagnose the 17-year simulations from the AMIP II phase that is in progress (e.g. Phillips *et al.*, 2000). AMIP II also has another Diagnostic Subproject specifically studying soil moisture simulations by participating AGCMs (Robock *et al.*, 1998).

There is a sound history of exploitation of various radionuclides in atmospheric model evaluation (e.g. Mahowald *et al.*, 1997). In particular, climate model intercomparisons have been conducted using radon surface emanations of: (a) two source strengths of 1 atom.cm^{-2}.s^{-1} (60° S to 60° N) and 0.5 atom.cm^{-2}.s^{-1} from 60° N to 70° N and (b) source strength a function of surface air temperature viz. 3.2 x 10^{-16} kg.m^{-2}.d^{-1} when the surface temperature is greater than 273 K and 1.0 x 10^{-16} kg.m^{-2}.d^{-1} when the surface temperature is less than or equal to 273° K (Rind and Lerner, 1996). These researchers found that radon proved to be a useful global circulation tracer.

Detailed observations have been made around the world of radon emanation rates as a function of soil moisture. Measurements of radon flux at 78 sites in Australia (Schery *et al.*, 1989), 42 Hawaiian sites (Whittlestone *et al.*, 1996) and 325 in Florida (Nielson *et al.*, 1996) give rise to expressions relating to radon emanation rates to soil moisture (Figure 3(a)). Detailed comparisons of radon emanation rates from similar soils with differing moisture and depth characteristics show that these factors can be segregated successfully and that the wetness (or dryness) of the soil is a significant factor in

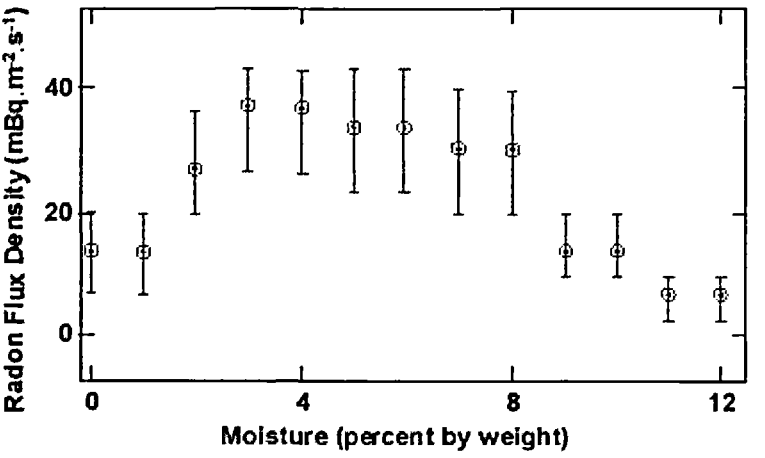

Figure 3a
Binned plot of radon emanation rates (mBq.m^{-2}.s^{-1}) and soil moisture content at 20 cm depth (percent by weight) (after Schery *et al.*, 1989).

radon release rates (Table 1). Strong and Levins (1982) find low radon emanation rates at both very low and medium soil moisture values with a turning point at about 8% water content by weight. From these sources, a functional dependence has been derived for use in global climate model studies (Figure 3(b)).

Soil	Radon flux ($mBq.m^{-2}.s^{-1}$)		
Location/Moisture	Dry	Wet	Ratio (dry/wet)
Thin soil	1.3	0.006	21.7
Deep soil	6.5	1.1	5.9
E or W of island	5.7	1.1	5.1

▌Table 1
Radon flux as a function of soil moisture from Hawaii (compiled from Whittlestone *et al.*, 1996).

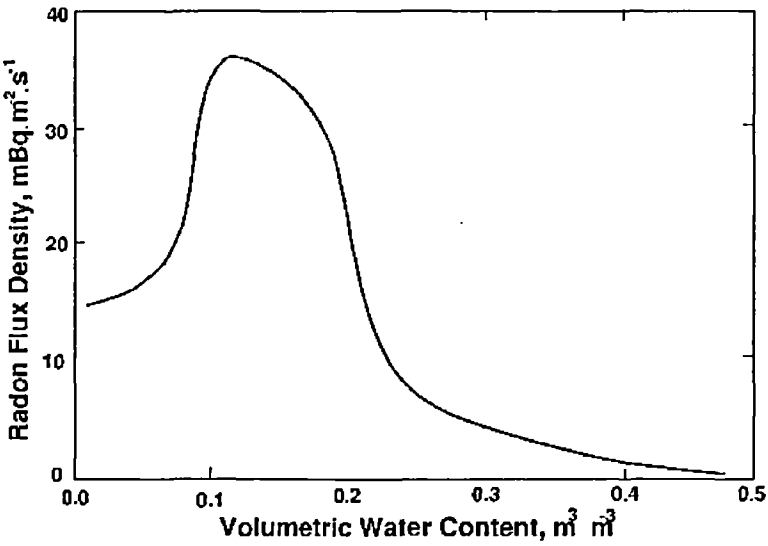

▌Figure 3b
Developed relationship between soil water (volumetric water content $m^3\ m^{-3}$ and radon release rates ($mBq.m^{-2}.s^{-1}$) used in the calculation of the near-surface radon maps shown in Figure 4.

As a result of many recommendations from project participants, the AMIP Co-ordinating Panel has provided for the possibility of some experimentation within the framework of Phase II of AMIP. In these global simulation sensitivity projects, the intention is to address fundamental issues associated with atmospheric GCMs and their development. It is envisaged that some working hypotheses warranting experimentation will result from the AMIP II Diagnostic Subprojects.

We propose that an AMIP II Experimental Subproject be performed in which the ^{222}Rn source strength is a function of simulated soil moisture. The nature of the relationship is open for discussion. Suggestions include: ^{222}Rn flux be inversely proportional to the square root of soil moisture (Nielson *et al.*, 1996); ^{222}Rn flux be given by the relationship in Schery *et al.* (1989) i.e. Figure 3(a); or the use of the function shown in Figure 3(b). Proposals for AMIP Experimental Subprojects are evaluated in terms of their capacity to address: 1) fundamental issues associated with AGCMs; 2) defined and practical questions; 3) implementation (demonstrated with at least one AMIP AGCM); 4) demonstrated need for intercomparative study; and 5) interest of at least three modelling groups participating in AMIP identified.

The first step in making such a proposal is to involve one AGCM group and ultimately two others. To this end, we propose the following hypotheses be examined by at least one AGCM in AMIP II:

(i) does the addition of a functional dependence of radon emanation on soil moisture improve the fit of predicted near-surface ^{222}Rn to observations?

(ii) does the addition of a functional dependence of radon emanation on soil moisture improve the fit of archived ^{210}Pb to observations? and, if either of these return an affirmative reply, then;

(iii) can ^{222}Rn or ^{210}Pb be used as a novel monitor of areal soil moisture and hence, ultimately, a tool for verification of global climate models?

The benefits of proposing a series of AGCMs experiments under the auspices of AMIP II are illustrated in Figure 4. This shows the simulated distributions of surface to atmosphere emanation rates of radon based on the soil moisture function given in Figure 3(b).

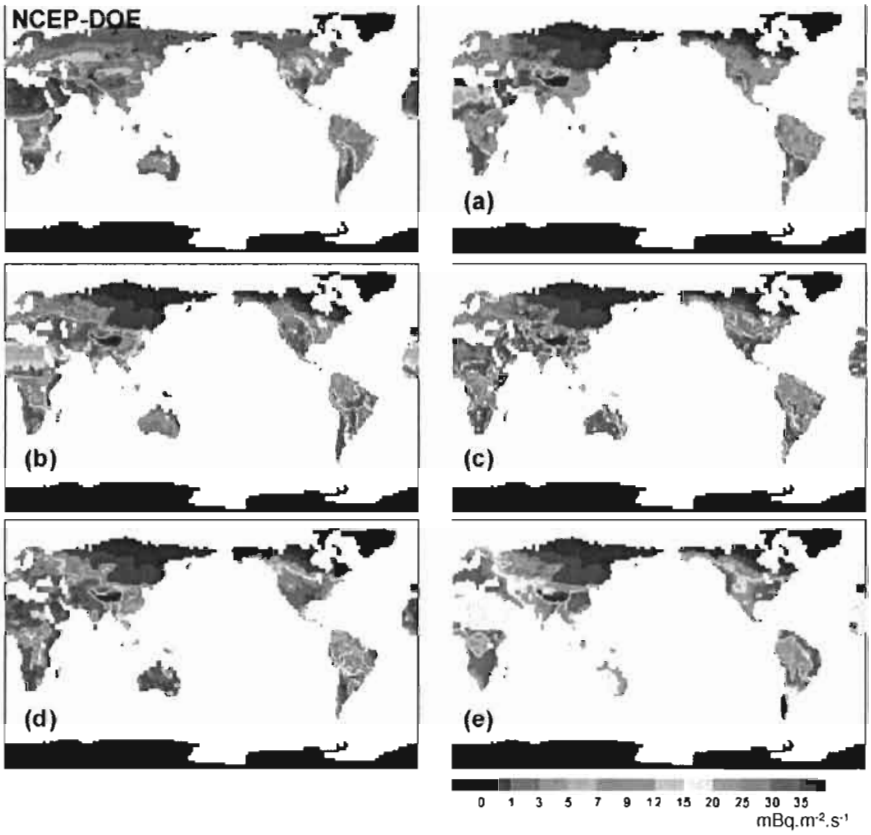

Figure 4
Computed global distributions of ^{222}Rn emanation rates from the surface ($mBq.m^{-2}.s^{-1}$) derived from 5 example AMIP II AGCMs (b)-(e) and one re-analysis data set (NCEP-DOE) (a). These distributions could form the basis for a global climate model soil moisture verification study using either the networks of atmospheric radon observations or archives of ^{210}Pb.

These maps have been derived using surface temperature and soil moisture conditions calculated by five example AMIP II models and one of the available reanalysis data sets (NCEP-DOE e.g. WCRP, 2000). The considerable variation in global radon distributions lends support to the proposal that comparison of such maps with

global observations of ^{222}Rn could provide a novel and valuable means of verification of a poorly understood but critically important surface climate characteristic: soil water content.

Bibliography

ARMENGAUD A., GENTHON C., 1993 – "Modelling global distributions of ^{222}Rn, ^{210}Pb and ^{7}Be in the atmosphere with general circulation models ". *In: Isotope Techniques in the Study of Past and Current Environmental Changes in the Hydrosphere and the Atmosphere*, Vienna International Atomic Energy Agency, SM-329: 15-24.

BELJAARS A. C. M., VITERBO P., MILLER M. J., 1993 – The anomalous rainfall over the United States during July 1993: Sensitivity to land surface parameterization and soil moisture anomalies. *Mon. Wea. Rev.*, 124: 362-383.

BROECKER W. E., LI Y. H., CROMWELL J., 1967 – Radium-226 and radon-222: concentrations in Atlantic and Pacific Oceans. *Science*, 158: 1307-1310.

DOUVILLE, H., CHAUVIN F., 2000 – "Relevance of soil moisture for seasonal climate predictions", Procs. Second WCRP International Conference on Reanalyses, Geneva, WCRP-109, WMO/TD-NO. 985: 169-172.

FEICHTER J., CRUTZEN P. J., 1990 – Parameterisation of vertical tracer transport due to deep cumulus convection in a global transport model and its evaluation with ^{222}radon measurements. *Tellus*, 42B: 100-117.

GATES W. L., HENDERSON-SELLERS A., BOER G. J., FOLLAND C. K., KITOH A., MCAVANEY B. J., SEMAZZI F., SMITH N., WEAVER A. J., ZENG Q.-C., 1996 – "Climate Models – evaluation". *In* J.T. Houghton *et al.* (eds.) : *Climate Change 1995: The Science of Climate Change*, Cambridge University Press: 229-284.

GATES W. L., BOYLE J. S., COVEY C., DEASE C. G., DOUTRIAUX C. M., DRACH R. S., FIORINO M., GLECKLER P. J., HNILO J. J., MARLAIS S. M., PHILLIPS T. J., POTTER G. L., SANTER B. D., SPERBER K. R., TAYLOR K. E., WILLIAMS D. N., 1999 — An overview of the results of the Atmospheric Model Intercomparison Project (AMIP). *Bulletin of the American Meteorological Society*, 80: 29–55.

GENTHON C., ARMENGAUD A., 1995 – Radon-222 as a comparative tracer of transport and mixing in two general circulation models of the atmosphere. *J. Geophys. Res.*, 100: 2849-2966.

HENDERSON-SELLERS A., JONES M. D. H., 1990 – History of the greenhouse effect. *Progress in Physical Geography*, 14: 1-18.

HENDERSON-SELLERS A., MCGUFFIE K., 2000 – Forty years of numerical climate modeling. *Int. J. Climatol.*, in the press.

HENDERSON-SELLERS A., MCGUFFIE K., PITMAN A. J., 1996 – The Project for Intercomparison of Land-surface Parametrization Schemes (PILPS): 1992 to 1995. *Climate Dynamics*, 12: 849-859.

HINTON T. G., WHICKER F. W., 1985 – A field experiment on Rn flux from reclaimed uranium mill tailings. *Health Phys.*, 48, 421-427.

HOUGHTON J. T., MERA FILHO L. G., CALLANDER B. A., HARRIS N., KATTENBERG A., MASKELL K., 1996 – *Climate Change 1995, The Science of Climate Change: Contribution of Working Group 1 to the Second Assessment Report of the Intergovernmental Panel on Climate Change*, Cambridge, Cambridge University Press: 572 p.

IRANNEJAD P., HENDERSON-SELLERS A., SHAO Y., LOVE P. K., 1995 – "Comparison of AMIP and PILPS off-line landsurface simulations". *In: Procs. of The First International AMIP Scientific Conference,* Monterey, CA, USA, 15-19 May 1995, (ed. W.L. Gates), WMO/TD, 732, Geneva, WCRP: 465-470.

JACOB D. J., *et al.*, 1997 – Evaluation and intercomparison of global atmospheric transport models using ^{222}Rn and other short lived tracers. *J. Geophys. Res.*, 102: 5953-5970.

KEELING C. D., BACASTOW R. B., BAINBRIDGE A. E., EKDAHL C. A., GUENTHER P. R., WATERMAN L. S., CHIN J. F. S., 1976 – Atmospheric carbon dioxide variations at Mauna Loa Observatory, Hawaii. *Tellus*, 28: 538-551.

KEELING C. D., WHORF T. P., WAHLEN M., VAN DER PLICHT J., 1995 – Interannual extremes in the rate of rise of atmospheric carbon dioxide since 1980. *Nature*, 375: 666–670.

LAMBERT G., POLION G., SANAK J., ARDOUIN B., BUISSON A., JEGOU A., LEROULLEY J. C., 1982 – Application à l'étude des échanges troposphère-stratosphère. *Annal. Geophys.*, 48: 497-531.

LOVE P. K., HENDERSON-SELLERS A., IRANNEJAD P., 1995 – "AMIP diagnostic subproject 12 (PILPS Phase 3): Land-surface Processes". *In: Proceedings of the First International AMIP Scientific Conference,* , Monterey, CA, USA, 15-19 May 1995, (ed. W.L. Gates), WMO/TD, 732, Geneva, WCRP: 101-106.

MCGUFFIE K., HENDERSON-SELLERS A., 1997 – *A Climate Modelling Primer*, Chichester, 2nd edition, John Wiley and Sons, 254 p.

MAHOWALD N. M., RASCH P. J., EATON B. E., WHITTLESTONE S., PRINN R. G., 1997 – Transport of ^{222}radon to the remote troposphere using the model of atmospheric transport and chemistry and assimilated winds from ECMWF and the National Center for Environmental Prediction. *J. Geophys. Res. (Atmosphere)*, 102 D23 (28): 139-157.

NIELSON K. K., ROGERS V. C., HOLT R. B., 1996 – Measurements and calculations of soil radon flux at 326 sites throughout Florida. *Env. Int.*, 22 (1): S471-S476.

PEARSON J. E., JONES G. E., 1966 – Soil concentration of emanating radium-226 and the emanation of radon from soils and plants. *Tellus*, 18: 655—662.

PHILLIPS T. J., HENDERSON-SELLERS A., IRANNEJAD P., MCGUFFIE K., ZHANG H., 2000 – On validation and diagnosis of land-surface climate simulations.

Climate Change Newsletter, 12(1): 3-5 and http://www.brs.gov.au/publications/ccn/ccn12v1/research.html.

PREISS N., MÉLIÈRES M-A., POURCHET M., 1996 – A compilation of data on lead 210 concentration in surface air and fluxes at the air-surface and water-sediment interfaces. *J. Geophys. Res.*, 101 D22 (28): 847-862.

QU W., HENDERSON-SELLERS A., 1998 – Comparing the scatter in PILPS off-line experiments with that in AMIP I coupled experiments. *Global and Planetary Change*, 19 (1-4): 209—223.

RIND D., LERNER J., 1996 – Use of on-line tracers as a diagnostic tool in general circulation model development. 1. Horizontal and vertical transport in the troposphere. *J. Geophys. Res.*, 101 (12): 667-683.

ROBOCK A., SCHLOSSER C. A., VINNIKOV K. YA., SPERANSKAYA N. A., ENTIN J. K., QIU, S., 1998 – Evaluation of the AMIP soil moisture simulations. *Glob. Plan. Chng.*, 19: 181-208.

SCHERY S. D., GAEDDERT D. H., 1982 – Measurements of the effect of cyclic atmospheric pressure variation on the flux of ^{222}Rn from soil. *Geophys. Res. Letts.*, 9: 835-838.

SCHERY S. D., GAEDDERT D. H., WILKENING M. H., 1984 – Factors affecting exhalation of radon from a gravelly sandy loam. *J. Geophys. Res.*, 89: 7299-7309.

SCHERY S. D., 1986 – Studies of thoron and thoron progeny: implications for transport of airborne radioactivity from soil to indoor air. *Indoor Radon*, SP-54, Air Poll. Cont. Assoc., Pittsburgh PA: 25-36.

SCHERY S. D., WHITTLESTONE S., HART K. P., HILL S. E., 1989 – The flux of radon and thoron from Australian soils. *J. Geophys. Res.*, 94(D6): 8567-8576.

SELLERS P. J., DICKINSON R. E., RANDALL D. A., BETTS A. K., HALL F. G., BERRY J. A., COLLATZ G. J., DENNING A. S., MOONEY H. A., NOBRE C. A., SATO N., FIELD C. B., HENDERSON-SELLERS A., 1997 – Modeling the exchange of energy, water and carbon between continents and the atmosphere. *Science*, 275: 502-509.

SHAO Y., HENDERSON-SELLERS A., 1996 – Modelling soil moisture: a Project for Intercomparison of Land Surface Parameterisation Schemes Phase 2(b). *J. Geophys. Res.*, 101 (D3), 7227-7250.

SOROOSHIAN S., 2000 – GEWEX Phase II, (editorial). *GEWEX News*, March 2000: 2-3

STOCKWELL D. Z., KRITZ M. A., CHIPPERFIELD M. P., PYLE J. A., 1998 – Validation of an off-line three-dimensional transport model using observed radon profiles. 2 Model results. *J. Geophys. Res.*, 103 (D7): 8433-8445.

STRONG K. P., LEVINS D. M., 1982 – Effect of moisture content on radon emanation from uranium ore and tailings. *Health Phys.*, 42: 27-32.

TAPLIN R., 1996 – "Climate science and politics: the road to Rio and beyond". *In* Giambellucca, T. and Henderson-Sellers, A. (eds): *Climate Change: Developing Southern Hemisphere perspectives*, Chichester, John Wiley & Sons: 377–396.

TUREKIAN K. K., NOZAKI Y., BENNINGER L. K., 1977 – Geochemistry of atmospheric radon and radon products. *Ann. Rev. Earth Plant Sci.*, 5: 227-255.

WASHINGTON W. M., PARKINSON C.L., 1986 – *An Introduction to Three-Dimensional Climate Modelling.* Mill Valley, CA, University Science Books, 422 p.

WCRP, 2000 – "Second WCRP International Conference on Reanlaysis". *Proceedings, WCRP-109*, World Meteorological Organisation, Geneva, 452 p.

WHITTLESTONE S., SCHERY S. D., LI Y., 1996 – Thoron and radon fluxes from the island of Hawaii. *J. Geophys. Res.*, 101(D9): 787-794.

WIGLEY T. M. L., 1998 – The Kyoto protocol: CO_2, CH_4 and climate implications, *Geophys. Res. Lett.*, 25: 2285-2288.

WOOD E. F., LETTENMAIER D. P., LIANG X., LOHMANN D., BOONE A., CHANG S., CHEN F., DAI Y., DICKINSON R. E., DUAN Q., EK M., GUSEV Y. M., HABETS F., IRANNEJAD P., KOSTER R., MITCHEL K. E., NASONOVA O. N., HOILHAN J., SCHAAKE J., SCHLOSSER A., SHAO Y., SHMAKIN A. B., VERSEGHY D., WARRACH K., WETZEL P., XUE Y., YANG Z.-L., ZENG Q.-C., 1998 – The Project for Intercomparison of Land-surface Parameterization Schemes (PILPS) Phase 2(c) Red—Arkansas River basin experiment: 1. Experiment description and summary intercomparisons. *Global and Planetary Change*, 19(1-4): 115-135.

Production and release of tritium from a research reactor

Masami Fukui

Ron Grazioso

Introduction

The Kyoto University Research Reactor (KURR) is a light water moderated research reactor. It commenced operation in 1964 at 1 MW_{th} and the power was raised to 5 MW_{th} in 1968. The ventilation system in the containment building works at ca.350 $m^3.mn^{-1}$ order to cover the duration of the reactor operation cycle of 70-80 $h.wk^{-1}$ from Tuesday through Friday. Using a Ge(Li) detector the concentrations of radionuclides in the exhaust air during operation at 5 MW_{th} have been confirmed to be in the order of 10^{-2} $Bq.cm^{-3}$ for ^{41}Ar, 10^{-6} $Bq.cm^{-3}$ for tritium, 10^{-8} $Bq.cm^{-3}$ for ^{133}I and 10^{-9} $Bq.cm^{-3}$ for ^{131}I. As a result of the routine monitoring by a 22-L ionization chamber set for the stack exhaust, the presence of most radionuclides in the stream is usually masked by the reading of ^{41}Ar; this is especially true for tritium vapor.

As shown in Figure 1 the reactor core is submerged in a moderating pool of 30 m^3 of demineralized light water. The reactor supports two major sources of tritium: a D_2O facility (Installed in 1964: ca. 2 m^3) and a Cold Neutron Source (CNS) facility (Installed in 1986: ca. 40 dm^3 liquid deuterium).

This report is divided into three major sections: 1) monitoring the tritiated water (HTO) vapor in the stack exhaust in order to assess

the annual quantity discharged, 2) monitoring the HTO concentrations in the air within the containment building in order to get insight into the distribution and variations in the controlled area for radiation workers, and 3) monitoring the HTO concentrations in the exhaust from ^{41}Ar decay tanks of both the D_2O and CNS facilities (Figure 1) set near the reactor core in order to assess the HTO production of major sources. The goal of the last section is to attempt to locate a possible tritium leak to decrease radiation exposure to both radiation workers and the public.

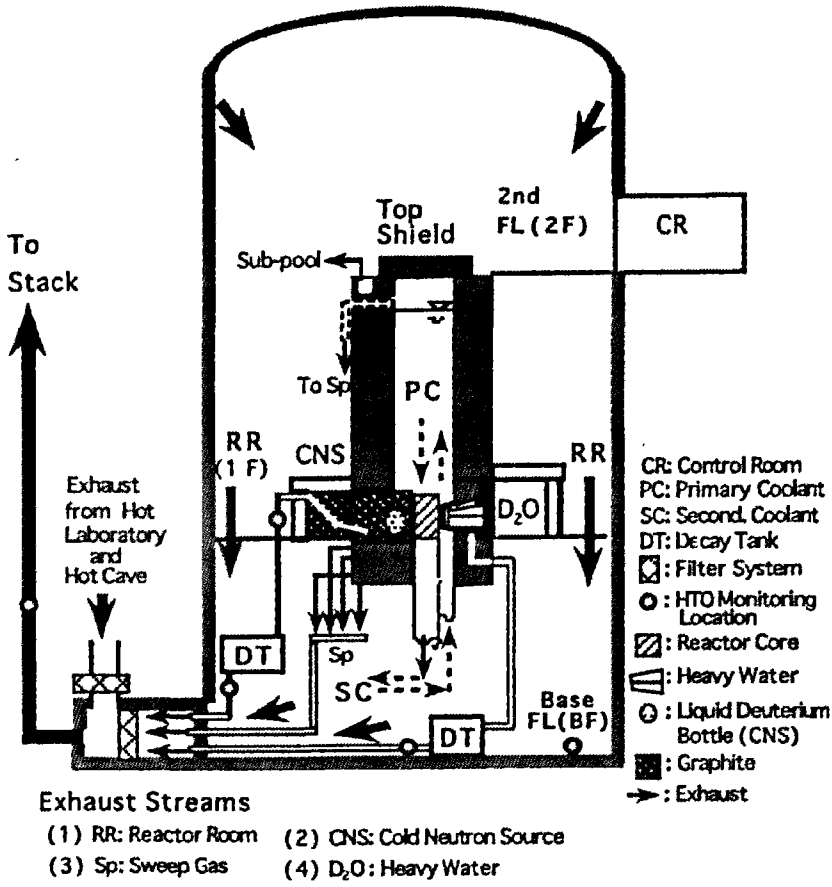

Figure 1
Cross section of the KURR with major exhaust streams.

All concentrations reported here are measured by the liquid scintillation counting (LSC) method for a cocktail of 10 ml scintillator and 1 ml condensate, collected using condensers and/or dehumidifiers for a few hours.

Monitoring HTO concentrations in stack exhaust

Figure 2 shows the HTO concentrations in condensate of the stack exhaust monitored routinely for twenty years using LSC. This Figure indicates that the concentration has not increased so much since the installation of these HTO source facilities except for a term of unexpected release of heavy water. During a one and half

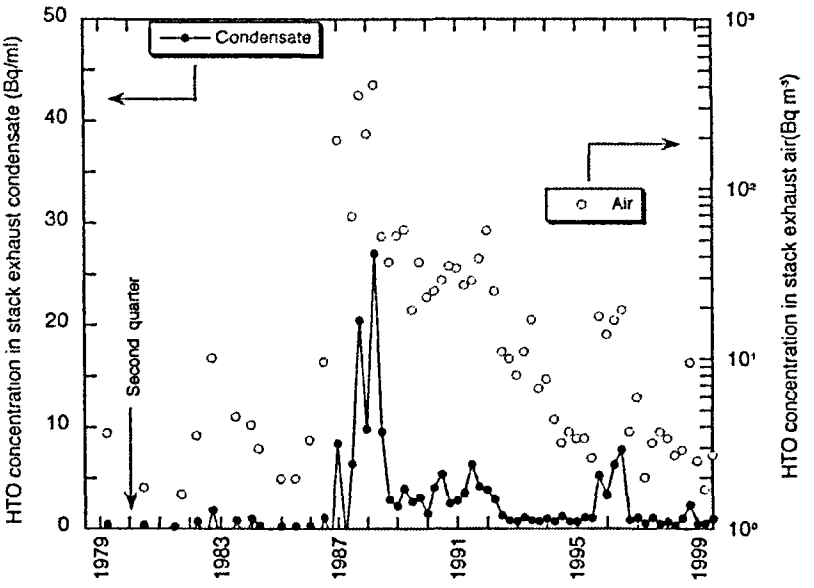

Figure 2
Evolution of HTO concentrations in the KURR stack exhaust over the last twenty years.

year period from May 1987 to November 1988, the D_2O facility leaked approximately 0.34 TBq of heavy water (ca.30 dm^3) into the KURR containment building (Fukui, 1992). As shown in Figure 2, peak concentration, 27 $Bq.ml^{-1}$ in the stack condensate (ca.400 $Bq.m^{-3}$ in air), was observed for the routine monitoring of the third quarter of 1988. After the leak event, monitoring of HTO vapor in the stack exhaust has been carried out on a quarterly basis during the operation of the KURR. A few times after1990, ranges from 5 to 10 $Bq.ml^{-1}$ were recorded due to the small leak of the heavy water during the period of renewal work of distribution pipes of D_2O during 1990 to 1992 and the storage tank in 1996. As recognized the exhaust monitoring is on a batch basis for the water samples

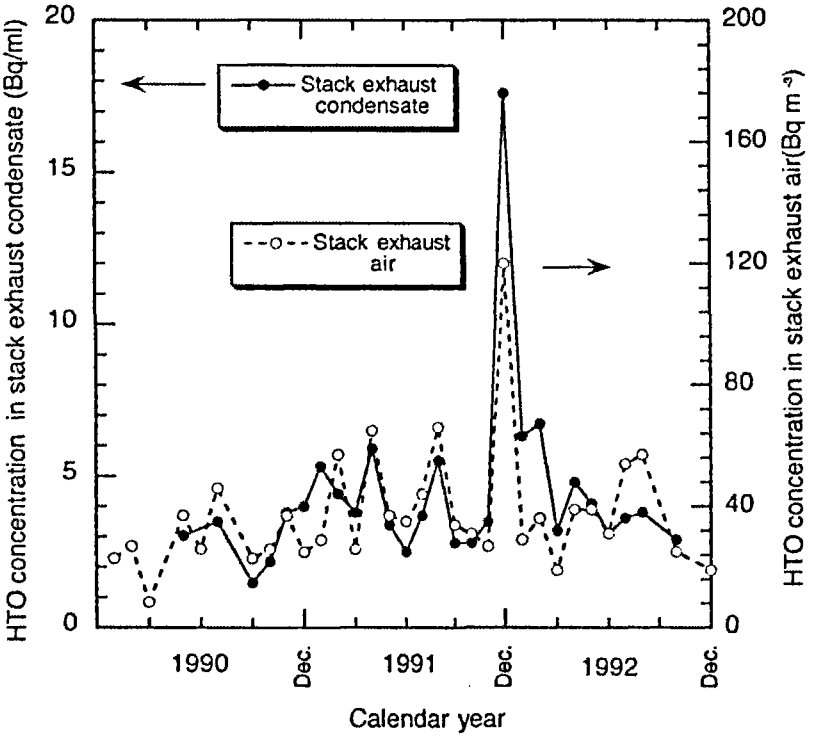

Figure 3
HTO concentrations in the stack exhaust monitored on a monthly basis during 1990-1992.

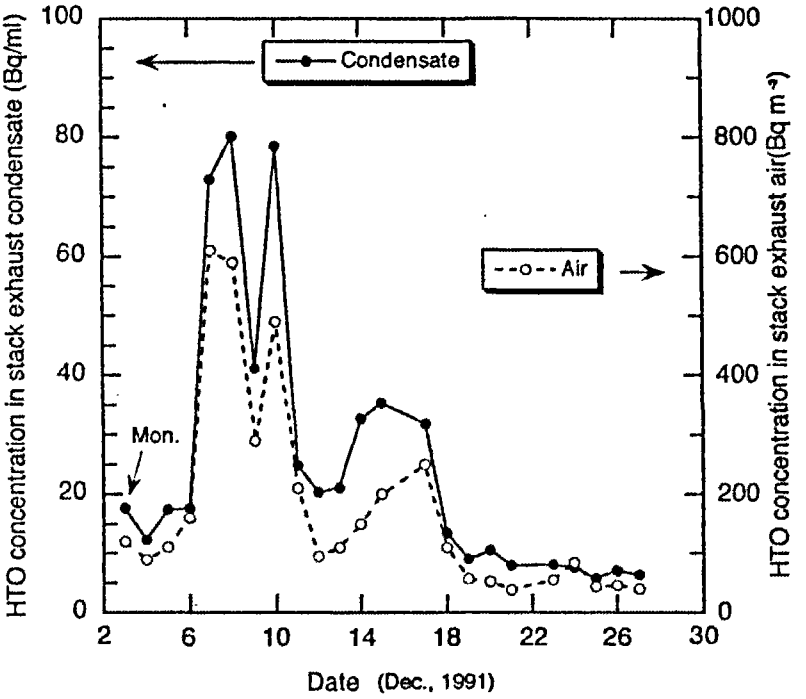

Figure 4
HTO concentrations in the stack exhaust monitored on a daily basis in December 1991.

collected as condensate and may overlook more high concentrations in the exhaust. This is confirmed by the results that showed the peak concentrations of 18 and 80 $Bq.ml^{-1}$, respectively, for monthly (1990-1992; Figure 3) and daily (December 1991; Figure 4) basis monitoring. This suggests that a greater frequency of sampling condensate is required (at least on a daily basis) in addition to the routine monitoring on the quarterly basis in case of a probable leakage of tritium.

Recent monitoring data show that the HTO concentrations in vapor are less than a few $Bq.ml^{-1}$, resulting in the annual HTO discharge from the KURR to be estimated as ca. 1 $GBq.yr^{-1}$.

Monitoring HTO concentrations in containment building air

Procedure for assessment of HTO concentrations in the air using laboratory dishes

The transfer of HTO vapor, Cv, from the air into dish water is primarily a function of two processes: exchange and evaporation. Exchange refers to the net transport of HTO into or out of the water dish. Exchange is dependent on the difference in specific activities between the water in the dish and the vapor in the air. Evaporation affects the amount of HTO that leaves the water and returns to the air. These phenomena were modeled mathematically (Fukui, 1992). The change in the HTO concentration, C_W, in the dish water exposed to the HTO concentration in vapor, C_V, is expressed as:

$$C_w = C_V \{ 1 - (1 - k_e t / H)^{kc/ke} \} / å, \qquad (1)$$

where:

- C_w : the HTO concentration of the water sample ($Bq.ml^{-1}$);
- å : the ratio of isotropic concentrations $(H^3)/(H^1)$ in the saturated vapor and liquid phases of tritiated;
- C_V : the HTO concentration in vapor ($Bq.ml^{-1}$);
- k_c : the exchange rate constant ($cm.h^{-1}$);
- k_e : the apparent evaporation rate constant ($cm.h^{-1}$);
- t : the elapsed time after exposure (h), and
- H : the initial depth of water in the dish (cm).

Thus from eqn. (1), the average concentration in vapor during exposure time, t, is given by:

$$C_V = åC_w / \{ 1 - (1 - k_e t / H)^{kc/ke} \}, \qquad (2)$$

Finally, the concentration of HTO in air, C_a, is related to C_V by the following equation:

$$C_a = KC_V, \qquad (3)$$

where:

$$K = 2.9 \times 10^{-4} P^{-1} (273 + T)^{-1} R/100, \qquad (4)$$

P is the saturated vapor pressure (mmHg) at temperature T(°C) (Anazawa *et al.*, 1972), and R is the relative humidity (%). The isotope ratios, $\hat{a}$, were found by measurement to be approximately 0.90 to 0.92 (Sepall, 1960). The ratio k_c/k_e is estimated approximately as 1.8 for the given ambient temperature and humidity in the containment building. Estimation of other parameter values including k_c and k_e is described elsewhere (Fukui, 1993). Thus, all constants can be calculated or are given in order to monitor C_a.

A liquid scintillation counter was used to determine the specific activity of the water sample, from which the tritiated water vapor concentration was calculated. The samples were counted for three 10-minute cycles for tritium (^3H) and carbon 14 (^{14}C) as a reassurance that tritium was the main radioactive nuclide in the water samples.

Distribution of HTO concentration in the containment building air during ventilation cessation using laboratory dishes

The distribution of the HTO concentration in the air of the containment building was determined from 30 laboratory dishes which were filled with 25 ml of tap water and placed on the floor and/or desks. The reactor was shutdown at 16:00 on Fri., July 18, 1997 and ventilation in the building ceased at 18:00 that day. After 40 hours the ventilation cessation, the dishes were exposed for 24 hours untill July 21, then they were weighed in order to estimate the evaporation rate and water sampling for radiometry on July 21. The average concentration of HTO, C_V, estimated by the methodology described above was 54.5 $Bq.ml^{-1}$ in the containment building and is shown for each of the locations as the difference ($Bq.ml^{-1}$) from the average concentration in Figure 5 together with the location numbers. The HTO concentrations in vapor in Figure 5 show a little dependence on the location of the sample. The values range from 30 (No.24) to 75 $Bq.ml^{-1}$ (No.8) with the lowest concentrations coming from the basement (heat exchange room). The heat exchange room is isolated by a wall in the basement and the lowest downstream of the containment building, i.e. is connected to the exhaust stack, suggesting air exchange between the heat exchange room in the containment building and field during venting cessation. The highest

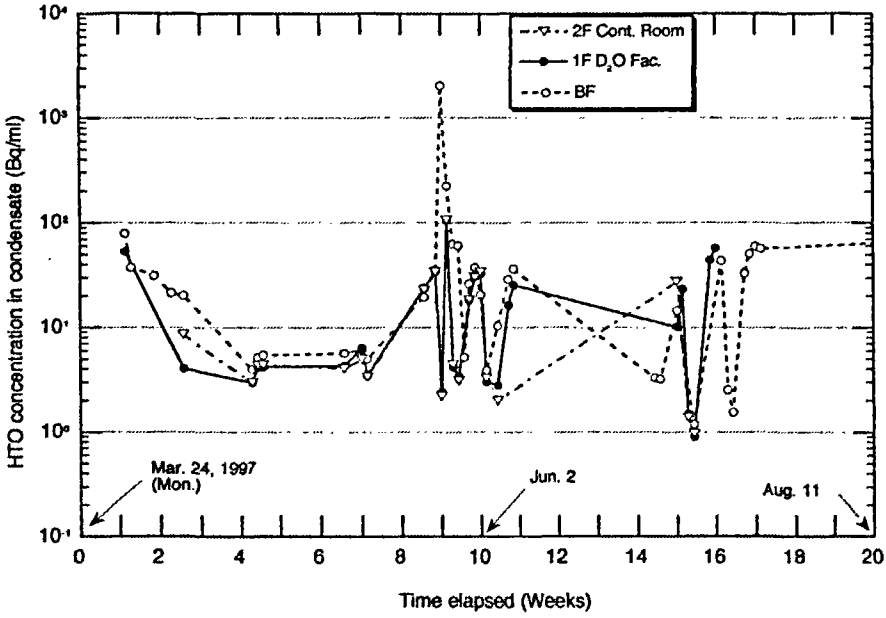

Figure 5
Distribution of HTO concentrations in the vapor, CV, estimated using laboratorydishes filled with tap water (25 ml) set at 30 locations for 24 hrs during ventingcessation in the KURR containment building. Bars indicate the difference in $Bq.ml^{-1}$ from the average concentration for the 30 locations (54.5 $Bq.ml^{-1}$).

concentration (No.8) that appeared near the D_2O facility on the first floor may link to No.16 in the basement, the location with the second highest concentration via. An open gallery under the A stairs. Thus, the local high concentration was found to be attributable to the small leak of heavy water and/or HTO impregnated wastes related to the D_2O facility. From the above, this technique using laboratory dishes provides an adequate distribution of HTO concentrations within the three floors of the containment building. Figure 6 shows the HTO concentrations in dish water, C_w, at 30 locations, the vapor concentration estimated from eqn. (2), C_V, and the HTO concentration in air, C_a, converted from eqn. (3). This indicates that the measured concentrations in dish water exposed for 24 hours fall

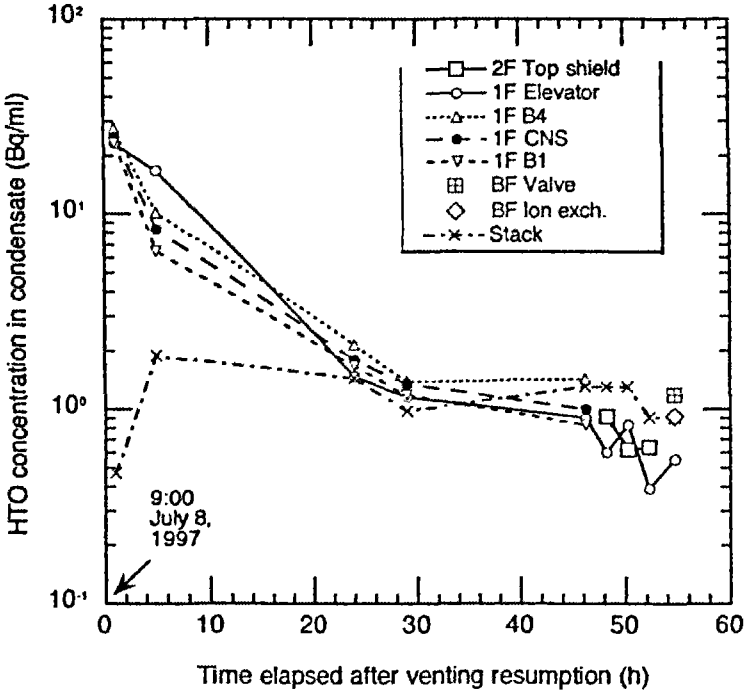

Figure 6
HTO concentrations in dish water, vapor and air at the 30 locations.

from 40 to 80% of C_V, depending on the temperature and humidity of each location. The highest concentration in air, 1.3 kBq.m^{-3}, was found at location No.16 in the basement. It is below the maximum concentration limit for an average over three months, restricted by the law, 700 kBq.m^{-3}.

Changes in HTO concentration in vapor in the containment building after venting resumption

Four dehumidifiers were set in the containment building to investigate the changes in concentrations with time after venting resumption. As seen in Figure 7, the concentrations at the four locations on

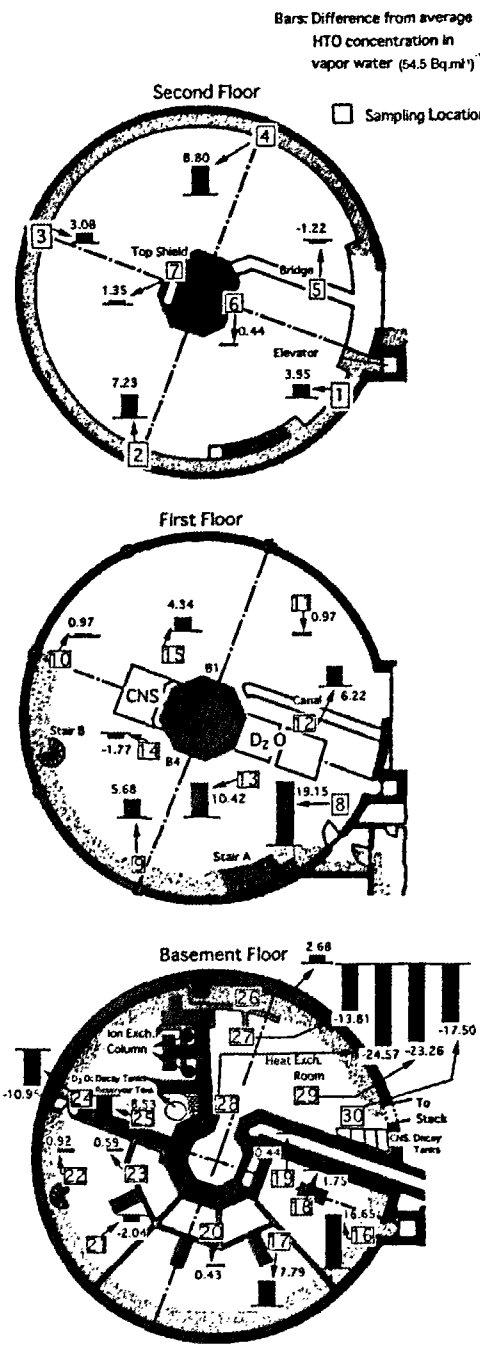

Figure 7
Changes in the HTO concentration in condensate within the containment building after venting resumption.

the first floor (No. 8-11 in Figure 5) decreased from a few ten to a few Bq.ml^{-1}, i.e., one order of magnitude less, 24 hours after venting resumption. No apparent differences can be seen in the concentrations in the air of the three floors. This indicates that if one detects a concentration exceeding 10 Bq.ml^{-1} in vapor 24 hours after venting resumption, it may come from an artificial cause of contamination.

Figure 8 shows the HTO concentrations monitored over period of four months from late March to late July 1997 using a dehumidifier on three floors (Base FL: No.19, 1st FL: No.12, 2nd FL: near No.1 in Figure 5). The highest concentration, more than 2000 Bq.ml^{-1}, was detected in late May 1997, resulting from a spill of heavy water during the renewal of a distribution pipe linked to the D_2O tank. The

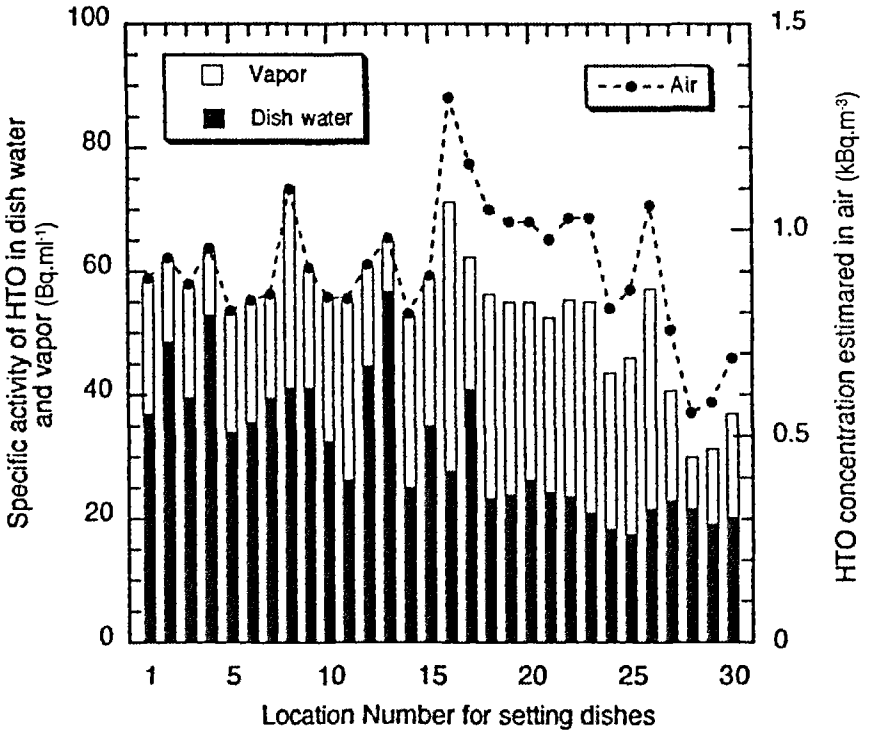

Figure 8
HTO concentrations in condensate at three floors for four months in 1997.

work for the renewal of the distribution pipe and tank finished in late July 1997. Nevertheless, ingrowth of the HTO concentration in vapor was shown in the containment building during venting cessation after reactor shutdown. Monitoring the concentrations in vapor near the reactor core was then planned to locate a possible tritium leak other than that from the D_2O facility.

Monitoring HTO concentrations in vapor in decay tank exhaust

Many source points in KURR were sampled in order to locate a higher source of tritium activity or any other radionuclide that could be causing a higher specific activity in the air. The sources that were sampled includeed the: exhaust stack, reactor room exhaust, reactor room filter chamber, experimental pipe to the biological shielding, exhaust from the CNS and D_2O facilities and air samples from all three floors of KURR. Among these, only the CNS and D_2O facilities showed an abnormally high specific activity. The 4 dm^3 liquid deuterium in a bottle as a neutron moderator set near the reactor core is isolated by three layered aluminum conduit (5 mm thick) including a vacuum, a He and a Ne gas layer. The CNS system surrounded by a graphite block layer is isolated by sealing from which exhaust air is introduced to decay tanks (1.3 m^3) at a rate of ca. 2 $dm^3.mn^{-1}$ in order to lower ^{41}Ar concentration. The exhaust line pump for the CNS and D_2O (flow rate: 0.53 $dm^3.mn^{-1}$, decay tank volume: 0.56 m^3) facilities only works to cover the reactor operation. Figure 9 shows the activity of the CNS and D_2O exhaust vapor. The higher specific activities ranging from 130 to 200 $kBq.ml^{-1}$ were found at the inlet of the decay tank from the CNS graphite. These values do not fluctuate because of the presence of the graphite which can absorb tritium near the CNS facility and release it depending on venting resumption by the pump set in the exhaust line. That is, the graphite may normalize the tritium concentration with time. On the other hand, the concentrations at the outlet of the

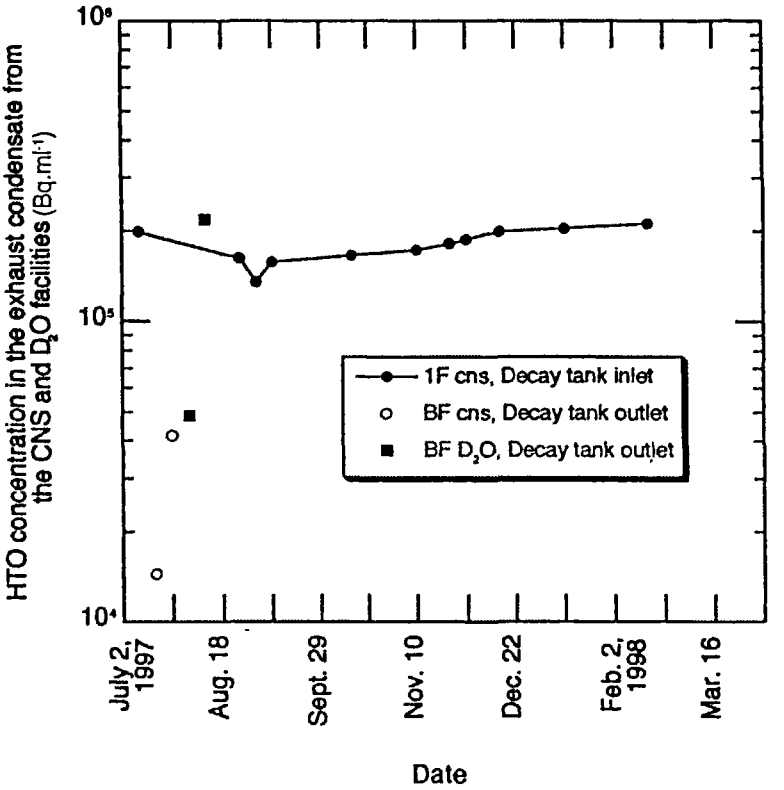

Figure 9
HTO concentrations in condensate in the CNS and D2O exhaust lines.

decay tanks for both facilities fluctuate so much due mainly to inhaling downstream air near the outlet of the exhaust line pipes because of pumping by the ionization chamber system from the line during exhaust line pumping cessation.

There may be two reasons why the tritium concentrations from the CNS and D_2O lines could be so high: 1) the leak of liquid deuterium and/or heavy water could exist, therefore expelling a large quantity of tritium, or 2) the leak could be negligible, but a higher concentration of tritium exists in the facilities that was produced by a nuclear reaction. That is, the ingrowth of HTO vapor during vent-

ing cessation in the containment building may be caused by the $^{14}N(n, {}^{3}H)^{12}C$ reaction of the irradiation of nitrogen in air. Assuming the constant concentration of 200 $kBq.ml^{-1}$ is in a steady state in the exhaust line vapor which is trapped by the CNS condenser, the production rate of HTO from the CNS line is estimated as 0.6 $GBq.yr^{1}$. Considering the above and HTO sources of other exhaust lines from the KURR, the annual release rate based on the monitoring data from the stack exhaust, 0.6 $GBq.yr^{1}$, may increase by a factor. The production of a large content of tritium from the D_2O facility could not be discarded through the $^{6}Li(n,\alpha)^{3}H$ reaction. The probable source of tritium, Li, was removed from the experimental devices in July 1997. All of the water samples collected were also counted for ^{14}C, which was thought to have contributed to the higher than expected activities. But the constituent of ^{14}C in the activity of the samples was less than a few percent and, therefore, considered to be minimal.

Precise estimation for the amount of discharge from the KURR is under investigation using not only a LSC method but also a 1.5 l portable ionization chamber focused on near core exhaust.

Conclusions

The use of laboratory dishes in estimating the HTO concentration in air proved to be very simple and effective. The laboratory dish method did provide us with the useful information of a low HTO concentration in the containment building air. Unfortunately, since the HTO concentrations within the containment building air were not so different, a positive location of a tritium leak could not be identified. Even after the renewal of distribution pipes, valves and tank for heavy water, which were likely points of HTO leakage, higher than concentrations were found in the exhaust air from facilities adjacent to the reactor core. This was a cause of ingrowth in the HTO concentration in the containment building during venting cessation. Our next step must be to concentrate the sampling around the reactor core in order to pinpoint the precise location of the leak

and/or to estimate the production rate by the neutron reaction. The production and leak should be located and rectified in order to lower the tritium concentration throughout the containment building. Though the annual discharge of tritium from the KURR was estimated to be around 1 GBq.yr^{-1}, This must be done in accordance with ALARA. It is hoped that the leak is small, and that a large percentage of the tritium leaking is from a nitrogen reaction not an artificial one.

Acknowledgements

This research was supported, in part, by Grant-in Aid for Scientific Research from the Ministry of Education, Science, Sports and Culture, Japan.

A portion of this work was done while R. Grazioso, University of New Mexico, USA was an exchange student at the Kyoto University. Mr. T. Yoshimoto provided technical assistance in monitoring activities.

Bibliography

Anazawa Y., Kokubu M., Fujita K., 1972 – Monitoring of Tritium in the Working Environment. *Hoken Butsuri (Japan J. Health Phys.)*, 7: 27-35.

Fukui M., 1992 — Modeling the Behavior of Tritiated Water Vapor in a Research Reactor Containment Building. *Health Phys.*, 62: 144-154.

Fukui, M., 1993 – Development of a Convenient Monitoring Method for Tritiated Water Vapour in Air using Small Water Dishes as Passive Samplers. *Radiat. Prot. Dosimetry*, 48: 169-178.

Sepall O., Mason S. G., 1960 – Vapor/Liquid Partition of Tritium in Triated Water. *Can. J. Chem.* 38: 2024-2025.

Oral/Poster presentations

Session 4

Particulate radionuclide monitoring in the South Pacific and compliance with the comprehensive nuclear-test-ban treaty (CTBT)

R. A. Tinker

Following the opening for signing of the Comprehensive Nuclear-Test-Ban Treaty (CTBT) by the United Nations member countries, in September 1996, verification of Treaty compliance is now an important international issue with NRL atmospheric monitoring stations becoming part of the global verification network. In 2000 major upgrades to stations at Kaitaia, New Zealand, and Rarotonga, Cook Islands, were completed, and a new atmospheric monitoring station installed at Chatham Islands, New Zealand. These stations now comply with the CTBT technical specifications. Major equipment at these stations consist of thin window 50% Broad Energy Canberra Ge detectors and PTI 900 m^3 high-volume air samplers. Stations operate daily with a 24 hours sampling period, a 24 hours decay period, and a 24 hours gamma spectrometric analysis. Acquisition data and station state of health information (eg. Indoor temperature and humidity) are sent via the Global Communication Infrastructure every 2 hours. Data is analysed by the International Data Centre (IDC), Vienna, and the NRL. A station is graded on its ability to achieve a Ba-140 (half-life = 12.8 days) Minimum Detectable Concentration (MDC) of less than 30 $\mu Bq.m^{-3}$ and to maintain 95% data availability (a maximum of 14 days down time a year). The Ba-140 MDC at Kaitaia and Chatham Islands stations were recorded at 5 $\mu Bq.m^{-3}$, while at Rarotonga an MDC of 10 $\mu Bq.m^{-3}$ was measured. To support a 95% data availability, a comprehensive spare parts inventory is maintained in addition to a

robust quality management system for preventative maintenance. An overview of CTBT requirements, station operations and management will be presented. Analytical data obtained at these stations, including minimum detectable concentrations and daily naturally occurring radionuclide trends, will be presented and interpretation of observations suggested.

Uranium and thorium series radionuclides in rainwater samples over several tropical storms

P. Martin

Most studies of radionuclides in precipitation involve sample collection periods of days or longer, in order to determine long-term average fluxes to the Earth's surface. However, where knowledge of the dynamics of precipitation scavenging is desired, other approaches may prove valuable. In the present study, rainwater samples were collected at two locations, Jabiru and Jabiru East, in the Northern Territory of Australia. The main purpose of the study was to improve our understanding of the dispersion and deposition of airborne dust originating from the nearby Ranger U mine. Collections were restricted to single rainstorm events. The measured $^{232}Th/^{230}Th$ ration in rainstorm samples from the two sites varied between 0.01 and 0.5, implying a contribution from dust originating from the minesite. Concentrations of ^{238}U, ^{234}U, ^{230}Th, ^{226}Ra and ^{210}Pb were generally in the range of 0.5~50 $mBq.l^{-1}$. Concentrations of ^{210}Pb were higher, reflecting the additional contribution of ingrowth from ^{222}Rn in the atmosphere. For six events, sequential intra-storm samples were collected, primarily in an attempt to distinguish the source of radioactivity as being from rainout (activity captured by precipitation below the raincloud) or washout (captured within the cloud). Concentrations of U, ^{230}Th and ^{226}Ra generally decreased over the course of rainstorms, implying rainout from the air column below the cloud, but the results for ^{210}Pb and ^{210}Po are more complex.

A moving-grid model of the dispersion of radon and radon progeny in the open atmosphere

P. Martin

Atmospheric dispersion of ^{222}Rn is one of the primary pathways leading to radiological dose to humans as a result of U mining operations. Most of the the dose results from inhalation of the short-lived progeny of Rn rather than from inhalation of the Rn itself. A type of grid-cell model (called here a "moving-grid" model) has been developed to enable prediction of concentrations of Rn and progeny in the open atmosphere downwind of a source such as a U mine. The model also yields predictions of the unattached fraction of the mine-origin Rn progeny. Application of the model to the case of the Ranger U mine in the Northern Territory of Australia shows reasonable agreement with previously-published data for Rn and Rn progeny concentrations at the receptor locations of Jabiru and Jabiru East. The model predicts an unusually high unattached fraction for mine-origin Rn progeny at these locations (annual averages of 0.29 and 0.43, respectively), this being a result of the extremely low aerosol particle concentrations in the air of the region. A sensitivity analysis showed that predictions of Rn and Rn progeny concentrations were most sensitive to changes in Rn emission rates from the source and to vertical dispersion in the atmosphere. Equilibrium factor and unattached fraction were most sensitive to the attachement rate, to dry deposition rates of progeny to the ground, and to vertical dispersion parameters.

^{210}Po and ^{210}Pb air-surface deposition fluxes in Japanese coastal area

Y. Tateda **K. Shimoike**

K. Iwao **M. Ouya**

Atmospheric deposition of ^{210}Pb is important in calculating downward transport fluxes of ^{210}Po-adsorptive debris in open water, while ^{210}Po atmospheric deposition is generally negligible in ocean surface. However, in coastal area, the ^{210}Pb deposition is higher and variable, and the excess ^{210}Po atmospheric deposition is sometimes detected probably because of land-born wind-driven re-suspended soil particle's deposition. In the estimation of particle removal rate by particle reactive these nuclides in coastal waters, the sight specific atmospheric deposition flux estimation will be necessary. In high latitude Asian coastal area of North Pacific Ocean, the Chinese continental air-mass and wind-driven particles are the significant source of ^{210}Po and ^{210}Pb. Briefly, the ^{210}Po and ^{210}Pb concentrations are expected to be raised under the conditions of land-originated wind blows from the Chinese continent. To clarify the generality and variations of these nuclide's atmospheric deposition fluxes around Japanese coastal area, we analyzed the ^{210}Po and ^{210}Pb concentrations in dry and wet fallout on Japanese coastal area. We estimate the balance of ^{210}Po and ^{210}Pb deposition flux on Japanese coastal area and discuss the origin and variations of these nuclide's deposition fluxes. The result indicated that the large seasonal variations of ^{210}Po and ^{210}Pb atmospheric depositions in Okinawa coastal area, which shows high in late winter and low in summer, indicating the main source of ^{210}Po and ^{210}Pb are estimated to be Chinese continent origin, because the NW monsoon from continent is dominant in winter. While in coastal area of mainland arc, ^{210}Po and ^{210}Pb deposition fluxes are high during winter and rainy seasons, indicating the mainland is other source of these nuclides.

Atmospheric $^{7}Be/^{210}Pb$ as a tool for determining the origin of detrital material in ombrogenous sediment: a hypothesis

C. W. Holmes

E. Shinn

M. E. Marot

^{7}Be and ^{210}Pb distribution in sediments and in the atmosphere are potentially useful in studying the dynamics of surface processes. ^{210}Pb in the atmosphere origin lies in the degassing of ^{222}Rn from continental surfaces. As the ^{222}Rn flux from the ocean is negligible, and thus ^{210}Pb may be a useful tracer of continental material transport. ^{7}Be, on the other hand, is produced via cosmic ray spallation reactions with nitrogen and oxygen. The measured ratio of these two isotopes in aerosols over the Atlantic is being used to examine the transport of African Dust to the southeastern United States. The $^{7}Be/^{210}Pb$ activity ratio of material collected in the Azores during a storm event at the end of February averaged 4.0 ± 0.2, with concentrations varying being 50-150 $Bq.g^{-1}$ for ^{210}Pb and 180 and 750 $Bq.g^{-1}$ for ^{7}Be. Comparing these ratios with the historical record in Miami indicated much of the material is transport across the Atlantic within a very short time. In south Florida, there is growing body of evidence that suggests that much of the trace metal load in ombrogeneous sediments of the Florida Everglades is derived from external sources. What is unknown at this time is whether this material is derived from regional sources or part of the worldwide atmospheric transport of material. Using these ratios and the measured elemental concentrations the sources appeared to be defined. In the ombrogeneous sediment of south Florida, there is significant evidence that metals may be derived from transported aerosols with some contribution as detrital material transported with Africa as dust during the summer.

A rapid estimation of ^{210}Po and ^{210}Po in rainwater

G. A. Peck

J. D. Smith

A method for determination of ^{210}Po and ^{210}Pb in rainwater samples is described. This method was developed to permit measurement of the radionuclides in rainwater samples collected at short time intervals (2 weeks) on a small area (0.5 m^2) and to give results with the minimum delay. ^{210}Pb was estimated from counts of the daughter ^{210}Bi after allowing 30 days for ingrowth. ^{210}Po was measured directly by alpha-spectrometry. The radionuclides were collected from rainwater samples by co-precipitation with manganese dioxide and dissolution of the precipitate in a small volume of HCl/H_2O_2. ^{210}Po was plated onto silver and counted immediately and stable Bi was added to the solution which was allowed to stand for 30 days. After this time ^{210}Bi was separated from the ^{210}Pb by extraction into 0.2% DDTC in chloroform and precipitated as bismuth oxychloride. The bismuth oxychloride was collected by filtration and the ^{210}Bi counted using a gas-flow proportional counter. ^{210}Pb activity was inferred from the ^{210}Bi activity. This procedure allowed rapid, sensitive and cost effective measurement of ^{210}Bi in rain water with a limit of detection 4.2 mBq and a coefficient of variation of 2% for four replicate analyses at the 1.0 Bq level.

Radioactivity in soils and related issues

Session 5

Chairman: P. Schuller

Session opening: T. Quine

Application of Chernobyl-derived ^{137}Cs for assessment of soil redistribution in agricultural catchments of central Russia

Valentin N. Golosov

Maxim Vladimirovich Markelov

Introduction

Problems of soil degradation and water pollution are very significant for agricultural zone of Russia, because of two reasons: relatively high soil erosion rates and Chernobyl contamination of vast areas within Russian Plain. The northern part of Srednerusskaya upland is one of the hot plots, where combination both high intensity of soil erosion and extremely high level of radionuclide contamination are observed. This area 200-300 km south of Moscow is characterized by very contrast relief with deep river and balka valley and the high erosion index of rain-storms. The cultivated area varies from 60% to 75% from total area of the small river basin. The most part of the land is cultivating during 300-350 years and as far as 120-130 years ago the area of arable lands reached the maximum up to 80%. Even extremely steep valley slopes were ploughed in this period. As a result the increase the sheet, rill and gully erosion was observed. About 40-50% of small creek and some of the small rivers were completely filled and they transformed into dry valley with relatively flat bottom without permanent flow, which are named locally balka. Now the balka basin is the main area of sedi-

ment and sediment-associated pollutant redistribution. This contribution aims to study the contemporary soil redistribution rates based on ^{137}Cs redistribution within typical slope catchments located within the Lokna river basin 250 km south of Moscow in the center of Plavsk ^{137}Cs plot.

Study site

Three slope catchments with different configuration were chosen for detail study in the Chasovenkov Verh balka basin, which is the right tributary of the Lokna River, 2 km west of Plavsk in the Tula region of Central Russia (Figure 1). This area was contaminated by Chernobyl fallout with maximum inventories in excess of 400 kBq.m^{-2} along the Lokna river valley. Pre-existing bomb-derived ^{137}Cs inventories were in 100 times lower. So it is not necessary to take bomb-derived ^{137}Cs into consideration for study spatial redistribution of ^{137}Cs within the study area. The Chasovenkov Verh

Figure 1
Location of the Chasovenkov Verh balka basin within Plavsk Chernobyl contamination plot.

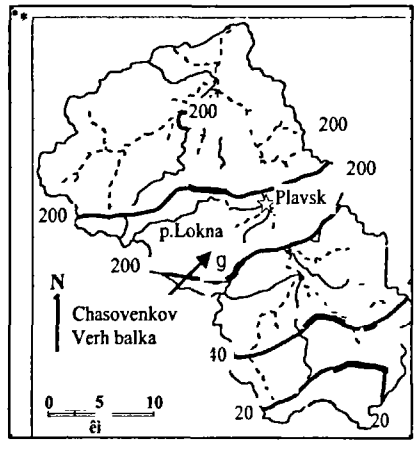

200 - ^{137}Cs inventory, kBq.m^{-2}.
■ - location of the Chasovenkov Verh baika within the Lokna river basin.

balka is the former river (according of the map produced in the middle of XIX century) which were completely filled by sediment due to intensive gully and rill erosion in the end of XIX century. Recently gullies stop their growth and most part of sediment delivered to the balka bottom from cultivated slope as a product of rill and sheet erosion. The underlying geology of the both catchments is limestone with clay layers overlying Holocene loess. Mean annual precipitation is 650 mm with about half of them during cold period as snow.

The soils are primarily typical and leaching chernozem, with a loamy texture. The most part of cultivated soil lost about half of their initial humus content in the upper 10 cm layer during the period of cultivation. The upper parts of cultivated slopes are occupied by typical chernozem and the lower relatively steep parts of cultivated slopes are occupied by leaching chernozem.

Three slope catchments of different configuration were chosen for detail study of erosion rates within the Chasovenkov Verh balka basin (Table 1). The first catchment has complex longitudinal form

	Area ha	Slope length, m	Slope gradient, %	Configuration	Soil	Humus content, %
Site 1	0.92	200-250	6-15	convex slope	leaching chernozem	2.4-3.8
Site 2	6.6	200-400	4-8	hollow catchment	leaching+ typical chernozem	2.4-3.8 4.6-5.5
Site 3	7.7	450-550	5-10	straight slope	leaching chernozem	2.4-3.8

Table 1
Catchments characteristics.

with maximum angle in the bottom of cultivated part (Figure 2). The small hollow watershed is the second site. This catchment has asymmetrical form with relatively steep short south slopes and more gentle north slopes (Figure 2). The catchment located on the lower part of slope and part of surface runoff and sediments from the upper slopes cross the ground road, located upper border of this

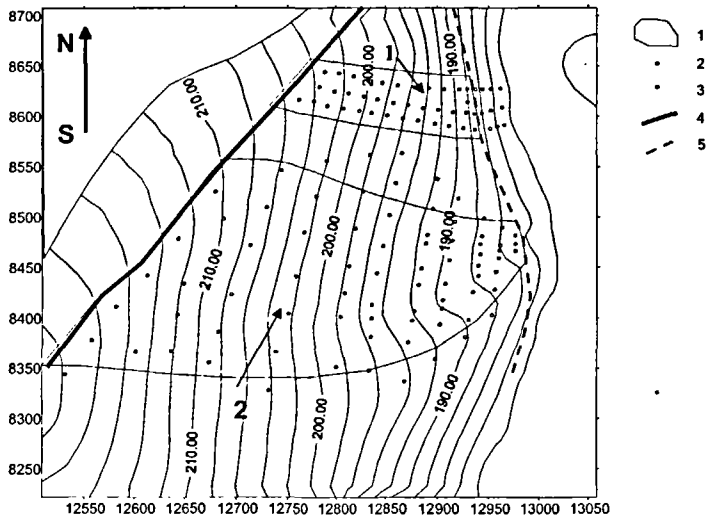

Key: 1- border of watershed, 2 – point of sampling and in situ measurements, 3 – points in situ measurements, 4 – ground road, 5 – lower border of cultivated slope.

Figure 2
Topographical plan of slope catchments 1 and 2.

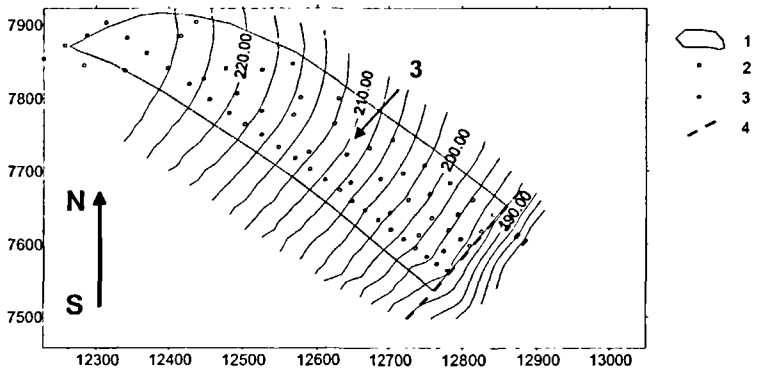

Key: 1- border of watershed, 2 – point of sampling and in situ measurements, 3 – points in situ measurements, 4 –lower border of cultivated slope.

Figure 3
Topographical plan of slope catchment 3.

catchment (Figure 2), in few places and flow through it. In the result the part of sediment, which delivered from upper slopes to the ground road, redeposit in the upper part of catchment 2. It is typical situation for sediment redistribution within cultivated fields of Sredne-Russkaya upland. The third catchment has relatively straight longitudinal profile with small increase of angle in the lower half of slope (Figure 3).

It should be noted that direction of tillage as well as tractor wheel tracks usually change direction of flow. In the result the catchment areas can vary from year to year.

Methods

The main task of sampling program was to evaluate the ^{137}Cs redistribution for different parts of key slope catchments using both laboratory measurements of ^{137}Cs inventory and *in situ* measurements of ^{137}Cs inventory. Sampling was undertaken during the periods May-June 1998. Particular attention was given to the identification of reference locations where the measured ^{137}Cs inventories should be representative of the total fallout input. The relatively flat cultivated field and adjacent forest-shelter belt were chosen for detail study of reference inventory 27 in situ measurements of ^{137}Cs inventory were done. In addition 9 samples for laboratory analisys were taken in the same points. Also the other reference points were selected on the alka sides within areas without deposition. The most of samples were bulk. Two cores (0-30 and 30-40 cm) were taken from few points within cultivated part of flat interfluve field to determine of vertical migration rate of ^{137}Cs. Bulk core samples were collected from each of the study watersheds, using a 36.2 cm^2 core tube inserted to a depth of 30 cm. Simultaneously with the collection of the depth incremental samples and the soil cores, *in situ* measurements of ^{137}Cs inventory were made adjacent to each sampling point and at additional sites using a Corad field-portable collimated spectrum sensitive NaI detector (Govorun *et al.*, 1994; Chesnokov *et al.*, 1997). Based on field experiments undertaken by

the designers of the Corad equipment, the detector is capable of measuring ^{137}Cs inventories in the range 0.37 - $5.55x10^2$ $kBq.m^{-2}$ to depths of up to 40 cm with a precision better than ±20%. Because of the high levels of ^{137}Cs present in the soil of the study area, problems associated with interference by other radionuclide are minimised and the *in situ* measurements required count times of only a few minutes. The possibilities of use *in situ* ^{137}Cs inventory measurements for analysis of ^{137}Cs redistribution were discussed elsewhere (Golosov *et al.*, 2000).

A detailed topographic survey of the each key watershed, the sampling and measurements points was made using a differential GPS system, which provided measurements of height and position with a maximum error of ±2cm. The resulting data were used to produce 1:2000 plans of the study catchment (Figure 2, 3).

All soil samples were dried and sieved to <2mm prior to laboratory measurement of their ^{137}Cs content by gamma spectrometry using an HPGe coaxial detector calibrated with Standard Reference Materials and laboratory standards made using standard solutions. Count times were sufficient to provide a typical analytical precision of ±4-5%.

The information about crop rotation and peculiarities of soil cultivation was collected for period 1986-1998 for each watershed from local farmers. Also additional meteorological information for period 1986-1998 were received from meteorological station, which is located in 1.5 km east of key catchments. Data about soil characteristics were taken from Agricultural Institute of the Central Region, which are located near the Lokna river basin.

The proportional and standard mass-balance models were used for calculation of erosion and deposition rates for each key catchment, using software elaborated by D.E. Walling and Q. He. The proportional model can be represented as follows:

$$Y = 10 \frac{BdX}{100\,TP} \qquad (1)$$

where: Y – mean annual soil loss ($tons.ha^{-1}.yr^{-1}$); d – depth of plough or cultivation layer (m); B– bulk density of soil ($kg.m^{-3}$); X – percentage reduction in total ^{137}Cs inventory; T – time elapsed since initiation ^{137}Cs accumulation (yr); P – particle size correction factor.

Percentage reduction in total ^{137}Cs inventory defined as:

$$X = \frac{A_{ref} - A}{A_{ref}} \times 100 \qquad (2)$$

where:
A_{ref} – local ^{137}Cs reference inventory ($Bq.m^{-2}$);
A – measured total ^{137}Cs inventory at the sampling point ($Bq.m^{-2}$).
Standard Mass Balance Model (MBM-1) was used for calculation erosion-deposition rates within each sites. For calculation of erosion rates the following equation was applied:

$$Y = \frac{10\,dB}{P}\left[1 - \left(1 - \frac{X}{100}\right)^{1/(t-1986)}\right] \qquad (3)$$

where:
Y – mean annual soil loss ($tons.ha^{-1}.yr^{-1}$); d – depth of plough or cultivation layer (m); B – bulk density of soil ($kg\ m^{-3}$); X – percentage reduction in total ^{137}Cs inventory defined as $(A_{ref}\text{-}A)/A_{ref} \times 100$); t – time (yr); P – particle size correction factor .
Deposition rate was estimated from the ^{137}Cs concentration of the deposited sediment according to:

$$P' = \frac{A_{ex}(t)}{\int_{1986}^{t} C_d(t')e^{\lambda(t-t')}dt} = \frac{A(t) - A_{ref}}{\int_{1986}^{t} C_d(t')e^{\lambda(t-t')}dt} \qquad (4)$$

where:
$A_{ex}(t)$ – excess ^{137}Cs inventory of the sampling point over reference inventory at year t' ($Bq.m^{-2}$); $C_d(t')$ – ^{137}Cs concentration of deposited sediment at year t' ($Bq.kg^{-1}$); λ – decay constant for ^{137}Cs (yr^{-1}), P' – particle size correction factor.

Calculation of soil erosion rate using modified version of USLE (for assessment of rain erosion) and model of State Hydrological Institute (for assessment of erosion during snow-melting period) (Larionov, 1993) was made for each key catchment. In the result the soil erosion maps for each site were produced.

Results

The comparison results of calculations with actual soil losses from different cultivated slope of Russian Plain demonstrate that in the cases erosion models (modified version of USLE and State Hydrological Institute model) results overestimated annual sediment output from slope catchments mostly on 20-40%, but sometimes even in two times (Golosov, 1998). However it probably can be explain the absent of correct information about crop rotation for the entire period of calculation. In our study we have the detail information about crop rotation from 1986. Soil erosion map with annual soil losses for the period 1986-1998 were produced for each key catchment. Using USLE, the mean annual erosion rates for all catchments are in one range: 11.5; 11.8 and 13.8 $Mg.ha^{-1}$ from catchment 1, 2 and 3 respectively.

Because *in situ* and laboratory measurement of ^{137}Cs inventory were made, it is necessary to compare both sets of data. First it should be noted that the measurements provided by the Corad equipment relate to a surface area of 2.1 m^2, which represents the field of view below the detector collimator, whereas those for the cores relate to an area of only 36.2 cm^2. In view of the microscale spatial variability of ^{137}Cs inventories, which has been widely reported in the literature (Sutherland, 1991, 1994; Owens and Walling *et al.*, 1996), the larger surface area sampled by the *in situ* detector could be expected to reduce the effects of this variability and should therefore result in lower values of standard deviation, coefficient of variation and range for the *in situ* measurements.

As our previous study demonstrate (Golosov *et al.*, 2000), in the case of the cultivated areas difference between *in situ* and laboratory measurement is not high. This reflects the mixing caused by ploughing and cultivation, which reduce the microscale variability of ^{137}Cs inventories and thus the potential contrast between the two sets of measurements. The enough good correlation between two data sets was received for two catchments of the Chasovenkov balka basin (Figure 4). The each sampling point represent the mean value between rill and interrill surfaces. *In situ* measurement char-

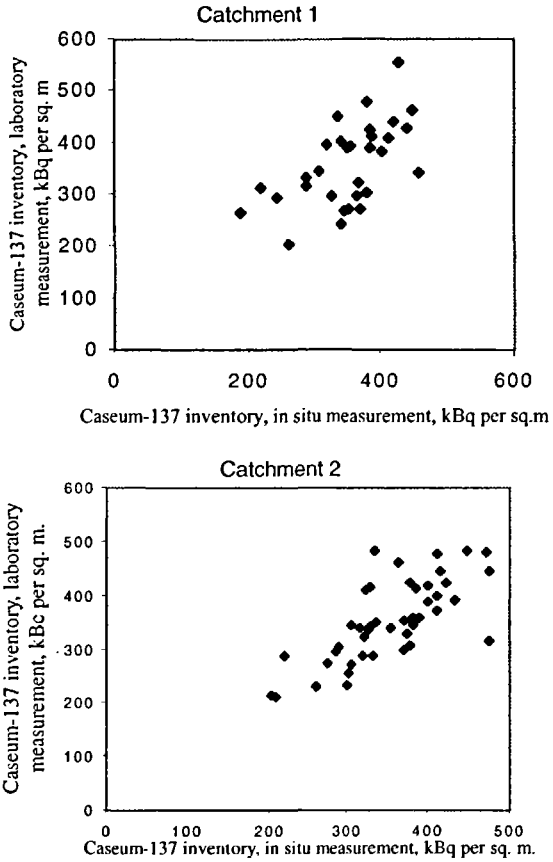

Figure 4 Relationship between *in situ* and laboratory measurements of ^{137}Cs inventory in catchments 1 and 2.

acterise the 2.1 m^2 area with accidental relationship between rill and interrill surfaces. So it is possible to use *in situ* measurement for the study of ^{137}Cs inventory within cultivated slope of the Chasovenkov balka basin. *In situ* measurements are used for analysis of sediment redistribution. ^{137}Cs reference inventories in undisturbed soil profiles around the key sites average ca 354 $kBq.m^{-2}$ with standart deviation 37.9 and coeffient variation 0.11.

Walling and He (1999) summarised the existence approaches to transform the ^{137}Cs distribution patterns to the soil distribution patterns. Also they suggested some improved models, which are able to take into consideration some peculiarities of interaction between

fresh bomb-derived ^{137}Cs fallout, grain size and tillage. However the proportional model (Mitchell *et al.*,1980; Walling and Quine *et al.*, 1990) and standard mass balance model (Kachanoski and de Jong, 1984; Quine, 1989; Walling and Quine,1990; Ostrova *et al.*, 1990) is enough correct for area with Chernobyl-derived ^{137}Cs, because Chernobyl radionuclide fallout accumulation was occurred during very short period of time (27 April- 15 May 1986) and the all bare slopes were cultivated shortly after the fallout input. Uncertainties associated with the fate of freshly deposited ^{137}Cs prior to its incorporation into the plough layer by cultivation are substantially reduced. This is also true for fields under winter corn and perennial grass, because according of observation erosion rate is very low under these crops during summer period. According of results of comparison of grain size distribution of suspended sediment, which were taken from flow near lower border of cultivated field, and samples of surface soil from cultivated field from Chasovenkov Verh balka basin demonstrates, that they are very similar (Walling *et al.*, in press). Tillage effect is not significant yet for cultivated slope of the Lokna river basin, because only twelve years pass from 1986 with only maximum two tillalage operations per year. However the tillage operation influence on the soil redistribution within shoulders of the local catchments. The proportional and standard mass-balance models were used for calculation of erosion and deposition rates for each key catchment, using software elaborated by D.E. Walling and Q. He.

The results of calculation the erosion and sedimentation rates are presented in Tables 2 and 3. If it is compare the patterns of soil redistribution, which were received used proportional and standard mass-balance models, there are no essential differences (Figure 5). However some disparity can be found between values of gross and net erosion rates and deposition rates. Mass-balance model give more contrast results (Table 3, 4). It is interesting that area of eroding sites decrease with complication of relief pattern from relatively simple catchment 3 to hollow catchment 2 (Table 3, 4). However area of aggrading sites is enough vast within the all sites. The soil aggradation in the upper part connects with transport of soil particle with runoff from the fields located upper the road and their redeposition within the top part of catchment 2. As we observed during rain storm, stream formed along road overflows through the road edge during extreme erosion events.

Measure	Catchment 1	Catchment 2	Catchment 3
Gross erosion rate (tons.h^{-1}.year^{-1})	11.0	4.7	10.2
Eroding sites			
Mean erosion rate (tons.h^{-1}.year^{-1})	18.0	11.5	14.0
% total area	62	41	73
Aggrading sites			
Mean deposition rate (tons.h^{-1}.year^{-1})	13.3	12.6	12.2
% total area	38	59	27
Net erosion rate (tons.h^{-1}.year^{-1})	6.1	-2.88	6.9
Sediment delivery ratio	55	0	68

Table 2
Integrated field data for the slope catchments at the Chasovenkov Verh balka basin (proportional model, *in situ* measurement of ^{137}Cs inventory).

Measure	Catchment 1	Catchment 2	Catchment 3
Gross erosion rate (tons.h^{-1}.year^{-1})	13.1	5.2	11.0
Eroding sites			
Mean erosion rate (tons.h^{-1}.year^{-1})	21.6	13.3	15.1
% total area	61	39	72
Aggrading sites			
Mean deposition rate (tons.h^{-1}.year^{-1})	16.1	15.0	13.3
% total area	39	61	28
Net erosion rate (tons.h^{-1}.year^{-1})	6.8	-3.9	7.4
Sediment delivery ratio	52	0	67

Table 3
Integrated field data for the slope catchments at the Chasovenkov Verh balka basin (mass-balance model-1, *in situ* measurement of ^{137}Cs inventory).

It is obviously, that only part of soil mobilised by erosion was exported from the field towards the balka valley bottom depending from relief. So the sediment delivery ratio is very different for slope catchments of different configuration (Table 2, 3). 67% of the soil mobilised by erosion was transported from the field. The maximum sediment accumulation rate in the bottom part of slope is

Method of assessment	Mean annual rates, tons.ha^{-1}.year^{-1}		
	Site 1	Site 2	Site 3
Modified version of USLE	11.5	11.8	13.8
^{137}Cs technique			
Corad measurement			
Proportional model			
Net erosion	6.1	- 2.9	6.9
Cross erosion	11.0	4.7	10.2
Mass balance model			
Net erosion	6.8	-3.9	7.4
Cross erosion	13.1	5.1	11.0

Table 4
Mean annual soil losses from cultivated catchments for period 1986-1997 established by different methods.

40-45 tons.ha^{-1}.yr^{-1}. The sediment accumulation in the bottom part of cultivated slope connects with dam effect of lower tillage edge. The other zone of sediment storage is in the upper part of slope, where gradient of slope is relatively lower. The combination effect of soil and tillage erosion is responsible for some deposition in this area. Deposition on the flat slope usually occur if direction of tillage operation cross the flow path along slope gradient.

The sediment delivery ratio for the slope catchment 1 is about 52-55% (Table 2, 3). The maximum deposition rate is observed within two storage zones. One of them is located near the slope bottom. The origin of this plot underpins the suggestion about wave nature of erosion/deposition processes. The storage zone in the upper part of slope is consequence of sediment transport from ground road, which is located upslope catchment. The sediments redeposit within this relatively flat upper part of catchment.

The catchment 2 is transit type field. The artificial runoff, which concentrated along the ground road upslope of hollow catchment 2, overflows the road edge and move toward of hollow bottom. Most part of sediment is stored in the upper part of catchment, because the flow transformed from concentrated to dispersal. In the result the sediment input exceed sediment output (Table 2, 3). Areas with

maximum erosion rates are located along the hollow bottom, because of flow concentrations, (*answer on question* L*)*. Typically even direction of tillage can influence on the increase or decrease of erosion/deposition rates within gentle slopes. From the other hand probably the density of measurement points was not enough within upper part of this catchment (Figure 2-II). It is obviously, that twelve years passed from 1986 is not enough time for forming the pattern of rill net within gentle slopes. At least it is possible to suggest that some ^{137}Cs input was delivered to the upper parts of catchments 1 and 2 during spring-summer 1986, because of dust transfer from ground road.

Discussion and conclusion

Attempt to use Chernobyl-derived ^{137}Cs for assessment sediment redistribution demonstrates that only 12 years after Chernobyl accident it is possible to identify the areas with high erosion and deposition rates. However some areas within slope catchments, which are named stable (Figure 5), can not be defined as loss/gain sites, because the changes of ^{137}Cs do not exceed the initial variability of Chernobyl-derived ^{137}Cs fallout.

Soil losses, which were received by calculation of erosion rates using modified version of USLE and SGI model, are much more close to gross erosion rates, which were received using ^{137}Cs technique (Table 4). Erosion models were validated for Russian conditions previously (Golosov, 1998). These erosion models do not take in account intra-field deposition. However deposition is actually observed within cultivated fields. Also it should be noted, that ^{137}Cs technique allow to determine soil deposition for transit catchments. Probably ^{137}Cs technique is unique opportunity to determine the actual pattern of soil loss/gain areas within cultivated field, because traditional soil-morphological method demand much more field work and so more expensive.

It should be noted that 15 years after Chernobyl accident ^{137}Cs technique can be apply for assessment of erosion and deposition rates

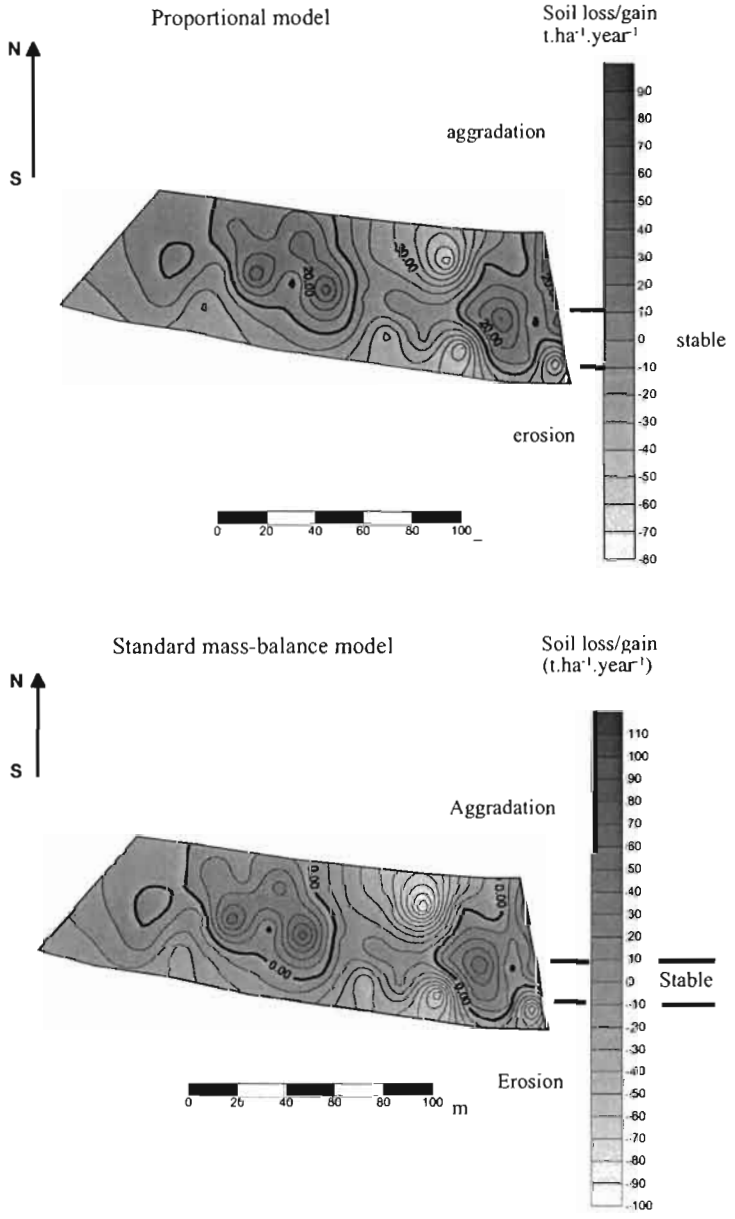

Figure 5
Maps of soil intra-field redistribution for period 1986-1997, catchment 1.

for sites with mean annual erosion rates exceed 10 tons.ha^{-1}. The absolutely correct results can be received for areas within part of fields with annual soil losses 20 tons.ha^{-1} (Litvin *et al.*, 1994). There are no essential differences between using *in situ* and laboratory measurements of ^{137}Cs inventory for calculation erosion/deposition rates. However *in situ* measurements allow defining more correct pattern of soil redistribution because the larger surface area sampled by the *in situ* detector could be expected to reduce the effects of random variability of ^{137}Cs inventory.

Application of ^{137}Cs technique for assessment of erosion/deposition rate allows to receive pattern of soil redistribution within study area, including influence sheet, rill and tillage erosion, as well as some possible input of soil because of sediment transit from topographically upper located fields or local wind erosion. Maps of intra-field erosion demonstrate that maximum soil losses are observed within lower half of midslopes. Usually few strips with high soil losses usually alternate with strips where erosion rates are lower. It is consequences of wave nature of erosion/deposition processes. The upper boundary of the area of high soil losses depends from configuration of slope profile and as a rule it is very close to shoulder between relatively gentle and relatively steep part of slope. Bottom of cultivated hollows is the other area of extreme erosion rates. However some compensation of soil losses in hollow bottoms happen in period between erosion events because of redistribution of soil by tillage erosion processes. So the actual soil losses from hollow bottom can be identified by ^{137}Cs technique only if monitoring of ^{137}Cs redistribution is organised for hollow site.

The values of sediment delivery ratio (SDR) change in very wide range for key catchments. The SDR coefficient increases proportionally to gradient of slope. However it is necessary to take into consideration the type of slope catchment and 3-dimension model of slope.

Aknowledgements

The authors gratefully acknowledge financial support from INTAS-RFBR (Grant no. 95-0734) and from the IAEA Co-ordinated Research Project on the Assessment of Soil Erosion through the Use of ^{137}Cs and Related Techniques (IAEA Contract 9044).

Bibliography

CHESNOKOV A. V., FEDIN V. I., GOVORUN A. P., IVANOV O. P., LIKSONOV V. I., POTAPOV V. N., SMIRNOV S. V., SCHERBAK S. B., URUTSKOEV V. I., 1997 — Collimated detector technique for measuring a ^{137}Cs deposit in soil under a clean protected layer. *Applied Radiation and Isotopes*, 48: 1265-1272.

GOLOSOV V. N., 1998 — Redistribution of sediments within small river catchments in the agricultural zone of Russia. *Geomorphologie: relief,processus, environnement*, 1: 53-64.

GOLOSOV V. N., WALLING D. E., KVASNIKOVA E. V., STUKIN E. D., NIKOLAEV A. N., PANIN, A. V., 2000 — Application of a field-portable scintillation detector for studying the distribution of ^{137}Cs inventories in a small basin in Central Russia. *J. Environmental Radioactivity*, 48 (1): 79-94.

GOLOSOV V. N., WALLING D. E., PANIN A. V., STUKIN E. D., KVASNIKOVA E. V., IVANOVA N. N., 1999 — The spatial variability of Chernobyl-derived ^{137}Cs inventories in a small agricultural drainage basin in Central Russia. *Applied Radiation and Isotopes*, 51 (3): 341-352.

GOVORUN A. P., LIKSONOV V. I., ROMASKO V. P., FEDIN V. I., URUTSKOEV L. I., CHESNOKOV A. V., 1994 — Spectrum sensitive portable collimated gamma-radiometer CORAD. *Pribory i Tekhnika Experimenta*, 5: 207-208. (in Russian).

KACHANOSKI R. G., DE JONG E., 1984 — Predicting tthe temporal relationship between soil caesium-137 losses and erosion rates. *Can. J. Soil Sci.*, 67: 117-137.

MITCHELL J. K., BUBENZER G. D., MCHENRY J. R., RITCHIE J. C., 1980 — "Soil losses estimation from the fallout cesium-137 measurements". *In* DeBoodt M., Gabriels D. (ed.): *Assessment of erosion*, Chichester,UK, 393-401, John Wiley & Sons.

OSTROVA I. V., SILANT'EV A. N., LITVIN L. F., GOLOSOV V. N., SHKURATOVA I. V., 1990 — Assessment of Soil Erosion and Sedimentation Intensity Using ^{137}Cs Content in the Soil. Vestnik MSU, *geography*, 5: 79-85 (in Russian).

LARONIOV, G.A., 1993 — *Soil and Wind Erosion: Main Regularities and Quantitative Estimation*. Izd-vo MSU, Moscow, 200 p. (in Russian).

LITVIN L. F., GOLOSOV V. N., DOBROVOL'SKAYA, IVANOVA N. N., KIRYUKHINA Z. P., KRASNOV S. F., 1994 — Redistribution of ^{137}Cs by the Processes of Water Erosion of Soils. *Water Resources*, 23 (3): 286-291.

OWENS P. N., WALLING D. E., 1996 — Spatial variability of caesium-137 inventories at reference sites: an example from two contrasting sites in England and Zimbabwe. *Applied Radiation and Isotopes*, 47: 699-707.

QUINE T. A., 1989 — Use of a simple model to estimate rates of soil erosion from caesium-137 data. *J. Water Resourc.*, 8: 54-81.

SUTHERLAND R. A., 1991 — Examination of caesium-137 areal

activities in control (uneroded) locations. *Soil Technology*, 4: 33-50.

Sutherland R. A., 1994 — Spatial variability of ^{137}Cs and the influence of sampling on estimates of sediment redistribution. *Catena*, 21: 57-71.

Walling D. E., He Q., 1999 — Improved Models for estimation Soil Erosion Rates from Cesium-137 Measurements. *J. Environ. Qual.*, 28: 611-622.

Walling D. E., Quine T. A., 1990 — Calibration of caesium-137 measurements to provide quantitaive erosion rate data. *Land Degrad. Rehab.*, 2: 161-175.

Walling D. E., Golosov V. N., Panin A. V., He Q., 1999 — "Use of radiocaesium to investigate erosion and sedimentation in areas with high levels of Chernobyl fallout". In Foster I.D.L. (ed.): *Tracers in Geomorphology*, John Wiley & Sons (in press).

Use of ^{137}Cs to estimate rates and patterns of soil redistribution on agricultural land in Central-South Chile: models and validation

Paulina Schuller

Rosa Eugenia Trumper

A. Castillo

Introduction

Soil conservation and sustainability is of maximum relevance to guarantee the increasing demand for food and raw materials in the world. Therefore, soil degradation and deterioration occurring during the past need to be evaluated. For this purpose, reliable techniques for quantifying soil erosion and sedimentation have to be improved. Developments made during the last decades in the use of the anthropogenic radionuclide ^{137}Cs as a tracer for determining rates and patterns of soil redistribution were considered by many authors as an important advance that overcomes many limitations of the conventional monitoring techniques (Loughran, 1989; Ritchie and McHenry, 1990; Quine, 1997; Walling, 1998).

The purpose of this research was to evaluate the applicability of the conventional ^{137}Cs technique and a simplified and faster method for

estimating spatial distribution of medium-term soil erosion and sedimentation rates on agricultural land in Central-South Chile. The potential for using ^{137}Cs as a tracer in soil redistribution investigations had not been explored in Chilean soils.

Material and methods

Four study sites were selected in the Coastal Mountain Range in Central-South Chile (38°40′S, 72°30′W), where sustainable development of agricultural production need to be assessed due to erosion problems affecting this area. The mean annual rainfall at the study area is 1160 mm.y^{-1} and the typical soil type a Palehumult, Metrenco Series (IREN, 1970) containing about 65% clay and 7% organic matter (Ellies and Contreras, 1997). The study fields were under contrasting land use and management: crop land and semi-permanent grassland, both under subsistence and commercial management. The main characteristics of the sites are summarised in Table 1.

Site code	A	B	C	D
Use	Crop land	Crop land	Grassland	Grassland
Management	Subsistence	Commercial	Subsistence	Commercial
Surface (m2)	22000	4000	5000	2000
Slope (%) U; M; L*	6; 19; 7	13; 16; 3	9; 13; 7	36; 48; 17
Plough depth (m)	0.12±0.3	0.17±0.5	0.12±0.3	0.15±0.4
Density (kg m-3)	1250	1000	1180	1060
Sampling grid (mxm)	16 x 20	7 x 10	10 x 10	6 x 6

* Determined at the upper (U), middle (M), and low (L) sector of the site.

Table 1
Characteristics of the study sites.

To estimate the ^{137}Cs reference inventory, four appropriate sites that had been under herbaceous cover for at least four decades were chosen. For measuring the ^{137}Cs inventories, soil cores of 0.072 m in diameter were collected with an auger down to at least the penetration depth between June and August 1998. At the reference site samples were taken on a 6 m by 6 m grid. The grid spacing at the study sites are shown in Table 1.

To save time on the gamma analysis, the feasibility of measuring ^{137}Cs inventories of composite soil samples for estimating soil redistribution was also tested at all four sites. For this purpose, in October and November 1999 soil samples were collected at the same grid spacing as previously, but all cores from transects along the same contour line were bulked proportionally. The viability of this approach relies on the similar topography in parallel downslope transects, and on the almost uniform soil properties of each analysed site. Additionally, it is based on the assumption that soil redistribution occurred approximately to the same extend in parallel downslope transects of the field.

Soil redistribution rates were quantified using the refined mass balance model for cultivated soils incorporating soil movement by tillage described by Walling and He (1999), adapted to the site specific conditions of the studied fields. The time-course of the ^{137}Cs deposit within the study area was estimated on the basis of the annual deposit of ^{90}Sr and ^{137}Cs reported at the nearest site, located at 41°26′S, 73°07′W (Health and Safety Laboratory, 1977; Juzdan, 1988; Larsen, 1985; Larsen and Juzdan, 1986; Monetti and Larsen, 1991; UNSCEAR, 1982), and considering the activity ratio $^{137}Cs/^{90}Sr$ in deposition constant at 1.6 (UNSCEAR, 1982).

In order to examine the validity of the results obtained by the ^{137}Cs method, experimental erosion plots of 10 m^2 were installed in the upper part of the fields A and C for obtaining reference values of the annual sediment flux at the corresponding area. In addition, the results obtained by the ^{137}Cs method were compared with redistribution rates obtained by pedological observations, comparing the depths of the horizon of the area affected by soil redistribution with that of a reference area with scarce intervention.

Results and discussion

The measured reference inventory was 525±12 Bq.m^{-2} (σ= 94 Bq.m^{-2}, n=61, reference date: January 1998). The plough depth determined at the studied fields (Table 1) varied according to the tillage technique employed, ranging from 0.12±0.03 m depth at sites ploughed by animal traction to 0.17±0.05 m in sites ploughed by mechanical traction. The ^{137}Cs penetration depth ranged according to the position along the slope transects, from 0.12 m at eroded points to 0.34 m at points of sediment accumulation. Other values for the parameters required were taken from the literature (Walling and He, 1999) or estimated by using information on local soil properties and annual distribution and intensity of the rainfall.

Figure 1 represents the soil erosion (negative values) and deposition rates (positive values) estimated at the four analysed areas as a function of the field topography using the conventional grid framework sampling and evaluation of ^{137}Cs inventory at each point. The graphics were obtained using Surfer 7, and kriging geostatistics.

The results shown in Figure 1 allow a comparison of the modelled estimates of the net soil redistribution rates and their spatial distribution at the four studied sites.

At the crop land site under subsistence management (A) high erosion rates were observed at the upper border, due to repeated ploughing normal to the downslope gradient and due to the obstruction of sediment flux from the adjacent area into this field by a dense shrub fence. The other sector of high erosion rates is located in the area of maximum slope, which also promotes higher amounts of soil erosion. The sedimentation area is positioned at the sector of minimal slope located at hillfoot in water run-on sites. Intensive annual cultivation processes and frequent transit of animal plough systems could influence the high erosion rates obtained in this field (Schuller *et al.*, 1999).

Similar spatial distribution of soil erosion rates was observed on the crop land under commercial management (B): The highest erosion rates were estimated at the top of the field and at the sector of maximum slope. The highest sedimentation rates were obtained at a

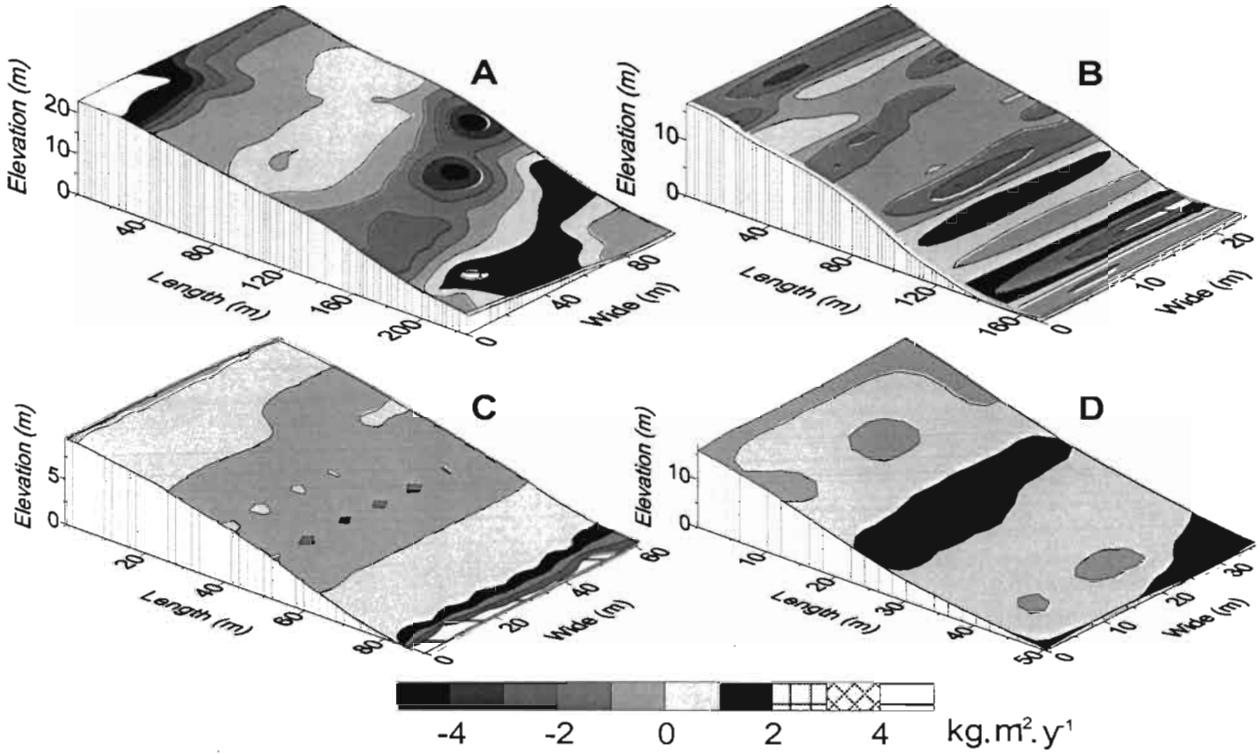

Figure 1
Soil redistribution rates estimated by ^{137}Cs inventory evaluation at grid points: crop land under subsistence (A) and commercial management (B), grassland under subsistance (C) and commercial management (D).

depression at the hillfoot. The erosion rates quantified in field B are lower than in field A. The soil loss estimated in field A is influenced by the site isolation from upper and lateral surrounding fields, which hinder sediment input into the study area. The field B is not isolated from surrounding crop fields, and therefore part of the soil loss could be compensated by sediment input moving from adjacent areas.

A form of expressing tolerable erosion is that the soil loss should not exceed their natural production (Hudson, 1971). Due to the difficulty in measuring this last parameter it is considered that the soil use is sustainable, when the annual loss does not exceed a thousandth of their total mass (Peralta, 1976). The values of the erosion rates measured in the crop land sites are mostly below this tolerable limit estimated at about 1 $kg.m^{-2}.yr^{-1}$, but in sectors with large slope it exceeds this value by far.

At the semi-permanent grassland site under subsistence management (C) the areas showing the highest erosion rates are located in the middle sector of the field, where the slope is steepest. At this field, high sedimentation rates caused by sediment flow into an adjacent stream and by sediment accumulation during the swelling periods of the stream were observed at the hillfoot.

At the non-permanent grassland site under commercial management (D) the predominant process caused by soil movement was sedimentation. This area could be affected by deposition of sediments moving from an upper flat adjacent cultivated area, which was ploughed perpendicular to the hillslope of the grassland throughout several decades. The highest sedimentation areas were located in water flow concentration sites: at footslope and at the midslope where the inclination is maximal. The midslope sector is positioned at a concavity of lateral hillslopes, and could be therefore affected by sediment coming from lateral pronounced slopes. Both grassland sites are not isolated from the surrounding fields, and are probably affected by soil movement from and towards the adjacent areas.

As shown in Figure 1, the ^{137}Cs method allows to discriminate between the long-term soil redistribution processes according to the use (crop or grassland) and management (commercial or subsistence) of the soil.

The soil erosion rates estimated by the ^{137}Cs method were first compared with sediment flux measured at erosion plots during three years. The mean annual sediment loss determined with an experimental plot located at the upper sector of site A was 0.28 ± 0.08 $kg.m^{-2}.yr^{-1}$. The calculated erosion rate at the sampling points adjacent to the plot area varied from 0.09 to 0.6 $kg.m^{-2}.yr^{-1}$ (mean value 0.25 $kg.m^{-2}.yr^{-1}$). The sediment flux determined with the experimental plot simulating the management conditions of grassland C was 0.10 ± 0.03 $kg.m^{-2}.yr^{-1}$ and the calculated erosion rates at sampling points of similar slope in that grassland fluctuated between 0.04 and 0.19 $kg.m^{-2}.yr^{-1}$ (mean value 0.11 $kg.m^{-2}.yr^{-1}$). The annual sediment loss measured with erosion plots is in good agreement with the estimated erosion rates at adjacent positions in the fields. Nevertheless, the measured flux represents net soil export from the plots, because of their isolation from the soil redistribution processes operating in the surrounding area. Moreover, sediment flux is time dependent and therefore valid for the period for which it is calculated.

The soil redistribution rates quantified by the ^{137}Cs technique represent a time-integrated, medium-term, average for the last 40-45 years, and are therefore less influenced by extreme events. Additional redistribution rates obtained by pedological observations, which also consider the accumulative effect of past soil redistribution processes, are represented in Figure 2. The rates estimated by the pedological observations reflect a similar pattern of spatial distribution, in relation to the soil redistribution rates quantified by the ^{137}Cs method. Nevertheless, the values of erosion and sedimentation rates obtained by this method are expressed on relative scales, because of the difficulty in determining the period of cultivation of each field and the depth of the reference horizons. Therefore, additional medium-term estimations of erosion and sedimentation rates are required for validating the values estimated by the ^{137}Cs method. In the future, it is also necessary to study the applicability of the method under other climatic conditions and soil types occurring in Chile in which erosion is not so evident, in order to prevent it.

The erosion and sedimentation rates caused by tillage, water and the net rates obtained along the slope transect at each study site using the simplified ^{137}Cs inventory evaluation are represented in Figure 3.

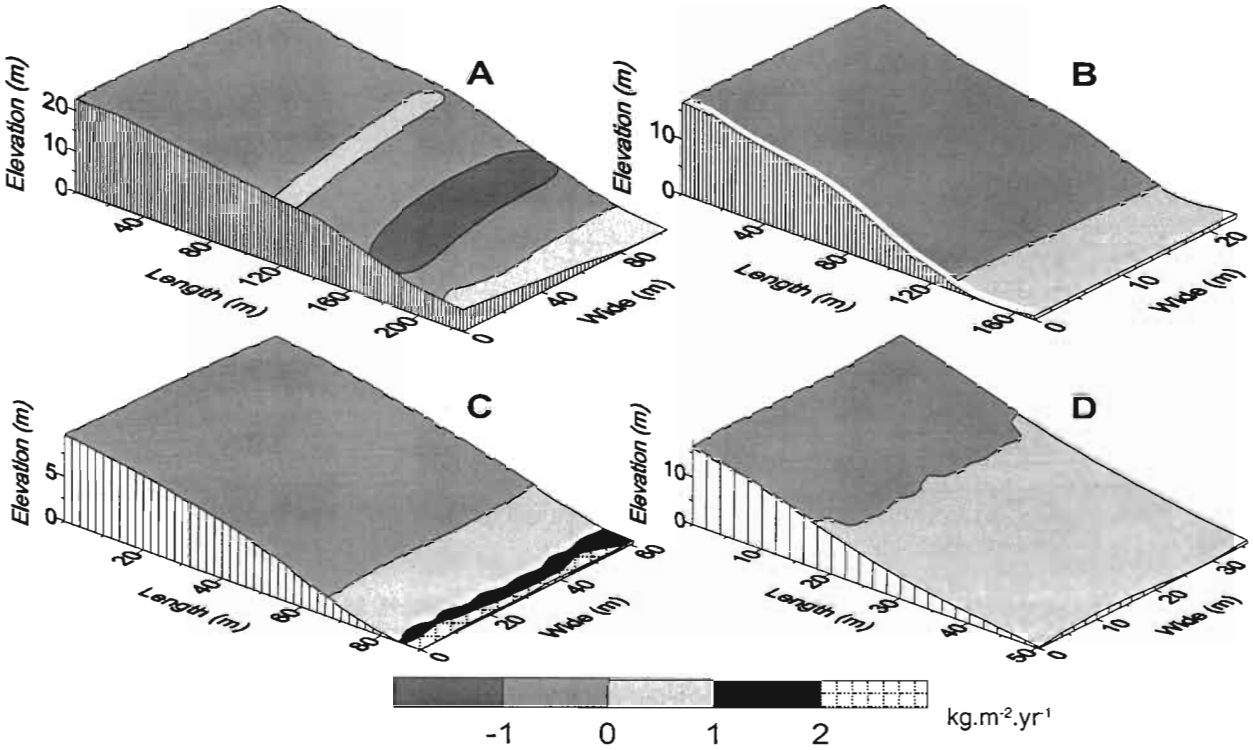

Figure 2
Soil redistribution rates estimated by pedological observations: crop land under subsistence (A) and commercial management (B), grassland under subsistance (C) and commercial management (D).

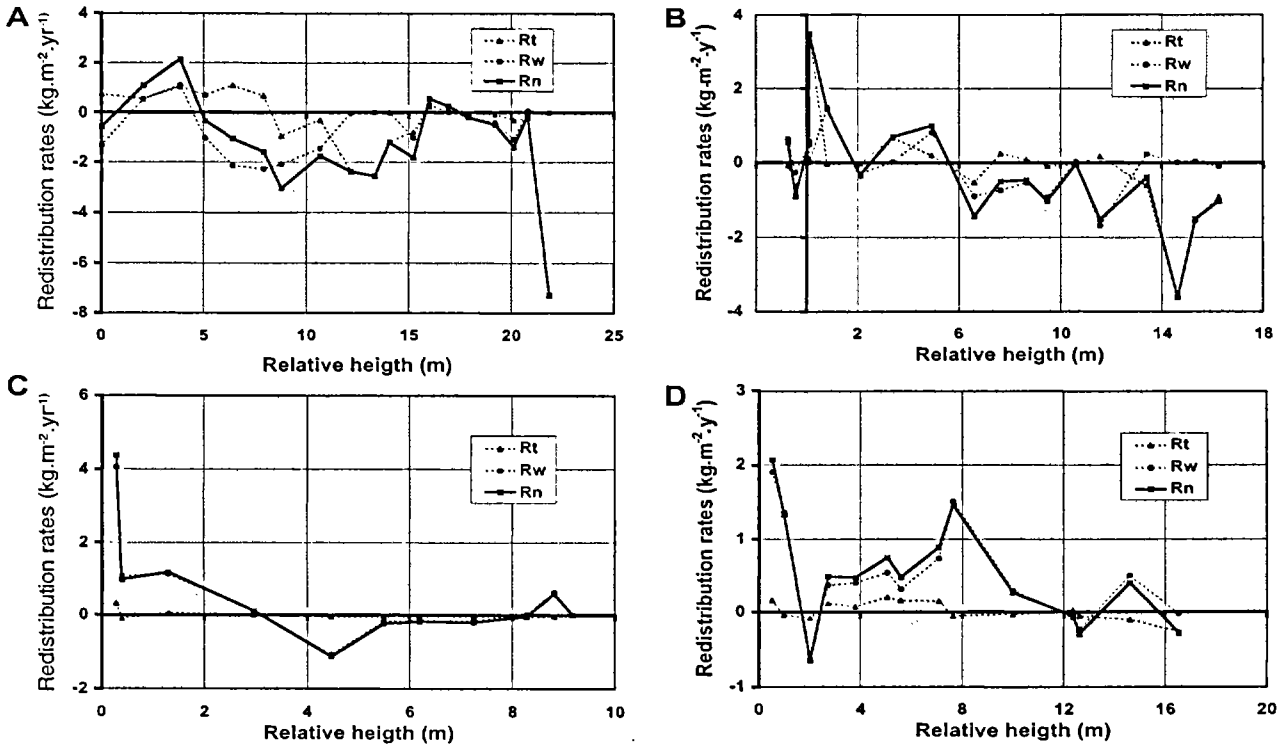

I Figure 3
Soil redistribution rates caused by tillage (Rt), by water (Rw), and net rates (Rn) along the slope transect estimated by ^{137}Cs inventory evaluation at contour lines: crop land under subsistence (A) and commercial management (B), grassland under subsistence (C) and commercial management (D).

Comparing the mean redistribution rates estimated at similar altitude along the slope transects obtained by a ^{137}Cs inventory evaluation of individual samples collected in a grid pattern with the ones obtained by an inventory evaluation in composed samples taken at contour lines, the correlations between the redistribution rates caused by tillage, by water and net rates are strongly significant at the 0.01 level in each site, with exception of redistribution caused by water (significant at level 0.05) in site A. The simplified method is suitable for giving assessment on soil loss and sediment accumulation in areas exhibiting simple topography, showing almost similar slopes at constant-altitude transects. It reduces considerably the measuring time to estimate the soil redistribution.

The simplified method allows a fast estimation of soil redistribution rates, providing the possibility to estimate soil redistribution in larger areas in a shorter time. Nevertheless, the sampling and ^{137}Cs inventory quantification strategy must be selected according to the resolution of the required information, and extension and complexity of the landscape relief.

Aknowledgements

This study was supported by the Fondo Nacional de Investigación Científica y Tecnológica, Chile (FONDECYT 1970662), the International Atomic Energy Agency (IAEA CHI-8899), and the Dirección de Investigación y Desarrollo, Universidad Austral de Chile. The authors wish to thank these institutions for their financial support.

Bibliography

ELLIES A., CONTRERAS C., 1997 — Modificaciones estructurales de un Palehumult sometido a distintos manejos. *Agricultura Técnica*, 57: 15-21.

HEALTH AND SAFETY LABORATORY, 1977 — Final tabulation of monthly ^{90}Sr fallout data: 1954-1976. U. S. Energy Research and Development Administration. New York, USA. *HASL-329 Report*, UC-11. 323 p.

HUDSON N., 1971 — *Soil conservation.* Cornell University Press, Ithaca, New York. 320 p.

IREN, 1970 — *Integrated studies on natural resources in Cautín.* Instituto de Recursos Naturales, Santiago, Chile. 29(2), 140 p. (in Spanish).

JUZDAN Z. R., 1988 — *Worldwide deposition de ^{90}Sr through 1985.* Department of Energy, New York, USA. Environmental Measurements Laboratory Report. EML-515. 34 p.

LARSEN R. J., 1985 — *Worldwide deposition de ^{90}Sr through 1983.* Department of Energy, New York, USA. Environmental Measurements Laboratory Report. EML-444. 159 p.

LARSEN R. J., JUZDAN Z. R., 1986 — *Worldwide deposition of ^{90}Sr through 1984.* Department of Energy, New York, USA. Environmental Measurements Laboratory Report. EML-457. 159 p.

LOUGHRAN R. J., 1989 — The measurement of soil erosion. *Prog. Phys. Geogr.* 13: 216-233.

MONETTI M. A., LARSEN R. J., 1991 — *Worldwide deposition de ^{90}Sr through 1986.* Department of Energy, New York, USA. Environmental Measurements Laboratory Report. EML-533. 31 p.

PERALTA M., 1976 — *Soil use, classification and conservation.* Servicio Agrícola y Ganadero. Santiago, Chile. 337 p. (in Spanish).

QUINE T. A., GOVERS G., WALLING D. E., ZHANG X., DESMET P. J. J., ZHANG Y., VANDAELE K., 1997 — Erosion processes and landform evolution on agricultural land – New perspectives from ^{137}Cs measurements and topographic-based erosion modelling. *Earth surface processes and landforms.* 22: 799-816.

RITCHIE J. C., MCHENRY J. R., 1990 — Application of radioactive fallout cesium-137 for measuring soil erosion and sediment accumulation rates and patterns: A review. *J. Environ. Qual.* 19: 215-233.

SCHULLER P., SEPÚLVED, A., ELLIES A., CASTILLO A., 1999 — Utilización de ^{137}Cs en cuantificación de erosión y sedimentación en un Palehumult de la IX Región. *Agro Sur* 27: 29-36.

UNITED Nations Scientific Committee on the Effects of Atomic Radiation 1982 — *Ionizing radiation: Sources and biological effects.* United Nations. 773 p.

WALLING D. E., 1998 — *Use of ^{137}Cs and other fallout radionuclides in soil erosion investigations: Progress, problems and prospects, in use of ^{137}Cs in the study of soil erosion and sedimentation,* IAEA TECDOC-1028, Vienna, 39-62.

WALLING D. E., HE Q., 1999) — Improved models for estimating soil erosion rates from cesium-137 measurements. *J. Environ. Qual.* 28(2): 611-622.

Soil-radionuclides interaction and subsequent impact on the contamination of plant food products based on a simulated accidental source

Francois Bréchignac
Yves Thiry
Nadia Waegeneers
Ramon Vallejo
Teresa Sauras
Jaume Casadesus
Graeme Shaw
Joanna Marchant
Sverker Forsberg
Chatal Madoz-Escande
Claude Colle
Marc André Gonze

Introduction

The Chernobyl accident, which resulted in a substantial release of radioactive materials in the atmosphere, demonstrated that large environmental areas may be contaminated by fall-out deposition of

radioactivity. In particular, contamination by ^{137}Cs and ^{90}Sr of agro-ecosystems where food production is taking place is most liable to contribute to population radiation dose (Strand *et al.*, 1996). Nuclear safety analysis shows that the possibility, although very small, of an accident occurring on a pressurized water reactor (PWR) cannot be completely ruled out. In such a situation, decision-making and management of the contaminated agricultural surfaces largely depends on our ability to predict how, and to which extent, the initial contamination may cause foodstuffs to be polluted. Furthermore, the efficiency of the prediction models relies on our level of understanding of the mechanisms governing the transfer of radionuclides in the soil-plant system.

Gaining an understanding of these mechanisms from *in situ* observations of environmental areas contaminated by past events is difficult due to the lack of knowledge and control on both, the contamination itself, arising from a critical situation, and the natural environment, which is highly variable, temporally and spatially. Such conditions prevent a clear identification of the most relevant parameters influencing the radionuclides transfer and thereby the prediction goal from being achieved. This is why IPSN developed a unique research facility capable of generating, in closed and controlled environmental conditions, a mini-accident with release of radioactive aerosols onto small-scale, but realistic, samples of crops. These crops are grown on undisturbed soil monoliths, featuring several soil types from various European countries, managed in advanced lysimeters, and placed in greenhouses where various climatic conditions can be reproduced artificially under computer control.

The PEACE Programme, gathering a European scientific collaboration around this facility, has been designed to tackle the consequences of an accidental release of ^{137}Cs and ^{90}Sr on the soil-plant system of agricultural lands. The research conducted has focused on the interaction of radionuclides with soils with a view to improve our understanding of the mechanisms governing their transfer to plants via the roots, and their modelling for prediction.

Materials and methods

A detailed description of the performances of the IPSN Controlled Lysimetric Environmental facility and its various technological components has already been published elsewhere (Bréchignac *et al.*, 1996; Bréchignac *et al.*, 1998; Madoz-Escande *et al.*, 1999). Only the essential features are briefly recalled in the following.

The climates and the soils in the controlled lysimetric environmental facility

Located at Cadarache (Bouches-du-Rhône, France), the facility is a 2000 m² leak-proof (depressurized) laboratory consisting in four experimental greenhouses where artificial reproduction of predefined climatic and hydric conditions is made possible by means of computer based regulation. These greenhouses host various lysimeters made of soil monoliths which have been sampled in one block (12 tons) without disturbing the pedological stratification, and further fitted in metallic casings (1.5 m deep, 3.2 m² area). Sampled in Belgium (Mol), Germany (Jülich), France (Belleville), Spain (Barcelona) and the United Kingdom (Wellesbourne), they correspond to several soil types commonly encountered in western Europe. Prior to installing a soil monolith in its dedicated greenhouse, the bottom face of the lysimeter is fitted with a water reservoir interfacing the soil via a porous ceramic layer. This unique system allows the exchange of water which occurs naturally between the water table and the soil to be simulated artificially. Thus, the soil moisture can be mastered. The top side of the lysimeter to be cultivated is next brought to fit a hole in the greenhouse floor in such a way that the soil surface appears in the greenhouse where the climatic conditions prevailing at its sampling site are artificially reproduced. The underground parts of all the lysimeters are located in a common hall where temperature can be controlled

independently from that which is controlled above the soil surface, in the greenhouses. Climatic control and corresponding data acquisition (temperature, hygrometry, light and rainfall) are performed automatically. For the purpose of this study, three different climates have been reconstructed (temperate, Mediterranean and transition temperate-Mediterranean) within independent greenhouses by means of a dedicated software which reproduces the nyctemerial and seasonal climatic parameters variations in real time.

Contamination of the lysimeters for accident simulation

Simulation of an accidental contamination is performed by using an induction furnace that produces aerosols similar to those which would be produced in the event of severe failure in a pressurized water reactor (PWR) with core fusion (about 3000°C). Aerosols are generated in a water-saturated atmosphere enclosed in a polyethylene envelope which can be made to communicate with a similar envelope covering the lysimeter surface to be contaminated. They are produced from a mixture of elements representative of the materials constituting a 900 MW reactor: the nuclear fuel (as uranium oxide), the structural materials of the reactor core, the components of the fuel sheath and the control bars. The proportions of elements within this mixture correspond to the relative quantities of the nuclear core inventory, reduced by 10^7. ^{137}Cs and ^{90}Sr, the two radioactive fission products most detrimental to the environment in a radiation protection perspective, are included in this experimental mixture. In order to produce such aerosols, the mixture is brought up, as powder, to a temperature of 2950 °C (reached within 30 minutes and maintained for 15 minutes) in a water-saturated atmosphere. A thorough physico-chemical characterization of these aerosols showed that they were produced as numerous oxides of combined elements, with a mean aerodynamic diameter of 3.5 µm. The total dissolution rates (in rain water) of the ^{137}Cs and the ^{90}Sr contained in these aerosols amounted to 85-95 % after 1 day, and 75-85 % after 5 days, respectively.

Experimental protocol for radio-contamination follow up

The general experimental protocol of lysimeter studies starts off with the aerosol deposition on the lysimeters soils and their crops, which took place in 1994 and 1995. Subsequent to contamination, several annual crops (barley, lettuce and beans) have been grown successively for several years, and in parallel on the various soils, with realistic rainfall cycles in order to simulate natural conditions. Two perennial crops (rye-grass and lucerne) have also been sown on some plots, either before or after the contamination event, and followed up to five successive years in order to simulate a cattle feeding semi-natural ecosystem. Migration profiles of radionuclides within untilled plots of the soils have been determined by sampling vertical soil cores (down to 50 cm), taking due care of potential compaction and in-depth contamination transport associated to this method. The same procedure has been applied to the tilled plots of the soils (down to 20-30 cm) in order to check for the vertical distribution homogeneity in this layer, and to determine the soil specific activity for each radionuclide. Plants have been sampled periodically, and annual crops harvested upon maturity, for determining their radio-contamination status.

Radionuclides and ionic determinations in soils and plants

Measurements of radionuclides and major ions species (K, Ca, Mg) have been carried out on various sample types: bulk dry soil, soil interstitial water (soil solution) and plants (leaves and seeds, separately as appropriate). The soil solution has been extracted by high speed centrifugation of moist soil samples. Stable ionic species have been determined based on atomic absorption spectroscopy. ^{137}Cs has been determined using a Germanium coaxial g emission detector, whilst ^{90}Sr has been measured by liquid scintillation after rapid separation/purification as previously described (Tormos *et al.*, 1995).

Results and discussion

Soils physico-chemical characterization

The soils studied show contrasted properties with respect to texture, clay content and pH (Table 1). The soils texture range from sandy/sandy-loamy (Mol, Belleville, Wellesbourne), typical of alluvial and fluvio-glacial sediments, to loamy, characteristic of loess sediments present in Central Europe (Jülich), or derived from ancient pedogenesis of alluvial sediments typical of Mediterranean areas (Barcelona). The clay content varies from 4.1% (Mol) up to 13.9% (Barcelona), whereas the soils pH ranges from acidic (Mol and Belleville) up to about neutral (Wellesbourne, Jülich and Barcelona). The soils retention properties for ^{137}Cs and ^{90}Sr have been quantified respectively by determining their RIP (Radiocaesium Interception Potential) and their CEC (Cationic

Geographical sampling site	Mol (Belgium)	Belleville (France)	Wellesbourne (U.K.)	Jülich (Germany)	Barcelona (Spain)
FAO classification	orthic podzol	fluvisol	eutric fluvisol	orthic luvisol	calcic luvisol
Soil texture	(Loamy) sand	Loamy sand	Sandy loam	Silt loam	Loam
Particle size					
% clay	4.1	5.8	9.5	11.2	13.9
% silt	14.6	13.7	19.7	78.8	28.8
% sand	78.4	79.0	66.6	8.4	47.7
Chemistry					
pH (KCl)	4.6	4.1	6.3	7.1	7.3
% organic matter	3	1.5	3.9	1.5	2.3
Total carbonates (%)	≈0	≈0	0.3	0.2	7.2
RIP ($\mu eq.g^{-1}$)	443	1126	2316	2328	2732
CEC ($cmol_c.kg^{-1}$)	11.7	5.8	17.8	13.4	16.4

Table 1
Main physico-chemical characteristics of the various European soils in the plough layer.

Exchange Capacity). The Radiocaesium Interception Potential is the product of the capacity of the Frayed Edge Sites (FES) of clay minerals to adsorb radiocaesium, and the selectivity coefficient of caesium with respect to K for these exchange sites (Wauters *et al.*, 1994). Highly selective, and located at the interlayer edges of weathered micaceous clay minerals, such sites have been demonstrated to govern radiocaesium sorption (Maes *et al.*, 1998; Maes *et al.*, 1999). This approach allows to take due account of the competitive effect of K and Ca+Mg ions for ^{137}Cs and ^{90}Sr sorption, respectively, which influence their respective solid-liquid partition coefficients (K_DCs=RIP/[K] and K_DSr=CEC/[Ca]+[Mg], Sweeck *et al.*, 1990).

Another approach to identifying the degree of radionuclides fixation on soil matrices relies on the estimation of the exchangeable fractions as displaced by NH_4Ac (1 N), and expressed as a percentage of the total amount initially fixed. These have been measured on the various soils and amounted to 12-20 % for ^{137}Cs, and to 35-60 % for ^{90}Sr (Figure 1), therefore featuring a chemical availability of ^{90}Sr in the soils larger than that of ^{137}Cs which should reflect their respective mobilities in the soil-plant system with respect to both, migration and root uptake. More detailed analysis on the chemical

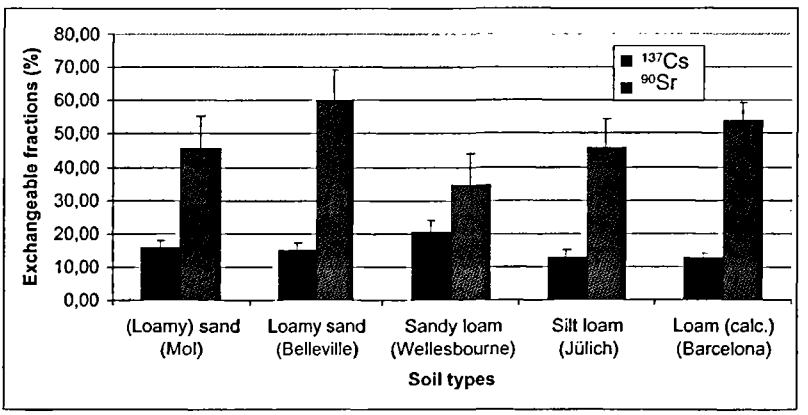

Figure 1
Exchangeable fractions of ^{137}Cs and ^{90}Sr in various soils as measured from displacement by NH_4 Acetate (1 N).

availabilities of ^{137}Cs and ^{90}Sr in these soils have already been reported (Sauras-Yera. *et al.*, 1999; Forsberg *et al.*, in press).

^{137}Cs and ^{90}Sr migration in soils

When attempting to understand the migration patterns, the first steps come from chemistry which indicates that the high potential mobility of radiocaesium, due to its significant solubility, is counteracted by its very specific and efficient sorption on clay particles (FES of illitic and vermiculitic clay, in particular). Conversely, the lower potential mobility of radiostrontium, due to its poorer solubility, is not counteracted to the same extent by specific fixation sites on the soil matrix. Overall, this results in radiostrontium being more mobile than radiocaesium with clearly distinct K_D values, as determined *in vitro*, from which a higher migration rate is expected for ^{90}Sr than for ^{137}Cs after several years. However, experimental observations do not fit this theoretical approach (Forsberg *et al.*, 2000).

On the one hand, the two radionuclides developed migration profiles, on a given agricultural soil (untilled plots), which still show similar shapes four years after the contamination deposition. Even the soil type, which yields various K_D coefficient values for the 5 soils of this study, does not significantly alter the observed profiles (Figure 2). On the other hand, the low rates of migration observed in the long term (around 1 $cm.yr^{-1}$, in the years following contamination) cannot explain the shapes of the profiles (Figure 3). In the shorter term, when experimentally forcing migration on soil columns with a high hydrological flux, the two radionuclides exhibit profiles which are established within one month, with very limited further evolution (Figure 4). Altogether, these observations strongly suggest that the migration profiles are established very early after contamination, under the influence of initial processes that do not depend primarily on the soils K_D coefficients, as determined *in vitro*. Their evolution is subsequently very slow. This indicates the importance of the early conditions prevailing immediately after contamination, such as soil moisture and first rain events, which may be paramount in determining the extent to which radionuclides will penetrate in depth.

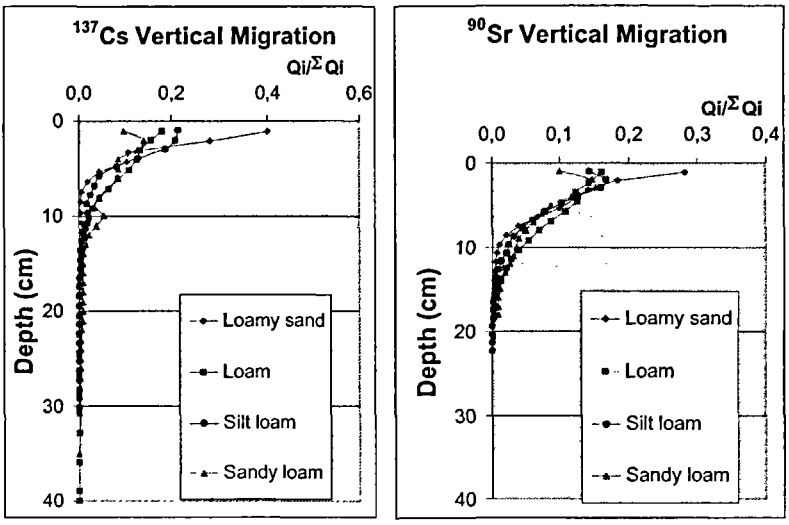

Figure 2
^{137}Cs and ^{90}Sr migration profiles observed four years after contamination on various agricultural soils.

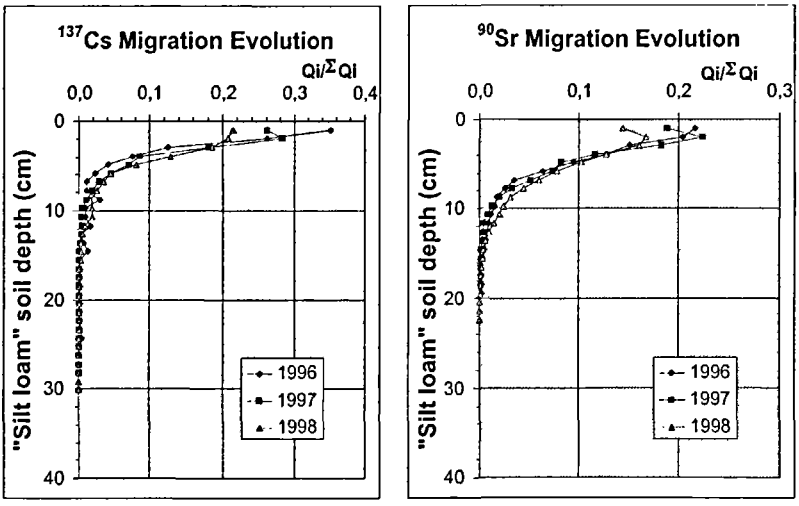

Figure 3
^{137}Cs and ^{90}Sr migration evolution during three successive years on an untilled silt loam soil.

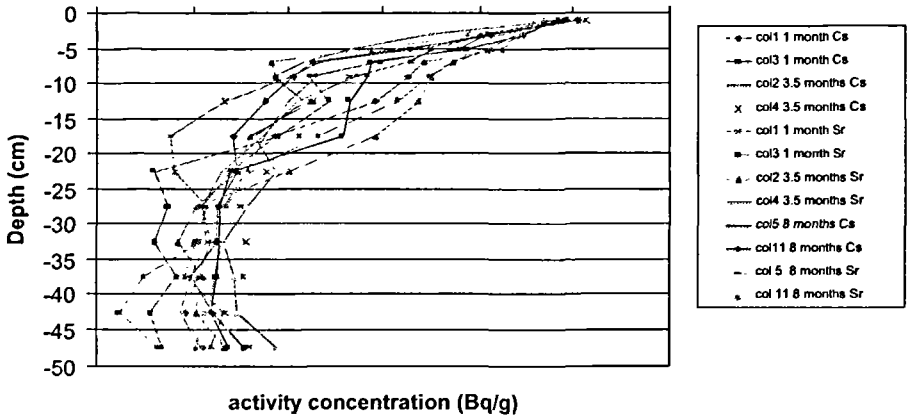

Figure 4
Cs and Sr profiles observed after 1, 3.5 and 8 months following contamination, in an undisturbed soil driven into experimental columns submitted to a high hydrological flux.

The simulation of the hourly-to-yearly vertical migration of ^{137}Cs and ^{90}Sr in a saturated/unsaturated soil column with vegetation has been undertaken based on a one-dimensional, dynamic physically-based model formulation (TRANSSOL model, Gonze, 1999). The major processes involved in water flow and transfer of radionuclides have been taken into account. Mechanisms such as downward migration enhancement due to macropores, water exchanges with surface atmospheric layer and time-dependent sorption of radionuclides onto the soil matrix are accounted for, as well as the slow initial dissolution of aerosols and the influence of soil moisture on the radionuclide concentrations in the soil solution (see below). Despite this accurate description effort, introducing the radionuclides' respective K_D coefficients, as derived from *in vitro* sorption/desorption experiments, produces calculated migration profiles which are underestimated for ^{137}Cs, and overestimated for ^{90}Sr (Figure 5). This suggests that migration is not governed by the soil traditional physico-chemical features only, as characterised by the *in vitro* radionuclides K_D coefficients. Additional soil properties are most probably of importance. The soil structure, which refers to the soil particles degree of aggregation, largely driven by the soil biological

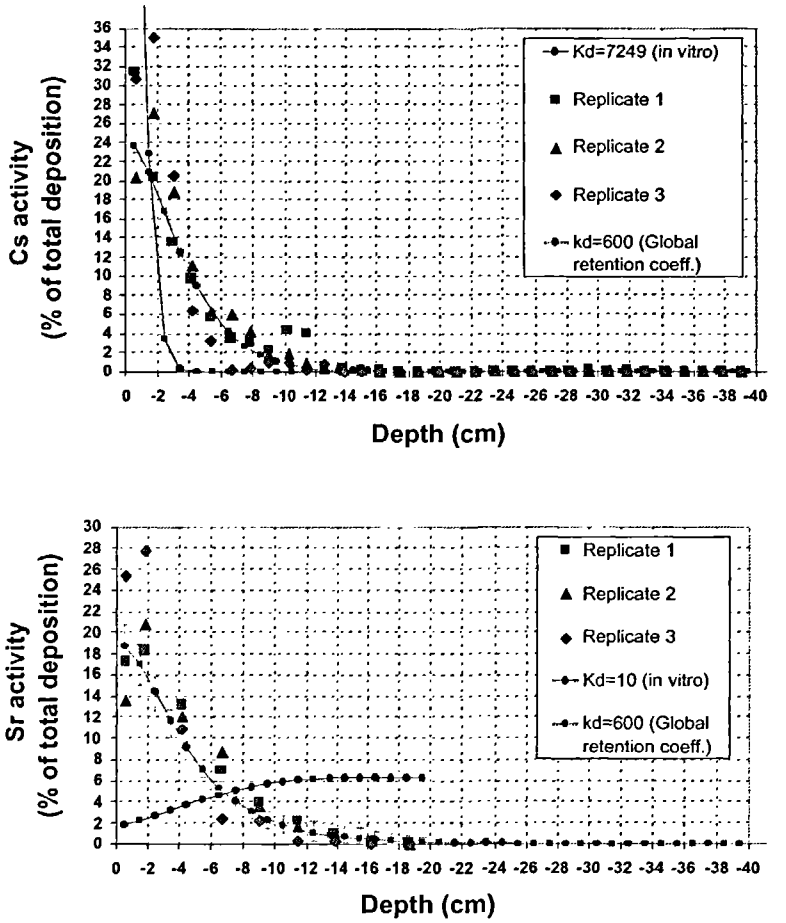

Figure 5
Model-based predictions of ^{137}Cs (up) and ^{90}Sr (down) migration against experimental data (three replicates).

activity present in the surface layer (microbial and root activity), is a good candidate. When taken into account in addition to processes inferred by the traditional K_D coefficients, the model predicts an "*in situ* global retention coefficient" of about 600 $l.kg^{-1}$ (noted k_d), which best fits the experimental profiles for both radionuclides in the first 15 cm soil layer (Gonze and Perrier, 1999).

Soil influence on ^{137}Cs and ^{90}Sr root transfer to annual crops

Once contamination has reached the soil, long term pollution of plant food products occurs essentially via root uptake. Prediction models have first tackled this problem by applying a "transfer factor" coefficient, similar to a "concentration ratio" defined as the ratio between the specific activity in the plant and the specific activity in the soil. This empirical approach, however, suffers from high and poorly documented variabilities, which can largely be accounted for by the plant species considered, but also by the complexity and diversity of the soil compartment (IUR, 1989; Eriksson and Rosen, 1991). This is illustrated by the ^{137}Cs and ^{90}Sr concentration ratios (CR) which have been simultaneously measured on the five soil types for three different plant consumables: barley grains, bean pods and lettuce (Figure 6). For ^{90}Sr, the classification of the observed Concentration Ratios (CR) lies in general agreement with the soils' respective CEC values. For this radionuclide, the CR values are also 2 orders of magnitude larger than for ^{137}Cs, irrespective of the plant considered, illustrating its larger mobility in agreement with the chemical availability studies previously mentioned. For ^{137}Cs, however, the soils physico-chemical characteristics of relevance (such as RIP and % clay) do not fully explain the observed CR values. Whilst confirming previous observations (Frissel *et al.*, 1990; Smolders *et al.*, 1997), such characteristics are not sufficient to establish an accurate prediction of ^{137}Cs transfer to plants. This lack of agreement results from complex variations of the soil solution composition which need to be elucidated. In particular, the soil water composition does not only depend on soil type, but also on a number of other parameters such as soil moisture, climate, fertilization (particularly with K and Ca) and root uptake activity.

Elucidating the parameters which influence the "soil solution" composition is of paramount importance since this is the very place where roots absorb radionuclides along with dissolved mineral nutrients. Current predictive assessment models usually involve the soil-specific K_D concept (soil solid/liquid partition coefficient) which reflects the radionuclide retention on the solid matrix (sorp-

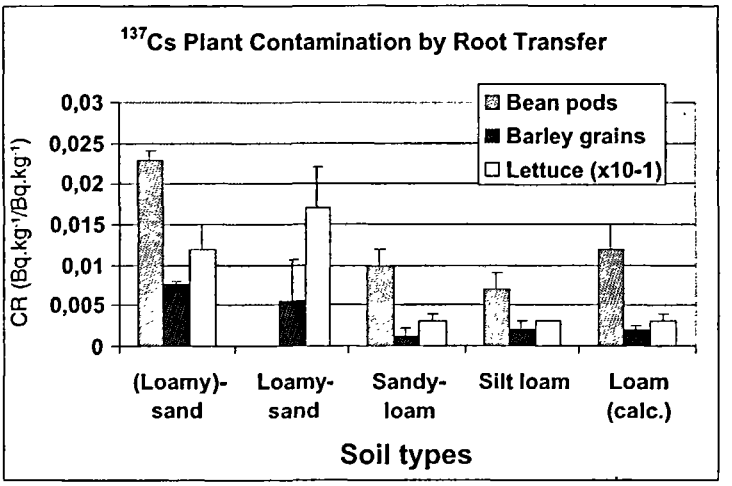

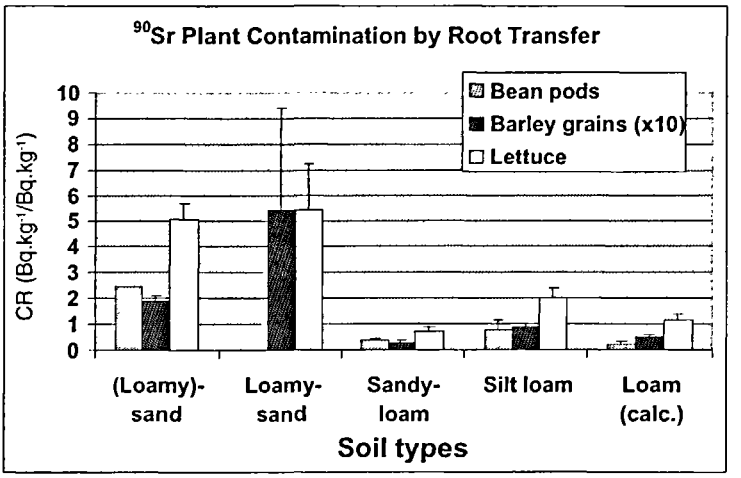

Figure 6
^{137}Cs and ^{90}Sr root transfer (as concentration ratios) obtained on five distinct agricultural soils for lettuce, bean pods and barley grains.

tion potential of a given soil) with respect to its solubility in interstitial water (potential availability to plant roots). The large sorption rate of ^{137}Cs on most mineral soils determine trace concentrations in interstitial water. The radionuclides dissolved concentrations in soil water are further influenced to a large extent by the abundance of other ionic nutritive elements. As previously mentioned, this roots from the often reported competition occurring between Cs and K for adsorption on the FES of clay particles (Smolders *et al.*, 1997; Delvaux *et al.*, 2000; Thiry *et al.*, 2000), or between Sr and Ca+Mg for adsorption on the argilo-humic complex. However, inherent limits to adequately describing the soil water composition also arise from the equilibrium nature of the K_D coefficient, which is usually determined in water saturated conditions. Such conditions are rarely encountered in real nature, due, for example, to the continuous pumping activity of the roots or to climate-driven variations in soil moisture.

A previous investigation on pasture plants in northern Germany indicated that Cs and Sr root uptake were controlled by their concentrations in soil water which were reported to increase at reduced soil moistures (Kirchner and Ehlken, 1997). Based on a series of *in vitro* experiments carried out on samples from the soils considered in the present study, soil moisture is indeed demonstrated to markedly influence the radionuclides concentrations in soil water. For example, reducing soil moisture promotes an increase in Cs concentration, thereby reducing its K_D (Figure 7), an effect which in a first approach would tend to favour root uptake. However, the K concentration is also increased in parallel, to an extent proportionally even greater than for Cs (Cs/K lower at reduced soil moisture), hence promoting a larger competition with Cs for fixation on clay minerals. Similar observations have been obtained for ^{90}Sr and Ca+Mg. When considering the soil matrix-liquid interface only, the radionuclides availability to root uptake will therefore result from the combination of both effects.

In turn, when considering the interface between the root surface and the soil water, an increased K concentration in the soil water (as measured upon plant harvest) promotes a reduction of ^{137}Cs uptake expressed as a concentration factor (Figure 8, with CF= specific activity in plants/specific activity in soil water). Similar

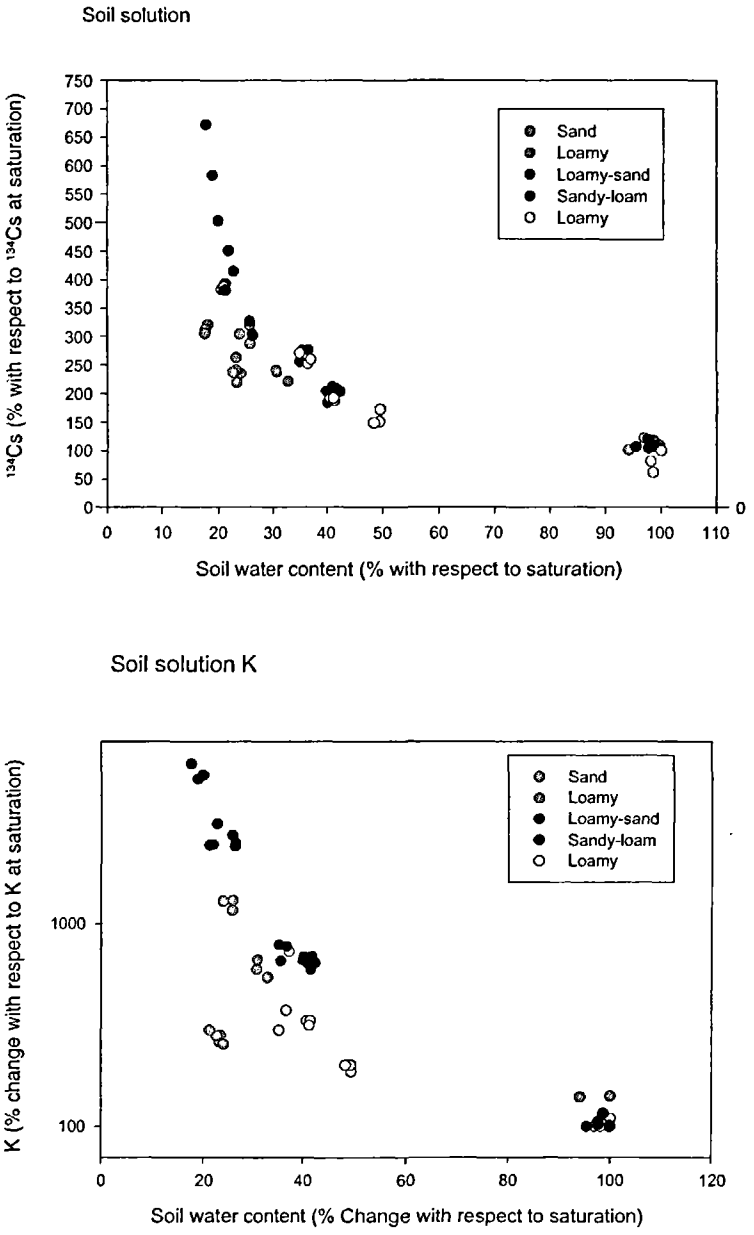

I Figure 7
Influence of soil moisture on Cs (up) and K (down) concentrations in soil water.

observations have been obtained for ^{90}Sr and Ca+Mg. The log-log plot of the ^{137}Cs CF versus K concentration in soil water shows that this effect is more pronounced in the low range of K concentrations, most likely in soils with reduced fertility. Having been obtained from measurements on different soil types, the correlation between CF and the concentration in analogue ionic species suggests that plant contamination is primarily susceptible to the status of analogues in the soil water, irrespective of the soil type. Recent studies undertaken on a wide spectrum of different soil types, either mineral or organic, have established a similar competition promoted by K in soil water for root uptake of ^{137}Cs, an effect most pronounced below 1mM K (Smolders *et al.*, 1997; Sanchez *et al.*, 1999). This agrees with the principle of radionuclide competition with its analogue ion occurring at the root level for membrane-based ionic transport systems.

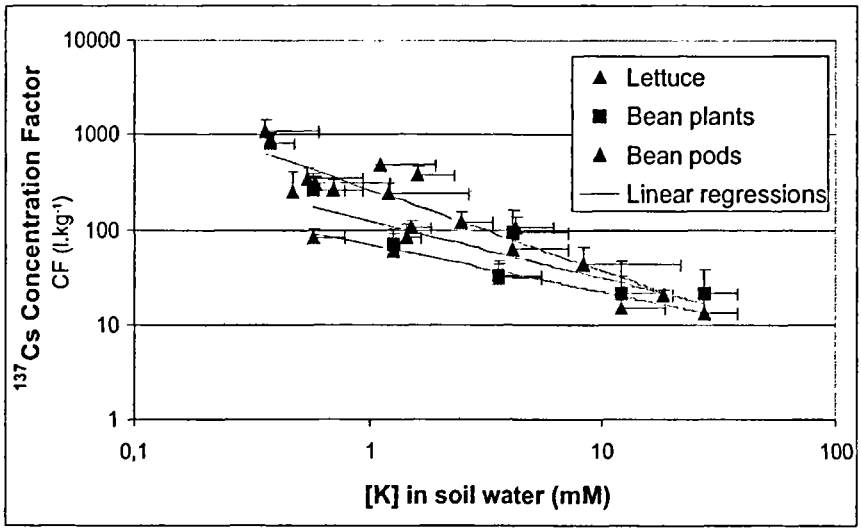

Figure 8
Influence of the K concentration in soil wateron the ^{137}Cs Concentration Factor in lettuce and bean.

When considering finally the overall soil-plant system, it has been suggested that plant uptake could be described, provided some assumptions, by a series of two reactions (as for Cs, Smolders *et al.*, 1997):

$$Cs_{soil} \xleftrightarrow{K_D} Cs_{soil\ water} \xleftrightarrow{CF} Cs_{plant}$$

From this model, the overall transfer factor (expressed as the concentration ratio $CR=Cs_{plant}$ [specific activity in plant]/Cs_{soil} [specific activity in soil]) can be derived: $CR=CF/K_D$. CF (plant root/soil water interface) and K_D (soil matrix/soil water interface) are both depending on the K status of soil water, but with opposite trends. In particular, when increasing K in soil water, the Cs availability at the soil matrix-liquid interface (K_D) is increased (a feature which would favour root uptake) concurrently with a stimulation of the competition at the root level which tends to reduce root uptake. The ultimate plant contamination rate results therefore from the complex combination of these two interface-related processes, further explaining why CR is not easily linked to soil properties. This demonstrates the central role played by the soil water chemical composition, not only with respect to the trace amounts of radionuclides, but also with regard to their ionic analogues (K, Ca+Mg), as a key element contributing to the variability of the observed transfer factors. In other words, an accurate prediction of the soil water composition, as experienced by the roots of the plants during growth, will most probably resolve a large part of the transfer factors variability.

Kinetics of ^{137}Cs and ^{90}Sr transfer to crops via root uptake.

Further to the influence of the soil parameters (such as texture, moisture, analogue ions availability, ...etc), the soil water composition is also influenced by the root uptake activity itself, as governed by the plant physiological requirements for homeostasis. Primarily designed to supply such nutrients as K and Ca to the plants in amounts suitable to support appropriate growth, the root uptake

activity is regulated by the plants physiological requirements. This can be illustrated by the variations during the growth cycle of the Cs accumulation rate in an annual crop (barley, Figure 9). Based on the finding that ^{137}Cs and ^{90}Sr are withdrawn respectively by the K- and Ca-membrane transport mechanisms, an analytical model describing Root Uptake of Radionuclides (RUR, Casadesus, 1999; Casadesus *et al.*, 1999) has been developed with particular emphasis on the depletion zone in the rhizosphere. This model accurately simulates the observed kinetics of radionuclides accumulation in plants. By integrating the physiology of plant growth, and in particular the regulatory mechanisms which overcome potential drastic depletion of nutrients in the root vicinity, this model accounts for the plant's ability to adjust the rate of supply to its demand.

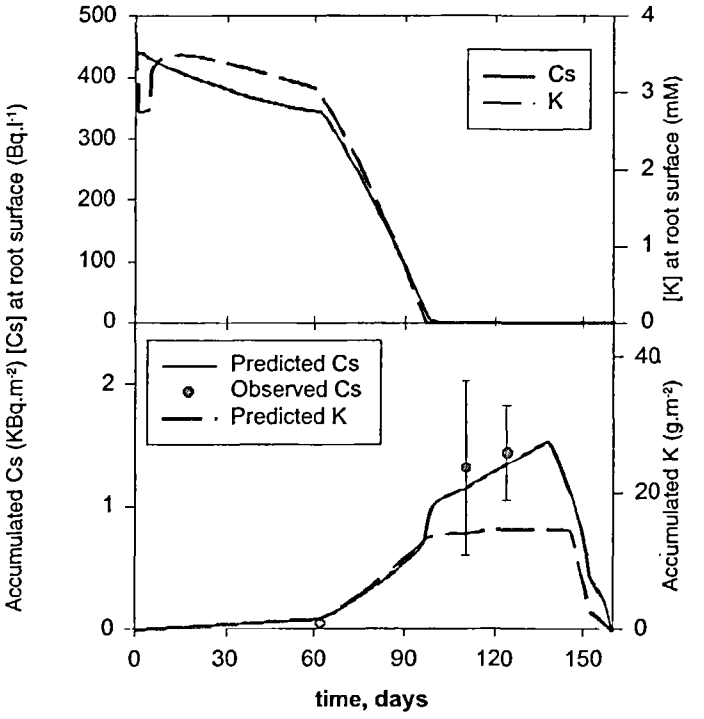

Figure 9
Cs and K evolution at the root vicinity during a barley crop, and their observed /predicted accumulation in plants.

In addition to spatial variability, most often associated to soil type, such an in-year seasonality also contributes to puzzling the accurate determination of the longer-term contamination evolution within perennial vegetation, a prerequisite for valid long-term predictions. This is illustrated by the ^{137}Cs and ^{90}Sr activity concentrations in a rye-grass crop, grown on a silt-loam (Jülich) and a sandy loam soil (Wellesbourne), which have been followed up to 4.5 years after the contaminating deposition (Figure 10). Already present upon deposition, the contamination of the crop grown on the sandy loam (Wellesbourne) exhibits a rate of decline which can be decomposed into several successive phases with distinct characteristic times. For ^{137}Cs contamination, the fast initial rate of decline during the first few months following deposition is attributed to foliar transfers as affected by rain wash-off and growth-mediated dilution. During this initial phase, the ^{137}Cs contamination absorbed by the foliage is also translocated towards the roots. This root-accumulated pool will next be discharged to the rest of the plants, therefore promoting a slower rate of decline in the vegetation up to 2 years after contamination. Interestingly, ^{90}Sr does not exhibit such an intermediate phase due to its reduced mobility within plants which prevents a similar pool

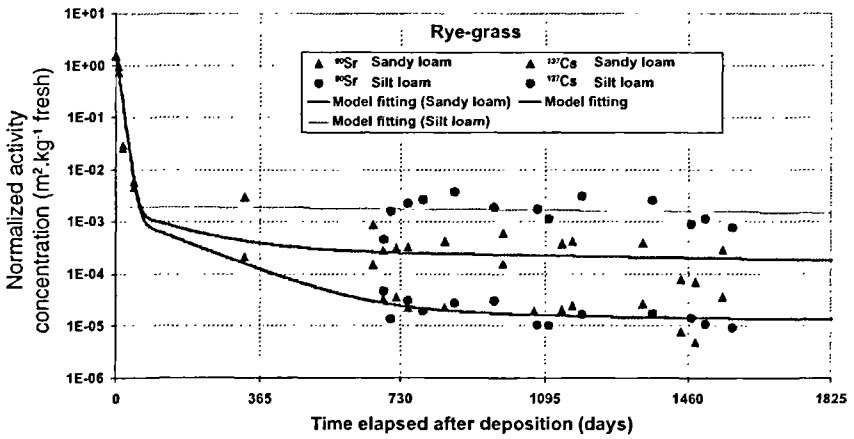

Figure 10
^{137}Cs and ^{90}Sr contamination evolution in Rye-grass during 4.5 years after deposition, and current model fitting of experimental values (ASTRAL Model).

build up within the roots. The last phase, from 2 years after deposition and further on, shows a contamination evolution which only comes from root uptake, and whose very slow rate of decline is usually attributed to migration and gradual irreversible fixation (both on top of physical decay). During this phase, within-year seasonal variations are particularly clear for both, ^{137}Cs and ^{90}Sr, on the silt loam soil (Jülich), where rye-grass had been sown after deposition (therefore ruling out any contribution from foliar transfers). This illustrates the difficulty to experimentally determine the long-term kinetics of contamination decline in the vegetation.

Conclusions and perspectives

PEACE constitutes the last piece of a series of international scientific programmes designed around the IPSN-controlled lysimetric environmental facility over the past decade. Focused on the behaviour of ^{137}Cs and ^{90}Sr, when accidentally released in the environment, these experimental investigations have generated a number of duly documented data (Bréchignac *et al.*, 1999). These are precious both, in enriching current radioecological data base and in providing a better understanding of mechanisms and processes, a key to making prediction models more accurate. The experimental designing of the soil-plant systems, as instrumented lysimetric soils in well-controlled climatic conditions, has allowed the use of a purely deterministic and mechanistic approach to modelling, because of both, the smaller space and time scales, and the reduced uncertainties on experimental data. Basically, such an approach has enabled the detailed study, with a relative accuracy, of the interactions between the various bio-physico-chemical processes of relevance, and their respective influence upon the contaminant behavior within such ecosystems. A sound scientific basis has now been reached, with prefiguration of appropriate research directions, in order to further elucidate the radionuclide "bioavailability" concept, which needs to move beyond the often misleading K_D-based formulation. Further work will address this particular issue.

Bibliography

BRÉCHIGNAC F., COLLE C., HUGON J., MADOZ-ESCANDE C., RONGIER P., SANCHEZ A., 1996 — "RESSAC: A research facility for studying radionuclides behaviour within ecosystems". *In Proceedings of IRPA International Congress on Radiation Protection*, Vienna, Austria, April 14-19, 1996, 3: 137-139.

BRÉCHIGNAC F., RONGIER P., HUGON J., DUBOIS E., COLLE C., MADOZ-ESCANDE C., 1998 — "Controlled lysimetric environmental facility at IPSN: assessing accidental radioactive contamination". *In Proceedings of International Meeting on Influence of Climatic Characteristics upon Behavior of Radioactive Elements*, Rokkasho, Aomori, Japan, October 14-16, 1997: 35-42.

BRÉCHIGNAC F., VALLEJO R.V., SAURAS YERA T., CASADESUS J., THIRY Y., WAEGENEERS N., FORSBERG S., SHAW G., MADOZ-ESCANDE C., GONZE M.-A., 1999 — *PEACE : Programme for Evaluating the impact of Accidents Contaminating the Environment-Soil-radionuclides processes of interaction and modelling of their impact on contamination of plant food products.* Final Report, European Atomic Energy Community Contract F14-CT96-0039a. (IPSN-DPRE/SERLAB Report 99-017(P)).

CASADESUS J., 1999 — *Root uptake of radionuclides – Model description.* Technical Note, European Atomic Energy Community Contract F14-CT96-0039a.

CASADESUS J., SAURAS YERA T., ROCA M. C.,VALLEJO V. R., 1999 — *Root uptake model validation.* Technical Note, European Atomic Energy Community Contract F14-CT96-0039a.

DELVAUX B., KRUYTZ N., CREMERS A., 2000 — Rhyzospheric mobilization of radiocaesium in soils. *Environmental Science and Technology*, 34: 1489-1493.

ERIKSSON A., ROSEN K., 1991 — "Transfer of caesium to hay grass and grain crops after Chernobyl". *In* Moberg L. (ed): *The Chernobyl fallout in Sweden – Results from a research programme on environmental radiology*, Stockholm, The Swedish Radiation Protection Institute: 291-304.

FORSBERG S., ROSÉN K., FERNANDEZ V., JUHAN H., 2000 — Migration of ^{137}Cs and ^{90}Sr in undisturbed soil profiles under controlled and close-to-real conditions. *Journal of Environmental Radioactivity*, 50 (3): 235-252.

FORSBERG S., ROSÉN K., BRÉCHIGNAC F., 2000 — Chemical availability of ^{137}Cs and ^{90}Sr in undisturbed lysimeter soils driven under controlled and close-to-real conditions. *Journal of Environmental Radioactivity*, in press.

FRISSEL M. J., NOORDIJK H., VAN BERGEIJK K. E., 1990 — "The impact of extreme environmental conditions, as occurring in natural ecosystems, on the soil-to-plant transfer of radionuclides". *In* Desmet G., Nassimbeni P., Belli M. (eds) : *Transfer of radionucides in natural and semi-natural environments*, Brussels and Luxembourg, Elsevier Science Publishers: 40-47.

GONZE M.-A., 1999 — *A physically-based model for simulating the soil-to-plant*

transfer of ^{137}Cs and ^{90}Sr radionuclides: the TRANSSOL code (updated release version 2.0), Technical Note, European Atomic Energy Community Contract F14-CT96-0039a.

GONZE M.-A., PERRIER T., 1999 — *Numerical simulations of ^{137}Cs and ^{90}Sr migration: TRANSSOL versus lysimeter experiments.* Technical Note, European Atomic Energy Community Contract F14-CT96-0039a.

IUR, 1989 — *Workgroup of the International Union of Radioecologists on soil-to-plants Transfer Factors.* Report VI. RIVM, Bilthoven, The Netherlands.

KIRCHNER G., EHLKEN S., 1997 — "Climatic influence on root uptake of Cs and Sr by pasture plants: evidence from field experiments in northern Germany". *In* Ohmomo Y., Sakurai N. (eds) : *Proceedings of International Meeting on Influence of Climatic Characteristics upon Behaviour of Radioactive Elements*, Aomori, Japan, Institute for Environmental Sciences: 83-90.

MADOZ-ESCANDE C., BRÉCHIGNAC F., COLLE C., DUBOIS E., HUGON J., JOUGLET H., MOUTIER M., RONGIER P., SANCHEZ A., SCHULTE E. H., ZANON R., 1999 — Experimental installation for radioecology research on defined ecosystems subjected to contamination in controlled conditions. *Nuclear Science and Engineering*, 133: 178-191.

MAES E., DELVAUX B., THIRY Y., 1998 — Fixation of radiocaesium in an acid brown forest soil. *European Journal of Soil Science*, 49: 133-140.

MAES E., ISERENTANT A., HERBAUTS J., DELVAUX B., 1999 — Influence of the nature of clay minerals on the fixation of radiocaesium traces in an acid brown earth-podzol weathering sequence. *European Journal of Soil Science*, 50: 117-125.

SANCHEZ A. L., WRIGHT S. M., SMOLDERS E., NAYLOR C., STEVENS P. A., KENNEDY V. H., DODD B. A., SINGLETON D. L., BARNETT C. L., 1999 — High plant uptake of radiocesium from organic soils due to Cs mobility and low soil K content. *Environmental Science and Technology*, 33: 2752-2757.

SAURAS YERA T., VALLEJO V. R., VALCKE E., COLLE C., FÖRSTEL H., MILLÀN R., JOUGLET H., 1999 — ^{137}Cs and ^{90}Sr root uptake under close to real controlled conditions. *Journal of Environmental Radioactivity*, 45(3): 191-218.

SMOLDERS E., VAN DEN BRANDE K., MERCKX R., 1997 — Concentrations of ^{137}Cs and K in soil solution predict the plant availability of ^{137}Cs in soils. *Environmental Science and Technology*, 31: 3432-3438.

STRAND P., BALONOV M., SKUTERUD L., HOVE L., HOWARD B., PRISTER B. S., TRAVNIKOVA I., RADNIKOV A., 1996 — "Exposures from consumption of agricultural ans semi-natural products". *In* Karaoglou A., Desmet G., Kelly G.N., Menzel H.G. (eds): *The Radiological Consequences of the Chernobyl Acciden*, EN-Luxembourg, Eur 16544: 261-269.

SWEECK L., WAUTERS J., VALCKE E., CREMERS A., 1990 — "The specific interception potential of soils for radiocaesium". *In* Desmet G., Nassimbeni P., Belli M. (eds): *Transfer of radionucides in natural and semi-natural environments*, Brussels and Luxembourg, Elsevier Science Publishers: 249-258.

THIRY Y., KRUYTS N., DELVAUX B., 2000 — Respective horizon contributions to cesium-137 soil-to-plant transfer: a pot experiment approach. *Journal of Environmental Quality*, 29, in press.

TORMOS J., JOUVE A., REVY D., MILLAN-GOMEZ R., ZANON R., ERARIO M. J., 1995 —

A rapid method for determining strontium-90 in contaminated samples of soil and plant. *Journal of Environmental Radioactivity,* 27(3): 193-206.

WAUTERS J., SWEECK L., VALCKE E., ELSEN A., CREMERS A., 1994 — Availability of radiocaesium in soils: a new methodology. *The Science of the Total Environment,* 157: 239-248.

Oral/Poster presentations

Session 5

Linking erosion and environmental change the potential of fallout radionuclides

T. A. Quine

Y. Zhang

P. Wallbrink

The need to document and predict erosional responses to environmental change presents an important challenge to research scientists, particularly in the light of growing concern over future climate change and increased pressure on land resources. Widespread applications of caesium-137 in erosion investigations and the more recent use of excess lead-210 have demonstrated the great potential of fallout radionuclides for assembling retrospective erosion rate data. However, if these data are to be used to address erosional responses to environmental change there is a need to derive information concerning changing rates of erosion. This paper considers approaches to deriving such data that include: comparison of radionuclide derived rates with contemporary experimental data; use of radionuclide data in erosion model validation; and comparison of data derived using different radionuclides. Examples from Europe and Australia will be used and attention will focus on tillage and water erosion. In comparison of data derived from different radionuclides, synchronous simulations are used in order to ensure internal consistency. The merits and limitations of this approach and the implications of dichotomies in data derived from different radionuclides are discussed.

Beyond erosion: relationships between soil redistribution, soil properties and crop production within an agricultural field in Devon, UK

T. A. Quine

Y. Zhang

This paper uses erosion data derived from caesium-137 measurements and field survey of rill networks to explore the role of tillage erosion and water erosion in the development of observed within-field spatial variation in soil properties and crop production. It is suggested that soil redistribution by tillage is a major contributor to the observed spatial variation in soil properties. Relationships between crop production and soil properties and erosion rates were found to be complex and non-linear. Simulation of a further 40 years of tillage erosion suggests that spatial variation in soil properties will become more extreme and is likely to have a deleterious impact on crop production.

Combining tracers and landscape modelling to predict sources of sediments and phosphorus to waterways

Ck. Bundella **C. J. Wilson**
P. J. Wallbrink **C. Martin**

The Liverpool plains in the Namoi River basin, NSW, is one of the most productive agricultural regions in Australia. However sedimentation in the streams and rivers running through it has resulted in severe environmental degradation. Eutrophication is also a major associated issue, algal blooms persistently occur. The occurrence of these blooms is associated with excess available Phosphorus. This phosphorus is derived as either particle bound from erosion of diffuse sources or as runoff of fertiliser p from cultivated and pastureland areas. The three major erosion sources of particle bound P are: i) sheet erosion of the 40% land surface under cultivation, ii) subsoil erosion from the significant number of channels and gullies that drain the region and iii) surface erosion from the pastureland and forested parts of the catchment. Fertilisers based on Nitrogen, P and K are used extensively in the catchment. The Bundella Ck catchment within the Namoi system, contains each of these landuses. As such it is an ideal location to determine the influence of these different diffuse sources to fluxes of sediments and p in this landscape. In this paper we use fallout tracers to quantify the proportionate contributions of sediments and diffuse P from these different sources. We also use measurements of REE and strontium isotopes to ascertain the contribution of fertilizer derived P compared to that from diffuse native P. We also create a topographic model to independently predict the contributions of sediment and P from these different sources. The strength of the model is its ability to charac-

terize not only fluxes of material from surface erosion, but also that from subsoil channel and gully erosion processes. We compare the results of sediment and P fluxes from the tracers and the topographic model and investigate the potential for applying the model to other parts of the landscape in which tracer data is not available.

Studies of natural and artificial radioactivity in Brazil

A. S. Paschoa

Studies of natural and artificial radioactivity started in Brazil, as well as in other countries, as a consequence of the 1956 recommendations of the United Nations Scientific Committee on the Effects of Atomic Radiation (UNSCEAR). Brazilian scientists from the Pontificia Universidade Católica do Rio de Janeiro and the Biophysics Institute of the then Universidade do Brasil (now, Universidade Federal do Rio de Janeiro – UFRJ) joined their efforts with American scientists from the New York University, with the support of the United States Atomic Energy Commission (USAEC) and the Brazilian Nuclear Energy Commission (Comissão Nacional de Energia Nuclear – CNEN). Such efforts resulted in wide research spectrum encompassing studies from radioactive fallout from weapons tests to natural radioactivity in soils and plants. The studies of natural radioactivity were carried out mostly in Morro do Ferro, Guarapari, and Araxá, which are known to be areas of elevated natural radioactive background. The radioactive fallout measurements were concentrated in Rio de Janeiro. In some cases the areas of elevated natural radioactivity are associated with rare earth sands (Guarapari), pyrochlore and apatite (Araxá), and bauxite (Morro do Ferro). Thus, such areas present opportunities to compare the original radioactive baseline vis-a-vis the current situation of the technologically enhanced naturally occurring radioactive materials (TENORM) in the same site. The studies of artificial radioactivity provide information on circulation of radionuclides from the weapons tests in the Southern Hemisphere. The paper will discuss the importance of re-examining the available data under new light.

Results of limited gamma spectrometry intercomparison on mineral sand products and associated issues

R. Kleinschmidt

G. Godwin

New radiation control legislation in Queensland, Australia provides for the exemption of abrasive blast material upon meeting a specified release criteria. Calculation of the release criteria is based on the measurement of uranium and thorium series radionuclides in the abrasive blast media. Past experience has shown that results from different facilities vary to the extent that the material may be exempt based on the results of one laboratory but not another. Queensland Health Scientific Services embarked on the trail of running a limited intercomparison for a sample of ilmenite, a commonly used mineral sand abrasive blast material, to establish sources of variation in reported results. The results of the program are presented with comment on their implications.

In situ determination of the depth distribution of ^{137}Cs by means of gamma spectrometry of primary and forward scattered photons

T. Hjerpe

C. Samuelsson

Stationary or mobile in situ gamma ray spectrometry is a useful tool for rapid estimations of environmental radioactivity inventories in the ground. A week point however, is that the vertical distribution of the activity in the ground must be known, in order to calculate the activity per unit surface area from an observed photon fluence rate. In the case of stationary measurements, the depth distribution in soil is commonly determined by analysing core samples by gamma spectrometry afterwards in the laboratory. In order to be representative, the number of samples to be analysed in the lab is roughly one hundred for each a 10x10 m^2 surface and a 30 cm depth module monitored. During mobile in situ spectrometry, large areas are covered and an on-line presentation of the result is given high priority. During such circumstances, traditional core sampling methods are not feasible and other more direct methods have to be used. One promising method for conversion of incoming spectral data in real time to both true area activity density and activity depth distribution is based on an analysis of the ratio between count rates from primary and forward scattered photons. The method is frequently referred to as the peak-to-valley ratio method. This contribution will describe our plans to adopt the peak-to-valley method to car-borne mobile gamma spectrometry using a large HPGe detector. Preliminary results from testing the method in the field, utilising a point source at different depths, will be presented.

Investigation of uranium and radium plant uptake from cover soil of uranium mining tailings ponds

P. Szerbin

E. Koblinger-Bokori

L. Juhász

The only Hungarian uranium mine in the vicinity of Pécs (South Hungary) was shut down in 1997. During the former operation residue of the ore processing was placed in natural environment. This action has lead to many environmental problems, first of all, it has created several environmentally unfriendly artificial formations. Such formations are the tailings ponds, which are potential sources of radioactive contaminants like uranium and radium. Uranium and ^{226}Ra contents of the pond water are 0.1 $mg.l^{-1}$ and 5.2 $Bq.l^{-1}$, respectively; those of the solid phase of the pond material are 70 $g.ton^{-1}$ and 12.7 $Bq.g^{-1}$, respectively. These contaminants may increase the radiation burden of population in this area via both aerial and terrestrial pathways. The partially dried-out tailings ponds are planned to be covered with different materials in order to reduce radon emanation and the plant uptake of the radioactive elements. Green plant cover is foreseen to reduce radionuclide release by wind and soil erosion. For this reason column experiments and pilot studies on the surface of the ponds have been carried out to find optimal solution for cover system. Environmental restoration of the uranium mining and milling sites will be performed on the basis of the results of those pilot studies In spite of these actions, the radioactive materials may still reach the upper layers by long-time migration and become available for plants. Bio-availability of radionuclides in soil is influenced by their chemical form and asso-

ciation with different geo-chemical phases. Consequently, the bio-available part of the radionuclides may enter the terrestrial food-chain pathway. The presentation deals with the results of investigations of plant uptake of uranium and radium from the soil of the uppermost pond covering layer. The investigation was carried out in laboratory conditions. The soil was labelled with uranium and ^{226}Ra. Four species of plants were selected for the study: Lolium multiflorum, Festuca rubra, Sinapis alba and Panikum miliaceum. The amount of mobile form of radionuclide in soil was determined by parallel extraction. Two types of extractants were used to determine radionuclide association with readily exchangeable forms and carbonate phases. The total amount of radionuclide was determined after extraction with nitric acid. A set of concentration factors was calculated from the ratio of soil and plant activity concentrations, for various soil extractants and plant types. Values of radium concentration factors related to the total amount of radionuclide in soil varied between $1.3\ 10^{-1}$ and $5.03\ 10^{-1}$, whereas the uranium concentration factors were between $3.8\ 10^{-1}$ and $1.2\ 10^{-1}$.These values are one order of magnitude higher if the concentration factors are related to the bio-available amount.

U-decay series studies of a redox front system in the Bangombé natural nuclear reactor zone (Gabon)

R. Bros
P. Roos
E. Holm
N. Yanase
T. Ohnuki

As part of a major natural analogue study of relevance to radioactive waste disposal, studies of naturally occurring U-series radionuclides have been carried out on the natural nuclear reactor found in the Bangombé uranium deposit (Gabon). Due to its shallow location within the zone saturated by groundwaters, this reactor has undergone extensive weathering phenomena. Radiochemical analyses by α and γ spectrometry show significant disequilibria of the $^{234}U/^{238}U$, $^{230}Th/^{234}U$, $^{226}Ra/^{230}Th$ pairs. Therefore, the Bangombé system has not been a closed system at least during the last 1 Ma until recently. The shales overlying the mineralization show oxidation effects related to the percolation of oxygenated waters from the surface. This has produced downward migrating redox fronts which dissolve inherited mineral phases, mostly Fe(II)-bearing chlorite, producing secondary alteration phases such as goethite, kaolinite and halloysite. U has been remobilized, transported and accumulated as U(VI) at the boundary between reduced black shales and oxidized pelites. The estimated rate of downward redox front movement is 15 m/Ma which also corresponds to the erosion rate if we assume a major role of erosion over the redox front movement. Selective chemical extractions with NH4 acetate and NH4 oxalate were performed in order to determine the U-bearing phases. The results indicate that most of U is extracted into the NH4 acetate phase and, therefore, U is mainly adsorbed onto clays.

Radioactivity and water column

Session 6

Chairman: R. Tinker

Session opening: P. Kershaw

Contrasting behaviour of artificial radionuclides in the Pacific and other ocean basins: radionuclides as tracers of environmental change?

Peter J. Kershaw
Hugh D. Livingston
Pavel Povinec
Hilde-Elise Heldal

Introduction

Ocean basins have received artificial radionuclides from a number of sources, including: global fallout from weapons testing, close-in fallout (e.g. Marshall Islands, Mururoa Atoll, Novaya Zemlya), dumped wastes (e.g. Sea of Japan, NE Atlantic, Kara Sea), accidental losses (e.g. SNAP-9A satellite, nuclear-powered vessels, nuclear weapons) and discharges into coastal regions (e.g. nuclear reprocessing facilities at Sellafield (UK) and La Hague (France)). In some cases the sources are well defined and in others it is more a case of estimating the size of the source from environmental measurements. These phenomena have provided a variety of tracers which can be used to describe the behaviour of artificial radionuclides in the water column and provide information on the underlying physics, biology and chemistry controlling their re-distribution.

This provides an opportunity to enquire whether artificial radiotracers can have a role in describing and quantifying the extent of environmental variability and change. In order to do this it is necessary to pose 2 fundamental questions:

What can observations of artificial radionuclide distributions tell us about ocean processes?

What can this information about observations and processes tell us about climate variability and environmental change?

To answer the first question we need to be able to clearly define the source terms and make adequate observations, both in space and time, of the radionuclide distributions. However, it is also essential to relate the observations to an adequate understanding of the underlying physics, biology and chemistry of the environment which are moderating the radionuclide behaviour. Some examples are presented below, from the Pacific and other ocean basins, to illustrate this point. To answer the second question we have to be able to define the variability, in space and time, of the observations and processes and link this to some index of environmental/climate variability. One example is presented, from the North Atlantic/ Arctic, where this approach is being attempted, comparing the distribution of mainly Sellafield-derived radionuclides with fluctuations in the North Atlantic Oscillation (NAO) as the index of environmental variability.

Radiotracers and ocean processes

Some datasets allow direct comparisons to be made between radionuclide distributions in different ocean basins. For example, Bourlat *et al.* (1996) presented ^{137}Cs, ^{90}Sr and $^{239,240}Pu$ concentrations in surface waters from the Pacific, Atlantic and Indian Oceans, from samples collected in 1992-1994. ^{137}Cs and ^{90}Sr both showed a latitudinal dependence but, in addition, concentrations in the Pacific were consistently higher (by ~ 0.5 $Bq.m^{-3}$) between 50° N and 30° S. The $^{137}Cs/^{90}Sr$ remained relatively constant (~ 1.7). The consistently

higher surface concentrations in these Pacific latitudes most likely results from the residual effects of the additional close-in tropospheric testing from the U. S. Pacific weapons tests in the Marshall Islands. This difference was evident in the 1950's and 60's (Volchok *et al.*, 1971), in the 1970's (Livingston *et al.*, 1985) and still remains (IAEA, 1985). A decrease in ^{137}Cs concentrations in surface waters has also been observed in the Mediterranean Sea, with a consequent increase in deeper waters. In this case the transfer is intimately linked to convection and the seasonal formation of deep and intermediate water (Papucci *et al.*, 1996). The Mediterranean also received a significant additional input of ^{137}Cs as a consequence of the Chernobyl accident. The penetration of tritium to deeper layers in the Atlantic provided good evidence of the degree to which ventilation was taking place, following the contamination of surface waters by bomb-tritium and subsequent formation of intermediate and deep water in the Nordic Seas (Nyffeler *et al.*, 1996).

In oligotrophic regions, covering much of the world ocean, most of the plutonium has remained in the water column, unlike in coastal and shelf regions where there is significant removal on biological particles in highly productive shelf areas and through contact with higher shelf sediment particulates. The situation in the NW Pacific with respect to plutonium is less straightforward, both because of the more complex environmental behaviour of plutonium, compared with Cs and Sr, and because there are 2 significant sources. In addition to stratospheric global fallout (maximum input in the early 1960s) there was a significant contribution from tropospheric fallout, originating from the Marshall Islands proving grounds from tests conducted in the early 1950s (Bikini and Enewetak Atolls). Many of these tests were conducted at or near ground level. This source has a higher $^{240}Pu/^{239}Pu$ ratio (0.24 vs. 0.18) and appears to be more rapidly removed from surface waters (Buesseler, 1997). It has also contributed to an increase in $^{239,240}Pu$ concentrations in bottom waters, as well as the underlying sediments. These surface tests tended to produce relatively large calcium-rich particles, unlike the smaller iron-rich particles associated with stratospheric fallout. An overview of plutonium behaviour in the Pacific was recently presented by (Livingston *et al.*, 1999). They also concluded that tropospheric fallout had contributed to plutonium inventories in the NW Pacific. This study benefited from having access to the large GLO-

MARD database (Global Marine Radioactivity Database), under development at the IAEA-MEL (IAEA in press; www.iaea.org/monaco/glomard). Sediment and water column inventories, based on GLOMARD data, decreased with both latitude and longitude from the Marshall Islands, consistent with an additional localised source. In contrast, the French weapons programme conducted at Mururoa and Fangataufa did not produce a significant tropospheric footprint, beyond a few km from the atolls. This was as a result of the conditions under which the detonations took place (underground, under water, and at a height of several 100s m). The lagoons act as a local source of radioactivity but this is not significant on a regional scale.

Livingston *et al.* (1999) compared water column profiles of plutonium concentrations from common sampling locations visited in 1973 (GEOSECS), 1978, 1980, 1982 and 1997. Certain common features were revealed, in particular the persistence of sub-surface ^{239,240}Pu concentration maxima (Figure 1). However, profiles from the central NW Pacific showed a consistent trend, with the sub-surface maxima both deepening and becoming less intense with time. The authors took all available data within a defined region (20° – 40° N and 135° – 175° E) and established a doubling-depth of the ^{239,240}Pu maximum of about 40 years, and a half-value of the concentration of about 22 years. Although it is tempting to conclude that this re-distribution is entirely biologically mediated – i.e. remineralisation of sinking biogenic particles (Hirose 1997) – there is reason to believe that physical processes may have a significant influence. Profiles of ^{137}Cs and ^{90}Sr, which are not expected to be involved in biomediation, also revealed a decrease in concentrations and inventories, having corrected for decay. This implies that water with lower concentrations has been advected into the region at depth. The need to consider a horizontal advective component when interpreting open ocean plutonium profiles has been discussed previously in respect of the NW Atlantic, and the southwards flow of high-plutonium North Atlantic Deep Water at intermediate depths (35-50% contribution) (Cochran *et al.*, 1987). The NW Pacific profiles also featured an increase in ^{239,240}Pu concentrations in bottom waters of about a factor of 2. This latter observation has not been recorded in the NE Pacific. Upper ocean profiles in the immediate vicinity of Bikini Atoll, which lies in the westward-flowing North

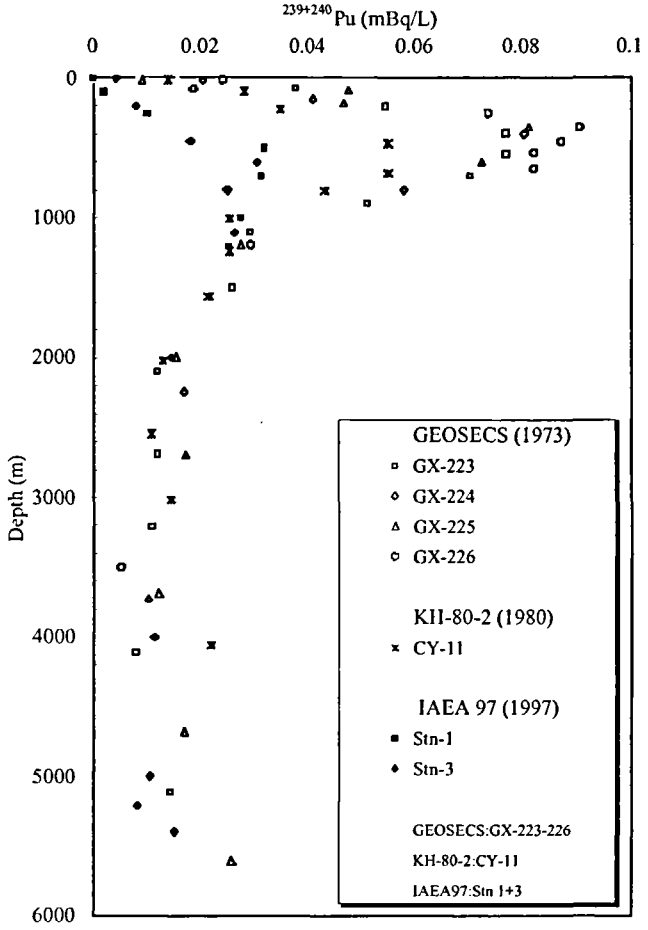

Figure 1
Vertical distribution of $^{239,240}Pu$ (Bq.m^{-3}) in the NW Pacific, in 1973, 1980 and 1997; from Livingston *et al.*, in press.

Equatorial Current, revealed that $^{239,240}Pu$ concentrations and inventories did not change significantly between 1973 and 1997. It is suggested that the concentrations were maintained by the continual re-supply of low-productivity water.

It is clear that observations of artificial radionuclide distributions as time-series at specific locations, vertical water-column profiles and

spatial surveys can all provide insights into ocean processes on a range of space and time scales. However, it is also apparent that interpretation of the data will be seriously compromised if due account is not taken of the underlying factors controlling the distribution. Some factors may be common to many regions of the world ocean but others may be specific to particular situations. One advantage of using water column measurements is that it may be easier to achieve sample homogeneity compared with sediment sampling.

Radiotracers and environmental variability

Water column radiotracer data can be used to identify transport mechanisms/pathways and sometimes to quantify the rate at which transport is taking place. This alone may require a considerable effort. However, to attempt to establish the degree of variability, and systematic change, in such processes presents a formidable challenge. The great advantage of utilising sediment core samples is that they can be dated, often independently, and a single core may encompass the entire period of interest. For water column work it is usually necessary to establish time-series of observations, as well as spatial distributions, and such data sets are often limited to particular locations or regions because of a specific radiological concern (e.g. Sellafield, La Hague, Marshall Islands, French Polynesia) or because of proximity to a research centre (e.g. La Spezia, Italy, annual sampling from 1960 to the present; Papucci *et al.*, 1996). These studies would have been undertaken for a variety of reasons in a variety of circumstances and this may limit their usefulness for environmental change investigations. However, they do provide an excellent basis for designing future programmes.

Fortunately there are examples of where the necessary combination of well-defined radiotracer inputs, oceanography and climate indices occur. The NE Atlantic has received a considerable input of artificial radionuclides as result of nuclear fuel reprocessing activi-

ties at Sellafield (UK, discharging into the Irish Sea since 1952) and La Hague (France, discharging into the English Channel since 1966). One of the main purposes of conducting distribution studies throughout the 1960s-1980s was to assess the likely impact of the releases, from the consumption of contaminated fish, by the whole population (i.e. calculating the Collective Dose). However, a number of investigators saw the value in using these freely-available tracers to examine transport pathways, transit times and transfer factors across the shelf and consequently the releases have been traced from the pipelines throughout the NW European Shelf, into the Baltic Sea, across the Nordic Seas (Norwegian, Greenland, Barents) and into the Arctic (see references cited in: Kershaw and Baxter, 1995). Of particular value from Sellafield were ^{134}Cs, ^{137}Cs, ^{90}Sr, ^{99}Tc and ^{129}I although Pu isotopes have also been used. The total quantities discharged from La Hague were much lower but also included characteristic tracers such as ^{125}Sb which has been measured extensively in the English Channel and the North Sea (Guegueniat *et al.*, 1997). In recent years there has been a tendency for discharges of most radionuclides from both sites to decrease substantially. This may have resulted in welcome reductions in the dose to human populations but it has meant that the analytical challenge of making the measurements has increased.

As a consequence of the reductions in direct discharges, the sediments of the Irish Sea, which represent a substantial repository of ^{137}Cs and transuranic elements, have become a significant source of ^{137}Cs and plutonium into the water column. This is in response to the lower water concentrations following flushing by Atlantic Water, characterised by background levels of activity. Despite this mechanism, the outflow from the Baltic Sea, contaminated by Chernobyl, has been the largest source of ^{137}Cs to the North Sea for the past decade. The $^{137}Cs/^{90}Sr$ ratio due to Chernobyl contamination falls in the same range as that from Sellafield, introducing ambiguity in applying this ratio to transport studies. Fortunately, developments during the 1990s, both analytical and in waste treatment procedures, have provided a further opportunity to utilise reprocessing tracers and compare the results of recent studies with those conducted in earlier years. There has been a steep increase in the quantity of ^{129}I discharged from La Hague, due to increased fuel throughput, and this nuclide can now be detected in small volume samples using the extremely sensitive technique of Accelerator

Mass Spectrometry (AMS) (Smith *et al.*, 1998). Likewise, at Sellafield there has been an increase in the quantity of ^{99}Tc discharged (Figure 2), although this has been in the form of a 'pulse' extending over a number of years, rather than the continuous increase in ^{129}I seen at La Hague. There has also been an increase in ^{129}I discharged from Sellafield (about 20% of the combined release). The development of AMS for ^{99}Tc has been problematic but several groups are now using ICP-MS routinely. Careful separation stages are required to remove interferences, as is the case for more standard radiometric methods.

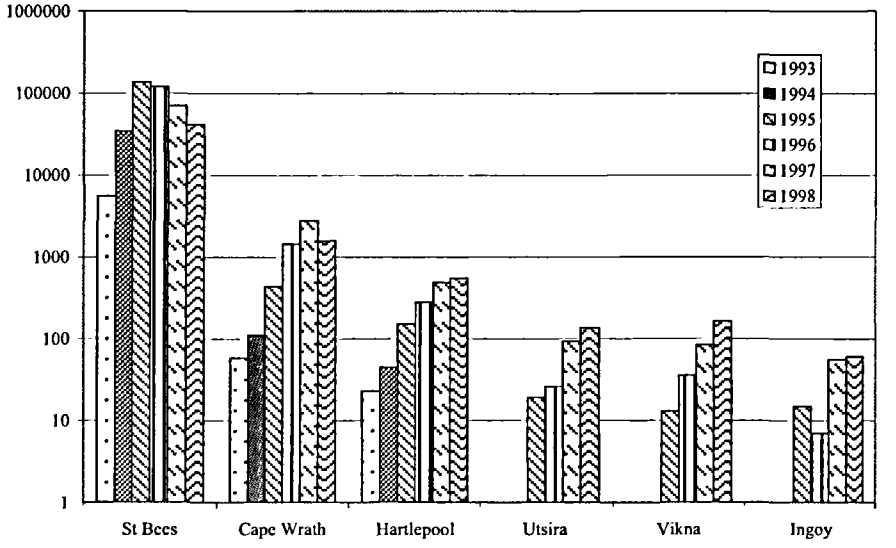

Figure 2
Discharge of ^{99}Tc (TBq.yr^{-1}) from Sellafield (UK) in to the Irish Sea 1978-1998.

The transport of the initial leading edge of the 1990s ^{99}Tc 'plume' (Figure 3) was much more rapid than had been anticipated, on the basis of the earlier transport time studies, especially within the first 2 years (Figure 4). Seawater samples were augmented with brown seaweed (*Fucus vesiculosus*) collected from around the coast of the

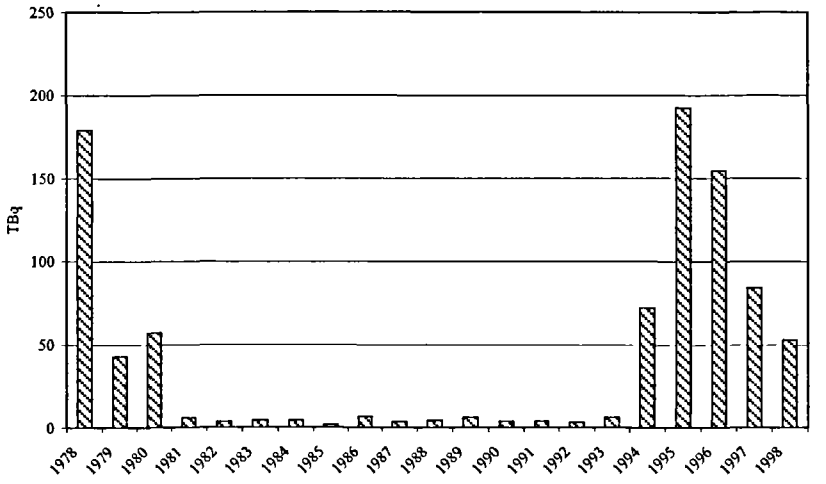

Figure 3
Concentration of ^{99}Tc (Bq.kg^{-1}, dry weight) in the brown seaweed *Fucus vesiculosus* collected from shoreline locations: near Sellafield (St Bees), NW Scotland (Cape Wrath), NE England (Hartlepool), SW Norway (Utsira, ~ 59° N), mid-Norway (Vikna) and northern Norway (Ingoy). The discharged increased in 1994.

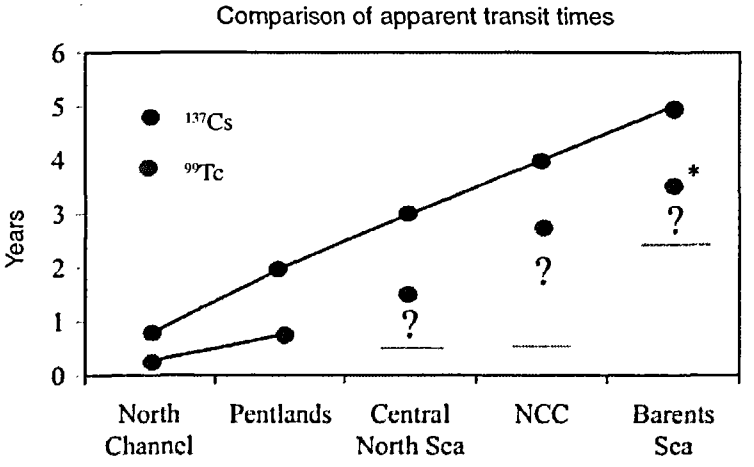

* Gordon Christensen pers. comm.

Figure 4
Comparison of apparent transit times from studies using Cs or ^{99}Tc: the North Channel is the northern exit of the Irish Sea, the Pentlands lie to the north of mainland Scotland, the NCC is the Norwegian Coastal Current.

UK and Norway (Heldal *et al.*, in prep) as this has a high concentration factor for ^{99}Tc (~ $1x10^5$) so provides an effective indicator of the spread of ^{99}Tc contamination. Heldal *et al.* (in prep) suggest that the difference in apparent transport rates is due, in part, to variations in the degree of atmospheric forcing, as indicated by the NAO. The NAO is a simple measure of mean, winter (December-March), surface pressure difference between Iceland (Stykkisholmur) and Lisbon (Portugal). Winters with a high mean pressure difference are described as having a high positive NAO index, and are characterised by increases in the number and intensity of storms, with accompanying higher precipitation, an increase in the flow of the North Atlantic Current and the formation of a shelf-edge jet-like current. There has been an overall increase in both the number of NAO positive years and the value attained by the index. The mid 1990s, when the ^{99}Tc releases increased, were marked by high positive values, in contrast to the lower values of the 1970s and 1980s, when most of the Cs-based transport studies were carried out. There may be other factors which are influencing the derived transit times but there seems to be sufficient consistency to justify further investigation, in particular with the application of mathematical models having adequate spatial and temporal resolution (Nies *et al.*, 1998). The NAO is one of about 12 indices which are routinely monitored, with the results being made freely available via the internet (e.g. National Centers for Environmental Prediction, www.ncep.noaa.gov). There is some evidence that the NAO variation is related to the fluctuations in the ENSO (El Niño Southern Oscillation). Radiotracers may provide a tool to describe the environmental response to these large-scale forcing events, and other climate-related phenomena. For example, it has been suggested that the degree of oligotrophy in the central Pacific is increasing in response to global warming and the consequential strengthening of the thermocline. One way to quantify this mechanism will be to determine whether there is an increase in radionuclide/metal residence times in surface waters, as might be anticipated.

Conclusions

Observations of artificial radionuclide distributions in the water column, in time and space, can provide valuable insights into the presence and rates of ocean processes - on physical scales from local to basin-wide and time-scales of days to decadal - providing something is known about the source term; i.e. the quantity, location and rate of entry into the marine environment, and the chemical behaviour of the radionuclides (i.e. conservative vs. non-conservative). Global stratospheric fallout represents the most significant source on a global scale, although it has had a strong latitudinal dependence and significantly higher deposition in the northern hemisphere (N:S, 3:1), as a result of the history of detonations and resulting yields. The distribution of ^{3}H has been particularly useful in illustrating the extent of ventilation in the North Atlantic. Vertical profiles of $^{239,240}Pu$ in the open ocean tend to exhibit a characteristic sub-surface maximum. This can be attributed partly to biological mediation but it is apparent that in the NW Pacific a component is due to lateral advection – a phenomenon also observed in the North Atlantic. It has been demonstrated, in the NW Pacific, that the magnitude of the sub-surface maxima has decreased and the position in the water column has deepened. Close-in fallout in the Pacific has had a minor impact in the environment around Mururoa and Fangataufa atolls, but near-ground tests in the Marshall Islands have contributed a significant input of plutonium to the NW Pacific. The addition of ^{238}Pu, preferentially into the southern hemisphere, as a result of the SNAP-9A satellite accident represents an underutilised tracer.

The controlled but variable releases of radionuclides from European reprocessing facilities, combined with the relative proximity of potential sampling sites to centres of population, have provided the

best opportunity so far to test whether radiotracers can be used as indicators of environmental variability. A comparison of transport times, from Sellafield to various locations in the North Atlantic and Nordic Seas, based on recent releases of ^{99}Tc (mid 1990s onwards) and older releases of ^{137}Cs (1970s-1980s) has revealed an apparent difference, with the former being faster. It is conjectured that this difference, at least in part, may be due to differences in environmental forcing linked to phenomena which can be characterised by fluctuations in the NAO. To test the validity of this initial conclusion it will be necessary to conduct simulations using sophisticated coupled ocean-ice models, covering the range of years for which Sellafield has been operating.

Aknowledgements
The first author (PJK) is indebted to the SPERA organisation for their generous support, allowing his participation. The project received support from the Ministry of Agriculture, Fisheries & Food (England & Wales) (PJK, project A1215), the IAEA (HDL & PPP) and the Norwegian Research Council (H-EH).

Bibliography

BOURLAT Y., MILLIES-LACROIX J.-C., LE PETIT G., BOURGUIGNON J., 1996 — "^{90}Sr, ^{137}Cs and ^{239,240}Pu in world ocean water samples collected from 1992 to 1994". *In* Gueguenіat P., Germain P., and Metivier H. (eds): *Radionuclides in the Oceans Inputs and Inventories*, Les Ulis, les editions de physique: 75-93.

BUESSELER K. O., 1997 — The isotopic signature of fallout plutonium in the North Pacific. *J. Environ. Radioact*, 36 (1): 69-83.

COCHRAN J. K., LIVINGSTON H. D., HIRSCHBERG D. J., SURPRENANT L. D., 1987 — Natural and anthropogenic radionuclide distributions in the Northwest Atlantic Ocean. *Earth Planet. Sci. Lett.*, 84: 2-3.

GUEGUENIAT P., KERSHAW P., HERMANN J., DU BOIS P. B., 1997 — New estimation of La Hague contribution to the artificial radioactivity of Norwegian waters (1992-1995) and Barents Sea (1992-1997). *Environmental Radioactivity in the Arctic*, Strand P. (ed), 202: 1-3.

HELDAL H.-E., KERSHAW P. J., CHRISTENSEN G.C. (in prep). — Transport of ^{99}Tc from Sellafield

along the Norwegian Coastal Current to the Arctic.

HIROSE K., 1997 — Complexation-scavenging of plutonium in the ocean. *Radioprotection*, 32 (C2): 225-230.

IAEA. (in press). — *Global Marine Radioactivity Database* (GLOMARD), IAEA, Vienna.

IAEA., 1995 — *Sources of radioactivity in the marine environment and their relative contributions to overall dose assessment from marine radioactivity (MARDOS).* Vienna, IAEA-TECDOC-838.

KERSHAW P., BAXTER A., 1995 — The transfer of reprocessing wastes from northwest Europe to the Arctic. *Deep Sea Res.*, 42 (6): 1413-1448.

LIVINGSTON H. D., BOWEN V. T., CASSO S. A., VOLCHOK H. L., NOSHKIN V. E., WONG K. M., BEASLEY T. M., 1985 — *Fallout Radionuclides in Atlantic and Pacific Water Columns from GEOSECS Data*, Technical Report, WHOI-85-19, Woods Hole.

LIVINGSTON H. D., POVINEC P. P., TOSHIMICHI I., TOGAWA O., 1999 — The behaviour of plutonium in the Pacific Ocean. *Plutonium in the environment*, Osaka, Japan.

NIES H., HARMS I. H., KARCHER M. J., DETHLEFF D., BAHE C., KUHLMANN G., OBERHUBER J. M., BACKHAUS J. O., KLEINE E., LOEWE P., MATISHOV D., STEPANOV A., VASILIEV O. F., 1998 — Anthropogenic radioactivity in the Nordic Seas and the Arctic Ocean-results of a joint project. *Deutsche Hydrographische Zeitschrift*, 50 (4): 313-343.

NYFFELER F., CIGNA A. A., DAHLGAARD H., LIVINGSTON H. D., 1996 — "Radionuclides in the Atlantic Ocean: a survey". *In* Guegueniat P., Germain P., Metivier H. (eds): *Radionuclides in the Oceans Inputs and Inventories*, Les Ulis, les editions de physique.

PAPUCCI C., CHARMASSON S., DELFANTI R., GASCO C., MITCHELL P., SANCHEZ-CABEZA J. A., 1996 — "Time evolution and levels of man-made radioactivity in the Mediterranean Sea". *In* Gueguenia P., Germain P., Metivier H. (eds): *Radionuclides in the Oceans Inputs and Inventories*, Les Ulis, les editions de physique.

SMITH J. N., ELLIS K. M., KILIUS L.R., 1998 — ^{129}I and ^{137}Cs tracer measurements in the Arctic Ocean. *Deep Sea Research*, 45 (I): 959-984.

VOLCHOK H. L., BOWEN V. T., FOLSOM T. R., BROECKER W. S., SCHUERT E. A., BIEN G. S., 1971 — *Oceanic Distributions of Radionuclides from Nuclear Explosions. Radioactivity in the Marine Environment.* National Academy of Sciences, Washington D.C. 42-89.

Export fluxes of organic carbon in the Western North Pacific determined by drifting sediment trap experiments and ^{234}Th profiles

Koh Harada

Yoko Shibamoto

Introduction

The s of carbon cycling on the Earth's surface is becoming more important because of increasing attention to the global climate change caused by the increasing CO_2 level in the atmosphere. Oceans are one of the largest sinks for atmospheric CO_2 making carbon cycling in the ocean also as important. Inorganic and organic carbon concentrations in seawater are controlled not only by physical and chemical processes, but also by biological processes. The biological processes vary season by season and day by day. This is a reason why a shorter time scale observation is needed.

In JGOFS studies, a time series observation in the subtropical region near Hawaii has been conducted (Karl and Lukas, 1996) and the Canadian group continues the observation at a station in the subarctic eastern North Pacific (Wong *et al.*, 1998). Since the difference between the eastern and western sides of the Pacific has been recognized, the Japanese group decided to initiate the time series

observation in the western side of the Pacific. We started the observation from June 1998 at 44°N, 155°E in the western North Pacific, where the biological activity in the surface ocean is relatively high. The station is named Stn. KNOT which means "Cooperative North Pacific Ocean Time Series".

In this time series study, we are investigating carbonate chemistry, gas constituents, nutrient dynamics, primary, new and export productions and biological communities.

In this paper, I will introduce primary results of the export flux. The export flux is a flux of materials from the surface layer to the deeper ocean, and it is mainly controlled by settling particles that is produced in the euphotic layer in the ocean surface. This process is very important because it controls the concentration of inorganic carbon in surface water and the concentration controls CO_2 exchange rate with the atmosphere. The drifting sediment tap experiment is very useful to estimate the export flux because we can collect the settling particles directly and many chemical components can be analyzed. However, the export flux estimated by the shallow sediment trap was doubtful because of the complicated flows in the upper ocean (Buesseler, 1991). Recently, ^{234}Th, a short-lived insoluble natural radionuclide in the uranium decay series, is widely used to estimate particulate fluxes and to calibrate the sediment trap fluxes (e.g. Coale and Bruland, 1985, Buesseler *et al.*, 1992, Cochran *et al.*, 1993). In this paper, I introduce the primary results of estimation of the export fluxes in the western North Pacific by the drifting sediment trap and ^{234}Th profiles.

Methods

Station KNOT, which is a station for time series observations of Japanese JGOFS activity, is located at 44°N, 155°E in the western North Pacific (Figure 1).

The drifting sediment trap experiments were carried out three times in November, December 1998 and May 1999 at the station in the

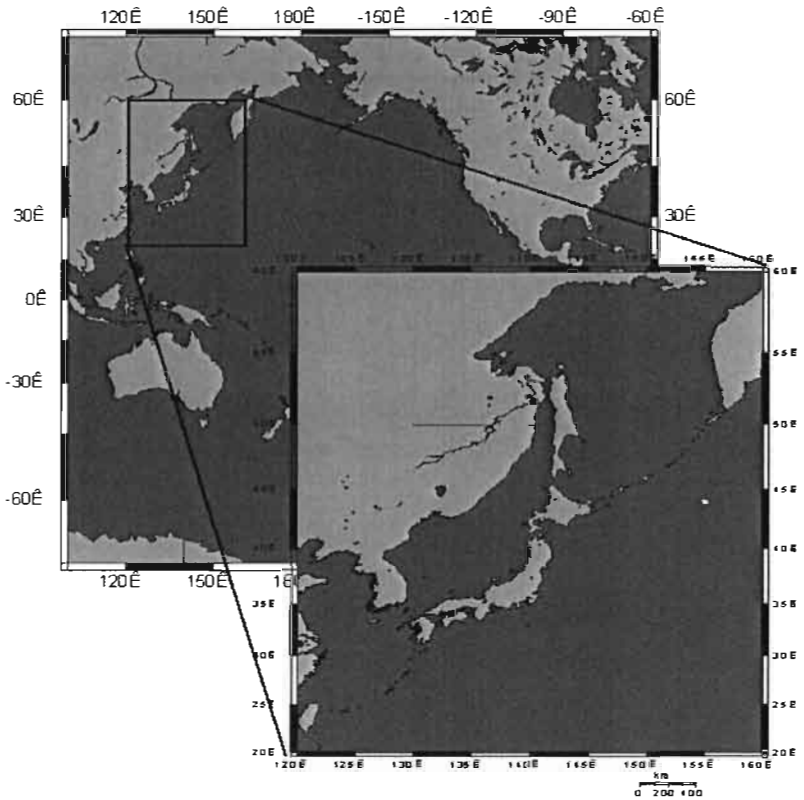

Figure 1
Map of the northwestern North Pacific showing a core location.

cruises of R/V Mirai. The sediment trap we used (Figure 2) is almost same design as one by Knauer *et al.* (1979). The array was deployed for two to three days at each experiment. Immediately after recovering the traps on the deck, particle samples were filtered on GF/F filters for organic carbon analysis and on Nuclepore filters for chemical and radiochemical analyses. The filter samples were brought to land laboratories and organic carbon and ^{234}Th were analyzed in Nagoya University and NIRE, respectively.

About 20 l of seawater samples were collected from 13 layers down to 300 m depth by Niskin bottles attached in a CTD-RMS. The seawater samples were through GF/F filters, and the filters

Figure 2
Picture of a drifting sediment trap used.

were used to determine "particulate ^{234}Th". "Dissolved ^{234}Th" was determined from the filtered seawater by the method of Harada and Tsunogai (1985) with some modification with liquid scintillation counting system.

Results and discussion

Vertical distributions of ^{234}Th in water column

In Figure 3, vertical distributions of particulate and dissolved ^{234}Th in the water column obtained in November 1998 were shown. The

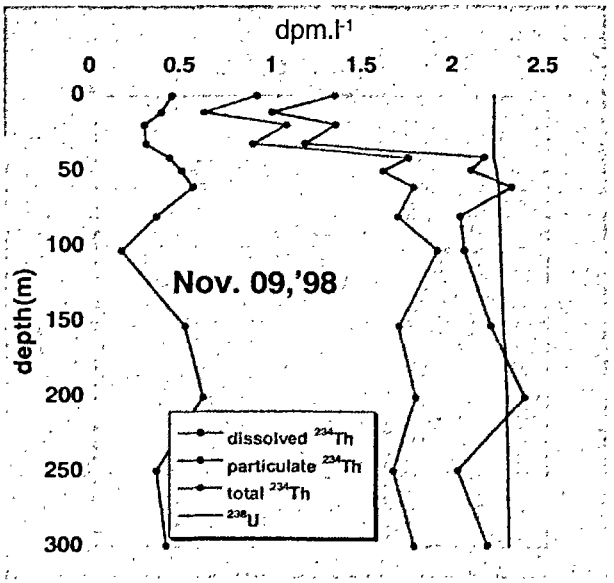

Figure 3
Vertical distributions of particulate, dissolved and total ^{234}Th at Stn. KNOT observed on November 9th 1998.

particulate ^{234}Th ranged from 0.2 to 0.6 dpm.l^{-1} and had no typical vertical trend. On the other hand, dissolved ^{234}Th in surface 30 m layer was significantly lower than one in the layer below 40 m depth. The sum of the concentrations of particulate and dissolved ^{234}Th in the deeper layer is almost the same as ^{238}U concentration, showing ^{234}Th is in equilibrium with its precursor. The removal flux of ^{234}Th can be calculated from a balance of ^{234}Th in the upper layer as follows, if steady state is assumed,

$$F_{Th} = \lambda_{Th} A_U - \lambda_{Th} A_{Th}$$

where, F_{Th} is ^{234}Th flux (dpm.m^{-2}.day^{-1}), λ_{Th} is decay constant of ^{234}Th (day^{-1}) and A_U and A_{Th} are activities (dpm.l^{-1}) of ^{238}U and ^{234}Th (total). From the vertical profile of ^{234}Th in November 1999, the ^{234}Th flux was calculated as 1,070 dpm.m^{-2}.day^{-1} and the estimations for other profiles are summarized in Table 1.

	234Th flux at 100m depth ($dpm.m^{-2}.day^{-1}$)		
	From Profile in water column	By sediment trap	ratio
November 1998	1070	730	0.68
December 1998	1050	710	0.68
May 1999	1490	1120	0.75

Table 1
Comparison of ^{234}Th flux obtained from water column profiles and sediment traps.

^{234}Th in the settling particles collected by the sediment trap

Results of the drifting sediment trap experiments are shown in Figure 4 and 5. The total mass fluxes decreased rapidly from surface to 100 m depth and below the depth the fluxes were almost constant or decreased gradually. The concentration of ^{234}Th in the settling particles were relatively constant in the surface layer, however, it tended to increase below the 100 m depth. The ^{234}Th flux by the traps was calculated multiplying the ^{234}Th concentration in the settling particles and the total mass flux. In Table 1, the ^{234}Th fluxes at 100 m depth are also summarized.

The ^{234}Th fluxes determined by sediment trap were always smaller than those obtained from ^{234}Th profiles in the water column. From this comparison, it was concluded that the trapping efficiency of the sediment trap we used was about 70 %.

Export flux of organic carbon at Stn. KNOT

Vertical profiles of organic carbon concentration and organic carbon/^{234}Th ratio in the settling particles are shown in Figure 6 and 7. The organic carbon concentration in the settling particles was almost constant at least down to 400 m depth and the POC/^{234}Th ratio decreased from the surface to 300 m depth gradually. If the ^{234}Th flux obtai-

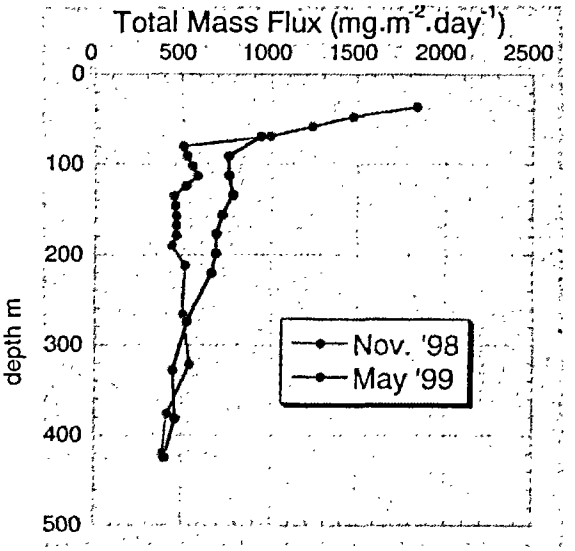

Figure 4
Total mass fluxes observed by the drifting sediment traps at Stn. KNOT in November 1998 and May 1999.

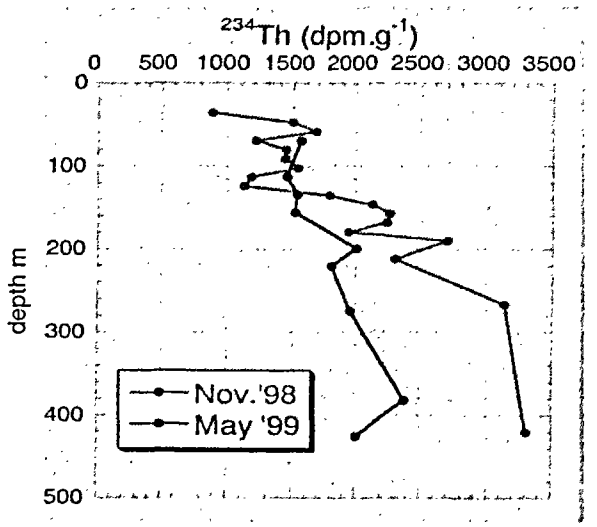

Figure 5
Concentration of ^{234}Th in the settling particles observed by the drifting sediment traps at Stn. KNOT in November 1998 and May 1999.

	^{234}Th flux ($dpm.m^{-2}.day^{-1}$)	POC/^{234}Th ($mmol.dpm^{-1}$)	POC flux ($mmol.m^{-2}.day^{-1}$)
November 1998	1070	6.1	6.5
December 1998	1050	5.2	5.5
May 1999	1490	6.2	9.2

Table 2
Estimation of export flux of organic carbon from ^{234}Th flux and org.C/^{234}Th in the settling particles.

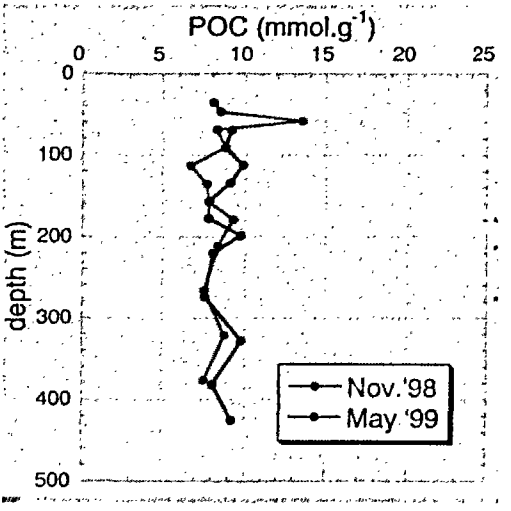

Figure 6
Concentration of organic carbon in the settling particles observed by the drifting sediment traps at Stn. KNOT in November 1998 and May 1999.

ned from the vertical distribution of ^{234}Th in seawater is correct, the organic carbon flux can be estimated from a the following equation,

$$F_{org.C} = F_{Th} \times (C_{org.C} / C_{Th})_{particle}$$

where $F_{org.C}$ is the organic carbon flux ($mmol.m^{-2}.day^{-1}$), F_{Th} is the ^{234}Th flux obtained from the water column profiles ($dpm.m^{-2}.day^{-1}$) and $(C_{org.C} / C_{Th})_{particle}$ is the organic carbon/^{234}Th ratio in the settling particles ($mmol.dpm^{-1}$). The estimated organic carbon flux was about 6 $mmol.m^{-2}.day^{-1}$ in winter and 9 $mmol.m^{-2}.day^{-1}$ in spring.
In the time series observation, primary production in the surface

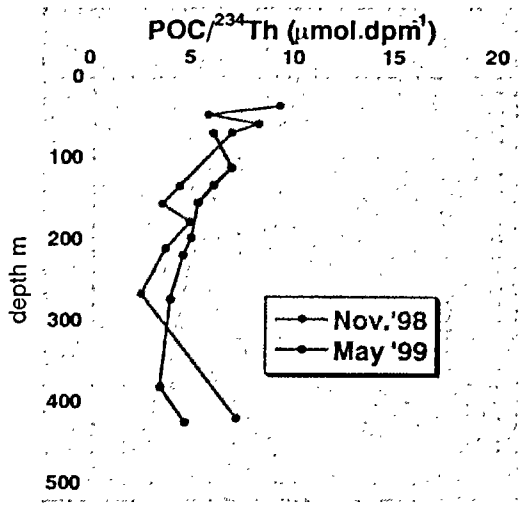

Figure 7
Ratio of organic carbon and ^{234}Th in the settling particles observed by the drifting sediment traps at Stn. KNOT in November 1998 and May 1999.

layer was also measured (Imai *et al.*, personal communication) and the export flux obtained here can be compared with the primary production. E-ratio, which is the ratio of the export flux to the primary production rate is 0.75 in winter and 0.21 in spring. In the observation in May 1999, we found many patches of phytoplankton bloom near Stn. KNOT although there was no bloom at St. KNOT, itself. From this observation, the western North Pacific near Stn. KNOT was in biologically active condition. In this condition, both the primary production and the export flux increase. However, it seems that the ratio becomes low, since regeneration of particulate organic matter in the surface layer also increases.

Conclusion

To investigate the export flux in the western North Pacific, drifting sediment trap experiments and 234Th observations were conducted.
1.Trapping efficiency of the drifting sediment trap was estimated as about 70 %.

2.Organic carbon flux at Stn. KONT was about 6 mmol.m^{-2}.day^{-1} in winter and 9 mmol.m^{-2}.day^{-1} in spring.
3.E-ratio in spring (0.21) was significantly lower than in winter (0.75), although the export flux in spring was high.

Aknowledgements
The authors would like to thank Dr. Narita, Hokkaido University, for helping sediment trap works and radiochemical analysis and also to thank scientists, technicians and crew on R/V Mirai for their help of sample collection.

Bibliography

BUESSELER K. O., 1991 — Do upper-ocean sediment traps provide an accurate record of particle flux ? *Nature*, 353: 420.

BUESSELER K. O., BACON M. P., COCHRAN J. K., LIVINGSTON H.D., 1992 — Carbon and nitrogen export during the JGOFS North Atlantic Bloom Experiment estimated from 234Th:238U disequilibria. *Deep-Sea Res. I*, 39: 1115.

COALE K. H., BRULAND K.W., 1985 — 234Th:238U disequilibria within the California Current. *Limnol. Oceanogr.*, 3081: 22.

COCHRAN J. K., BUESSELER K. O., BACON M. P., LIVINGSTON H. D., 1993 — Thorium isotopes as indicators of particle dynamics in the upper ocean: Results from the JGOFS North Atlantic Bloom Experiment. *Deep-Sea Res.*, 40: 1569.

HARADA K., TSUNOGAI S., 1985 — A practical method for the simultaneous determination of ^{234}Th, ^{226}Ra, ^{210}Pb and ^{210}Po in seawater. *J. Oceanogr. Soc. Japan*, 41: 98.

KARL D. M., LUKAS R., 1996 — The Hawaii Ocean Time-series (HOT) program: Background, rationale and field implementation. *Deep-Sea Res. II*, 43 (2-3): 129.

KNAUER G. A., MARTIN J. H., BRULAND K. W., 1979 — Fluxes of particulate carbon, nitrogen and phosphorus in the upper water column of the northeast Pacific. *Deep-Sea res.*, 26: 97.

WONG C. S., MATEAR R. J., WHITNEY F. A., ISEKI. K., 1998 — Enhancement of new production in the Northeast Subarctic Pacific Ocean during negative North Pacific Index events. *Limnol. Oceanogr.*, 43 (7): 1418.

Uranium decay series radionuclides in the Western Equatorial Pacific Ocean and their use in estimating POC fluxes

Gillian Peck

J. David Smith

Introduction

The naturally occurring radionuclides ^{226}Ra, ^{210}Pb and ^{210}Po are members of the ^{238}U decay series and have been used to study the kinetic aspects of material cycling in the ocean (Bacon *et al.*, 1976; Ritchie and Shimmield, 1991). These studies utilise the observed radioactive disequilibria in the ^{226}Ra, ^{210}Pb and ^{210}Po system. Particle fluxes may also be studied using disequilibria among naturally occurring radionuclides. $^{226}Ra/^{210}Pb$ and $^{210}Pb/^{210}Po$ ratios cover time scales of months to years and are suitable tracers for studying particle fluxes in the upper layer of the ocean.

^{210}Pb is added to the upper ocean by fallout from the atmosphere and by decay of ^{226}Ra in the water column. ^{210}Po is produced in seawater by decay of the ^{210}Pb. Both ^{210}Pb and ^{210}Po are removed from the upper ocean by radioactive decay and by adsorption onto particles followed by sinking. The input of ^{210}Pb from the atmosphere and removal by sinking particles combine to give a vertical concentration profile that can be used to calculate the ratios of the contributing processes. Measurements of the fractions of the radionuclides in the dissolved and particulate phases have been used in steady-state

box-models of adsorption/settling and radioactive decay to calculate radionuclide residence times (Bacon *et al.*, 1976; Ritchie and Shimmield, 1991; Towler and Smith, 1997). A likely mechanism for the removal of these radionuclides is adsorption onto other non-living biogenic material followed by sinking. Carbon dioxide in the atmosphere dissolves in the surface layer of the ocean. Transfer of carbon to the deep ocean is facilitated by fixation into particulate organic matter in the euphotic zone. Sinking of these biogenic particles from the upper layers of the ocean to the deeper layers is an important pathway in the global carbon cycle. Particle fluxes must be quantified if accurate carbon cycle models are to be developed.

Analyses were carried out on water samples of 30-40 l for particulate matter and 10 l for dissolved species using specially developed methods. These methods were developed with the specific aim of using small volumes of seawater to reduce the sampling time required when at sea. ^{226}Ra, ^{210}Pb and ^{210}Po profiles for the Bismarck Sea and western equatorial Pacific Ocean are presented. Using the ^{226}Ra, ^{210}Pb and ^{210}Po data, and a box-model based on that proposed by Bacon *et al.*, 1976, the average residence times of dissolved ^{210}Po and ^{210}Pb and particulate ^{210}Po in two layers of the upper 300 m of the ocean were estimated. The residence time of particulate ^{210}Po was used with the concentration of particulate organic carbon (POC) to estimate the flux of POC from the upper layer of the water column to the deeper layer. This work was a contribution to the international Tropical River-Ocean Processes in Coastal Settings (TROPICS) project.

Sampling

Water samples were collected at 5 locations in the Bismarck Sea and western equatorial Pacific Ocean during a strong El Niño phase on the August 1997 cruise of the *R.V. Franklin* (FR07/97) (Table 1). 10 l poly-vinyl chloride Niskin bottles on a rosette sampler were used to collect water from five depths at each station. This permitted collection of 3 bottles at 5m, 50m and 100m depth, and 4 bottles at 200m and 300m depth in two casts.

Station No. (Lat;Long)	Depth (m)	Specific Activity ($Bq.m^{-3}$)						
		^{226}Ra[a]	^{210}Pb			^{210}Po		
			Dissolved	Particulate	Total	Dissolved	Particulate	Total
1.	5	-	2.78± 0.09	0.033± 0.004	2.81	0.71± 0.03	0.34± 0.01	1.05
2°48'S;	50	-	2.86± 0.09	0.042± 0.004	2.90	0.84± 0.04	0.28± 0.01	1.12
145°06'E	100	-	2.45± 0.08	0.066± 0.005	2.52	0.82± 0.04	0.19± 0.01	1.01
	200	-	2.82± 0.09	0.162± 0.007	2.98	1.69± 0.11	0.20± 0.01	1.89
	300	-	2.81± 0.08	0.159± 0.007	2.97	1.60± 0.08	0.22± 0.01	1.82
2.	5	1.73	3.82± 0.09	0.031± 0.004	3.85	0.82± 0.04	0.34± 0.01	1.16
2°09'S;	50	1.73	2.65±0.08	0.035± 0.003	2.69	0.92± 0.05	0.35± 0.02	1.27
144°00'E	100	1.82	1.82± 0.07	0.047± 0.004	1.87	1.52± 0.06	0.17± 0.01	1.69
	200	1.82	2.37± 0.07	0.055± 0.003	2.43	2.47± 0.12	0.12± 0.01	2.59
	300	2.06	2.24± 0.07	0.057± 0.004	2.30	1.37± 0.06	0.15± 0.01	1.52
3.	5	1.41	3.14± 0.10	0.044± 0.003	3.18	0.74± 0.03	0.33± 0.01	1.07
0°00' N;	50	1.64	2.96± 0.09	0.028± 0.004	2.98	1.06± 0.04	0.45± 0.02	1.51
142°59'E	100	1.61	2.81± 0.09	0.035± 0.004	2.85	1.16± 0.05	0.24± 0.01	1.40
	200	1.97	2.10± 0.07	0.060± 0.003	2.16	1.90± 0.10	0.18± 0.01	2.08
	300	2.71	2.15± 0.07	0.060± 0.004	2.21	1.26± 0.06	0.10± 0.01	1.36
4.	5	0.96	3.01±0.09	0.031± 0.004	3.04	0.71± 0.04	0.41± 0.01	1.12
0°00'N;	50	1.18	3.58± 0.09	0.061± 0.004	3.64	1.18± 0.06	0.34± 0.01	1.52
146°60'E	100	1.52[b]	2.76± 0.10	0.032± 0.003	2.79	1.53± 0.06	0.19± 0.01	1.72
	200	2.21	2.56± 0.09	0.085± 0.005	2.65	1.48± 0.07	0.18± 0.01	1.66
	300	2.35	2.83± 0.09	0.072± 0.004	2.90	1.42± 0.07	0.17± 0.01	1.59
5.	5	1.02	3.21± 0.09	0.026± 0.004	3.24	0.70± 0.04	0.35± 0.01	1.05
0°00'S	50	1.11	3.73± 0.10	0.019± 0.003	3.75	1.12±0.04[c]	0.32± 0.01	1.32
152°00'E	100	1.44	3.39± 0.10	0.058± 0.004	3.45	1.13± 0.04	0.22± 0.01	1.35
	200	1.22	3.28± 0.08	0.057± 0.004	3.34	1.40± 0.06	0.13± 0.01	1.53
	300	1.21	2.53± 0.07	0.050±0.003	2.58	1.57± 0.07	0.12± 0.01	1.69

[a] ^{226}Ra data lost at station 1.
[b] Value taken as average of stations 3 and 5.
[c] Value taken as average of stations 4 and 5.

Table 1
Activity of radionuclides in depth profiles collected on FR07/97.
Particulate matter retained on 0.45 mm Millipore filter.

Experimental

Upon recovery sub-samples (~5 l) were removed for nutrient and particulate organic carbon analyses. The remaining volume was pressure filtered through Millipore HA membrane filters (47 mm diameter, pore diameter 0.45 µm). 10 l of filtered seawater from each depth was transferred to a glass vessel for the pre-concentration of

radionuclides. The filters containing the samples of particulate matter were placed in filter holders and stored at 4°C for later processing ashore.

Dissolved ^{226}Ra, ^{210}Po and ^{210}Pb were pre-concentrated from the filtered seawater samples using a modification of the method of Towler *et al.* (1996). Only a brief summary is given here. Filtered seawater (10 l) was acidified with HCl and standard additions of the yield tracers ^{208}Po (0.2 Bq), ^{133}Ba (8.0 Bq) and stable Pb (3 mg). After 1-2 h, the samples were neutralised by addition of sodium hydroxide solution. MnO_2-coated magnetite was added to each sample and stirred vigorously for 1 h. The magnetite was then simply collected using a magnet. The loaded magnetite adsorbent was stored under pure water in 50 ml plastic bottles and returned to the shore laboratory for further processing.

In the laboratory, the MnO_2 was dissolved in H_2O_2/ HCl and Po was spontaneously plated onto a spinning silver disc (Hamilton and Smith, 1986) that was presented for alpha-spectrometry. ^{210}Po was counted immediately and the activity of ^{210}Pb in the seawater sample was inferred from a second plating and measurement of ^{210}Po after allowing a suitable time for ingrowth. Recovery of the stable Pb yield tracer was measured using atomic absorption spectrometry and the appropriate correction made to the ^{210}Pb activity. ^{226}Ra in the residual solution was measured by liquid scintillation counting (Cooper and Wilks, 1981) after successive precipitations with $PbSO_4$ and $BaSO_4$ followed by re-solution in EDTA. A toluene-naphthalene scintillant was used. ^{226}Ra concentrations were corrected using the measured recovery of the ^{133}Ba yield tracer (Tinker & Smith, 1996).

Filters containing particulate ^{210}Pb and ^{210}Po were spiked with standard additions of stable Pb (3 mg) and ^{208}Po (0.2 Bq) and digested in gently boiling 2M HCl for 2 hours. The samples were filtered and the Po measured after plating on a silver disc as described previously. ^{210}Pb was inferred from a second count of ^{210}Po after ingrowth. All sample activity calculations involved correction from the mid-point of the count time to the time of sample plating/separation and also a correction for the period between plating and sampling. POC was determined after warming the defrosted

filters in super clean HCl in alumina ceramic micro boats, to remove PIC. This was followed by analysis of samples in the solid sample chamber of a Shimadzu 500 high temperature (900°C) catalytic analyser.

Results

Radionuclide data for the two Bismarck Sea and three equatorial Pacific Ocean profiles are summarised in Table 1. All errors are based on 1σ counting errors. These results are discussed in more detail elsewhere (Peck and Smith, 2000).

Modeling

Material balance equations based on the steady-state model of Bacon *et al.* (1976) were used to estimate the residence times and fluxes of ^{210}Pb and ^{210}Po from the upper layer of the ocean via the sinking of particles. A number of assumptions were required and are discussed in greater detail elsewhere (Peck and Smith, 2000). Density profiles plotted as σ_t *vs.* depth indicated that the base of the thermocline was at approximately 100 m depth, this corresponding to the base of the main pycnocline. Calculations, therefore, assumed a surface layer that was 100 m thick. This surface layer is referred to as Layer 1 in the model. The remaining samples were collected from 100-300 m depth. This range was chosen as the second layer and is referred to as Layer 2. The inventories in each layer were calculated for dissolved ^{226}Ra, dissolved and particulate ^{210}Pb and dissolved and particulate ^{210}Po. These inventories were then entered in the material balance equations that follow to calculate the flux and residence times of dissolved and particulate ^{210}Pb and ^{210}Po. Using the flux of ^{210}Pb, ^{210}Po and the concentrations of particulate organic

carbon, estimations of particulate organic carbon flux were made. The particulate organic carbon (POC) flux, R (mg C $cm^{-2}.year^{-1}$), was estimated using the equation shown below (15).

$$R = P_{Po}\left(\frac{C}{A_p}\right)$$

Where P_{Po} is the removal rate of particulate ^{210}Po ($mBq.cm^{-2}.year^{-1}$), from each layer, calculated in the box model, C is the inventory of the POC (mg C cm^{-2}) calculated for each layer and A_P is the inventory of the radionuclide ($mBq.cm^{-2}$) for each layer. These results are multiplied by 27.4 to convert from mg C $cm^{-2}.year^{-1}$ to mg C $m^{-2}.day^{-1}$. The results are summarised in Table 1.

Discussion

The equatorial Pacific Ocean is the largest oceanic source of CO_2 to the atmosphere and has also been proposed to be a major site of organic carbon export to the deep sea (Murray *et al.*, 1994). Much of what is known about the equatorial Pacific has come from the US Joint Global Ocean Flux Study (JGOFS-EqPac). The JGOFS studies set out to better characterise carbon fluxes in the high nutrient low chlorophyll (HNLC) regions of the central and eastern equatorial Pacific Ocean. These studies have suggested that the variability of remote winds in the western Pacific Ocean and tropical instability waves are major factors controlling physical and biological variability of these waters (Murray *et al.*, 1994). Carbon fluxes strongly depend on climate variability and in the equatorial Pacific Ocean the El Niño Southern Oscillation (ENSO) plays a major role in seasonal and annual variability in the productivity of these waters.

In contrast to the eastern/central equatorial Pacific Ocean, much less work has been done in the western equatorial Pacific Ocean. Barber and Kogelschutz, 1990, suggested that the ENSO, through modulation of the east-west tilt of the equatorial nitracline, was a

primary source of new production variability, reducing new production in the eastern Pacific and increasing it in the western Pacific during El Niño. Primary production in the western equatorial Pacific has been reported from the Australian JGOFS program during non El Niño and El Niño phases (Mackey *et al.*, 1997). In 1990 (FR08/90) from 5°S to 5°N along 155°E primary productivities of 96-241 mg C $m^{-2}.day^{-1}$ were recorded, productivities for the 1992 (FR05/92) and 1993 (FR08/93) cruises were in the range 220-620 mg C $m^{-2}.day^{-1}$ (Mackey *et al.*, 1997). The 1990 cruise was after the 1988/89 La-Niña but before the 1991/92 El-Niño. The 1992 and 1993 cruises were at the middle to end of a prolonged El-Niño event. This increase in productivity during an El-Niño phase supports the link proposed by Barber and Kogelschutz (1990).

Until recently POC fluxes in the western equatorial Pacific had not been recorded (Dunne *et al.*, 2000). In this study POC fluxes were calculated using the POC inventory with the removal rate and inventory of particulate ^{210}Po. The average POC flux sinking out of Layer 1 was 104 mg C $m^{-2}.day^{-1}$ and from Layer 2 was 180 mg C $m^{-2}.day^{-1}$, an increase of POC flux with depth. In the western equatorial Pacific Ocean POC fluxes of 49.2 mg C $m^{-2}.day^{-1}$ at 0°N,167°E (Rodier and Leborgne, 1997), 118.8 mg C $m^{-2}.day^{-1}$ for 0°N,165°E and 97.2 mg C $m^{-2}.day^{-1}$ at 0°N,175°E (Dunne *et al.*, 2000) have been reported for depths of 100 m, 120 m and 120 m respectively. These POC fluxes are in a similar range to the fluxes reported in this study for Layer 1. However, increase in carbon flux down the water column is not expected in the western equatorial Pacific Ocean and the results from this work are not strongly supported by the productivity results for this region. Increased fluxes of particulate matter of 130 mg C $m^{-2}.day^{-1}$ at 50 m and 210 mg C $m^{-2}.day^{-1}$ at 250 m in the Mediterranean Sea, off Monaco have been reported by Fowler *et al.*, 1986. POC fluxes for the central and eastern equatorial Pacific Ocean have been more widely studied and those cited in this paper range from 23-146 mg C $m^{-2}.day^{-1}$. POC fluxes calculated from data collected on FR07/97 and comparative results from the literature are summarised in Table 2.

Carbon flux depends strongly on the physical processes; horizontal advection, diffusion, upwelling rates and wind speeds. In the equatorial Pacific these processes have been shown to cause variation in

Location	Depth (m)	POC Flux (mg C $m^{-2}day^{-1}$)	Year of Sampling	Method
This Study[a]				
2°48'S, 145°06'E	100	70-125	August 1997	Box Model:
2°09'S, 144°00'E		104 ± 21	(El-Niño)	Polonium-210
0°00'N, 142°59'E				
0°00'N, 146°60'E	300	150-210		
0°00'S, 152°00'E		180 ± 22		
Rodier & Leborgne 1997				
0°N, 167°E	100	49.2	October 1994	Drifting
0°N, 150°W	100	204	(El-Niño)	sediment trap
Dunne *et al.* 2000				
0°N, 165°E	120	70.8	October 1994	Combined
0°N, 150°W	120	146.4	El-Niño	drifting sediment
0°N, 165°E	120	118.8	April 1996	trap/Th-234
0°N, 175°E	120	97.2	Mild La-Niña	
Murray *et al.* 1996				
0°N, 140°W	120	72	February 1992	Combined
0°N, 140°W	120	120	August 1992 (El-Niño)	drifting sediment trap/Th-234
Bacon *et al.* 1996				
0°N, 140°W	120	23	March-April 1992	
	120	29	October 1992 (El-Niño)	Th-234
Raimbault *et al.* 1999				
0°N, 150°W	200	80-90	November 1994 (El-Niño)	Drifting sediment trap
Fowler *et al.* 1986				
Off Monaco	50	130	N/A	Sediment trap
	150	136		
	250	210		
Buesseler et al. 1995				
0°N, 140°W	100	36-60	1992	Th-234
Karl *et al.* 1996				
Station ALOHA	150	29	Average over	Drifting
22°45'N, 158°W			1990-1992	sediment trap
Central North Pacific				

[a]POC fluxes reported are the range and average values for the five sampling sites.

Table 2
Particulate organic carbon fluxes for oceanic seawater samples.

primary productivity with strong interannual and seasonal variability (Mackey *et al.*, 1997). Variability in the physical processes of horizontal advection, diffusion and wind speed would play a greater

role in the variability of POC flux from the upper layer of the ocean at the equator in the Pacific Ocean. These processes would not effect the lower layer to the same extent. Possible explanations for the observed increase in POC flux from the lower layer are; upwelling of nutrient rich water or diel migration of zooplankton. Estimates of POC export flux using ^{234}Th found an increase in upwelling by a factor of two causing the POC export flux to increase by 50% at the equator (Buesseler *et al.*, 1995).

Steinberg *et al.* (2000) found that approximately 15-50% of zooplankton biomass above 500 m vertically migrates into surface waters at night. Zooplankton biomass in the upper 160 m can nearly double at night due to vertically migrating zooplankton. This migration can cause increased POC fluxes in the mid-layers of the ocean.

Conclusion

There is a wide range of reported POC fluxes in the upper layers of the ocean. It is a common feature of the use of radionuclides as tracers of marine processes, that radionuclides of different half-lives yield particle fluxes of different magnitudes. Particle fluxes estimated using the same radionuclide system by different workers are generally similar. Care must be taken if particle fluxes obtained using one radionuclide system are to be compared with those obtained using different radionuclides or from the use of sediment traps.

Comparisons of POC fluxes obtained from the same study site using different radionuclide systems and using sediment trap measurements would help quantify the aspects of particle sinking that each method actually determines. This work has added to the literature for estimates of POC fluxes in the western equatorial Pacific Ocean, but highlights that future studies aimed at further understanding the relationship between the chemical, physical and biological processes in the ocean are warranted.

Aknowledgements

We thank the Hydrography Group of CSIRO, Marine Research, Hobart and particularly D. Mackey as cruise leader. We thank the master and crew on the *R.V. Franklin.* We also thank Dr Kathy Burns of the Australian Institute of Marine Science for POC determinations and the Australian Research Council for financial support.

Bibliography

BACON M. P., SPENCER D. W., BREWER P. G., 1976 – $^{210}Pb/^{226}Ra$ and $^{210}Po/^{210}Pb$ disequilibria in seawater and suspended particulate matter. *Earth & Planetary Science Letters* 32: 277-296.

BACON M. P., COCHRAN J. K., HIRSCHBERG D., HAMMAR T. R., FLEER A. P., 1996 – Export flux of carbon at the equator during the EqPac time-series cruises estimated from ^{234}Th measurements. *Deep-Sea Research II.*, 43: 1133-1153.

BARBER R.T., KOGELSCHATZ J.E., 1990 – "Nutrients and productivity during the 1982/83 El-Niño ". *In*: Glynn P.W. (ed.) : *Global consequences of the 1982/83 El Niño-Southern Oscillation Event.* Elsevier, Amsterdam.

BUESSELER K. O., ANDREWS J. A., HARTMAN M. C., BELASTOCK R., CHAI F., 1995 – Regional estimates of the export flux of particulate organic carbon derived from thorium-234 during the JGOFS EqPac program. *Deep-Sea Research II.*, 42 (2-3): 777-804.

COOPER M. B., WILKS M. J. 1981 – *An analytical method for radium (^{226}Ra) in environmental samples by the use of liquid scintillation counting. Australian* Radiation Laboratories, Melbourne, ARL/TR040.

DUNNE J., MURRAY J. W., RODIER M., HANSELL, D. A., 2000 – Export flux in the western and central equatorial Pacific: zonal and temporal variability. *Deep-Sea Research I.*, 47: 901-936.

FOWLER S. W., HEUSSNER S., HEYRAUD M., LAROSA J., BOJANOWSKI R., 1986 – "Vertical transport studies in the coastal Mediterranean". International Laboratory of Marine Radioactivity. Biennial Report 1983-1984. IAEA, Vienna, IAEA-TECDOC-380.

HAMILTON T. F., SMITH J. D., 1986 – Improved alpha energy resolution for the determination of polonium isotopes by alpha-spectrometry. *Applied Radiation and Isotopes.*, 37: 628-630.

KARL D. M., CHRISTIAN J. R., DORE J. E., HEBEL D. V., LETELIER, R. M., TUPAS, L. M., WINN, C. D., 1996 – Seasonal and interannual variability in primary production and particle flux at Station ALOHA. *Deep-Sea Research II*, 43 (2-3) 539-568.

MACKEY D. J., PARSLOW J., GRIFFITHS F. B., HIGGINS H. W., TILBROOK B., 1997 –

Phytoplankton productivity and the carbon cycle in the western equatorial Pacific under El Niño and non-El Niño conditions. *Deep-Sea Research II.*, 44 (9-10): 1951-1978.

Murray J. W., Barber R. T., Roman M. R., Bacon M. P., Feely R. A., 1994 – Physical and biological controls on carbon cycling in the equatorial Pacific. *Science.*, 266: 58-65.

Murray J. W., Young J., Newton J., Dunne J., Chapin T., Paul B., McCarthy J. J., 1996 – Export flux of particulate organic carbon from the central equatorial Pacific determined using a combined drifting trap-^{234}Th approach. *Deep-Sea Research II.*, 43, (4-6): 1095-1132.

Peck G. A. Smith J. D., 2000 – Distribution of dissolved and particulate ^{226}Ra, ^{210}Pb and ^{210}Po in the Bismarck Sea and western equatorial Pacific Ocean. *Marine & Freshwater Research.*, 51: 647-658.

Raimbault P., Slawyk G., Boudjellal B., Coatanoan C., Conan P., Coste B., Garcia N., Moutin T., Pujo-Pay M., 1999 – Carbon and nitrogen uptake and export in the equatorial Pacific at 150°W: Evidence of an efficient regenerated production cycle. *Journal of Geophysical Research.*, 104: 3341-3356.

Ritchie G. D., Shimmield G. B., 1991 – "The use of ^{210}Po/^{210}Pb disequilibria in the study of the fate of marine particulate matter". *In*: Kershaw P. J., Woodhead D. S. (eds.) *Radionuclides in the Study of Marine Processes.* Elsevier Applied Science: 142-153.

Rodier M., Leborgne R., 1997 – Export flux of particles at the equator in the western and central equatorial Pacific Ocean. *Deep-Sea Research II.*, 44 (9-10): 2085-2113.

Steinberg D. K., Carlson C. A., Bates N. R., Goldthwait S. A., Laurence P. M., Micheals A. F., 2000 – Zooplankton vertical migration and the active transport of dissolved organic and inorganic carbon in the Sargasso Sea. *Deep-Sea Research I.*, 47: 137-158.

Tinker R. A., Smith J. D., 1996 – Simultaneous measurement of radium-226 and barium-133 using liquid scintillation counting with pulse shape discrimination., *Analytica Chimica Acta.*, 332: 291-297.

Towler P. H., Smith J. D., Dixon D. R., 1996 – Magnetic recovery of radium, lead and polonium from seawater samples after preconcentration on a magnetic adsorbent of manganese dioxide coated magnetite. *Analytica Chimica Acta.*, 328: 53-59.

Towler P. H., Smith J. D., 1997 – Distribution of ^{226}Ra and ^{210}Pb in the mixed layer of the western equatorial Pacific Ocean. *Marine and Freshwater Research.*, 48: 371-375.

Origin and transport of radium in the water column of Buena Coastal Lagoon

Dejanira C. Lauria

José Marcus de Oliveira Godoy

Introduction

The radium concentration in surface waters normally ranges from 0.01 to 0.1Bq.l^{-1} (Iyengar, 1990), with high values found in waters close to uranium mining and milling (Iyengar, 1990; Paschoa *et al.*, 1979 and Benes, 1990). In groundwater, the Ra concentration can reach values up to 38 Bq.l^{-1}, depending on factors such as the kind of aquifer rock as well as chemical and physical characteristics of water (Gascoyne, 1989). Based on groundwater data, a correlation between salinity and radium is expected (Kramer and Reid, 1984; Langmuir, 1985); therefore, among others the lower concentration of radium in surface waters than in ground waters could be credited to the lower values of salinity normally found in surface waters. Well known is the increase of the dissolved radium concentrations in the estuarine region due to salinity effects (Hancock and Murray, 1996; Moore and Shaw,1998).

The so-called Buena Lagoon is a high salt coastal lagoon located close to the border between Rio de Janeiro and Espirito Santo States, Brazil, in a monazite rich region. Its waters are used by a hydrogravimetric monazite sand separation mill. In the waters of

Buena lagoon abnormal concentrations of ^{226}Ra and ^{228}Ra were found, which at first could be credited to the activities at this mill. However, the high chemical and mechanical stability of the monazite is responsible for the negligible releasing of radionuclides from it and consequently the short contact time of the water with the sand minerals during the hydrogravimetric processing would not be sufficient to promote the releasing of radionuclides from the ore. Additionally, higher radium concentrations were observed upstream instead of downstream from the effluent discharge point. So, the aim of this research was to identify the origin of the observed high radium concentrations and to study its transport in the water column of the lagoon.

Material and methods

The study area

Buena Lagoon is located in Rio de Janeiro State, Brazil, between the coordinates 21° 23'- 21° 24' S and 41° 00'- 41° 03' W (Figure 1). Its watercourse surface area is 0.11 km^2 (113 000 m^2), its length is 5.4 km and it is on average 21 m wide. Its wetland has an area of 0.67 km^2, largely covered by aquatic vegetation, mainly *Typha Dominguesis* Pers., and its catchment area comprises 7.5 km^2. The lagoon is separated from the ocean by a barrier of sand approximately 15 meters wide. Once or two times a year, fishers open its mouth and its water inflows in the direction of the sea. A physical separation plant aiming the heavy mineral separations uses the water of Buena Lagoon and after the water is used, it is returned to the place where it was taken from (sampling station 5, Figure 1). The regions climate is tropical, warm and wet, with rainy (approximately October-February) and dry (approximately March-September) seasons. Mean annual rainfall is about 760 mm.

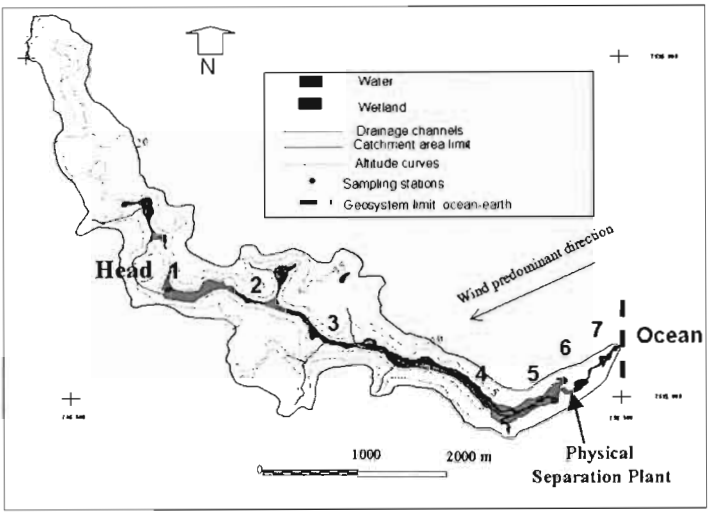

Figure 1
Map of Buena lagoon containing the localization of the sampling points.

Sampling

About 4.5 l samples, 4 l in a polyethylene bottle and 0.5 l in a dark glass bottle, were collected at each sampling point, in the rainy and in the dry seasons, from June/95 to December/97. Sediment and water samples were collected in the seven sampling stations along the lagoon. Eh, pH and conductivity were measured directly at the site. On a time scale shorter than one hour, the samples were taken to a clean lab and the aliquot storage in the glass bottle was filtered with glass fiber for the determination of nitrate, phosphate and organic and inorganic carbon; afterward the aliquot was again put in a dark glass flask and preserved frozen until the day of the determinations. The other 3.5 l samples were filtered (Millipore membrane) and were then acidified with nitric acid supra pure for the determination of the radionuclides and cations. 0.5 l Samples were stored without acidification fror the sulfate and chlorine determination.

Chemical analysis methods

Anions: Classical chemical methods were applied to the determination of anions in the water samples. Sulfate was determined by turbidimetry, chloride by the Volhard's argentometric method, nitrate by spectrophotometric method after its reduction to nitrite on a cadmium/copper column and phosphate by the ammonium molibdate/ascorbic acid method and the alkalinity by acid tritation (Standard Methods, 1975).

Organic and inorganic carbon: Both organic and inorganic carbon were determined by a Carbon Analyzer Beckman 915B.

Cations: Cations in general, including major cations, rare earth elements, uranium and thorium were analyzed by inductively coupled plasma-mass spectrometry, ICP-MS, Perkin-Elmer ELAN 5000, after a dilution 1:20 with water quality Milli-Q, applying the so-called "TotalQuant" method using In and Tl as internal standards. A total of 27 elements were used for the equipment mass efficiency calibration.

^{228}Ra and ^{226}Ra: Using 1-liter sample, ^{228}Ra and ^{226}Ra were analyzed applying the procedure described by Godoy (1990). The accuracy of such determination is routinely tested by inter-laboratory exercises organized by the EPA/USA and the Radionuclide Metrology Division of IRD/CNEN (Vianna, Tauhata, de Oliveira, Clain and Ferreira, 1998).

Results and discussion

Among seven and four sampling campaigns were performed at each sampling station, as station one was the last station discovered, only four sampling campaigns were performed at this station. The complete data set was composed by 1065 single measurements of the 28 variables (Na, K, Mg, Ca, Mn, Fe, Al, Si, La, Ce, Pr, Nd, Sm, Th, U, ^{226}Ra, ^{228}Ra, ^{210}Pb, F^-, Cl^-, SO_4^{2-}, NO_3^-, Dissolved Organic Carbon, Inorganic Carbon, pH, Eh, Alkalinity and Conductivity).

Comparing the values of the variables at the same station, no significant differences among the values in the dry and in the rainy seasons was observed. The normality distribution tests for each variable showed that the data were log-normally distributed. Statistical tests were performed with the data transformed into their logarithms allowing the central tendency and dispersion to be represented by the geometric mean and geometric standard deviation for each station (Wayne,1990). The exception was the pH data set. The central tendency and dispersion were represented by arithmetic mean and standard deviation as the pH data set was already in the logarithm form. The central tendency and the dispersion for the most representative variables (Th, U, ^{228}Ra, ^{226}Ra, Cl^- and pH) at the sampling stations are shown in Table 1.

The comparison of the geometric mean and the geometric standard deviation of each variable among the sampling stations (respectively by t-test and F-test) showed four different distribution patterns along the lagoon: *i)* the mean is the representative value of concentration for all stations, including the behavior of Th, Fe, Mn and dissolved organic carbon; *ii)* the highest values of concentration were found at station 1, while in all the other stations the concentrations had the same mean value. The variables of this set are Si, Eh and nitrate. Uranium belongs to this set, however its behavior is a little bit different, since at station 7 its concentration value increased; iii) the concentrations increased with the proximity of the sea. To this data set belongs the major ions (Na, K, Ca, Mg, Cl^-, F^- , SO_4^{2-}) and the pH and iv); the fourth data set showed a behavior opposite to the last distribution, the values of the concentration decreased with proximity to the sea. To this variable set belongs the radium isotopes and the light rare earth elements.

Investigating the radium origin

In order to identify the main sources of ions to the lagoon water, factor analysis was employed, using the complete data set. Factor analysis is a technique suitable for simplifying large and complex data sets, creating a limited number of factors, each representing a cluster of interrelated variables within a data set (Zhu *et al.*, 1997). For the extraction methods the Principal Component Analysis method (PCA)

Station	Distance from the Lagoon head (m)	Th µg.l⁻¹	U µg.l⁻¹	^{226}Ra Bq.l⁻¹	^{228}Ra Bq.l⁻¹	La µg.l⁻¹	PH	Cl^- mg.l⁻¹
1	0	0.05	1.10	0.36	1.52	26	4.2	487
		(1.50)	(2.39)	(1.23)	(1.33)	(1.86)	(0.1)	(1.76)
2	800	0.14	0.04	0.26	0.63	2.37	5.9	650
		(4.41)	(4.38)	(1.20)	(1.35)	(2.51)	(0.2)	(2.40)
3	1900	0.08	0.03	0.25	0.49	1.75	5.9	864
		(3.06)	(5.70)	(1.93)	(1.68)	(5.89)	(0.2)	(2.22)
4	3700	0.14	0.03	0.15	0.20	0.16	6.3	1217
		(4.31)	(6.09)	(1.32)	(1.41)	(3.25)	(0.2)	(1.37)
5	4500	0.08	0.04	0.17	0.18	0.54	6.7	1060
		(3.58)	(3.65)	(2.31)	(1.82)	(7.14)	(0.2)	(1.85)
6	4900	0.07	0.12	0.14	0.10	0.09	6.9	1627
		(2.00)	(1.50)	(1.46)	(1.47)	(5.59)	(0.4)	(1.26)
7	5400	0.10	0.42	0.08	0.12	0.14	7.3	2295
		(3.08)	(2.24)	(1.36)	(1.27)	(3.17)	(0.3)	(1.61)

( ) standard deviation

Table 1
Values of the geometric mean and geometric standard deviation of the Th, U, ^{226}Ra, ^{228}Ra and Cl^- concentrations and of the arithmetic mean and standard deviation of pH in the lagoon water.

was applied and those variables with a large number of values close or below the detection limits, such as Th and Al, were excluded. The extraction showed that 82 % of the variance could be explained by only three components (Component 1: 39 %, Component 2: 32 % and Component 3: 11 %). Component 1 joins all the light rare earth elements and the radium isotopes, showing a strong relationship with the constituent elements of the monazite. Component 2 aggregates the set of seawater variables and it represents the seawater influence on the lagoon water composition and Component 3 unites elements which can be released from the rock weathering such as Fe and Mn (Figure 2). Uranium has two different sources, one from the same source of the Component 1 and the other from the Component 2 (sea water).

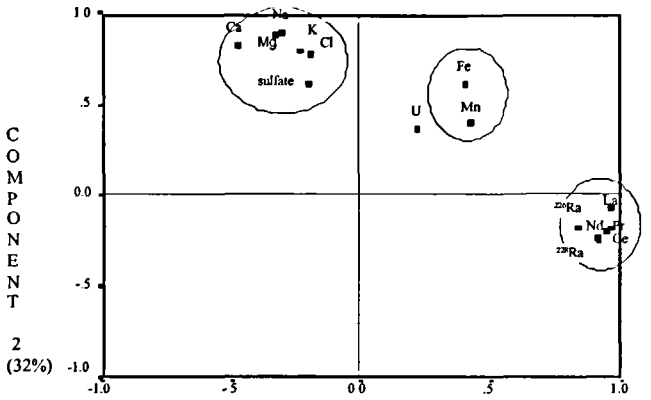

Figure 2
Plot of loadings on component 1 to 2.

The factor analysis indicated that the gradient of the variable concentrations along the lagoon were due to two water sources located at opposite sides of the lagoon. The seawater can supply the major ions by seawater infiltration and atmosphere deposition. The groundwater supplies the radium isotopes and the light rare earth elements (LREEs).

Based on this data set, the approximate location of the radium source may be in the area surrounding station one. This was confirmed by the discovery of several water springs feeding a channel (consructed by local farmers) flowing in the direction of the lagoon head (station one). The distance from the springs to the lagoon head was around 100 meters. The channel was totally covered by vegetation, making its location difficult. The spring waters had between 1.7 and 2.5 Bq.l^{-1} of ^{228}Ra and around 0.5 Bq.l^{-1} of ^{226}Ra and its pH value was around 3.7.

The water springs are salt water (salinity 14 ‰) and have a low pH (3,7). It is well established that increasing cation concentrations will lead to competition with Ra for adsorption sites. Consequently, in saline groundwaters, high Ra concentrations have been found (Moore and Shaw, 1998). On the other hand, increases in Ra lea-

ching from ores was observed at a pH lower than 4 (Benes, 1984). The low pH value observed for the water springs can also contribute to the high Ra concentrations in it. The strong relationship among the Ra isotopes, the light rare earth elements and U is compelling evidence that these elements derive from the same source. Then the possibility of the monazite being the source of Ra in the groundwater and consequently to the lagoon water have to be considered.

Evaluating the radium transport along the lagoon

The activity ratio of $^{228}Ra/^{226}Ra$ can be used as a tracer of Ra mobility in the water column if it does not vary with the evaporation, precipitation or biological activity, but varies only with the radium decays. To use this ratio some assumptions must be made: i) the ratio of the concentrations of ^{228}Ra and ^{226}Ra is constant at the source and ii) there is only one source of radium which is located at the head of the lagoon.

The Ra concentrations observed in other lagoons of the region, located around 20 Km from Buena Lagoon, showed a mean value (for four measurements) of $^{226}Ra = 0.16 \pm 0.05$ and $^{228}Ra = 0.21 \pm 0.11$ $Bq.l^{-1}$. Considering this concentration as the regions background and subtracting this value from the Ra concentrations at the different stations (Table 1), the "real concentration" of Ra in the water can be estimated as well as the concentration ratios (Table 2).

Once the concentration ratio of the Ra isotopes at each station is known and knowing that the decay of ^{226}Ra is negligible (^{226}Ra half-life 1600 years), the time spent by the radium to move from one station to another can be evaluated (using the activity decay equation). As the distances among the stations are known, the migration velocity can be estimated. Therefore it was estimated a period of around 6.7 years for the radium to move 1900 meters, resulting in a mean migration velocity of 283 meters per year.

$$\left(\frac{Ra228}{Ra226}\right)_{\text{station}} = \left(\frac{Ra228}{Ra226}\right)_{\text{station}} 1 \frac{e^{-\lambda Ra228T}}{e^{-\lambda Ra226T}}$$

Station	Altitude (m)	Distance from the lagoon head (m)	$^{228}Ra/^{226}Ra$	Spent time to move from station 1 (years)	Migration velocity m.yr^{-1}
1	7.5	0	7	-	-
2	5.0	800	4.2	4.4	182
3	1.5	1900	3.1	6.7	478
4	1.0	3700	-	-	-
5	<1.0	4500	-	-	-
6	<1.0	4900	-	-	-
7	<1.0	5400	-	-	-

Table 2
Estimate of the time and migration velocity needed to move Radium from station one to other stations.

From station 4 the ^{226}Ra and ^{228}Ra concentrations were very close to background one and the migration velocity could not be estimated.

The data from the decay equation estimates has to be treated carefully and some factors are discussed. The potential influences on Ra isotope activity concentrations in the water column would be the presence of other sources of Ra in the water, such as the contribution from the catchment and the Ra releasing from the sediment.

1) The contribution from the catchment would be: *i)* groundwater flux containing high Ra concentrations along the lagoon: The decrease of Ra concentration along the lagoon suggests the non existence of other groundwater sources, as the ones found at the lagoon heard. *ii)* contribution from run off: The low rate of radionuclides released from the monazite sand in normal conditions, for example by the leaching from rain water, makes it difficult to believe that a significant contribution of Ra to the lagoon is due to water run off.

2) The contribution from the sediment: the Ra desorption from the sediment is possible in such salt waters and the disequilibrium found between U/^{226}Ra (from 1.2 to 2.1) and Th/^{228}Ra (here in two stations -3 and 6- the relation was 0.6, while for the others the relation ranged from 1.2 to 1.6) in the lagoon sediment showed the existence of this process. The Th activity in the Buena sediments is 1.1 to 3.8 more elevated than the U activity. The ^{228}Ra has a short half-

life and is almost directly produced by the ^{232}Th decay, while ^{226}Ra has a long half-life and its ingrowth depends on the decay of three radionuclides of long half-life: ^{238}U, ^{234}U and ^{230}Th. Because of that, the production rate of ^{228}Ra in the sediment is more elevated than ^{226}Ra and probably the ^{228}Ra amount is also desorpted from the sediment. Thus, the value of the ratio activity $^{228}Ra/^{226}Ra$ found in the water would be due to the decay of the spring's ^{228}Ra and to the radium desorpted from the sediment. Considering the activity ratio $^{228}Ra/^{226}Ra$ desorpted from the sediment is higher than one, the time and the migration velocity —estimated from equation 1 and presented in Table 2— would be underestimated. The radium migration in the water column of the lagoon is very low and the remaining time in the water column is long. This long radium remaining time in the column water of the lagoon could be explained by the high water salinity and the consequent competition among the cations for the exchange sites of the sediment as observed in salt groundwater.

Quantifying the radium amount in the water column

The distribution of the radium concentrations (Table 1) can be fitted by exponential functions, where the variation of the radionuclide concentrations with the distance can be expressed as:

$^{228}Ra\ (Bq.m^{-3}) = 1180.e^{-0.0005.d}$ and $^{226}Ra\ (Bq.m^{-3}) = 351e^{-0.0002.d}$

where d is the distance from the sampling point to the head of the lagoon (m). The values of the correlation coefficients were respectively $R^2 = 0.9565$ and 0.8632.

If these functions were integrated along the 5,400 m of the lagoon, it is possible to estimate the total amount of the radionuclide in the water. The area of the lagoon is 113,000 m^2 and the mean width is around 21 meters. The depth of the lagoon is variable (between 10 cm and 3 m), however it is possible to estimate it at around 0.80 m, resulting in a transverse section of 16.8 m^2. So in the water of the lagoon the total amount of the Ra isotopes are estimated as : $3.7\ 10^7$ Bq of ^{228}Ra (40MBq) and $1.9\ 10^7$ Bq (20 MBq) of ^{226}Ra.

Conclusion

The outcropping of groundwater containing high concentrations of Ra is responsible for the observed Ra concentrations in the water of the lagoon. The water of the lagoon is basically composed by two sources of ions located at opposite sides of the lagoon. The seawater supplies the major ions and the groundwater supplies the radium and the rare earth elements, possibly by the leaching of the monazite. The data points to a slow migration velocity of the radium isotopes in the water column, which could be attributed to the high salinity of the water. A total activity of 40MBq of ^{228}Ra and 20MBq of ^{226}Ra remains in the water column.

Aknowledgements

The authors thank the Fundação de Amparo e Pesquisa do Estado do Rio de Janeiro (FAPERJ) and the International Atomic Energy Agency (IAEA), which partially provided funding for this research. Thanks are also due to colleagues at Divisão de Análise Ambiental/DEPRA/IRD, who analyzed part of the samples of this study. The constructive suggestions of Luigi Monte is especially acknowledged.

Bibliography

BENES P., 1984 –
Migration of Radium in the Terrestrial Hydrosphere. The Behavior of Radium in Waterways and Aquifers. IAEA-TECDOC-301, Vienna, 119-173.

BENES P., 1990 –
Radium in (Continental) Surface Water. The Environmental Behavior of Radium, IAEA. Technical Reports Series, n° 310: 373-418.

GASCOYNE M., 1989 –
High Levels of Uranium and Radium in Groundwater at Canada's Underground Research Laboratory, Lac du Bonnet, Manitoba, Canada. *Applied Geochemistry.*, 4: 557-591.

GODOY J. M., 1990 –
Methods for Measuring Radium Isotopes: Gross Alpha and Beta Counting. International Environmental Behavior of Radium. IAEA, Vienna, Technical Reports Series, n° 310 (1): 205-221.

HANCOCK G. J., MURRAY A. S., 1996 –
Source and distribution of dissolved radium in the Bega river estuary, Southeastern Australia. *Earth and planetary science Letters.*, 138: 145-155.

IYENGAR M. A. R., 1990 –
The Natural Distribution of Radium, The Environmental Behavior of Radium. IAEA, Technical Reports Series, n° 310: 59-128.

KRAEMER T. F., REID D. F., 1984 –
The Occurrence and Behavior of Radium in Saline Formation Water of the U.S. Gulf Coast Region. *Isotope Geoscience.*, 2: 153-174.

LANGMUIR D., 1985 –
The Thermodynamic Properties of Radium. *Geochimica et Cosmochimica Acta.*, 49: 1593-1601.

MONTE L., BALDINI E., BATTELLA C., FRATARCANGELI S., POMPEI F., 1997 –
"Modelling the Radionuclide Balance in some Water Bodies of Central Italy", *J. Environ. Radioactivity.*, 37 (3): 269-285.

MOORE W. S. E SHAW T. J., 1998 –
Chemical Signals from Submarine Fluid Advection onto the Continental Shelf. *Journal of Geophysical Research, September.*, 103 (C10): 21543-21552.

PASCHOA A. S., BAPTISTA G. B., MONTENEGRO E. C., MIRANDA A. C. SIGAUD G. M., 1979 –
"Radium-226 Concentrations in the Hydrographic Basins near Uranium Mining and Milling in Brazil". *In: Mid Year Topical Symp.*, Low Level Radioactive Waste Management, Williamsburg, VA: 337-343

Standard Methods for Examination of Water and Wastewater, 1975 –
14th edition, American Public Health Association, Washington.

VIANNA M. E. C. M., TAUATA L., OLIVEIRA A. E., OLIVEIRA J. P., CLAIN A. F., FERREIRA A. C. M., 1998 –
Evaluation of Brazilian Intercomparison Program Data from 1991 to 1995 of Radionuclide Assays in Environmental Samples. *Appl. Radiat. Isto.*, 49 (9-11): 1463-1466.

WAYNE R. O., 1990 –
A Physical Explanation of the Lognormality of Pollutant Concentrations, *J. Air Waste Manage. Assoc.*, 40: 1378-1383.

ZHU W., KENNEDY M., LEER E. W. B., ZHOU H., ALAERTS G. J. F. R., 1997 –
Distribution and Modelling of Rare Earth Elements in Chinese River Sediments. *The Science of Total Environment.*, 204: 233-243.

Hydric resources radioactive contamination in the central region of Cuba as a consequence of fallout after the atmospheric nuclear bombs tests

C. Alonso Hernández

A. Muñoz Caravaca

M. Díaz Asencio

H. Cartas Aguila

E. Suárez Morell

Introduction

With the birth of the nuclear era a new group of contaminants have been introduced into the atmosphere, they are the artificial radionuclides. From 1945 up to 1980, with the high scale nuclear bombs tests, more than 960 PBq of ^{137}Cs has been released into the atmosphere in 545 Mt predicted released power (UNSCEAR, 1983). Besides, the nuclear fuel cycle (mainly as a result of nuclear power plant accidents) has promoted radioactivity releases become another important source of artificial radionuclides contaminating our atmosphere.

Not all radionuclides releases in the atmosphere remain for indefinite time, their presence in the atmosphere depend upon physical-chemical properties in relation with their interaction capacity in this media. For these reasons the radioactivity releases have caused one of the greatest changes of all times in the atmosphere composition, and have brought about the contamination of almost every environmental component, not only in the testing or power plant sites, but also all around the world because of the Global Fallout.

The Cuban water masses, as well as the rest of the natural components of our ecosystems, are not free of this source of global contamination. Although the contamination coming from this source is not an imminent danger to the populations using these water, it has been seen as an increase in the radiological background of the main hydrological resources of the country. These resources are used for direct consumption, food production and irrigation of crops. Furthermore, it is perceivable the presence of artificial radionuclides in the underground waters, despite their different self-cleaning mechanisms and the slow speed of the contamination processes characterizing these water masses (CRESL, 1993; CRESL, 1994; CRESL, 1995a2,3,4,5).

The use of radioactive tracers implies the implementation and evaluation of every measurement methodology. It permits us to determine their distributions in the environment and to understand the dynamic processes that control their behavior in the environment. The *Radiological and Environmental Surveillance Laboratory* have developed a monitoring program for some environmental variables, among which the ^{137}Cs concentration in several environmental samples such as soil, grass, milk, foods, surface and underground waters and air, are measured. Therefore the natural cycle of these radionuclides has been studied thoroughly. This article main goal is to present the ^{137}Cs activity level determined in atmospheric and hydric samples, as well as some considerations about transference processes of these radionuclides throughout some environmental components.

Methods

The studied zone, was located around the Juraguá Nuclear Power Plant (Central-South region of the country, Cienfuegos province) and it was 10 000 km^2 wide. We fixed six sampling places distributed as follow: three sampling places for surface waters in the most important dams (Hanabanilla Dam, Abreus Dam and Avilés Dam), two samples places in the Juraguá water bearing for underground waters, and one place for continuous air monitoring in our laboratory.

The period of study was five years long (1994-1998). The air samples were collected weekly. Aerosol samples were collected by PRIMUS, an air pump designed in our laboratory (CRESL, 1995b). It has a 800-1400 mμ.h^{-1} air flux, a collecting area 0.65m^2 and uses a Petrianov filter (FPP-15-1.5) able to retain the particles with dimensions greater than 3mm (99%) and avoid the resuspension in dry season. Each filter was exposed for 168 hours (1200 mμ.h^{-1} air flux average), after that each samples was dry ashed and measured by gamma spectrometry. Fallout samples were collected in try covered with the same Petrianov filter. Each filter was exposed during 30 days, after that each sample was dry ashed (350 °C). Due to ^{137}Cs low level, each quarter samples xere unified and measured by gamma spectrometry.

The waters were sampled after three months and were collected in 50 l cleaned bottles (CPHR, 1990a; CPHR, 1990b; EML, 1990). To determine ^{137}Cs, 20 l samples were filtered trough a qualitative filter paper and nitric acid or hydrochloric acid up to 1.5 pH was added. To determine ^{137}Cs in water, AMP was used to concentrate it and then it was measured by gamma spectrometry. A germanium detector was used for comparative measurements: HPGe detector having 11.1% relative efficiency, geometry Hole P-Type, and energy Resolution FWHM of 2.26 keV on 1.33 MeV photopeak of ^{60}Co, (CPHR, 1990a; CPHR, 1990c; CRESL, 1995c). The pulses were analyzed with a multichannel buffer, Silena Spectrometer

System. The background contribution was reduced by surrounding the detector with 1 mm thickness copper, 5 cm thickness lead, and 15 cm thickness iron castle.

Results and discussion

Aerosols samples

Let's begin our analysis with aerosols samples, because they are the first indicator of all kind of atmospheric contamination. The ^{137}Cs and ^{7}Be concentration behavior in aerosol samples during the period of study is very regular, (Figure 1). The ^{137}Cs averaged concentration

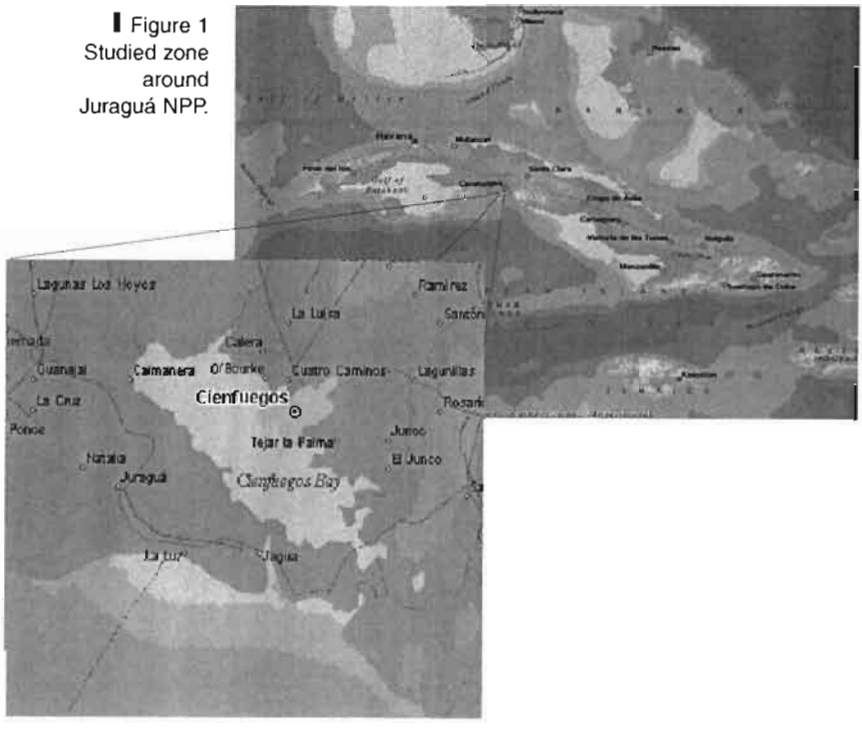

Figure 1
Studied zone around Juraguá NPP.

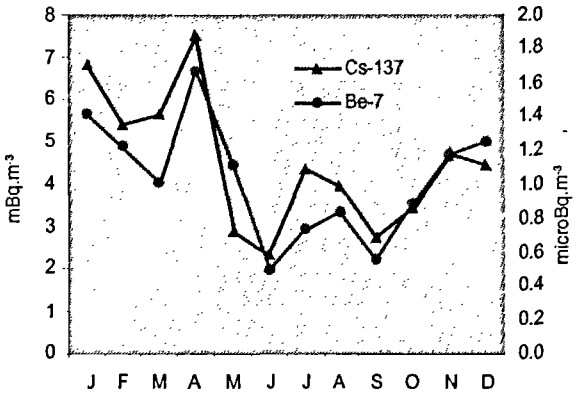

Figure 2
^{137}Cs and ^{7}Be concentration behavior in aerosol samples.

is 1 $\mu Bq.m^{-3}$, this value is representative of normal radiological regions, affected by global fallout only. It is observed that both radionuclides have the same behavior, implying that they are both affected by the same vertical transport processes. A correlation coefficient between these two series is 0.8. The results obtained are coincident with others authors like Feely *et al.* (1988), who reported a correlation coefficient of 0.79 for the same variables in Miami city.

^{7}Be seasonal behavior depends upon several factors not studied completely yet, but the transference processes in the tropopause and the regional climatic conditions are the most important ones (Marenco & Fontan, 1974; Feely *et al.*, 1988). Figure 3 shows the monthly behavior for ^{7}Be versus rain quantity in the study period. The 73.9% of ^{7}Be levels could be predicted by the rain variations, while the no correlation probability is less than 0.2%. These behaviors and r^2 and r values are similar to those reported by Feely *et al.* (1988) for tropical zones from 08° to 25° north latitude.

The results obtained for Cienfuegos have the same temporal behavior that other measurements in cities of the Caribbean region, have like Panama, Miami and San Juan cities, where the maximum ^{7}Be levels are reached in the first quarter of the year coinciding with the minimum levels of precipitation reported for the region (Kendrew,

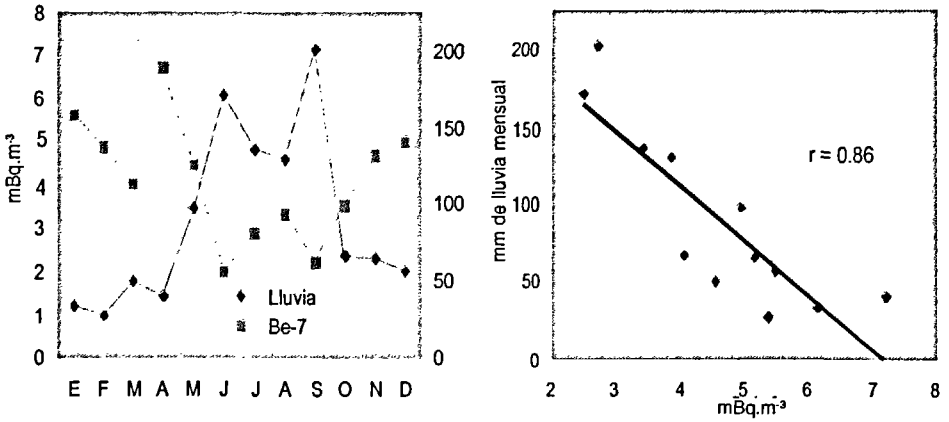

Figure 3
Monthly behavior for ^{7}Be versus rain quantity in the study period.

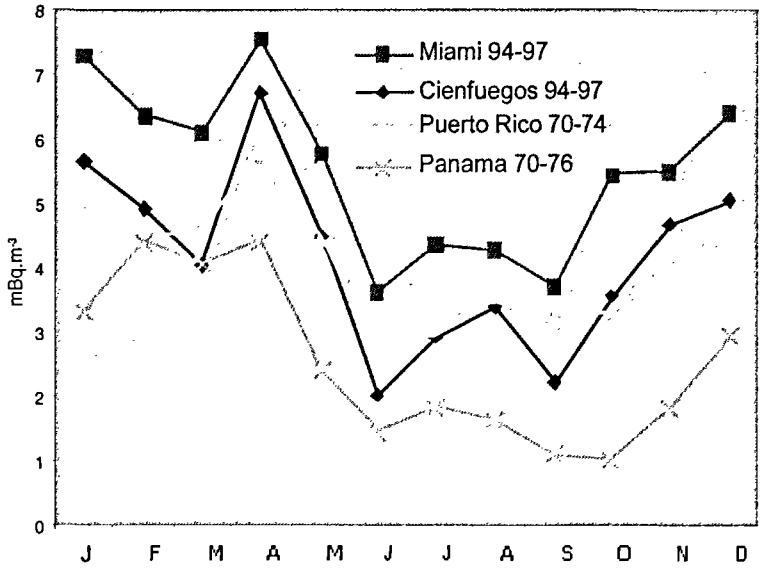

Figure 4
^{7}Be aerosols monthly behavior for the period in Cienfuegos, Miami, Puerto Rico and Panama cities.

1963). The increase observed in April has been explained by Aegerter *et al.* (1966) and Feely *et al.* (1988), due to breaking of tropopause at the end of the winter season when the vertical transport from the stratosphere to tropopause is higher.

The $^{137}Cs/^{7}Be$ ratio for Miami and Cienfuegos has a correlation coefficient of 0.93, see Figure 5. Using the linear equation fit and systematizing by monthly ratio $^{7}Be_{Cienf}/^{7}Be_{Miami}$, the ^{137}Cs in aerosols for Cienfuegos could be expressed by :

$$^{137}Cs_{Cienf}=0.729\,^{137}Cs_{Miami}.R \quad [1]$$

The ^{137}Cs levels in aerosols obtained by the expression [1] coincide with those reported by (SASP, 1998) for Puerto Rico (1970-1974), Bahamas (1968-1972), Panama (1965-1967) and Hawaii (1970-1994). The maximum level was 4.7 $mBq.m^{-3}$, calculated for the year 1963 when higher numbers of atmospheric nuclear weapons were tested (UNSCEAR, 1982). But the most relevant component of this study was that the Chernobyl accident signal in our country was

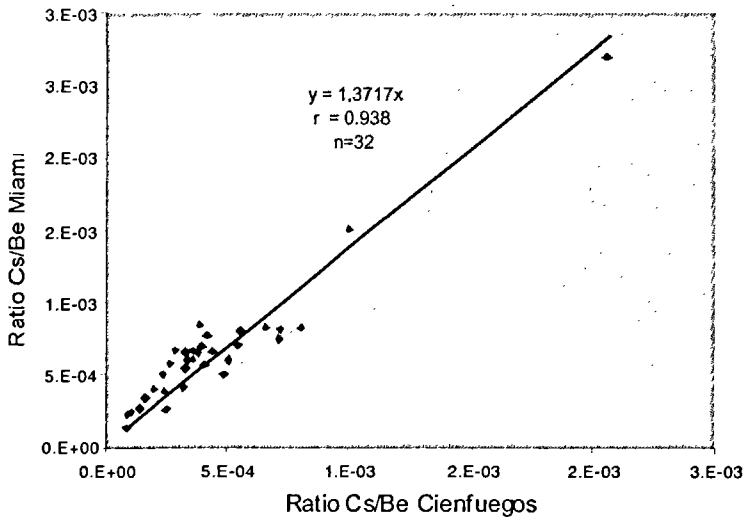

Figure 5
$^{137}Cs/^{7}Be$ ratio for Miami and Cienfuegos.

observed. It was predicted for May, 1986, 0.74 mBq.m^{-3} of ^{137}Cs, two orders higher than the average level for the region in the period of this study. This result is concordant with observations made by Feely *et al.* (1988, 1988a) and Larsen *et al.* (1986) for the east coast of the United State from Maine (47°N,68°W) to Miami (26°N,80°W) in May, 1986. The presence in our latitude of Chernobyl radionuclides has been explained by Larsen *et al.* (1989), Pearson *et al.* (1987) and Roy *et al.* (1988) where the global transport processes transferred the initial plume forward northeast of Canada, after that part of the plume was associated with a quasistacionary low pressure in the northeast of the Atlantic ocean which promoted the descent of contaminated air around all of the north American east coast.

Fallout

In the studied period the ^{137}Cs was detected by gamma spectrometry, the ^{137}Cs averaged concentration was 0.12 Bq.m^{-3}.month^{-1} and range 0.015 and 0.207 Bq.m^{-3}.month^{-1}. Figure 6 shows the temporal

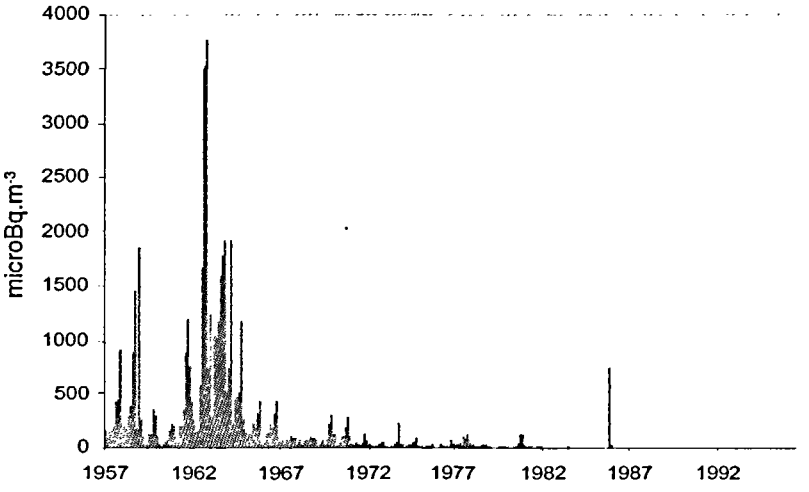

Figure 6
Retrospective ^{137}Cs predicted values in aerosols for Cienfuegos in the period July 57 - May 94.

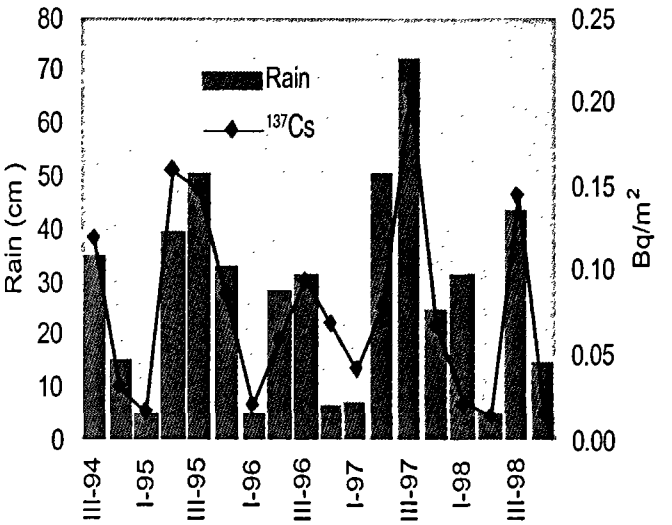

Figure 7
^{137}Cs total fallout and precipitation
for period June 94 – December 98 in Cienfuegos.

behavior of fallout deposition. A good correlation with precipitation levels in the period was observed, where the higher values are in wet season (May-October) and diminish rapidly in the dry season. A correlation analysis indicates that the 71% ^{137}Cs fluctuations are explained by the fluctuations in precipitation regime. This variable is the principal in the vertical transport processes of ^{137}Cs from low troposphere to the surface ground and agrees with observations made by Feely *et al.* (1988) in the 1970-1985 period for Miami city.

Waters

The ^{137}Cs radionuclide was detected by gamma spectrometry in surfaces and underground waters after radiochemical extraction. The concentrations range determined in surface waters was 0.34 – 9.04 $mBq.l^{-1}$, averaging 7.9 $mBq.l^{-1}$ Underground waters have a 2.73 $mBq.l^{-1}$ average concentration and a 1.38 – 5.28 $mBq.l^{-1}$ range.

There are no significative differences between the results obtained for the different sampling places in both media. It is observed that underground waters have a ^{137}Cs concentration lower than surface waters. This shows that the speed of the contamination processes is slow and that their self-cleaning mechanisms characterize these water masses.

Averaged concentration ^{137}Cs [mBq.l^{-1}]		
Control Media	Period	Activity levels
Underground waters	88-97	2.83 ± 1.86
	1998	1.68 ± 0.30
	1999	3.88 ± 1.40
Surface waters	88-97	6.46 ± 2.58
	1998	3.75 ± 1.54
	1999	0.84 ± 0.50

Table 1
^{137}Cs range and averaged concentration in underground and surface waters.

The ^{137}Cs in aquatic fish and aquatic vegetation is *0.18 ± 0.1* and *0.18 ± 0.06 10 Bq.kg^{-1} wet weight* respectively. Those values are representative of zones affected by Global Fallout only.

Conclusions

The results drawn by our studies show the presence of ^{137}Cs nuclear fission product in all the studied areas, and it having an activity above the detection limits of our measurement systems.

The ^{137}Cs concentration in aerosols samples show a good correlation with the behavior of local atmospheric perturbations, which

are more frequent in the summer season (May-September). This behavior has been associated with a greater transport in the precipitation processes from the atmosphere to earth. The increase observed in April has been explained by Aegerter *et al.* (1966) and Feely *et al.* (1988), due to breaking of tropopause at the end of the winter season when the vertical transport from the stratosphere to tropopause is higher.

It is perceivable that the presence of ^{137}Cs in the underground waters and in aquatic biognosis, despite their different self-cleaning mechanisms, is due to the slow speed of the contamination processes that characterize these water masses.

We conclude that our hydrological resources have been contaminated by the ^{137}Cs nuclear fission product coming from the past nuclear weapons tests by means of Global Fallout. The level of specific activity of this radionuclide is very similar with those reported in the scientific literature for zones affected by Global Fallout only (UNSCEAR, 1983; UNSCEAR, 1993).

Bibliography

AEGERTER S., BHANDARI N., RAMA H., TAMHANE A. S., 1966 — Be^7 and P^{32} in ground level air. *Tellus*, 18: 212-15.

CPHR, 1990a — *Guide for collection and register of environmental samples around nuclear sites.* CPHR-MA-87, Havana, Cuba.

CPHR, 1990b — *Methodological guide for environmental samples pretreatment.* Havana, Cuba.

CPHR, 1990c — *Guide for ^{137}Cs determination in environmental samples.* CPHR-MA04-87, Havana, Cuba.

CRESL, 1993 — *Natural radioactive levels around Juraguá Nuclear Power Plant site.* Central Radiological and Environmental Surveillance Laboratory, LVRAC Cienfuegos, Cuba,

CRESL, 1994 — *Radiological Monitoring Program. Juraguá Nuclear Power Plant site.* Report 1994, Central Radiological and Environmental Surveillance Laboratory, LVRAC Cienfuegos, Cuba.

CRESL, 1995a — *Radiological Monitoring Program. Juraguá Nuclear Power Plant site.* Report 1995, Central Radiological and Environmental Surveillance

Laboratory, LVRAC Cienfuegos, Cuba.

CRESL, 1995b —
Design and put in practice of aerosol collector system PRIMUS. Central Radiological and Environmental Surveillance Laboratory, LVRAC Cienfuegos, Cuba, 1995.

CRESL, 1995c —
Procedures Manual. MIP SA-32. Central Radiological and Environmental Surveillance Laboratory, LVRAC Cienfuegos, Cuba.

EML, 1990 —
Procedures Manual. Environmental Measurements Lab., Hasl-300-Ed-27, NY, USA.

Feely H. W., Lasen R. J., Sanderson C. G, 1988 —
Annual Report of the surface air sampling programs. New York, Department of Energy Repot. EML-447.

Feely H. W., Helfer I. K., Juzdan Z. R., Klusek C. S., Lasen R. J., Leifer R., Sanderson C. G., 1988a —
Fallout in the New York Metropolitan Area Following the Chernobyl Accident. *J. Environ. Radioactivity,* 7: 177-191.

Feely H. W., Lasen R. J., Sanderson C.G., 1989 —
Factors that cause seasonal variations in beryllium-7 in surface air. *J. Environ. Radioactivity,* 9: 223-249.

Kendrew W. G., 1963 —
The climates of the Continents. Oxford, The Claredon Press.

Larsen R. J., Sanderson C. G., Rivera W., Zamiquieli M., 1986 —
"The caracterization of radionuclides in the North American and Hawaiian surface air and deposition following the Chernobyl accident".
In Volchok H. L., Chieco N. A. (eds) : *A Compendium of the Environmental Measurement Laboratory's Research Projects Related to the Chernobyl Nuclear Accident,* New York, US Department of Energy Report EML-460: 1-104.

Larsen R. J., Haagenson P L., Reiss N. M., 1989 —
Transport Processes Associated with the initial elevated concentrations of Chernobyl Radioactivity in Surface air in the United States. *J. Environ. Radioactivity,* 10 (1): 1-18.

Marenco A., Fontan J., 1974 —
Étude des variations des ^{7}Be, ^{32}P,^{90}Sr, ^{210}Pb et ^{10}Po dans la troposphère. *Tellus.*, 26: 386-401.

Persson C., Rodhe H., DeGeer L., 1987 —
The Chernobyl accident- A meteorological analysis of how radionuclides reached and were deposited in Sweden. *AMBIO,* 16: 20-31.

Roy J., Cote J. E., Mahfoud A., Villenuve S., Turcotte J., 1988 —
On the trasport of Chernobyl radioactivity to the eastern Canada. *J. Envirom. Radioactivity,* 6: 121-30.

SASP, 1998 —
Surface Air Sampling Program. (EML-572) (on line). http://www.eml.doe.gov/databases/SASP/sasp_data_search.htm

UNSCEAR, 1983 —
United Nations Scientific Committee on the Effect of Atomic Radiation, 1982. NY, USA.

UNSCEAR, 1983 —
United Nations Scientific Committee on the Effect of Atomic Radiation, 1993. NY, USA.

Oral/Poster presentations

Session 6

Estimating the Indonesian throughflow from the Indo-Pacific tritium concentration gradient

P. Jean-Baptiste

V. Leboucher

The Indonesian throughflow is a major feature of the Indian and Pacific oceans equatorial circulation and an important component of world ocean circulation (Gordon, 1986). It results from the pressure gradient which exists between the Indian and Pacific oceans, as the mean sea level is higher on the Pacific side than on the Indian side. The various methods used to estimate its strength lead to much scatter, with values comprised between -2.6±9 Sv and 18.6±7 Sv.

Here, we focus on the tritium (^3H) distribution. ^3H was injected in the atmosphere by atmospheric thermonuclear weapons tests during the 1950s and 1960s. First, the ratio of thermonuclear ^{14}C to ^3H inventories is used to trace the North Pacific origin of the throughflow waters. Then, the comparison of the ^3H inventory on both sides of the Indonesian seas, in Pacific and Indian oceans, allows us to derive a new estimate of the Indonesian throughflow. Unlike direct current measurements or geostrophy, the present approach gives a value which is averaged over the transit time of the waters through the Indonesian archipelago (i.e., over several years) and makes it possible to remove much of the seasonal and interannual variability of the throughflow.

Circulation in the Arctic and North Atlantic Oceans revealed by ^{129}I and ^{137}Cs tracers from European nuclear fuel reprocessing plants

J. N. Smith

The development during the past 10 years of analytical techniques to measure ^{129}I by accelerator mass spectrometry has led to recent advances in its use as an oceanographic tracer, particularly in the Arctic Ocean. Large quantities of ^{129}I ($t1/2 = 16 \times 10^6$ yr) have been discharged from the Sellafield (UK) and La Hague (France) nuclear fuel reprocessing plants into the Irish Sea and English Channel, respectively since the 1960s. Together with ^{137}Cs ($t1/2 = 30$ yr), derived mainly from Sellafield, the ^{129}I reprocessing signal is transported into the North Sea and Norwegian Coastal Current and then enters the Arctic Ocean through Fram Strait and the Barents Sea where both tracers independently reflect the circulation of Atlantic origin halocline and intermediate water. Combined measurements of ^{129}I and ^{137}Cs, together with a knowledge of the historical record of reprocessing plant discharges, can be used to identify a given year of transport through the Norwegian Coastal Current (NCC), thereby permiting the determination of a transit time from the NCC to a given sampling location, similar to a ventilation age determined using atmospherically-derived tracers such as tritium and chlorofluorocarbon compounds (CFC's). Measurements of ^{129}I and ^{137}Cs conducted on seawater samples collected during icebreaker and US Navy nuclear submarine cruises to the Central Arctic Ocean clearly delineate circulation features such as the boundary between Atlantic and Pacific-origin water that is presently aligned with the Mendeleyev Ridge. These results have been interpreted using a

transit time model which provided estimates of 6-7 yr (± 0.5 y) for the passage of Atlantic Water from the Norwegian Coastal Current (60°N) to the Eurasian slope of the Makarov Basin, 8-10 years to the Mendeleyev Ridge and > 10 yr to the interior of the Canada Basin.

Application of $^{238}U/^{234}Th$ ratios to determine particle flux and trace element residence times in tropical marine systems

R. Szymczak

M. Zaw

Particles of all sizes and various sources play a central role in the scavenging of natural and pollutant chemical species in marine systems. In estuaries and coastal waters particle concentrations are generally several orders of magnitude higher than in the deep sea and consequently very important in determining the biogeochemical behaviour of associated pollutants. Further offshore, biological processes become increasingly important in regulating the flux of these materials. An understanding of the formation and residence times of particles in marine environments will greatly assist in the interpretation of several key issues associated with (1) the fate of natural terrestrial material during mixing of rivers and oceans in the coastal zone, and (2) the chemical behaviour and environmental consequence of pollutants in coastal and oceanic systems. The parent-daughter association of primordial, chemically conservative and long-lived (half-life 4.5×10^9 years) uranium-238 and thorium-234, with a half-life of 24.1 days and high affinity to bind with seawater particles, provides an excellent tracer to study these processes with temporal ranges from days to months. When combined with phase associations measurements of other elements (heavy metals, rare earth elements and noble metals) observations of disequilibrium in uranium-238/thorium-234 ratios provide an understanding of the time dependence of particle formation and elemental scavenging, or removal, processes.

Contamination of waterways in the Czech Republic with radionuclides from uranium mining and milling

P. Benes **F. Sebesta**
J. John **J. Vesely**

Data on the contents of uranium, thorium, ^{226}Ra, ^{228}Ra and ^{228}Th in bottom sediments in the catchment of Labe (Elbe) River in the Czech Republic are analyzed. It is shown that some rivers and reservoirs are extensively contaminated with uranium and ^{226}Ra from the past uranium mining and milling, whereas the activities of thorium, ^{228}Ra and ^{228}Th are rather evenly distributed without apparent anthropogenic effects. The background concentrations of all the radionuclides are established and the sources of local contamination are identified. Some of the sources represent old liabilities of the mining and milling whose remediation remains important task for future. Analysis of radioactive equilibria ($^{238}U/^{226}Ra$ and $^{232}Th/^{228}Ra$) in the sediments have indicated that the uncontaminated river sediments contain ^{226}Ra mainly bound inside mineral particles in equilibrium with ^{238}U, but a large part of ^{226}Ra in the contaminated river sediments is adsorbed on the surface of sediment grains. The fraction adsorbed is large also in all reservoir sediments and particularly in suspended solids of river water. ^{228}Ra is bound by adsorption more than ^{226}Ra in uncontaminated sediments. Comparison of the activities of uranium and ^{226}Ra in the river sediments with similar activities in the adjacent river water revealed rather small variability of the ratio of the sediment/water activities among different sampling sites. The ratio represents a kind of modified "Kd" value. Significance and possible uses of this value are discussed.

U-series disequilibria in deep fracture zone in the Vienne granitoids as an indicator of uranium migration processes

J. Casanova

J. F. Aranyossy

Uranium concentration and activity ratios ($^{234}U/^{238}U$ and $^{230}Th/^{234}U$) in groundwater, fracture coatings and adjoining rock matrix were studied in the Vienne granitoids, France. The aim was to develop and test a conceptual model of the groundwater flow system. The small to moderate disequilibrium ($1.87 < ^{234}U/^{238}U < 3.36$) observed in the deep groundwater, together with very low uranium concentration, is characteristic of reducing conditions. It is very likely that deep groundwaters with uranium contents as low as 0.022 ppb, underwent activity ratio increase due to the alpha-recoil process, while shallow groundwaters, with uranium content close to 24 ppb, result from preferential ^{234}U -solution processes. Activity ratios as a function of distance from fractures surface (sample at 342m) show clear absolute uranium release up to 5 to 6 cm's from the fracture surface. Both $^{230}Th/^{234}U$ and $^{234}U/^{238}U$ profile indicates episodic ^{234}U mass flow events within the last 350,000 years. A working hypothese to relate observed absolute uranium release and isotopic fractionation between isotopes ^{234}U and ^{238}U is based on the radioactive decay induced oxidation of ^{234}U to U(VI), that is the more soluble oxidation state of uranium. In this situation the oxygen concentration in groundwater plays an important role. If there is much oxygen it can actually oxidise and release the bulk of uranium which would not lead to marked isotopic fractionation. If there are

small amounts of oxygen, the already oxidised ^{234}U is easier to remove leading to clear isotopic fractionation. If finally there is very little or no oxygen, it would have no effect even for ^{234}U in which case there would not be absolute release nor preferential ^{234}U release.

Iodine-131 and technetium-99: sewerage plume tracers?

R. Kleinschmidt

The radioisotopes ^{131}I and ^{99m}Tc are frequently used in diagnostic and therapeutic medical procedures. Waste products associated with these procedures are typically discharged to the sewer. Gamma spectrometry of passive bioaccumulators collected in the vicinity of a local sewerage treatment plant outfall have shown that the concentration of these, plus other medical radionuclides, is significant (e.g. ^{131}I in macro algae, $1 kBq.kg^{-1}$). A pilot study based in Brisbane, Australia suggests that the discharge of these waste products and their progeny into the Brisbane River may provide a sensitive means of mapping the sewerage plume distribution within the river and nearby Moreton Bay.

Results of a limited gamma spectrometry intercomparison on mineral sand products and associated issues

Kleinschmidt

G. Godwin

New radiation control legislation in Queensland, Australia provides for the exemption of abrasive blast material upon meeting a specified release criteria. Calculation of the release criteria is based on the measurement of uranium and thorium series radionuclides in the abrasive blast media. Past experience has shown that results from different facilities vary to the extent that the material may be exempt based on the results of one laboratory but not another. Queensland Health Scientific Services embarked on the trail of running a limited intercomparison for a sample of ilmenite, a commonly used mineral sand abrasive blast material, to establish sources of variation in reported results. The results of the program are presented with comment on their implications.

Thermodynamic and hydrogeochemical controls of the redox speciation of uranium in the marine environment

G. Kniewald

M. Branica

The chemical speciation and redox equilibria of uranium in seawater (and natural waters in general) are controlled by a suite of physico-chemical processes. Among these, of primary significance from the thermodynamic point of view are major and trace constituent interactions, redox processes and sorption phenomena. The complex redox system of uranium in natural waters, involving at least three of the five known oxidation states of this element, is highly sensitive to changes of the redox potential (Eh) of the milieu. Several hydrogeochemical equilibrium models were applied to the calculation of uranium distribution between the oxidation states VI, V and IV. Subroutines for inclusion of varying redox potentials, solubility products and stability constants were used to identify thermodynamically feasible reactions, the predominating oxidation states of uranium and the respective solubility-limiting solids. The results indicate that the redox equilibria of uranium do not necessarily follow the classic concept of soluble U(VI) vs. insoluble U(IV) species. The presence and geochemical relevance of transient redox state of uranium (V) has to be accounted for in models predicting the redox speciation of uranium and its mass tranfser reactions in the marine environment. Significant environmental implications include the reaction pathways of uranium precipitation and remobilization in anoxic environments, but also coastal waters, with a possibly detrimental effect on the environmental quality of such areas.

3-D modelling of ^{137}Cs and ^{90}Sr transport in Dnieper-Boog Estuary

N.Yu. Margvelashvili

V. S. Maderich

M. J. Zheleznyak

The developed recently 3-D numerical model of hydrodynamics, sediment transport and pollutant dispersion (THREETOX) is applied to simulate radionuclide fate in stratified water bodies. Hydrodynamics of THREETOX is similar to Blumberg-Mellor model, also known as Princeton Ocean Model. Suspended sediment transport is described by advection- diffusion equations. Transport of the radionuclides is calculated separately for the liquid and solid phases. The paper presents the methodology and results of the model implementation to Dnieper –Boog Estuary (Dnieper River, Ukraine), that is the largest estuary of the Black Sea with a surface area of 1006.3 km^2, and a volume of 4.24 km^3. The regime of this drowned-river water body varies from stratified to partially mixed. The sources of fresh water discharge are the Dnieper and Southern Boog rivers. Dnieper-Boog Estuary (DBE) is the end of Chernobyl radionuclide's riverine pathway from Chernobyl into the Black Sea. The simulation of the ^{137}Cs and ^{90}Sr distribution in the DBE and calculation of the relevant radionuclide fluxes to\from Black Sea were done on the basis of the measured radionuclide influxes into the DBE from the Dniper River in 1986-1989. The simulated radionuclide concentrations on sediments and in dilute where compared with the measured data. It was shown that the spatial correlation between ^{137}Cs and salinity in DBE is strongly nonlinear due to sorption of the radionuclides on the fine sediment particles. The water stratification, compared with the wind action, has minor effect on the sediment and radionuclide fluxes in major part of the estuary except the ship channel, where the salt wage is formed.

Numerical study of radionuclide dispersion in Chernobyl Cooling Pond

N.Yu. Margvelashvili **S. A. Yushenko**
V. S. Maderich **M. J. Zheleznyak**

Three-dimensional model of radionuclide dispersion (THREETOX) was applied to simulate fate of ^{137}Cs in the Cooling Pond of the Chernobyl Nuclear Power Plant (NPP). The length of Chernobyl Cooling Pond (CCP) is 11.5 km, the maximum width is 2.2 km, the capacity is 0.16 km^3. The water level in the CCP is supported by the permanent pumping of water from Pripyat River to compensate the losses due to seepage and evaporation. The currents in the CCP are driven by releases of hot water from the NPP, by the cooled water intake to it and by the wind. The CCP was heavy contaminated during the Chernobyl accident in April-May, 1986. Till today the levels of ^{137}Cs and ^{90}Sr concentrations in the bottom deposition are rather high. The measurements revealed redistribution and accumulation of the radionuclide in deepest parts of the cooling pond. The modelling studies of the radionuclide fate in the CPP are stimulated now by the needs to have assessments of the radionuclide re-distributions after Chernobyl NPP shut down and resulting shut down of the water pumping from the river. The simulation of the radionuclide fate in the CCP during 1986-1992 was provided on the basis of the initial atmospheric fallout data. The reasonable agreement between measured and simulated data is reached for the radionuclide concentration in the water and bed. Both cohesive sediments and radionuclides are accumulated with higher rate in deepest parts of the cooling pond. Spatial distribution of ^{137}Cs in the bed since mid of 1987 correlates well with the fine sediment distribution and does not correlate with initial fallout data. The analysis of the efficiency of the chosen mud transport model is provided treating the radionuclide as a tracer.

Radium isotopes in the Ulsan Bay

J.S. Lee

K. H. Kim

D. S. Moon

During high discharge period, radium isotopes are shown distinct positive curvature within the mixing zone, representing the desorption of radium isotopes within the Ulsan Bay. The activities of radium isotopes increased gradually up to the salinity of 26.41. Above salinity of 26.41 the radium isotopes activities decreased to the values of the oceanic end-member. This addition increases the estuarine flux of ^{224}Ra, ^{226}Ra, and ^{228}Ra to the outer sea by a factor of 7, 15, and 92, respectively.

In order to estimate residence time of the Ulsan Bay waters, we applied mass balance model to the distribution of ^{224}Ra and ^{226}Ra activities in bay waters. The residence times of the Ulsan Bay waters were in range of 6.8 to 11 days. This result may provide useful information concerning the transport of estuarine waters and dissolved pollutants from the estuarine waters to the open sea.

Spatial variations of ^{137}Cs and ^{90}Sr concentrations in coastal waters of Japan

N. Inatomi

Y. Nagaya

F. Kasamatsu

The artificial radionuclides concentrations (^{137}Cs and ^{90}Sr) in sea waters and sediments in coastal waters of Japan has been monitoring since 1984 as a part of the marine environmental radioactive monitoring program sponsored by the Science and Technology Agency of Japan. The spatial and temporal variations of ^{137}Cs and ^{90}Sr concentration in seawaters and the factors affecting the variations have been investigated. The concentrations in cold water currents (Oyashio currents system) are lower than those in warm water currents (Kuroshio currents system). The concentrations of ^{137}Cs and ^{90}Sr in coastal waters of northeast Japan have been substantially influenced by the occurrence and strength of the Kuroshio currents system/Oyashio currents system. Relatively constant concentrations of ^{137}Cs and ^{90}Sr were observed in waters above 200m depth with sharp gradient below 200m depth. We also discuss the characteristics of the vertical distribution of $^{239+240}Pu$ in coastal waters of Japan.

Abstracts

Vladimir L. Zimin: "Fishes as radionuclide bioindicators in the area of Leningrad nuclear power plant (Gulf of Finland, Baltic Sea)"

Since the early 1980s the long time dynamics of migration of radionuclides in water, aquatic plants, fish and bottom sediments, sampled in the Koporskaya Bay of the Gulf of Finland as well as in rivers and lakes of the bay drainage basin have been traced. This work comprises the Monitoring Program in the NPP sanitary zone. In this paper a part of data, precisely fish materials, were analyzed. The results reflect the complex character of the radioactive contamination in Sosnovy Bor Region (the Koporskaya Bay drainage basin). Fish were chosen as specific concentrators and bio-transferors of anthropogenic radionuclides, and to obtain information on exposure doses for the human population of the Region resulting from consumption of the local food products.

Keywords: Radionuclide — Fish — Contamination — Bioindicator.

Vasile Patrascu: "Synthetyc results in the radioactivity assessment of the Romanian Black Sea sector after 1992"

The ecosystem state and marine environmental quality research developed in our institute involve the follwing directions:

- monitoring of the physico-chemicals factors (temperature, currents, salinity, nutrients);
- monitoring of the living resources (phyto and zooplankton, macrophite algae, molluscs, fish);
- monitoring of pollution (radioactivity, heavy metals, oil, organic substance, microbiology);
- study of the pollution effects (ecotoxicology);
- coastal zone and marine environmental protection (erosion, ICZM, aquaculture, biodiversity).

Water, sediments and marine organisms are sampling from network stations between Danube mouth and Vama Veche (245 km). Marine radioactivity is measured by gross beta, gamma spectrometry and radiochemical methods.

Keywords: Radionuclide — Marine sciences — Black Sea.

Claire Garrigue: "Impact of the human activities on cetaceans in the South West Pacific Ocean by measuring ^{137}Cs, ^{40}K and ^{210}Pb"

Radioactivity occurs naturally in the environment, however some artificial radionuclides have also been introduced since the 60's. One of the most widespread is the isotope ^{137}Cs the source of which is the global atmospheric fallout generated from airbone nuclear explosions. In the more recent past the Chernobyl nuclear accident injected important amounts of artificial radioactivity in the Northern hemisphere. The analyses of long-lived artificial and natural redionuclides can be used as tracers of the global human impact on the marine environment. In particular ^{137}Cs and ^{210}Pb have been traced in muscle tissues and the livers of whales stranded along the coast of New Caledonia. The highest concentrations of ^{137}Cs were systematically found in the muscle tissues (0.08 to 0.26 $Bq.kg^{-1}$ wet wt) in agreement with the literature values. However an exception was observed in a pregnant female whose liver showed concentrations similar to those measured in its muscle. Despite the relatively low number of cetaceans sampled, globally the concentrations in ^{137}Cs are at least two times lower than those observed in the animals netted in the Northern hemisphere. This results probably reflects the differences in the nuclear past (weapons testing, nuclear plant accidents) between the two hemispheres.

Keywords: Radionuclides — ^{137}Cs, ^{40}K, ^{210}Pb — South Pacific Ocean — Short-finned pilot whale — Pygmy sperm whale.

Bruno Danis: "^{14}C radiolabelling: a sensitive tool for studying pcb bioaccumulation in echinoderms"

Uptake kinetics of PCB were investigated in the common NE Atlantic sea star *Asterias rubens*, using congener #153 (viz. the most abundant congener in biota) as a model. Organisms were exposed to the ^{14}C labelled contaminant for 34 days via either sea water or sediments. Kinetics were followed in eight body compartments (oral body wall, aboral body wall, cardiac stomach, pyloric caeca, rectal caeca, gonads, podia, and coelomic fluid). Results indicate that bioaccumulation of PCB#153 varied with both the body compartment and the exposure mode. *A. rubens* accumulated the

PCB more efficiently (by 3 to 4 orders of magnitude) when exposed via water than via sediments. Uptake of PCB#153 tended to display saturation kinetics. Steady-state was reached faster for body compartments such as aboral body wall, gonads, and rectal caeca. Finally, some body compartments (viz. aboral body wall and podia) accumulated the PCB congener more intensely. It is concluded that ^{14}C radiolabelling is a promising tool in the study of PCB biokinetics. This extremely sensitive method also allows taking into account key organs which are too small for classical detection techniques.

Keywords: Radionuclide — Bioaccumulation — Echinoderms — PCB — ^{14}C.

Paco Bustamante: "Cadmium bioaccumulation at different stages of the life cycle of cephalopods: a radiotracer (^{109}Cd) investigation"

Cephalopods are a primary food source for cetaceans, and it has been proposed that a cephalod diet may be linked to the high heavy metal concentrations found in many cetacean species. Nevertheless, only very few studies have examined heavy metal behaviour and fate in cephalopods. For example, these organisms are well known to concentrate cadmium to extremely high levels in their digestive gland; however, the reason for such a high bioaccumulation potential is still poorly understood. Therefore, the present study has examined the biokinetics of ^{109}Cd uptake, loss and retention in a typical cephalopod, the common cuttlefish Sepia officinalis, in order to characterise the bioaccumulation potential of Cd in this organism. Cadmium bioaccumulation via sea water and food exposures was studied at different stages of the life cycle of S. officinalis, viz. in embryos, early juveniles and adults. During embryonic development, Cd was efficiently taken up from sea water by the eggs (concentration factor reaching 46 after 8 days of exposure). Surprisingly, only 0.4 % of the ^{109}Cd burden was found in the embryo and 99 % of the metal tracer was found associated with the capsule membrane of the egg. Thus, the capsule acts as a very efficient shield against Cd incorporation,

which in turn suggests that this metal could be highly toxic for early embryos. Once this shield is lost (after hatching), the cuttlefish may bioconcentrate waterborne Cd. Indeed, juveniles as well as adults take up Cd efficiently, particularly in the muscle (62 % of body burden) and digestive gland (25 %). When S. officinalis is replaced in non-contaminated sea water, the whole body loss of Cd is relatively slow (biological half life: ca. 65 days) and proportion of ^{109}Cd body burden increases in digestive gland during the depuration period (42 % after 6 days and 70 % after 29 days of loss). This indicates either a longer retention time of Cd in digestive gland than in other organs, or a preferential translocation of Cd from the organs to the digestive gland. Loss of ^{109}Cd ingested with food (brine shrimp for juveniles; mussels for adults) was even slower than Cd taken up via sea water (biological half life > 257 days), indicating a very strong retention of dietary Cd by juvenile and adult S. officinalis. Assimilation efficiencies were as high as 60 % for both age groups, and the proportion of ^{109}Cd body burden reached 90% in the digestive gland after 29 days of loss. Our results clearly demonstrate that food is the major route of Cd bioaccumulation in the cephalopod S. officinalis. Whatever the source of Cd (water or food), the digestive gland is the primary organ that accumulates Cd. This form of metal storage may be related to the detoxification function of the digestive gland (e.g., metal trapping by metalloproteins) and could explain why Cd reaches extremely high concentrations in this organ.

Keywords: Radionuclide — Bioaccumulation — Cadmium — Cephalopode — Radiotracer.

Ali Temara: "Heavy metals in the sea star *Asterias Rubens* (echinodermata): basis for the construction of an efficient biomonitoring program"

Asterias rubens has been considered as a useful bioindicator of heavy metal contamination by various teams around the NE Atlantic. However, a sound sampling strategy based upon the actual parameters that affect uptake and loss kinetics of heavy metals by asteroids has not yet been designed. The most critical factor that accounts for heavy metal

concentration variability in *A. rubens* living either in background environments or exposed to a metal source is the body compartment. The main route of Cd and Pb uptake, either directly from the water or indirectly through the diet, appears to be the digestive wall; though transfers to other compartments including the body wall and the gonads have been quantified. At steady state, there is a simple relationship between Cd and Pb concentrations in the body and concentrations in the environment (water column or sediments, as observed in the laboratory or in the field). Asteroids have developed efficient detoxification mechanisms (including constitutive or inducible metallothioneins, incorporation of heavy metals into the skeleton) and thus are able to settle and survive in highly impacted environments. According to its ecotoxicological features (ubiquity, temporal and geographical stability, abundance, sampling easiness, size, affinity for and sensitivity to heavy metals, presence in polluted zones), *A. rubens* qualifies as a valuable bioindicator of heavy metal contamination. A sampling strategy and critical values, developed in accordance with the biology of the asteroid and biokinetics of heavy metals described in *A. rubens*, are proposed to assist ecotoxicological risk assessment in marine environments.

Keywords: Radionuclide — *Asterias rubens* — Bioindicator — Heavy Metals — Detoxification — Echinoderms.

Pedro Rivas Romero: "Radioactive waste management: the role of CIEMAT in the Spanish and European R+TD programs for radwaste disposal"

The Spanish concept for RADWASTE disposal is based on a multibarrier confinement system that can be applied to different host rocks acting as final barrier against radionuclide movement. Such systems require a detailed characterisation of each barrier subsystem to know the potential transference of radioisotopes from the spent fuel towards the environment. From this starting point CIEMAT is involved in providing scientific support to the research projects undertaken in the frameworks of ENRESA (Spain) and EU R+TD programs for RADWASTE management. With this purpose CIEMAT's research groups focus their investigations in the

more relevant fields for the safety of a repository in deep geological formations. The main research lines cover the behaviour of engineered barrier sealing materials, the hydrogeochemical characterisation of geological formations and studies of radionuclide retardation processes in the formations considered. There is also a research line for the study of natural analogues, to validate the results obtained in other research lines. The studies of naturally occurring radionuclides (U series, Tritium or ^{14}C) as well as artificial radionuclides or their chemical analogues are used to ascertain the role played by the main transport mechanisms characteristic of each type of formation. Advective processes are studied in crystalline formations (El Berrocal, ASPÖ or HIDROCAR Projects). Diffusive phenomena are being studied, both in laboratory and "in situ", in projects where clay backfill materials are involved (FEBEX-I, RESEAL) or clay formations are regarded as potential host rocks (Mt Terri, MAR Projects). Natural analogues (MATRIX, OKLO and PALMOTTU projects) are employed to evaluate the evolution of natural radionuclides in several scenarios (redox fronts, meteoric weathering, etc..) at a geological time scale.

Keywords: Radionuclide — Rradioactive waste — Management.

John R. Harris: "Radionuclide migration in arid soils"

For a near-surface repository in an arid climate, the unsaturated zone is an important barrier to the release of radionuclides to the environment. The rate of migration of radionuclides depends on the water velocity and the retardation of the radionuclides with respect to water flow. This paper outlines experimental studies of the radionuclide retardation properties of soil and regolith samples from the region being investigated for the Australian repository. Retardation was measured using both batch sorption experiments (high liquid-to-solid ratio) and column experiments (low liquid-to-solid ratio). The use of radionuclides in these experiments enabled sorption and migration properties to be measured at trace concentrations. Batch sorption measurements using ^{137}Cs and ^{238}U were undertaken over a range of pH, ionic strength and radionuclide concentrations. The

column experiments using tritium, ^{137}Cs and ^{60}Co enabled the retardation of these nuclides to be measured under unsaturated flow conditions that are more representative of field conditions.

Keywords: Radionuclide — Arid soils.

Riitta Pilviö: "Actinide separation using extraction chromatography"

Low concentrations and complex sample matrices have made the determination of actinide concentration in the environment a time consuming and complicated task. This paper presents three methods for actinide analyses in environmental samples using extraction chromatography: (i) for the separation of Th, U, Pu and Am in bone ash, (ii) for the separation of Pu and Am from MOX material and (iii) for the separation of Th from soil. These methods are fast and simple and give reliable results with high recoveries and pure spectra.

Keywords: Radionuclide — Actinide — Analytical methods.

John N. Smith: "Seasonally moduladed sedimentation in an estuarine depositional regime"

Sediment cores have been collected at a single station in the Saguenay Fjord over a period of 18 years (1979-1997) in an effort to characterise the preservation of textural and geochemical unconformities associated with river discharge, landslide and flood events. Measurements of the ^{210}Pb sediment-depth distribution permit the determination of an extremely detailed sediment time-stratigraphy for each core that can be used to cross-correlate between different cores in the time series. The accuracy of the time-stratigraphies has been validated using various horizons, such as the 1954 initial appearance of the fallout radionuclides, ^{137}Cs. These results provide a method for real time profiling of the sediment transport events, particularly those promoted by the Spring river discharge, that shape the Saguenay drainage basin and fjord.

Keywords: Radionuclide — Lake — Sediment cores — Time-stratigraphy — ^{210}Pb.

Pedro Francisco Rodríguez-Espinosa: "Regionalization of natural and artificial radionuclides in marine sediments of the Southern Gulf of Mexico"

This paper summarizes the results of regional studies of radioactivity (^{40}K and ^{137}Cs) in 12 of 25 marine-sediments of the Southern Gulf of Mexico. The ^{137}Cs and ^{40}K concentrations measured ranged from 2-6.5 $Bq.kg^{-1}$ and 100-800 $Bq.kg^{-1}$, respectively. These concentrations are similar to those reported in the World inventory for same type of marine sediments. The radioactivity concentrations varied as a function of sedimentary environment. The highest ^{40}K concentrations are associated mainly with the sediments of the Pánuco River fan in the south west of Gulf of México; while the lowest ^{40}K concentrations were found in the Yucatán Escarpment sediments in the south east Gulf of México. The highest ^{137}Cs levels were found in the continental shelf sediments, and the lowest in the continental slope sediments

Keywords: Radionuclide — Distribution — Marine sediments — Gulf of Mexico.

Sandor Mulsow: "Mixing models (advection/diffusion/non-local exchange) and ^{210}Pb sediment profiles from a wide range of marine sediments"

Diffusive and non-local mixing models have been applied to systematically explore the role of mixing in the interpretation of activity profiles of ^{210}Pb. The sediment samples were from the Northwest Pacific Ocean (3 cores), Arabian Sea (1 core) Mediterranean Sea (2 cores) and three cores from the Kara Sea. In 5 cases a significant improvement was achieved when a non-local exchange (injection flux) parameter was added to a diffusive mixing model. In 4 cases simple diffusive mixing was necessary to improve the advection/decay interpretation. In only one case, a more complex interpretation was needed. The latter may be also the result of a sampling artefact. In the study sediment profiles, 6 to 99 % of the surface flux enters the sediment column by injection rather than by simple diffusion/advection process. In summary, diffusion/advection coupled to

non-local mixing processes appears to be more common in marine sediments, thus complicating and stressing the use of ^{210}Pb radiotracer as a geochronological tool. The systematic exploration of mixing models in the interpretation of radiotracer profiles should be a prerequisite to study accumulation rates in marine sediments. Ancillary parameters such as porosity gradients are useful techniques to rule out sampling artefacts from real variations on radiotracer activity profiles in sediments

Keywords: Radionuclide — Marine sediments — Cores — Mixing models — ^{210}Pb.

Jean-Michel Fernandez: "Advantages of combining ^{210}Pb and geochemical signature determinations in sediment record studies; application to coral reef lagoon environments"

Human activities have impacted our natural environment, especially since the middle of the 19th century. The memory of past environmental conditions is partly recorded in the layers of the sediment reservoirs of lakes and seas. Geochemical approaches applied to sediment cores can provide information on past changes in heavy metal concentrations and other environmental tracers that are indicative of specific environmental modifications. However, these studies cannot be self-supported and have to be combined with dating techniques such as the ^{210}Pb method. In the present paper we provide several application examples from coral reef environments that illustrate different cases. Sediment cores were sampled in the lagoons of New-Caledonia and Fiji which differ in their, geological, morphological and environmental contexts. Each core, representative of a particular set of environmental conditions, has been studied in terms of heavy metal concentration (sequential extractions) and ^{210}Pb unsupported radioactivity. ^{210}Pb data allowed the impact of real human activities to be distinguished from phenomena due to natural occurrences (e.g. slumps) and deficiency in sampling techniques. Although relatively distant from the main terrigeneous sources (La Coulée & Les Pirogues rivers), Sainte-Marie Bay still proves to be strongly influenced by past mining activities. In Laucala Bay (Fiji),

the results showed that the inputs of terrigeneous particulate matter originating from the Rewa river remained high and constant over time, resulting in an extremely limited bioturbation layer. In contrast, profiles from a submarine valley in the middle lagoon of New Caledonia and from Suva Harbour in Fiji displayed anomalies that can be attributed to two different type of phenomena: natural occurrence of slumps in the valley and sampling artefact in Suva Harbour.

Keywords: Radionuclide — Marine sediments — Cores — Coral reef lagons — ^{210}Pb.

Sitaram Garimella: "Concentrations of heavy metals and trace elements in the marine sediments of the Suva Lagoon, Fiji"

Sediment samples from 30 sites in the Suva lagoon were collected and their elemental abundances analysed by the technique of instrumental neutron activation. The sediment samples were irradiated for 4 h at a thermal neutron flux of $4x10^{12}$ $n.s^{-1}.cm^{-2}$ in a nuclear reactor in Australia. Five days later, the samples were flown back to Fiji for analysis using a HPGe gamma-ray spectrometer of the Department of Physics. From the above measurements, concentrations of two major elements (Na and Fe) and 23 trace elements (As, Br, Ce, Co, Cr, Cs, Eu, Hf, Hg, La, Mo, Nd, Rb, Sb, Sc, Sm, Sr, Ta, Tb, Th, Yb, Zn and Zr) were determined in the above sediments. Concentrations of several elements at most sites were higher than the EPA (Environmental Protection Agency) limits.

Keywords: Radionuclide — Heavy metals — Neutron activation — Marine sediments — Coral reef lagon.

Hervé Michel: "Comparaison of ^{210}Pb chronology with $^{238,239-240}$Pu, ^{241}Am and ^{137}Cs sedimentary record capacity in a lake system"

^{238}Pu, $^{239-240}$Pu, and ^{241}Am were measured, by counting after radiochemical separation, in two lake sediment cores. The profiles of these transuranics were compared to those of the fission product ^{137}Cs and natural radionuclide ^{210}Pb. Datation of nuclear events and data on behaviour of the studied elements were deduced.

Keywords: Radionuclide — Lake — Time stratigraphy.

Koh Harada: "Excess ^{210}Pb and ^{210}Po in sediment from the Western North Pacific"

Concentrations of ^{210}Pb and ^{210}Po in sediment core samples from the western North Pacific, highly biologically productive subarctic ocean, were determined. Excess ^{210}Pb with respect to its precursor ^{226}Ra and excess ^{210}Po to ^{210}Pb were observed in the sediment down to 6 cm depth. It clearly shows that the sediment particles are mixed by relatively strong bioturbation, since sedimentation rate should be low, < 1 cm.kyr^{-1}. Assuming diffusion-like mixing and a constant coefficient, the bioturbation coefficient was estimated to be 0.04 to 0.4 cm^2.yr^{-1} from the excess ^{210}Pb profile and also to be 1.2 cm^2.yr^{-1} from the excess ^{210}Po profile. Fluxes from overlying water of ^{210}Pb and ^{210}Po were calculated to be 70 and 590 dpm.g^{-1}, respectively, from the standing crop of these nuclides in the sediment.

Keywords: Radionuclide — Marine sediments — Cores — Mixing.

Wlodek Zahorowski: "Radon measurements for atmospheric tracing"

Natural radioactivity in the atmosphere is predominantly due to radon and radon progeny. Radon (^{222}Rn) is a noble gas, which does not interact chemically with particulates or aerosols. A decay product of uranium, radon, with a half life of 3.8 days, is released into the pore space of rocks and soils where most of it decays. The proportion of the radon which diffuses to the surface is dependent on soil moisture. Once in the troposphere, the predominant loss mechanism is radioactive decay, with only a small fraction mixing to the stratosphere or being adsorbed by the surface. The decay products (progeny) are the major component of the natural radiation dose. Lead-212, a decay product of thoron (^{222}Rn), is a complementary tracer to radon with a shorter time scale, defined by the 10.64 hour half-life of lead-212. Radon is an excellent tracer of air transport in the troposphere. Because the radon emanation rate from land is about one hundred times the rate from oceans, the presence of radon in air samples at levels above a threshold value is indicative of contact with land within the previous two weeks. An inter-

national network of baseline monitoring stations has been established to record the concentration of climate-sensitive gases far away from their sources. An air sample that has not been perturbed by recent passage over land is considered baseline and the lack of radon is a direct indication that an air sample has not recently travelled over land. ANSTO has extensive experience in the measurement of radon and thoron in the atmosphere. Radon concentration in baseline air can be as low as a few radon atoms per litre of air. This makes the task of measuring radon levels with a time resolution matching prevailing weather conditions a demanding task. Radon measuring techniques and instrumentation developed for radiation protection are inadequate for the climate research. ANSTO has developed new radon detectors with the sensitivity and ruggedness required for climate research. In these detectors, the function of supplying filtered air to the detector is separated from the function of delivering air to the collecting wire screen used for plating-out the radon progeny. The high diffusivity of radon progeny makes it possible to use a wire screen to remove the progeny with high efficiency and very low flow impedance. The present detectors can measure radon concentration in baseline air down to 10 $mBq.m^{-3}$ with a time resolution of less than 1 hour. These detectors have been installed at several atmospheric baseline stations and will be used in the international Aerosol Characterisation Experiment (ACE-Asia) in East Asia and the Northern Pacific. Radon is a better indicator of baseline air than other parameters commonly used for the same purpose, such as condensation nuclei, wind direction and speed. The application of radon as a criterion for baseline air generally improves the quality of trace gases data attributed to baseline conditions. Measurement of both radon and ^{212}Pb at the Mauna Loa Observatory in Hawaii was able to quantify the degree of contact of the air parcels with local (Hawaiian) land. A local knowledge of radon and thoron flux in the vicinity of a baseline station can be important. Low level thoron flux measurements led to an evaluation of the thoron source term from barren lava around the Mauna Loa Observatory in Hawaii. A thoron emanometer specifically assembled for the survey achieved a lower limit of detection of 1 $mBq.m^{-2}.s^{-1}$. Radon transport can be simu-

lated by general circulation models by implementing the parameterisation for passive tracers. Such a procedure can be used for calibrating and verifying the transport component of the model, as well as providing a better understanding of the atmospheric features that control the distribution of radon. With the lack of radon emanation data, it is commonly assumed that the radon production term is constant on the global scale, which is clearly a poor approximation to reality. Good quality data regarding the radon flux is required. ANSTO has developed experimental methods for measuring radon and thoron flux emanation in the context of climate research. The spot flux measurements have been combined with data from airborne gamma surveys to construct a self-consistent map of radon flux from 5° X 4° grid boxes over Australia. Even on such a scale, the radon flux estimate vary by more than one order of magnitude from one grid box to another.

Keywords: Radionuclide — Radon — Atmosphere — Climate.

Gilbert Le Petit: "Trace elements in total atmospheric suspended particules in a suburban area of Paris: a study carried out by INAA"

The atmospheric particulate matter of industrialised cities have become a mixture of potentially basic substances whose concentration have to be monitored to assess the pollution levels. Anthropogenic elements, particularly trace metal, are part of these pollutants and the knowledge of their total concentration in the air is necessary to evaluate the pollution risk in term of maximum levels and long term exposure. In the present work a preliminary study initiated for monitoring the trace element levels present in total atmospheric suspended particles (TSP) of the suburban areas of Paris in France is presented. More than 30 elements have been determined using a high volume air sampler, about 600 $m^3.h^{-1}$, installed near a busy highway and equipped with large filters for weekly collection of atmospheric aerosols. The study covers a period of a whole year (1998) and different weather conditions. Instrumental Neutron Activation Analysis (INAA) from the OSIRIS research reactor (neutron

flux: $1.2x10^{14}$ $n.s^{-1}.cm^{-2}$) at the Commissariat à l' Energie Atomique, Saclay centre, has been used for the determination of the great part of element whereas ICP-MS has been employed for determination of lead. The reliability of our INAA methodology was demonstrated using a standard internal reference. Enrichment factors were used to investigate trends, emission sources. Evolution in time of stable element concentrations and possible origin of certain pollution sources, has been investigated.

Keywords: Radionuclide — Trace elements — Neutron activation — Atmosphere — Particles.

Ann Henderson-Sellers: "Assessing soil moisture in global climate models: is radon a possible verification tool?"

A noble gas with a half life of 3.8 days, radon has been used successfully in many atmospheric tracer studies. Radon is generated in soil by the radioactive decay of radium and escapes by diffusion through soil pores and plant transpiration. Emanation rates are a function of soil temperature, soil porosity, depth of soil, soil moisture and the underlying geology. It is proposed here that radon data be investigated as a possible source of information about large-scale soil moisture: a quantity important for global climate model verification and difficult to measure by other means. Measurements of radon flux at seventy eight sites in Australia, thee hundred and twenty five sites in Florida and forty two Hawaiian sites have generated expressions relating radon emanation rates to soil moisture. It is both feasible and potentially valuable to exploit this relationship in a new Global Climate Model (GCM) intercomparison. We propose that a new Experiment Subproject of the Atmospheric Model Intercomparison Project (AMIP) II programme be created in which the ^{222}Rn source strength is a function of model-simulated soil moisture. Hypotheses to be examined include (i) does the addition of a functional dependence of radon emanation on soil moisture improve the fit of predicted near-surface ^{222}Rn to observations; (ii) does the addition of a functional dependence of radon emanation on soil moisture improve the fit

of archived ^{210}Pb to observations; and, if either generate an affirmative reply, then (iii) can ^{222}Rn or ^{210}Pb be used as a novel monitor of areal soil moisture and hence as a new means of verifying global climate model simulations?

Keywords: Radionuclide — Climate — Models — ^{222}Rn — Soil moisture.

Masami Fukui: "Production and release of tritium from a research reactor"

The Kyoto University Research Reactor Institute (KURRI) supports three major sources of tritium: a D2O (heavy water) facility, a Cold Neutron Source (CNS) facility and a tritium target fabricated in an accelerator. This paper focuses on determination of the distribution and variation in the concentration of tritium in the air near sources in the containment building. To assess the degree of attenuation of HTO concentrations in the field is another point of interest in radiation protection for the public. The radioactive gas concentrations in the exhaust from the CNS and D2O facilities were measured using an ionization chamber with an effective volume of 1.5 dm^3. The specific activities of the water samples from the condensates in the air were obtained using a liquid scintillation counter. During the overhaul on August 1998 continuous extraction of the air from the CNS facility revealed the presence of radioactive gas showing a maximum concentration, $2.6x10^4$ $Bq.dm^3$. This attenuated to two orders of lower after one month of the overhaul. On the other hand the specific activities in condensates of this exhaust air line had been detected on the order of $2 x10^5$ $Bq.ml^{-1}$ of which value is two orders higher than that observed for the D2O decay exhaust line. This indicates that the CNS exhaust line may be the primary source for the HTO concentration in the KURR containment building air to increase during Saturday and Sunday when the venting ceases. That is, the specific activities in condensates in the air ranged from less than 1 $Bq.ml^{-1}$ during venting operation to few tens of $Bq.ml^{-1}$ after two days of discontinued venting.

Keywords: Radionuclide — Tritium — Radio-protection.

Valentin N. Golosov: "Application of Chernobyl-derived ^{137}Cs for assessment of soil redistribution in agricultural catchments of Central Russia"

Vast areas of Russian Plain were contaminated by radionuclides after Chernobyl Power Station explosion. Because more than 99 % of radionuclides fall on the ground during very short period of time, the layer with contaminants can serve as a marker for assessment of soil and sediment redistribution for period from May 1986. Detail study of erosion and deposition rates within 4 agricultural catchments with different slope configuration were made in the Lokna river basin, Tula region, Central .Russia. Initial fallout inventory within the Lokna river basin was more than 200 kBq.m^2. Both grid and transect sampling procedures were applied for collection of samples for laboratory analysis of gamma-spectrometry. In addition in situ measurement of ^{137}Cs inventories were made. Results of assessment demonstrate that ^{137}Cs technique can be used for assessment of soil redistribution in areas affected by Chernobyl contamination. Two approaches can be applied. First is the use of proportional and mass-balance model[1] for assessment of soil redistribution for each site. Second is the calculation of the ^{137}Cs budget for the cultivated areas and adjacent area of deposition within dry creek valley. Independent calculation of soil erosion rates for each site were made using modified version of USLE and State Hydrological Institute model. Results of assessment of erosion rates using different approaches demonstrate that proportional and mass-balance calibration models can be applied for sites with erosion rates 20 kg per m2 and more because only 13 years have passed from the Chernobyl explosion. ^{137}Cs budget approach are more useful for areas with low erosion rates. The detail study of deposition area should be done in the latter case.

Keywords: Radionuclide — ^{137}Cs — Chernobyl — Contamination — Soil transport — Modelling.

Paulina Schuller: "Use of ^{137}Cs to estimate rates and patterns of soil redistribution on agricultural land in Central-South Chile: models and validation"

The objective of the present study was to evaluate the applicability of a conventional and a simplified technique to estimate rates and patterns of soil redistribution on agricultural land in Central-South Chile. Four fields of Palehumult soil showing contrasting land use and management were selected in the Coastal Mountain Range (38° 40′S, 72° 30′W): crop fields and semi-permanent grasslands, both under subsistence and commercial management. A software was designed to estimate the amounts and spatial distribution of the soil erosion and sedimentation based on existing models. The rates and patterns of soil redistribution estimated by a ^{137}Cs inventory evaluation of individual samples collected in a grid pattern were very similar to the ones obtained by an inventory evaluation in composed samples taken at constant-elevation transects. The second method is suitable for giving assessment on soil loss and sediment accumulation in areas exhibiting simple topography, showing almost similar slopes at constant-altitude transects. It reduces considerably the measuring time and the costs of the soil redistribution quantification. The results obtained using both methods were in accordance with the local annual sediment loss measured in erosion plots and with the pattern of soil redistribution rates estimated by pedological observations. The ^{137}Cs technique is seen as an efficient method to obtain long-term soil redistribution rates under the climatic conditions and the soil type selected in Chile. In order to optimise the costs and benefits of the ^{137}Cs technique, the sampling and inventory quantification strategy must be selected according to the resolution of the required information, and extension and complexity of the landscape relief.

Keywords: Radionuclide — ^{137}Cs — Chile — Soil transport — Modelling.

Francois Bréchignac: "Soil-radionuclides interaction and subsequent impact on the contamination of plant food products based on a simulated accidental source"

The PEACE* European Programme has studied the consequences on the agricultural environment of the atmospheric release of radio-contaminants which would occur in case of a severe accident in a PWR nuclear reactor. Beyond the quantification of traditional radioecological features (transfer factors), this programme has looked for a better understanding of the mechanisms which govern the kinetic behaviour of ^{137}Cs and ^{90}Sr in soils, and their transfer to plants, in view of improving the accuracy of assessment model predictions. A mechanistic modelling of migration and root absorption has been confronted to the results of original experiments undertaken in the unique IPSN facility designed for simulating a radioactive contamination in controlled conditions and following it up during several years. Contamination in ^{90}Sr of all investigated plants by root uptake exceeds that of ^{137}Cs, with variations which cannot be accounted for based on the physico-chemical properties of the soils solid matrix only. The complex and essential role of the soil solution has been identified. As an interface compartment, its composition results from the double interaction with the soil solid matrix, in the one hand, and the root absorbing surfaces, in the other hand. It is through their effects on the soil solution chemical composition (competitive ions K, Ca and Mg, in particular) that parameters such as soil type, agricultural practices, time and climatic conditions, promote a variability of the radionuclides transfer factors. Vertical migration is reduced in mineral agricultural soils. Profiles are established early on after the contamination event (less than one month) suggesting the importance of the initial soil moisture and the first rains. Furthermore, they remain similar on all the studied soils, without a clear differentiation between ^{137}Cs and ^{90}Sr despite their quite distinct respective KD values. Reliable predictions, therefore, cannot be achieved from a soil description reduced to the only classical KD concept.

(* PEACE: Programme for Evaluating the impact of Accidents Contaminating the Environment).

Keywords: Radionuclide — Soil — Plant — ^{137}Cs — Contamination — Modelling — ^{90}Sr.

Peter J. Kershaw: "Contrasting behaviour of artificial radionuclides in the Pacific and other ocean basins: radionuclides as tracers of environmental change?"

Ocean basins have received artificial radionuclides from a number of sources, including: global fallout from weapons testing, close-in fallout (e.g. Marshall Islands, Mururoa Atoll, Novaya Zemlya), dumped wastes (e.g. Sea of Japan, NE Atlantic, Kara Sea), accidental losses (e.g. SNAP-9A satellite, nuclear-powered vessels, nuclear weapons) and discharges into coastal regions. These various sources will be summarised and the consequent distribution and behaviour of artificial radionuclides (^{137}Cs, ^{90}Sr, ^{238}Pu, ^{239,240}Pu), in the water column, will be described. Time- and space-dependent changes have been observed in the distribution patterns in both surface waters and in vertical profiles. These will be related to environmental factors, where possible, and the nature of the source term(s). Examples will be taken primarily from the Pacific Ocean, and these will be compared with observations from other ocean basins, as appropriate.

Keywords: Radionuclide — Pacific ocean — Environment.

Koh Harada: "Export fluxes of organic Carbon in the Western North Pacific determined by drifting sediment trap experiments and ^{234}Th profiles"

To investigate seasonal change of biogeochemical processes in the western North Pacific, a time-series observation is being conducted at 44°N, 155°E from 1998 by Japanese JGOFS team. In the activity, export fluxes of particulate organic carbon, which is the POC flux transported from surface euphotic layer to deeper ocean were estimated from drifting sediment trap experiments and measurements of ^{234}Th in the water column in November and December 1998 and twice in May 1999. Concentrations of ^{234}Th in seawater increased with increasing water depth down to 100 m depth, showing the preferential removal of Th from the surface layer. Total mass flux, POC flux and ^{234}Th flux determined by the sediment traps were gradually decreased down to the 100 m depth and were almost constant or increased below the depth. The ^{234}Th flux at 100 m depth determined by the

sediment trap were about 30 % smaller than the flux estimated from the water column profiles of ^{234}Th. This suggested that collection of particulate materials by the sediment trap was not quantitative. Therefore, the export flux of POC was estimated from the ^{234}Th flux from the water column profile and the POC/^{234}Th ratio in the settling particle to be 6.6, 5.5 and 9.2 mmol.m^{-2}.day^{-1}, respectively in November, December 1998 and May 1999.

Keywords: Radionuclide — Pacific ocean — Sediment trap — ^{234}Th — Organic carbon.

Gillian Peck: "Uranium decay series radionuclides in the Western Equatorial Pacific Ocean and their use in estimating poc fluxes"

The uranium decay series radionuclides, ^{226}Ra, ^{210}Pb and ^{210}Po were measured in dissolved phase (< 0.45 mm) and ^{210}Pb and ^{210}Po in the particulate phase (> 0.45 mm), in the upper 300 m of the Bismarck Sea and the western equatorial Pacific Ocean, along the equator from 143°E to 152°E. Box model calculations were then used to estimate the flux of particulate ^{210}Po and ^{210}Pb from the upper layers of the ocean. The downward flux of particulate organic carbon was then estimated using the flux of particulate ^{210}Po and the ratio of POC/^{210}Po in each layer.

The downward flux of particulate organic carbon was calculated to be 104 mg.m^{-2}.d^{-1} from the upper 100 m and 180 mg.m^{-2}.d^{-1} from the 100-300 m layer of the Western Equatorial Pacific Ocean and Bismarck Sea.

Keywords: Radionuclide — Pacific ocean — Uranium — Particule Flux — Organic carbon.

Dejanira C. Lauria: "Origin and transport of radium in the water column of Buena coastal lagoon"

The origin and transport of radium in the surface water of a coastal lagoon was studied. The water analysis showed a decrease in the radium concentration, and an increase of the pH and salinity in the seaward direction The gradient of the radium concentration along the lagoon pointed to the source of radium in the lagoon water, leading to the discovery of

spring waters located at the less brackish zone of the lagoon. The groundwater supplies the Ra isotopes, probably from monazite leaching, while the seawater supplies major ions. Both of ion sources are located in opposite sides of the lagoon. From the $^{228}Ra/^{226}Ra$ concentration ratios, a radium migration velocity of around 300 m/years along the lagoon's first 1.9 km was estimated. The high salinity of the water seems to play an important role for the long residence time of radium in the waters of the Buena lagoon. The total amount of ^{228}Ra and ^{226}Ra in the water column was estimated as 40 MBq and 20 MBq respectively

Keywords: Radionuclide — Lagoon — Radium — Residence time.

C. Alonso Hernández: "Hydric resources radioactive contamination in the central region of Cuba as a consequence of fallout after the atmospheric nuclear bombs tests"

The ^{137}Cs activity levels determined in atmospheric and hydric samples, collected in Cienfuegos province (Central-South region of the country), during five years (1994-1998) are presented. Some graphics of the ^{137}Cs behavior in the period of study are shown, as well as some considerations about their transference processes throughout some environmental components are explained. It has been concluded that our hydrological resources have been contaminated by nuclear fission products coming from the past nuclear bombs tests by means of Global Fallout.

Keywords: Radionuclide — Cuba — Freshwater — Atmosphere — ^{137}Cs.

Achevé d'imprimer en février 2002

Imprimé par l'atelier de reprographie

du Centre IRD de Nouméa

Dépot légal: février 2002

SPERA 2000 forming the 6th biennial Conference from the South Pacific Environmental Radioactivity Association (SPERA) was organised at the Institut de recherche pour le développement (IRD) in Noumea, New Caledonia on the 19th to 23rd of June 2000. The contributions to this conference which focused on "Environmental Changes and Radioactive Tracers" are gathered in the present publication. For several decades, naturally occurring radionuclides have been studied primarily to assess their distributions in the environment but also to understand the dynamic processes that control their behaviour. More recently, injection of both natural and artificial radionuclides due to human activities have provided new tools for the study of environmental processes at local, regional and global scales. The most recent environmental radionuclide studies using both natural and artificial emitters in various research fields were presented during SPERA 2000. The Conference included 6 sessions covering atmospheric, water, sediment, soils, waste disposal and biological radionuclides in addition to a workshop on "Radiological techniques in sedimentation studies: Methods and applications".

Radionuclide — radioactivity — tracers — environment — atmosphere — water — sediment — biology — soil — waste.

Le congrès SPERA 2000, qui constituait la VI[e] conférence de la South Pacific Environmental Radioactivity Association (SPERA), s'est tenu à l'Institut de recherche pour le développement (IRD) à Nouméa, Nouvelle-Calédonie, du 19 au 23 juin 2000. Cet ouvrage rassemble les contributions à ce congrès ayant pour thème central « Modifications environnementales et traceurs radioactifs ». Le SPERA 2000 a permis de présenter les travaux les plus récents sur l'étude des radionucléides artificiels et naturels dans différents champs d'investigation des sciences de l'environnement. La conférence rassemblait 6 sessions liées à l'étude des compartiments atmosphérique, aquatique, biologique ou sédimentaire, ou traitant des problèmes d'érosion des sols ou de stockage des déchets ainsi qu'une table ronde dédiée à « L'apport des techniques radiologiques dans les études sédimentaires : méthodes et applications ».

Radionucléide — radioactivité — traceurs — environnement — atmosphère — eau — sédiment — biologie — sol — déchets.

IRD Éditions
213, rue La Fayette
75480 Paris cedex 10

Diffusion
IRD, 32, avenue Henri-Varagnat
93143 Bondy cedex
fax : 01 48 02 79 09
diffusion@bondy.ird.fr

20,00 €

ISSN : 0767-2896
ISBN : 2-7099-1493-X

9 782709 914932